NOVEL PLANT MOLECULES REGULATING THE INTERACTION WITH PATHOGENIC AND BENEFICIAL FUNGI

EDITED BY: Silvia Proietti, Ivan Baccelli, Richard Hickman,
Antonio Leon-Reyes and Laura Bertini

PUBLISHED IN: Frontiers in Plant Science and Frontiers in Microbiology

frontiers Research Topics

frontiers

ISSN 1664-8714
ISBN 978-2-88966-568-6
DOI 10.3389/978-2-88966-568-6

About Frontiers

Frontiers is more than just an open-access publisher of scholarly articles: it is a pioneering approach to the world of academia, radically improving the way scholarly research is managed. The grand vision of Frontiers is a world where all people have an equal opportunity to seek, share and generate knowledge. Frontiers provides immediate and permanent online open access to all its publications, but this alone is not enough to realize our grand goals.

Frontiers Journal Series

The Frontiers Journal Series is a multi-tier and interdisciplinary set of open-access, online journals, promising a paradigm shift from the current review, selection and dissemination processes in academic publishing. All Frontiers journals are driven by researchers for researchers; therefore, they constitute a service to the scholarly community. At the same time, the Frontiers Journal Series operates on a revolutionary invention, the tiered publishing system, initially addressing specific communities of scholars, and gradually climbing up to broader public understanding, thus serving the interests of the lay society, too.

Dedication to Quality

Each Frontiers article is a landmark of the highest quality, thanks to genuinely collaborative interactions between authors and review editors, who include some of the world's best academicians. Research must be certified by peers before entering a stream of knowledge that may eventually reach the public - and shape society; therefore, Frontiers only applies the most rigorous and unbiased reviews.
Frontiers revolutionizes research publishing by freely delivering the most outstanding research, evaluated with no bias from both the academic and social point of view. By applying the most advanced information technologies, Frontiers is catapulting scholarly publishing into a new generation.

What are Frontiers Research Topics?

Frontiers Research Topics are very popular trademarks of the Frontiers Journals Series: they are collections of at least ten articles, all centered on a particular subject. With their unique mix of varied contributions from Original Research to Review Articles, Frontiers Research Topics unify the most influential researchers, the latest key findings and historical advances in a hot research area! Find out more on how to host your own Frontiers Research Topic or contribute to one as an author by contacting the Frontiers Editorial Office: frontiersin.org/about/contact

NOVEL PLANT MOLECULES REGULATING THE INTERACTION WITH PATHOGENIC AND BENEFICIAL FUNGI

Topic Editors:
Silvia Proietti, University of Tuscia, Italy
Ivan Baccelli, Istituto per la Protezione sostenibile delle Piante, Sede Secondaria Firenze, Italy
Richard Hickman, Utrecht University, Netherlands
Antonio Leon-Reyes, Universidad San Francisco de Quito, Ecuador
Laura Bertini, University of Tuscia, Italy

Citation: Proietti, S., Baccelli, I., Hickman, R., Leon-Reyes, A., Bertini, L., eds. (2021). Novel Plant Molecules Regulating the Interaction with Pathogenic and Beneficial Fungi. Lausanne: Frontiers Media SA. doi: 10.3389/978-2-88966-568-6

Table of Contents

frontiers in Plant Science

EDITORIAL
published: 27 January 2021
doi: 10.3389/fpls.2021.644546

Editorial: Novel Plant Molecules Regulating the Interaction With Pathogenic and Beneficial Fungi

Ivan Baccelli[1]*, *Laura Bertini*[2]*, *Richard Hickman*[3], *Antonio Leon-Reyes*[4] and *Silvia Proietti*[2]

[1] Institute for Sustainable Plant Protection, National Research Council of Italy, Florence, Italy, [2] Department of Ecological and Biological Sciences, University of Tuscia, Viterbo, Italy, [3] Plant-Microbe Interactions, Department of Biology, Utrecht University, Utrecht, Netherlands, [4] Laboratorio de Biotecnología Agrícola y de Alimentos-Ingeniería en Agronomía, Colegio de Ciencias e Ingenierías El Politécnico, Universidad San Francisco de Quito USFQ, Quito, Ecuador

Keywords: molecular plant-microbe interaction, microbiome, endophytes, mycorrhizae, plant diseases, plant evolution, plant immunity, stress resistance

Editorial on the Research Topic

Novel Plant Molecules Regulating the Interaction with Pathogenic and Beneficial Fungi

Plants started colonizing land ∼450–470 million years ago (Humphreys et al., 2010; Rubinstein et al., 2010; Parfrey et al., 2011). With remarkable coincidence, the first symbiotic interaction between fungi and plants can be dated back to 400–460 million years ago (Remy et al., 1994; Redecker et al., 2000).

In 1975, Pirozynski and Malloch hypothesized that colonization of land by plants was possible only because a symbiotic association between a "semi-aquatic ancestral alga" and a "mycorrhizal partner" (referred to as an "aquatic fungus" by the authors) occurred. For the authors, terrestrial plants are "the product of this ancient and continuing partnership" which has allowed plants "to cope with the problems of desiccation and starvation associated with terrestrial existence" (Pirozynski and Malloch, 1975). Moreover, "land plants never had any independence" (from mutualistic symbiosis), and "if they had, they could never have colonized the land." According to recent data, arbuscular mycorrhizal fungi actually appeared as drivers of plant terrestrialization in early Palaeozoic land ecosystems (Humphreys et al., 2010; Field et al., 2012; Loron et al., 2019).

Coevolution between plants and fungi has obviously led both partners to evolve mechanisms of interaction that nowadays appears extremely sophisticated. Plants can produce molecules able to promote beneficial interactions and molecules able to counteract pathogenic interactions. They can sense pathogens and trigger the activation of defenses as well as communicate with beneficial fungi and modify the plant transcriptome and metabolome in order to accommodate symbiotic associations. The outcome of the interaction may have implications in terms of plant growth, development, and stress resistance.

In this issue we will highlight discoveries in the field of plant-fungi interactions, particularly around the role of plant molecules, with the belief that the development of novel plant protection strategies will be greatly assisted in the future by understanding the mechanisms of plant-microbe communication.

PATHOGENIC PLANT-FUNGI INTERACTIONS

Plant molecules may act as either resistance or susceptibility factors during the plant-pathogen interaction, and their role may also go beyond this and affect plant growth and developmental

Edited and reviewed by:
Essaid Ait Barka, Université de Reims Champagne-Ardenne, France

***Correspondence:**
Ivan Baccelli
ivan.baccelli@ipsp.cnr.it
Laura Bertini
lbertini@unitus.it

Specialty section:
This article was submitted to Plant Pathogen Interactions, a section of the journal Frontiers in Plant Science

Received: *21 December 2020*
Accepted: *04 January 2021*
Published: *27 January 2021*

Citation:
Baccelli I, Bertini L, Hickman R, Leon-Reyes A and Proietti S (2021) Editorial: Novel Plant Molecules Regulating the Interaction With Pathogenic and Beneficial Fungi. Front. Plant Sci. 12:644546. doi: 10.3389/fpls.2021.644546

traits or tolerance to abiotic stresses. Their identification and characterization is thus essential to develop sustainable control strategies for plant protection.

Wild tomato species are a valuable source of resistance to powdery mildew caused by *Oidium neolycopersici*. This is the case of *Solanum habrochaites* G1.1560 which carries the resistance gene *Ol-1*. Zhang Y. et al. identified a new gene required for *Ol-1*-mediated resistance. The gene, named ShORR-1 (*Solanum habrochaites Oidium* Resistance Required-1) was shown to encode a membrane-localized protein. By overexpression and silencing studies, it was demonstrated that ShORR-1 plays a role in resistance in *S. habrochaites* G1.1560. However, a ShORR-1 homolog differing in 13 aa residues from the susceptible tomato cultivar Moneymaker was shown to confer instead pathogen susceptibility, revealing how gene variants may differently turn the interaction into resistance or susceptibility.

A Type I Rac/Rop GTPase named TaRac6was studied in *Triticum aestivum* by Zhang Q. et al. *Puccinia striiformis* f. sp. *tritici* isolates CYR23 (leading to incompatible interaction, i.e., resistance) and CYR31 (leading to compatible interaction, i.e., disease) were used to investigate the role of TaRac6. Transient expression of TaRac6 inhibited Bax-triggered plant cell death in *N. benthamiana*. In addition, the gene was up-regulated 24 h after infection only in the compatible interaction. Importantly, silencing of TaRac6 by virus induced gene silencing (VIGS) led to higher production of hydrogen peroxide and enhanced resistance to *P. striiformis* f. sp. *tritici* CYR31, suggesting that TaRac6 functions as a susceptibility factor.

Membrane-bound transcription factors (MTFs) belonging to the basic leucine zipper (bZIP) family act as key components of stress signaling pathways in endoplasmic reticulum (ER). Wang et al. revealed how mRNA encoding a bZIP MTF in wheat, named TabZIP74, may undergo splicing and encode a new protein lacking the transmembrane domain which is mobilized to the nucleus. Knocking down TabZIP74 by VIGS enhanced wheat seedling susceptibility to *P. striiformis* f. sp. *tritici*, and decreased both drought tolerance and lateral root formation, demonstrating that TabZIP74 mRNA is induced to splice during biotic and abiotic stresses and acts as a positive regulator of wheat stripe rust resistance and drought tolerance, being also implied in root development.

Invertases irreversibly catalyze the cleavage of sucrose into glucose and fructose, exerting a pivotal role in carbon utilization and distribution, as well as immune responses to pathogens. Their activities are determined by proteinaceous inhibitors named C/VIFs (cell wall/vacuolar inhibitor of β-fructosidases). Su et al. characterized two putative invertase inhibitors from *Populus trichocarpa* named PtC/VIF1 and PtC/VIF 2, and showed that the two encoding genes were down-regulated in poplar roots during *Fusarium solani* infection, suggesting that invertase inhibitors may be involved in a sucrose-mediated defense pathway.

Pastor-Fernández et al. reported on the protective effects of two signaling peptides, systemin, and hydroxyproline-rich systemins (HypSys) from tomato, on *Arabidopsis thaliana*. The peptides were able to induce resistance against *Plectosphaerella cucumerina* infection indicating that *Arabidopsis* plants can sense peptides from phylogenetically distant plant species. In addition, it emerged how resistance was dependent on jasmonic acid signaling and led to enhanced PAMP-triggered immunity (PTI) responses upon infection.

Trdá et al. shed new light on a group of plant molecules named saponins, demonstrating that besides antifungal activity they may also possess resistance inducing ability. In particular, the terpenoid saponin aescin was able to induce resistance in *Brassica napus* against the fungus *Leptosphaeria maculans* by activating the SA pathway and oxidative burst. In *A. thaliana*, aescin induced SA-dependent resistance to the bacterium *Pseudomonas syringae* pv *tomato* DC3000.

Serine protease inhibitors (PIs) belonging to the Kunitz-type (PKPI) and Potato type I (Pin1) families are known to possess insecticidal and nematicidal activity. Turrà et al. investigated the ability of PKPI and Pin1 proteins to limit fungal and bacterial infection and influence plant growth. Transgenic *Nicotiana benthamiana* plants transiently expressing PKPI and Pin1 proteins turned out to be more resistant to *Botrytis cinerea*, *Alternaria alternata* and *Pseudomonas syringae* pv. *tabaci* infections. Systemic expression of these proteins resulted in plants with enhanced shoot and root biomass, revealing that members of PKPI and Pin1 family proteins can influence cell development, differentiation, and disease resistance to fungal and bacterial pathogens.

Finally, a new effector named AGLIP1, able to induce cell death in *Nicotiana benthamiana* and to suppress PAMP-triggered immunity in transgenic *Arabidopsis* lines was identified from *Rhizoctonia solani* by Li et al.

BENEFICIAL PLANT-FUNGI INTERACTIONS

Plant-associated fungi can bestow important benefits upon host plants. Nevertheless, plants need to manage the microbes residing inside them or surrounding their roots, i.e., the so-called microbiome. Among the strategies to achieve this, plants can produce exudates and other molecules that are able to shape root-associated microbial communities.

In their comprehensive review, Pascale et al. summarized the current knowledge on plant-microbiome interactions. More specifically, they described the mechanisms by which plants select their microbiome (via structural/chemical components) and presented well-characterized examples of microbiome recruitment by plants. Finally, they suggested approaches to exploit plant microbiomes and design synthetic communities that can be used to boost plant health and growth in a sustainable and reproducible manner.

Some of the molecules employed by plants to communicate with surrounding microorganisms originate from carotenoid precursors by oxidative cleavage, yielding a range of compounds known as apocarotenoids. Apocarotenoids are emerging as key regulators of plant–microbe interactions, in particular of the arbuscular mycorrhizal (AM) symbiosis: abscisic acid (ABA), strigolactones, blumenols, mycorradicins,

and zaxinone play roles during different stages of the colonization process by AM fungi, as reviewed by Fiorilli et al.

Finally, in a context of increasing demand for animal-friendly endophytes harboring deterrent and insecticidal properties for the market of artificially infected grass cultivars (Johnson et al., 2013), Cagnano et al. performed a large-scale screening of *Epichloë* endophytes infecting *Schedonorus pratensis* and other forage grasses and investigated genetic diversity, geographic variation, and loline alkaloid levels.

AUTHOR CONTRIBUTIONS

The authors jointly defined the content of this Research Topic and all participated in the editing process. All authors made substantial, direct, intellectual contribution to the composing of this editorial and approved it for publication.

ACKNOWLEDGMENTS

The editors would like to thank all reviewers who evaluated manuscripts for this Research Topic.

REFERENCES

Field, K. J., Cameron, D. D., Leake, J. R., Tille, S., Bidartondo, M. I., and Beerling, D. J. (2012). Contrasting arbuscular mycorrhizal responses of vascular and non-vascular plants to a simulated Palaeozoic CO_2 decline. *Nat. Commun.* 3:835. doi: 10.1038/ncomms1831

Humphreys, C. P., Franks, P. J., Rees, M., Bidartondo, M. I., Leake, J. R., and Beerling, D. J. (2010). Mutualistic mycorrhiza-like symbiosis in the most ancient group of land plants. *Nat. Commun.* 1:103. doi: 10.1038/ncomms1105

Johnson, L. J., De Bonth, A. C. M., Briggs, L. R., Caradus, J. R., Finch, S. C., Fleetwood, D. J., et al. (2013). The exploitation of epichloae endophytes for agricultural benefit. *Fungal Divers.* 60, 171–188. doi: 10.1007/s13225-013-0239-4

Loron, C. C., François, C., Rainbird, R. H., Turner, E. C., Borensztajn, S., and Javaux, E. J. (2019). Early fungi from the Proterozoic era in Arctic Canada. *Nature*. 570, 232–235. doi: 10.1038/s41586-019-1217-0

Parfrey, L. W., Lahr, D. J., Knoll, A. H., and Katz, L. A. (2011). Estimating the timing of early eukaryotic diversification with multigene molecular clocks. *Proc. Natl. Acad. Sci. U.S.A.* 108, 13624–13629. doi: 10.1073/pnas.1110633108

Pirozynski, K. A., and Malloch, D. W. (1975). The origin of land plants: a matter of mycotrophism. *Biosystems* 6, 153–164. doi: 10.1016/0303-2647(75)90023-4

Redecker, D., Kodner, R., and Graham, L. E. (2000). Glomalean fungi from the Ordovician. *Science* 289, 1920–1921. doi: 10.1126/science.289.5486.1920

Remy, W., Taylor, T. N., Hass, H., and Kerp, H. (1994). Four hundred-million-year-old vesicular arbuscular mycorrhizae. *Proc. Natl. Acad. Sci. U.S.A.* 91, 11841–11843. doi: 10.1073/pnas.91.25.11841

Rubinstein, C. V., Gerrienne, P., de la Puente, G. S., Astini, R. A., and Steemans, P. (2010). Early Middle Ordovician evidence for land plants in Argentina (eastern Gondwana). *New Phytol.* 188, 365–369. doi: 10.1111/j.1469-8137.2010.03433.x

Conflict of Interest: The authors declare that the research was conducted in the absence of any commercial or financial relationships that could be construed as a potential conflict of interest.

frontiers in Plant Science

ORIGINAL RESEARCH
published: 12 June 2019
doi: 10.3389/fpls.2019.00765

Large Scale Screening of *Epichloë* Endophytes Infecting *Schedonorus pratensis* and Other Forage Grasses Reveals a Relation Between Microsatellite-Based Haplotypes and Loline Alkaloid Levels

Giovanni Cagnano[1,2], Niels Roulund[1], Christian Sig Jensen[1], Flavia Pilar Forte[2], Torben Asp[2] and Adrian Leuchtmann[3]*

[1] DLF Trifolium A/S, Roskilde, Denmark, [2] Department of Molecular Biology and Genetics, Faculty of Science and Technology, Research Centre Flakkebjerg, Aarhus University, Slagelse, Denmark, [3] Institute of Integrative Biology, ETH Zurich, Zurich, Switzerland

OPEN ACCESS

Edited by:
Silvia Proietti,
Università degli Studi della Tuscia, Italy

Reviewed by:
Barry Scott,
Massey University, New Zealand
Jonathan A. Newman,
University of Guelph, Canada

***Correspondence:**
Giovanni Cagnano
gca@dlf.com

Specialty section:
This article was submitted to Plant Microbe Interactions, a section of the journal Frontiers in Plant Science

Received: *17 April 2019*
Accepted: *24 May 2019*
Published: *12 June 2019*

Citation:
Cagnano G, Roulund N, Jensen CS, Forte FP, Asp T and Leuchtmann A (2019) Large Scale Screening of Epichloë Endophytes Infecting Schedonorus pratensis and Other Forage Grasses Reveals a Relation Between Microsatellite-Based Haplotypes and Loline Alkaloid Levels. Front. Plant Sci. 10:765. doi: 10.3389/fpls.2019.00765

Species belonging to the Festuca-Lolium complex are often naturally infected with endophytic fungi of genus *Epichloë*. Recent studies on endophytes have shown the beneficial roles of host-endophyte associations as protection against insect herbivores in agriculturally important grasses. However, large-scale screenings are crucial to identify animal friendly strains suitable for agricultural use. In this study we analyzed collected populations of meadow fescue (*Schedonorus pratensis*) from 135 different locations across Europe, 255 accessions from the United States Department of Agriculture and 96 accessions from The Nordic Genetic Resource Centre. The analysis also included representatives of *S. arundinaceus*, *S. giganteus*, and *Lolium perenne*. All plants were screened for the presence of *Epichloë* endophytes, resulting in a nursery of about 2500 infected plants from 176 different locations. Genetic diversity was investigated on 250 isolates using a microsatellite-based PCR fingerprinting assay at 7 loci, 5 of which were uncharacterized for these species. Phylogenetic and principal components analysis showed a strong interspecific genetic differentiation among isolates, and, with *E. uncinata* isolates, a small but significant correlation between genetic diversity and geographical effect (r = 0.227) was detected. Concentrations of loline alkaloids were measured in 218 infected meadow fescue plants. Average amount of total loline and the proportions of the single loline alkaloids differed significantly among endophyte haplotypes ($P < 0.005$). This study provides insight into endophyte genetic diversity and geographic variation in Europe and a reference database of allele sizes for fast discrimination of isolates. We also discuss the possibility of multiple hybridization events as a source of genetic and alkaloid variation observed in *E. uncinata*.

Keywords: *Epichloë*, genetic diversity, grass endophytes, interspecific hybrids, microsatellite markers, *Schedonorus*, loline

INTRODUCTION

Many grasses of the subfamily Pooideae form symbiotic relationships with filamentous fungi of the Clavicipitaceae family belonging to the genus *Epichloë* (Schardl et al., 1997). Among grasses and endophytic fungi there is a continuum of symbiotic interactions that range from antagonistic to clearly mutualistic (Schardl and Clay, 1997; Schmid et al., 2017). *Epichloë* endophytes grow asymptomatically in the intercellular spaces of the aerial tissues of the host plants and, in most of the asexual species, they do not spread by infecting neighboring plants but they are exclusively seed-transmitted from previously infected hosts (Schardl, 1996). At seed maturity, the endophyte is found between the pericarp and the aleurone layer, and between the cells of the embryo/scutellum, an area called "the infection layer" (Johnson et al., 2013). In some species the efficiency of vertical transmission is close to 100% and usually all seeds are infected (Schardl, 1996). Asexual *Epichloë* species may arise from sexual species that lost the ability to sexually reproduce (e.g., *E. festucae* var. *lolii*) or from interspecific hybridizations between sexual and/or asexual *Epichloë* species (Craven, 2003). Hybridizations may occur within host plants that are co-infected by different strains through a process known as vegetative hyphal fusion (VHF) or anastomosis followed by nuclear fusion (Shoji et al., 2015). Interspecific hybrids have an allopolyploid-like genome which is the result of the combination of two or more parental chromosome sets. Several studies support the evidence of the prevalence of interspecific hybrids amongst *Epichloë* species (Moon et al., 2004; Ghimire et al., 2011): hybridization might reduce the effects of deleterious mutations that accumulate in clonal genomes, the so-called "Muller's ratchet" (Muller, 1964), and provide the endophyte with an additional set of genes for alkaloid biosynthesis which will eventually improve host fitness, and through it, the endophyte fitness itself (Selosse and Schardl, 2007).

Presence of *Epichloë* endophyte was generally assumed to be undesirable in the late 70s, when they were identified as the causal agent of fescue toxicosis and ryegrass stagger (Bacon et al., 1977; Fletcher and Harvey, 1981; Gallagher et al., 1981). In order to preserve the health of livestock, endophyte free varieties of tall fescue and perennial ryegrass were released, but their yield and persistence were not comparable to the endophyte infected grasses especially in areas with strong environmental pressure, such as New Zealand (Latch and Christensen, 1982; Bouton et al., 1993). The increasing knowledge on *Epichloë* endophytes and their secondary metabolites led researchers to reconsider their use in agriculture. This led private and public research organizations to focus on large-scale screenings in order to isolate animal-friendly endophytes still harboring deterrent and insecticidal properties, opening a new market for artificially infected grass cultivars (Bouton et al., 2002; Johnson et al., 2013). The "ideal endophyte" to be exploited in a more sustainable agriculture would be an asexual *Epichloë* strain with high production of water soluble insecticide and nematocide alkaloids; low to no production of alkaloid toxic to livestock; high compatibility with different species of the Festuca-Lolium complex; a stable profile and amount of secondary metabolites when inoculated in non-native grasses; high persistence in top varieties through the generations. Particularly interesting, in this respect, are two species of endophytes isolated from meadow fescue (*Schedonorus pratensis* Huds.): *E. uncinata* (Gams et al., 1990) and *E. siegelii* (Craven et al., 2001). These species produce high levels of lolines, a group of aminopyrrolizidine derivatives with deterrent and insecticidal properties without side effects on livestock (Patchett, 2007; Schardl et al., 2007). Loline alkaloids occur in several forms, the most common and abundant ones are N-formylloline (NFL), N-acetylloline (NAL), N-acetylnorloline (NANL), and N-methylloline (NML). These alkaloids normally accumulate in the aerial parts of the plant but they can also be found, in variable amounts, in the roots: the amount stored in below ground tissues can increase according to the presence of insects feeding on the roots themselves (Patchett et al., 2008).

In this study we (i) determined the incidence of *Epichloë* endophytes in Pooideae grasses (primarily *S. pratensis* but also *S. giganteus, S. arundinaceus*, and *L. perenne*) collected at various sites in Europe; (ii) screened meadow fescue accessions labeled as wild or landraces from the United States Department of Agriculture (USDA) and Nordic Genetic Resource Centre (NordGen); (iii) identified isolates from *S. arundinaceus* var. *glaucescens* as FaTG-5 through a phylogenetic analysis of *tubB* and *tefA* sequences, along with morphological examinations and microsatellites fingerprinting; (iv) tested the descriptive and discrimination power of 5 microsatellite markers on *E. uncinata, E. coenophiala*, *E. siegelii*, *E. festucae*, and *E. festucae* var. *lolii*; (v) investigated the genetic diversity of these species; and (vi) measured the amount of loline alkaloids in the isolates and tested their associations with endophyte microsatellite profiles.

MATERIALS AND METHODS

Plant Material

Schedonorus pratensis, *Schedonorus arundinaceus*, *Schedonorus Giganteus,* and *Lolium perenne* plants were collected during the summer 2016 and summer 2017 in Denmark, Sweden, Norway, Italy, Germany, and Austria. The 135 collection sites were meadows located near roadsides, in isolated environments, supposedly not contaminated by cultivated grasses. Whenever possible, approximately 15 to 20 plants were sampled from each location. Latitude, longitude, and altitude data of all collection sites were recorded. Plants were planted in pots (9 cm × 11 cm) with standard peat (En brown 06 W 30P, Kekkilä Group, Vantaa, Finland), watered regularly and grown in the greenhouse with 16 light hours at approximately 15–24°C.

A total of 255 *S. pratensis* accessions were requested from USDA and 92 from NordGen. Only accessions labeled as wild or semi-wild were chosen. Seeds were germinated in the same conditions as described above. A map and a detailed database of the plant material used in this study are provided in **Supplementary Figure S1** and **Supplementary Table S1**.

Endophyte Detection, Isolation, and Identification

The presence of *Epichloë* endophytes was determined in two tiller sections from each of the collected plants, 6 weeks after the transplant, using the immunoblot assay "Phytoscreen Field Tiller Endophyte Detection Kit" (Cat. #ENDO797-3; Agrinostics Ltd. Co.) described by Hiatt et al. (1999) according to manufacturer's description. A PCR-based approach was used to screen the high number of genotypes from the genebank accessions (approximately 17,000). The presence of the endophyte was initially tested with an *in planta* assay using microsatellite markers B10 and B11 described by Moon et al. (1999) on 50 stems per accession, split in 5 bulk samples of 10 stems each. Accessions where no amplifications was detected were considered endophyte-free and discarded, whereas accessions that produced amplicons were moved in single plant trays, 50 plants per accession, and tested with the "Phytoscreen Field Tiller Endophyte Detection Kit." The infection rate of every population was scored as the ratio of infected to total number of tested plants, descriptive statistics such as mean, confidence interval of 95% (95% CI), standard error (SE), and sample size (n) were calculated using Microsoft Excel (2016). High-resolution DNA flow cytometry was used to confirm the species of the infected populations according to Jensen et al. (2007).

Pure cultures of endophytes were obtained from pieces of surface-sterilized pseudostems on potato dextrose agar (PDA) as described elsewhere (An et al., 1993; Schardl and An, 1993). To study colony growth, 2 mm^2 plugs of mycelium were placed at the center of PDA plates and grown in the dark at 24°C. Colony diameter was measured from 5 replicate plates after 14, 21, and 28 days. For microscopic examinations of conidia and conidiophores, agar plates were inoculated with a suspension obtained by macerating 2 mm^3 of culture in 100 μL of sterile water and kept in a dark growth chamber at 24°C for 7 days until conidiation occurred. The examination was performed with an Olympus BH-2 microscope (Olympus Optical Co., Hamburg) and photographs taken with a Canon EOS 600D camera. Measurements of conidiogenous cells (length and width at tip and base) and conidia and conidiophores (length and width) were taken from 20 structures each in 3 different isolates using an ocular micrometer at 1000×.

DNA Amplification, Sequencing and Analysis of *tefA*, and *tubB* Genes

DNA extraction, PCR reaction, and gene cloning were performed using the method described by Oberhofer and Leuchtmann (2012). The nuclear genes for β-tubulin (*tubB*) and translation elongation factor 1-alpha (*tefA*) were PCR-amplified from genomic DNA. Both genes have been widely used for phylogenetic analysis of broad taxonomic range of endophytes worldwide. The primers used for the PCR reaction were 5′-TGG TCA ACC AGC TCA GCA CC-3′ (forward) and 5′-TGG TCA ACC AGC TCA GCA CC-3′ (reverse) for *tubB*, and primers 5′-GGG TAA GGA CGA AAA GAC TCA-3′ (forward) and 5′-CGG CAG CGA TAA TCA GGA TAG-3′ (reverse) for *tefA* (Craven et al., 2001). Isolates of the accession PI347572 were cloned into bacterial plasmids for separating alleles into different *Escherichia coli* colonies. Correct product size was verified by gel electrophoresis. Copies of both genes were sequenced and manually edited with Sequencher 10.4.1 (Gene Codes Corporation, United States). Sequences were aligned in GENEIOUS version 6.1.3 (Biomatters Ltd, Auckland, New Zealand) along with sequences from representative *Epichloë* species using default alignment parameters, gaps were removed, and ambiguously aligned sites were checked manually and adjusted if needed. Sequences were deposited in GenBank: *tef* A: MK423914 and MK423915; *tub*B: MK423916 and MK423917.

Maximum likelihood (ML) trees were constructed with MEGA X (Kumar et al., 2018) with default parameters and 1,000 bootstrap replicates. Gene sequences available in Genbank of endophyte species related to the ones analyzed in this study and relevant putative ancestors were included in the dataset, each tree is provided with corresponding Genbank numbers.

Microsatellite Analysis

Genomic DNA was extracted from infected stems on a Quadra 96 Model 320 robotic system (Tomtec Inc., Hamden, CT, United States) using the method described previously by Brazauskas et al. (2011). Two hundred fifty samples were characterized for their allelic variation at 7 microsatellites loci: B10 and B11 published by Moon et al. (1999) and E08, E29, E33, E36, and E39 published by Schirrmann et al. (2014). PCRs were performed in 10 μl volumes containing 4 μl of genomic DNA, 2 mM $MgCl_2$, 0.25 mM of each deoxynucleotide triphosphate (dATP, dCTP, dGTP, and dTTP), 4 μM of each primer (Eurofins genomics, Ebersberg, Germany), 0.4 U of Taq DNA polymerase with 1× key buffer (Mg^{2+} free) (Cat. No. 733-1313, VWR International, Leuven, Belgium). Each primer pair was fluorescently labeled either with DY-682 or with DY-782 (Eurofins genomics, Ebersberg, Germany). Reactions were carried out in a Mastercycler gradient 5331 (Eppendorf AG, Hamburg, Germany) programmed with 2 min of initial denaturation at 95°C followed by 34 cycles of 95°C for 20 s, 56°C for 30 s, and 72°C for 1 min, with a final extension of 72°C for 10 min.

Lab internal standards (*E. uncinata*, *E. siegelii*, *E. festucae* var. *lolii*, *E. coenophiala*, FaTG-2, endophyte free plant and negative control) were used in each PCR reaction. The products were then electrophoresed using a LI-COR model 4200 automated fluorescent DNA sequencer (Middendorf et al., 1992) (LI-COR, Lincoln, NE, United States). Gel dimensions were 25 cm long and 0.25 mm thick. The gel contained 7 M urea and 7.0% SequaGel XR concentrate (National Diagnostics, Atlanta, Georgia). The running buffer was 0.4X TBE. The gel was run at 2000 V constant voltage, and the gel temperature was maintained at 50°C. The size of the amplicons was estimated by comparison to a size ladder with 42, 44, 125, 126, 150, 151, 193, 251, 280, 327, 328, 414, and 551 base pair fragments markers. The accuracy of the size estimates is specific to the electrophoretic separation conditions and a confidence interval of ±5 bp should be considered.

Loline Alkaloid Analysis

In March 2018, 218 endophyte infected *S. pratensis* plants were trimmed, moved in bigger pots (35 cm × 30 cm) with standard peat (En brown 06 W 30P, Kekkilä Group, Vantaa, Finland), watered regularly and grown in the same greenhouse room with 16 light hours at approximately 15–24°C. In June 2018 samples from the basal part of the tiller were harvested and freeze-dried in the same day and subsequently powdered in a laboratory mill. About 50 mg of each sample were sent in duplicate to AgResearch Grasslands (Palmerston North, New Zealand), were the analysis was performed using a gas chromatographic method described by Baldauf et al. (2011).

Data Analysis

Microsatellite data were coded with a tetraploid-like format so that *E. coenophiala* samples, which present three alleles in 5 out of 7 microsatellites, could be included in the analysis. Null-alleles were regarded as missing values. Number of multi-locus genotypes (MLG), allelic richness, Simpson's (1949) Index, evenness (Grünwald et al., 2003), Shannon-Wiener Index of MLG diversity (Shannon, 1948), Stoddart and Taylor's (1988) Index of MLG diversity were determined using the *poppr* package (Kamvar et al., 2014) in R (R version 3.4.2). The Simpson's Index was corrected for sample size multiplying it by n/(n–1) as well as the Stoddart and Taylor's diversity index, which was scaled by sample size and expressed as percentage. The software GenAlex v. 6.5 (Peakall and Smouse, 2012) was used to determine the Nei's (1978) unbiased genetic identity and diversity, the number of alleles, the number of effective alleles and the Shannon's information index (Sherwin et al., 2006) at each locus. Assessment of genetic relatedness between MLGs was performed using the function *provesti.dist* which calculates Provesti's genetic distance. The function *aboot* runs a bootstrap analysis set up on 10,000 bootstrap replicates, treating loci as independent units, it was visualized with a dendrogram created using the unweighted pair-group method with arithmetic average (UPGMA). Principle component analysis (PCA) was performed to complement model-based clustering methods and to test the ability to distinguish haplotypes. Matrixes comparison using Mantel test was performed between the genetic similarity matrix with the cophenetic matrix. The change in genetic similarity associated with increasing spatial distance between individuals was investigated by testing and plotting spatial autocorrelation at above distance intervals. A geographical distance matrix of Euclidean distances (km) was computed between all pairwise combinations sites from their GPS coordinates with the R package *geosphere* (Hijmans et al., 2017) and tested against a genetic similarity matrix. The R function *mantel.correlog* in the package *vegan* (Oksanen et al., 2018) was used to compute multivariate Mantel correlogram using Pearson correlation, the Sturge equation to estimate distance classes, the Bonferroni progressive correction ($\alpha = 0.05$) and 9999 permutations for significance tests. The concentrations of loline alkaloids were compared between haplotypes using the Kruskal-Wallis test by rank, a non-parametric alternative to one-way ANOVA test which could not be used because its assumptions were not met. The output of the function *kruskal.test* tells if the concentration of loline alkaloids were significantly different between haplotypes, but the Wilcoxon rank sum test (function *pairwise.wilcox.test*) was needed to calculate pairwise comparisons between haplotypes.

RESULTS

Infection Rates of Grass Populations and Accessions

A total of 2008 plants (1764 *S. pratensis*, 42 *S. giganteus*, 63 *S. arundinaceus*, and 139 *L. perenne*) were collected from 135 different locations at different altitudes (from 0 to 1740 m) and longitudes and screened for the presence of *Epichloë* endophytes with a tissue-print immunoblot assay. Infection rates (IRs), calculated for each location as the ratio of infected (E+) plants, and the number of analyzed plants, showed a large variation among the sites, spanning from 0 to 100% (**Table 1**). Sweden was the country where wild and semi-wild habitats containing meadow fescue were easiest to find and infected plants with IRs from 24 to 100% (mean = 87.6%; 95% CI ± 5.1%; *SE* = 2.5%; $n = 42$) were found in 42 of 42 sites. Also in Norway all

TABLE 1 | *Epichloë* endophyte frequencies in populations of *Schedonorus pratensis, S. arundinaceus, S. giganteus*, and *Lolium perenne* collected in Austria, Denmark, Germany, Italy, Norway, and Sweden (Average infection rates among infected populations; SD, standard deviation; ND, not determined).

Species	Country	No. of collected populations	Infected populations (%)	Average IR (%)	SD (%)	No. of infected plants
S. pratensis	Austria	12	100.0	69.3	23.1	149
	Denmark	10	70.0	84.5	23.2	78
	Germany	10	70.0	74.6	10.4	93
	Italy	28	85.7	76.3	24.5	320
	Norway	9	100.0	90.6	10.8	125
	Sweden	42	100.0	87.5	16.3	611
S. arundinaceus	Denmark	9	66.7	63.8	37.9	55
S. giganteus	Denmark	2	100.0	64.3	20.2	17
	Germany	2	50.0	80.0	ND	12
L. perenne	Denmark	7	14.3	8.3	ND	1
	Germany	4	75.0	26.4	23.7	11

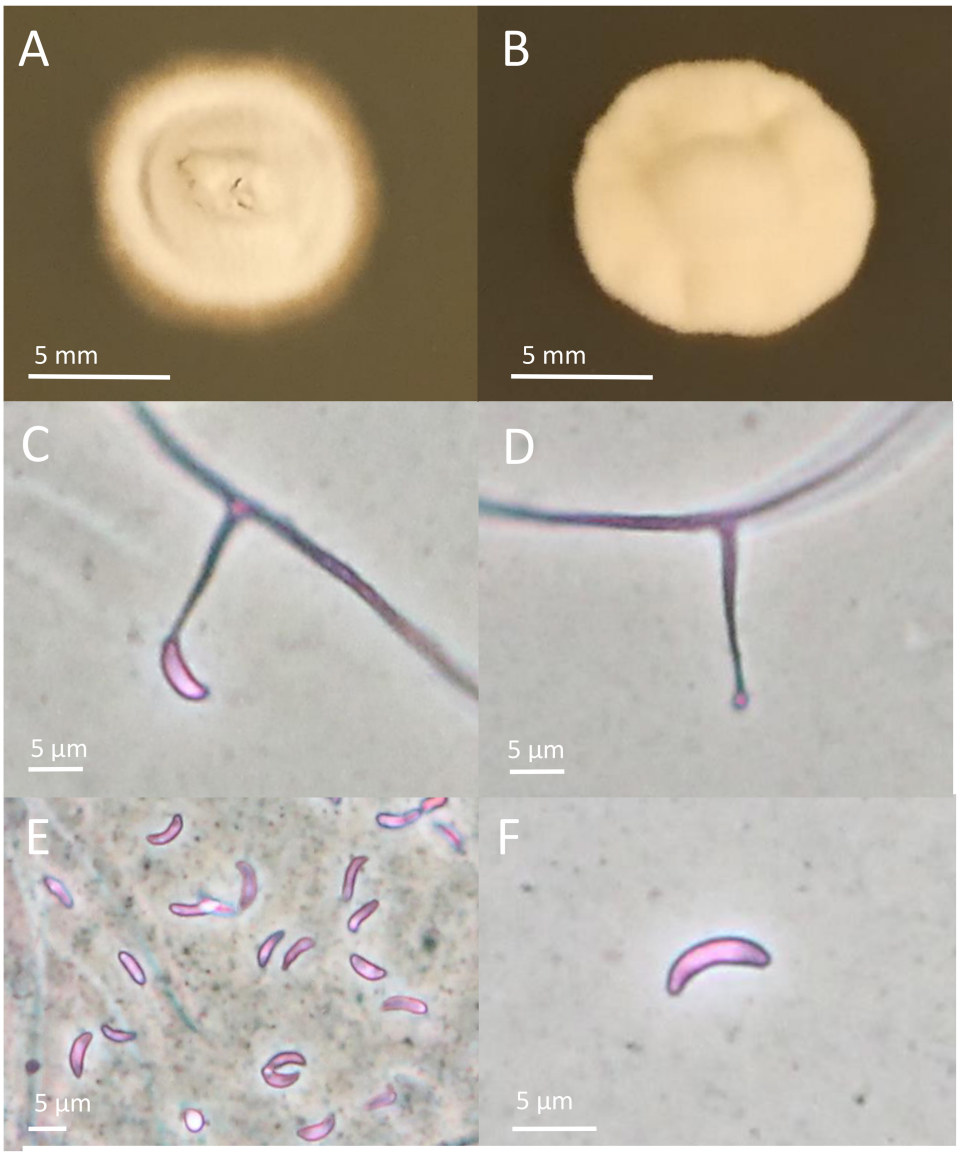

FIGURE 1 | Colony and conidial morphology of *Epichloë* isolates from *Schedonorus arundinaceus* var. *glaucescens*. **(A,B)** Different colony morphologies of FaTG-5 isolates. **(C,D)** Conidiophores from the two isolates. **(E,F)** Conidia from the two isolates. Pictures of colonies were taken after growing on PDA for 4 weeks.

the collection sites were found to host infected plants with high IRs, from 68 to 100% (mean = 90.6%; 95% CI ± 8.3%; *SE* = 3.6%; *n* = 9), but the occurrence of meadow fescue was lower and it was difficult to find isolated habitats due to the higher frequency of farms and grass cultivated fields in the Østfold area close to the border with Sweden. The average IR was slightly lower in the collections made in the Alpine regions, across the Italian and Austrian border where it ranged from 6.7 to 100% (mean = 76.3%; 95% CI ± 10.3%; *SE* = 5%; *n* = 24) and 25 to 95% (mean = 69.3%; 95% CI ± 14.7%; *SE* = 6.7%; *n* = 12), respectively. Regarding the collections made in Germany and in Denmark, the number of infected sites was 4 out of 11 for *L. perenne* and 14 out of 20 for *S. pratensis*. The scarcity of isolated wild and semi-wild habitats made collection trips rather inefficient in these countries, especially when the target is meadow fescue.

A large-scale screening was performed analyzing 255 *S. pratensis* accessions from USDA and 96 from NordGen. Infected accessions were detected with an *in planta* microsatellite-based PCR assay using the loci B10 and B11. The detection threshold of this method, when using bulk samples, was tested with different combinations of *in vitro*–composed admixtures of endophyte infected (E+) and endophyte free (E-) stems. A clear and strong amplification was detected up to bulks with 14 E- stems and 1 E+ stem. This approach allows also to identify the presence of different species or strains in the mixture if they have different amplicon sizes at the chosen loci. Bulks of stems infected with *E. uncinata*

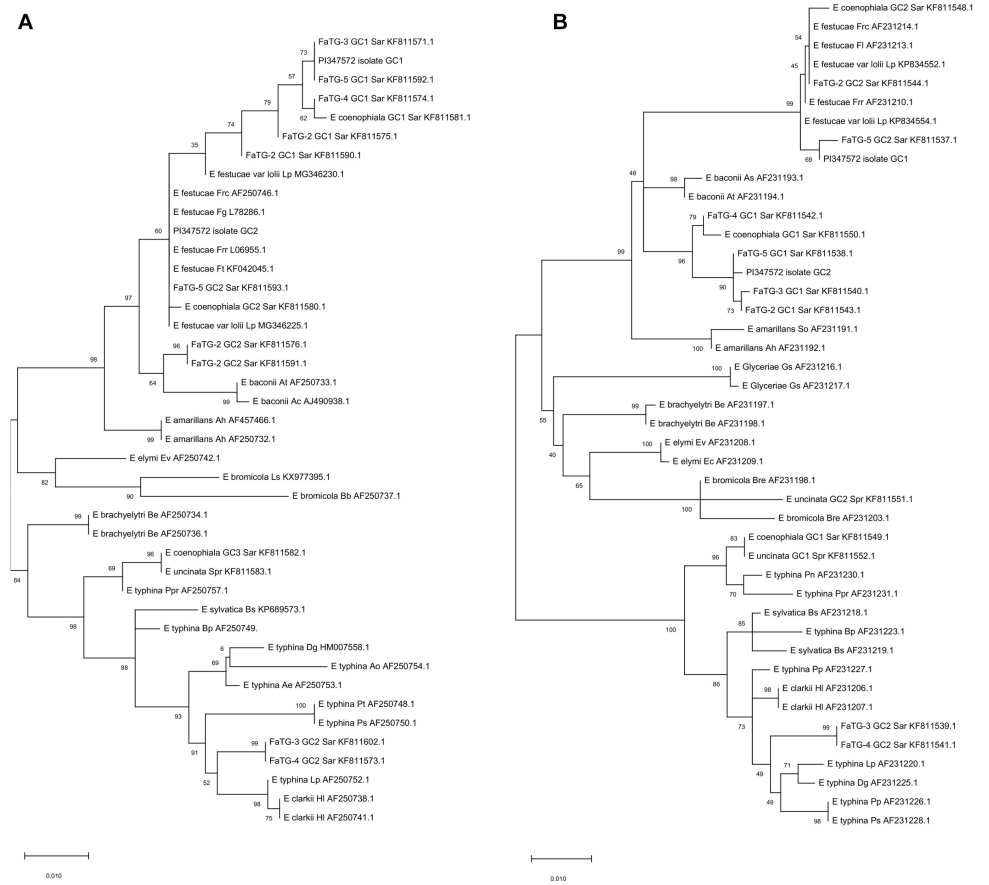

FIGURE 2 | Phylograms derived from maximum likelihood (ML) analysis and Tamura-Nei model of the partial sequence of tubB **(A)** and tefA **(B)** genes from representative haploid *Epichloë* species and hybrid species included in this study. The two copies obtained from *S. arundinaceus* var. *glaucescens* are labeled as "PI347572 isolate." The tree is midpoint rooted and drawn to scale, with branch lengths measured in the number of substitutions per site. Bootstrap values (1000 replicates) are shown next to the branches. GC stands for gene copy. GenBank accession numbers are provided for each sequence. Letters after each endophyte refer to host designations as follows: Lp, *Lolium perenne*; Dg, *Dactylis glomerata*; Ps, *Poa sylvicola*; Pp, *Phleum pratense*; Sar, *Schedonorus arundinaceus*; Hl, *Holcus lanatus*; Bp, *Brachypodium pinnatum*; Bs, *Brachypodium sylvaticum*; Spr, *Schedonorus pratensis*; Pn, *Poa nemoralis*; Ppr, *Poa pratensis*; Gs, *Glyceria striata*; Be, *Brachyelytrum erectum*; Ev, *Elymus virginicus*; Ec, *Elymus canadensis*; Bre, *Bromus erectus*; So, *Sphenopholis obtusata*; Ah, *Agrostis hiemalis*; As, *Agrostis stolonifera*; At, *Agrostis tennuis*; Frr, *Festuca rubra* subsp. *rubra*; Fl, *Festuca longifolia*; Frc, *Festuca rubra* subsp. *commutata*; Fg, *Schedonorus giganteus;* Bb, *Bromus benekenii*; Ls, *Leymus secalinus*; Pt, *Poa trivialis*; Ao, *Anthoxanthum odoratum.*

and *E. siegelii* were tested and species distinction was possible up to 14:1 ratio. Further ratios were not tested because of the increasing amount of plant material which exceeded the threshold recommended in the DNA extraction protocol. Of the 255 USDA seedlots, 215 were able to grow enough seedlings to be analyzed: 159 were endophyte free, 12 had ambiguous results, and 44 had clear evidence of endophyte presence. Subsequent verification of the 56 (12+44) putative E+ accessions by immunoblotting only confirmed *Epichloë* infection in 12 accessions. The infection rates ranged from 2.5 to 77.5% (mean = 38%; 95% CI ± 16.4%; *SE* = 7.4%; n = 12). Regarding the 96 NordGen accessions, only 4 of them did not germinate. Of the remaining, 53 out of 92 (57.6%) were found infected with *Epichloë* endophytes both with the PCR assay and the immunoblot, the infection rates ranged from 3.1 to 100% (mean = 71.2%; 95% CI ± 7.9%; *SE* = 4%; n = 52). Twelve accessions had an infection rate of 100% while 4 of them had few weak seedlings that eventually died and could not be used for further analysis. The final outcome was therefore 49 E+ accessions, for a total of 1256 plants.

Ploidy Level

Two plants per each infected population/accession were analyzed with a flow cytometer to confirm the host ploidy. All the *S. pratensis* collected had 14 chromosomes, thus no *S. pratensis* subsp. *apennina* (2N = 4× = 28 chromosomes) was collected in the Alpine regions. *S. arundinaceus* ecotypes sampled in Denmark were hexaploid with a chromosome number of 2N = 6× = 42, as well as the *S. giganteus* ecotypes collected in Denmark and Germany. All the infected accessions from NordGen and USDA were confirmed to be *S. pratensis* with 2N = 4× = 14 chromosomes except for 3 USDA accessions, collected in Morocco (PI347571, PI347572, and PI347573), which were tetraploid, with a chromosomes number estimated to be

2N = 4× = 28, and a clearly different phenotype from typical meadow fescue. After detailed morphological analysis these accessions were identified as *S. arundinaceus* var. *glaucescens*.

Characterization of *S. arundinaceus* var. Glaucescens Endophyte

The endophytes harbored in PI347571 and PI347573 were formerly classified as FaTG-2 and FaTG-5, respectively (Ekanayake et al., 2012), therefore isolates from the accession PI347572 that have not been examined before were cultured on PDA and characterized (**Figure 1**). The diameters of the colonies after 4 weeks at 24°C were 10–15 mm, the mycelium was white, densely velvety, slightly raised in the center, more flattened toward the perimeter, ca. 1 mm submerged at the margin, whereas the reverse side of the colonies were light brown with some fractures of the agar medium. Sporulation was moderately abundant. Conidiogenous cells were 10–25 μm long, ca. 2 μm wide at the base, tapering to ca 0.5 μm at the apex, arising solitarily from hyphae, and usually lacking basal septum. The conidia (6.4–8.5 μm × 1.8–3.5 μm) were 6–10 μm long, 1–3 μm wide, luniform to reniform, hyaline, aseptate, and smooth. The presence of two amplicons at B10 and B11 suggested that the isolates were interspecific hybrids, this was confirmed by the phylogenetic analysis of the *tef*A and *tub*B (**Figure 2**) genes. Both genes were present in two copies. In the *tefA* based phylogeny, copy 1 (GC1) was placed in a clade with FaTG-5 among *E. festucae* and a *E. festucae* var. *lolii* strains. Gene copy 2 (GC2) formed a separate subclade with all the other *S. arundinaceus* isolates (*E. coenophiala*, FaTG-2, FaTG-3, FaTG-4, and FaTG-5) nested within a larger clade including *E. baconii* and *E. amarillans* reference strains. In the *tub*B phylogram the GC1 formed again a separate subclade with all the other *S. arundinaceus* taxonomic groups next to *E. festucae* var. *lolii*. that seemed to be genetically close. The GC2 of *tub*B showed genetic similarities with those of FaTG-5 and *E. festucae*. By contrast, FaTG-2 strains in the *tub*B tree were more similar to *E. baconii* and FaTG-3/FaTG-4 more similar to *E. typhina*. Moreover, SSR profiles of the endophyte from PI347573 that has been previously identified as FaTG-5 showed close similarity with the isolate from PI347572. Taken together, evidence suggest that the newly characterized endophyte from *S. arundinaceus* var. *glaucescens* is correctly assigned to FaTG-5.

SSR and Population Genetic Analysis

The allelic diversity of 250 isolates (224 *E. uncinata,* 9 *E. coenophiala,* 7 *E.* festucae, 6 *E. festucae* var. *lolii*, 1 *E. siegelii*, 1 FaTG-2, and 2 FaTG-5) was investigated using 7 microsatellites. The isolates were a representative subset of the screened populations. A detailed list of the samples and their allelic profiles at each locus is provided in **Supplementary Table S2**, Supporting information. All seven microsatellites yielded amplicons in the above mentioned species except for E08 in *E. festucae* and *E. festucae* var. *lolii*. The number of alleles at the 7 loci spanned from 0 to 5, according to the endophyte species. Also, the information index at each locus varied among species (**Table 2**): B11 and E33 were the most polymorphic loci in *E. festucae* var. *lolii* and *E. festucae*, whereas for *E. uncinata* there was higher variability at B10. It was impossible to obtain the same information for *E. siegelii,* FaTG-2 and FaTG-5 because only one haplotype was available, and for *E. coenophiala,* because the software GenAlex cannot process triploid data.

Unique combinations of alleles across the 7 different loci were called different haplotypes (**Table 3**). A total of 21 haplotypes were identified among the 250 isolates. The expected number of alleles was detected in 97% of cases and it was consistent with the information currently available on the closest extant relatives or the ancestral species when the sample was a hybrid. The locus E08 was not detected in the *E. festucae* strains analyzed, accordingly, all the hybrids that have *E. festucae* among their ancestors (*E. siegelii,* FaTG-2, FaTG-5, and *E. coenophiala*) lacked this allele. B11 was not detected in *E. typhina* (Moon et al., 1999) therefore only one amplicon was detected in its derived hybrids *E. uncinata* and *E. coenophiala*. Fewer alleles than expected were only observed at B10 in *E. siegelii*, at E33 in FaTG-2 and at E39 in three haplotypes of *E. uncinata* (Eu_H1, Eu_H2, and Eu_H4 where one amplification product instead of two was detected). *E. coenophiala* had 3 haplotypes which were characterized by three alleles at loci B10, E33, E36, and E39 and two at the remaining ones. The most abundant tall fescue haplotype collected in Zealand (Denmark) was Ec_H1, isolated in 5 different locations. Ec_H2 was isolated from two samples collected in a relatively small area around Stevns Klint (Stevns Municipality, Zealand, Denmark) and it can be distinguished from the previous haplotypes for a different amplicon size at

TABLE 2 | Number of alleles, number of effective alleles, and informativeness at the seven SSR loci analyzed for each endophyte species.

Pop	Locus	*N*	Na	Ne	*I*
E. festucae	B10	7	2	1.324	0.410
	B11	7	3	2.333	0.956
	E33	7	3	2.333	0.956
	E36	7	1	1.000	0.000
	E29	7	3	1.815	0.796
	E39	7	1	1.000	0.000
	E08	0	0	0.000	0.000
E. festucae var. *lolii*	B10	8	2	1.280	0.377
	B11	8	5	3.200	1.386
	E33	8	2	1.280	0.377
	E36	8	1	1.000	0.000
	E29	8	3	1.684	0.736
	E39	8	3	1.471	0.602
	E08	0	0	0.000	0.000
E. uncinata	B10	224	4	3.838	1.365
	B11	224	3	1.018	0.057
	E33	224	3	2.657	1.037
	E36	224	3	2.089	0.784
	E29	224	2	2.000	0.693
	E39	224	2	1.577	0.552
	E08	224	3	2.623	1.027

N, sample size; Na, number of alleles; Ne, number of effective alleles; I, Shannon's information index.

TABLE 3 | Haplotypes of *Epichloë* isolates based on microsatellite profiles of seven loci.

Host	Endophyte	Haplotype	No. of isolates	Alleles size (bp)							Country	Closest non-hybrid groups
				B10	B11	E33	E36	E29	E39	E08		
Sa	*E. coenophiala*	Ec_H1	5	164 173 188	150 194	326 329 344	398 407 414	122 150	419 424 426	211 238	DK	Efe, ETC, LAE
		Ec_H2	2	164 173 188	150 179	326 329 344	398 407 414	122 150	419 424 426	211 238	DK	Efe, ETC, LAE
		Ec_H3	2	175 181 185	125 194	326 329 344	398 407 414	122 134	419 424 426	211 238	ES	Efe, ETC, LAE
Sag	FaTG-2	Fa_H1	1	178 181	131 150	344	398 405	134 137	424 430	245	MO	Efe, LAE
Sag	FaTG-5	Fa_H2	2	176 190	131 150	344 349	398 405	134 150	424 430	245	MO	Efe, LAE
Sg	*E. festucae*	Ef_H1	4	181	150	344	398	137	419	–	DK, DE	Efe
		Ef_H2	1	181	119	341	398	134	419	–	DE	Efe
		Ef_H3	1	181	150	341	398	137	419	–	DK	Efe
		Ef_H4	1	187	154	348	398	130	419	–	DK	Efe
Lp	*E. festucae* var. *lolii*	El_H1	4	181	179	344	398	134	430	-	DK, DE	Efe
		El_H2	1	181	160	344	398	134	430	-	ES	Efe
		El_H3	1	181	209	344	398	131	430	-	IT	Efe
Sp	*E. siegelii*	Es_H1	1	188	117 125	335 346	398 410	122 140	430 434	202	DE	Efe, Ebr
Sp	*E. uncinata*	Eu_H1	113	164 200	121	326 335	407 410	122 146	426	209 228	DK, DE, SE, NO, FI, RU	Ebr, ETC
		Eu_H2	1	164 200	117	326 335	407 410	122 146	426	209 228	SE	Ebr, ETC
		Eu_H3	1	164 200	109	326 333	407 410	122 146	421 426	209 228	RU	Ebr, ETC
		Eu_H4	2	164 200	121	326 335	398 407	122 146	426	209 228	SE	Ebr, ETC
		Eu_H5	7	164 200	121	326 335	398 407	122 146	421 426	209 228	DE, FI, KZ, RU, SE	Ebr, ETC
		Eu_H6	10	164 200	121	326 333	407 410	122 146	421 426	209 228	DE, IT, RU	Ebr, ETC
		Eu_H7	89	176 196	121	326 333	407 410	122 146	421 426	206 228	AT, DE, DK, IT, KZ, NO, RU, SE	Ebr, ETC
		Eu_H8	1	176 196	121	326 335	398 407	122 146	421 426	206 228	RU	Ebr, ETC

Sa, S. arundinaceus; Sag, S. arundinaceus var. glaucescens; Sg, S. giganteus; Lp, L. perenne; Sp, S. pratensis; Efe, E. festucae; ETC, E. typhina complex; LAE, Lolium-associated clade; Ebr, E. bromicola.

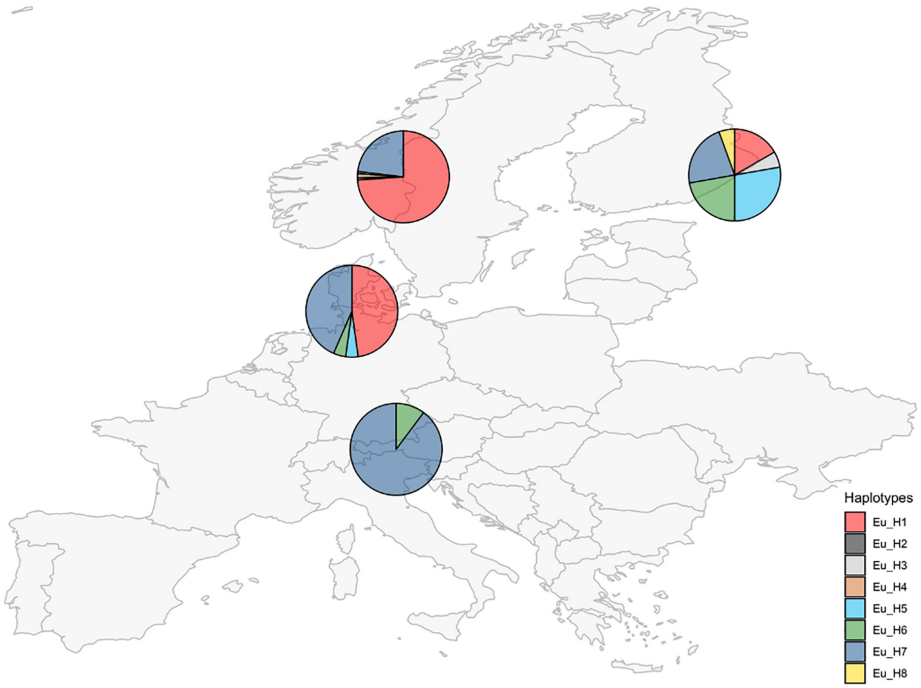

FIGURE 3 | Occurrence of *E. uncinata* haplotypes (defined in **Table 3**) in four macro areas.

B11 (150–179 bp vs. 150–194 bp, respectively). In comparison, isolates from Spain had a different profile at B10, B11, and E29. The most abundant *E. festucae* haplotype found in this study was Ef_H1 isolated both in Denmark and in Germany. Ef_H1 is very similar to Ef_H2 and Ef_H3, from which it differs at only one locus, but very different from Ef_H4 with differences at 4 loci. Interestingly, Ef_H4 was isolated from a single location in Fyn (Denmark) where the majority of the plants collected nearby were infected with Ef_H3. Isolates from *E. festucae* var. *lolii* collected in Denmark and Germany had the same genetic profile, named El_H1, and differed from isolates used as internal standard, collected in Spain (El_H2) and in Italy (El_H3), at one locus. *E. uncinata* showed an unbalanced distribution of the 8 detected haplotypes. The 224 *E. uncinata* isolates were grouped in 4 populations (**Figure 3**) according to the macro area of their geographic origins (**Supplementary Table S2**). Samples collected in Italy, Austria, and southern Germany were grouped in the population *Alps*, samples from Denmark and northern Germany form the population *North-West*, samples from Norway and Sweden were grouped in the population *Scandinavia* and the remaining samples from Finland, Russia, and Kyrgyzstan were grouped in the population *East*. The most frequent haplotypes were Eu_H1 (113 samples) and Eu_H7 (88 samples). Eu_H1 is the most abundant haplotype in *Scandinavia*, found in 73.9% of the isolates, represents 47.8% of the isolates from the population *North-West* and 16.7% of the isolates from *East*, but is completely absent in the *Alps*. Eu_H7 is the only haplotype shared among the four populations, it is the most abundant in the *Alps* (87.8%), it is as abundant as Eu_H1 in the population *North-West* (43.5%), and present with lower percentages in *Scandinavia* (23.1%) and *East* (22.2%). Eu_H2 and Eu_H3 were the only two haplotypes with a polymorphism at B11, they were isolated from a single population, respectively in *Scandinavia* and *East*. Eu_H4 was only found in two locations in *Scandinavia*. Eu_H5 was the most abundant haplotype in *East* (27.8%), isolated in a single population both in *Scandinavia* and *North-West*, but completely absent in the *Alps*. Eu_H6 was the only other haplotype isolated on the *Alps* (12.2%), fairly abundant in *East* (22.2%), present in only one isolate in *North-West* but completely absent in *Scandinavia*. Eu_H8 was only found in a single population in *East*. During the screening, genotypes from 47 locations were found infected with more than one haplotype. Among the Scandinavian collected samples, when two haplotypes were detected in the same location, one was Eu_H1 and the other was always Eu_H7, except for one case when a Eu_H4 was found. In the *Alps*, the second haplotype in addition to the common Eu_H7 was always Eu_H6.

The number of multi-locus genotypes (MLG) detected span from 2 to 6 and incidence was independent of the population size ($R^2 = 0.0034$). Genotypic diversity indices (**Table 4**) displayed consistently low diversity in all populations: Shannon-Weiner's index (H) ranged from 0.37 (*Alps*) to 1.64 (*East*; Stoddart and Taylor's corrected index (G′) ranged from 1.25% (*Scandinavia*) to 26.44% (*East*; and Simpson's corrected index (λ′) ranged from 0.22 (*Alps*) to 0.84 (*East*). Therefore *East* was clearly the population with the highest diversity and Alps was the population with the lowest diversity according to all indexes except for G′, but this is due to the different sensitiveness of the index to changes in abundant genotypes or in rare alleles. Overall, the populations were very similar to each other as

TABLE 4 | Statistics summarizing genotypic richness, diversity, and evenness in 224 *E. uncinata* isolates collected in 4 macro areas: population name as defined in **Supplementary Table S1** (Pop), number of multi-locus genotypes observed (MLG), Shannon-Wiener Index of MLG diversity (H), Stoddart and Taylor's Index scaled by sample size (G'), Simpson's index corrected for sample size (λ'), and Eveness (E.5).

Pop	N	MLG	H	G′ (%)	λ′	E.5	Alps	North-West	East	Scandinavia
Alps	49	2	0.37	2.59	0.22	0.61	–	0.95	0.94	0.88
North-West	23	4	0.99	10.30	0.60	0.82	0.05	–	1.00	1.00
East	18	6	1.64	26.44	0.84	0.90	0.06	0.00	–	0.98
Scandinavia	134	5	0.70	1.25	0.40	0.66	0.13	0.00	0.02	–

On the right, pairwise comparison of the four populations based on Nei's unbiased genetic identity (above diagonal) and Nei's unbiased genetic distance (below diagonal) calculated in GenAlEx V6.5 (Peakall and Smouse, 2012).

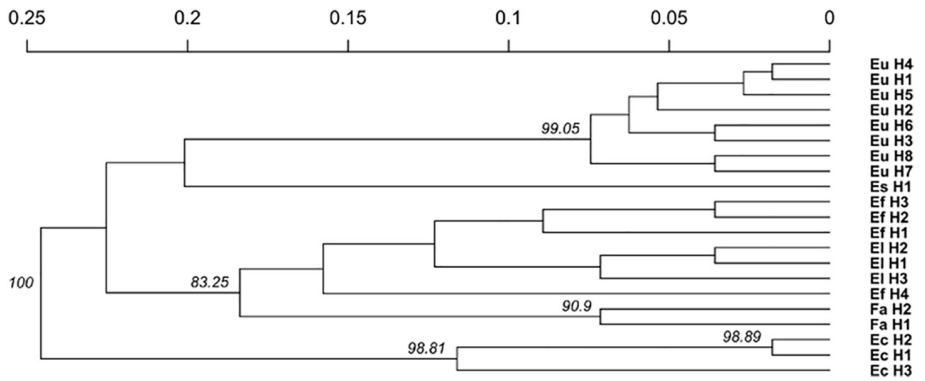

FIGURE 4 | Unweighted pair group mean average (UPGMA) cladogram with 10000 bootstrap replicates based on a microsatellite profile-based distance matrix, genetic bootstrap values greater than 75% are shown. The labels refers to the name of the haplotypes described in **Table 3**.

shown by the pairwise comparisons (**Table 4**) based on Nei's unbiased genetic identity, where all values where close to 1, and on Nei's unbiased genetic distance, where all values were close to 0. The two populations that differed the most are the *Scandinavia* and the *Alps*. Evenness (E.5) ranged from 0.61 (*Alps*) to 0.90 (*East*) showing a relatively unbalanced distribution of haplotypes in the *Alps*.

Population Structure

The relationship between isolates was investigated using the Provesti's distance inferred from clone-corrected microsatellite data. The phenogram (**Figure 4**) generated with the UPGMA method, resolved 3 main clusters that split into sub clusters that were consistent with the host species from which the haplotypes were isolated. Cluster 1 consisted of the two *S. pratensis* endophytes, separated in two clades. The first clade included the eight *E. uncinata* haplotypes. Eu_H1, Eu_H2, Eu_H4, and Eu_H5 cluster together because they only differs at one or two loci, Eu_H3 and Eu_H6 are closely related because they have the same profile at E33 and E39, suggesting that the first might derive from the other through modification at locus B11; the haplotypes Eu_H7 and Eu_H8 group separately from the others having amplicons of different size at B10 and E29. The second clade of cluster 1 includes the only *E. siegelii* isolate currently known. Cluster 2 included *E. festucae, E. festucae* var. *lolii* and the newly characterized isolates from *S. arundinaceus* var. *glaucescens*. Although FaTG-2 and FaTG-5 haplotypes were in a distinct clade, *E. festucae* and *E. festucae* var. *lolii* showed to be closely related, as expected, but still different enough to group in two different subclades. The only exception is haplotype Ef_H4 that appeared to be different from the other *E. festucae* and *E. festucae* var. *lolii* isolates and clustered separately from them. Cluster 3 included *E. coenophiala*, its allotriploid-like genome makes it very distinct from the others. The phenogram was supported by Mantel test statistics with the original and derived matrices showing a high cophenetic correlation ($r = 0.992$).

Similarly, the PCoA (**Figure 5**) showed varying degrees of population separation according to principal component PC1 and PC2, which explained 52 and 27% of the variance, respectively. The 7 species clustered consistently with their species and genetic composition on the *x*-axis and with their ploidy on the *y*-axis: on the left side *E. uncinata* haplotypes, whose ancestors are *E. bromicola* and *E. typhina,* group together; on the right side there are the *E. festucae* strictly related species, whereas at the center of the plot there are *E. siegelii,* whose ancestors are *E. festucae* and *E. bromicola*, and, in the upper part, the allotriploid-like *E. coenophiala* which share the same *E. typhina* ancestor as *E. uncinata,* the same LAE ancestor as FaTG-2 and FaTG-5. The Mantel correlation between pairwise Provesti's genetic distance and pairwise geographic distances (measured in kilometers) between populations was equal to 0.226 ($p < 0.0001$). Thus, populations close to each other tend to be genetically more similar than expected by chance, and genetic differences increase with geographic distances. In order to study the

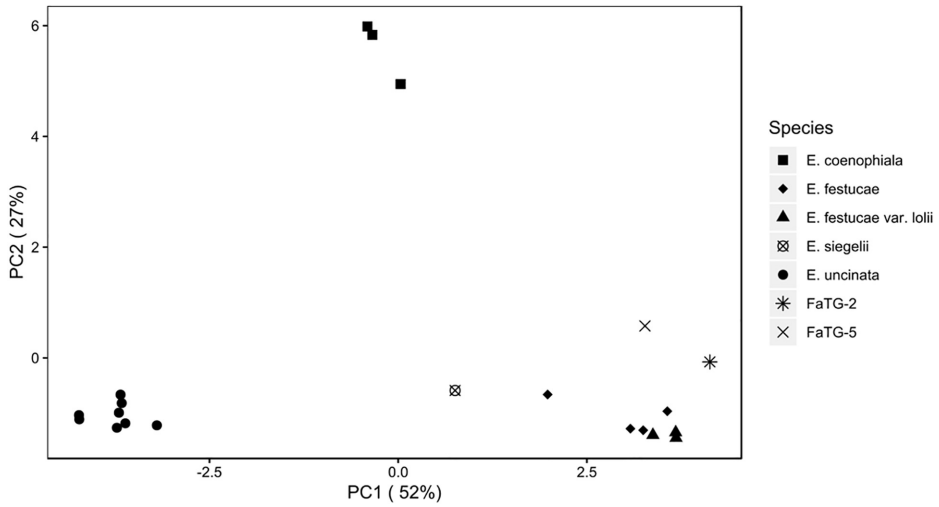

FIGURE 5 | Analysis of principal components (PCoA) scatterplot of the *Epichloë* haplotypes.

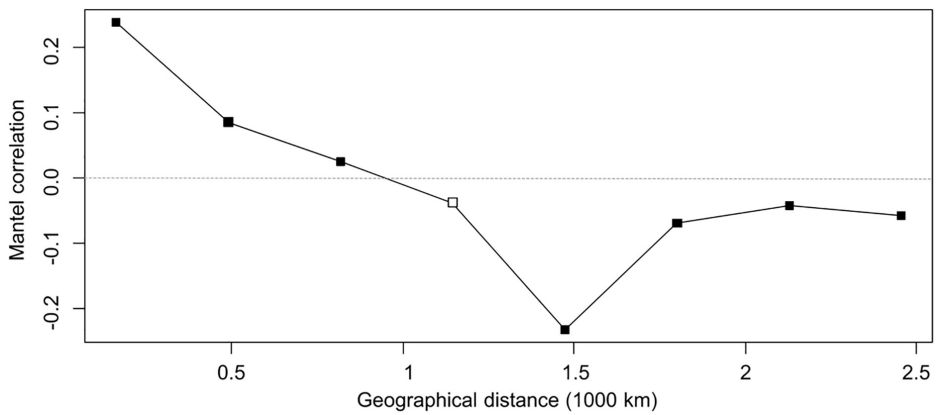

FIGURE 6 | Mantel correlogram. Filled squares indicate significant positive or negative correlations (based on sequential Bonferroni corrections with $\alpha = 0.05$) between genetic and geographical distance of *E. uncinata* isolates. Open squares indicate non-significant correlation.

relationship between genetic and geographic distances across space and its variations in the correlations a Mantel correlogram (**Figure 6**) was computed on 216 *E. uncinata* samples whose coordinates were available.

The correlogram, with five distance classes, showed an overall significance since 7 out of 8 correlation coefficients were significant. Populations distant by 164 km tend to be similar ($r = 0.24$; $p < 0.0001$ with 9999 permutations), this indicates that the haplotypes composition is more similar than they would by chance at the shortest distances. Mantel correlation decreased almost linearly up to -0.23 ($p < 0.0001$) for populations distant approximately 1500 km from each other. From 1800 km onward the correlation tends to stabilize on an average level of about -0.06 ($p < 0.005$) which can be related to patches of genetic variation such as those areas in Sweden and *East* where some atypical haplotypes (Eu_H2-3-4-8) were isolated. A negative correlation indicates more dissimilar haplotypes than expected by chance on farther distances. Mantel correlations were however, not high, therefore the spatial structure is not strong, and only 5% of the genetic divergence is explained by geographic distance.

Loline Analysis

Levels of NAL, NANL, and NFL were measured in 218 samples of endophyte-infected S. pratensis (**Supplementary Table S3**). The total concentration of loline, calculated as sum of the concentrations of the single compounds, varied widely among isolates, spanning from barely detectable traces (<25 μg/g) up to 5629 μg/g. The average profile composition of the isolates was NAL = 10.9% (95% CI ± 0.6%; *SE* = 3%); NANL = 16.2% (95% CI ± 0.6%; *SE* = 3%); and NFL = 73% (95% CI ± 0.7%; *SE* = 3%). These proportions changed with the increase of the total amount of loline with a calculated $P < 0.005$ (**Figure 7**): in the range 100–1000 μg/g the average percentage of NANL was 14% (95% CI ± 1.3%; *SE* = 0.7%; $n = 67$) and NFL was 70.9% (95% CI ± 1.4%;

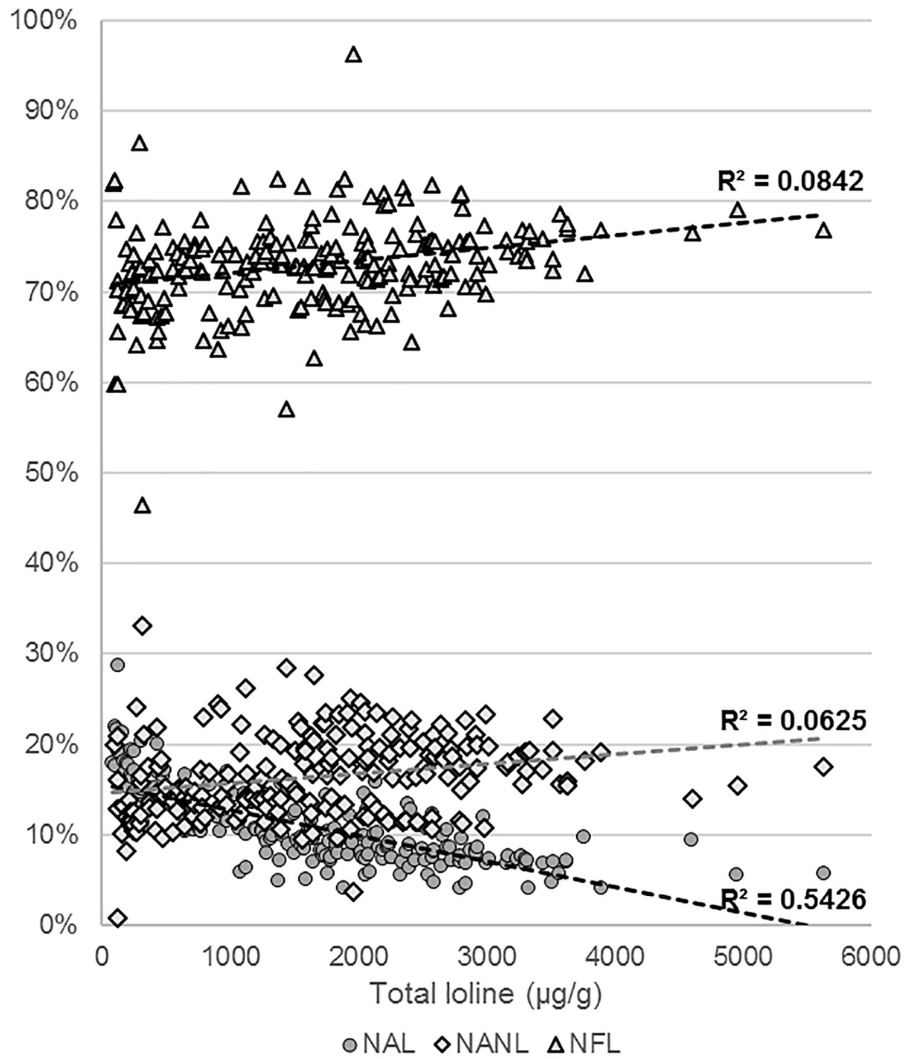

FIGURE 7 | Variation of the NAL, NANL, and NFL proportions with the increase of the total amount of loline.

SE = 0.7%; *n* = 67), but in the range 3000–4000 μg/g they increased to 18.1% (95% CI ± 1%; *SE* = 0.5%; *n* = 17) and 75.3% (95% CI ± 1%; *SE* = 0.5%; *n* = 17), respectively. By contrast, in the same ranges, the average percentage of NAL decreased from 15.2% (95% CI ± 0.8%; *SE* = 0.4%; *n* = 67) to 6.7% (95% CI ± 0.7%; *SE* = 0.3%; *n* = 17). Data suggested that the production of high levels of loline is correlated with a slight increase of the proportion of NANL and NFL ($R^2 < 0.1$) and with a greater decrease of NAL ($R^2 < 0.54$).

Significant differences in the average amount of total loline and in the proportion of the loline alkaloids were also found among haplotypes (**Figure 8**). Specifically, Eu_H1 had a lower amount of total loline ($P < 0.005$) and percentage of NANL ($P << 0.001$) but a higher percentage of NAL ($P < 0.005$) compared to Eu_H5, Eu_H6 and Eu_H7. As it concerns the percentage of NFL, significant differences were found only between Eu_H1 and Eu_H7 ($P = 0.01$).

Traces of NFL (30 μg/g) were detected in the FaTG-2 sample isolated from the accessions PI 347571, but no loline alkaloids were detected in the FaTG-5 isolates.

DISCUSSION

Occurrence of Epichloë Endophytes in Wild and Semi-Wild European Meadows

Epichloë endophytes are a valuable resource, useful to bring new resistances in forage and turf grasses. Their use in agriculture is well-established and breeding companies are looking for new strains with improved characteristics to introduce in their varieties. Animal-friendly *Epichloë* endophytes are rare and substantial sampling effort is required to identify genotypes with an appropriate alkaloid profile. In this study we screened wild- and semi-wild grass ecotypes collected in different countries or

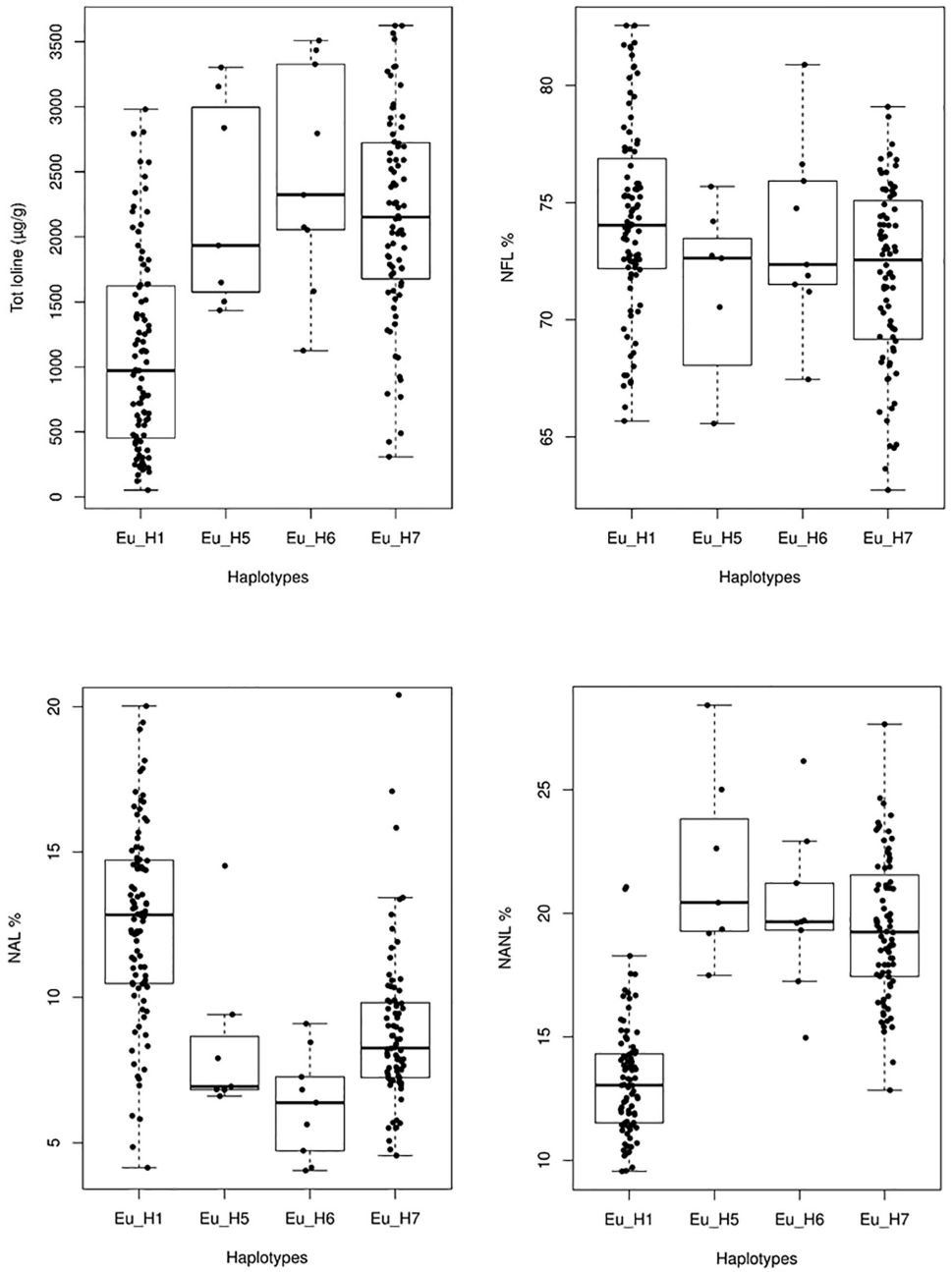

FIGURE 8 | Variation of the total amount of loline and NAL, NANL, and NFL proportions in 4 different haplotypes. Outlier values are not shown.

provided by seed banks, after establishing a nursery of *Epichloë* infected plants.

The frequency and the occurrence of *Epichloë* endophytes in Europe is consistent with the results of previous screening (Oliveira and Castro, 1997; Saikkonen et al., 2000; Jensen and Roulund, 2004; Jensen et al., 2007; Zurek et al., 2012). Among all the countries, the highest infection rates were scored in southern Sweden where all sites were found to be infected with *Epichloë* endophytes. A similar incidence was found in Norway although, due to more intensive agriculture in areas where collection was conducted, it was much harder to find isolated areas colonized with semi-wild meadow fescue. The lowest number of infected locations was scored in Denmark, probably due to the lack of isolated habitats and the intensive use of E- forage cultivars which may successfully invade uncultivated areas. Most of the collected perennial ryegrass plants were, indeed, endophyte-free. Surprisingly, the Alps at the Austrian-Italian border was a good source of infected material, although most of the pastures were supposedly cultivated, or derived from cultivated fields. It seems that the use of permanent pastures led to a complex genetic

relationship between naturalized and cultivated meadow fescue in these regions, as it has been found for Scandinavian meadow fescue (Fjellheim et al., 2009).

Epichloë uncinata and *Epichloë coenophiala* are described to be vertically transmitted within their host, therefore infected meadow and tall fescue plants likely arise from infected seeds. Several studies, mostly focused on tall fescue and perennial ryegrass, stress the selective advantage of infected grasses over endophyte free grasses correlating high infection rates with better performances to water-supply deficit (West et al., 1993; Lewis et al., 1997), increased photosynthetic rate (Belesky et al., 1987) and resistance to insects, nematodes (Elmi et al., 2000), and seed predators (Madej and Clay, 1991). It is known that E+ grasses can have a higher competitive ability and, because of that, infection frequencies should rise over time (Cunningham et al., 1993) especially if strong biotic and abiotic stresses impose selective pressure on E- individuals (Bouton et al., 1993).

It has to be taken into account that all the infection rate values might be biased by the relatively low number of plants (15–20) sampled in each location and by the small sampling area (on average 1000–2000 m^2), which increases the probabilities that the sampled plants were siblings, although efforts were made to collect plants as widespread as possible. Infection rates lower than 100% occur when E+ and E- plants coexist in the same population. This could happen if the population is in a transition period toward complete infection or, on the opposite side, toward a loss of infection. Another possible explanation is the occurrence of imperfect vertical transmission to seeds (Ravel et al., 1997) or the loss of the endophyte viability in the seeds, which generates E- plants. Moreover, several commercially available varieties are infected with *Epichloë* endophytes although most of them are endophyte free (Holder et al., 1994; Saikkonen et al., 2000), and their extensive use might have affected the species composition and the ratio between infected and non-infected grasses in the area of sampling. According to our results in Sweden, Norway and on the Alps it is highly unlikely to find wild extensive habitats containing *Epichloë*-free meadow fescues.

Occurrence of *E. uncinata* in *S. pratensis* Accessions

With regard to the accessions from the germplasm banks, the number of infected USDA accessions was surprisingly low, especially according to the immunoblot test, which only confirmed 12 out of 44 PCR-positives. The reason for the discrepancy between the two assays could be that the infection rates of some seedlots were very low due to the loss of viability of the endophytes during the storage. Another possible explanation is that the immunoblot may not have been able to detect the endophyte in the seedlings because of low biomass. Seven accessions were already known to be endophyte infected from previous studies, but when tested with the immunoblot they were negative. Moreover, Holder et al. (1994) tested seeds of 198 meadow fescue accessions, only 30 of them were found to be E+ and they experienced the same phenomenon when assessing the infection status of the seedlings, realizing that infection rates were lower than the ones in the seeds. The loss of endophyte viability is a known problem related to seeds storage conditions which are optimized to preserve seeds' germination rate rather than endophytes' viability (Clement et al., 2008). Plants were also severely weakened by a severe powdery mildew (*Blumeria graminis*) infestation and by a long and cold winter. Long exposure to sub-optimal temperatures can strongly affect the amount of endophyte mycelia in the plant, as described by Breen (1992) who demonstrated a difference in the concentration of endophyte in plants grown at constant temperature of 7 or 28°C than in plants growing at a constant temperature of 14 or 21°C. Bacon and Siegel (1988) described the disintegration of the mycelium in leaf sheaths during periods of plant stress and fungal dormancy, which can also justify the failure in detecting the endophytes with the immunoblot method. This is supported by the observation that PCR and immunoblot results concurred for the NordGen accessions, which were assayed during the summer on healthy and vigorous plants. The accessions from NordGen confirmed the trend seen from the collection trips according to which meadow fescue ecotypes in Scandinavian countries, particularly Sweden, were highly infected with *Epichloë* endophytes. For this investigation, only accessions labeled as "wild" or "semi wild" were chosen, but more endophytes can be found also in commercial varieties (Holder et al., 1994). In the NordGen database there are no records of endophyte infected accessions, therefore endophyte infection data have been shared with both genebanks so that they can be incorporated into their databases to enable endophyte and grass scientists to screen for desirable plant-endophyte combinations.

Identification of FaTG-2 and FaTG-5 Isolates

Identification of endophyte species through morphological traits and host specificity (Christensen et al., 1993) can be difficult and misleading due to similarities among species and intra-species variations of different strains. Most of the current knowledge on taxonomy and phylogenetic relationship among the genus *Epichloë* relies on analysis of intron sequences from the β-tubulin (*tub*B), translation elongation factor 1-α (*tef* A, former *tef* 1) and γ-actin (*act*A) (Schardl et al., 1991). Another rapid, cheap, and reliable method to detect and characterize isolates is through microsatellite markers (Moon et al., 1999). Microsatellite fingerprints can be done both in pure cultures and *in planta*. Primers used in this study were specific for endophytes and no amplifications in E- samples were detected. Generally, primers designed for a specific locus work for more than one species and may be used to discriminate isolates not only on a species level but also between taxa and strains (van Zijll de Jong et al., 2003). The level of polymorphisms at each locus, and therefore its informativeness, may be different and change from species to species (**Table 2**) so that some loci are more suitable to investigate genetic differences in a species than others. The result shown in this study may help to choose an adequate set of loci and help the identification of new isolates by comparison of their genetic profile with the haplotypes described.

In order to correctly identify isolates of the accession PI347572, all three approaches were applied (morphological

traits, microsatellite profiles and housekeeping genes phylogeny). Conidia dimensions are consistent with the ones described by Christensen et al. (1993), suggesting that both FaTG-2, and FaTG-5 are characterized by similar shorter conidia (5–8 μm) compared to the ones of *E. coenophiala* (6–15 μm). The microsatellite analysis was able to distinguish the two closely related taxonomic groups, their genetic profiles at B10 and B11 can be compared to the result of other studies (Moon et al., 2004; Jensen et al., 2007) where the strain Tf15, with isozyme phenotype FaC, seems to be closer to FaTG-2, whereas the strain Tf13, with isozyme phenotype FaA, seems to be closer to FaTG-5. Phylogenies inferred from housekeeping genes showed a close relationship of FaTG-2 and FaTG-5 with Lolium-associated endophyte (LAE) clade (Schardl et al., 2008), which seems to be a common ancestor to all the *S. arundinaceus* associated endophytes described so far, and *E. festucae*. This result was consistent with other phylogeny studies based on housekeeping gene sequences (Ekanayake et al., 2013) and SSR-based phenetic analysis (Ekanayake et al., 2012).

Microsatellite Fingerprinting

Our analysis revealed 21 different haplotypes and amplified a number of amplicons consistent with the one provided in previous studies. Fewer alleles than expected were only observed at B10 in *E. siegelii*, at E33 in FaTG-2 and at E39 in three haplotypes of *E. uncinata*. According to Moon et al. (2004) there could be polymorphisms at the primer sites which prevent a correct ligation of the primer(s) and subsequent amplification of the locus, leading to a false negative; if the amplified fragments, at two or more loci, have the same size they are scored as one allele; a third possibility is the loss of a chromosomal parts.

A direct comparison of the haplotypes is possible at loci B10 and B11 with the results reported in other studies using the same loci (Moon et al., 1999, 2004; Young et al., 2014; Clayton et al., 2017). In *S. arundinaceus,* haplotype Ec_H1 has the same profile as *E. coenophiala* profile 1-1 (Young et al., 2014) at both loci, whereas Ec_H2 has a polymorphism at B11 never described before. Ec_H3 has the same profile as the isolate Tf28 (isozyme phenotype coC) (Moon et al., 1999) and it was only detected from plants collected in Spain. In *S. giganteus, E. festucae* haplotypes Ef_H1 and Ef_H3 have the same profile as the isolate Frc7 (Moon et al., 1999), which was isolated from *Festuca rubra* subsp. *commutata*. Regarding isolates from *L. perenne*: El_H1 has the same profile as strains Lp5, Lp6 and Lp13 (isozyme phenotype loA) (Moon et al., 1999) whereas the other haplotypes are different from the ones previously described. The only isolate of *E. siegelii* had the same profile as ATCC 74483, an attempt to re-isolate *E. siegelii* from the original accession was made but it was unsuccessful. Regarding *S. pratensis* isolates, at locus B11 only one allele with size 121 pb has been described so far in *E. uncinata*, which was the most common found in this study as well, but two isolates had an amplicon of 117 pb (Eu_H2) and 109 (Eu_H3), respectively. These polymorphisms are likely to arise by errors during the replication process, due for instance to DNA polymerase slippage. At B10 the haplotypes split into two groups, one with amplicons of approximately 164 and 200 bp and the other with amplicons of approximately 176 and 196 bp, which reflect the same allele sizes as the two strains isolated from Fp1 and Fp4 described by Moon et al. (1999) with allozymes profile unA and unB, respectively.

Clayton et al. (2017) have described two similar haplotypes naming them "ecotype 1" and "ecotype 3," and their B10 sequences are compared to the ones of the closest *E. uncinata* ancestors *E. typhina* and *E. bromicola*. There are several variations in repeated structures between the two copies of the locus among the two haplotypes and this raises the question whether these variations occurred in *E. uncinata* or in its ancestors, assuming different independent interspecific hybridization events. If two independent anastomosis events occur in different locations an unbalanced geographical distribution of the haplotypes may be expected since *E. uncinata* is only vertically transmitted. Eu_H1 is the most abundant haplotype in the northern countries and it is completely absent in Italy and Austria, whereas Eu_H7 can be found throughout Europe, even in Russia and Kyrgyzstan. Its wide distribution might be anthropogenic if, for example, this haplotype was infecting one or more cultivars commercialized in several countries. Contamination of natural populations with plants from infected varieties could also explain the presence of two haplotypes in the same location. Clayton et al. (2017) come to a similar conclusion, associating different geographical origins to the 4 ecotypes detected: the strain U2 with a similar profile as Eu_H1 may come from Norway and U4, similar to Eu_H7, from Germany.

It can also be speculated that a possible explanation for the observed genetic variation in relation to the geographical distribution involves local adaptation to specific stresses which may positively select one haplotype over another. This could explain the absence of Eu_H1 on the Alps. Clayton et al. (2017) showed that polymorphisms at B10 can lead to changes in the polypeptide sequences since it lies within the exon of an expressed gene, and the two haplotypes have two different allozyme profiles (unA and unB), which could represent a phenotypic diversity on which selection could act.

The above mentioned uneven distribution of the haplotypes and the fact that 5 of the 8 haplotypes scored came from very diverse USDA accessions, reported to be collected in Russia, affected the relation between geographical distribution and genetic diversity investigated with the Mantel correlogram. Having on the shortest distance individuals which are genetically closer than random individuals is partially coherent with what it is expected from clonally propagated species. But the fact that on the longer distance they are more diverse than random individuals does not fit with the idea of a single strain vertically transmitted throughout Europe, it rather supports the hypothesis of different hybridization events.

It has to be taken into account that the number of haplotypes strongly depends on the number and on the information content of the profiled loci, and the number of individuals and populations sampled. Using a wider panel of SSRs on more samples may lead to a deeper characterization of the isolates. The 7 microsatellites used in this study allowed a clear separation between species as shown in the phylogenetic tree and in the PCoA, but as it is clear from the latter, and genetic variation within isolates of vertically propagated species is usually very

low due to the absence of sexual reproduction (van Zijll de Jong et al., 2008). For a deeper characterization and to investigate the genetic variation within asexual species it is suggested to either screen more loci or to use a different fingerprinting approach. The phenetic relationships between haplotypes were consistent with those described in other studies (van Zijll de Jong et al., 2003; Karimi et al., 2012) with *E. festucae* and *E. festucae* var. *lolii* being closely related, *E. coenophiala* clustering in a different clade, FaTG-2 and FaTG-5 being genetically very similar and related to *E. festucae*.

Loline Analysis

One of the features that makes *E. uncinata* an endophyte appealing for agricultural uses is its production of high level of loline alkaloids. Measuring the alkaloids at a given time is like taking a screenshot on a state that it is known to vary greatly during the host lifespan. There are several factors that can directly affect the concentration of these compounds, which include the season of the year (Patchett et al., 2009), pest feeding on the host or abiotic stresses (Patchett et al., 2008; Helander et al., 2016), or that can indirectly affect the amount of alkaloids that the endophyte can produce by altering the mycelium biomass in the host (Ryan et al., 2015). Nevertheless, comparing the amount of loline alkaloids in plants grown at the same conditions is one way to select suitable candidates for being artificially inoculated in elite varieties and re-tested for loline content in the new host.

The total amount of loline measured in this study is consistent with the results of similar studies based on plants grown in pots at greenhouse conditions (Leuchtmann et al., 2000; Patchett et al., 2011). Usually, plants grown in open fields have higher levels of total loline that can easily exceed 10,000 μg/g (Barker et al., 2015). NFL was found to be the alkaloid with the highest concentration in all the isolates, but the proportion of NANL and NAL changed significantly with the increase of the amount of total loline and among haplotypes (**Figures 7**, **8**). Findings from Eu_H1 support the trend found in the literature previously mentioned, where concentrations of NAL are similar or higher than those of NANL, whereas in Eu_H5, Eu_H6 and Eu_H7 from this study the trend was the opposite way. Haplotypes synthesizing higher levels of loline produce significantly more NANL and less NAL than the ones with low level of total loline. These phenotypic differences may be additional evidence for a greater genetic diversity than previously assumed among haplotypes and may be related to differences in their ancestors.

CONCLUSION

The Scandinavian northern regions and the Alps are a good source of *Epichloë* infected meadow fescue. Also, germplasm repositories represent a valuable resource for endophytes even though their viability in the seeds is reduced over time, particularly at suboptimal storage conditions. Results from this study provide valuable information to germplasm banks which will allow to provide additional support to forage and turf breeders. The genetic diversity and allelic composition of asexual, vertically transmitted species appears to be more complex than previously assumed. In this study we discuss the possibility of multiple hybridization events as source of intraspecific variability. It is not possible to infer from our results where the hybridization events took place, because meadow fescue and other grasses have been spread by human beings throughout the continent(s). Since our current knowledge of endophyte distribution is incomplete, population genetic studies on ancestor species from a wide geographic range are needed to understand the evolutionary origin of the hybrid endophytes of the *Festuca-Lolium* complex. Moreover, the different genetic background of the haplotypes may affect the production of loline alkaloids. Finally, sharing of the genetic profiles of screened isolates is crucial for identifications of new isolates that may have improved characteristics and could be used for grass breeding and future research.

DATA AVAILABILITY

The datasets generated for this study can be found in NCBI: https://www.ncbi.nlm.nih.gov/nuccore/MK423914.1, https://www.ncbi.nlm.nih.gov/nuccore/MK423915.1, https://www.ncbi.nlm.nih.gov/nuccore/MK423916.1, and https://www.ncbi.nlm.nih.gov/nuccore/MK423917.1.

AUTHOR CONTRIBUTIONS

GC, NR, CJ, and TA designed the experiment. GC, NR, FF, and AL collected the data. GC and AL analyzed the data. All authors contributed to manuscript preparation, editing, and gave final approval for publication.

FUNDING

This study was received funding from the European Union's Horizon 2020 Research and Innovation Programme under the Marie Skłodowska-Curie grant agreement number 676480.

ACKNOWLEDGMENTS

We thank I. Lenk, E. W. Larsen, and I. Nagy for their methodological advice and scientific discussions.

SUPPLEMENTARY MATERIAL

The Supplementary Material for this article can be found online at: https://www.frontiersin.org/articles/10.3389/fpls.2019.00765/full#supplementary-material

FIGURE S1 | Map of the collection sites of the sampled grass ecotypes (blue) and of the screened accessions from USDA (green) and NordGen (red) whose coordinates were available.

TABLE S1 | Ecotypes and accessions screened in this study followed by coordinates, altitude, infection status and infection rate.

TABLE S2 | List of fingerprinted isolates and their allelic profiles at 7 microsatellites loci. Information about host, endophyte and location of the collection are provided together with the genetic profile of each sample.

TABLE S3 | Levels of N-formylloline (NFL), N-acetylloline (NAL), N-acetylnorloline (NANL) in 218 pseudostems of *Epichloë*-infected grasses.

REFERENCES

An, Z., Siegel, M. R., Hollin, W., Tsai, H., Schmidt, D., and Schardl, C. L. (1993). Relationships among non-*Acremonium sp.* fungal endophytes in five grass species. *Microbiology* 59, 1540–1548.

Bacon, C. W., Porter, J. K., Robbins, J. D., and Luttrell, E. S. (1977). *Epichloe typhina* from toxic tall fescue grasses. *Appl. Environ. Microbiol.* 34, 576–581.

Bacon, C. W., and Siegel, M. R. (1988). Endophyte parasitism of tall fescue. *Jpa* 1:45. doi: 10.2134/jpa1988.0045

Baldauf, M. W., Mace, W. J., and Richmond, D. S. (2011). Endophyte-mediated resistance to black cutworm as a function of plant cultivar and endophyte strain in tall fescue. *Environ. Entomol.* 40, 639–647. doi: 10.1603/EN09227

Barker, G. M., Patchett, B. J., and Cameron, N. E. (2015). *Epichloe uncinata* infection and loline content protect festulolium grasses from crickets (Orthoptera: Gryllidae). *J. Econ. Entomol.* 108, 789–797. doi: 10.1093/jee/tou058

Belesky, D. P., Devine, O. J., Pallas, J. E., and Stringer, W. C. (1987). Photosynthetic activity of tall fescue as influenced by a fungal endophyte. *Photosynthetica* 21, 82–87.

Bouton, J. H., Gates, R. N., Belesky, D. P., and Owsley, M. (1993). Yield and persistence of tall fescue in the southeastern coastal plain after removal of its endophyte (AJ). *Agron. J.* 85, 52–55. doi: 10.2134/agronj1993.00021962008500010011x

Bouton, J. H., Latch, G. C. M., Hill, N. S., Hoveland, C. S., McCann, M. A., Watson, R. H., et al. (2002). Reinfection of tall fescue cultivars with non-ergot alkaloid–producing endophytes. *Agron. J.* 94:567. doi: 10.2134/agronj2002.0567

Brazauskas, G., Lenk, I., Greve Pedersen, M., Studer, B., and Lübberstedt, T. (2011). Genetic variation, population structure, and linkage disequilibrium in European elite germplasm of perennial ryegrass. *Plant Sci.* 181, 412–420. doi: 10.1016/j.plantsci.2011.06.013

Breen, J. P. (1992). Temperature and seasonal effects on expression of *Acremonium* endophyte-enhanced resistance to *Schizaphis graminum* (homoptera: aphididae). *Environ. Entomol.* 21, 68–74. doi: 10.1093/ee/21.1.68

Christensen, M. J. J., Leuchtmann, A., Rowan, D. D. D., and Tapper, B. A. A. (1993). Taxonomy of *Acremonium* endophytes of tall fescue (*Festuca arundinacea*), meadow fescue (*F. pratensis*) and perennial ryegrass (*Lolium perenne*). *Mycol. Res.* 97, 1083–1092. doi: 10.1016/S0953-7562(09)80509-1

Clayton, W., Eaton, C. J., Dupont, P.-Y., Gillanders, T., Cameron, N., Saikia, S., et al. (2017). Analysis of simple sequence repeat (SSR) structure and sequence within *Epichloë* endophyte genomes reveals impacts on gene structure and insights into ancestral hybridization events. *PLoS One* 12:e0183748. doi: 10.1371/journal.pone.0183748

Clement, S. L., Martin, R. C., Dombrowski, J. E., Elberson, L. R., Kynaston, M., and Azevedo, M. D. (2008). *Neotyphodium* endophytes in tall fescue seed: viability after seed production and prolonged cold storage. *Seed Sci. Technol.* 36, 710–720. doi: 10.15258/sst.2008.36.3.20

Craven, K. D. (2003). *Coevolution and Genetic Diversity in Grass-Endophyte Symbioses*. Doctoral Dissertations, University of Kentucky, Lexington, KY, Vol. 431.

Craven, K. D., Blankenship, J. D., Leuchtmann, A., Hignight, K., and Schardl, C. L. (2001). Hybrid fungal endophytes symbiotic with the grass *Lolium pratense*. *Sydowia* 53, 44–73.

Cunningham, P. J., Foot, J. Z., and Reed, K. F. M. (1993). Perennial ryegrass (*Lolium perenne*) endophyte (*Acremonium lolii*) relationships: the Australian experience. *Agric. Ecosyst. Environ.* 44, 157–168. doi: 10.1016/0167-8809(93)90044-P

Ekanayake, P. N., Hand, M. L., Spangenberg, G. C., Forster, J. W., and Guthridge, K. M. (2012). Genetic diversity and host specificity of fungal endophyte taxa in fescue pasture grasses. *Crop Sci.* 52, 2243–2252. doi: 10.2135/cropsci2011.12.0664

Ekanayake, P. N., Rabinovich, M., Guthridge, K. M., Spangenberg, G. C., Forster, J. W., and Sawbridge, T. I. (2013). Phylogenomics of fescue grass-derived fungal endophytes based on selected nuclear genes and the mitochondrial gene complement. *BMC Evol. Biol.* 13:270. doi: 10.1186/1471-2148-13-27

Elmi, A. A., West, C. P., Robbins, R. T., and Kirkpatrick, T. L. (2000). Endophyte effects on reproduction of a root-knot nematode (*Meloidogyne marylandi*) and osmotic adjustment in tall fescue. *Grass Forage Sci.* 55, 166–172. doi: 10.1046/j.1365-2494.2000.00210.x

Fjellheim, S., Pašakinskienė, I., Grønnerød, S., Paplauskienė, V., and Rognli, O. A. (2009). Genetic structure of local populations and cultivars of meadow fescue from the Nordic and Baltic regions. *Crop Sci.* 49, 200–210. doi: 10.2135/cropsci2007.08.0422

Fletcher, L. R., and Harvey, I. C. (1981). An association of a lolium endophyte with ryegrass staggers. *N. Z. Vet. J.* 29, 185–186. doi: 10.1080/00480169.1981.34839

Gallagher, R. T., White, E. P., and Mortimer, P. H. (1981). Ryegrass staggers: isolation of potent neurotoxins lolitrem A and lolitrem B from staggers-producing pastures. *N. Z. Vet. J.* 29, 189–190. doi: 10.1080/00480169.1981.34843

Gams, W., Petrini, O., and Schmidt, D. (1990). Acremonium uncinatum, a new endophyte in *Festuca pratensis*. *Mycotaxon* 37, 67–71.

Ghimire, S. R., Rudgers, J. A., Charlton, N. D., Young, C., and Craven, K. D. (2011). Prevalence of an intraspecific *Neotyphodium* hybrid in natural populations of stout wood reed (*Cinna arundinacea* L.) from eastern North America. *Mycologia* 103, 75–84. doi: 10.3852/10-154

Grünwald, N. J., Goodwin, S. B., Milgroom, M. G., and Fry, W. E. (2003). Analysis of genotypic diversity data for populations of microorganisms. *Phytopathology* 93, 738–746. doi: 10.1094/PHYTO.2003.93.6.738

Helander, M., Phillips, T., Faeth, S. H., Bush, L. P., McCulley, R., Saloniemi, I., et al. (2016). Alkaloid quantities in endophyte-infected tall fescue are affected by the plant-fungus combination and environment. *J. Chem. Ecol.* 42, 118–126. doi: 10.1007/s10886-016-0667-1

Hiatt, E. E., Hill, N. S., Bouton, J. H., and Stuedemann, J. A. (1999). Tall fescue endophyte detection: commercial immunoblot test kit compared with microscopic analysis. *Crop Sci.* 39, 796–799. doi: 10.2135/cropsci1999.0011183X003900030030x

Hijmans, R. J., Williams, E., and Vennes, C. (2017). *Package "geosphere"*. Available at: http://www.movable-type.co.uk/scripts/latlong.html (accessed November 14, 2018).

Holder, T. L., West, C. P., Turner, K. E., McConnell, M. E., and Piper, E. L. (1994). Incidence and viability of *Acremonium* endophytes in tall fescue and meadow fescue plant introductions. *Crop Sci.* 34, 252–254. doi: 10.2135/cropsci1994.0011183X003400010046x

Jensen, A. D. M., and Roulund, N. (2004). Occurrence of *Neotyphodium* endophytes in permanent grassland with perennial ryegrass (*Lolium perenne*) in Denmark. *Agric. Ecosyst. Environ.* 104, 419–427. doi: 10.1016/j.agee.2004.01.044

Jensen, A. M. D., Mikkelsen, L., and Roulund, N. (2007). Variation in genetic markers and ergovaline production in endophyte (*Neotyphodium*)-infected fescue species collected in Italy, Spain, and Denmark. *Crop Sci.* 47, 139–147. doi: 10.2135/cropsci2005.10.0352

Johnson, L. J., De Bonth, A. C. M., Briggs, L. R., Caradus, J. R., Finch, S. C., Fleetwood, D. J., et al. (2013). The exploitation of epichloae endophytes

for agricultural benefit. *Fungal Divers.* 60, 171–188. doi: 10.1007/s13225-013-0239-4

Kamvar, Z. N., Tabima, J. F., and Grünwald, N. J. (2014). Poppr?: an R package for genetic analysis of populations with clonal, partially clonal, and/or sexual reproduction. *PeerJ* 2:e281. doi: 10.7717/peerj.281

Karimi, S., Mirlohi, A., Sabzalian, M. R., Sayed Tabatabaei, B. E., and Sharifnabi, B. (2012). Molecular evidence for *Neotyphodium* fungal endophyte variation and specificity within host grass species. *Mycologia* 104, 1281–1290. doi: 10.3852/11-316

Kumar, S., Stecher, G., Li, M., Knyaz, C., and Tamura, K. (2018). MEGA X: molecular evolutionary genetics analysis across computing platforms. *Mol. Biol. Evol.* 35, 1547–1549. doi: 10.1093/molbev/msy096

Latch, G. C. M., and Christensen, M. J. (1982). Ryegrass endophyte, incidence, and control. *New Zeal. J. Agric. Res.* 25, 443–448. doi: 10.1080/00288233.1982.10417910

Leuchtmann, A., Schmidt, D., and Bush, L. P. (2000). Different levels of protective alkaloids in grasses with stroma-forming and seed-transmitted *Epichloe/Neotyphodium* endophytes. *J. Chem. Ecol.* 26, 1025–1036. doi: 10.1023/A:1005489032025

Lewis, G. C., Ravel, C., Naffaa, W., Astier, C., and Charmet, G. (1997). Occurrence of *Acremonium* endophytes in wild populations of *Lolium spp.* in European countries and a relationship between level of infection and climate in France. *Ann. Appl. Biol.* 130, 227–238. doi: 10.1111/j.1744-7348.1997.tb06828.x

Madej, C. W., and Clay, K. (1991). Avian seed preference and weight loss experiments: the effect of fungal endophyte-infected tall fescue seeds. *Oecologia* 88, 296–302. doi: 10.1007/BF00320825

Middendorf, L. R., Bruce, J. C., Bruce, R. C., Eckles, R. D., Grone, D. L., Roemer, S. C., et al. (1992). Continuous, on-line DNA sequencing using a versatile infrared laser scanner/electrophoresis apparatus. *Electrophoresis* 13, 487–494. doi: 10.1002/elps.11501301103

Moon, C. D., Craven, K. D., Leuchtmann, A., Clement, S. L., and Schardl, C. L. (2004). Prevalence of interspecific hybrids amongst asexual fungal endophytes of grasses. *Mol. Ecol.* 13, 1455–1467. doi: 10.1111/j.1365-294X.2004.02138.x

Moon, C. D., Tapper, B. A., and Scott, B. (1999). Identification of *Epichloë* endophytes in planta by a microsatellite-based PCR fingerprinting assay with automated analysis. *Appl. Environ. Microbiol.* 65, 1268–1279.

Muller, H. J. (1964). The relation of recombination to mutational advance. *Mutat. Res. Mol. Mech. Mutagen.* 1, 2–9. doi: 10.1016/0027-5107(64)90047-8

Nei, M. (1978). Estimation of average heterozygosity and genetic distance from a small number of individuals. *Genetics* 89, 583–590.

Oberhofer, M., and Leuchtmann, A. (2012). Genetic diversity in epichloid endophytes of *Hordelymus europaeus* suggests repeated host jumps and interspecific hybridizations. *Mol. Ecol.* 21, 2713–2726. doi: 10.1111/j.1365-294X.2012.05459.x

Oksanen, J., Blanchet, F. G., Friendly, M., Kindt, R., Legendre, P., and McGlinn, D. (2018). *Vegan: Community Ecology Package. R package version 2.4–2*. Available at: https://CRAN.R-project.org/package=vegan

Oliveira, J. A., and Castro, V. (1997). Incidence and viability of *Acremonium* endophytes in tall fescue accessions from North Spain. *Genet. Resour. Crop Evol.* 44, 519–522. doi: 10.1023/A:1008620725857

Patchett, B., Gooneratne, R., Fletcher, L., and Chapman, B. (2009). Seasonal changes in leaf and stem loline alkaloids in meadow fescue. *Crop Pasture Sci.* 62, 261–267. doi: 10.1071/CP10266

Patchett, B., Gooneratne, R., Fletcher, L., and Chapman, B. (2011). Seasonal distribution of loline alkaloid concentration in meadow fescue infected with *Neotyphodium uncinatum*. *Crop Pasture Sci.* 62:603. doi: 10.1071/CP11017

Patchett, B. J. (2007). *Loline Alkaloids: Analysis and Effects on Sheep and Pasture Insects*. Ph. D thesis, Lincoln University, Canterbury.

Patchett, B. J., Chapman, R. B., Fletcher, L. R., and Gooneratne, S. R. (2008). Root loline concentration in endophyte-infected meadow fescue (Festuca pratensis) is increased by grass grub (Costelytra zealandica) attack. *New Zeal. Plant Prot.* 61, 210–214.

Peakall, R., and Smouse, P. E. (2012). GenAlEx 6.5: genetic analysis in Excel. Population genetic software for teaching and research–an update. *Bioinformatics* 28, 2537–2539. doi: 10.1093/bioinformatics/bts460

Ravel, C., Michalakis, Y., and Charmet, G. (1997). The effect of imperfect transmission on the frequency of mutualistic seed-borne endophytes in natural populations of grasses. *Oikos* 80, 18–24. doi: 10.2307/3546511

Ryan, G. D., Rasmussen, S., Parsons, A. J., and Newman, J. A. (2015). The effects of carbohydrate supply and host genetic background on *Epichloë* endophyte and alkaloid concentrations in perennial ryegrass. *Fungal Ecol.* 18, 115–125. doi: 10.1016/j.funeco.2015.07.006

Saikkonen, K., Ahlholm, J., Helander, M., Lehtimaki, S., and Niemelainen, O. (2000). Endophytic fungi in wild and cultivated grasses in Finland. *Ecography* 23, 360–366. doi: 10.1111/j.1600-0587.2000.tb00292.x

Schardl, C. L. (1996). Epichloë species: fungal symbionts of grasses. *Annu. Rev. Phytopathol.* 34, 109–130. doi: 10.1146/annurev.phyto.34.1.109

Schardl, C. L., and An, Z. (1993). "Molecular biology and genetics of protective fungal endophytes of grasses," in *Genetic Engineering*, ed. J. K. Setlow (Boston, MA: Springer), 191–212. doi: 10.1007/978-1-4899-1666-2_9

Schardl, C. L., and Clay, K. (1997). "Evolution of mutualistic endophytes from plant pathogens," in *Plant Relationships Part B*, eds G. C. Carroll and P. Tudzynski (Berlin: Springer), 221–238. doi: 10.1007/978-3-642-60647-2_14

Schardl, C. L., Craven, K. D., Speakman, S., Stromberg, A., Lindstrom, A., and Yoshida, R. (2008). A novel test for host-symbiont codivergence indicates ancient origin of fungal endophytes in grasses. *Syst. Biol.* 57, 483–498. doi: 10.1080/10635150802172184

Schardl, C. L., Grossman, R. B., Nagabhyru, P., Faulkner, J. R., and Mallik, U. P. (2007). Loline alkaloids: currencies of mutualism. *Phytochemistry* 68, 980–996. doi: 10.1016/j.phytochem.2007.01.010

Schardl, C. L., Leuchtmann, A., Chung, K.-R., Penny, D., and Siegel, M. R. (1997). Coevolution by common descent of fungal symbionts (*Epichloe spp.*) and grass hosts. *Mol. Biol. Evol.* 14, 133–143. doi: 10.1093/oxfordjournals.molbev.a025746

Schardl, C. L., Liu, J.-S., White, J. F. Jr., Finkel, R. A., An, Z., and Siegel, M. R. (1991). Molecular phylogenetic relationships of nonpathogenic grass mycosymbionts and clavicipitaceous plant pathogens. *Plant Syst. Evol.* 178, 27–41. doi: 10.1007/BF00937980

Schirrmann, M. K., Zoller, S., Fior, S., and Leuchtmann, A. (2014). Genetic evidence for reproductive isolation among sympatric *Epichloë* endophytes as inferred from newly developed microsatellite markers. *Microb. Ecol.* 70, 51–60. doi: 10.1007/s00248-014-0556-5

Schmid, J., Day, R., Zhang, N., Dupont, P.-Y., Cox, M. P., Schardl, C. L., et al. (2017). Host tissue environment directs activities of an *Epichlöe* endophyte, while it induces systemic hormone and defense responses in its native perennial ryegrass host. *Mol. Plant Microbe Interact.* 30, 138–149. doi: 10.1094/MPMI-10-16-0215-R

Selosse, M. A., and Schardl, C. L. (2007). Fungal endophytes of grasses: hybrids rescued by vertical transmission? An evolutionary perspective. *New Phytol.* 173, 452–458. doi: 10.1111/j.1469-8137.2007.01978.x

Shannon, C. E. (1948). A mathematical theory of communication. *Bell Syst. Techn. J.* 27, 379–423.

Sherwin, W. B., Jobot, F., Rush, R., and Rossetto, M. (2006). Measurement of biological information with applications from genes to landscapes. *Mol. Ecol.* 15, 2857–2869. doi: 10.1111/j.1365-294X.2006.02992.x

Shoji, J. Y., Charlton, N. D., Yi, M., Young, C. A., and Craven, K. D. (2015). Vegetative hyphal fusion and subsequent nuclear behavior in *Epichloë* grass endophytes. *PLoS One* 10:e0121875. doi: 10.1371/journal.pone.0121875

Simpson, E. H. (1949). Measurement of diversity. *Nature* 163, 688–688. doi: 10.1038/163688a0

Stoddart, J. A., and Taylor, J. F. (1988). Genotypic diversity: estimation and prediction in samples. *Genetics* 118, 705–711.

van Zijll de Jong, E., Guthridge, K. M., Spangenberg, G. C., and Forster, J. W. (2003). Development and characterization of EST-derived simple sequence repeat (SSR) markers for pasture grass endophytes. *Genome* 46, 277–290. doi: 10.1139/g03-001

van Zijll de Jong, E. V., Dobrowolski, M. P., Sandford, A., Smith, K. F., Willocks, M. J., Spangenberg, G. C., et al. (2008). Detection and characterisation of

novel fungal endophyte genotypic variation in cultivars of perennial ryegrass (*Lolium perenne* L.). *Aust. J. Agric. Res.* 59, 214–221. doi: 10.1071/Ar07270

West, C. P., Izekor, E., Turner, K. E., and Elmi, A. A. (1993). Endophyte effects on growth and persistence of tall fescue along a water-supply gradient. *Agron. J* 85, 264–270. doi: 10.2134/agronj1993.00021962008500020019x

Young, C. A., Charlton, N. D., Takach, J. E., Swoboda, G. A., Trammell, M. A., Huhman, D. V., et al. (2014). Characterization of *Epichloë?coenophiala* within the US: are all tall fescue endophytes created equal? *Front. Chem.* 2:95. doi: 10.3389/fchem.2014.00095

Zurek, M., Wiewióra, B., Zurek, G., and Prończuk, M. (2012). Occurrence of endophyte fungi on grasses in Poland - Review. *Fungal Ecol.* 5, 353–356. doi: 10.1016/j.funeco.2011.07.007

Conflict of Interest Statement: GC, NR, and CJ are employees of DLF Trifolium A/S.

The remaining authors declare that the research was conducted in the absence of any commercial or financial relationships that could be construed as a potential conflict of interest.

frontiers in Microbiology

ORIGINAL RESEARCH
published: 26 September 2019
doi: 10.3389/fmicb.2019.02228

The Effector AGLIP1 in *Rhizoctonia solani* AG1 IA Triggers Cell Death in Plants and Promotes Disease Development Through Inhibiting PAMP-Triggered Immunity in *Arabidopsis thaliana*

Shuai Li[1], Xunwen Peng[1], Yingling Wang[1], Kangyu Hua[2], Fan Xing[1], Yuanyuan Zheng[1], Wei Liu[1], Wenxian Sun[3]* and Songhong Wei[1]**

[1] Department of Plant Pathology, College of Plant Protection, Shenyang Agricultural University, Shenyang, China, [2] Department of Chemistry & Biochemistry, The Ohio State University, Columbus, OH, United States, [3] College of Plant Protection, Jilin Agricultural University, Changchun, China

OPEN ACCESS

Edited by:
Silvia Proietti,
Università degli Studi della Tuscia, Italy

Reviewed by:
Christos Zamioudis,
Democritus University of Thrace, Greece
Cécile Segonzac,
Seoul National University, South Korea

***Correspondence:**
Songhong Wei
shw@syau.edu.cn
Wenxian Sun
wxs@cau.edu.cn
Shuai Li
lishuai@syau.edu.cn

Specialty section:
This article was submitted to Plant Microbe Interactions, a section of the journal Frontiers in Microbiology

Received: 08 July 2019
Accepted: 11 September 2019
Published: 26 September 2019

Citation:
Li S, Peng X, Wang Y, Hua K, Xing F, Zheng Y, Liu W, Sun W and Wei S (2019) The Effector AGLIP1 in Rhizoctonia solani AG1 IA Triggers Cell Death in Plants and Promotes Disease Development Through Inhibiting PAMP-Triggered Immunity in Arabidopsis thaliana. Front. Microbiol. 10:2228. doi: 10.3389/fmicb.2019.02228

Rhizoctonia solani, one of the most detrimental necrotrophic pathogens, causes rice sheath blight and poses a severe threat to production. Focus on the function of effectors secreted by necrotrophic pathogens during infection has grown rapidly in recent years. However, little is known about the virulence and mechanisms of these proteins. In this study, we performed functional studies on putative effectors in *R. solani* and revealed that AGLIP1 out of 13 putative effectors induced cell death in *Nicotiana benthamiana*. AGLIP1 was also demonstrated to trigger cell death in rice protoplasts. The predicted lipase active sites and signal peptide (SP) of this protein were required for the cell death-inducing ability. *AGLIP1* was greatly induced during *R. solani* infection in rice sheath. The AGLIP1's virulence function was further demonstrated by transgenic technology. The pathogenesis-related genes induced by pathogen-associated molecular pattern and bacteria were remarkably inhibited in AGLIP1-expressing transgenic *Arabidopsis* lines. Ectopic expression of AGLIP1 strongly facilitated disease progression in *Arabidopsis* caused by the type III secretion system-defective mutant from *Pseudomonas syringae* pv. tomato DC3000. Collectively, these results indicate that AGLIP1 is a possible effector that plays a significant role in pathogen virulence through inhibiting basal defenses and promoting disease development in plants.

Keywords: *Rhizoctonia solani*, effector, innate immunity, defense responses, fungal virulence and pathogenicity

INTRODUCTION

Rhizoctonia solani (teleomorph: *Thanatephorus cucumeris*) is classified as a saprophytic fungus, which resides in the soil in the form of sclerotia and does not produce asexual spores. It is complex, with more than 100 species which infect crops, such as rice, wheat, corn, cotton and soybean, ornamental, and horticultural plants. *R. solani* is divided into 14 anastomosis groups (AG1 to AG13

and AGBI). Based on differences in culture characters, host, physiology and biochemistry, they are divided into different subgroups (Ogoshi, 1987; Anderson et al., 2017). Among them, AG1 IA is the most destructive group of pathogens that causes diseases in many monocot and dicot plants. The second most serious rice disease, rice sheath blight, which can reduce rice production up to 50%, is also brought on by AG1 IA (Bernardes-de-Assis et al., 2009).

Pathogenic mechanisms are significantly different among various types of pathogens which allows for characterization of plant pathogens into biotrophic, hemibiotrophic, and necrotrophic pathogens according to their life styles. Biotrophic pathogens obtain nutrients from host living cells and tissues by manipulating host physiology, while hemibiotrophic pathogens absorb nutrients from living cells in the early biotrophic stage of infection, and then obtain nutrients by killing host cells in the later necrotrophic stage of infection (Schulmeyer and Yahr, 2017). Usually, biotrophic and hemibiotrophic pathogens secrete effectors to facilitate infection by manipulating the structure and function of the host cells and suppressing plant defenses. Effectors that are secreted and transported into host cells play important roles in pathogenicity of biotrophic and hemibiotrophic fungi (Koeck et al., 2011). Necrotrophic pathogens, such as *R. solani*, have long been known as plant killers. Necrotrophic fungi complete their life cycle by killing host cells and take nutrients from dead plant tissue. Such pathogens secrete large amounts of cell wall degrading enzymes or toxins, which promote cell necrosis for their own development (Oliver and Solomon, 2010).

However, recent studies indicate that the infection process of necrotrophic pathogens is complex. There may be a transient transition from biotrophy to necrotrophy in the life cycle of such pathogens (Kabbage et al., 2015). For example, *Botrytis cinerea* produces an exopolysaccharide, which regulates the antagonistic effects of jasmonic (JA) and salicylic acid (SA) signaling pathways to enhance its pathogenicity in tomato (El et al., 2011). Moreover, effectors are also crucial weapons which play important roles in promoting pathogen infection. SSITL secreted by *Sclerotinia sclerotiorum* is a possible effector that inhibits host resistance mediated by the JA/ethylene (ET) signaling pathway during the early stage of pathogen infection (Zhu et al., 2013). SsCP1, A cerato-platanin protein, which targets pathogenesis-related protein 1 (PR1), regulates the concentration of SA and contributes to the virulence of *S. sclerotiorum* (Yang et al., 2018). Interestingly, it has recently been shown that NIS1, a core effector in *Colletotrichum* spp. interacts with pattern recognition receptor (PRR)-associated kinases BAK1 and BIK1. Such interaction inhibits kinase activities and the BIK1-NADPH oxidase interaction in host plants (Irieda et al., 2019). *C. orbiculare* expresses specific effectors at different stages. *C. orbiculare* accumulate virulence-related effectors in a pathogen-host interface during the early biotrophic phase and are secreted into plant cells. This process is regulated by the Rab GTPase SEC4 protein (Irieda et al., 2014). The *Parastagonospora nodorum* effectors SnToxA and SnTox3 interact with PR-1-5 and PR-1-1, respectively, and play a decisive role in pathogenicity (Lu et al., 2014; Breen et al., 2016). SnTox1 secreted by *P. nodorum* is a dual-function protein that facilitates infection and counters wheat-produced chitinases (Liu Z. et al., 2016).

Some plants initiate innate immunity through specific interactions of pathogen effectors by nucleotide binding-leucine rich repeat (NB-LRR) proteins. The recognition usually leads to plant cell death, also known as hypersensitive responses (HRs). For biotrophic and hemibiotrophic fungi, HRs is an obstacle for further development in early infection stages (Stergiopoulos and de Wit, 2009). However, host cell death may be beneficial rather than detrimental for necrotrophic pathogenesis. Effectors in necrotrophic fungi may facilitate host cell wall degradation and ultimately promote infection (McDonald and Solomon, 2018). For example, a small protein SsSSVP1 in *S. sclerotiorum* interacts with QCR8, a subunit of the cytochrome b-c1 complex of the mitochondrial respiratory chain in plants. This interaction results in significant plant cell death and facilitates pathogen infection (Lyu et al., 2016). Furthermore, Ss-Caf1 and Xyn11A secreted by *S. sclerotiorum* and *B. cinerea*, respectively, may interact with specific host proteins or unknown substances in host cells which, subsequently, could result in host cell death and contribute to pathogenesis (Noda et al., 2010; Xiao et al., 2014). In *P. tritici-repentis*, the effector proteins ToxA interacts with *Tsn1,* a dominant wheat susceptibility gene, while effector protein ToxB interacts with *TscB* in a gene-for-gene relationship to cause chlorosis in susceptible wheat lines (Sperschneider et al., 2017).

Rhizoctonia solani encodes multiple secreted proteins which are considered as effectors, some of which cause necrotic phenotypes in rice, corn, and soybean (Zheng et al., 2013). However, whether effectors in the necrotrophic pathogen can trigger defense signaling after being recognized by host and non-host plants is still unclear. In this study, we investigated 13 putative effectors in *R. solani* and their ability to induce cell death through transient expression assays. An effector named AGLIP1 (Gene ID: AG1IA_05142) was discovered to trigger cell death in *Nicotiana benthamiana* and rice protoplasts, respectively. The secretion signal peptide (SP) and predicted lipase active sites of AGLIP1 were found to play an important role in inducing cell death. Importantly, our findings also demonstrated that heterologous expression of AGLIP1 in transgenic *Arabidopsis* plants promotes bacterial pathogens progression through suppressing defense responses, which includes flg22- and chitin-triggered PR genes expression. The findings will provide new perspectives in understanding the molecular mechanisms of *R. solani* pathogenesis.

RESULTS

A Putative Effector AGLIP1 in *R. solani* Induces Cell Death in *N. benthamiana*

Many effectors in different pathogens induce non-host hypersensitive cell death in *N. benthamiana* (Li et al., 2015; Fang et al., 2016). To identify if any effectors in *R. solani* have the ability to induce cell death, we chose 13 putative effectors specifically that contained conserved domain and predicted

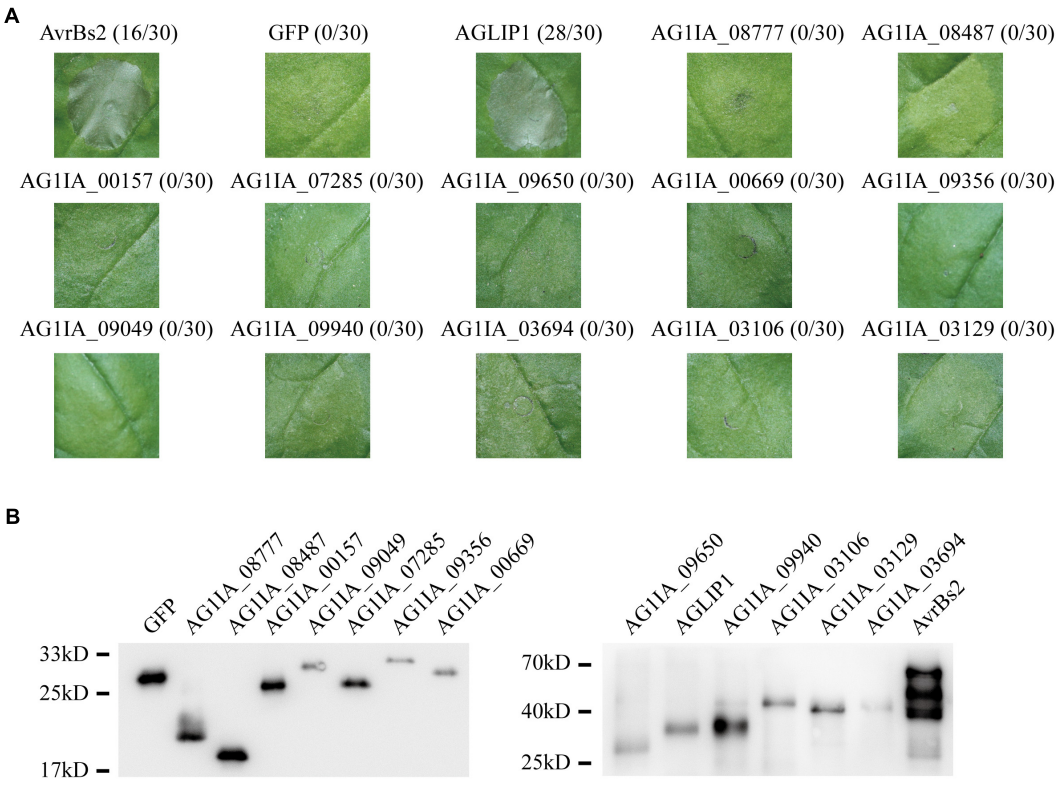

FIGURE 1 | Putative effectors in *Rhizoctonia solani* induce cell death symptoms on *Nicotiana benthamiana* leaves. **(A)** One protein out of 13 tested putative effectors, i.e., AGLIP1, induced the cell death in *N. benthamiana*, while the other 12 proteins did not. GFP, which did not trigger cell death, was shown as a negative control. AvrBs2 in *X. oryzae* pv. *oryzicola* was shown as a positive control. Numbers, e.g., 16/30, indicate that 16 of 30 infiltrated leaves exhibited cell death phenotypes. Representative photos were taken 3 days after DEX treatment. **(B)** Transient expressions of 13 tested putative effectors, AvrBs2 and GFP in *N. benthamiana* were confirmed by Western blot assay. For AGLIP1, the sample for protein extraction was collected at 1 day after DEX treatment, while samples for other proteins extraction were collected at 3 days after DEX treatment. The proteins with 3 × HA tag were detected by immunoblotting with an anti-HA antibody.

functions (**Supplementary Table S1**). 13 putative effectors were transiently expressed in *N. benthamiana* through *Agrobacterium tumefaciens*-mediated transfection after amplifying and subcloning into the glucocorticoid-inducible pTA7001 binary vector (Aoyama and Chua, 1997). The cell death symptoms were recorded within 3 days post-treatment with dexamethasone (DEX), which induces expression of effectors in *N. benthamiana*. Among the 13 tested effectors, AGLIP1 was shown to trigger cell death in *N. benthamiana* leaves at 1–2 days after DEX spraying, while the expression of green fluorescent protein (GFP) did not induce necrosis in *N. benthamiana*. AvrBs2 in *Xanthomonas oryzae* pv. *oryzicola* was shown as a positive control (Li et al., 2015). Other investigated putative effectors did not induce cell necrosis in *N. benthamiana*, although expressions of those proteins were all detected by Western blotting (**Figures 1A,B**).

To discriminate whether the induction of cell death is caused by the hypersensitive response triggered by activation of the resistance gene following recognition of effector presence, or the possible toxicity of AGLIP1 in the plant cell, two effector-triggered immunity (ETI) marker genes, *NbPR1*, and *NbHsr203J* (Wei et al., 2013) were detected by quantitative real time reverse transcription-polymerase chain reaction (qRT-PCR) after 1 day induced-expression of AGLIP1 and control protein GFP in *N. benthamiana*. However, expression of the two genes showed no significant differences compared with DEX-induced expression of AGLIP1 and mock treatment (**Supplementary Figure S1**). This result indicated that AGLIP1-triggered cell death might not result from ETI but rather from cellular toxicity.

AGLIP1 Is Highly Conserved in Plant Fungal Pathogens

AGLIP1 encodes a 302 amino acid protein which contains a predicted N-terminal SP and a C-terminal lipase domain (**Supplementary Figure S2A**). Previous study demonstrates that core effector proteins are highly conserved among many pathogenic fungi (Lyu et al., 2016). BLAST searches against the NCBI database found that the lipase domain proteins appeared in many fungi and bacterial. Phylogenetic analysis indicated that homolog of AGLIP1 were widely present in plant pathogenic fungi, in particular necrotrophic pathogens (**Supplementary Figure S2B**). In order to investigate sequence conservation of these homologous proteins, we performed multiple amino acid alignment analysis, which showed AGLIP1 is highly conserved, and similar to known plant fungal pathogens proteins (**Supplementary Figure S2C**).

The Predicted Lipase Active Sites and Signal Peptide of AGLIP1 Are Required for Its Ability of Cell Death-Eliciting

To test the function of AGLIP1's lipase activity and SP in cell death induction, point and deletion mutations were constructed, respectively. The residues Asp105, Ser107, Lys108, Pro111, Asp117, Ser174, and Asp230 which were predicted as active sites of the conserved lipase domain were substituted with alanine (**Supplementary Figure S2A**). Cell death symptoms on *N. benthamiana* leaves were monitored within 3 days after infiltration of *Agrobacterium* containing the AGLIP1 mutation and DEX treatment. Interestingly, expression of AGLIP1^{S174A}, AGLIP1^{D230A}, and the truncated variant without signal peptide (NSP) did not cause cell necrosis, while expression of other variants also caused cell death symptoms in *N. benthamiana* (**Figure 2A**). Western blot analysis showed that all of the different AGLIP1 mutations were expressed at similar levels in the infiltrated leaves (**Figure 2B**).

To further verify whether AGLIP1 and its variants induce cell death in host, we utilized a polyethylene glycol (PEG)-mediated transfection system for transiently expressing these proteins in rice protoplasts (Chen et al., 2013). The recombinant plasmids containing the full-length sequence of *AGLIP1* and its variants were co-transformed into rice protoplasts with luciferase (LUC) protein driven by *Cauliflower mosaic virus* 35S promoter, respectively (Luehrsen et al., 1992). LUC activity was tested for identifying the ability of cell death-inducing in rice protoplasts which is isolated from rice cv. Nipponbare. As compared with the LUC intensity in the protoplasts which were co-transfected with GFP, LUC activities were significantly low when AGLIP1, AGLIP1^{D105A}, AGLIP1^{S107A}, AGLIP1^{K108A}, AGLIP1^{P111A}, and AGLIP1^{D117A} were co-expressed with LUC, respectively. By contrast, LUC activity did not have any inhibitory effect in rice protoplasts which expressed AGLIP1^{S174A}, AGLIP1^{D230A}, and AGLIP1^{NSP} (**Figure 2C**). These results demonstrated that AGLIP1 could trigger cell death and the putative lipase active sites S174, D230, and the protein's SPs are indispensable for its ability to elicit plant cell death.

AGLIP1 Is Up-Regulated During *R. solani* Infection and Located at Endoplasmic Reticulum (ER)

The effector genes are often up-regulated during filamentous plant pathogen infection (Stergiopoulos and de Wit, 2009). To investigate regulation of *AGLIP1* expression during *R. solani* infection, the strain collected from a heavily infected rice plant in Liaoning province, China, was artificially inoculated into rice sheath. *AGLIP1* expression at 0, 12, 24, 48, 72, and 96 h post-inoculation was measured via qRT-PCR. The result showed that *AGLIP1* expression was transcriptionally induced from approximately 2- to 8-fold at different times during infection (**Figure 3A**). This result demonstrated that *AGLIP1* expression was regulated during *R. solani* infection and indicated that AGLIP1 might have essential functions in the interaction between rice and the fungal pathogen.

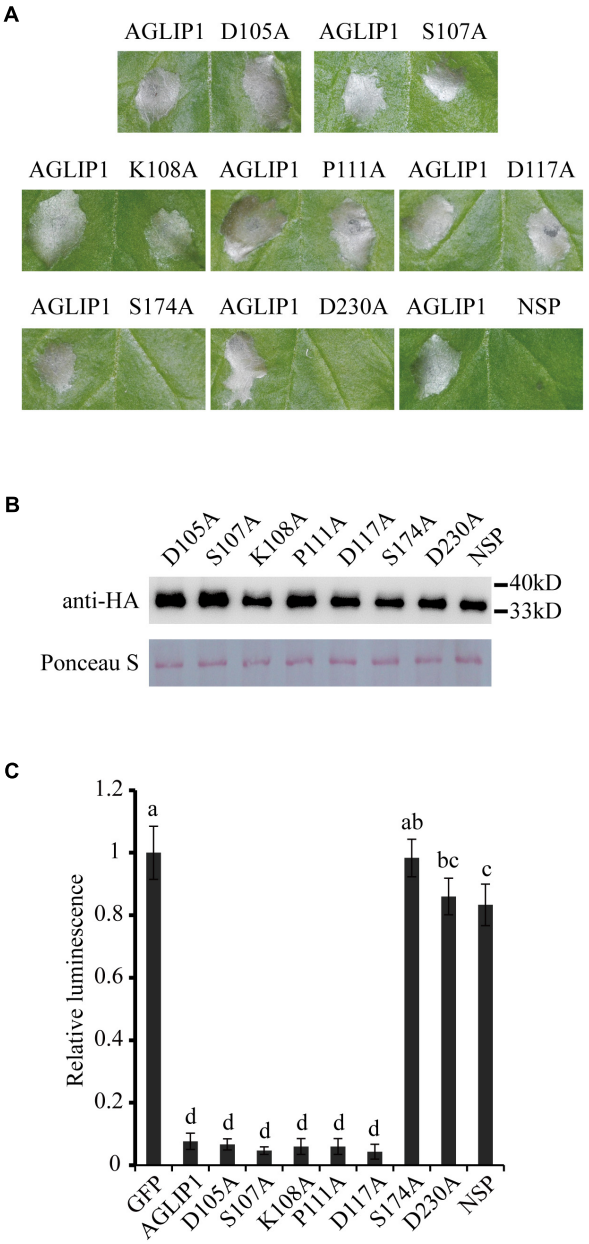

FIGURE 2 | The predicted lipase active sites and signal peptide of AGLIP1 are required for its cell death-inducing ability. **(A)** The mutant proteins AGLIP1^{S174A}, AGLIP1^{D230A} and AGLIP1^{NSP} lost the ability to induce cell death, while other variants, including AGLIP1^{D105A}, AGLIP1^{S107A}, AGLIP1^{K108A}, AGLIP1^{P111A} and AGLIP1^{D117A}, triggered cell death symptoms on *N. benthamiana* leaves. **(B)** The protein expression level of mutant proteins in the infiltrated leaves detected by Western blotting. The equal loading of the total proteins was showed by Ponceau S staining. The samples for protein extraction were collected before the cell death symptoms were visible. The proteins with 3 × HA tag were detected by immunoblotting with an anti-HA antibody. **(C)** The luciferase activity in rice protoplasts was significantly inhibited by the co-expression of AGLIP and its mutant variants AGLIP1^{D105A}, AGLIP1^{S107A}, AGLIP1^{K108A}, AGLIP1^{P111A} and AGLIP1^{D117A}, while the mutant variants AGLIP1^{S174A}, AGLIP1^{D230A}, and AGLIP1^{NSP} did not. Data are means ± standard error (SE). Different letters (a through d) indicate significant differences in the luciferase activity at $P < 0.05$, according to Duncan's multiple-range test.

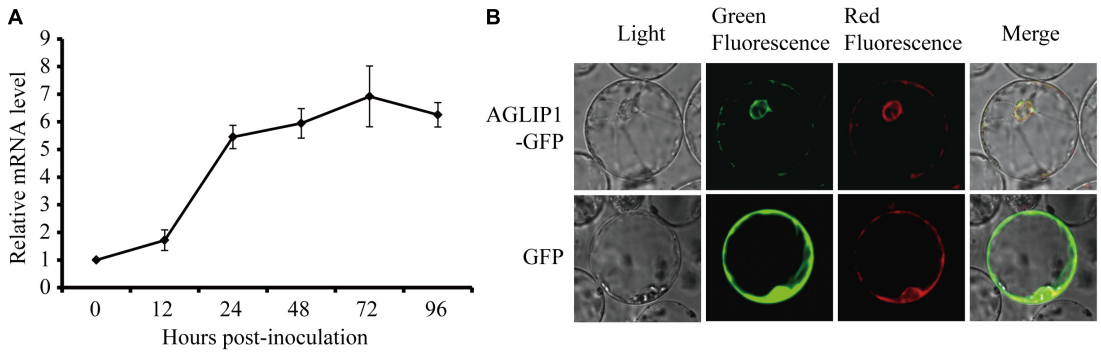

FIGURE 3 | Expression analyses of *AGLIP1* during *R. solani* infection and subcellular localization of AGLIP1 in rice cell. **(A)** Expression analyses of *AGLIP1* during *R. solani* infection in rice cv. Nipponbare. The *R. solani*-inoculated rice sheaths were collected at 0, 12, 24, 48, 72, and 96 h post-inoculation for gene expression analyses using quantitative real time reverse transcription-polymerase chain reaction assay. The expression level of *gpd* was used as an internal reference for normalizing within the samples. Data are means ± standard error. **(B)** Subcellular localization of AGLIP1-GFP transiently expressed in rice protoplasts. The vector pUC19 carrying GFP was used as a control. The overlapped fluorescence was observed in rice protoplasts when co-expressed with AGLIP1-GFP and HDEL-mCherry via laser scanning confocal microscopy. The photo was taken before cell death symptom was induced.

To investigate subcellular localization of AGLIP1 in rice cells, *AGLIP1* coding sequence was amplified, and fused in frame with the GFP gene at its C terminus, then subcloned into the pUC19 plasmid driven by 35S promoter. The recombinant AGLIP1-GFP protein was transiently co-expressed in rice protoplasts with the known ER marker HDEL-mCherry (Haseloff et al., 1997). The result showed that green fluorescence from AGLIP1-GFP and red fluorescence from HDEL-mCherry overlapped, suggesting AGLIP1 is ER located (**Figure 3B**). The similar subcellular localization pattern of AGLIP1-GFP has also been observed in *N. benthamiana* (**Supplementary Figure S3**). Induced expression of AGLIP1-GFP in *N. benthamiana* could also trigger cell death, demonstrating the AGLIP1-GFP fusion protein is functional (data not shown).

Ectopic Expression of AGLIP1 Suppresses PTI Signaling in *Arabidopsis thaliana* Seedlings

To investigate if AGLIP1 suppresses plant immunity, we generated *AGLIP1* transgenic *Arabidopsis* lines through *Agrobacterium*-mediated transformation. In 7 transgenic overexpression lines, AGLIP1 expression was driven by a DEX-inducible promoter. Expressions of AGLIP1 in these transgenic lines were detected by immunoblotting (**Supplementary Figure S4**). Three independent T3 homozygous overexpression lines, Line 3, Line 4 and Line 5, were chosen for subsequent functional analyses.

As an important weapon, effectors secreted by pathogens usually suppress plant defense responses including *PR* genes expression (Boller and He, 2009). Here, we chose four early defense-response genes, *FRK1* (Flg22-induced receptor-like kinase 1), *At2g17740* (cysteine/histidine-rich C1 domain family protein), *At5g57220* (member of CYP81F) and *At1g51890* (leucine-rich repeat protein kinase), which can be induced by pathogen-associated molecular patterns (PAMPs) such as bacterial flagellin and fungal chitin but not by stress-related signals (He et al., 2006; Akimoto-Tomiyama et al., 2012). Expression patterns of the four genes were detected by qRT-PCR in the *AGLIP1* transgenic plants after DEX treatment followed by flg22 and chitin stimulation. Remarkably, expression of the four genes induced by flg22 and chitin were dramatically suppressed in all transgenic lines after DEX-induced expression of AGLIP1 (**Figures 4A–D**). These results indicated that AGLIP1 contributes to virulence by inhibiting PAMP-triggered immune signaling in plants.

Ectopic Expression of AGLIP1 Promotes Disease Development via Suppressing PTI Responses in *Arabidopsis* Plants

To verify the virulence function of AGLIP1 in suppressing plant immunity further, the AGLIP1-expressing transgenic *Arabidopsis* plants were first inoculated with the *Pseudomonas syringae* pv. tomato (*Pst*) DC3000 *hrcC* mutant that is defective in the type III secretion system (T3SS) apparatus via pressure infiltration (He et al., 2006; Hatsugai et al., 2018). The results indicated increased levels of disease symptoms on inoculated transgenic leaves after DEX treatment compared to plants under mock spraying (**Figure 5A**). The leaf bacterial growth assay proved that the population of *Pst* DC3000 *hrcC* mutant in the transgenic plants with DEX treatment was also remarkably enhanced compared to the mock-treated or wild-type transgenic plants at 3 days post-inoculation. Furthermore, the bacterial population in the transgenic Line 5 was higher than the other two lines, Line 3, and Line 4. These results are consistent with the higher AGLIP1 expression level in Line 5 after DEX induction (**Supplementary Figure S4**). Moreover, the bacterial population in the wild-type plants was similar after DEX and mock treatments, indicating the lack of influence that DEX has on proliferation of the bacterium (**Figure 5B**). In addition, we showed that the expression of *FRK1*, *At2g17740*, *At5g57220*, and *At1g51890* induced by *Pst* DC3000 *hrcC* mutant in transgenic lines with mock treatment was markedly inhibited by DEX-induced AGLIP1 expression,

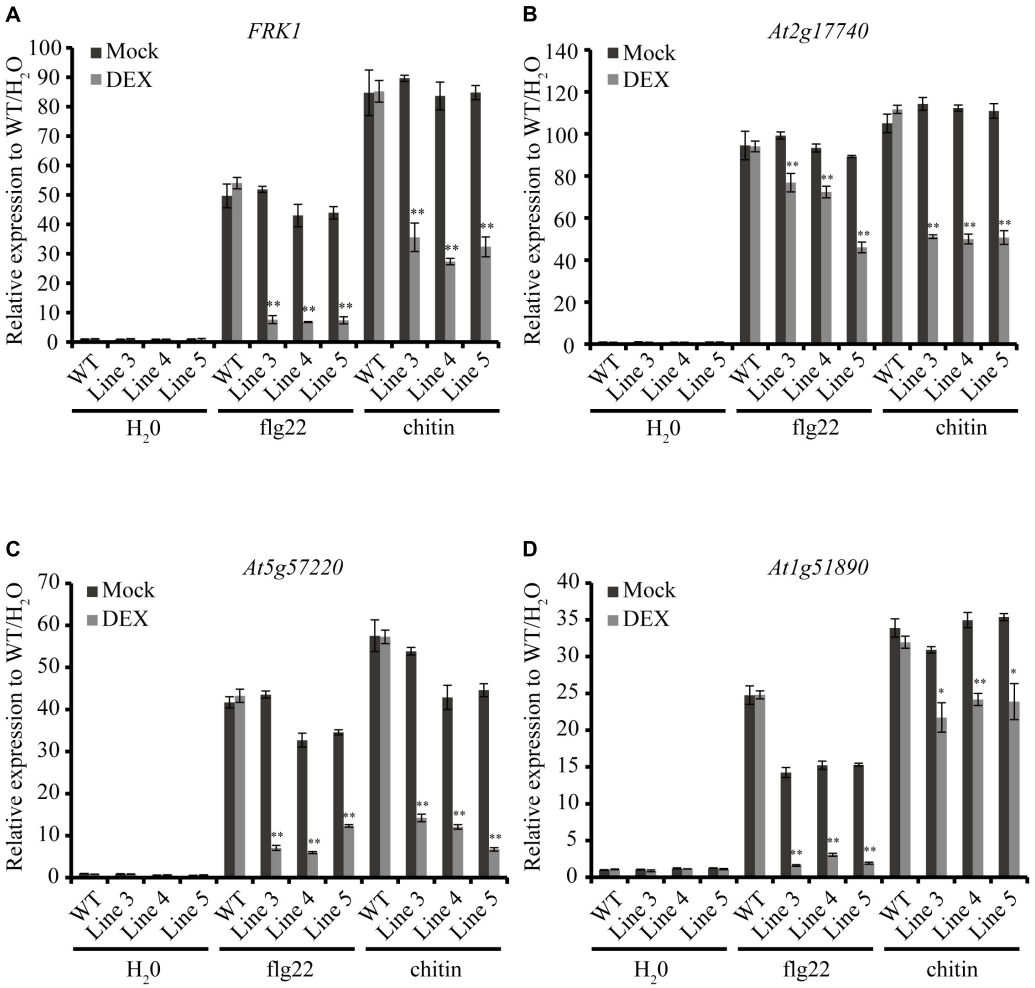

FIGURE 4 | Heterologous expression of AGLIP1 suppresses PAMP-induced defense genes expression in transgenic *Arabidopsis thaliana* seedlings. **(A–D)** Upregulation of the defense marker genes *FRK1*, *At2g17740*, *At5g57220*, and *At1g51890*, respectively, induced by flg22 and chitin were dramatically suppressed in transgenic Line 3, Line 4, and Line 5 after DEX-induced expression of AGLIP1. The transgenic plant seedlings were treated with 10 μM DEX or 0.03% ethanol as mock control for 24 h, followed by the treatment of 1 μM flg22 or chitin for 3 h. The expression level of *AtUBQ5* was used as an internal reference for normalizing within the samples. Asterisks (*) indicate P value < 0.05 and (**) indicate P value < 0.01; means ± standard error are shown.

which was consistent with the results obtained from transgenic *Arabidopsis* seedlings (**Figures 5C–F**). Taken together, these findings demonstrated that AGLIP1 expressed in transgenic *Arabidopsis* plants facilitated bacterial multiplication and the development of disease symptom through inhibiting plant basal defenses during pathogen infection.

DISCUSSION

Rice, one of the major food crops, is continuously threatened by various pathogenic microbes. Pressingly, *R. solani* causes rice sheath blight, one of the most severe fungi diseases in rice, and poses a significant threat to grain yield (Shu et al., 2019). Breeding for disease-resistant varieties is considered to be the most effective and eco-friendly method for disease control. However, no endogenous resistance gene for rice sheath blight has been identified in rice besides a selection of moderately resistant rice varieties (Zheng et al., 2019). *R. solani* has been described as a saprophyte that takes nutrients from dying plant debris/cells to complete their life cycle. Recent studies have shown that the effector proteins secreted by necrotrophic pathogens mainly designed as host-specific or host-selective toxins are able to promote necrosis and play important roles in the host-pathogen interactions (Lyu et al., 2016; Anderson et al., 2017). Almost 900 secreted proteins are predicted in the *R. solani* genome, many of which are thought to be candidates of effector proteins. The genes of many putative effectors are up-regulated during rice infection via expression profiling analyses, indicating effectors may play significant roles in the interaction between rice and the pathogen (Zheng et al., 2013; Anderson et al., 2017).

In this study, a heterogeneous transient expression assay was used to investigate the *R. solani* putative effectors activity

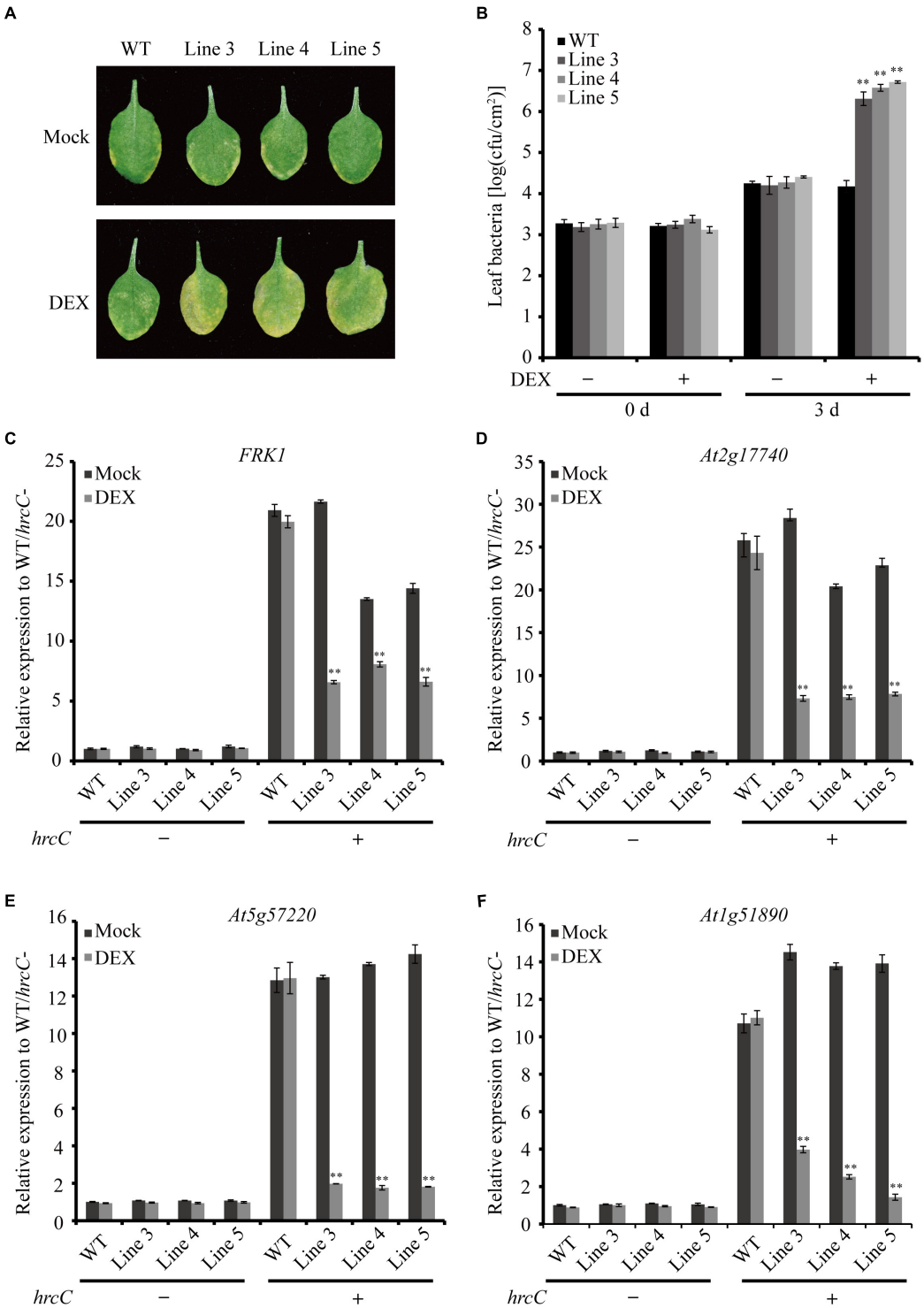

FIGURE 5 | Heterologous expression of AGLIP1 suppresses PTI signaling and promotes disease development in transgenic *Arabidopsis* plants. **(A)** Disease symptoms in the wild-type and AGLIP1 transgenic *Arabidopsis* plant lines after inoculation with bacterial pathogens *Pseudomonas syringae* pv. tomato (*Pst*) DC3000 *hrcC* mutant. Disease symptoms exhibited on the leaves of the wild-type and *AGLIP1* transgenic lines Line 3, Line 4 and Line 5 with mock or DEX treatment after pressure infiltration with the *Pst* DC3000 *hrcC* mutant. Photos were taken at 3 days after inoculation. **(B)** *In planta* bacterial population of *Pst* DC3000 *hrcC* mutant in the wild-type and *AGLIP1* transgenic lines at 0 day and 3 days after inoculation. **(C–F)** Upregulation of the defense marker genes *FRK1*, *At2g17740*, *At5g57220*, and *At1g51890*, respectively, induced by *Pst* DC3000 *hrcC* mutant were completely inhibited in transgenic Line 3, Line 4 and Line 5 after DEX-induced expression of AGLIP1. The 4–5 weeks transgenic plant were treated with 30 μM DEX or 0.1% ethanol as mock control for 24 h, followed by the spray inoculation of *Pst* DC3000 *hrcC* mutant for 6 h. The expression level of *AtUBQ5* was used as an internal reference for normalizing within the samples. Asterisks (**) indicate *P* value < 0.01; means ± standard error are shown.

of cell death-eliciting in the non-host *N. benthamiana* plants and revealed that one of them, i.e., AGLIP1, caused cell death (**Figure 1**). Furthermore, AGLIP1 was found to possess the function of eliciting cell death in host rice protoplasts (**Figure 2C**). Similar results were found in putative effectors from *R. solani* AG1 IA and AG8 strains which induce cell death symptoms in rice and non-host *N. benthamiana*, respectively (Zheng et al., 2013; Anderson et al., 2017). Through Pfam and BLAST searches against the NCBI database,AGLIP1 was predicted to have a lipase domain. Effector proteins which contain the lipase domain have been reported in regulating innate immunity in humans and in plants (Blumke et al., 2014; Chen and Alonzo, 2019). However, studies on induction of cell death by fungal effectors with the lipase domain have not been reported so far. We predicted 7 enzymatically active sites in the protein and 2 of them, i.e., S174 and D230, were essential for inducing cell death both in *N. benthamiana* and in rice protoplasts (**Figure 2**). Extended results showed that the expression level of two ETI marker gene, *NbPR1* and *NbHsr203J*, were not different between DEX-induced expression of AGLIP1 and mock treatment leaf tissue, demonstrating the cell death was likely toxin-induced necrosis rather than active hypersensitive response triggered by the activation of a resistance gene (**Supplementary Figure S1**). These findings indicate that lipase domain activity of AGLIP1 is essential for its cell death-inducing activity in plants.

The SP of AGLIP1 was also required for its cell death-inducing ability in *N. benthamiana* and in rice protoplasts (**Figure 2**). Similar results have been reported that the full-length effectors MoCDIPs in *Magnaporthe oryzae* and UV_44 in *Ustilaginoidea virens* are able to trigger cell death in rice protoplasts, respectively, but truncated versions of these proteins without SPs do not (Chen et al., 2013; Fang et al., 2016). The function of SP for secreted proteins in inducing cell death suggests that these effector proteins are likely to function in plant intercellular space. Effectors without SPs cannot be secreted into the intercellular space and thus are not recognized by PRRs in the plasma membrane (Fang et al., 2016). However, our result showed that AGLIP1 was located at ER when expressed in rice protoplasts and *N. benthamiana* (**Figure 3B** and **Supplementary Figure S3**), indicating that the protein secreted by *R. solani* may have multiple functions in plant. Alternatively, it is also possible that this effector protein was translocated into the cell after secretion and recognized by cytoplasmic receptors to trigger cell death.

Pathogen effectors often inhibit PTI during compatible interactions, thus enhancing pathogenesis. AGLIP1 was considered as a putative effector because *AGLIP1* was up-regulated during *R. solani* infecting to rice sheaths (**Figure 3A**), which is a common characteristic of filamentous fungal pathogens effector proteins (Fang et al., 2016). Ectopic expression of pathogen effectors in host plants has been widely used to investigate the virulence of bacterial and fungal effectors (Li et al., 2015; Fang et al., 2019). Subsequently, we demonstrated that immune responses, including *PR* genes expression, induced by flg22 and chitin were dramatically suppressed when AGLIP1 expression was induced in transgenic *Arabidopsis* seedlings (**Figure 4**). Furthermore, the AGLIP1-expressing transgenic *Arabidopsis* plants showed almost complete inhibition of defense genes expression triggered by the *Pst* DC3000 *hrcC* mutant. Most importantly, ectopic expression of AGLIP1 in the transgenic plants accelerated bacterial colonization and multiplication *in planta* and facilitated disease progression (**Figure 5**). Similar results have shown that *PR* genes expression induced by *X. campestris* pv. *campestris hrcC* mutant are significantly inhibited in the *X. oryzae* pv. *oryzae* effector XopR expressed in *Arabidopsis* (Akimoto-Tomiyama et al., 2012). The phenomenon that transgenic plants are more susceptible to *Pst* DC3000 *hrcC* mutant than in the wild-type counterpart when AGLIP1 is expressed, indicating AGLIP1 is a critical virulence factor in *R. solani*.

AGLIP1 is likely cytotoxic to rice and *N. benthamiana* but surprisingly displays no toxicity in *Arabidopsis*. It is possible that the DEX-induced expression of AGLIP1 in transgenic lines of *Arabidopsis* suppresses immunity at early infection stages when the transcripts are low, while AGLIP1 promotes cell death at the later stages when transcripts accumulate. The kinetics of the AGLIP1 expression in **Figure 3A** is further supportive to this notion. Alternatively, AGLIP1 may induce cell death via targeting a specific protein in rice and *N. benthamiana*; such interaction results in decreased accumulation of the targeted protein, which triggers plant cell death. In other words, the function of AGLIP1 may depend on the host. A similar function is found in SsSSVP1 secreted by *S. sclerotiorum* (Lyu et al., 2016). Furthermore, there are other effectors that display cytotoxic activity but also have additional functions. The core effector NIS1 in *Colletotrichum* spp. triggers the cell death of *N. benthamiana* and soybean, and suppresses PAMP-triggered immunity via targeting plant immune kinases (Yoshino et al., 2012; Irieda et al., 2019). The necrosis- and ethylene-inducing protein 1 (Nep1)-like proteins (NLPs) have both cytotoxic and non-cytotoxic functions to different plants (Seidl and Van den Ackerveken, 2019). Therefore, the precise function of AGLIP1 in plant cells needs to be further explored.

Taken together, the findings in this study further deepen our understanding of the effector function in plant pathogenesis of the necrotrophic fungus *R. solani*, highlighting the necessity of large-scale screening and functional analysis of candidate effectors in necrotrophic pathogen with a wide range of hosts. The exact molecular mechanism of how AGLIP1 regulate the rice-*R. solani* interaction remains to be further investigated.

MATERIALS AND METHODS

Bacterial Strains, Plant Materials, and Growth Conditions

The virulent *R. solani* researched in this study were isolated from a heavily infected rice plant in Liaoning province and cultured in PDA medium (200 g potato infusion, 20 g dextrose and 20 g agarı per liter). *N. benthamiana* plants were grown in growth chambers under 14 h/10 h photoperiod and kept at 25°C and

23°C at daytime and nighttime, respectively. *Arabidopsis* plants were grown under 12 h/12 h photoperiod and were kept at 23°C at daytime and 22°C at nighttime, respectively. *A. tumefaciens* EHA105 and GV3101 were cultured in LB medium (10 g tryptone, 10 g NaCl and 5 g yeast extract per liter). *Pst* DC3000 *hrcC* mutant were cultured in KB medium (2% proteose peptone, 0.2% $K_2HPO_4{\cdot}3H_2O$, 0.15% $MgSO_4{\cdot}7H_2O$, 1% glycerol). The concentrations of antibiotics used in this study are: ampicillin, 100 μg/ml; kanamycin, 50 μg/ml; and rifampin, 25 μg/ml. All data is based on at least three times repeats with similar results.

Plasmid Construction of *R. solani* Putative Effector Genes

Rhizoctonia solani total RNA extraction was based on the manufacturer's instructions of RNA extraction kit (TaKaRa). Complementary DNA synthetization was performed by using PrimeScript™ 1st Strand cDNA Synthesis Kit (TaKaRa). Phanta Max Super-Fidelity DNA Polymerase (Vazyme) was used for full-length and truncated putative effector-encoding genes amplification. PCR products were digested with *Xho*I and *Spe*I and subcloned into pTA7001 (Aoyama and Chua, 1997), which was constructed with 3 × HA. All constructs were confirmed with sequencing. Primers used in this study are listed in **Supplementary Table S2**.

Site-Directed Mutagenesis

Site-directed mutagenesis was performed by splicing overlap extension (SOE) PCR (Li et al., 2015). Two DNA fragments of each effector gene were amplified from the pTA7001-3 × HA gene constructs, respectively. Fusion PCR reaction was performed to combine DNA fragments containing the open reading frame (ORF). The resultant PCR products were cloned into pTA7001-3 × HA after *Xho*I and *Spe*I digestion.

Transient Expression of Effector Proteins in *N. benthamiana*

Using the freeze-thaw method, the constructed plasmids were transformed into the *Agrobacterium* spp. strain EHA105 (Deblaere et al., 1985). *Agrobacterium* strains were collected and resuspended in MMA buffer (10 mM MES, pH 5.7, 10 mM $MgCl_2$, and 150 μM acetosyringone) to an optical cell density of 0.3 at 600 nm after overnight culture, then perform infiltration with needleless syringes after incubation for 3–6 h. All leaves were sprayed with 30 μM DEX at 24 h after infiltration. Leaves within 3 days post DEX spraying were observed and photographed the cell-death phenotypes.

Rice Protoplast Transfection, Luminescence Measurement, and Subcellular Localization

Rice protoplast isolation and transfection were carried out as described previously (Wang et al., 2018). Briefly, protoplasts were extracted from *Oryza sativa* cv. Nipponbare etiolated seedlings and then transfected with plasmid DNA by polyethylene glycol-mediated transfection. Upon washing with W5 solution, the protoplasts were incubated in W5 solution and under low light for 12 h.

Extracted proteins (20 μl) from protoplast were used for luminescence (LUC) activity detection after mixing with the substrate luciferin (1 mM, 20 μl) and 100 μl of Tricine buffer (20 mM Tricine, 27 mM $MgSO_4{\cdot}7H_2O$, 0.1 mM EDTA, 2 mM DTT, 5 μM ATP, pH 7.8) as described previously (Fang et al., 2016). A microplate reader was used for data determination.

For subcellular localization, the coding sequence *AGLIP1* was amplified and introduced into pUC19-35S-GFP after digestion with *Bam*HI and *Sal*I (Li et al., 2015). The construct was confirmed by sequencing. Transfected rice protoplasts with GFP and RFP fluorescence were observed using confocal microscopy (Olympus FV3000).

R. solani Inoculation

Inoculation of the *R. solani* isolate into rice sheaths of *Oryza sativa* cv. Nipponbare was performed as previously described (Zhang et al., 2017). The inoculated sheaths samples were collected at 0, 12, 24, 48, 72, and 96 h post-inoculation, after immediately liquid nitrogen frozen treatment, then kept in −80°C ultra-low temperature refrigerator for further RNA isolation.

Development of the *AGLIP1* Transgenic *Arabidopsis* Plants

Agrobacterium-mediated floral dipping transformation which described previously was used for the *AGLIP1* transgenetic *Arabidopsis* seedlings generation (Liu L. et al., 2016). Half-strength Murashige and Skoog (MS) medium with 25 μg/mL hygromycin was used for transgenic seedlings screening.

Plant Inoculation and Bacterial Growth Assays

In planta bacterial inoculation and population sizes were analyzed as previously described (Liu L. et al., 2016). The 4–5 weeks old *Arabidopsis* plants were treated with 30 μM DEX or mock solution before bacterial inoculation after 24 h. Bacterial cells were collected and resuspended in 10 mM $MgCl_2$ to OD600 = 0.0005 after overnight culture. Bacterial inoculation was performed by pressure infiltration via plastic needleless syringes. The inoculated plants were covered with plastic sheets to maintain high humidity for 1 day, and then transported to normal growth conditions.

RNA Extraction and Quantitative Real Time RT-PCR

Samples from seedlings or plants were collected at different periods after *Arabidopsis* seedlings (10 days old) were treated with 1 mM flg22 or chitin or mock solution. Alternatively, 4–5 weeks old *Arabidopsis* plants were spray-inoculated with *Pst* DC3000 *hrcC* mutant at OD600 = 0.2. Total RNA isolation and cDNA was synthesized and performed according to the method described above.

Quantitative real time qRT-PCR was performed according to the manufacturer's instructions of Bio-Red CFX96 sequence

detection system and using ChamQ SYBR Color qPCR Master Mix from Vazyme Biotech Co., Ltd. The expression level of *AtUBQ5* and *gpd* were used as an internal reference for *Arabidopsis* and *R. solani*, respectively. The primer sets used for qRT-PCR are listed in **Supplementary Table S2**.

Protein Extraction and Immunoblotting

Samples from *N. benthamiana* leaves which were infiltrated with *Agrobacterium* or from the *AGLIP1* transgenic *Arabidopsis* seedlings were harvested at 24 h after DEX or mock (0.03% ethanol) treatment and were frozen in liquid nitrogen, then grounded in centrifuge tubes with small stainless steel balls by utilizing a milling apparatus (Retsch, Haan, Germany) for total protein extraction. The powders were incubated with 1 × sodium dodecyl sulfate (SDS)-polyacrylamide gel electrophoresis sample buffer (50 mM Tris–HCl, pH 7.4, 2% sodium dodecyl sulfate, 6% glycerol, 0.1 M dithiothreitol, and 0.01% bromophenol blue) and boiled for 10 min.

The extracted proteins were separated in a 12% polyacrylamide gel and electrophoretically transferred onto Immun-Blot PVDF Membrane (Millipore, Bedford, MA, United States) as described previously (Li et al., 2015).

DATA AVAILABILITY STATEMENT

All datasets generated for this study are included in the manuscript/**Supplementary Files**.

AUTHOR CONTRIBUTIONS

SL, WS, and SW designed and conceived the project, and wrote the manuscript with contributions of all other authors. SL, XP, YW, KH, FX, YZ, and WL performed the experiments and analyzed the data. All authors read and approved the final version of the manuscript for publication.

FUNDING

This work was supported by the earmarked fund for China's Agricultural Research System (CARS-01), the National Natural Science Foundation of China (NSFC) grant 31901956, the Natural Science Foundation of Liaoning Province, China (20180550304), and the Fundamental Research Project of College of Liaoning Province, China (LSNQN201715).

ACKNOWLEDGMENTS

We thank Yuxi Duan, Lijie Chen, Xiaofeng Zhu, and Haiyan Fan at the Shenyang Agricultural University (Liaoning, China) for the growth chambers.

SUPPLEMENTARY MATERIAL

The Supplementary Material for this article can be found online at: https://www.frontiersin.org/articles/10.3389/fmicb.2019.02228/full#supplementary-material

FIGURE S1 | The two ETI marker genes, **(A)** *NbPR1*, and **(B)** *NbHsr203J*, were not induced after DEX-induced expression of AGLIP1. Leaf tissue was collected from the inoculated sites after 1 day induced-expression of AGLIP1 and control protein GFP in *N. benthamiana*. Expression analyses of *NbPR1* and *NbHsr203J* were analyzed by qRT-PCR assay. Data are means ± standard error (SE). The expression level of *NbActin* was used as an internal reference for normalizing within the samples.

FIGURE S2 | Analysis conversation and similarity of AGlP1 with known plant fungal pathogens proteins. **(A)** The predicted domain structure of AGLIP1. SP, signal peptide; lipase domain including Asp105, Ser107, Lys108, Pro111, Asp117, Ser174, and Asp230, were predicted key residues necessary for the lipase activity. **(B)** The evolutionary relationship of AGLIP1 and its homologs from other fungi was inferred using the Neighbor-Joining method. The optimal tree with the sum of branch length = 6.66810195 is shown. The percentage of replicate trees in which the associated taxa clustered together in the bootstrap test (1000 replicates) is shown next to the branches. The tree is drawn to scale, with branch lengths in the same units as those of the evolutionary distances used to infer the phylogenetic tree. The evolutionary distances were computed using the Poisson correction method and are in the units of the number of amino acid substitutions per site. The analysis involved 18 amino acid sequences. All positions containing gaps and missing data were eliminated. There were a total of 157 positions in the final dataset. Evolutionary analyses were conducted in MEGA software. **(C)** Conserved amino acid residues of lipase have been showed. Asterisks (*) indicate the predicted lipase active sites of AGLIP1 which play an important role in inducing cell death.

FIGURE S3 | Subcellular localization of AGLIP1-GFP transiently expressed in *N. benthamiana*. The vector pCAMBIA1301 carrying GFP was used as a control. The overlapped fluorescence was observed in *N. benthamiana* when co-expressed with AGLIP1-GFP and HDEL-mCherry. The photo was taken under confocal microscopy before cell death symptom was visible.

FIGURE S4 | Induced expression level of AGLIP1 in the T2 transgenic homozygous lines Line 1 to Line 7 after DEX or mock treatment. The AGLIP1-3 × HA fusion was detected by Western blotting with an anti-HA antibody. DEX, dexamethasone; Mock, 0.03% ethanol. Each sample was harvested at 24 h after 10 μM DEX or mock treatment. The expression level of *AtUBQ5* was used as an internal reference for normalizing within the samples. CBB (coomassie brilliant blue) staining shows the equal loading of the total proteins. "M" means premixed protein marker.

TABLE S1 | Putative effector genes in *Rhizoctonia solani* AG1 IA used for testing cell death-inducing ability.

TABLE S2 | The designed primers used in this study.

REFERENCES

Akimoto-Tomiyama, C., Furutani, A., Tsuge, S., Washington, E. J., Nishizawa, Y., Minami, E., et al. (2012). XopR, a type III effector secreted by *Xanthomonas oryzae* pv. *oryzae,* suppresses microbe-associated molecular pattern-triggered immunity in *Arabidopsis thaliana*. *Mol. Plant Microbe Interact.* 25, 505–514. doi: 10.1094/MPMI-06-11-0167

Anderson, J. P., Sperschneider, J., Win, J., Kidd, B., Yoshida, K., Hane, J., et al. (2017). Comparative secretome analysis of *Rhizoctonia solani* isolates with different host ranges reveals unique secretomes and cell death inducing effectors. *Sci. Rep.* 7:10410. doi: 10.1038/s41598-017-10405-y

Aoyama, T., and Chua, N. H. (1997). A glucocorticoid-mediated transcriptional induction system in transgenic plants. *Plant J.* 11, 605–612. doi: 10.1046/j.1365-313X.1997.11030605.x

Bernardes-de-Assis, J., Storari, M., Zala, M., Wang, W., Jiang, D., Shidong, L., et al. (2009). Genetic structure of populations of the rice-infecting pathogen *Rhizoctonia solani* AG-1 IA from China. *Phytopathology* 99, 1090–1099. doi: 10.1094/PHYTO-99-9-1090

Blumke, A., Falter, C., Herrfurth, C., Sode, B., Bode, R., Schafer, W., et al. (2014). Secreted fungal effector lipase releases free fatty acids to inhibit innate immunity-related callose formation during wheat head infection. *Plant Physiol.* 165, 346–358. doi: 10.1104/pp.114.236737

Boller, T., and He, S. Y. (2009). Innate immunity in plants: an arms race between pattern recognition receptors in plants and effectors in microbial pathogens. *Science* 324, 742–744. doi: 10.1126/science.1171647

Breen, S., Williams, S. J., Winterberg, B., Kobe, B., and Solomon, P. S. (2016). Wheat PR-1 proteins are targeted by necrotrophic pathogen effector proteins. *Plant J.* 88, 13–25. doi: 10.1111/tpj.13228

Chen, S., Songkumarn, P., Venu, R. C., Gowda, M., Bellizzi, M., Hu, J., et al. (2013). Identification and characterization of *in planta*-expressed secreted effector proteins from *Magnaporthe oryzae* that induce cell death in rice. *Mol. Plant Microbe Interact.* 26, 191–202. doi: 10.1094/MPMI-05-12-0117-R

Chen, X., and Alonzo, F. R. (2019). Bacterial lipolysis of immune-activating ligands promotes evasion of innate defenses. *Proc. Natl. Acad. Sci. U.S.A.* 116, 3764–3773. doi: 10.1073/pnas.1817248116

Deblaere, R., Bytebier, B., De Greve, H., Deboeck, F., Schell, J., Van Montagu, M., et al. (1985). Efficient octopine *Ti* plasmid-derived vectors for *Agrobacterium*-mediated gene transfer to plants. *Nucleic Acids Res.* 13, 4777–4788. doi: 10.1093/nar/13.13.4777

El, O. M., El, R. T., Rigano, L., El, H. A., Rodriguez, M. C., Daayf, F., et al. (2011). *Botrytis cinerea* manipulates the antagonistic effects between immune pathways to promote disease development in tomato. *Plant Cell* 23, 2405–2421. doi: 10.1105/tpc.111.083394

Fang, A., Gao, H., Zhang, N., Zheng, X., Qiu, S., Li, Y., et al. (2019). A novel effector gene SCRE2 contributes to full virulence of *Ustilaginoidea virens* to rice. *Front. Microbiol.* 10:845. doi: 10.3389/fmicb.2019.00845

Fang, A., Han, Y., Zhang, N., Zhang, M., Liu, L., Li, S., et al. (2016). Identification and characterization of plant cell death-inducing secreted proteins from *Ustilaginoidea virens*. *Mol. Plant Microbe Interact.* 29, 405–416. doi: 10.1094/MPMI-09-15-0200-R

Haseloff, J., Siemering, K. R., Prasher, D. C., and Hodge, S. (1997). Removal of a cryptic intron and subcellular localization of green fluorescent protein are required to mark transgenic *Arabidopsis* plants brightly. *Proc. Natl. Acad. Sci. U.S.A.* 94, 2122–2127. doi: 10.1073/pnas.94.6.2122

Hatsugai, N., Nakatsuji, A., Unten, O., Ogasawara, K., Kondo, M., Nishimura, M., et al. (2018). Involvement of adapter protein complex 4 in hypersensitive cell death induced by avirulent bacteria. *Plant Physiol.* 176, 1824–1834. doi: 10.1104/pp.17.01610

He, P., Shan, L., Lin, N. C., Martin, G. B., Kemmerling, B., Nurnberger, T., et al. (2006). Specific bacterial suppressors of MAMP signaling upstream of MAPKKK in *Arabidopsis* innate immunity. *Cell* 125, 563–575. doi: 10.1016/j.cell.2006.02.047

Irieda, H., Inoue, Y., Mori, M., Yamada, K., Oshikawa, Y., Saitoh, H., et al. (2019). Conserved fungal effector suppresses PAMP-triggered immunity by targeting plant immune kinases. *Proc. Natl. Acad. Sci. U.S.A.* 116, 496–505. doi: 10.1073/pnas.1807297116

Irieda, H., Maeda, H., Akiyama, K., Hagiwara, A., Saitoh, H., Uemura, A., et al. (2014). *Colletotrichum orbiculare* secretes virulence effectors to a biotrophic interface at the primary hyphal neck via exocytosis coupled with SEC22-mediated traffic. *Plant Cell* 26, 2265–2281. doi: 10.1105/tpc.113.120600

Kabbage, M., Yarden, O., and Dickman, M. B. (2015). Pathogenic attributes of *Sclerotinia sclerotiorum*: switching from a biotrophic to necrotrophic lifestyle. *Plant Sci.* 233, 53–60. doi: 10.1016/j.plantsci.2014.12.018

Koeck, M., Hardham, A. R., and Dodds, P. N. (2011). The role of effectors of biotrophic and hemibiotrophic fungi in infection. *Cell Microbiol.* 13, 1849–1857. doi: 10.1111/j.1462-5822.2011.01665.x

Li, S., Wang, Y., Wang, S., Fang, A., Wang, J., Liu, L., et al. (2015). The type III effector AvrBs2 in *Xanthomonas oryzae* pv. *oryzicola* suppresses rice immunity and promotes disease development. *Mol. Plant Microbe Interact.* 28, 869–880. doi: 10.1094/MPMI-10-14-0314-R

Liu, L., Wang, Y., Cui, F., Fang, A., Wang, S., Wang, J., et al. (2016). The type III effector AvrXccB in *Xanthomonas campestris* pv. *campestris* targets putative methyltransferases and suppresses innate immunity in *Arabidopsis*. *Mol. Plant Pathol.* 18, 768–782. doi: 10.1111/mpp.12435

Liu, Z., Gao, Y., Kim, Y. M., Faris, J. D., Shelver, W. L., de Wit, P. J., et al. (2016). SnTox1, a *Parastagonospora nodorum* necrotrophic effector, is a dual-function protein that facilitates infection while protecting from wheat-produced chitinases. *New Phytol.* 211, 1052–1064. doi: 10.1111/nph.13959

Lu, S., Faris, J. D., Sherwood, R., Friesen, T. L., and Edwards, M. C. (2014). A dimeric PR-1-type pathogenesis-related protein interacts with ToxA and potentially mediates ToxA-induced necrosis in sensitive wheat. *Mol. Plant Pathol.* 15, 650–663. doi: 10.1111/mpp.12122

Luehrsen, K. R., de Wet, J. R., and Walbot, V. (1992). Transient expression analysis in plants using firefly luciferase reporter gene. *Methods Enzymol.* 216, 397–414. doi: 10.1016/0076-6879(92)16037-k

Lyu, X., Shen, C., Fu, Y., Xie, J., Jiang, D., Li, G., et al. (2016). A small secreted virulence-related protein is essential for the necrotrophic interactions of *Sclerotinia sclerotiorum* with its host plants. *PLoS Pathog.* 12:e1005435. doi: 10.1371/journal.ppat.1005435

McDonald, M. C., and Solomon, P. S. (2018). Just the surface: advances in the discovery and characterization of necrotrophic wheat effectors. *Curr. Opin. Microbiol.* 46, 14–18. doi: 10.1016/j.mib.2018.01.019

Noda, J., Brito, N., and Gonzalez, C. (2010). The *Botrytis cinerea* xylanase Xyn11A contributes to virulence with its necrotizing activity, not with its catalytic activity. *BMC Plant Biol.* 10:38. doi: 10.1186/1471-2229-10-38

Ogoshi, A. (1987). Ecology and pathogenicity of anastomosis and intraspecific groups of *Rhizoctonia Solani* Kühn. *Annu. Rev. Phytopathol.* 25, 125–143. doi: 10.1146/annurev.py.25.090187.001013

Oliver, R. P., and Solomon, P. S. (2010). New developments in pathogenicity and virulence of necrotrophs. *Curr. Opin. Plant Biol.* 13, 415–419. doi: 10.1016/j.pbi.2010.05.003

Schulmeyer, K. H., and Yahr, T. L. (2017). Post-transcriptional regulation of type III secretion in plant and animal pathogens. *Curr. Opin. Microbiol.* 36, 30–36. doi: 10.1016/j.mib.2017.01.009

Seidl, M. F., and Van den Ackerveken, G. (2019). Activity and phylogenetics of the broadly occurring family of microbial Nep1-like proteins. *Annu. Rev. Phytopathol.* 57, 367–386. doi: 10.1146/annurev-phyto-082718-100054

Shu, C., Zhao, M., Anderson, J. P., Garg, G., Singh, K. B., Zheng, W., et al. (2019). Transcriptome analysis reveals molecular mechanisms of sclerotial development in the rice sheath blight pathogen *Rhizoctonia solani* AG1-IA. *Funct. Integr. Genomics.* 19, 743–758. doi: 10.1007/s10142-019-00677-0

Sperschneider, J., Catanzariti, A. M., DeBoer, K., Petre, B., Gardiner, D. M., Singh, K. B., et al. (2017). LOCALIZER: subcellular localization prediction of both plant and effector proteins in the plant cell. *Sci. Rep.* 7:44598. doi: 10.1038/srep44598

Stergiopoulos, I., and de Wit, P. J. (2009). Fungal effector proteins. *Annu. Rev. Phytopathol.* 47, 233–263. doi: 10.1146/annurev.phyto.112408.132637

Wang, J., Wang, S., Hu, K., Yang, J., Xin, X., Zhou, W., et al. (2018). The kinase OsCPK4 regulates a buffering mechanism that fine-tunes innate immunity. *Plant Physiol.* 176, 1835–1849. doi: 10.1104/pp.17.01024

Wei, H. L., Chakravarthy, S., Worley, J. N., and Collmer, A. (2013). Consequences of flagellin export through the type III secretion system of *Pseudomonas syringae* reveal a major difference in the innate immune systems of mammals and the model plant *Nicotiana benthamiana*. *Cell Microbiol.* 15, 601–618. doi: 10.1111/cmi.12059

Xiao, X., Xie, J., Cheng, J., Li, G., Yi, X., Jiang, D., et al. (2014). Novel secretory protein Ss-Caf1 of the plant-pathogenic fungus *Sclerotinia sclerotiorum* is required for host penetration and normal sclerotial development. *Mol. Plant Microbe Interact.* 27, 40–55. doi: 10.1094/MPMI-05-13-0145-R

Yang, G., Tang, L., Gong, Y., Xie, J., Fu, Y., Jiang, D., et al. (2018). A cerato-platanin protein SsCP1 targets plant PR1 and contributes to virulence of *Sclerotinia sclerotiorum*. *New Phytol.* 217, 739–755. doi: 10.1111/nph.14842

Yoshino, K., Irieda, H., Sugimoto, F., Yoshioka, H., Okuno, T., and Takano, Y. (2012). Cell death of *Nicotiana benthamiana* is induced by secreted protein NIS1 of *Colletotrichum orbiculare* and is suppressed by a homologue of CgDN3. *Mol. Plant Microbe Interact.* 25, 625–636. doi: 10.1094/MPMI-12-11-0316

Zhang, J., Chen, L., Fu, C., Wang, L., Liu, H., Cheng, Y., et al. (2017). Comparative transcriptome analyses of gene expression changes triggered by *Rhizoctonia solani* AG1 IA infection in resistant and susceptible rice varieties. *Front. Plant Sci.* 8:1422. doi: 10.3389/fpls.2017.01422

Zheng, A., Lin, R., Zhang, D., Qin, P., Xu, L., Ai, P., et al. (2013). The evolution and pathogenic mechanisms of the rice sheath blight pathogen. *Nat. Commun.* 4:1424. doi: 10.1038/ncomms2427

Zheng, L., Shu, C., Zhang, M., Yang, M., and Zhou, E. (2019). Molecular characterization of a novel *endornavirus* conferring hypovirulence in rice sheath blight fungus *Rhizoctonia solani* AG-1 IA Strain GD-2. *Viruses* 11:178. doi: 10.3390/v11020178

Zhu, W., Wei, W., Fu, Y., Cheng, J., Xie, J., Li, G., et al. (2013). A secretory protein of necrotrophic fungus *Sclerotinia sclerotiorum* that suppresses host resistance. *PLoS One* 8:e53901. doi: 10.1371/journal.pone.0053901

Conflict of Interest: The authors declare that the research was conducted in the absence of any commercial or financial relationships that could be construed as a potential conflict of interest.

frontiers in Plant Science

MINI REVIEW
published: 27 September 2019
doi: 10.3389/fpls.2019.01186

Apocarotenoids: Old and New Mediators of the Arbuscular Mycorrhizal Symbiosis

Valentina Fiorilli[1†], Jian You Wang[2†], Paola Bonfante[1], Luisa Lanfranco[2] and Salim Al-Babili[2*]*

[1] Department of Life Sciences and Systems Biology, University of Torino, Torino, Italy, [2] The BioActives Lab, Division of Biological and Environmental Science and Engineering, King Abdullah University of Science and Technology, Thuwal, Saudi Arabia

OPEN ACCESS

Edited by:
Silvia Proietti, Università degli Studi della Tuscia, Italy

Reviewed by:
Juan Antonio Lopez Raez, Experimental Station of Zaidín (EEZ), Spain
Jose Manuel García-Garrido, Experimental Station of Zaidín (EEZ), Spain
Eloise Foo, University of Tasmania, Australia

***Correspondence:**
Luisa Lanfranco
luisa.lanfranco@unito.it
Salim Al-Babili
salim.babili@kaust.edu.sa

†These authors have contributed equally to this work

Specialty section:
This article was submitted to Plant Microbe Interactions, a section of the journal Frontiers in Plant Science

Received: *15 July 2019*
Accepted: *29 August 2019*
Published: *27 September 2019*

Citation:
Fiorilli V, Wang JY, Bonfante P, Lanfranco L and Al-Babili S (2019) Apocarotenoids: Old and New Mediators of the Arbuscular Mycorrhizal Symbiosis. Front. Plant Sci. 10:1186. doi: 10.3389/fpls.2019.01186

Plants utilize hormones and other small molecules to trigger and coordinate their growth and developmental processes, adapt and respond to environmental cues, and communicate with surrounding organisms. Some of these molecules originate from carotenoids that act as universal precursors of bioactive metabolites arising through oxidation of the carotenoid backbone. This metabolic conversion produces a large set of compounds known as apocarotenoids, which includes the plant hormones abscisic acid (ABA) and strigolactones (SLs) and different signaling molecules. An increasing body of evidence suggests a crucial role of previously identified and recently discovered carotenoid-derived metabolites in the communication with arbuscular mycorrhizal (AM) fungi and the establishment of the corresponding symbiosis, which is one of the most relevant plant–fungus mutualistic interactions in nature. In this review, we provide an update on the function of apocarotenoid hormones and regulatory metabolites in AM symbiosis, highlighting their effect on both partners.

Keywords: carotenoids, apocarotenoids, strigolactones, abscisic acid, mycorradicin, blumenols, zaxinone, arbuscular mycorrhizal symbiosis

INTRODUCTION

Carotenoids are a group of lipophilic, isoprenoid pigments characterized by bright colors ranging from yellow to red. Plant carotenoids consist of a common C_{40} skeleton and differ with respect to the number and stereo-configuration of conjugated double bonds, the presence of oxygen, and structure of end groups (Hirschberg, 2001; Moise et al., 2014). These pigments are best known for their essential role in photosynthesis where they protect the photosynthetic apparatus from photooxidative damage, act as accessory pigments absorbing photons and transferring them to chlorophyll, and stabilize thylakoid membranes. In addition, carotenoids are frequently accumulated in flowers and fruits, serving as optical signal in plant–animal communication (Fraser and Bramley, 2004; DellaPenna and Pogson, 2006; Nisar et al., 2015). Besides these plant specific functions, carotenoids are the precursors for different biologically important compounds in all clades of life, which include retinoids, hormones, and signaling molecules (Nisar et al., 2015). These carotenoid-derivatives are formed by oxidative cleavage of their precursor, which produces a wide range of compounds generally called apocarotenoids (Giuliano et al., 2003; Nisar et al., 2015).

Carotenoid cleavage can take place as a non-enzymatic process induced by reactive oxygen species that arise especially under stress conditions (Ramel et al., 2012; Havaux, 2014). However, the formation of most of the plant apocarotenoid hormones and signaling molecules involves

carotenoid cleavage dioxygenases (CCDs), an evolutionarily conserved family of non-heme Fe^{2+}-dependent enzymes, present in all taxa (Giuliano et al., 2003; Moise et al., 2005; Hou et al., 2016). A recent survey on plant CCDs identified six subfamilies: NCED (nine-*cis*-epoxycarotenoid dioxygenases), CCD1, CCD4, CCD7, CCD8, and zaxinone synthase (ZAS) (Wang et al., 2019). In brief, NCEDs catalyze the first step in abscisic acid (ABA) biosynthesis by cleaving 9-*cis*-violaxanthin or 9'-*cis*-neoxanthin at the C11, C12 or C11', C12' double bond, respectively, forming the ABA precursor xanthoxin, which is further metabolized by short chain dehydrogenase reductase (SDR) and abscisic aldehyde oxidase (AAO) leading to ABA (Nambara and Marion-Poll, 2005) (**Figure 1**). CCD1 enzymes convert a wide spectrum of carotenoid and apocarotenoid substrates and are also less specific with respect to the targeted double bonds. As shown by *in vitro* studies and functional expression in carotenoid accumulating *Escherichia coli* strains, CCD1 enzymes from different plant species produce the volatiles 6-methyl-5-hepten-2-one (C_8), geranial (C_{10}), and a series of C_{13} cyclohexenones including α- and β-ionone. CCD1 activity leads also to different dialdehyde products, such as rosafluene-dialdehyde that arises simultaneously with the corresponding C_{13}-ionone(s) upon the cleavage of C_{40} carotenoids or apo-10'-carotenoids (Vogel et al., 2008; Ilg et al., 2009; Ilg et al., 2014) (**Figure 1**). There are two types of CCD4 enzymes. The first type mediates the cleavage of bicyclic all-*trans*-carotenoids, e.g., all-*trans*-β-carotene, at the C9, C10 or C9', C10' double bond leading to apo-10'-carotenoids (C_{27}), e.g., β-apo-10'-carotenal, and the corresponding C_{13} cyclohexenone product, e.g., β-ionone (Bruno et al., 2015; Bruno et al., 2016) (**Figure 1**). The second type of CCD4 enzymes forms the *Citrus* pigment citraurin (3-OH-β-apo-8'-carotenoid; C_{30}), by cleaving the C7, C8 or C7', C8' double bond in hydroxylated bicyclic carotenoids (Rodrigo et al., 2013). CCD7 and CCD8 are strigolactone (SL) biosynthesis enzymes that act sequentially

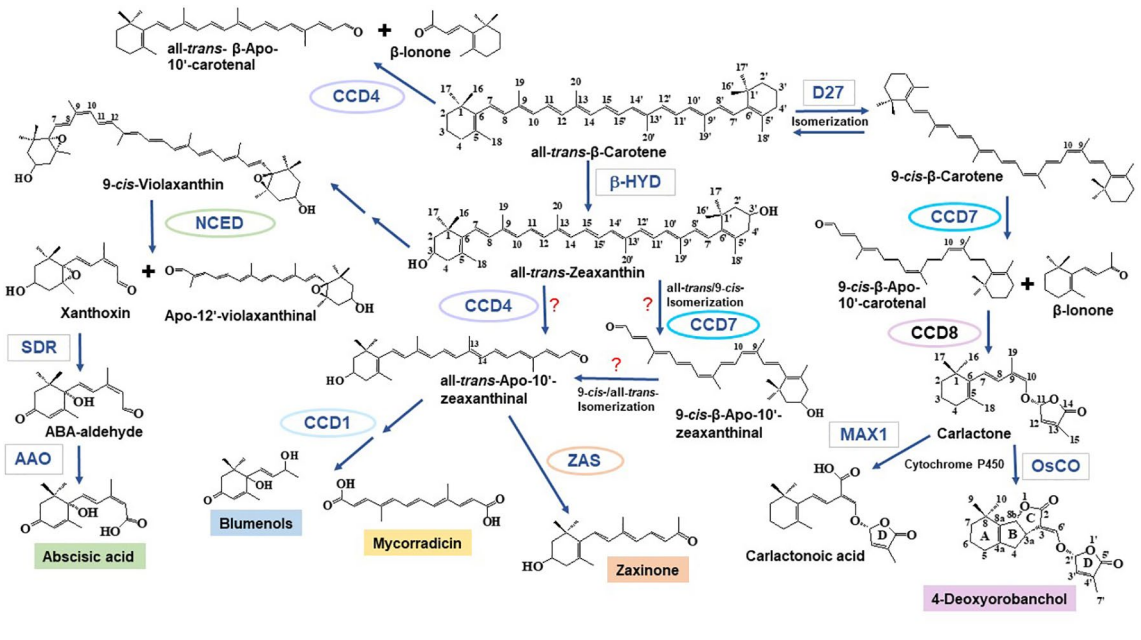

FIGURE 1 | Formation of apocarotenoids involved in mycorrhization. Nine-*cis*-epoxycarotenoid dioxygenase (NCED) enzymes catalyze the cleavage of 9-*cis*-violaxanthin—formed from all-*trans*-zeaxanthin through epoxidation and isomerization reactions—and 9'-*cis*-neoxanthin (not shown) into the ABA precursor xanthoxin and apo-12'-violaxanthinal (or apo-12-neoxanthinal, not shown) (Nambara and Marion-Poll, 2005). Xanthoxin is then further converted to ABA by SDR and AAO. Carotenoid cleavage dioxygenase (CCD) enzymes catalyze a set of different carotenoid and apocarotenoid cleavage reactions. The C_{27} apocarotenoids β-apo-10'-carotenal and/or β-apo-10'-zeaxanthinal may be formed by CCD4 enzymes that cleave all-*trans*-bicyclic carotenoids (Bruno et al., 2015; Bruno et al., 2016). CCD7 has been also implicated in the formation of all-*trans*-β-apo-10'-carotenoids, which include the zaxinone precursor all-*trans*-β-apo-10'-zeaxanthinal (see below); however, in this case, a *cis* to *trans* isomerization must be postulated, as the apo-10'-carotenoids produced by CCD7 enzymes are 9-*cis*-configured (Alder et al., 2012; Bruno et al., 2014). Several enzymatic studies show that CCD1 enzymes can produce C_{14} directly from carotenoids or—in a secondary cleavage reaction—from all-*trans*-β-apo-10'-carotenoids. In the case of mycorrhizal tissues, it is assumed that they use β-apo-10'-carotenoids as substrate to form precursors of mycorradicin and blumenols (structure shown as blumenol C), which accumulate in AM-colonized root and act as symbiosis signal in plant leaves, respectively (Floss et al., 2008b; Walter et al., 2010; Hou et al., 2016; Wang et al., 2018). Following β-carotene isomerization catalyzed by D27, the SL biosynthetic enzyme, CCD7, cleaves 9-*cis*-β-carotene into 9-*cis*-β-apo-10'-carotenal and β-ionone. This step is followed by the CCD8-catalyzed conversion of 9-*cis*-β-apo-10'-carotenal into carlactone. Carlactone, a central intermediate in SL biosynthesis, is further modified by cytochrome P450 enzymes of the 711 clade (i.e., the Arabidopsis MAX1 (Abe et al., 2014), the rice carlactone oxidase (Zhang et al., 2014), which yield canonical, e.g., 4-deoxyorobanchol, and non-canonical, e.g., carlactonoic acid, SLs. Carlactonoic acid is further modified into different products (Alder et al., 2012; Bruno et al., 2014; Al-Babili and Bouwmeester, 2015; Bruno et al., 2017; Abuauf et al., 2018; Jia et al., 2018). ZAS, a recently identified CCD, cleaves apo-10'-zeaxanthinal, yielding the novel signaling molecule, zaxinone (Wang et al., 2019). β-Apo-10'-zeaxanthinal could be formed from zeaxanthin or lutein (not shown) by CCD4 enzymes. Enzymes are surrounded either by ellipses (CCDs) or rectangles (other enzymes). SDR, short chain dehydrogenase reductase; AAO, Abscisic aldehyde oxidase; β-HYD, β-hydroxylase; D27, DWARF27; MAX1, more axillary growth1; OsCO, rice carlactone oxidase, a MAX1 homolog.

in converting 9-*cis*-β-carotene produced by the carotene isomerase DWARF27 (D27) into the SL precursor carlactone that is the substrate of cytochrome P450 enzymes from the 711 clade, such as the rice carlactone oxidase (OsCO), that form 4-deoxyorobanchol (Alder et al., 2012; Abe et al., 2014; Bruno et al., 2014; Zhang et al., 2014; Bruno and Al-Babili, 2016; Bruno et al., 2017; Abuauf et al., 2018) (**Figure 1**). In addition, CCD7 is also involved in the formation of C_{13} cyclohexenones (Floss et al., 2008b; Walter et al., 2015). ZASs constitute a recently identified CCD subfamily (Wang et al., 2019). A study of the enzymatic activity of a rice ZAS shows that this enzyme converts 3-OH-all-*trans*- β-apo-10'-carotenal (apo-10'-zeaxanthinal) into zaxinone (3-OH-all-*trans*-apo-13-carotenone), a regulatory metabolite required for normal rice growth (Wang et al., 2019).

Besides their role as color and volatile attractants in plant–animal communications (Nisar et al., 2015), apocarotenoids are emerging as key regulators of plant–microbe interactions, in particular of the arbuscular mycorrhizal (AM) symbiosis. AM fungi (AMF) form a widespread root symbiotic association that provides several benefits to the host plants, by improving the mineral nutrition and the tolerance to biotic and abiotic stresses. Furthermore, AMF colonization has an impact on plant developmental processes that determine root architecture, flowering time, fruit and seed formation, and quality (Ruíz-Lozano et al., 2012; Zouari et al., 2014; Fiorilli et al., 2018). The key feature of AM symbiosis is nutrients exchange, in which AMF provide the plant with minerals, mainly phosphorus (P) and nitrogen (N), and receive, in turn, carbohydrates and lipids (Wang et al., 2017 and references within). The AM interaction starts with a chemical dialogue based on plant and fungal diffusible molecules, which triggers the development of fungal adhesion structures on root epidermis. These structures, called hyphopodia, enable the fungus to enter the host root tissues where it spreads *via* intercellular and/or intracellular routes. In the inner cortical layers, fungal hyphae penetrate cortical cells and divide dichotomously, which results in the formation of arbuscules, highly branched structures that are assumed to mediate nutrient exchange (Lanfranco et al., 2018a).

The establishment of the AM symbiosis triggers a cellular, molecular, and metabolic reprogramming of the host plant. Many phytohormones are indeed modulated during the AM colonization and may have themselves a role in regulating the establishment and function of the AM symbiosis (Pozo et al., 2015; Chialva et al., 2018; Liao et al., 2018; Müller and Harrison, 2019). The role of carotenoid metabolism in the AM symbiosis process is not restricted to providing the known plant hormones ABA and SLs. Indeed, several lines of evidence suggest the involvement of other carotenoid-derived metabolites including the recently identified zaxinone (Akiyama et al., 2005; Floss et al., 2008a; Floss et al., 2008b; Walter et al., 2010; Wang et al., 2018; Wang et al., 2019).

In this review we describe the involvement of SLs, ABA, blumenols (C_{13}), mycorradicins (C_{14}), and zaxinone in AM symbiosis and depict their functional significance during different stages of the AMF colonization process.

Strigolactones

Natural SLs are carotenoid-derived compounds characterized by the presence of a methylbutenolide ring (D-ring) linked by an enol ether bridge in (*R*)-configuration to a structurally variable second moiety (Al-Babili and Bouwmeester, 2015). So far, approximately 30 SLs have been isolated from the root exudates of different plant species (Yoneyama et al., 2018). Depending on the structure of the second moiety, natural SLs are classified as canonical SLs that contain a tricyclic lactone (ABC-ring) and non-canonical SLs that have other structures instead (**Figure 1**). Canonical SLs are further divided based on the stereochemistry of the B/C junction into orobanchol- and strigol-like SLs (Al-Babili and Bouwmeester, 2015; Jia et al., 2018). SLs are involved in different developmental processes, including shoot branching, secondary growth, and the establishment of root system architecture (Waters et al., 2017), as well as in plant's response to biotic and abiotic stress factors (Ha et al., 2014; Decker et al., 2017). In addition, plants release SLs into the soil where they were originally discovered as seed germination stimulants of root parasitic weeds (Xie and Yoneyama, 2010) and later identified as hyphal branching factor for AMF (Akiyama et al., 2005) (**Figure 2**). Since then, SLs have become the best known molecules in early plant–AMF interaction (Lanfranco et al., 2018a; Lanfranco et al., 2018b) and have been shown to be involved in the communication with further beneficial microorganisms, such as rhizobia and in the interaction with detrimental organisms (Marzec, 2016; López-Ráez et al., 2017).

In addition to inducing hyphal branching, SLs trigger a range of responses in AMF, which include spore germination, hyphal elongation, and hyphopodia formation (Lanfranco et al., 2018b and references therein). However, it is still unclear how SLs are perceived by AMF and how they influence AMF. Nevertheless, it has been shown that SLs boost the AMF ATP production and mitochondrial division, activate the expression of mitochondrial and effector genes (Besserer et al., 2006, Besserer et al., 2008; Tsuzuki et al., 2016; Salvioli et al., 2016), and promote the release of chitin oligomers (Genre et al., 2013) that are perceived by the plant partner (Sun et al., 2015). The specific role of SLs during the colonization process within plant roots is still ambiguous; however, SLs deficient mutants show normal arbuscule morphology but lower colonization levels.

It has been shown that carlactonoic acid (CLA), the carlactone oxidation product formed by the *Arabidopsis thaliana* MAX1 (**Figure 1**) and its orthologous in other species, and its derivative methyl carlactonoate (MeCLA) have moderate activity in inducing AMF hyphal branching (Mori et al., 2016). Similarly, lotuslactone, a non-canonical SL that has been recently characterized as a *Lotus japonicus* SL, is a moderate inducer of hyphal branching of AMF (Xie et al., 2019). C_{20} non-canonical SLs, such as heliolactone (sunflower) and zealactone (maize), are also weak inducers of hyphal branching (Xie et al., 2019). However, it is worth to note that hyphal branching of *Gigaspora* species, which is used as a biological assay to determine SL effect, often shows high experimental variability and that only SL-induced hyphal elongation could be confirmed in another AMF species, such as *Rhizophagus irregularis* (Tsuzuki et al., 2016). Therefore, the development of a more reliable assay is desirable for a better comprehension of the biological activity of canonical and non-canonical SLs on AMF.

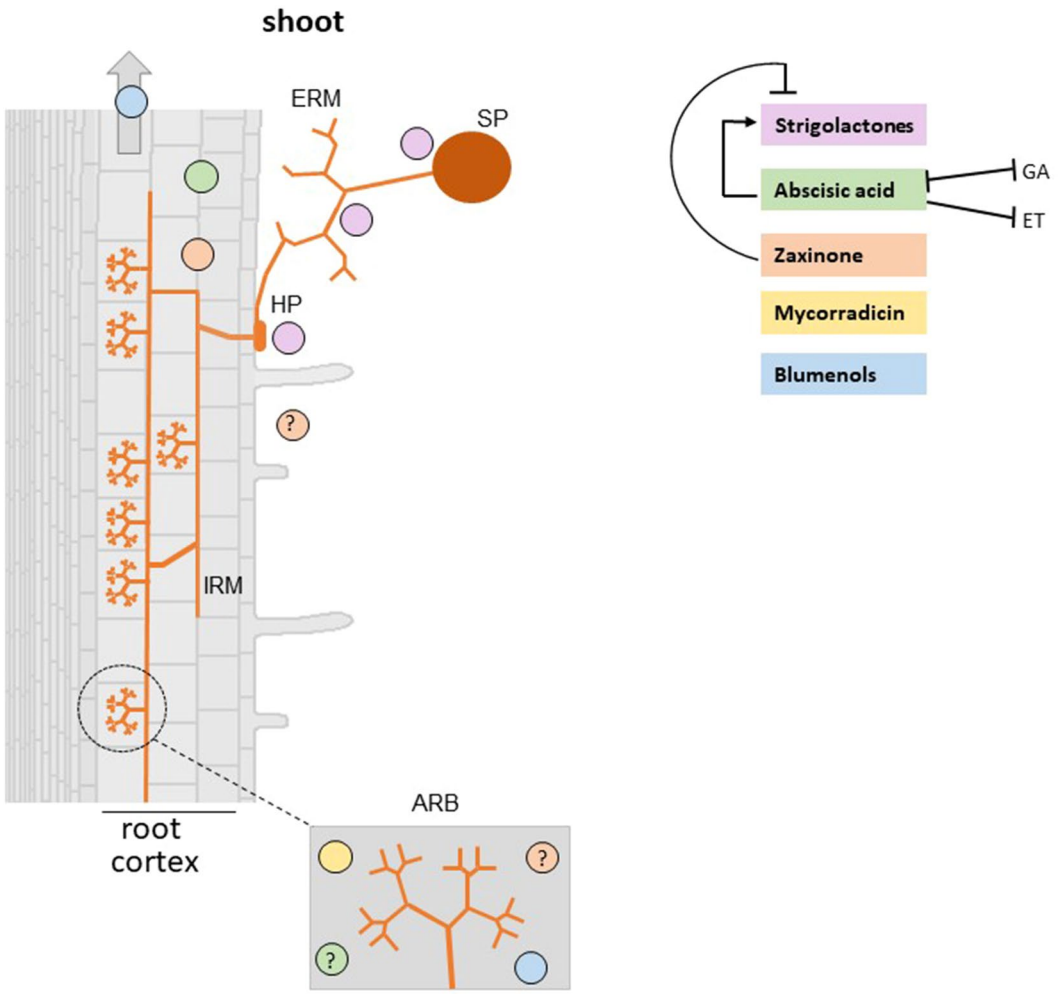

FIGURE 2 | Carotenoid derived-hormones and apocarotenoid signaling molecules involved in the establishment of AM symbiosis. Plant roots release SLs which stimulate AMF spore germination, hyphal branching, hyphopodia formation, and metabolism that in the end promote root colonization. Abscisic acid (ABA) deficient mutants show a reduction of AMF colonization and arbuscule formation and functionality (Herrera-Medina et al., 2007; Martín-Rodríguez et al., 2011). However, it is unclear whether ABA effect on the AM symbiosis is mediated by a cross-talk with SLs, ethylene, and gibberellins. Mycorradicins and blumenols are accumulated in arbuscule-containing cells (Walter et al., 2010). Moreover, Wang et al. (2018) demonstrated that blumenols accumulate also in shoots of several mycorrhizal plants and proposed them as foliar markers for a rapid screening of functional AMF associations. Recent findings showed that zaxinone is produced in mycorrhizal roots and a rice zaxinone defective mutant displays lower AM colonization levels (Wang et al., 2019). SP, spore; HP, hyphopodium; IRM, intraradical mycelium; ERM, extraradical mycelium; ARB, arbuscule-containing cells. Note that the specific localization of ABA and zaxinone is not known (indicated with a question mark). Positive and negative effects are illustrated by arrows and blunt-ended bars, respectively.

Taken together, SLs act as positive regulators of the AM symbiosis; they are essential to achieve the full extent of mycorrhization and, probably, more relevant during the early stage of interaction by activating the fungal metabolism and enhancing its ability to colonize roots. Further investigations are needed to clarify the molecular evolution and the biological role of canonical and non-canonical SLs as communication molecules in the rhizosphere.

Abscisic Acid

The best-studied plant apocarotenoid is the plant hormone ABA (C_{15}), which is a key player in plant response to abiotic stress (Peleg and Blumwald, 2011), regulation of plant growth, and development and promotion of pathogen defence responses (Ton et al., 2009; Ma et al., 2018). Strong evidence has emerged from different host plants for a direct role of ABA in mycorrhizal root colonization. *Solanum lycopersicum* (tomato) ABA defective mutants show a reduction of AMF colonization and arbuscule formation and functionality, which may be partially dependent on an increase of ethylene (Herrera-Medina et al., 2007; Martín-Rodríguez et al., 2011). In *Medicago truncatula*, it has been found that ABA promotes AM colonization, but only at low concentration, and that this positive effect is mediated by the protein phosphatase 2A (PP2A) that is activated during the AM symbiosis and upon ABA treatment (Charpentier et al., 2014). More recently, it

was reported that *Solanum tuberosum* (potato) plants pre-treated with ABA show higher colonization and arbuscule level (Mercy et al., 2017), suggesting that ABA creates a favorable metabolic environment, possibly during the early stage of mycorrhizal formation. It is worth to note that endogenous ABA levels increase in mycorrhizal roots (Ludwig-Müller, 2010) (**Figure 2**) and that a correlation between ABA and SLs levels was observed (López-Ráez et al., 2010). Both hormones are important for the AM symbiosis and seem to be regulated by each other (López-Ráez et al., 2010; Visentin et al., 2016): this cross-talk may also influence the outcome of the symbiosis. It is also worth to note that antagonistic interactions between ABA and other hormones involved in the AM symbiosis, such as ethylene (Martín-Rodríguez et al., 2011) and gibberellins (GA), have also been demonstrated (Floss et al., 2013; Martín-Rodríguez et al., 2016). In particular, it has been proposed that ABA could regulate AM development by inhibiting ethylene production (Martín-Rodríguez et al., 2011) and contribute in particular to arbuscule formation by modifying bioactive GA levels (Martín-Rodríguez et al., 2016).

Blumenols (C_{13}) and Mycorradicins (C_{14})

Accumulation of specific classes of apocarotenoids, such as mycorradicins and blumenols, is strongly associated with the establishment and maintenance of AMF colonization and can be considered a signature of AM symbiosis (Walter et al., 2007; Hill et al., 2018; Wang et al., 2018). These AMF-induced apocarotenoids can be divided based on their structure in two types: (i) colorless C_{13} cyclohexenone derivatives, such as blumenols, and (ii) yellow C_{14} polyene derivatives, called mycorradicins (Walter et al., 2010; Hill et al., 2018). Mycorradicin and its derivatives are mycorrhizal specific-apocarotenoid mixtures, which are detected thanks to a yellow or yellowish pigmentation of roots (Klingner et al., 1995; Walter et al., 2000; Walter et al., 2007; Walter et al., 2010). Mycorradicin is stored as globules in root chromoplasts and its accumulation leads to changes in root plastid morphology (Scannerini and Bonfante-Fasolo, 1977). Although Fester et al. (2002) identified very low mycorradicin concentrations also in non mycorrhizal roots of some species, its accumulation seems to be specific for the AM symbiosis and not for other symbiotic (such as ectomycorrhizas and nodules) or pathogenic interactions, or for the growth under abiotic stress conditions (Maier et al., 1997; Walter et al., 2010).

In addition to mycorradicins, C_{13} cyclohexenone derivatives, called blumenols, are also accumulated in roots after AMF inoculation (Klingner et al., 1995; Maier et al., 1995; Walter et al., 2000; Strack and Fester, 2006). Blumenols are classified into three major types: blumenol A, blumenol B, and blumenol C (**Figure 1**). However, studies have reported that only the content of blumenol C glycosides is increasing during mycorrhizal colonization. Recently, Wang et al. (2018) found a group of blumenols accumulating in roots and shoots of mycorrhizal plants from different species, i.e., tomato, barley, and potato. Abundance of the five blumenol C-glycosides (11-hydroxyblumenol C-9-O-Glc, 11-carboxyblumenol C-9-O-Glc, 11-hydroxyblumenol C-9-O-Glc-Glc, blumenol C-9-O-Glc-Glc, and blumenol C-9-O-Glc) showed a high correlation with AMF colonization rate, as shown by determining the transcript levels of well-known mycorrhization marker genes. It would be very interesting to know more about the biological function of these compounds that may be responsible for or contribute to the systemic effects (defence, attraction or signaling) exerted by the AM symbiosis on the epigeous portions of mycorrhizal plants. Experiments with exogenous treatments and genetic approaches using mutant lines with reduced or increased accumulation of blumenols will be instrumental to clarify the role of these compounds. In any case, blumenols are foliar markers that extend the possibilities of detecting AM symbiosis and can be used for high-throughput screening for functional AMF-associations (Wang et al., 2018).

Several lines of experimental evidence suggest that C_{13} and C_{14} apocarotenoids originate from a common C_{40} carotenoid precursor through a sequential two-steps cleavage: the current model proposes that a C_{40} carotenoid is cleaved by a CCD enzyme (CCD7 or possibly CCD4), leading to a C_{27} apocarotenoid and C_{13} cyclohexenone; then, the C_{27} apocarotenoid is subsequently converted by CCD1 into rosafluene-dialdehyde (C_{14}), the precursor of mycorradicin, and C_{13} cyclohexenone (Floss et al., 2008b; Walter et al., 2010; Hou et al., 2016) (**Figure 1**). The knockdown of *M. truncatula MtDXS2* gene, encoding a 1-Deoxy-D-xylulose 5-phosphate synthase that catalyzes the first step in the plastid isoprenoid biosynthesis, resulted in equal strong reductions of both C_{13} and C_{14} accumulation, which was mirrored by a reduction of the mycorrhizal functionality during later stages of the symbiosis (Floss et al., 2008a). In addition, C_{13} and C_{14} apocarotenoids seem to be strictly linked: both accumulate locally in arbuscules-containing cells (**Figure 2**) where their assumed biosynthetic enzymes are present (Walter et al., 2010). In contrast, *M. truncatula CCD1* knockdown lines displayed a strong reduction in the content of C_{14} mycorradicin derivatives while the C_{13} cyclohexenone level was only moderately affected, indicating that other enzyme(s) are also involved in C_{13} biosynthesis. CCD7, which provides the 9-*cis*-configured C_{27} intermediate in SL biosynthesis, is also a candidate enzyme for synthesizing the C_{27} precursor for the CCD8-mediated formation of the C_{18}-ketone β-apo-13-carotenone (Alder et al., 2008) and for the CCD1-catalyzed and AM-induced C_{13} and C_{14} apocarotenoids in mycorrhizal roots (Floss et al., 2008b; Hou et al., 2016). However, it should be mentioned here that CCD7 is a stereospecific enzyme that solely cleaves 9-*cis*-configured carotenoids and forms accordingly configured C_{27}-apocarotenoids (Bruno et al., 2014). Therefore, the involvement of CCD7 in the latter two metabolic processes implies a *cis* to *trans* isomerization of the formed C_{27}-apocarotenoids, which makes them suitable for being converted into β-apo-13-carotenone and C_{13} and C_{14} mycorrhizal apocarotenoids.

Interestingly, a reduced C_{14} mycorradicin content alone does not hamper the establishment of the AM symbiosis (Floss et al., 2008b), suggesting that C_{13} cyclohexenone derivatives may be more important for a successful AM symbiosis. Indeed, by comparing the distribution of developmental stages of arbuscules in mycorrhizal roots of *M. truncatula DXS* knockdown lines

(where both C_{13} and mycorradicin were strongly reduced) and *CCD1* silenced lines (where C_{13} moderately decreased while mycorradicin was strongly reduced), it was found that *DXS* lines displayed a higher ratio between degenerating and dead arbusculues *versus* mature arbuscules. These results provide a hint for a potential function of C_{13} apocarotenoids (or other isoprenoids/apocarotenoids) in arbuscule turnover, and ascribe to mycorradicin a minor contribution in AM establishment and functioning.

Zaxinone

Zaxinone was recently identified as an important growth-regulating apocarotenoid metabolite in rice. The enzyme responsible for its biosynthesis, ZAS, represents an overlooked sixth CCD subfamily common across the plant kingdom (Wang et al., 2019). ZAS shows the same *in vitro* enzymatic activity of CCD8 with respect to the cleavage of all-*trans*-C_{27} apocarotenoids at position C_{13}-C_{14} (Alder et al., 2008; Alder et al., 2012; Wang et al., 2018). Indeed, zaxinone corresponds to a hydroxylated form of the CCD8 product β-apo-13-carotenone (Alder et al., 2008; **Figure 1**).

A rice loss-of-function *zas* mutant shows a lower root zaxinone content, a severely retarded root and shoot growth and higher SL levels. Exogenous application of zaxinone not only rescued the mutant root defects but also promoted root growth in wild-type plants and reduced SL biosynthesis and exudation under low phosphate supply, pointing to a crucial role of zaxinone in rice development and growth. Despite a higher level of SLs, the rice *Oszas* mutant displayed a lower level of AM colonization compared to wild-type plants, although arbuscule morphology was unaltered. This result demonstrates that the cross-talk between zaxinone and SLs during mycorrhization is complex and shows that our understanding of the role of both apocarotenoids in this process is quite limited. So far, *OsZAS* involvement in the AM symbiosis has been only partially characterized: gene expression analyses of rice mycorrhizal roots revealed that *OsZAS* was induced especially during early (7 day post inoculation, dpi) and, to some extent, during late (35 dpi) stages of mycorrhizal colonization (Fiorilli et al., 2015; Wang et al., 2019). However, zaxinone content turned out to increase only during the early phase of the AM interaction, likely before fungal penetration inside the root. This discrepancy might be due to post-transcriptional regulation events of *OsZAS* gene expression and/or a fine balance between zaxinone synthesis and degradation. Another important clue that highlights the role of *OsZAS* in the AM symbiosis is that ZAS orthologues are absent in genomes of non-AMF host species, such as *A. thaliana* (Wang et al., 2019). Further studies are needed to clarify the precise role of zaxinone in the AM symbiosis and to answer the question whether its effect is direct or mediated by additional factors, i.e. alterations of the level of SLs and/or other hormones. The latter question arises from the finding that zaxinone reduces SLs content by acting as a negative regulator of the transcript level of SLs biosynthetic genes. This inhibition may not require the F-box protein D3 (Wang et al., 2019), which is known to be necessary for the SL-dependent negative feedback regulation of SL biosynthesis (Zhao et al., 2015). However, the root growth promoting effect of exogenously applied zaxinone likely requires functional SLs biosynthesis, as it was not observed in SLs deficient mutants (Wang et al., 2019).

Interestingly, a carotenoid compound (D'orenone), with a chemical structure similar to zaxinone, was recently shown to affect ectomycorrhizal formation possibly by modulating auxin metabolism in both partners (Wagner et al., 2016). It can be speculated that zaxinone and D'orenone may have functional similarities in regulating plant development or the interaction with microorganisms. Understanding the biology of zaxinone will provide new insights into plant development and AM symbiosis. Moreover, zaxinone, through its capability to control SLs biosynthesis, has a large application potential as a tool to combat infestations by root parasitic weeds such as *Striga* (Wang et al., 2019), whose weeds require host-released SLs as a germination signal (Al-Babili and Bouwmeester, 2015), which cause enormous crop yield losses in warm and temperate zones (Parker, 2012).

CONCLUSIONS AND PERSPECTIVES

The carotenoid biosynthesis pathway is an important source of known and postulated hormones and signaling molecules. Some of these carotenoid-derived regulatory metabolites have been recruited for the communication between plants and AMF and as regulators of the process leading to the establishment of a functional AM symbiosis. However, our knowledge on how these metabolites are affecting the symbiosis is still limited. Indeed, the mechanism of action has been unraveled only for SLs during the early stage of the AMF-plant interaction. Further investigations are needed to clarify the precise biological function of ABA, blumenols (C_{13}), and mycorradicins (C_{14})-derivatives and the recently identified zaxinone in this process. In addition, the relationships between all these molecules, which originate from the same metabolic pathway, and their interaction with other hormones known to be involved in the AM symbiosis are largely elusive. For this purpose, the characterization of genes encoding CCDs and other carotenoid-modifying enzymes and of their products will remain instrumental for AM symbiosis research and related agricultural application.

AUTHOR CONTRIBUTIONS

LL and SA-B proposed the concept. VF and JW organized and drafted the manuscript. PB, LL, and SA-B contributed to the editing of the manuscript. LL and SA-B supervised the work. All authors read and approved the manuscript.

FUNDING

This work was supported by baseline funding and Competitive Research Grant (CRG2017) given to SA-B and from King Abdullah University of Science and Technology.

REFERENCES

Abe, S., Sado, A., Tanaka, K., Kisugi, T., Asami, K., and Ota, S. et al. (2014) Carlactone is converted to carlactonoic acid by MAX1 in Arabidopsis and its methyl ester can directly interact with AtD14 in vitro. *Proc. Natl. Acad. Sci. U. S. A.* 111, 18084–18089.

Abuauf, H., Haider, I., Jia, K. P., Ablazov, A., Mi, J., Blilou, I., et al. (2018). The *Arabidopsis DWARF27* gene encodes an all-trans-/9-cis-β-carotene isomerase and is induced by auxin, abscisic acid and phosphate deficiency. *Plant Sci.* 277, 33–42. doi: 10.1016/j.plantsci.2018.06.024

Akiyama, K., Matsuzaki, K. I., and Hayashi, H. (2005). Plant sesquiterpenes induce hyphal branching in arbuscular mycorrhizal fungi. *Nature* 435, 824–827. doi: 10.1038/nature03608

Al-Babili, S., and Bouwmeester, H. J. (2015). Strigolactones, a novel carotenoid-derived plant hormone. *Annu. Rev. Plant Biol.* 66, 161–186. doi: 10.1146/annurev-arplant-043014-114759

Alder, A., Jamil, M., Marzorati, M., Bruno, M., Vermathen, M., Bigler, P., et al. (2012). The path from beta-carotene to carlactone, a strigolactone-like plant hormone. *Science* 335, 1348–1351. doi: 10.1126/science.1218094

Alder, A., Holdermann, I., Beyer, P., and Al-Babili, S. (2008). Carotenoid oxygenases involved in plant branching catalyse a highly specific conserved apocarotenoid cleavage reaction. *Biochem. J.* 416, 289–296. doi: 10.1042/BJ20080568

Besserer, A., Bécard, G., Jauneau, A., Roux, C., and Séjalon-Delmas, N. (2008). GR24, a synthetic analog of strigolactones, stimulates the mitosis and growth of the arbuscular mycorrhizal fungus *Gigaspora rosea* by boosting its energy metabolism. *Plant Physiol.* 148, 402–413. doi: 10.1104/pp.108.121400

Besserer, A., Puech-Pagès, V., Kiefer, P., Gomez-Roldan, V., Jauneau, A., and Roy, S. et al. (2006). Strigolactones stimulate arbuscular mycorrhizal fungi by activating mitochondria. *PLoS Biol* 4, 1239–1247.

Bruno, M., and Al-Babili, S. (2016). On the substrate specificity of the rice strigolactone biosynthesis enzyme DWARF27. *Planta* 243, 1429–1440. doi: 10.1007/s00425-016-2487-5

Bruno, M., Vermathen, M., Alder, A., Wüst, F., Schaub, P., Van-der-Steen, R., et al. (2017). Insights into the formation of carlactone from in-depth analysis of the CCD8-catalyzed reactions. *FEBS Lett.* 591, 792–800. doi: 10.1002/1873-3468.12593

Bruno, M., Beyer, P., and Al-Babili, S. (2015). The potato carotenoid cleavage dioxygenase 4 catalyzes a single cleavage of β-ionone ring-containing carotenes and non-epoxidated xanthophylls. *Arch. Biochem. Biophys.* 572, 126–133. doi: 10.1016/j.abb.2015.02.011

Bruno, M., Hofmann, M., Vermathen, M., Alder, A., Beyer, P., Al-Babili, S., et al. (2014). On the substrate- and stereospecificity of the plant carotenoid cleavage dioxygenase 7. *FEBS Lett.* 588, 1802–1807. doi: 10.1016/j.febslet.2014.03.041

Bruno, M., Koschmieder, J., Wuest, F., Schaub, P., Fehling-Kaschek, M., Timmer, J., et al. (2016). Enzymatic study on AtCCD4 and AtCCD7 and their potential to form acyclic regulatory metabolites. *J. Exp. Bot.* 67, 5993–6005. doi: 10.1093/jxb/erw356

Charpentier, M., Sun, J., Wen, J., Mysore, K. S., and Oldroyd, G. E. (2014). Abscisic acid promotion of arbuscular mycorrhizal colonization requires a component of the protein phosphatase 2A complex. *Plant Physiol.* 166, 2077–2090. doi: 10.1104/pp.114.246371

Chialva, M., Salvioli di Fossalunga, A., Daghino, S., Ghignone, S., Bagnaresi, P., Chiapello, M., et al. (2018). Native soils with their microbiotas elicit a state of alert in tomato plants. *New Phytol.* 220 (4), 1296–1308. doi: 10.1111/nph.15014

Decker, E. L., Alder, A., Hunn, S., Ferguson, J., Lehtonen, M. T., Scheler, B., et al. (2017). Strigolactone biosynthesis is evolutionarily conserved, regulated by phosphate starvation and contributes to resistance against phytopathogenic fungi in a moss, *Physcomitrella patens*. *New Phytol.* 216, 455–468. doi: 10.1111/nph.14506

DellaPenna, D., and Pogson, B. J. (2006). Vitamin synthesis in plants: tocopherols and carotenoids. *Annu. Rev. Plant Biol.* 57, 711–738. doi: 10.1146/annurev.arplant.56.032604.144301

Fester, T., Schmidt, D., Lohse, S., Walter, M. H., Giuliano, G., Bramley, P.M. et al. (2002). Stimulation of carotenoid metabolism in arbuscular mycorrhizal roots. *Planta* 216, 148–154.

Fiorilli, V., Vallino, M., Biselli, C., Faccio, A., Bagnaresi, P., and Bonfante, P. (2015). Host and non-host roots in rice: cellular and molecular approaches reveal differential responses to arbuscular mycorrhizal fungi. *Front. Plant Sci.* 6, 636. doi: 10.3389/fpls.2015.00636

Fiorilli, V., Vannini, C., Ortolani, F., Garcia-Seco, D., Chiapello, M., Novero, M., et al. (2018). Omics approaches revealed how arbuscular mycorrhizal symbiosis enhances yield and resistance to leaf pathogen in wheat. *Sci. Rep.* 8, 9625. doi: 10.1038/s41598-018-27622-8

Floss, D. S., Hause, B., Lange, P. R., Kuster, H., Strack, D., and Walter, M. H. (2008a). Knock-down of the MEP pathway isogene 1-deoxy-D-xylulose 5-phosphate synthase 2 inhibits formation of arbuscular mycorrhiza- induced apocarotenoids, and abolishes normal expression of mycorrhiza-specific plant marker genes. *Plant J.* 56, 86–100. doi: 10.1111/j.1365-313X.2008.03575.x

Floss, D. S., Levy, J. G., Lévesque-Tremblay, V., Pumplin, N., and Harrison, M. J. (2013). DELLA proteins regulate arbuscule formation in arbuscular mycorrhizal symbiosis. *Proc. Natl. Acad. Sci. U. S. A.* 110, 5025–5034. doi: 10.1073/pnas.1308973110

Floss, D. S., Schliemann, W., Schmidt, J., Strack, D., and Walter, H. (2008b). RNA interference-mediated repression of *MtCCD1* in mycorrhizal roots of *Medicago truncatula* causes accumulation of C27 apocarotenoids, shedding light on the functional role of CCD1. *Plant Physiol.* 148 (3), 1267–1282. doi: 10.1104/pp.108.125062

Fraser, P. D., and Bramley, P. M. (2004). The biosynthesis and nutritional uses of carotenoids. *Prog. Lipid Res.* 43, 228–265. doi: 10.1016/j.plipres.2003.10.002

Genre, A., Chabaud, M., Balzergue, C., Puech-Pagès, V., Novero, M., Rey, T., et al. (2013). Short-chain chitin oligomers from arbuscular mycorrhizal fungi trigger nuclear Ca^{2+} spiking in *Medicago truncatula* roots and their production is enhanced by strigolactone. *New Phytol.* 198, 190–202. doi: 10.1111/nph.12146

Giuliano, G., Al-Babili, S., and Lintig, J. V. (2003). Carotenoid oxygenases: cleave it or leave it. *Trends Plant Sci.* 8, 145–149. doi: 10.1016/S1360-1385(03)00053-0

Ha, C. V., Leyva-González, M. A., Osakabe, Y., Tran, U. T., Nishiyama, R., Watanabe, Y., et al. (2014). Positive regulatory role of strigolactone in plant responses to drought and salt stress. *Proc. Natl. Acad. Sci. U. S. A.* 111, 851–856. doi: 10.1073/pnas.1322135111

Havaux, M. (2014). Carotenoid oxidation products as stress signals in plants. *Plant J.* 79, 597–606. doi: 10.1111/tpj.12386

Herrera-Medina, M. J., Steinkellner, S., Vierheilig, H., Ocampo, J. A., and García-Garrido, J. M. (2007). Abscisic acid determines arbuscule development and functionality in the tomato arbuscular mycorrhiza. *New Phytol.* 175, 554–564. doi: 10.1111/j.1469-8137.2007.02107.x

Hill, E. M., Robinson, L. A., Abdul-Sada, A., Vanbergen, A. J., Hodge, A., and Hartley, S. E. (2018). Arbuscular mycorrhizal fungi and plant chemical defence: effects of colonisation on aboveground and belowground metabolomes. *J Chem. Ecol.* 44 (2), 198–208. doi: 10.1007/s10886-017-0921-1

Hirschberg, J. (2001). Carotenoid biosynthesis in flowering plants. *Curr. Opin. Plant Biol.* 4, 210–218. doi: 10.1016/S1369-5266(00)00163-1

Hou, X., Rivers, J., León, P., McQuinn, R. P., and Pogson, B. J. (2016). Synthesis and function of apocarotenoid signals in plants. *Trends Plant Sci.* 21, 792–803. doi: 10.1016/j.tplants.2016.06.001

Ilg, A., Beyer, P., and Al-Babili, S. (2009). Characterization of the rice carotenoid cleavage dioxygenase 1 reveals a novel route for geranial biosynthesis. *FEBS J.* 276, 736–747. doi: 10.1111/j.1742-4658.2008.06820.x

Ilg, A., Bruno, M., Beyer, P., and Al-Babili, S. (2014). Tomato carotenoid cleavage dioxygenases 1A and 1B: relaxed double bond specificity leads to a plenitude of dialdehydes, mono-apocarotenoids and isoprenoid volatiles. *FEBS Open Bio.* 4, 584–593. doi: 10.1016/j.fob.2014.06.005

Jia, K. P., Baz, L., and Al-Babili, S. (2018). From carotenoids to strigolactones. *J. Exp. Bot.* 69 (9), 2189–2204. doi: 10.1093/jxb/erx476

Klingner, A., Bothe, H., Wray, V., and Marner, F. J. (1995). Identification of a yellow pigment formed in maize roots upon mycorrhizal colonization. *Phytochemistry* 38, 53–55. doi: 10.1016/0031-9422(94)00538-5

Lanfranco, L., Fiorilli, V., and Gutjahr, C. (2018a). Partner communication and role of nutrients in the arbuscular mycorrhizal symbiosis. *New Phytol.* 220 (4), 1031–1046. doi: 10.1111/nph.15230

Lanfranco, L., Fiorilli, V., Venice, F., and Bonfante, P. (2018b). Strigolactones cross the kingdoms: plants, fungi, and bacteria in the arbuscular mycorrhizal symbiosis. *J. Exp. Bot.* 69, 2175–2188. doi: 10.1093/jxb/erx432

Liao, D., Wang, S., Cui, M., Liu, J., Chen, A., and Xu, G. (2018). Phytohormones regulate the development of arbuscular mycorrhizal symbiosis. *Int. J. Mol. Sci.* 19, 3146. doi: 10.3390/ijms19103146

López-Ráez, J. A., Kohlen, W., Charnikhova, T., Mulder, P., Undas, A. K., Sergeant, M. J., et al. (2010). Does abscisic acid affect strigolactone biosynthesis? *New Phytol.* 187, 343–354. doi: 10.1111/j.1469-8137.2010.03291.x

López-Ráez, J. A., Shirasu, K., and Foo, E. (2017). Strigolactones in plant interactions with beneficial and detrimental organisms: the yin and yang. *Trend Plant Sci.* 22, 527–537. doi: 10.1016/j.tplants.2017.03.011

Ludwig-Müller, J. (2010). "Hormonal responses in host plants triggered by arbuscular mycorrhizal fungi," in *arbuscular mycorrhizas: physiology and function*. Eds. H. Koltai and Y. Kapulnik (Dordrecht: Springer Science C Business Media B.V), 169–190. doi: 10.1007/978-90-481-9489-6_8

Ma, Y., Cao, J., He, J., Chen, Q., Li, X., and Yang, Y. (2018). Molecular mechanism for the regulation of ABA homeostasis during plant development and stress responses. *Int. J. Mol. Sci.* 19 (11), 3643. doi: 10.3390/ijms19113643

Maier, W., Hammer, K., Dammann, U., Schulz, B., and Strack, D. (1997). Accumulation of sesquiterpenoid cyclohexenone derivatives induced by an arbuscular mycorrhizal fungus in members of the Poaceae. *Planta* 202, 36–42. doi: 10.1007/s004250050100

Maier, W., Peipp, H., Schmidt, J., Wray, V., and Strack, D. (1995). Levels of a terpenoid glycoside (blumenin) and cell wall-bound phenolics in some cereal mycorrhizas. *Plant Physiol.* 109, 465–470. doi: 10.1104/pp.109.2.465

Martín-Rodríguez, J.Á., León-Morcillo, R., Vierheilig, H., Ocampo, J. A., Ludwig-Müller, J., and García-Garrido, J. M. (2011). Ethylene-dependent/ethylene-independent ABA regulation of tomato plants colonized by arbuscular mycorrhiza fungi. *New Phytol.* 190 (1), 193–205. doi: 10.1111/j.1469-8137.2010.03610.x

Martín-Rodríguez, J. A., Huertas, R., Ho-Plágaro, T., Ocampo, J. A., Turečková, V., Tarkowská, D., et al. (2016). Gibberellin-Abscisic Acid balances during arbuscular mycorrhiza formation in tomato. *Front. Plant Sci.* 7, 1273. doi: 10.3389/fpls.2016.01273

Marzec, M. (2016). Strigolactones as part of the plant defence system. *Trends Plant Sci.* 21 (11), 900–903. doi: 10.1016/j.tplants.2016.08.010

Mercy, L., Lucic-Mercy, E., Nogales, A., Poghosyan, A., Schneider, C., and Arnholdt-Schmitt, B. (2017). A functional approach towards understanding the role of the mitochondrial respiratory chain in an endomycorrhizal symbiosis. *Front. Plant Sci.* 8, 417. doi: 10.3389/fpls.2017.00417

Moise, A. R., Al-Babili, S., and Wurtzel, E. T. (2014). Mechanistic aspects of carotenoid biosynthesis. *Chem. Rev.* 114, 164–193. doi: 10.1021/cr400106y

Moise, A. R., Von, L. J., and Palczewski, K. (2005). Related enzymes solve evolutionarily recurrent problems in the metabolism of carotenoids. *Trends Plant Sci.* 10, 178–186. doi: 10.1016/j.tplants.2005.02.006

Mori, N., Nishiuma, K., Sugiyama, T., Hayashi, H., and Akiyama, K. (2016). Carlactone-type strigolactones and their synthetic analogues as inducers of hyphal branching in arbuscular mycorrhizal fungi. *Phytochemistry* 130, 90–98. doi: 10.1016/j.phytochem.2016.05.012

Müller, L. M., and Harrison, M. J. (2019). Phytohormones, miRNAs, and peptide signals integrate plant phosphorus status with arbuscular mycorrhizal symbiosis. *Curr. Opin. Plant Biol.* 50, 132–139. doi: 10.1016/j.pbi.2019.05.004

Nambara, E., and Marion-Poll, A. (2005). Abscisic acid biosynthesis and catabolism. *Annu. Rev. Plant Biol.* 56, 165–185. doi: 10.1146/annurev.arplant.56.032604.144046

Nisar, N., Li, L., Lu, S., Khin, N. C., and Pogson, B. J. (2015). Carotenoid metabolism in plants. *Mol. Plant.* 8, 68–82. doi: 10.1016/j.molp.2014.12.007

Parker, C. (2012). Parasitic weeds: a world challenge. *Weed Sci.* 60, 269– 276. doi: 10.1614/WS-D-11-00068.1

Peleg, Z., and Blumwald, E. (2011). Hormone balance and abiotic stress tolerance in crop plants. *Curr. Opin. Plant Biol.* 14 (3), 290–295. doi: 10.1016/j.pbi.2011.02.001

Pozo, M. J., López-Ráez, J. A., Azcón-Aguilar, C., and García-Garrido, J. M. (2015). Phytohormones as integrators of environmental signals in the regulation of mycorrhizal symbioses. *New Phytol.* 205, 1431–1436. doi: 10.1111/nph.13252

Ramel, F., Birtic, S., Ginies, C., Soubigou-Taconnat, L., Triantaphylidès, C., and Havaux, M. (2012). Carotenoid oxidation products are stress signals that mediate gene responses to singlet oxygen in plants. *Proc. Natl. Acad. Sci. U. S. A.* 109, 5535–5540. doi: 10.1073/pnas.1115982109

Rodrigo, M.J., Alquézar, B., Alós, E., Medina, V., Carmona, L., Bruno, M., et al. (2013) A novel carotenoid cleavage activity involved in the biosynthesis of Citrus fruit-specific apocarotenoid pigments. *J. Exp. Bot.* 64 (14), 4461–4478. doi: 10.1093/jxb/ert260

Ruíz-Lozano, J. M., Porcel, R., Azcón, C., and Aroca, R. (2012). Regulation by arbuscular mycorrhizae of the integrated physiological response to salinity in plants: new challenges in physiological and molecular studies. *J. Exp. Bot.* 63, 695–709. doi: 10.1093/jxb/ers126

Salvioli, A., Ghignone, S., Novero, M., Navazio, L., Venice, F., Bagnaresi, P., et al. (2016). Symbiosis with an endobacterium increases the fitness of a mycorrhizal fungus, raising its bioenergetic potential. *ISME J.* 10, 130–144. doi: 10.1038/ismej.2015.91

Scannerini, S., and Bonfante-Fasolo, P. (1977). Unusual plastids in an endomycorrhizal root. *Can. J. Bot.* 552471, 2474. doi: 10.1139/b77-280

Strack, D., and Fester, T. (2006). Isoprenoid metabolism and plastid reorganization in arbuscular mycorrhizal roots. *New Phytol.* 172, 22–34. doi: 10.1111/j.1469-8137.2006.01837.x

Sun, J., Miller, J. B., Granqvist, E., Wiley-Kalil, A., Gobbato, E., Maillet, F., et al. (2015). Activation of symbiosis signaling by arbuscular mycorrhizal fungi in legumes and rice. *Plant Cell* 27, 823–838. doi: 10.1105/tpc.114.131326

Ton, J., Flors, V., and Mauch-Mani, B. (2009). The multifaceted role of ABA in disease resistance. *Trends Plant Sci.* 14 (6), 310–317. doi: 10.1016/j.tplants.2009.03.006

Tsuzuki, S., Handa, Y., Takeda, N., and Kawaguchi, M. (2016). Strigolactoneinduced putative secreted protein 1 is required for the establishment of symbiosis by the arbuscular mycorrhizal fungus Rhizophagus irregularis. *Mol. Plant Micr. Inter.* 29, 277–286. doi: 10.1094/MPMI-10-15-0234-R

Visentin, I., Vitali, M., Ferrero, M., Zhang, Y., Ruyter-Spira, C., Novák, O., et al. (2016). Low levels of strigolactones in roots as a component of the systemic signal of drought stress in tomato. *New Phytol.* 212 (4), 954–963. doi: 10.1111/nph.14190

Vogel, J. T., Tan, B. C., McCarty, D. R., and Klee, H. J. (2008). The carotenoid cleavage dioxygenase 1 enzyme has broad substrate specificity, cleaving multiple carotenoids at two different bond positions. *J. Biol. Chem.* 283, 11364–11373. doi: 10.1074/jbc.M710106200

Wagner, K., Krause, K., David, A., Kai, M., Jung, E.-M., Sammer, D., et al. (2016). Influence of zygomycete-derived D'orenone on IAA signalling in Tricholoma-spruce ectomycorrhiza. *Environ. Microbiol.* 18, 2470–2480. doi: 10.1111/1462-2920.13160

Walter, M. H., Floss, D. S., and Strack, D. (2010). Apocarotenoids: hormones, mycorrhizal metabolites and aroma volatiles. *Planta* 232, 1–17. doi: 10.1007/s00425-010-1156-3

Walter, M. H., Fester, T., and Strack, D. (2000). Arbuscular mycorrhizal fungi induce the non-mevalonate methylerythritol phosphate pathway of isoprenoid biosynthesis correlated with the accumulation of the 'yellow pigment' and other apocarotenoids. *Plant J.* 21, 571–578. doi: 10.1046/j.1365-313x.2000.00708.x

Walter, M. H., Floss, D. S., Hans, J., Fester, T., and Strack, D. (2007). Apocarotenoid biosynthesis in arbuscular mycorrhizal roots: contributions from methylerythritol phosphate pathway isogenes and tools for its manipulation. *Phytochemistry* 68, 130–138. doi: 10.1016/j.phytochem.2006.09.032

Walter, M. H., Stauder, R., and Tissier, A. (2015) Evolution of root-specific carotenoid precursor pathways for apocarotenoid signal biogenesis. *Plant Sci.* 233, 1–10. doi: 10.1016/j.plantsci.2014.12.017

Wang, J. Y., Haider, I., Jamil, M., Fiorilli, V., Saito, Y., Mi, J., et al. (2019). The apocarotenoid metabolite zaxinone regulates growth and strigolactone biosynthesis in rice. *Nat. Commun.* 10, 810. doi: 10.1038/s41467-019-08461-1

Wang, M., Schäfer, M., Li, D., Halitschke, R., Dong, C., McGale, E., et al. (2018). Blumenols as shoot markers of root symbiosis with arbuscular mycorrhizal fungi. *eLife* 28 (7). doi: 10.7554/eLife.37093

Wang, W., Shi, J., Xie, Q., Jiang, Y., Yu, N., and Wang, E. (2017). Nutrient Exchange and Regulation in Arbuscular Mycorrhizal Symbiosis. *Mol. Plant.* 12 (9), 1147–1158. doi: 10.1016/j.molp.2017.07.012

Waters, M. T., Gutjahr, C., Bennett, T., and Nelson, D. C. (2017). Strigolactone signaling and evolution. *Annu. Rev. Plant Biol.* 68, 291–322. doi: 10.1146/annurev-arplant-042916-040925

Xie, X., and Yoneyama, K. (2010). The strigolactone story. *Annu. Rev. Phytopathol.* 48, 93–117. doi: 10.1146/annurev-phyto-073009-114453

Xie, X., Mori, N., Yoneyama, K., Nomura, T., Uchida, K., Yoneyama, K., et al. (2019). Lotuslactone, a non-canonical strigolactone from *Lotus japonicus*. *Phytochemistry* 157, 200–205. doi: 10.1016/j.phytochem.2018.10.034

Yoneyama, K., Mori, N., Sato, T., Yoda, A., Xie, X., Okamoto, M., et al. (2018). Conversion of carlactone to carlactonoic acid is a conserved function of MAX1 homologs in strigolactone biosynthesis. *New Phytol.* 218 (4), 1522–1533. doi: 10.1111/nph.15055

Zhang, Y., van Dijk, A. D., Scaffidi, A., Flematti, G. R., Hofmann, M., Charnikhova, T., et al. (2014). Rice cytochrome P450 MAX1 homologs catalyze distinct steps in strigolactone biosynthesis. *Nat. Chem. Biol.* 10, 1028–1033. doi: 10.1038/nchembio.1660

Zhao, L. H., Zhou, X. E., Yi, W., Wu, Z., Liu, Y., Kang, Y., et al. (2015). Destabilization of strigolactone receptor DWARF14 by binding of ligand and E3-ligase signalling effector DWARF3. *Cell Res.* 25, 1219–1236. doi: 10.1038/cr.2015.122

Zouari, I., Salvioli, A., Chialva, M., Novero, M., Miozzi, L., Tenore, G. C., et al. (2014). From root to fruit: RNA-Seq analysis shows that arbuscular mycorrhizal symbiosis may affect tomato fruit metabolism. *BMC Genomics* 15, 221. doi: 10.1186/1471-2164-15-221

Conflict of Interest: The authors declare that the research was conducted in the absence of any commercial or financial relationships that could be construed as a potential conflict of interest.

frontiers in Plant Science

ORIGINAL RESEARCH
published: 07 November 2019
doi: 10.3389/fpls.2019.01400

ShORR-1, a Novel Tomato Gene, Confers Enhanced Host Resistance to *Oidium neolycopersici*

*Yi Zhang[1,2†], Kedong Xu[1,2†], Dongli Pei[3†], Deshui Yu[1,2], Ju Zhang[1,2], Xiaoli Li[1,2], Guo Chen[1,2], Hui Yang[1,2], Wenjie Zhou[1,2] and Chengwei Li[4]**

[1] Key Laboratory of Plant Genetics and Molecular Breeding, Zhoukou Normal University, Zhoukou, China, [2] Henan Key Laboratory of Crop Molecular Breeding & Bioreactor, Zhoukou, China, [3] Department of Life Science, Shangqiu Normal University, Shangqiu, China, [4] Henan Engineering Research Center of Grain Crop Genome Editing, Henan Institute of Science and Technology, Xinxiang, China

A previous complementary cDNA-amplified fragment length polymorphism (cDNA-AFLP) analysis examined responses to the powdery mildew pathogen *Oidium neolycopersici* (*On*) of the resistant cultivar *Solanum habrochiates* G1.1560, carrying the *Ol-1* resistance gene, and susceptible cultivar *S. lycopersicum* Moneymaker (MM). Among other findings, a differentially expressed transcript-derived fragment (DE-TDF) (M14E72-213) was upregulated in near isogenic line (NIL)-*Ol-1*, but absent in MM. This DE-TDF showed high homology to a gene of unknown function, which we named *ShORR-1* (*Solanum habrochaites Oidium Resistance Required-1*). However, MM homolog of *ShORR-1* (named *ShORR-1-M*) was still found with 95.26% nucleic acid sequence similarity to *ShORR-1* from G1.1560 (named *ShORR-1-G*); this was because the cut sites of restriction enzymes in the previous complementary cDNA-AFLP analysis was absent in *ShORR-1-M* and differs at 13 amino acids from *ShORR-1-G*. Transient expression in onion epidermal cells showed that ShORR-1 is a membrane-localized protein. Virus-induced gene silencing (VIGS) of *ShORR-1-G* in G1.1560 plants increased susceptibility to *On*. Furthermore, overexpressing of *ShORR-1-G* conferred MM with resistance to *On*, involving extensive hydrogen peroxide accumulation and formation of abnormal haustoria. Knockdown of *ShORR-1-M* in MM did not affect its susceptibility to *On*, while overexpressing of *ShORR-1-M* enhanced MM's susceptibility to *On*. We also found that changes in transcript levels of six well-known hormone signaling and defense-related genes are involved in *ShORR-1-G*-mediated resistance to *On.* The results indicate that *ShORR-1-M* and *ShORR-1-G* have antagonistic effects in tomato responses to *On*, and that *ShORR-1* is essential for *Ol-1*-mediated resistance in tomato.

Keywords: ***Oidium neolycopersici*, *Ol-1*-mediated resistance, susceptible tomato, resistant tomato, H_2O_2 accumulation, abnormal haustoria**

OPEN ACCESS

Edited by:
Richard Hickman, Utrecht University, Netherlands

Reviewed by:
Rosa Rao, University of Naples Federico II, Italy
Barbara Molesini, University of Verona, Italy

***Correspondence:**
Chengwei Li
lichengweihist@163.com

†These authors have contributed equally to this work

Specialty section:
This article was submitted to Plant Microbe Interactions, a section of the journal Frontiers in Plant Science

Received: *14 June 2019*
Accepted: *10 October 2019*
Published: *07 November 2019*

Citation:
Zhang Y, Xu K, Pei D, Yu D, Zhang J, Li X, Chen G, Yang H, Zhou W and Li C (2019) ShORR-1, a Novel Tomato Gene, Confers Enhanced Host Resistance to Oidium neolycopersici Front. Plant Sci. 10:1400. doi: 10.3389/fpls.2019.01400

INTRODUCTION

Plants have evolved a multilayered immune system that prevents or hinders colonization by most potential pathogens. To date, two types of innate immune response have been recognized in plants. One is pathogen-associated molecular pattern-triggered immunity, which is activated by a number of pathogen-associated molecular patterns such as flagellin, EF-Tu, and chitin, and perceived by

pattern recognition receptors (Jones and Dangl, 2006; Dodds and Rathjen, 2010; Peng et al., 2018). The other is effector-triggered immunity, which is modulated by recognition of pathogen-derived avirulence effectors by plant R proteins (Jones and Dangl, 2006; Dodds and Rathjen, 2010).

Powdery mildew caused by *Oidium neolycopersici* (*On*) is one of the most severe diseases of tomato. Six resistance genes (termed *Ol-X*) and three quantitative resistance loci from wild tomato species have been identified, all of which mediate various resistance responses to *On* (Bai et al., 2003; Bai et al., 2004; Bai et al., 2005; Li, 2005). *Ol-1*, one of the resistance genes, derived from *Solanum habrochaites* G1.1560 (Lindhout et al., 1994), mediates partial resistance to *On*, including a slow hypersensitive response (HR) (Li et al., 2007). *Ol-4*, introgressed from wild tomato species *S. peruvianum* LA2172, confers complete resistance to *On* and is associated with a rapid HR (Bai et al., 2004). In previous studies, we found that near-isogenic lines (NILs) carrying *ol-2*, *Ol-1* and *Ol-4* genes in the genetic background of the susceptible cultivar MM had varying degrees of resistance to *On* (Li et al., 2006; Li et al., 2007). We also examined gene expression patterns in these lines by cDNA-amplified fragment length polymorphism (cDNA-AFLP) analysis. Transcript-derived fragments (TDFs) showing differential presence or intensity between resistant tomato NILs and susceptible MM after mock-inoculation and inoculation with *On* were identified (Li et al., 2006; Li et al., 2007). UniGene sequences in the Solanaceae Genomics Network (SGN) database showing high homology to each differentially expressed TDF were then identified. Tobacco rattle virus (TRV)-based virus-induced gene silencing (VIGS) constructs targeting these UniGenes were subsequently generated, and used to determine whether silencing the targeted genes altered the *On* resistance of relevant genotypes. These efforts revealed that acetolactate synthase (ALS) (Gao et al., 2014), a glutathione S-transferase (GST) gene (Pei et al., 2011a), and an NADP-malic enzyme gene (Pei et al., 2011b) are required for *Ol-1*-mediated resistance to *On*.

In the study presented here, we focused on another differentially expressed TDF (M14E72-213) and analyzed its involvement in *On* resistance. M14E72-213 is present in NIL-*Ol-1*, but not MM or NIL-*Ol-4* (Li et al., 2006; Li et al., 2007). We found that silencing it resulted in loss of resistance, to varying degrees, in *S. habrochaites* G1.1560 (which carries the *Ol-1* gene). Microscopic observation showed that the pathogen could complete its life cycle on leaves of the plants with silenced *Ol-1*. In addition, the HR was slow in epidermal cells of the leaves from this line, while rapid HR in attacked epidermal cells of control plants prevented completion of *On*'s life cycle. Thus, the gene is apparently required for *Ol-1* mediated resistance to *On*, and was named *ShORR-1* (*S. habrochaites Oidium Resistance Required gene*). According to open reading frame (ORF) finder, it encodes a putative 268 amino acid protein, which has 93% identity with an uncharacterized gene (XM_004242006), suggesting that it may be a novel gene. The results indicated that differences in *ShORR-1* variants of susceptible and resistant tomato account for at least some of the differences in their resistance. Further analyses indicate that increases in H_2O_2 accumulation and formation of abnormal haustoria are involved in *Ol-1*-mediated resistance to powdery mildew in tomato, which requires an appropriate variant of *ShORR-1*, such as *ShORR-1-G*.

MATERIALS AND METHODS

Plant Materials, Pathogen, Inoculation, and Treatments

The *On*-susceptible tomato *S. lycopersicum* Mill (MM) and resistant cultivar *S. habrochaites* G1.1560, which carries the *Ol-1* gene, were grown in a greenhouse providing 16 h and 23°C day/8 h and 20°C night cycles, with constant 80% relative humidity (RH). The tomato powdery mildew used in this research was identified as *On* isolate China (Li et al., 2008) on the basis of its morphological, histological, and molecular characteristics. The fungus was maintained on the susceptible tomato cultivar MM. For inoculation of *On*, whole plants were sprayed with a suspension of spores (5×10^3 conidia/ml) collected from infected tomato plants in a climate chamber in the conditions mentioned above, except that the RH was 85 and 95% during the day and night periods, respectively. Control plants were sprayed with sterile water.

Vector Construction and Virus-Inducing Gene Silencing Assays

The target DE-TDF was amplified by reverse transcription PCR (RT-PCR) with primers listed in **Table 1**. The recombinant vector TRV-LIC-*ShORR-1* carrying the target sequence was constructed as described elsewhere (Dong et al., 2007). The vectors TRV1 and TRV2-LIC-*ShORR-1* were introduced into *Agrobacterium tumefaciens* strain GV3101 by heat shock and cocultured overnight. Overnight cultures (5 ml) were grown at 28°C in appropriate antibiotic selection medium in 15 ml glass tubes for 1 day, then briefly centrifuged, and the collected cells were resuspended in infiltration medium (10 mM MES, 10 mM $MgCl_2$, 200 μM acetosyringone) to an OD_{600} of 1. After incubation at room temperature for 3 h, the cultures were used for agro-infiltration, as previously reported (Liu et al., 2010). Briefly, plants at the four-leaf stage were infiltrated with a 1:1 mixture of TRV1 and TRV2-LIC-*ShORR-1* fragments, and plants treated with cultures with empty vector provided negative controls. Ten days after agro-infiltration, plants were inoculated with *On*. Four plants per trial were inoculated and at least three trials were conducted.

H_2O_2 Accumulation Assay and Microscopic Analysis

An endogenous peroxidase-dependent 3,3-diaminobenzidine (DAB) assay was used to investigate H_2O_2 production in plants (Thordal-Christensen et al., 2010). To detect H_2O_2 accumulation, leaflets taken 65 h after *On* infection were immersed in DAB solution (1 mg/ml, pH 3.8) for 8–12 h until DAB staining was visible at the vein of the top leaflet. The DAB-stained leaflets were fixed and stained with Coomassie Brilliant Blue R250 in methanol (0.6%, w/v), following Li (2005) with minor

modifications. Samples were observed under a differential-interference contrast microscope (Carl Zeiss, Germany), and images were acquired with a Color Video Camera equipped with image analysis software (Image-Pro Plus 4.1, Media Cybernetics, L.P.). In each microscopically examined sample, we observed more than 200 primary haustoria and secondary haustoria, and recorded percentages of host cells showing HR. Three biological replicates of microscopic samples of both *ShORR-1* silenced and control plants were used in these examinations.

Gene Analog-Based Cloning of *ShORR-1*

RNA was extracted from G1.1560 and MM tomato leaves with TRIzol reagent (Life Technologies, Grand Island, NY) following the manufacturer's recommendations. After extraction, the RNA samples were treated with DNase I (TaKaRa) to eliminate trace contaminants of genomic DNA. cDNA was synthesized using a PrimeScript RT Perfect Real Time reagent kit (TaKaRa), and the resulting cDNAs were used as templates in the following PCR reactions. The TDF fragment M14E72-213 was aligned to the tomato genome (Consortium, 2012) and ShORR-1-F1/R1 primers (**Table 1**) were designed to clone the complete ORF based on the UniGene with highest identity. To detect genes homologous to *ShORR-1*, sequences from G1.1560 and MM, respectively designated *ShORR-1-G* and *ShORR-1-M*, were amplified with the *ShORR-1*-F2/R2 primers (**Table 1**). The PCR reactions involved denaturation at 94°C for 5 min, followed by 30 amplification cycles of 30 s at 94°C, 45 s at 58°C, 1 min at 72°C, and a final extension step of 10 min at 72°C. The resulting amplicons were inserted into the pMD18-T vector (TaKaRa) and recombinant plasmids were sequenced using the universal T7 primer.

Transient Expression Vector Construction and Subcellular Localization of *ShORR-1*

ORFs of *ShORR-1-G* and *ShORR-1-M* were used to construct transient expression vectors by insertion into the pSAT6-GFP-N1 vector (Xu et al., 2014), which contains a gene encoding a modified green fluorescent protein (GFP) at *Nco* I–*Xba* I sites, with *ShORR-1*-F3/R3 primers (**Table 1**). pSAT6-GFP-N1 was digested with *Kpn* I and *BamH* I to construct pSAT6-GFP-N1-*ShORR-1-G* and pSAT6-GFP-N1-*ShORR-1-M* vectors, then the recombinant plasmids were transformed into onion epidermal cells by an *Agrobacterium*-mediated *in planta* transient transformation protocol (Xu et al., 2014). Microscopic observations and image acquisition were performed on a fluorescence microscope (Olympus BX61, Japan).

Generation of Stable Transgenic Plants and Gene Function Verification

To validate functions of *ShORR-1-G* and *ShORR-1-M*, the full length target genes were introduced into the pCAMBIA2300 vector with *Kpn* I and *Sal* I restriction enzymes. Then a 381

TABLE 1 | Names and sequences of primers used in this study.

Primer name	Sequence (5′–3′)	Purpose
ShORR-1-F	CGACGACAAGACCCTCCCAATTTTCATAATCCTGTCA	VIGS vector construction of *ShORR-1*
ShORR-1-R	GAGGAGAAGAGCCCTCCATTTTGATAAATACCCCTCCA	
ShORR-1-F1	ATTACTCTCTTCATAAACTCATTTCCA	Cloning of full-length sequences of *ShORR-1*
ShORR-1-R1	TCTGCTGCTATTTCTGCCACT	
ShORR-1-F2	ATGTTTGATCCAAGAAAA	Cloning *ShORR-1* from different species
ShORR-1-R2	TCAGCAATCTAAATCAGT	
ShORR-1-F3	GTCCATGGATGTTTGATCCAAGAAAA	Subcellular localization vector
ShORR-1-R3	ATCTAGATCAGCAATCTAAATCAGT	
ShORR-1-F4	GTTCATTTCATTTGGAGAGGACAGGGTACCATGTTTGATCCAAGAAAACAAATACCCAA	Construction of *ShORR-1* overexpressing vector
ShORR-1-R4	CATTAAAGCAGGGCATGCCTGCAGGTCGACTCAGCAATCTAAATCAGTCATCACTTTGTTTT	
ShORR-1-F5	CACCAGCCTTATGGCAAAAT	qRT-PCR analysis
ShORR-1-R5	AGTTCCCATTGCCCTCTAGC	
SlPR1-F	TGCAACAACGGGTGGTACTT	qRT-PCR analysis
SlPR1-R	ATGGACGTTGTCCTCTCCAG	
SlPR2-F	CTGCGATGGATCGAACAGGA	qRT-PCR analysis
SlPR2-R	TGTGTTGCACCAAAAGCACC	
SlCOI1-F	GTAGTCTCGGAGCATCCAGC	qRT-PCR analysis
SlCOI1-R	GGGTCCAAAGGCTTGACAGT	
SlHSR203J-F	TGGTTCATCAAAAGCAAGTTAAAGA	qRT-PCR analysis
SlHSR203J-R	ACCAGTCCATGTCCGGTCTA	
SlROR2-F	AGACAAAAGATGGCGTCGGA	qRT-PCR analysis
SlROR2-R	TCCTTCACAGCTTCATGCCT	
SlBI1-F	GCTCCTCCTTATCAAGAGCAAAA	qRT-PCR analysis
SlBI1-R	AGCAGCTGAGAAGCAACCAA	
SlActin-F	CCATTCTCCGTCTTGACTTGG	Tomato reference gene
SlActin-R	TCTTTCCTAATATCCACGTCAC	

bp partial sequence of *ShORR-1-M* was cloned into RNAi vector pCAMBIA2300 using the sense and antisense strands. PCR products were amplified with KAPA HiFi PCR kits (Kapa Biosystems, USA), then transformed into *Escherichia coli* Trans T1 competent cells to generate recombinant plasmids, which were introduced into *Agrobacterium* strain GV3101. All applied oligonucleotide primers are listed in **Table 1**. Different homozygotes transgenic plants lines were produced by the Plant Genetic Transformation Center of the Henan Key Laboratory of Crop Molecular Breeding & Bioreactor. To investigate *ShORR-1*'s function in resistance to *On*, the positive transgenic plants were inoculated and microscopically analyzed, as previously described (Shen et al., 2007). Fresh leaves from wild-type and transgenic tomato plants were collected and placed on 1% agar plates containing 85 μM benzimidazole. The leaves were incubated in a climate chamber providing constant light at 20°C for at least 4 h, then inoculated with a suspension of *On* spores (5×10^3 conidia/ml). After allowing the *On* fungus to develop on the leaves for 65 h under the same conditions (Bai et al., 2005), the leaves were fixed in ethanol/acetic acid (1:1, v/v), stained with Coomassie Brilliant Blue R250 in methanol (0.6%, w/v) for 10 s, then rinsed in deionized water. Samples were subsequently observed with a BX61 microscope (Olympus, Tokyo, Japan), and microcolonies were counted. More than 1,000 germinated spores on each leaf segment from every plant were observed, and three biological replicates of control and transgenic plants were used.

Quantitative Reverse Transcription PCR

To quantify levels of *ShORR-1* transcript produced in response to *On*, susceptible and resistant tomato leaves were sampled at 0, 8, 24, 36, 72, and 120 h postinoculation (hpi), according to previous microscopic observations of tomato-*On* interaction (Gao et al., 2014). Estimates of fungal biomass in the samples were obtained by extracting *On* DNA and quantifying levels of the *EF-1a* gene following Trond and Cathrine (2009). To explore the resistance mechanisms involving *ShORR-1*, the expression of six marker genes associated with different disease resistance and hormone pathways was quantified in wild-type and *ShORR-1-G*-overexpressing plants in the presence and absence of *On*. For this, total RNA was extracted from samples of transgenic and wild-type plants with TRIzol reagent following recommendations of the manufacturer, and 1 μg total RNA was used for cDNA synthesis. It was then subjected to quantitative reverse transcription PCR (qRT-PCR) using a CFX96™ Real-Time PCR Detection System (Bio-Rad, Hercules, CA) with SYBR® Premix Ex Taq™ (Takara Bio Inc., Shiga, Japan). The amplification conditions consisted of 95°C for 3 min, followed by 40 cycles of 95°C for 10 s, and 60°C for 30 s. Fold changes in levels of target transcripts were calculated using the $2^{-\Delta\Delta Ct}$ and $2^{-\Delta Ct}$ method (Livak and Schmittgen, 2001), with normalization against the tomato *Actin* (*SlActin*) transcript levels. Three biological and technical replicates were run for each cDNA sample. All the applied qRT-PCR primers are listed in **Table 1**.

Data Analysis

Relative expression levels of genes were statistically analyzed using one-way analysis of variance (ANOVA) and Dunnett's *post hoc* or Tukey's HSD tests ($P < 0.01$ and $P < 0.05$). All analyses were performed using SPSS Statistics 17.0 following instructions in the SPSS Survival Manual.

RESULTS

Cloning and Sequence Analysis of *ShORR-1* in Resistant and Susceptible Tomato Genotypes

In our previous cDNA-AFLP study, we found that TDF fragment M14E72-213—designated No. 25 by Li et al. (2007), Appendix 1)—was present in *On*-resistant NIL-*Ol-1*, but not in the *On*-susceptible cultivar MM. BLAST analysis indicated that the 134 bp sequence had been annotated in SGN before the tomato genome sequence became publicly available, and was described as having 97% identity with a UniGene of unknown function (SGN-U319851). Using the sequence of this UniGene, in the study presented here we cloned the 807 bp ORF designated *ShORR-1-G* from the *Ol-1* resistant line G1.1560 (accession no. MK205292). We found it encodes a putative protein of 268 amino acids with a molecular weight of 30.55 kDa, isoelectric point (pI) of 9.53, and 95% identity to a protein of unknown function encoded by Solyc06g059860.2 according to a BLASTP search against the SGN database. In contrast, the ORF sequence of *ShORR-1-M* is 819 bp long (accession no. MK205293), and encodes a putative protein of 272 amino acids with a molecular weight of 30.96 kDa, isoelectric point (pI) of 9.48, and 99% identity with Solyc06g059860.2 (differing in only one nucleotide base). *ShORR-1-G* and *ShORR-1-M* have no conserved domain, according to a search of the NCBI database. The DNAMAN software package was applied to align the nucleotide and protein homologs of ShORR-1 cloned from the two tomato varieties (**Figure 1**). The ORF and protein sequence homologies of the susceptible and resistant species' ShORR-1 variants were 95.26 and 94.87%, respectively. The alignment results showed that ShORR-1-G has one more amino acid residue (a lysine) than ShORR-1-M at the 5′ end, while there are five more amino acids in ShORR-1-M at the 3′ end, and seven other amino acids differ between them. Additionally, the amino acid sequences of ShORR-1-G and ShORR-1-M shared 95.22 and 97.42% identity with a hybrid signal transduction histidine kinase of *S. pennellii* with a BLASTP search in NCBI, respectively. The ShORR-1-G and ShORR-1-M sequences respectively contain 19 and 20 potential serine phosphorylation sites (http://www.dabi.temple.edu/disphos), and in both cases putative MAPK phosphorylation sites (Mao et al., 2011, Nobuaki et al., 2011) in the N terminus (**Figure S1**). Moreover, ShORR-1-M and ShORR-1-G proteins both have potential ubiquitination (**Figure S2**) and SUMOylation sites (**Figure S3**) by UbPred (http://www.ubpred.org/) and GPS-SUMO (http://sumosp.biocuckoo.org/online.php) (Radivojac et al., 2010; Zhao et al., 2014). Neither ShORR-1-M and ShORR-1-G proteins have any transmembrane helices according to TMHMM 2.0 predictions (http://www.cbs.dtu.dk/services/TMHMM/).

FIGURE 1 | Nucleotide **(A)** and amino acid **(B)** sequences alignment of ShORR-1-M and ShORR-1-G share high homology using DNAMAN software.

ShORR-1 Localized in Plasma Membrane

To determine the subcellular localization of ShORR-1, the full-length sequences isolated from G1.1560 and MM were fused to the 5′ terminus of the *GFP* gene in the pSAT6-GFP vector, under control of the constitutive CaMV: 35S promoter. The ShORR-1 protein was transiently transferred into onion epidermal cells by *A. tumefaciens*-mediated transformation (Xu et al., 2014). Microscopic observation of the fluorescent signal emitted by the ShORR-1-GFP fusion protein revealed that ShORR-1-M and ShORR-1-G were both localized on the plasma membrane, while fluorescence signals from the control pSAT6-GFP vector were ubiquitous in examined cells (**Figure 2**). These results show that ShORR-1 is a membrane-localized protein.

Expression Pattern of *ShORR-1* in Tomato

To investigate *ShORR-1*'s role in resistance to infection by the powdery mildew fungus *On*, we measured its transcript levels in tissues of leaves infected by *On* at selected time-points by qRT-PCR. Previous research had revealed that *On* haustoria form at 24–41 hpi (Huang et al., 1998; Bai et al., 2005). Expression of *ShORR-1* was detected in both *On*-susceptible and -resistant species, but the transcription patterns and expression levels (relative to levels in controls) differed. Generally, relative expression levels of *ShORR-1* were much higher in G1.1560 than in MM, although they were similar at 36 hpi (**Figures 3A**, **B**). The relative expression level of *ShORR-1* in MM increased as early as 8 hpi, and peaked (at 7.8-fold) at 120 hpi, compared to levels in control leaves (**Figure 3A**), while the relative expression level of *ShORR-1* in G1.1560 also increased at 8 dpi and peaked at 72 hpi (**Figure 3B**). These results indicate that *ShORR-1* could be upregulated earlier and generally more strongly in resistant tomato plants than in susceptible tomato plants in response to *On*. Quantitative analysis of *ShORR-1* expression patterns in MM tissues by qRT-PCR showed that it is expressed mainly in leaves and stems, and to a lesser extent in mature red fruits, roots, flowers, and green fruits (**Figure 3C**).

Loss of Resistance to Powdery Mildew in *ShORR-1*-Silenced Tomato Leaves

For the TDF fragment M14E72-213, which had 97% identity with SGN-U319851, primers were designed based on U319851 to construct a TRV2-VIGS vector to silence *ShORR-1* in *S. habrochaites* G1.1560. Twenty silenced plants of this previously resistant line were inoculated with *On* 10 days after VIGS infiltration. Seven days postinoculation (dpi) with the fungus, *On* colonies were clearly visible on leaves of all 20 silenced plants, with 5–30% of their foliar area affected, while no fungal colonies were observed on plants infiltrated with the empty vector (TRV2-EV) (**Figure 4A**). These results clearly indicate that silencing of *ShORR-1* abolished *Ol-1*-mediated resistance to *On* at the macroscopic level. qRT-PCR analyses showed that

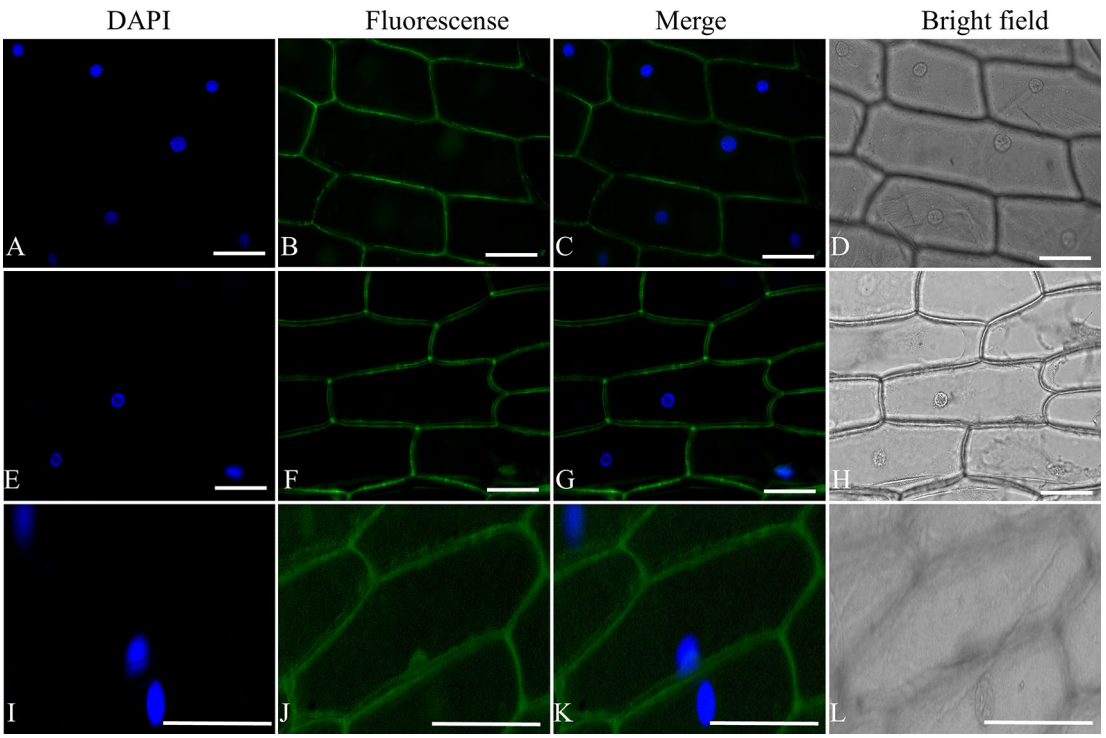

FIGURE 2 | ShORR-1-M and ShORR-1-G both localized to the plasma membrane. Subcellular localization GFP fusions with ShORR-1 variants isolated from G1.1560 and MM in onion epidermal cells, as shown by 4′,6-diamidino-2-phenylindole (DAPI) nuclear staining **(A**, **E**, and **I)**, green fluorescent protein (GFP) fluorescence **(B**, **F**, and **J)**, merger of DAPI staining and fluorescence **(C**, **G**, and **K)**, bright field microscopy **(D**, **H**, and **L)**. The proteins displayed in panels **(A**–**D)**, **(E**–**H)**, and **(I**–**L)** were transiently expressed using pSAT6-GFP-N1-ShORR-1-G, pSAT6-GFP-N1-ShORR-1-M, and a construct designed to express GFP alone (as a control), respectively. Scale bar = 25 μm.

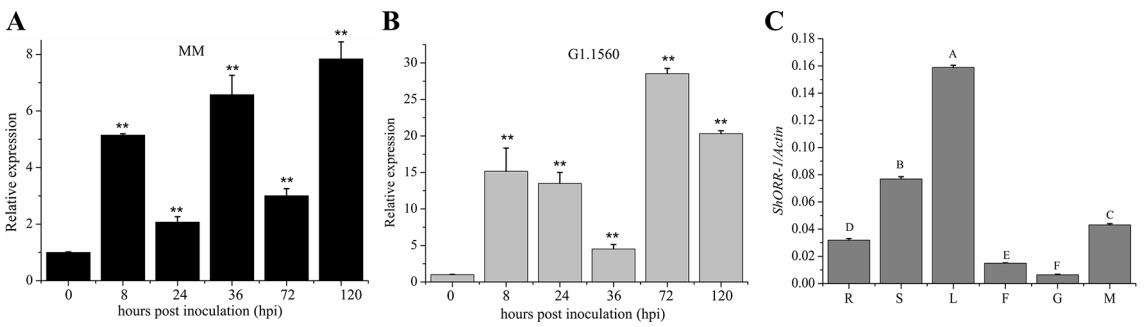

FIGURE 3 | Expression profiles of *ShORR-1* at indicated *On* infection stages and tissues in MM **(A)** and G1.1560 **(B)**. Samples were harvested at 0, 8, 24, 36, 72, and 120 hpi **(A**–**B)**. The relative expression levels of *ShORR-1* at each time-point were normalized relative to *SlActin*. Asterisks indicate significant difference from the control determined by one-way ANOVA followed by an independent-samples Dunnett's *post hoc* test (**: $P < 0.01$). **(C)** The transcript accumulation of *ShORR-1* was examined by quantitative real-time PCR from MM tissues, including roots (R), stems (S), leaves (L), flowers (F), green fruits (G), and red fruits (M). *Actin* was used as an internal control. Mean and standard error were calculated using data from three independent biological replicates. Letters indicate significant differences between different tissues determined by one-way ANOVA followed by Tukey's HSD test ($P < 0.01$).

ShORR-1 transcript levels were significantly lower in the silenced plants than in controls (**Figure 4B**). Moreover, microscopic analysis showed that numerous conidiophores with conidia were present on *ShORR-1*-silenced resistant plants, and the histological morphology of the fungus on *ShORR-1*-silenced resistant plants was similar to that on susceptible plants. Thus, the fungus successfully completed its life cycle on them, and silencing of *ShORR-1* did not lead to morphological alteration of *On*. In contrast, fungal growth was clearly prevented, and no conidiospores formed, on TRV2-EV G1.1560 plants (**Figure 4C**). In conclusion, silencing *ShORR-1* allowed fungal growth and sporulation, resulting in visible disease symptoms, indicating that *ShORR-1* plays an important role in resistance to powdery mildew caused by *On*.

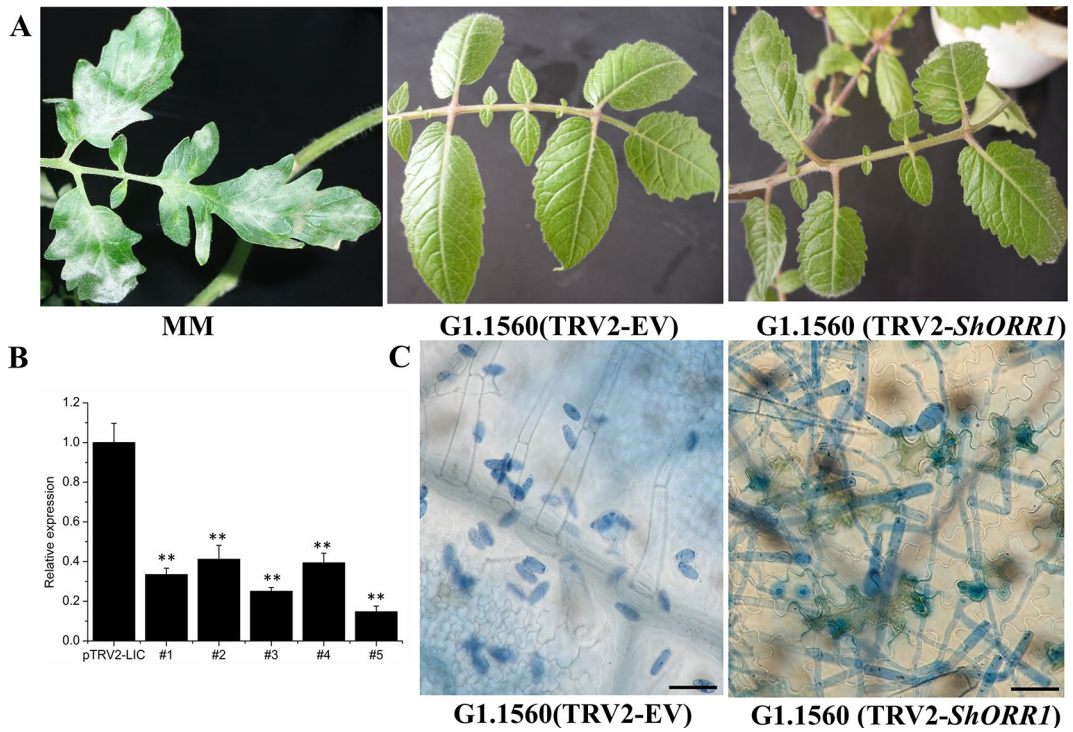

FIGURE 4 | Downregulation of *ShORR-1* by VIGS compromises *Ol-1*-mediated resistance. **(A)** *On* susceptible phenotypes of MM and *ShORR-1*-silenced (TRV2-*ShORR-1*) G1.1560 plants, and resistant phenotype of G1.1560 controls transformed with an empty vector (TRV2-EV). **(B)** Levels of *ShORR-1* transcripts in control and TRV2-*ShORR-1* leaves. Error bars represent standard deviations, obtained from analysis of three biological replicates. Asterisks indicate significant difference from the control by one-way ANOVA followed by an independent-samples Dunnett's *post hoc* test (**: $P < 0.01$). **(C)** Microscopic morphologies of *On* in control and TRV2-*ShORR-1* plants. Bar = 25 μm.

H_2O_2 Accumulation Analysis, *On* Growth and Host Response

Li (2005) noted that the TDF fragment M14E72-213 accumulated more rapidly, and to higher levels, in resistant tomato than in susceptible plants after inoculation with *On*. Microscopic analysis presented here showed that *S. habrochaites* G1.1560 control plants displayed a rapid HR following exposure to *On*. In this response, most cells invaded by primary haustoria of *On* rapidly accumulated H_2O_2 and died, thereby preventing further growth of *On* (**Figure 5A**). Contrary to expectations, *On*-induced cell death and H_2O_2 accumulation were observed in *ShORR-1*-silenced resistant plants (**Figure 5A**), although fungal growth and conidiophore formation were similar to those on susceptible plants. However, the proportion of dead cells among cells attacked by fungal haustoria was lower in *ShORR-1*-silenced resistant plants than in control resistant plants. We investigated more than 200 cells attacked by primary haustoria in each microscopic sample, and found that average percentages of cells showing HR in control and *ShORR-1*-silenced plants were about 68 and 30%, respectively, at 64 hpi. We then observed more than 200 cells attacked by secondary haustoria in each microscopic sample, and found that percentages of cells showing HR in control and *ShORR-1*-silenced plants were about 32 and 22%, respectively, at 147 hpi (**Figure 5B**). In contrast to those in resistant control plants, most cells invaded by fungal haustoria remained alive in *ShORR-1*-silenced resistant plants, and the haustoria showed normal morphology, resulting in further fungal growth and conidiophore formation in *ShORR-1*-silenced resistant plants. The results also indicated that the *On*-induced HR in the *ShORR-1*-silenced resistant plants was slower, and possibly weaker, than in the control resistant plants.

Overexpressing of *ShORR-1-G*, But Not *ShORR-1-M*, Enhanced Resistance to *On*

To further investigate the role of *ShORR-1-G* in resistance to *On*, stable RNAi and overexpressing MM transformants of *ShORR-1-G* and *ShORR-1-M* were generated. Samples collected at 65 hpi were microscopically examined, and percentages of germinated *On* conidiospores that developed into microcolonies on them were recorded. There were significantly fewer *On* microcolonies on leaves of transgenic plants overexpressing *ShORR-1-G* than on leaves of wild-type plants (**Figures 6A**, **C**). In addition, numerous clear mycelial colonies were macroscopically observed on leaves of control plants, while few were found on leaves of *ShORR-1-G* overexpressing plants (**Figure 6B**). The efficiency of gene overexpressing was confirmed by qRT-PCR analyses, which showed that *ShORR-1-G* transcript levels were 6.5-fold higher in the overexpressing lines than in control plants (**Figure 6D**). Moreover, fungal biomass was 4- to 5-fold lower on the

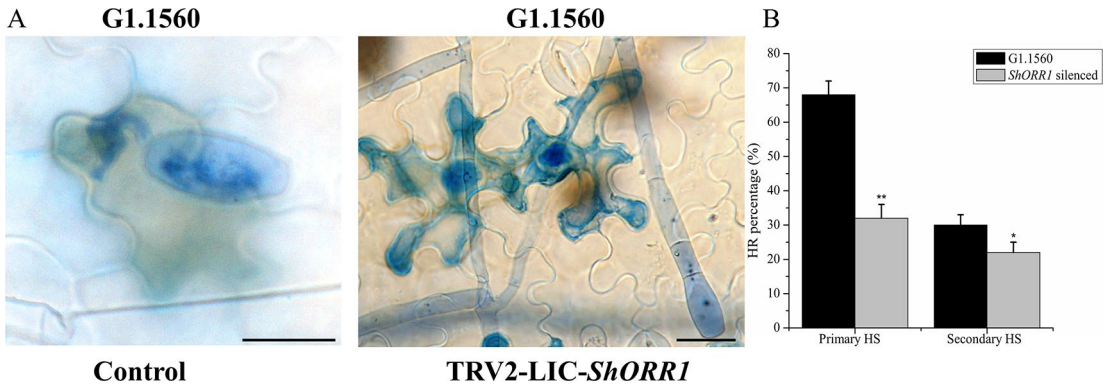

FIGURE 5 | *ShORR-1*-silenced plants show decreased *On*-induced HR formation and H_2O_2 accumulation. **(A)** Micrographs of resistant *S. habrochaites* G1.1560 without *ShORR-1* silencing (left) and *ShORR-1*-silenced *S. habrochaites* G1.1560 (right). Bar = 15 μm. **(B)** Percentages of HR-associated primary and secondary haustoria (HS) in *ShORR-1*-silenced and G1.1560 control plants. Asterisks indicate significant difference from the control by one-way ANOVA followed by an independent-samples Dunnett's *post hoc* test (**: $P < 0.01$, *: $P < 0.05$). Three biological replicates of microscopic samples of both *ShORR-1* silenced and control plants were observed.

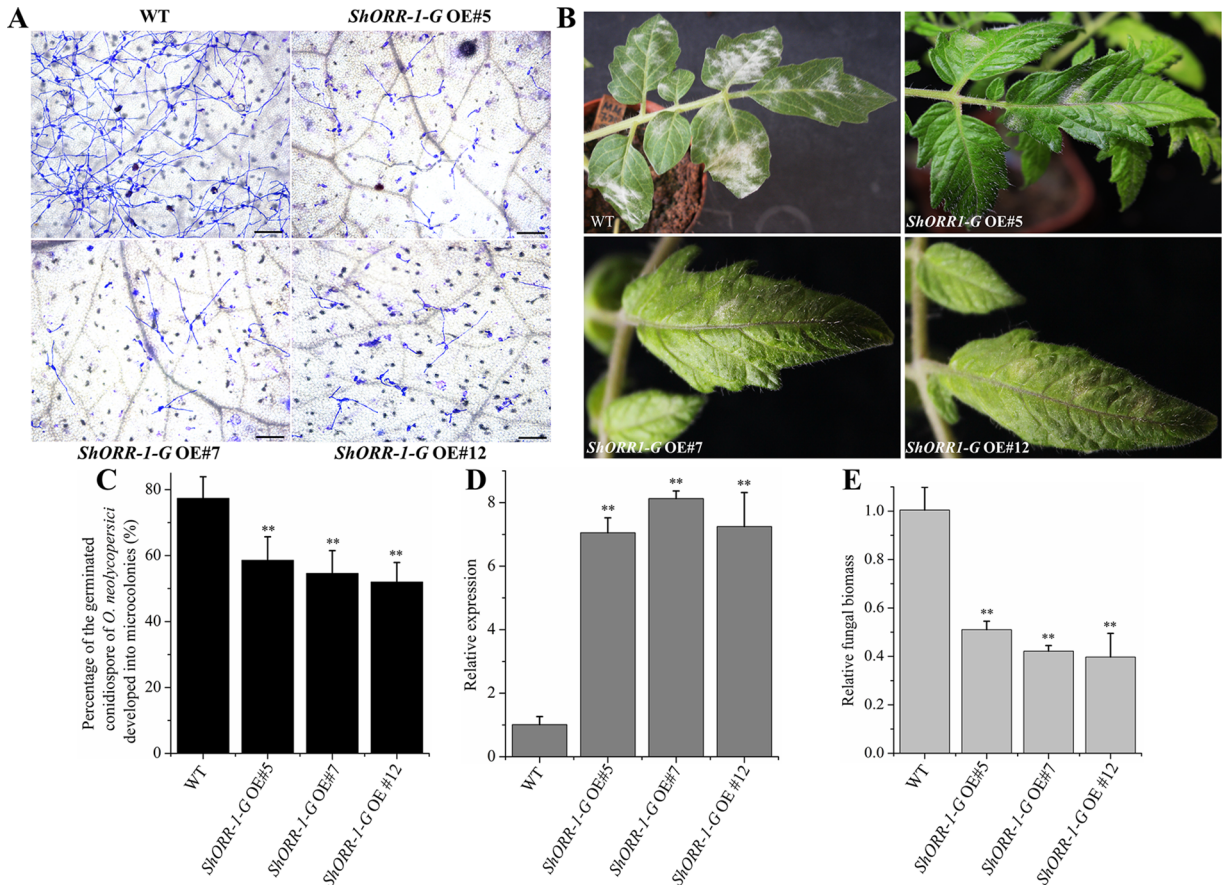

FIGURE 6 | Overexpressing of *ShORR-1-G* enhanced tomato plants' resistance to *On*. **(A)** Micrographs of powdery mildew on leaves of T2 *ShORR-1-G* overexpressing plants and untransformed MM plants, 65 h after inoculation. Scale bar = 25 μm. **(B)** Macroscopic phenotypes of *On* infected leaves of untransformed MM plants and T2 *ShORR-1-G* overexpressing plants. **(C)** Percentages of germinated *On* conidiospores on untransformed MM plants and T2 *ShORR-1-G* overexpressing plants at 65 h after infection. **(D)** Levels of *ShORR-1* transcripts in three transformed plants and controls. Double asterisks indicate significant differences from the control by one-way ANOVA followed by an independent-samples Dunnett's *post hoc* test ($P < 0.01$). **(E)** Estimated *On* fungal biomass on control plants and three transformed lines. All the above results are based on analyses of three biological replicates of control and transgenic plants.

ShORR-1-G overexpressing plants, according to genetically based estimates (**Figure 6E**).

However, microscopic observation indicated that overexpressing *ShORR-1-M* transgenic plants were more susceptible to *On* than control plants, while the plants with silenced *ShORR-1-M* had similar susceptibility to the controls (**Figures 7A**, **C**). Macroscopic observation confirmed these findings (**Figure 7B**). The gene silencing and overexpressing levels were confirmed by qRT-PCR analyses, which showed that *ShORR-1-M* transcript levels were dramatically lower in the gene-silenced plants and higher in the overexpressing transgenic plants than in the controls (**Figure 7D**). Quantification of fungal biomass confirmed that *ShORR-1-M* overexpressing increased the plants' susceptibility, but silencing of *ShORR-1-M* did not increase resistance to *On* (**Figure 7E**). These results clearly indicate that *ShORR-1-G* is required for *Ol-1* mediated resistance to *On* in tomato plants, while its homolog *ShORR-1-M* promotes susceptibility to *On*, presumably due to the differences in their sequences.

In addition, DAB staining revealed that H_2O_2 levels were higher in epidermal cells of *ShORR-1-G* overexpressing plants than in those of wild-type plants at 65 hpi with *On* (**Figure 8**). Thus, *ShORR-1-G* positively regulates resistance to *On* in tomato, and the resistance is associated with H_2O_2 accumulation. Moreover, upregulation of *ShORR-1-G* resulted in more abnormal haustoria (**Figure 9**, red arrows) in attacked cells than in untransformed plants. These haustoria were irregular and oval, had high H_2O_2 contents, and some seemed to be plasmolyzed (**Figure 9B**).

Overexpressing of *ShORR-1* Triggered or Suppressed Expression of Six Resistance Marker Genes

Induced plant defenses are regulated by a highly interconnected signaling network in which the plant hormones jasmonic acid (JA) and salicylic acid (SA) play central roles (Pieterse et al., 2009, Pieterse et al., 2012). To investigate pathways that may be recruited in defenses against powdery mildew in *ShORR-1-G* overexpressing tomato plants, we used qRT-PCR to analyze the expression of six defense genes involved in JA (*COI1*) and SA (*PR1*, *PR2*) pathways, HR (*HSR203J*, *BI1*) and other important aspects of disease resistance (*ROR2*). Three *ShORR-1-G* overexpressing transgenic lines and MM were chosen to probe expression levels of these six marker genes in the presence and absence of *On* infection. The qRT-PCR results revealed that

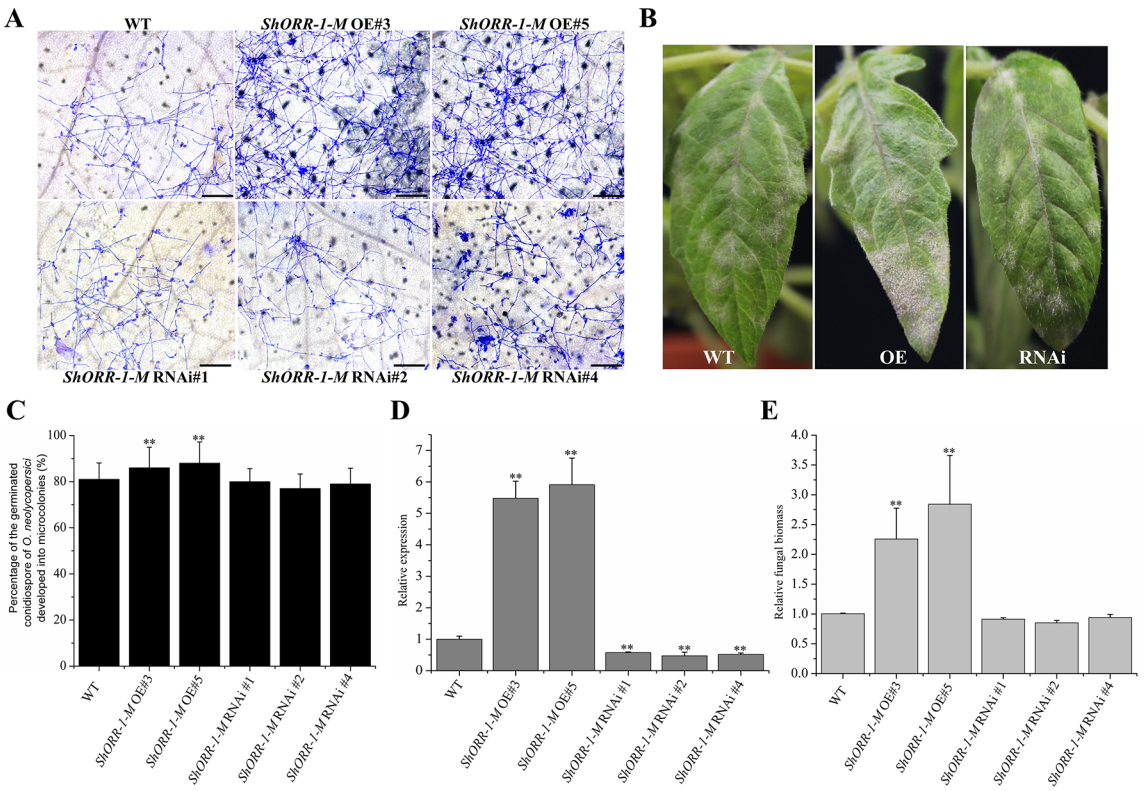

FIGURE 7 | Overexpressing of *ShORR-1-M* increased susceptibility to *On*, but silencing it did not increase resistance to *On*. **(A)** Micrographs of powdery mildew on leaves of T2 *ShORR-1-M* overexpressing and silenced plants, compared with untransformed MM plants, 65 h after inoculation. Scale bar = 25 μm. **(B)** Macroscopic phenotypes of *On* infected leaves of T2 *ShORR-1-M* overexpressing and silenced plants. **(C)** Percentages of germinated *On* conidiospores on *ShORR-1-M* overexpressing and silenced plants, 65 h after infection. **(D)** Levels of *ShORR-1* transcripts in transgenic plants and controls. Double asterisks indicate significant differences from the control by one-way ANOVA followed by an independent-samples Dunnett's *post hoc* test ($P < 0.01$). **(E)** Estimated *On* fungal biomass on transgenic and control plants. All the above results are based on analyses of three biological replicates of control and transgenic plants.

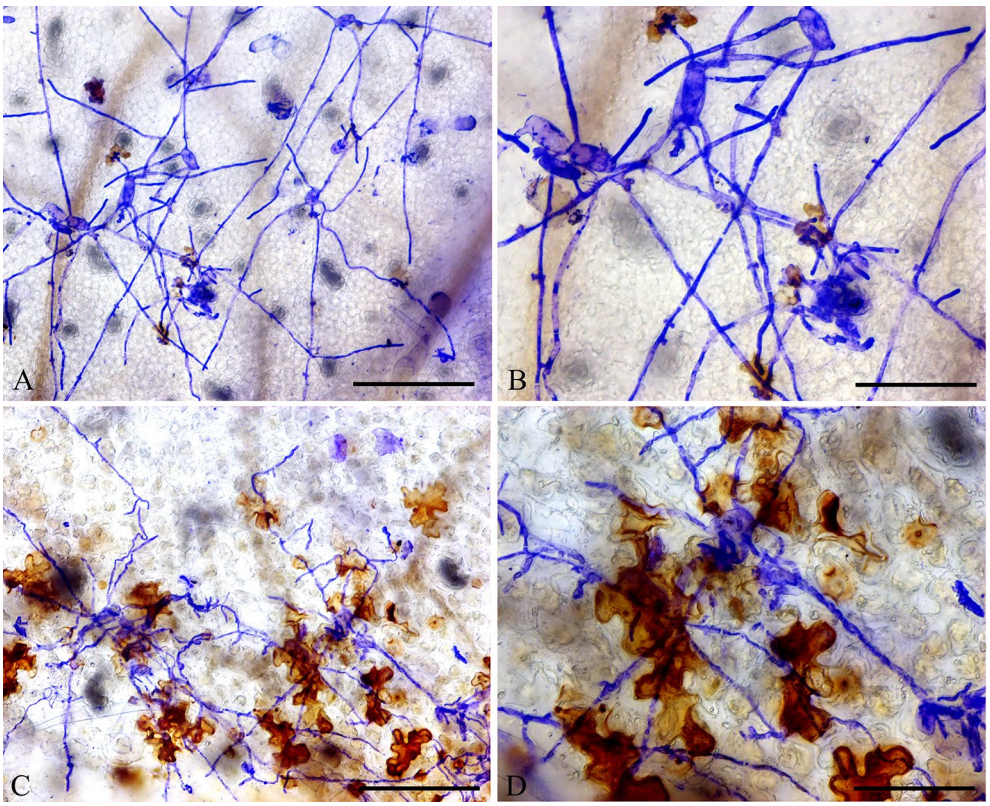

FIGURE 8 | Overexpressing of *ShORR-1-G* increased H_2O_2 accumulation in transgenic tomatoes. **(A)** Wild-type tomato leaves were inoculated with *On* and sampled 65 hours after infection. **(B)** Enlarged view of A. **(C)** *ShORR-1-G* overexpressing tomato leaves challenged with *On* and sampled 65 h after infection. **(D)** Enlarged view of **(C)**, showing H_2O_2 accumulation in epidermal cells, as manifested by 3,3-diaminobenzidine (DAB) staining. Scale bars = 25 μm in **(A** and **C)**, 12.5 μm in **(B** and **D)**.

SA, JA, and HR might be involved in tomato resistance to *On* mediated by *ShORR-1* (**Figure 10**).

PR1 and *PR2* (encoding β-1,3-glucanase; also called *BGL2*) have been widely used as molecular marker genes for the SA hormone pathway in plants (Glazebrook, 2005; López-Cruz et al., 2017; Yang et al., 2018; Miao et al., 2019; Wang et al., 2019). Our results showed that expression levels of *SlPR1* and *SlPR2* were higher in *On*-infected wild-type plants and *ShORR-1-G* overexpressing plants than in wild-type plants without *On* infection. Furthermore, *SlPR1* and *SlPR2* expression levels were dramatically higher (350- and 400-fold, respectively) in *On*-infected transgenic plants. Thus, powdery mildew infection dramatically induced expression of *SlPR1* and *SlPR2*, and overexpressing of *ShORR-1* enhanced this induction, in accordance with previous findings that the powdery mildew *Erysiphe orontii* can elicit accumulation of *PR1* and *PR2* in *Arabidopsis* (Lynnereuber et al., 2010). However, *On* inoculation did not significantly affect transcript levels of *SlCOI1*, encoding coronatine insensitive 1, a key component of JA-mediated defense pathways (Li et al., 2004), in wild-type plants, while it substantially suppressed *SlCOI1* expression in *ShORR-1-G* overexpressing plants. Moreover, we did not detect significant difference in expression levels of *SlHSR203J* and *SlBI1*—two important HR marker genes that are highly and rapidly induced in plant defense responses to various bacterial and fungal pathogens (Sanchez et al., 2000, Pontier et al., 2001)—between wild-type and *ShORR-1-G* overexpressing transgenic plants. However, *SlBI1* and (especially) *SlHSR203J* were induced more strongly by *On* in *ShORR-1-G* transgenic plants than in wild-type plants, and their expression levels correlated with the extent of HR. Required for *mlo*-specified resistance (*ROR2*), an essential component of *mlo*-mediated basal penetration resistance to barley powdery mildew, has a specialized resistance function that is conserved between monocotyledons and dicotyledons (Collins et al., 2003). We found that *SlROR2* was significantly induced in the *ShORR-1-G* overexpressing plants, with and without *On* inoculation, suggesting *ShORR-1-G* overexpression triggered this basal resistance.

DISCUSSION

Several DE-TDFs between powdery mildew-resistant NILs and the susceptible cultivar MM have been previously identified, including M14E72-213 (Li et al., 2006, Li et al., 2007). In the study presented here we found that M14E72-213 has high

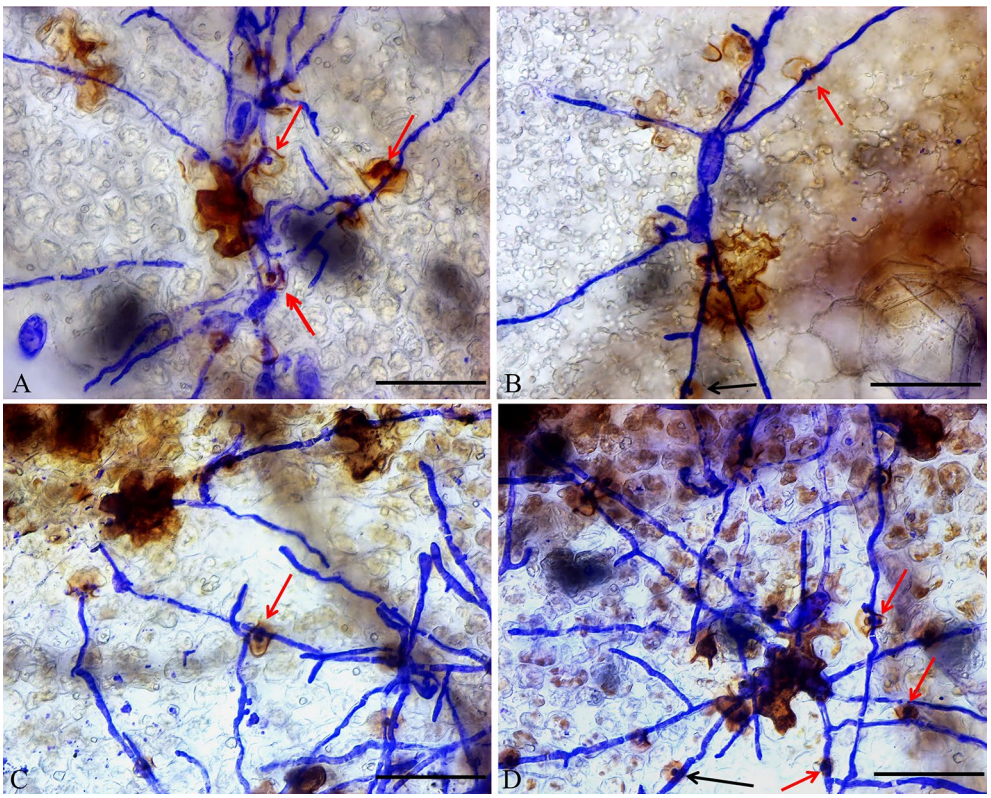

FIGURE 9 | Micrographs of haustorium phenotypes in *ShORR-1-G* overexpressing plants. Red and black arrows show morphologically abnormal and normal haustoria with high H_2O_2 contents, respectively. Scale bar = 12.5 μm. Panels **A**–**D** show the different haustorium phenotypes in *ShORR-1-G* overexpressing lines 5, 7, 12 and 13.

homology to a previously uncharacterized gene, which we named *ShORR-1*. By VIGS and overexpressing approaches, we demonstrated that a resistant variant of *ShORR-1* is essential for *Ol-1*-based resistance (**Figures 4** and **6**). Moreover, its overexpressing is associated with H_2O_2 accumulation (**Figure 8**) and abnormal haustoria (**Figure 9**), and hence enhances the resistance.

ShORR-1 Is a Novel and Indispensable Gene in *Ol-1*-Mediated Tomato Resistance to *On*

Silencing of *ShORR-1* in the resistant tomato cultivar *S. habrochaites* G1.1560 resulted in a susceptible phenotype, as shown by whole plant disease assays and microscopic analysis of *On*-infected plants (**Figure 4**). Downregulation of *ALS* and *ShGST*, two other DE-TDFs induced in NIL-*Ol-1*, both compromised tomato's resistance to powdery mildew caused by *On*, indicating that multiple resistance genes are involved in *Ol-1*-mediated resistance to *On* (Pei et al., 2011a; Gao et al., 2014).

We also found that silencing *ShORR-1-G* attenuated defense responses, i.e. rapid HR and H_2O_2 accumulation, which are normally induced strongly by infection with *On* in G1.1560 plants (**Figure 5**). The weakened responses (lacked by susceptible plants) were not sufficient to prevent growth and development of *On*. Similarly, knock-down of *ShGST* in G1.1560 tomato plants reduced resistance to *On*, and resulted in slow rather than rapid HR (Pei et al., 2011a). This response differed from the slow HR of the NIL-*Ol-1*, developed by backcrossing *S. habrochaites* G1.1560 with MM, in which cells invaded by primary fungal haustoria remained alive, and only cells invaded by secondary haustoria died (Li et al., 2006).

Furthermore, overexpressing of *ShORR-1-G* increased the *On* resistance of susceptible MM plants (**Figure 6**), and resulted in higher levels of H_2O_2 in their epidermal cells upon *On* attack than in wild-type plants (**Figure 8**). HR, which is frequently observed around the infection site when microbial pathogens attack, arrests development of the pathogen at the epidermal cell attacked (Perfect and Green, 2001; Salguero-Linares and Coll, 2019). H_2O_2 production closely accompanies HR, and is believed to be an important diffusive signal in programmed cell death. Our results suggest that *ShORR-1-G* (or another resistant variant of *ShORR-1*) is vital for resistance to powdery mildew caused by *On* in tomato, since its overexpressing enhanced HR, H_2O_2 levels and resistance to *On* infection, whereas there was less H_2O_2 accumulation in the highly susceptible MM. Moreover, in *ShORR-1-G* overexpressing plants we examined, and NIL-*Ol-1* plants examined by Li (2005), more abnormal haustoria were observed than in wild-type counterparts (**Figure 9**). Haustoria

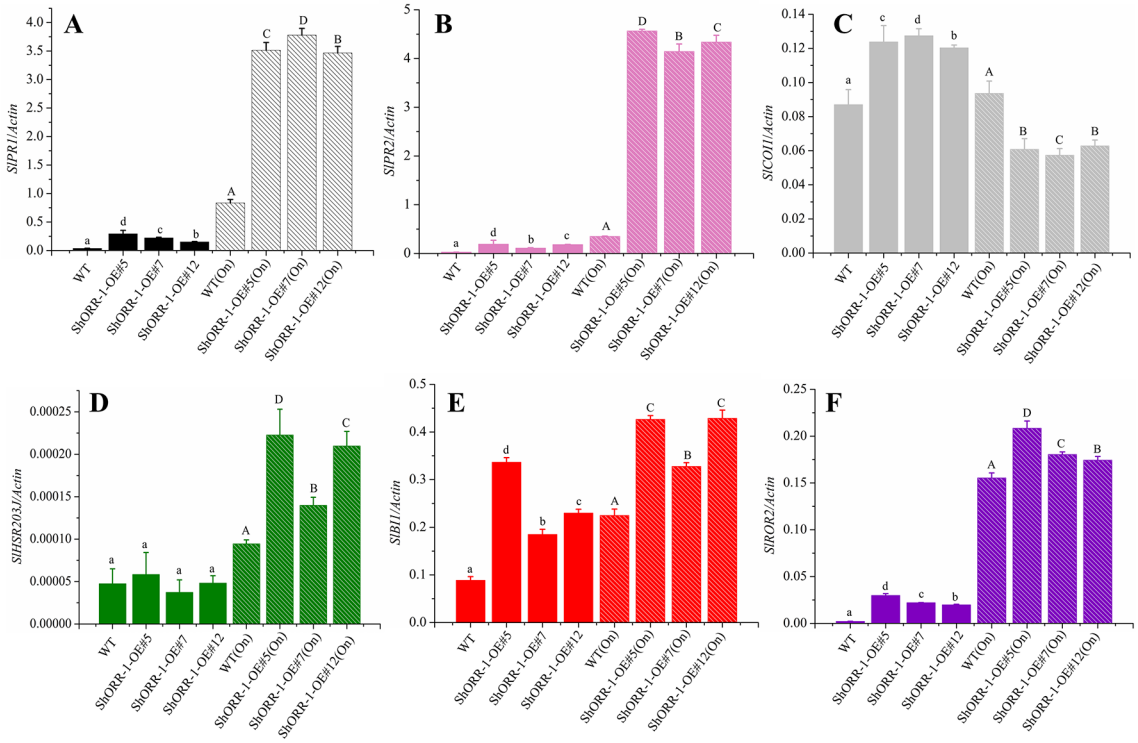

FIGURE 10 | Quantitative real-time PCR analysis of expression levels of the following selected defense marker genes in wild-type and *ShORR-1-G* overexpressing (OE) transgenic tomatoes with and without *On* infection: **(A)** *SlPR1*, **(B)** *SlPR2*, **(C)** *SlCOI1*, **(D)** *SlHSR203J*, **(E)** *SlROR2*, **(F)** *SlBI1*. *Actin* was used as an internal control. Value for each sample is mean of three biological replicates. Mean and standard error were calculated using data from three independent biological replicates. Lowercase letters were used to indicate significant differences between lines in untreated (without *On* infection) conditions, and capital ones indicate significant differences between lines after *On* infection. Upper and lowercase letters indicate significant differences relative to control (WT) plants determined by one-way ANOVA followed by Tukey's HSD test ($P < 0.05$).

are generally fungal pathogens' main structures for nutrient uptake (Roman-Reyna and Rathjen, 2017) and signal exchange (especially delivery of virulence effectors) with host plants (Hacquard et al., 2013). Our results suggest that the haustorial abnormalities in *ShORR-1-G* overexpressing plants at least partially prevented the fungus from absorbing nutrients and water from the host, thus reducing the extent of its growth and infection. However, in the NIL-*Ol-1* plants the abnormal haustoria were reportedly filled with small vesicles, which were not observed in the plants we examined, although abnormal plasmolyzed haustoria were found in both NIL-*Ol-1* (Li, 2005) and *ShORR-1* overexpressing plants. These findings suggest that the *Ol-1* and *ShORR-1* resistance mechanisms may have both similarities and differences.

ShORR-1 Variants in MM and G1.1560 Have Antagonistic Effects in Responses to *On*

M14E72-213 DE-TDF was found in NIL-*Ol-1*, but not either NIL-*Ol-4* or MM plants (Li et al., 2006, Li et al., 2007). However, ORFs of *ShORR-1* were isolated from both *On*-resistant NIL-*Ol-1* and *On*-susceptible MM plants (**Figure 1**), with mutations at 13 amino acid sequence sites. It indicated the above contrary was caused by the following, sequence analysis of ShORR-1-M and ShORR-1-G suggested that the mutation between two homologs at the 234th nucleotide base of ShORR-1-M was just at the annealing sequence region of selective primer E72 designed based on the recognition site of restriction enzyme (*EcoR* I) and selective nucleotide, sequence analysis also indicated that E72 can anneal at digested fragments of ShORR-1-G but not at those of ShORR-1-M (Li, 2005), which resulted in the DE-TDF of M14E72-213 was only identified in *ShORR-1-G* but not in *ShORR-1-M* in the cDNA-AFLP analysis using M14 (designed based on the recognition site of restriction enzyme (*Mse* I) and selective nucleotide) and E72 selective primer combination. Functional analysis showed that overexpressing of *ShORR-1-M* increased susceptibility to *On*, while *ShORR-1-M*-silenced plants phenotypically resembled untransformed controls (**Figure 7**). All the results indicate that *ShORR-1-G* plays a vital role in resistance to *On*, but not *ShORR-1-M*. Similarly, the *R* gene *PigmR* confers broad-spectrum resistance (*inter alia* to the blast fungus *Magnaporthe oryzae* in rice), while *PigmS* (which differs in four amino acids) competitively attenuates *PigmR* homodimerization to suppress resistance (Deng et al., 2017). Whether the mutation sites in resistant lines play important roles in *ShORR-1*-mediated *On* resistance needs

to be verified by site-specific mutation in future studies. In addition, sequences of ShORR-1-G and ShORR-1-M proteins respectively contain 20 and 19 serine phosphorylation sites (**Figure S1**), including in both cases a cluster of four potential MAPK phosphorylation sites (Ser-57, Ser-64, Ser-68, Ser-76) in the N terminus (**Figure S1**). Thus, ShORR-1 could be phosphorylated by MPKs, but this also requires verification.

JA, SA, HR, and Basal Resistance Are Involved in *ShORR-1*-Mediated Resistance to Powdery Mildew

Plants are not passive victims when attacked by microbial pathogens. SA-dependent signaling plays significant roles in plant resistance to biotrophic pathogens, especially powdery mildew, while the JA signaling pathway is important in resistance to necrotrophic pathogens, but there is complex crosstalk between the JA and SA signaling pathways (Glazebrook, 2005). When a plant is attacked by a biotrophic pathogen, this crosstalk leads to activation of the SA defense pathway and inhibition of the JA signaling pathway (Fu and Dong, 2013). We observed the same patterns in tomato plants infected by the powdery mildew *On*, especially *ShORR-1-G* overexpressing plants, in which the SA-related defense genes *SlPR1* and *SlPR2* were strikingly activated, but the JA-related defense gene *SlCOI1* was repressed. Various biotrophic pathogens have evolved intricate mechanisms that enable them to evade plant defenses by hijacking the JA pathway (Yan and Xie, 2016). Moreover, increasing evidence indicates that they inject effectors and toxins into plant cells that prevent the triggering of host defenses by targeting JA pathway components (Cole et al., 2014, Gimenez-Ibanez et al., 2014). Whether *ShORR-1* is associated with the SA- and JA-dependent pathways requires validation in further studies, for example by overexpressing *ShORR-1-G* in tomato lines with perturbances in the pathways, and/or screening for proteins that interact with ShORR-1 to elucidate the pathway(s) that ShORR-1 influences.

When attacked by fungal pathogens, HR is one of the most effective resistance responses (Salguero-Linares and Coll, 2019). The HR marker gene *SlHSR203J* is reportedly activated in tomato plants by the leaf mold pathogen *Cladosporium fulvum* (Pontier et al., 1998), and (in both susceptible and resistant tomato taxa) following exposure to *On* (Li, 2005). Our results confirmed that *On* significantly induced expression of *SlHSR203J*, accompanied by increases in numbers of epidermal cells displaying hypersensitive responses (**Figure 9**).

Another important gene in powdery mildew resistance is *Mildew Locus O* (*MLO*). Recessive loss-of-function (*mlo*) mutations in the gene confer resistance to powdery mildew in barley (Miklis et al., 2007), tomato (Bai et al., 2008), pepper (Zheng et al., 2013), pea (Pavan et al., 2011), wheat (Várallyay et al., 2012), and *Arabidopsis* (Consonni et al., 2006). The resistance mechanism is based on early abortion of fungal pathogenesis, with formation of papillae at attempted penetration sites (Bai et al., 2005). *ROR2* plays a major role in *mlo*-mediated disease resistance, and the barley *ror2* mutant reportedly has less penetration resistance but stronger HR than wild-type plants when attacked by barley powdery mildew (Collins et al., 2003). We found that both *On* infection and *ShORR-1-G* overexpressing induced expression of *SlROR2*, accompanied by higher frequencies of cells showing HR, especially in *ShORR-1-G* overexpressing tomatoes challenged by *On*. These findings suggest that upregulation of *SlROR2* might lead to formation of papillae, resulting in enhancement of resistance to *On*, but this hypothesis requires further validation.

In summary, *ShORR-1* (originally detected in the form of a DE-TDF in our previous cDNA-AFLP analysis) plays an essential role in *Ol-1*-mediated resistance. *ShORR-1-G* and *ShORR-1-M*, respectively cloned from G1.1560 and MM, have antagonistic roles in responses to *On*, presumably due to differences (13) in their amino acid sequences. Future research will decipher roles of mutation sites and analysis of the relationship of *ShORR-1* and *Ol-1* might provide new insights into the mechanisms of *Ol-1*-mediated tomato resistance to powdery mildew.

DATA AVAILABILITY STATEMENT

The datasets generated for this study can be found in the Genbank.

AUTHOR CONTRIBUTIONS

CL conceived and designed the research. YZ, KX, DP, GC, HY, and WZ performed the experiments. DY, JZ, and XL provided fungal materials, reagents, and analytical tools. YZ and DP analyzed the data, prepared figures, and wrote the paper. All authors read and reviewed the final manuscript.

FUNDING

This research was supported by the National Natural Science Foundation of China (grant nos. 31902030, 31571997, 31872129, 31071807, and 31272168), Natural Science Foundation of Henan province (grant no. 182300410058), Foundation of Henan Science and Technology Committee (grant nos. 192102110001 and 192102110124), and Training Program of Youth Backbone Teacher of Henan Province (grant no. 2017GGJS146).

ACKNOWLEDGMENTS

The authors gratefully acknowledge Professor David Baulcombe and Professor Liu Yule for providing the VIGS vectors and Dr. Bai Yuling for the seeds of wild-type tomato. We also thank the Plant Genetic Transformation Center of the Henan Key Laboratory of Crop Molecular Breeding & Bioreactor for providing the stable T2 transgenic tomatoes.

SUPPLEMENTARY MATERIAL

The Supplementary Material for this article can be found online at: https://www.frontiersin.org/articles/10.3389/fpls.2019.01400/full#supplementary-material

FIGURE S1 | Potential serine phosphorylation sites in ShORR-1-G **(A)** and ShORR-1-M **(B)** were predicted by DISPHOS (Version 1.3). The blue circles indicate putative MAPK phosphorylation sites in ShORR-1.

FIGURE S2 | Potential lysine ubiquitination sites of ShORR-1-G **(A)** and ShORR-1-M **(B)** were predicted by UbPred and graphed by IBS (Version 1.0). The threshold of confidence was set to be more than 0.69, and U indicates ubiquitination sites.

FIGURE S3 | Potential lysine SUMOylation sites of ShORR-1-G **(A)** and ShORR-1-M **(B)** were predicted by GPS-SUMO 2.0 Online Service and graphed by IBS (Version 1.0). Medium stringency (*Ac* > 89.12%, *Sn* > 67.93%, *Sp* > 90%, *MCC* > 0.3446, *Pr* > 21.96%) was chosen as the threshold for GPS-SUMO prediction, and S indicates SUMOylation sites.

REFERENCES

Bai, Y., Huang, C. C., van der Hulst, R., Meijer-Dekens, F., Bonnema, G., and Lindhout, P. (2003). QTLs for tomato powdery mildew resistance (Oidium lycopersici) in Lycopersicon parviflorumG1.1601 co-localize with two qualitative powdery mildew resistance genes. *Mol. Plant-Microbe Interact.* 16, 169–176. doi: 10.1094/MPMI.2003.16.2.169

Bai, Y., Pavan, S., Zheng, Z., Zappel, N. F., Reinstadler, A., Lotti, C., et al. (2008). Naturally occurringbroad-spectrum powdery mildew resistance in a Central American tomato accession is caused by loss of mlo function. *Mol. Plant-Microbe Interact.* 21, 30–39. doi: 10.1094/MPMI-21-1-0030

Bai, Y., van der Hulst, R., Bonnema, G., Marcel, T. C., Meijer-Dekens, F., Niks, R. E., et al. (2005). Tomato defense to Oidium neolycopersici: dominant Ol genes confer isolate-dependent resistance via a different mechanism than recessive ol-2. *Mol. Plant-Microbe Interact.* 18, 354–362. doi: 10.1094/MPMI-18-0354

Bai, Y., d., H. R., Huang, C. C., Wei, L., Stam, P., and Lindhout, P. (2004). Mapping Ol-4, a gene conferring resistance to Oidium neolycopersici and originating from Lycopersicon peruvianum LA2172, requires multi-allelic, single-locus markers. *Theor. Appl. Genet.*109, 1215–1223. doi: 10.1007/s00122-004-1698-5

Cole, S. J., Yoon, A. J., Faull, K. F., and Diener, A. C. (2014). Host perception of jasmonates promotesinfection by Fusarium oxysporum formae speciales that produce isoleucine- and leucine-conjugatedjasmonates. *Mol. Plant Pathol.* 15, 589–600. doi: 10.1111/mpp.12117

Collins, N. C., Thordal-Christensen, H., Lipka, V., Bau, S., Kombrink, E., Qiu, J. L., et al. (2003). SNARE-protein-mediated disease resistance at the plant cell wall. *Nat.* 425, 973–977. doi: 10.1038/nature02076

Consonni, C., Humphry, M. E., Hartmann, H. A., Livaja, M., Durner, J., Westphal, L., et al. (2006). Conserved requirement for a plant host cell protein in powdery mildew pathogenesis. *Nat. Genet.* 38, 716–720. doi: 10.1038/ng1806

Consortium, T. G. (2012). The tomato genome sequence provides insights into fleshy fruit evolution. *Nat.* 485, 635–641. doi: 10.1038/nature11119

Deng, Y., Zhai, K., Xie, Z., Yang, D., Zhu, X., Liu, J., et al. (2017). Epigenetic regulation of antagonistic receptors confers rice blast resistance with yield balance. *Sci.* 355, 962–965. doi: 10.1126/science.aai8898

Dodds, P. N., and Rathjen, J. P. (2010). Plant immunity: towards an integrated view of plant-pathogen interactions. *Nat. Rev. Genet.* 11, 539–548. doi: 10.1126/science.aai8898

Dong, Y., Burchsmith, T. M., Liu, Y., Mamillapalli, P., and Dineshkumar, S. P. (2007). A ligation-independent cloning tobacco rattle virus vector for high-throughput virus-induced gene silencing identifies roles for NbMADS4-1 and -2 in floral development. *Plant Physiol.* 145, 1161–1170. doi: 10.2307/40065758

Fu, Z. Q., and Dong, X. (2013). Systemic acquired resistance: turning local infection into global defense. *Annu. Rev. Plant Biol.* 64, 839–863. doi: 10.1146/annurev-arplant-042811-105606

Gao, D., Huibers, R. P., Loonen, A. E., Visser, R. G., Wolters, A. M., and Bai, Y. (2014). Down-regulation of acetolactate synthase compromises Ol-1-mediated resistance to powdery mildew in tomato. *BMC Plant Biol.* 14, 32. doi: 10.1186/1471-2229-14-32

Gimenez-Ibanez, S., Boter, M., Fernandez-Barbero, G., Chini, A., Rathjen, J. P., and Solano, R. (2014). The bacterial effector HopX1 targets JAZ transcriptional repressors to activate jasmonate signaling and promote infection in Arabidopsis. *PLoS Biol.* 12, e1001792. doi: 10.1371/journal.pbio.1001792

Glazebrook, J. (2005). Contrasting mechanisms of defense against biotrophic and necrotrophic pathogens. *Annu. Rev. Phytopathol.* 43, 205–227. doi: 10.1146/annurev.phyto.43.040204.135923

Hacquard, S., Kracher, B., Maekawa, T., Vernaldi, S., Schulzelefert, P., and Themaat, E. V. L. V. (2013). Mosaic genome structure of the barley powdery mildew pathogen and conservation of transcriptional programs in divergent hosts. *Proc. Natl. Acad. Sci. USA* 110, E2219–E2228. doi: 10.1073/pnas.1306807110

Huang, C. C., Groot, T., Meijer-Dekens, F., Niks, R. E., and Lindhout, P. (1998). The resistance to powdery mildew (Oidium lycopersicum) in Lycopersicon species is mainly associated with hypersensitive response. *Eur. J. Plant Pathol.* 104, 399–407. doi: 10.1023/a:1008092701883

Jones, J. D., and Dangl, J. L. (2006). The plant immune system. *Nat.* 444, 323–329. doi: 10.1038/nature05286

Li, C. (2005). "Transcriptional, microscopic and macroscopic investigations into monogenic and polygenic interactions of tomato and powdery mildew," in *Doctoral dissertation* (Netherlands: Wageningen University).

Li, C., Bai, Y., Jacobsen, E., Visser, R., Lindhout, P., and Bonnema, G. (2006). Tomato defense to the powdery mildew fungus: differences in expression of genes in susceptible, monogenic- and polygenic resistance responses are mainly in timing. *Plant Mol. Biol.* 62, 127–140. doi: 10.1007/s11103-006-9008-z

Li, C., Bonnema, G., Che, D., Dong, L., Lindhout, P., Visser, R., et al. (2007). Biochemical and molecular mechanisms involved in monogenic resistance responses to tomato powdery mildew. *Mol. Plant-Microbe Interact.* 20, 1161–1172. doi: 10.1094/mpmi-20-9-1161

Li, C., Pei, D., Wang, W., Ma, Y., Wang, L., Wang, F., et al. (2008). First report of powdery mildew caused by Oidium neolycopersici on tomato in China. *Plant Dis.* 92, 1370–1370. doi: 10.1094/PDIS-92-9-1370C

Li, L., Zhao, Y., Mccaig, B. C., Wingerd, B. A., Wang, J., Whalon, M. E., et al. (2004). The tomato homolog of CORONATINE-INSENSITIVE1 is required for the maternal control of seed maturation, jasmonate-signaled defense responses, and glandular trichome development. *Plant Cell* 16, 126–143. doi: 10.1105/tpc.017954

Lindhout, P., Beek, V. D. H., and Pet, G. (1994). Wild Lycopersicon species as sources for resistance to powdery mildew (Oidium lycopersicum): mapping of the resistance gene Ol-1 on chromosome 6 of L hirsutum. *Acta Hortic.* 376, 387–394. doi: 10.17660/ActaHortic.1994.376.53

Liu, Y., Schiff, M., Marathe, R., and Dinesh-Kumar, S. P. (2010). Tobacco Rar1, EDS1 and NPR1/NIM1 like genes are required for N-mediated resistance to tobacco mosaic virus. *Plant J.* 30, 415–429. doi: 10.1046/j.1365-313X.2002.01297.x

Livak, K. J., and Schmittgen, T. D. (2001). Analysis of relative gene expression data using real-time quantitative PCR and the 2(-Delta Delta C(T)) Method. *Methods* 25, 402–408. doi: 10.1006/meth.2001

López-Cruz, J., Óscar, C., Emma, F., Pilar, G., and Carmen, G. (2017). Absence of Cud Carmen, G. (2dismutase BCSOD1 reduces Botrytis cinerea virulence in Arabidopsis and tomato plants, revealing interplay among reactive oxygen species, callose and signalling pathways. *Mol. Plant Pathol.* 18, 16–31. doi: 10.1111/mpp.12370

Lynnereuber, T., Plotnikova, J. M., Dewdney, J., Rogers, E. E., Wood, W., and Ausubel, F. M. (2010). Correlation of defense gene induction defects with powdery mildew susceptibility in *Arabidopsis* enhanced disease susceptibility mutants. *Plant J.* 16, 473–485. doi: 10.1046/j.1365-313x.1998.00319.x

Mao, G., Meng, X., Liu, Y., Zheng, Z., Chen, Z., and Zhang, S. (2011). Phosphorylation of a WRKY transcription factor by two pathogen-responsive MAPKs drives phytoalexin biosynthesis in Arabidopsis. *Plant Cell* 23, 1639–1653. doi: 10.1105/tpc.111.084996

Miao, Y., Xu, L., He, X., Zhang, L., Shaban, M., Zhang, X., et al. (2019). Suppression of tryptophan synthase activates cotton immunity by triggering cell death via promoting SA synthesis. *Plant J.* 98, 329–345. doi: 10.1111/tpj.14222

Miklis, M., Consonni, C., Bhat, R. A., Lipka, V., Schulze-Lefert, P., and Panstruga, R. (2007). Barley MLO modulates actin-dependent and actin-independent antifungal defense pathways at the cell periphery. *Plant Physiol* 144, 1132–1143. doi: 10.1104/pp.107.098897

Nobuaki, I., Reiko, Y., Miki, Y., Shinpei, K., and Hirofumi, Y. (2011). Phosphorylation of the Nicotiana benthamiana WRKY8 transcription factor by MAPK functions in the defense response. *Plant Cell* 23, 1153–1170. doi: 10.1105/tpc.110.081794

Pavan, S., Schiavulli, A., Appiano, M., Marcotrigiano, A. R., Cillo, F., Visser, R. G. F., et al. (2011). Pea powdery mildew er1 resistance is associated to loss-of-function mutations at a MLO homologous locus. *Theor. Appl. Genet.* 123, 1425–1431. doi: 10.1007/s00122-011-1677-6

Pei, D., Ma, H., Zhang, Y., Ma, Y., Wang, W., Geng, H., et al. (2011a). Virus-induced gene silencing of a putative glutathione S-transferase gene compromised Ol-1-mediated resistance against powdery mildew in tomato. *Plant Mol. Biol. Rep.* 29, 972–978. doi: 10.1007/s11105-011-0331-4

Pei, D. L., Ma, H. Z., Zhang, Y., Ma, Y. S., Wang, W. J., Geng, H. X., et al. (2011b). Silencing a putative cytosolic NADP-malic enzyme gene comprised tomato resistance to Oidium neolycopersici. *Life Sci. J.* 8, 652–657.

Peng, Y., Wersch, R. V., and Zhang, Y. (2018). Convergent and divergent signaling in pamp-triggered immunity and effector-triggered immunity. *Mol. Plant-Microbe Interact.* 31, 403–409. doi: 10.1094/MPMI-06-17-0145-CR

Pieterse, C. M., Leon-Reyes, A., Van der, E. S., and Van Wees, S. C. (2009). Networking bysmall-molecule hormones in plant immunity. *Nat. Chem. Biol.* 5, 308–316. doi: 10.1038/nchembio.164

Pieterse, C. M., Van, d., D. D., Zamioudis, C., Leon-Reyes, A., and Van Wees, S. C. (2012). Hormonal modulation of plant immunity. *Annu. Rev. Cell Dev. Biol.* 28, 489–521. doi: 10.1146/annurev-cellbio-092910-154055

Perfect, S. E., and Green, J. R. (2001). Infection structures of biotrophic and hemibiotrophic fungal plant pathogens. *Mol. Plant Pathol.* 2, 101–108. doi: 10.1046/j.1364-3703.2001.00055x

Pontier, D., Balagu, C., Bezombes-Marion, I., Tronchet, M., Deslandes, L., and Roby, D. (2001). Identification of a novel pathogen-responsive element in the promoter of the tobacco gene HSR203J, a molecular marker of the hypersensitive response. *Plant J.* 26, 495–507. doi: 10.1046/j.1365-313x.2001.01049.x

Pontier, D., Tronchet, M., Rogowsky, P., Lam, E., and Roby, D. (1998). Activation of hsr203, a plant gene expressed during incompatible plant-pathogen interactions, is correlated with programmed cell death. *Mol. Plant-Microbe Interact.* 11, 544–554. doi: 10.1094/MPMI.1998.11.6.544

Radivojac, P., Vacic, V., Haynes, C., Cocklin, R. R., Mohan, A., Heyen, J. W., et al. (2010). Identification, analysis, and prediction of protein ubiquitination sites. *Proteins.* 78, 365–380. doi: 10.1002/prot.22555

Roman-Reyna, V., and Rathjen, J. P. (2017). Apoplastic sugar extraction and quantification from wheat leaves infected with biotrophic fungi. *Methods Mol Biol*. 1659, 125–134. doi: 10.1007/978-1-4939-7249-4_11

Salguero-Linares, J., and Coll, N. S. (2019). Plant proteases in the control of the hypersensitive response. *J. Exp. Bot.* 70, 2087–2095. doi: 10.1093/jxb/erz030

Sanchez, P., De Torres Zabala, M., and Grant, M. (2000). AtBI-1, a plant homologue of Bax Inhibitor-1, suppresses Bax-induced cell death in yeast and is rapidly upregulated during wounding and pathogen challenge. *Plant J.* 21, 393–399. doi: 10.1046/j.1365-313x.2000.00690.x

Shen, Q., Saijo, Y., Mauch, S., Biskup, C., Bieri, S., Keller, B., et al. (2007). Nuclear activity of MLA immune receptors links isolate-specific and basal disease-resistance responses. *Sci.* 315, 1098–1103. doi: 10.1126/science.1136372

Thordal-Christensen, H., Zhang, Z., Wei, Y., and Collinge, D. B. (2010). Subcellular localization of H2O2 in plants. H2O2 accumulation in papillae and hypersensitive response during the barley-powdery mildew interaction. *Plant J.* 11, 1187–1194. doi: 10.1046/j.1365-313X.1997.11061187.x

Trond, L., and Cathrine, L. (2009). Reference gene selection for quantitative real-time PCR normalization in tomato subjected to nitrogen, cold, and light stress. *Anal. Biochem.* 387, 238–242. doi: 10.1016/j.ab.2009.01.024

Várallyay, E., Giczey, G., and Burgyán, J. (2012). Virus-induced gene silencing of Mlo genes induces powdery mildew resistance in Triticum aestivum. *Arch. Virol.* 157, 1345–1350. doi: 10.1007/s00705-012-1286-y

Wang, L., Wen, R., Wang, J., Xiang, D., Wang, Q., Zang, Y., et al. (2019). Arabidopsis UBC13 differentially regulates two programmed cell death pathways in responses to pathogen and low-temperature stress. *New Phytol.* 221, 919–934. doi: 10.1111/nph.15435

Xu, K., Huang, X., Wu, M., Wang, Y., Chang, Y., Liu, K., et al. (2014). A rapid, highly efficient and economical method of Agrobacterium-mediated in planta transient transformation in living onion epidermis. *PLoS One* 9, e83556. doi: 10.1371/journal.pone.0083556

Yan, C., and Xie, D. (2016). Jasmonate in plant defence: sentinel or double agent? *Plant Biotechnol. J.* 13, 1233–1240. doi: 10.1111/pbi.12417

Yang, Y., Chen, T., Ling, X., and Ma, Z. (2018). Gbvdr6, a Gene Encoding a Receptor-Like Protein of Cotton (Gossypium barbadense), Confers Resistance to Verticillium Wilt in Arabidopsis and Upland Cotton. *Front. Plant Sci.* 8, 2272. doi: 10.3389/fpls.2017.02272

Zhao, Q., Xie, Y., Zheng, Y., Jiang, S., Liu, W., Mu, W., et al. (2014). GPS-SUMO: a tool for the prediction of sumoylation sites and SUMO-interaction motifs. *Nucleic Acids Res* 42, W325–W330. doi: 10.1093/nar/gku383

Zheng, Z., Nonomura, T., Appiano, M., Pavan, S., Matsuda, Y., Toyoda, H., et al. (2013). Loss of function in Mlo orthologs reduces susceptibility of pepper and tomato to powdery mildew disease caused by Leveillula taurica. *PLoS One* 8, e70723. doi: 10.1371/journal.pone.0070723

Conflict of Interest: The authors declare that the research was conducted in the absence of any commercial or financial relationships that could be construed as a potential conflict of interest.

frontiers in Plant Science

ORIGINAL RESEARCH
published: 27 November 2019
doi: 10.3389/fpls.2019.01551

TabZIP74 Acts as a Positive Regulator in Wheat Stripe Rust Resistance and Involves Root Development by mRNA Splicing

Fengtao Wang[1], Ruiming Lin[1], Yuanyuan Li[1], Pei Wang[1,2], Jing Feng[1], Wanquan Chen[1] and Shichang Xu[1]*

[1] State Key Laboratory for Biology of Plant Diseases and Insect Pests, Institute of Plant Protection, Chinese Academy of Agricultural Sciences, Beijing, China, [2] China Agricultural University, College of Plant Protection, Beijing, China

OPEN ACCESS

Edited by:
Laura Bertini, Università degli Studi della Tuscia, Italy

Reviewed by:
Lei Huang, Purdue University, United States
Urmil Bansal, University of Sydney, Australia
Lili Huang, Northwest A&F University, China

***Correspondence:**
Ruiming Lin
linruiming@caas.cn

Specialty section:
This article was submitted to Plant Microbe Interactions, a section of the journal Frontiers in Plant Science

Received: *20 July 2019*
Accepted: *06 November 2019*
Published: *27 November 2019*

Citation:
Wang F, Lin R, Li Y, Wang P, Feng J, Chen W and Xu S (2019) TabZIP74 Acts as a Positive Regulator in Wheat Stripe Rust Resistance and Involves Root Development by mRNA Splicing. Front. Plant Sci. 10:1551. doi: 10.3389/fpls.2019.01551

Basic leucine zipper (bZIP) membrane-bound transcription factors (MTFs) play important roles in regulating plant growth and development, abiotic stress responses, and disease resistance. Most bZIP MTFs are key components of signaling pathways in endoplasmic reticulum (ER) stress responses. In this study, a full-length cDNA sequence encoding bZIP MTF, designated *TabZIP74*, was isolated from a cDNA library of wheat near-isogenic lines of Taichung29*6/*Yr10* inoculated with an incompatible race CYR32 of *Puccinia striiformis* f. sp. *tritici* (*Pst*). Phylogenic analysis showed that *TabZIP74* is highly homologous to *ZmbZIP60* in maize and *OsbZIP74* in rice. The mRNA of *TabZIP74* was predicted to form a secondary structure with two kissing hairpin loops that could be spliced, causing an open reading frame shift immediately before the hydrophobic region to produce a new TabZIP74 protein without the transmembrane domain. *Pst* infection and the abiotic polyethylene glycol (PEG) and abscisic acid (ABA) treatments lead to *TabZIP74* mRNA splicing in wheat seedling leaves, while both spliced and unspliced forms in roots were detected. In the confocal microscopic examination, TabZIP74 is mobilized in the nucleus from the membrane of tobacco epidermal cells in response to wounding. Knocking down *TabZIP74* with barley stripe mosaic virus-induced gene silencing (BSMV-VIGS) enhanced wheat seedling susceptibility to stripe rust and decreased drought tolerance and lateral roots of silenced plants. These findings demonstrate that *TabZIP74* mRNA is induced to splice when stressed by biotic and abiotic factors, acts as a critically positive regulator for wheat stripe rust resistance and drought tolerance, and is necessary for lateral root development.

Keywords: common wheat, *Puccinia striiformis* f. sp. *tritici*, bZIP transcription factor, endoplasmic reticulum stress, mRNA splicing, disease resistance

INTRODUCTION

Plant pathogens, including fungi, viruses, bacteria, oomycetes, and nematodes, cause severe yield losses in crop production. To defend themselves against disease, plants have evolved different defense mechanisms against attackers. The first layer of defense is activated by athogen-associated molecular patterns (PAMPs) or microbe-associated molecular patterns (MAMPs). This kind of defense is referred

to as PAMP triggered immunity (PTI) or MAMP triggered immunity (MTI) and defend the plant against non-specialized pathogens. This type of defense is perceived by plasma membrane receptors, which rely on protein maturation and endoplasmic reticulum (ER) protein folding quality control (Li et al., 2009; Lu et al., 2009; Nekrasov et al., 2009; Saijo et al., 2009) and the secretion of anti-microbial proteins to the apoplast (van Loon et al., 2006).

Secretory proteins are synthesized and folded in ERs, and proper folding is needed to transport the proteins to their final destinations. Perturbations of this folding process result in ER stress, which is critical for rapid and effective basal immune responses of plant hosts (Wang et al., 2005). Regulation of ER capacity is important for immune signaling (Korner et al., 2015). The ER stress triggers cytoprotective signaling pathways, titled the unfold protein response (UPR), this signaling pathway restores and maintains ER homeostasis. There is growing recognition that ER stress responses are involved in normal plant development (Deng et al., 2016; Kim et al., 2018; Bao et al., 2019); for example, ER stress is involved in the cells synthesizing and secreting materials comprising the pollen coat (Deng et al., 2016).

There are two arms of the ER stress signaling pathway in plants, one of which encompass membrane-associated transcription factors (MTFs) through proteolytic cleavage, such as the MTFs of AtbZIP17 (Liu et al., 2007b), AtbZIP28 (Liu et al., 2007a; Tajima et al., 2008), ZmbZIP17 (Yang et al., 2013), and OsbZIP39 (Takahashi et al., 2012), which are mobilized from ERs to golgi apparatus in plant cell where they are released by site 1 and site 2 proteases (S1P and S2P) (Liu et al., 2007a; Sun et al., 2015). The other ER stress signaling pathway functions through inositol requiring enzyme 1 (IRE1) and the splicing of target RNA, such as *bZIP60*, which encodes an MTF of basic leucine zipper (bZIP) (Liu and Howell, 2010; Howell, 2013). Splicing of target mRNA lead a frame shift of ORF and produces a new protein without a transmembrane domain (TMD) in its C-terminal. Many MTF genes, such as *XBP1* in yeast (Yoshida et al., 2001), *AtbZIP60* in Arabidopsis (Deng et al., 2011), *OsbZIP50/OsbZIP74* in rice (Hayashi et al., 2012), and *ZmbZIP60* in maize (Li et al., 2012) are activated by the IRE1 depended mRNA splicing pathway.

The bZIP TF family is one of the largest families in plants, with the most diverse biological functions (Jakoby et al., 2002); several of its members, including *AtbZIP60*, *NtbZIP60,* and *OsbZIP50*, are membrane-associated bZIP factors, which fundamentally contribute to ER stress in plant basal immune responses. For example, *Arabidopsis thaliana* gene *bZIP60* encoding an MTF is strongly induced to express by tunicamycin, an ER stress-inducing chemicals (Iwata and Koizumi, 2005), before translocating its protein without TMD into the cell nucleus and upregulating mRNA expression levels of several ER-resident chaperones, sucn as binding protein (BiP) and protein-disulfide isomerases (Iwata and Koizumi, 2005; Lu and Christopher, 2008). In tobacco, expression of *NtbZIP60* was significantly upregulated upon infection with a non-host pathogen *Pseudomonas cichorii*, but not induced by a compatible pathogen *Pseudomonas syringae* pv. *Tabaci* (Tateda et al., 2008). Defense-related plant hormones salicylic acid, induced mRNA splicing of *AtbZIP60* and *OsbZIP50/OsbZIP74* (Hayashi et al., 2012; Lu et al., 2012; Moreno et al., 2012; Parra-Rojas et al., 2015), being the hallmark of IRE1-linking activation of an ER stress regulation defense responses in both Arabidopsis and rice (*Oryza sativa* L.). Abiotic stresses of heat and drought may also lead to splicing of *ZmbZIP60* and *TabZIP60,* (Geng et al., 2018; Li et al., 2018) and *BhbZIP60* mRNAs (Wang et al., 2017), respectively.

In this study, we characterized a gene designated *TabZIP74* from common wheat (*Triticum aestivum* L.), encoding a homologous TF protein of *AtbZIP60* or *OsbZIP74*. The results indicated that the mRNA sequence of *TabZIP74* was spliced in the progress of *Pst* infection and drought stress, which encoded a nucleus-localized factor by frame shift. The spliced mRNA was also detected in stem nodes, roots, and stigmas during normal wheat development. Knocking down the spliced form of *TaZIP74* increased the susceptibility level to stripe rust and decreased drought tolerance. Thus, *TaZIP74* functions as a positive regulator for stripe rust infection and drought tolerance.

MATERIALS AND METHODS

Plant Growth, Biotic Stress, and Chemical Treatments

Wheat near-isogenic lines (NILs) containing the resistant gene *Yr10* (Taichung 29*6/*Yr10*) are resistant to some races of *Pst* in China, while its backcross parent Taichung 29 is highly susceptible (Wan et al., 2004; Chen et al., 2014). We constructed a full-length cDNA library of NIL Taichung 29*6/*Yr10* infected with *Pst* races CYR34 (compatible race) and CYR17 (incompatible race). Wheat seedlings were grown in 8-cm pots and cultivated at 20°C under a 14 h/10 h day/night photoperiod cycle. Seven-day-old seedlings were inoculated with *Pst* races CYR34 and CYR17, or two-week-old wheat seedlings were treated with 5 μg ml^{-1} tunicamycin (TM, ER stress agent) for 4 h. Samples were collected at 0, 6, 12, 24, 36 and 48 h post-inoculation (hpi). To analyze the expression patterns of *TabZIP74* under exogenous plant hormone application and drought stress, 10-day-old seedlings of Taichung 29*6/*Yr10*, cultured in fresh quarter-strength Hoagland solution, were treated with 0.1 mM abscisic acid (ABA) or 20% polyethylene glycol (PEG). Both the leaves and roots of treated plants were sampled at 0, 3, and 6 h post-treatment (hpt). Flag leaves, anthers, stigmas, stem internodes, stem nodes, and roots were sampled at the flowering stage (Feeks 10.5.1). All samples were immediately frozen in liquid nitrogen and stored at –80°C for RNA isolation.

Gene Expression Analysis

Total RNA of each wheat sample was extracted using TRIZOL reagent according to the manufacturer's protocol (Invitrogen, USA). The RNA was used to synthesize first-strand cDNA using a TransScript II One-Step gDNA Removal and cDNA Synthesis SuperMix Kit (TransGen Biotech). Reverse transcription (RT)-PCR was performed using TransTaq HiFi PCR SuperMix (TransGen Biotech) and detected by 1.5% agarose gel for gene-spliced assays (Wang et al., 2015). Two pairs of specific primers flanking the splice site were designed to distinguish unspliced (bzipSPassayf1/bzipSPassayr1) and spliced (bzipSPassayf1/bzipSPassayr2) forms of *TabZIP74*. *Ta54227* transcripts of the AAA-superfamily of ATPases (Paolacci et al., 2009) and *NbEF1*

were used as controls in the semi-quantitative RT-PCR analyses of unspliced and spliced mRNA forms for expression in wheat or tobacco. Primer sequences are listed in **Table 1**.

Quantitative RT-PCR (qRT-PCR) was performed on the basis of reported by Wang et al., 2015, GoTaq® qPCR Master Mix (Promega) and ABI7500 Real-Time PCR System (Applied BioSystems) were used. Dissociation curves were generated to ensure specific amplification for each reaction. Each PCR reaction was performed three times. The threshold values (C_T) were used to quantify relative gene expression using the comparative threshold ($2^{-\Delta\Delta CT}$) method (Schmittgen and Livak, 2008). *Ta54227* transcripts of the AAA-superfamily of ATPases (Paolacci et al., 2009) were used as a control for the qRT-PCR analyses of the expression level of *TabZIP74* in VIGS plants. Each experiment were performed three replicates. The statistic software SPSS 16.0 (SPSS Inc., USA, http://spss.en.softonic.com/) was used to assy significant differences using one-way ANOVA, taking $P < 0.05$ as significant according to Duncan's multiple range test.

Sequence Analysis of *TabZIP74*

Gene sequences were analyzed on the basis of reported by Wang et al., 2015, mainly including DNAMAN software (Lynnon Biosoft, USA) and on line analysis by BLAST and ORF Finder on the NCBI website (http://www.ncbi.nlm.nih.gov/). Multiple sequence alignments were deduced, and a phylogenetic tree generated using the neighbor-joining method with Clustal X version 2.0 (Larkin et al., 2007). The phylogenetic comparison of isolated full-length *TabZIP74*, reported bZIP proteins (Sornaraj et al., 2015) and those derived from GenBank were constructed from the neighbor-joining algorithm using MEGA7 program (Kumar et al., 2016), the bootstrap re-sampling analysis was performed with bootstrap trials = 1000. The sequence of *TabZIP74* was blasted on the Ensembl Plants website (http://plants.ensembl.org/index.html) to get chromosome location of *TabZIP74*.

Subcellular Localization

To confirm subcellular localization of TabZIP74, fusion-plasmid expression vectors of TabZIP74-eGFP, TabZIP74-eGFPΔC, and eGFP-TabZIP74, containing either a complete or C-terminal truncated sequence of *TabZIP74* cDNA, were constructed (**Figure 3A**). For TabZIP74-eGFP expression vector construction, the encoding region delete the stop codon was amplified by PCR with forward primer sequence TabZIP74subf (5'-TA*GCATCC*ATGGACACCGACCTCGACCT-3', *BamH* | site in italics) and reverse primer sequence TabZIP74subr (5'-TA*TCTAGA*CTAGCAAGCGGCAGCTGCA-3', *Xba* | site in italics). For the C-terminal deleted sequence expression vector (TabZIP74-eGFPΔC) construction, the forward primer TabZIP74subf and reverse primer sequence TabZIP74ΔCsubr (5'-TAT*TCTAGA*CGAAAGTACGGCAGACTCCT-3', *Xba* | site in italics) were used. To construct the eGFP-TabZIP74 expression vector, the encoding region delete the stop codon was amplified by high-fidelity DNA polymerase HIFI Taq (TransGen Biotech) using forward primer eG-bZIP74f(5'-TA*GGATCC*ATGGACACCGACCTCGACCT-3', *BamH* | site in italics) and reverse primer eG-bZIP74r (5'-AT*TCTAGA*CTAGCAGCGGCAGCTGCA-3', *Xba* | site in italics). The PCR product was cloned into the binary vectors with eGFP in front or in the back of inserted sequences to produce different fusion vectors. These fusion vector plasmids were introduced into *A. tumefaciens* strain GV3101. Tobacco epidermal cells were infiltrated with *A. tumefaciens* strain GV3101 containing a binary vector encoding GFP-fusion construct for transient expression. 24 h post incubation at 25°C, fluorescence of the GFP images of the transformed tobacco epidermal cells was observed with a confocal microscope (Zeiss LSM 880 Confocal Microscope).

TABLE 1 | RT-PCR and qRT-PCR primers used for analyzing *TabZIP74* expression in wheat and tobacco.

Name	Sequence (5'-3')
Ta54227f	CAAATACGCCATCAGGGAGAACATC
Ta54227r	CGCTGCCGAAACCACGAGAC
bzipSPassayf1	ATGAAGTCCAGGGAGAGGAAGA
bzipSPassayr1	GACAGGGAAACCAGCGGCAGAC
bzipSPassayr2	CAGGGTTTCCGAAAGTACGGCA
NbEF1f	TGGTGTCCTCAAGCCTGGTAT
NbEF1r	ACGCTTGAGATCCTTAACCGC

Transcriptional Activation Analysis in Yeast

To investigate the transcriptional activity of TabZIP74, the complete open reading frame (ORF) and C-terminal deleted cDNA fragment of *TabZIP74* were amplified using the primer combinations (for complete ORF primers: TF1 5'-ATA*GTCGAC*ATGGACACCGACCTCGAC-3'andTR15'-TA*CTGCAG*CTAGCAAGCGGCAGCTGCA -3'; for C-terminal deleted sequence primers: TF1 5'- ATA*GTCGAC*ATGGACACCGACCTCGAC -3' and primer TR2 5'- TA*CTGCAG*GTTCTGGCGCAGTGCCATGTT -3', *Pst* I and *Sal* I sites in italics) and fused in the encoding region of GAL4 DNA-binding domain (GAL4-BD) in yeast expression vector pGBKT7, and vectors of pGBKT7-TabZIP74 and pGBKT7-TabZIP74ΔC were constructed for analyzing transcriptional activity of TabZIP74. The empty vector pGBKT7 was used as a negative control. All the vectors were transformed into yeast strain AH109. The different transformants were streaked on medium plates containing SD/Trp- (yeast synthetic drop-out medium supplement without tryptophan) (Clontech, USA) or SD/Trp-/His-/Ade- (yeast synthetic drop-out medium supplement without tryptophan, histidine, or adenine) (Clontech, USA). Incubation at 28°C for 3 d, then evaluated the growth status of the transformants.

Functional Analysis in Response to *Pst* Infection

Wheat Barley Stripe Mosaic Virus (BSMV)-induced gene silencing assay was conducted as described by Yuan et al. (2011). Specific sequences of wheat *TaPDS* (primer pairs: vTaPDSf, 5'-*AAGGAAGTTTAA*CTGCATAAACGCTTAAAAG-3', and vTaPDSr, 5'-*AACCACCACCACCGT*TCTCCAGTTATTTGAG-3', LIC adapters in italics), *TabZIP74* (primer pairs: vTabZIP74f 5'-*AAGGAAGTTTAA*CCAACCGAAGTCTGGTGGCT-3' and vTabZIP74r, 5'-*AACCACCACCACCGT*CTAGCAAGCGGCAG

CTGCA-3', ligation-independent cloning (LIC) adapters in italics) were amplified and inserted into vector pCa-γbLIC. For gene function analysis with VIGS, two-week-old common wheat cultivar Fengchan 3 were planted in a growth chamber under a 16 h/8 h day/night photoperiod cycle at 16 ± 2°C. The second leaf surface was inoculated with *Nicotiana benthamiana* leaf sap containing BSMV particles (Mock, BSMV, BSMV-*TabZIP74*, BSMV-*TabZIP74sp*) by gently sliding pinched fingers from the leaf base to the tip. Treated with sterile water as Mock control. The inoculated seedlings were placed in a growth chamber in the dark at 60% humidity, 22 ± 2°C and kept under a 16 h/8 h day/night photoperiod. Nine d after virus inoculation, the phenotypes of wheat seedlings were observed and photographed. Fengchan 3 is highly susceptible to the virulent *Pst* race of CYR32, and its seedlings pre-inoculated with BSMV were successfully infected. Fresh urediniospores of stripe rust race CYR34 were inoculated onto the surface of the third leaves with a paintbrush 14 d after pre-inoculating with the virus. Three independent biological replications were performed for each treatment. The *Pst* infection phenotypes were recorded and photographed from 8 to 16 d post-inoculation (dpi). The latend period and number of uredinia on 6-cm long inoculated leaf fragments was recorded at 16 dpi.

Functional Analysis in Response to Drought

To examine whether *TabZIP74* is involved in wheat responses to drought stress, the leaf relative water content (RWC) of Mock, BSMV, and BSMV-TabZIP74 plants was determined (Mao et al., 2012). Different virus-pretreated plants were subjected to drought stress by withholding water supply for 10 d, after 10 d rewatering. Development of the treated plants was routinely monitored by record the symptoms of leaf rolling and leaf RWC.

Measurement of Primary and Lateral Root Lengths

To evaluate the role of *TabZIP74* in the wheat rooting pattern, five-day-old seedlings of Mock, BSMV, and BMSV-TabZIP74 were transferred to fresh quarter-strength Hoagland solution and grown vertically for 20 d at 22°C, under a 16 h/8 h day/night photoperiod. Photographs were recorded with a digital camera, lateral root number in the distal end of primary roots were determined by ImageJ software (http://rsbweb.nih.gov/ij/download.html). The number of lateral roots on 10 plants was calculated, and the mean of lateral roots was used to measure lateral root growth. Three biological replications were performed.

RESULTS

Sequence Analysis of Putative *TabZIP74*

According to the EST sequence of a differentially expressed bZIP gene in responsing to stripe rust infection, the sequence was cloned from a cDNA library of NIL Taichung 29*6/*Yr10*. The 1,096- base-pair (bp) cDNA clone contains a 909-bp ORF, encoding a putative bZIP74 TF of 302 amino acid residues sharing high identity with MTFs such as *OsbZIP74*, *ZmbZIP60*, *NtbZIP60*, *HvbZIP74,* and *SibZIP50* (**Figure 1A**). Furthermore, genomic sequence blast results indicated *TabZIP74* is located on wheat chromosome 7D.

The phylogenetic tree constructed with TabZIP74 protein and other reported bZIP protein in *Arabidopsis* and rice indicated that different groups of bZIP factors were distinguished and named based on their phylogenetic relationships and functional divergence. The maximum likelihood analysis of bZIP proteins, including TabZIP74, identified 10 bZIP factors from rice, three from maize, one from tobacco and 73 from Arabidopsis in 11 distinct clades (A–I, S, and U), all of which had high bootstrap value support (**Figure 1B**).

The phylogenetic analysis revealed that *TabZIP74* was most homologous to *OsbZIP74* (LOC_Os06g41770) in the rice genome (Correa et al., 2008) and *ZmbZIP60* in maize (*Zea mays* L.) (**Figures 1A, B**). OsbZIP74 also named as bZIP50 (Os06g0622700) in the Rice Annotation Project Database (Wakasa et al., 2011) and is an important ER stress regulator in rice (Lu et al., 2012).

TabZIP74 mRNA Splicing in Response to Biotic and Abiotic Factors

TabZIP74 has a high level of identity to OsbZIP74 with regard to amino acid sequences. Interestingly, the mRNA sequence of *TabZIP74* can form two kissing hairpin loops through an RNA secondary structure prediction program Centroidfold (http://rtools.cbrc.jp/centroidfold/) (Hamada et al., 2009), and potentially produce its unspliced (*TabZIP74-USP*) and spliced (*TabZIP74-SP*) forms. The spacer between two hairpin loops in *TabZIP74* comprises only two nucleotides, the same as *OsbZIP74* (**Figures 2A, B**).

Speicific primers flanking the predicted *TabZIP74* splice sites was designed and used for RT-PCR analysis to assay the splicing of *TabZIP74* (**Figure 2C**). When wheat seedling leaves were treated with 5 μg ml^{-1} tunicamycin (TM) for 4 h, one normal cDNA band and another smaller one were detected with RT-PCR in agarose gel electrophoresis. The sequencing result showed that a 20 bp fragment was spliced from the original *TabZIP74* mRNA molecule in response to TM treatment (**Figure 2A**). The specific primers were also used to discriminate the unspliced (USP) and spliced (SP) forms of *TabZIP74* after infection with *Pst*. When wheat seedlings were inoculated with two *Pst* races (CYR17, avirulent; CYR34, virulent), both induced *TabZIP74* mRNA molecules for splicing (**Figures 2D, E**). In contrast, the abiotic factor PEG triggered *TabZIP74* to be spliced in the roots of treated wheat seedlings (**Figure 2F**), while ABA induced splicing in both leaves and roots of stressed seedlings (**Figure 2G**). *TabZIP74* mRNA splicing also occurred in stigmas, stem nodes, and roots of adult wheat plants (**Figure 2H**), but not in unstressed seedling leaves (**Figures 2 D–F, H**).

Subcellular Localization of TabZIP74

To investigate the subcellular localization of TabZIP74 in plant cells, different types of fusion protein with eGFP were constructed and these fusion vectors were transiently expressed in *Nicotiana benthamiana* leaf epidermal cells infiltrated with *Agrobacterium tumefaciens* cells of strain GV3101, containing a vector of TabZIP74-eGFP, TabZIP74-eGFPΔC or eGFP-TabZIP74 (**Figure 3A**). Confocal microscopic examination showed that the TabZIP74-GFP protein bound only to the plasma membrane and the TabZIP74-ΔC-GFP

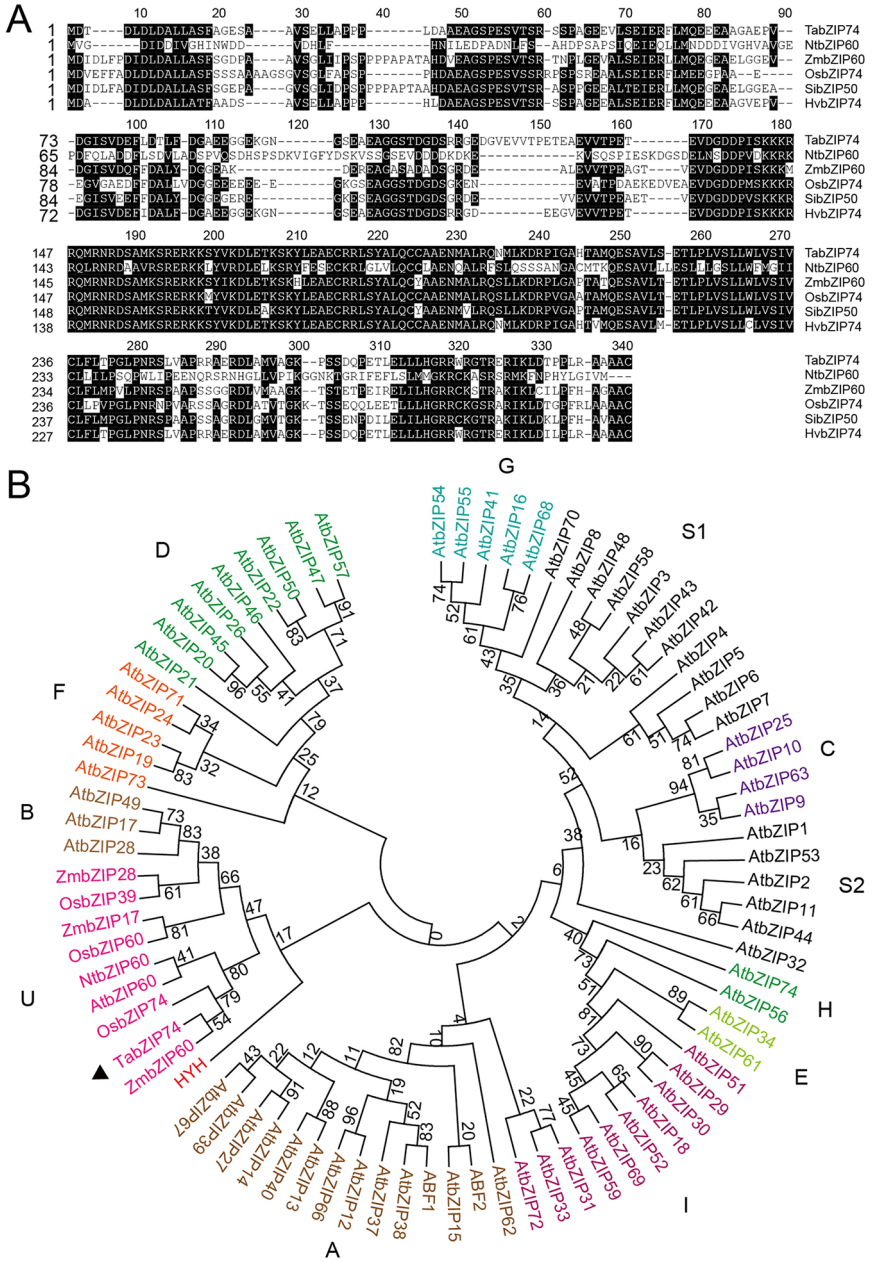

FIGURE 1 | Phylogenetic tree of bZIP transcription factors and alignment of amino acid sequences of TabZIP74. **(A)** Amino acid alignment of TabZIP74 with other bZIP family members of NtbZIP60, OsbZIP74, ZmbZIP60, HvbZIP74, and SibZIP50 from tobacco (*Nicotiana tabacum*, NP_001311663.1), rice (*Oryza sativa*, XP_015641141.1), maize (*Zea mays*, NP_001147256.1), barley (*Hordeum vulgare*, BAJ96708.1), and millet (*Setaria italica*, XP_004965858.1), respectively. The numbers on the left indicate amino acid positions. Identical amino acid residues are shaded black, representing >50% similarity of conserved amino acids. **(B)** Phylogenetic tree of TabZIP74 with selected bZIP TFs from rice (OsbZIPs), Arabidopsis (AtbZIPs), tobacco (NtbZIPs), and maize (ZmbZIPs). Genbank accession numbers of the factors are listed in **Supplementary Table 1**. The subgroups were designated as A, B, C, D, E, F, G, H, S1, S2, and U, according to the analysis results (Jakoby et al., 2002; Zhou et al., 2017).

protein bound to the nuclei of tobacco epidermal cells, whereas eGFP-TabZIP74 was localized in both the plasma membrane and nucleus (**Figure 3B**). These results suggest that TabZIP74 is a membrane-bound and nucleus-localized protein.

The mRNA levels of USP and SP forms of *TabZIP74* in tobacco leaf epidermal cells infiltrated with the strain GV3101 with a fusion vector of *eGFP-TabZIP74* was assayed by semi-RT-PCR. Fourteen hours after infiltrating, USP-type mRNA molecules of *TabZIP74* were detected at the inoculation site center with a high expression level and at the edge of infiltrated leaves with a relatively lower level. The SP-type molecules of *TabZIP74* were not detected at the inoculation site center until 36 h after

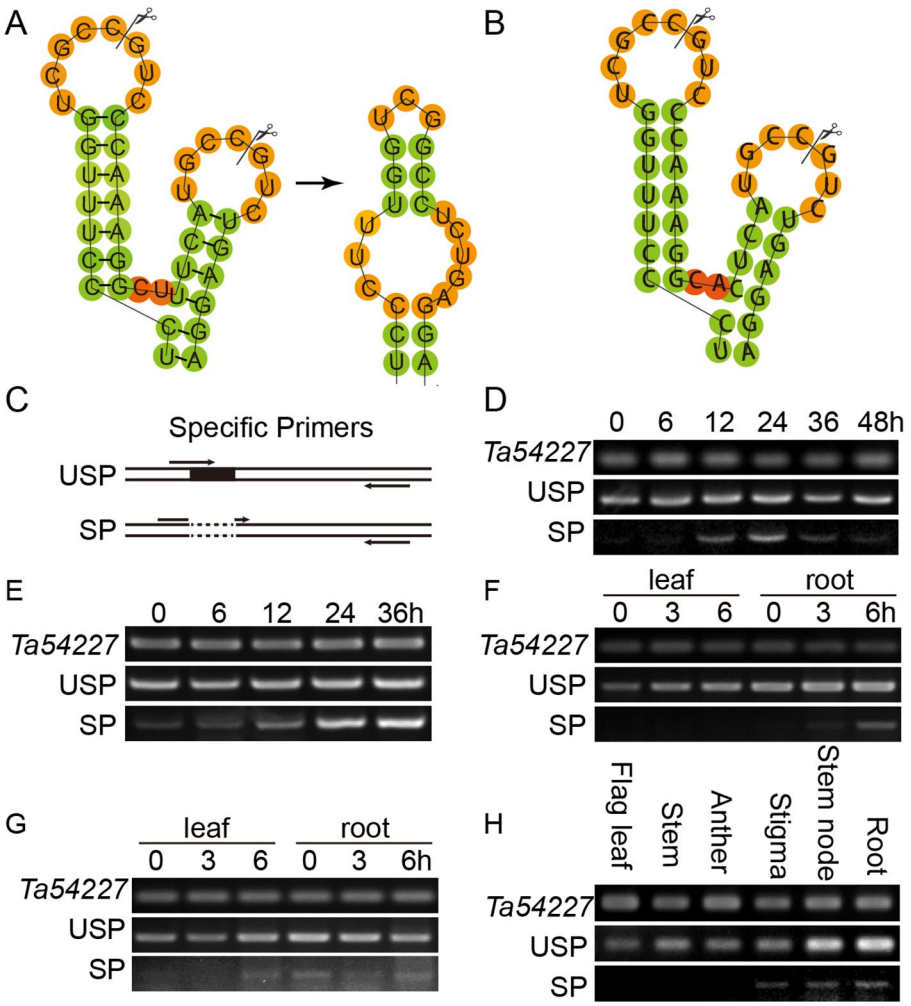

FIGURE 2 | Splicing prediction and molecular assay of *TabZIP74* in response to *Pst* infection, abiotic treatments, and development. **(A**, **B)** Predicted twin hairpin loop structures of unspliced (USP, left) and spliced (SP, right) forms of *TabZIP74* **(A)** and its homolog of *OsbZIP74* mRNA **(B)**. Each structure contains two stems and two loops. The spliced and predicted cleavage sites are highlighted with scissors. Schematic representation of the USP and SP primers **(C)**, Time-course experiments of the *TabZIP74* splicing in response to infection by *Pst* with an avirulent race CYR17 **(D)** and a virulent race CYR32 **(E)**. Splicing test in wheat seedling leaves and roots under PEG-induced drought stress **(F)** and ABA **(G)**. **(H)** Splicing test in flag leaves, stems, anthers, stigmas, stem nodes, and roots of adult wheat plants.

infiltration, and no SP forms were found at the edge of the infiltrated area; both types of *TabZIP74* mRNA were not detected at the inoculation site center or the edge of infiltrated leaves until 14 h after infiltration (**Figures 3C**, **D**). Therefore, wounding by infiltration possibly induces *TabZIP74* mRNA splicing in tobacco cells, and the proteins encoded by the confusion gene *eGFP-TabZIP74* were bound to the tobacco epidermal cell membrane and accumulated in the nuclei, while those encoded by *TabZIP74-eGFP* were only bound to the plasma membrane (**Figure 3B**).

Transcription Activity of TabZIP74

The full-length ORF and its truncated cDNA fragment without TMD (*TabZIP74ΔC*) were fused into the GAL4-DB in the vector pGBKT7, and the constructs were transformed into yeast strain AH109 cells to assay TabZIP74 transcriptional activity. The yeast transformant cells containing the fusion plasmids of full-length cDNA of *TabZIP74*, *TabZIP74ΔC,* and the vector control pGBKT7 grew well on selection SD medium plate without tryptophan (Trp−) (**Figure 4**). However, only the yeast cells encoding the fusion protein of TabZIP74ΔC grew well on the selection medium without tryptophan, histidine, and adenine (Trp−/His−/Ade−) (**Figure 4**), indicating that TabZIP74ΔC had transcriptional activity in yeast cells.

TabZIP74 Knockdown Plants Increased Susceptibility to *Pst*

To identify the regulatory roles of *TabZIP74* in the wheat response to *Pst* infection, the specific C-terminal fragment of *TabZIP74* was used to construct the BSMV-*TabZIP74* fusion vector to silence *TabZIP74* expression in wheat seedlings.

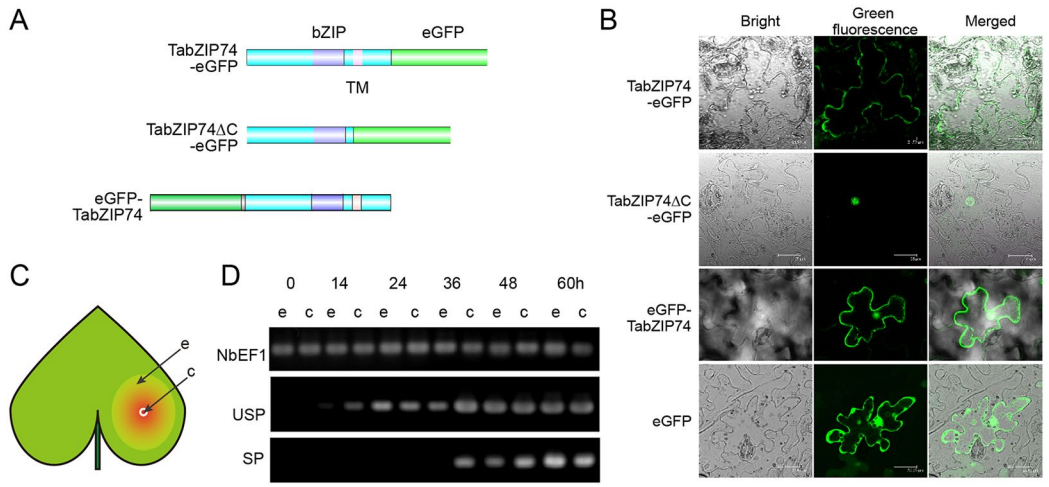

FIGURE 3 | Subcellular localization of TabZIP74 and its mRNA splicing in tobacco leaf epidermal cells. **(A)** Plasmids encoding fusion proteins of eGFP with TabZIP74 were constructed, including two structures of full-length TabZIP74 fused to the N- or C-terminal of eGFP (top and bottom) and truncated TabZIP74(ΔC) (middle) fused to the N-terminal of eGFP protein. **(B)** Subcellular localization of TabZIP74 protein. **(C)** Schematic diagram of tobacco leaf infiltration. 'c' and 'e' represent the 'center' and the 'edge' of infiltrating area inoculated with *A. tumefaciens* cells containing GFP-fusion vectors, respectively. **(D)** mRNA splicing assay of *TabZIP74* induced by wounding in tobacco leaf cells. USP and SP, unspliced, and spliced mRNA forms of *TabZIP74*. *NbEF1* was used as control genes in the tobacco leaf RT-PCR analyses.

Mild chlorotic mosaic symptoms were observed in the BSMV-inoculated plants 10 d post virus inoculated, and there was no obvious defects in further seedling leaf growth. Typical photobleaching was observed on the leaves of wheat seedlings pre-inoculated with BSMV-*TaPDS* (a specific fragment of wheat phytoene desaturase gene *PDS*) 14 d after virus inoculation, indicating the feasibility of the gene knockdown system applied in this study (**Figure 5A**). Interestingly, 11 dpi with the virulent *Pst* race of CYR 32, uredinium pustules erupted on the *TabZIP74*-knocked down seedling leaves of variety Fengchan 3, while no uredinia were visible on the Mock or vector control plants (**Figure 5B**). As a result, the latent period of *Pst* infection in silenced plants was significantly shorter than in the BSMV vector control and Mock seedlings (**Figure 5C**). Sixteen d post-inoculation, most *Pst* uredinia had matured and erupted from the seedling leaf surface (**Figure 4B**). There were no significant differences in the number of *Pst* uredinia on Mock, BSMV control and *TabZIP74*-knocked down seedling leaves. However, the *TabZIP74*-knocked down seedling leaves had longer uredinia than the Mock and BSMV control seedlings (**Figure 5D**). The expression level of *TabZIP74* before *Pst* inoculation was ranked BSMV > Mock > *TabZIP74*-knocked down seedlings. At 48 hpi, no differences in expression level were detected between BSMV and Mock treatments, but the *TabZIP74* expression level remained relatively low in its knockdown seedlings (**Figure 5E**).

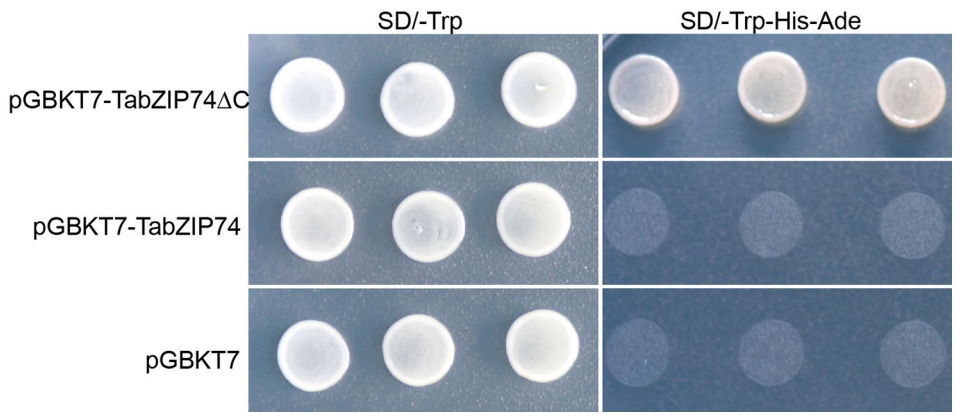

FIGURE 4 | Transcription activity assay of TaZIP74 protein. The full-length encoding region and truncated cDNA fragment of *TabZIP74* were fused with the GAL4 DNA-binding domain in vector pGBKT7. The plasmid containing the fusion gene and the empty vector control pGBKT7 were introduced into yeast cells of strain AH109. The yeast transformants were plated and incubated for 2 d at 28°C on SD/Trp– plate and SD/Trp–/His–/Ade– plate.

TabZIP74 Knockdown Plants Decreased Drought Tolerance and Lateral Roots

Leaf RWC is an important indicator of plant drought response, reflecting the water balance in leaf tissues. Wheat seedlings withholding water for 10 d to drought stress, and then rewatering for 3 d, and the RWC of seedling leaves was assayed at different drought stages. There was no notable phenotypical difference in leaf rolling or wilting between treatments, but the drought-stressed plants pre-silenced by BSMV-*vTabZIP74* had lower RWC than Mock and BSMV control plants; 3 d after rewatering, RWC did not differ between treatments (**Figure 6A**). There were clear differences in primary root length of treated plants, namely, *TabZIP74* > Mock > BSMV (**Figure 6B**). Plants knocked down with *TabZIP74* developed longer primary roots but had less drought tolerance than Mock- and BSMV-treated plants. Furthermore, 9 d post-virus inoculation, *TabZIP74*-knockdown plants had significantly fewer lateral roots than BSMV-infected and Mock plants (**Figures 6C, D**).

DISCUSSION

Upon pathogen recognition, plants responsed rapid and complex immune responses. One type of plant defense response is the programmed burst in transcription and translation of pathogenesis-related proteins, most of which rely on ER processing (Korner et al., 2015). Two plant ER stress sensors, bZIP28 and IRE1, are involved in ER stress-induced signaling (Yoshida et al., 2001; Deng et al., 2011), but only IRE1 has been shown to operate in plant immune responses (Moreno et al., 2012). Plant bZIP TFs, such as AtbZIP60 and OsbZIP50/OsbZIP74, are involved in Regulated IRE1-Dependent Splicing (RIDS) in response to ER stress (Deng et al., 2011; Hayashi et al., 2012).

mRNA Splicing of *TabZIP74* Was Initiated by *Pst* Infection and Wounding

TabZIP74 encodes an ORF consisting of 302 amino acids, beside bZIP DNA-binding domain there was a TMD in C terminal.

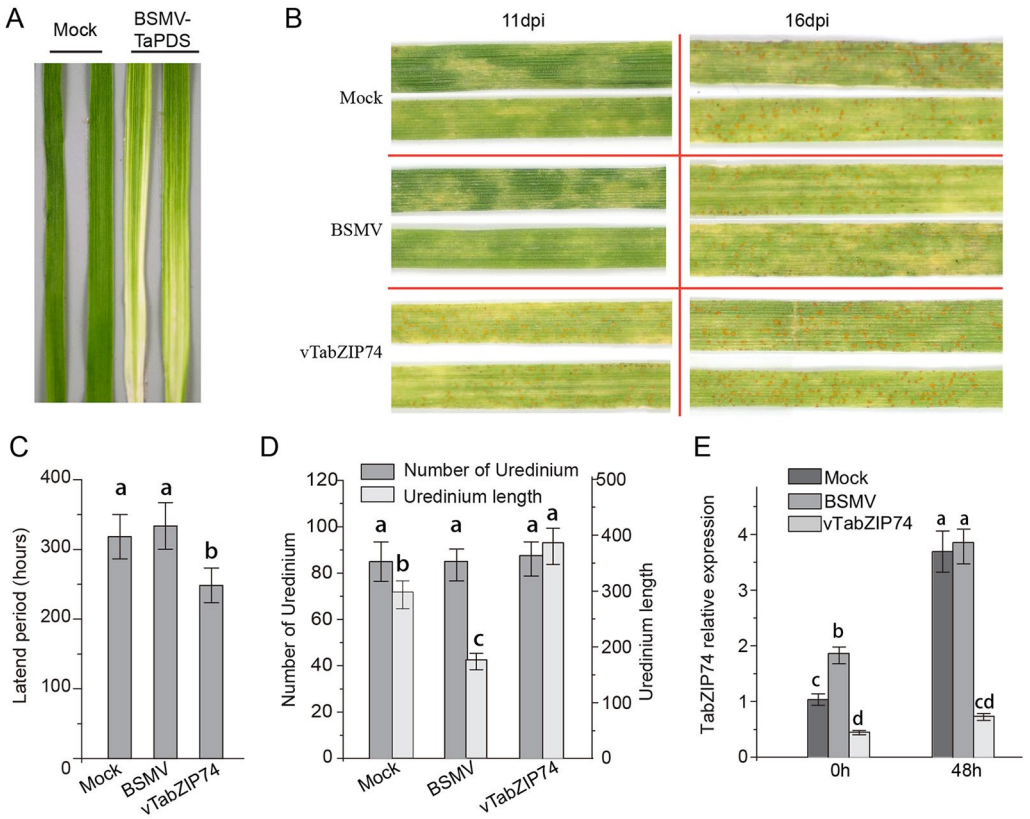

FIGURE 5 | Functional characterization of *TabZIP74* in response to *Pst* infection using the BSMV-VIGS system. **(A)** Third leaves of wheat seedlings of cultivar Fengchan 3 pre-inoculated with positive control vector (BSMV-*TaPDS*) at 14 d post-virus treatment (dpi). **(B)** Phenotypes for the third leaves inoculated with *Pst* race CYR32 were observed at 11 dpi and 16 dpi, respectively; the second leaves of these seedlings were pre-inoculated with water (Mock), empty BSMV vector and silencing vector of BSMV-*vTabZIP74*. **(C)** *Pst* latent infection period of different treatments. **(D)** Statistics of uredinium number and length on third leaves inoculated with *Pst*. Representative experiments were replicated three times ($n = 3$), at least 60 uredinia on 6-cm leaf segments from Mock, BSMV vector and BSMV-*vTabZIP74* treated seedlings were counted in each replicate. Error bars indicate SD, letters indicate significant differences between Mock, BSMV, and BSMV-*TabZIP74* samples determined by one-way ANOVA, taking $P < 0.05$ level according to Duncan's multiple range tests. **(E)** Silencing efficiency of *TabZIP74* expression in knockdown leaves was determined by qRT-PCR; third leaves were sampled at 0 and 48 h after inoculation with BSMV virus. All experiments of *TabZIP74* functions for *Pst* infection were replicated five times, and the results of three representatives were selected.

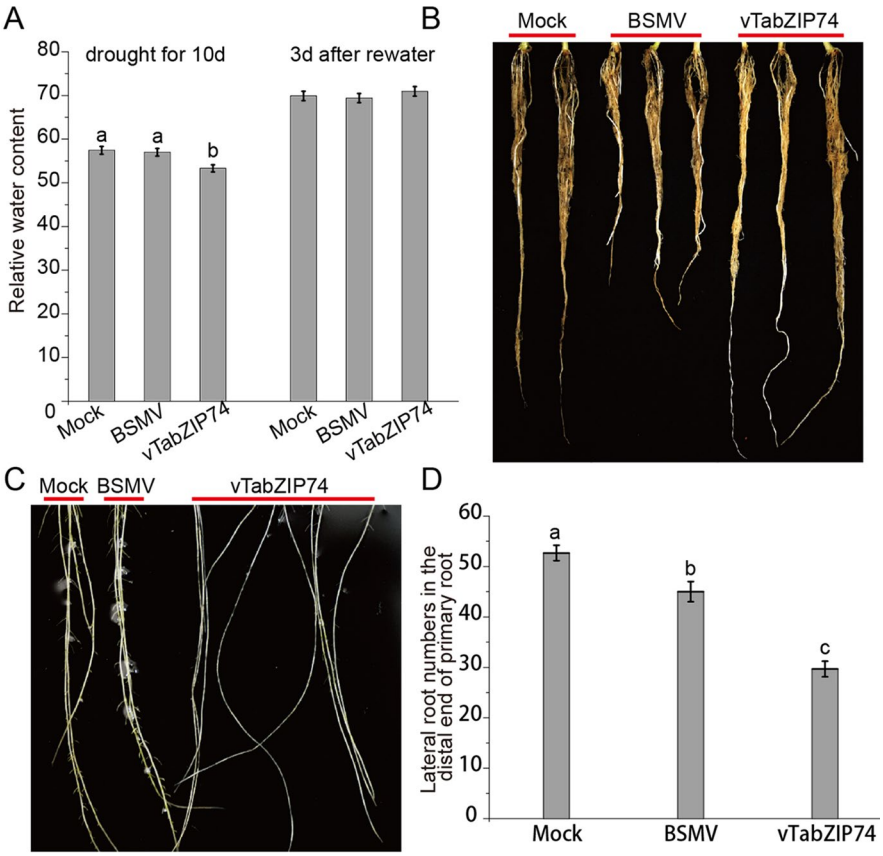

FIGURE 6 | The effects of *TabZIP74* silencing on wheat seedling drought tolerance and root development. **(A)** RWC of plants exposed to drought for 10 d and rewatered 3 d later. The experiments were performed in triplicate. Each value is the mean ± standard deviation of three independent measurements (SD, n = 3). Different letters indicate significant differences by one-way ANOVA, taking $P < 0.05$ level according to Duncan's multiple range test for comparisons between treatment times. **(B)** Morphological differences in primary root development between Mock, BSMV, and BSMV-*vTabZIP74* plants. **(C)** Morphological differences in lateral root development between Mock, BSMV, and BSMV-*vTabZIP74* plants cultured in quarter-strength Hoagland solution for 20 d after sowing. **(D)** Lateral root numbers in the distal end of the primary root of Mock, BSMV, and BSMV-*vTabZIP74* plants cultured in 10-cm pots for 20 d after sowing.

The ER stress lead TabZIP74 mRNA splicing, and the spliced gene encode noval protein without TMD. The phylogenetic tree indicated that TabZIP74 belong to the subgroup U, most of its members have been characterized to regulate UPR. For example, *ZmbZIP60* mRNA is spliced in maize in response to ER stress (Li et al., 2012), OsbZIP74 is an important ER stress regulator in rice (Lu et al., 2012), OsbZIP39 regulates the ER stress response in rice (Takahashi et al., 2012), and NtbZIP60 is an ER-localized transcription factor in tobacco (Tateda et al., 2008; Xu et al., 2013). Therefore, TabZIP74 may be involved in ER stress responses.

IRE1 has been proved as a dual protein kinase/RNase. The predicted structure of the IRE1 splicing site was based on two 'kissing' hairpin loops with conserved bases, and its predicted cleavage sites located close to the ribonuclease catalytic sites in its cytosolic domain (Lee et al., 2008). *TabZIP74* shares high similarity with *OsbZIP74* in the nucleotide sequence, neither of which had a higher sequence identity than the bZIP TF of yeast *HAC1* or mammalian *XBP1* at nucleotide or protein levels in response to ER stress (Kawahara et al., 1998; Yoshida et al., 2001). *TabZIP74* and *OsbZIP60* mRNAs, being like *HAC1* and *XBP1* mRNAs, can fold and form an IRE1 recognition site with two stem loops, each containing the bases remarkably conserved from yeast to mammals at three positions.

The splicing of *TabZIP74* mRNA in wheat leaves or roots was evident from RT-PCR and sequencing after ER stress, *Pst* infection, or drought and ABA treatments. The mRNA splicing of *TabZIP74* was also detected in tobacco leaves infiltrated with *A. tumefaciens* cells containing the *GFP-TabZIP74* fusion vector. Consequently, the *TabZIP74* mRNA sequence in infiltrated tobacco leaves may have been spliced by IRE1 under ER stress triggered by wounding.

TabZIP74 mRNA Splicing Produces the Active Form of Transcription Factor bZIP74

The full length of TabZIP74 was located on the membrane, and the truncated form of TaZIP74 can enter the nucleus (**Figure 3A**); OsbZIP74, AtbZIP60, ZmbZIP60, and NtbZIP60 showed similar results. In this research, we fused eGFP in the N terminus and found the splicing of TabZIP74 lead to new proteins entering the nucleus. The IRE1 splicing in mammals produces the active form

of the transcription factor by adding the transcriptional activation domain in the newly formed longer C-terminus (Lu et al., 2012). In this research, the truncated but not full length of TabZIP74 acts as a transcriptional activator in yeast; similar results were observed in NtbZIP60. However, the TMD in OsbZIP74 and AtbZIP74 did not affect activation activity in yeast. So, the splicing of TabZIP74 produces the active form of transcription factor bZIP74.

BSMV Infection Enhanced the Expression Level of *TabZIP74*

Plant-infecting viruses can activate the ER stress signaling mechanism. Upon infection, viruses hijack cellular machinery to replicate their genomes and translate viral proteins (Korner et al., 2015). In Arabidopsis, when leaves were infected with potyvirus *Turnip mosaic virus* (Gaguancela et al., 2016) the spliced bZIP60 mRNA were accumulated. ER stress marker genes were also induced in *N. benthamiana* infected with potexvirus *Potato virus X* (PVX) and fijivirus *Rice black-streaked dwarf virus* (Ye et al., 2011; Sun et al., 2013). And it has proved that ER stress activation acts as a positive regulator of virus replication (Korner et al., 2015).

Our results showed that the infection of BSMV induced a higher expression level of *TabZIP74* than Mock or BSMV-*TabZIP74* (**Figure 4F**). Moreover, the stripe rust disease severity of BSMV-treated seedlings was lower than Mock and BSMV-*TabZIP74* seedlings (**Figure 4E**). As such, the wheat seedlings pre-infected with BSMV may reduce the disease severity of stripe rust.

TabZIP74 Involved in Wheat Drought Tolerance and Development

In plants, UPR is provoked by a heavy demand in anther tapetal cells to synthesize and secrete pollen coat materials (Deng et al., 2016). Our study is also showed that UPR contributes to normal plant development. Under normal development conditions, low levels of the spliced form of *TabZIP74* were detected in wheat stem nodes, roots, and stigmas. It is interesting to note that *TabZIP74* knockdown seedlings developed fewer lateral roots, while other studies have found that IRE1a and IRE1b support root growth in ways other than the splicing of *bZIP60* mRNA (Deng et al., 2016). The growth of single or double *bZIP60* mutants in combination with either *bZIP17* or *bZIP28* appear to be normal in unstressed conditions (Kim et al., 2018; Bao et al., 2019). Biotic stress, ER stress-inducing agent, ABA treatment, and drought could induce *TabZIP74* mRNA splicing. However, in rice, the ER stress-inducing agent and SA treatment induced the splicing of *OsbZIP74*, the homolog of *TabZIP74*, whereas stress hormone ABA and drought did not. So differences in biological function may exist between TabZIP74 and OsbZIP74.

The wheat root system includes the primary root, crown, and lateral roots, and root hairs. When *TabZIP74* expression was silenced with VIGS, the wheat seedlings developed longer primary roots, but with significantly fewer lateral roots. This may be the reason why the *TabZIP74* knockdown plants showed less drought tolerance (**Figure 5**). Besides, *TabZIP74* knockdown plants also increased susceptibility to *Pst* infection. Water deficiency, pathogen infection, or stress-induced agent ABA usually cause the disorder of protein synthesis, degradation, and folding. In the endoplasmic reticulum, it is termed ER stress. Thus, it is particularly important to maintain protein stability in plant cells. ABA plays a major role in abiotic stress signaling, in particular in drought and salinity stress responses. ABA also has a pivotal role in the regulation of the plant immune signaling network (Pieterse et al., 2012). In Arabidopsis, ABA signaling antagonizes plant immunity by suppressing SA-dependent defenses. *Boea hygrometrica* bZIP transcription factor, BhbZIP60, is a splicing-activated ER stress regulator involved in drought tolerance. So, we propose that the splicing form of *TabZIP74* is involved in the ABA pathway to respond to abiotic and biotic stresses.

In brief, *TabZIP74* encodes a membrane-associated bZIP-type transcription factor. Based on the results presented in this study, we conclude that *TabZIP74* might positively regulate wheat defenses against *Pst* and drought stress tolerance and is necessary for lateral root development.

DATA AVAILABILITY STATEMENT

The raw data supporting the conclusions of this manuscript will be made available by the authors, without undue reservation, to any qualified researcher.

AUTHOR CONTRIBUTIONS

RL and WC designed the experiment. RL and FW wrote the manuscript. FW, YL, PW, JF, and SX performed the experiments and analyzed the data.

FUNDING

The study was financially supported by the National Key Research and Development Program of China (projects 2018YFD0200501, 2018YFD0200401) and National Natural Science Foundation of China (31871949).

ACKNOWLEDGMENTS

We thank Professor Zejian Guo and Professor Dawei Li of the Chinese Agricultural University for providing the eGFP expression vector and vectors of BSMV-VIGS system.

SUPPLEMENTARY MATERIAL

The Supplementary Material for this article can be found online at: https://www.frontiersin.org/articles/10.3389/fpls.2019.01551/full#supplementary-material

Supplementary Material includes one table listing Locus ID of bZIP genes.

REFERENCES

Bao, Y., Bassham, D. C., and Howell, S. H. (2019). A functional unfolded protein response is required for normal vegetative development. *Plant Physiol.* 179 (4), 1834–1843. doi: 10.1104/pp.18.01261

Chen, W., Wellings, C., Chen, X., Kang, Z., and Liu, T. (2014). Wheat stripe (yellow) rust caused by *Puccinia striiformis* f. *sp. Tritici. Mol. Plant Pathol.* 15 (5), 433–446. doi: 10.1111/mpp.12116

Correa, L. G., Riano-Pachon, D. M., Schrago, C. G., dos Santos, R. V., Mueller-Roeber, B., and Vincentz, M. (2008). The role of bZIP transcription factors in green plant evolution: adaptive features emerging from four founder genes. *PloS One* 3 (8), e2944. doi: 10.1371/journal.pone.0002944

Deng, Y., Humbert, S., Liu, J. X., Srivastava, R., Rothstein, S. J., and Howell, S. H. (2011). Heat induces the splicing by IRE1 of a mRNA encoding a transcription factor involved in the unfolded protein response in Arabidopsis. *Proc. Natl. Acad. Sci. U.S.A.* 108 (17), 7247–7252. doi: 10.1073/pnas.1102117108

Deng, Y., Srivastava, R., Quilichini, T. D., Dong, H., Bao, Y., Horner, H. T., et al. (2016). IRE1, a component of the unfolded protein response signaling pathway, protects pollen development in Arabidopsis from heat stress. *Plant J.* 88 (2), 193–204. doi: 10.1111/tpj.13239

Gaguancela, O. A., Zuniga, L. P., Arias, A. V., Halterman, D., Flores, F. J., Johansen, I. E., et al. (2016). The IRE1/bZIP60 pathway and Bax Inhibitor 1 suppress systemic accumulation of potyviruses and potexviruses in *Arabidopsis* and *Nicotiana benthamiana* plants. *Mol. Plant Microbe Interact.* 29 (10), 750–766. doi: 10.1094/MPMI-07-16-0147-R

Geng, X., Zang, X., Li, H., Liu, Z., Zhao, A., Liu, J., et al. (2018). Unconventional splicing of wheat *TabZIP60* confers heat tolerance in transgenic Arabidopsis. *Plant Sci.* 274, 252–260. doi: 10.1016/j.plantsci.2018.05.029

Hamada, M., Kiryu, H., Sato, K., Mituyama, T., and Asai, K. (2009). Prediction of RNA secondary structure using generalized centroid estimators. *Bioinformatics* 25 (4), 465–473. doi: 10.1093/bioinformatics/btn601

Hayashi, S., Wakasa, Y., Takahashi, H., Kawakatsu, T., and Takaiwa, F. (2012). Signal transduction by IRE1-mediated splicing of *bZIP50* and other stress sensors in the endoplasmic reticulum stress response of rice. *Plant J.* 69 (6), 946–956. doi: 10.1111/j.1365-313X.2011.04844.x

Howell, S. H. (2013). Endoplasmic reticulum stress responses in plants. *Annu. Rev. Plant Biol.* 64, 477–499. doi: 10.1146/annurev-arplant-050312-120053

Iwata, Y., and Koizumi, N. (2005). An Arabidopsis transcription factor, AtbZIP60, regulates the endoplasmic reticulum stress response in a manner unique to plants. *Proc. Natl. Acad. Sci. U.S.A.* 102 (14), 5280–5285. doi: 10.1073/pnas.0408941102

Jakoby, M., Weisshaar, B., Droge-Laser, W., Vicente-Carbajosa, J., Tiedemann, J., Kroj, T., et al. (2002). bZIP transcription factors in *Arabidopsis*. *Trends Plant Sci.* 7 (3), 106–111. doi: 10.1016/s1360-1385(01)02223-3

Kawahara, T., Yanagi, H., Yura, T., and Mori, K. (1998). Unconventional splicing of *HAC1/ERN4* mRNA required for the unfolded protein response. Sequence-specific and non-sequential cleavage of the splice sites. *J. Biol. Chem.* 273 (3), 1802–1807. doi: 10.1074/jbc.273.3.1802

Kim, J. S., Yamaguchi-Shinozaki, K., and Shinozaki, K. (2018). ER-anchored transcription factors bZIP17 and bZIP28 regulate root elongation. *Plant Physiol.* 176 (3), 2221–2230. doi: 10.1104/pp.17.01414

Korner, C. J., Du, X., Vollmer, M. E., and Pajerowska-Mukhtar, K. M. (2015). Endoplasmic reticulum stress signaling in plant immunity–At the crossroad of life and death. *Int. J. Mol. Sci.* 16 (11), 26582–26598. doi: 10.3390/ijms161125964

Kumar, S., Stecher, G., and Tamura, K. (2016). MEGA7: Molecular Evolutionary Genetics Analysis Version 7.0 for bigger datasets. *Mol. Biol. Evol.* 33 (7), 1870–1874. doi: 10.1093/molbev/msw054

Larkin, M. A., Blackshields, G., Brown, N. P., Chenna, R., McGettigan, P. A., McWilliam, H., et al. (2007). Clustal W and Clustal X version 2.0. *Bioinformatics* 23 (21), 2947–2948. doi: 10.1093/bioinformatics/btm404

Lee, K. P., Dey, M., Neculai, D., Cao, C., Dever, T. E., and Sicheri, F. (2008). Structure of the dual enzyme Ire1 reveals the basis for catalysis and regulation in nonconventional RNA splicing. *Cell* 132 (1), 89–100. doi: 10.1016/j.cell.2007.10.057

Li, J., Chu, Z. H., Batoux, M., Nekrasov, V., Roux, M., Roux, M., et al. (2009). Specific ER quality control components required for biogenesis of the plant innate immune receptor EFR. *Proc. Natl. Acad. Sci. U.S.A.* 106 (37), 15973–15978. doi: 10.1073/pnas.0905532106

Li, Y., Humbert, S., and Howell, S. H. (2012). ZmbZIP60 mRNA is spliced in maize in response to ER stress. *BMC Res. Notes* 5, 144. doi: 10.1186/1756-0500-5-144

Li, Z., Srivastava, R., Tang, J., Zheng, Z., and Howell, S. H. (2018). *Cis*-effects condition the induction of a major unfolded protein response factor, *ZmbZIP60*, in response to heat stress in maize. *Front. Plant Sci.* 9, 833. doi: 10.3389/fpls.2018.00833

Liu, J. X., and Howell, S. H. (2010). Endoplasmic reticulum protein quality control and its relationship to environmental stress responses in plants. *Plant Cell* 22 (9), 2930–2942. doi: 10.1105/tpc.110.078154

Liu, J. X., Srivastava, R., Che, P., and Howell, S. H. (2007a). An endoplasmic reticulum stress response in *Arabidopsis* is mediated by proteolytic processing and nuclear relocation of a membrane-associated transcription factor, bZIP28. *Plant Cell* 19 (12), 4111–4119. doi: 10.1105/tpc.106.050021

Liu, J. X., Srivastava, R., Che, P., and Howell, S. H. (2007b). Salt stress responses in Arabidopsis utilize a signal transduction pathway related to endoplasmic reticulum stress signaling. *Plant J.* 51 (5), 897–909. doi: 10.1111/j.1365-313X.2007.03195.x

Lu, D. P., and Christopher, D. A. (2008). Endoplasmic reticulum stress activates the expression of a sub-group of protein disulfide isomerase genes and AtbZIP60 modulates the response in *Arabidopsis thaliana*. *Mol. Genet. Genomics* 280 (3), 199–210. doi: 10.1007/s00438-008-0356-z

Lu, X., Tintor, N., Mentzel, T., Kombrink, E., Boller, T., Robatzek, S., et al. (2009). Uncoupling of sustained MAMP receptor signaling from early outputs in an Arabidopsis endoplasmic reticulum glucosidase II allele. *Proc. Natl. Acad. Sci. U. S. A.* 106 (52), 22522–22527. doi: 10.1073/pnas.0907711106

Lu, S. J., Yang, Z. T., Sun, L., Sun, L., Song, Z. T., and Liu, J. X. (2012). Conservation of IRE1-regulated bZIP74 mRNA unconventional splicing in rice (*Oryza sativa* L.) involved in ER stress responses. *Mol. Plant* 5 (2), 504–514. doi: 10.1093/mp/ssr115

Mao, X., Zhang, H., Qian, X., Li, A., Zhao, G., and Jing, R. (2012). *TaNAC2*, a NAC-type wheat transcription factor conferring enhanced multiple abiotic stress tolerances in *Arabidopsis*. *J. Exp. Bot.* 63 (8), 2933–2946. doi: 10.1093/jxb/err462

Moreno, A. A., Mukhtar, M. S., Blanco, F., Boatwright, J. L., Moreno, I., Jordan, M. R., et al. (2012). IRE1/bZIP60-mediated unfolded protein response plays distinct roles in plant immunity and abiotic stress responses. *PloS One* 7 (2), e31944. doi: 10.1371/journal.pone.0031944

Nekrasov, V., Li, J., Batoux, M., Roux, M., Chu, Z. H., Lacombe, S., et al. (2009). Control of the pattern-recognition receptor EFR by an ER protein complex in plant immunity. *EMBO J.* 28 (21), 3428–3438. doi: 10.1038/emboj.2009.262

Paolacci, A. R., Tanzarella, O. A., Porceddu, E., and Ciaffi, M. (2009). Identification and validation of reference genes for quantitative RT-PCR normalization in wheat. *BMC Mol. Biol.* 10, 11. doi: 10.1186/1471-2199-10-11

Parra-Rojas, J., Moreno, A. A., Mitina, I., and Orellana, A. (2015). The dynamic of the splicing of bZIP60 and the proteins encoded by the spliced and unspliced mRNAs reveals some unique features during the activation of UPR in *Arabidopsis thaliana*. *PloS One* 10 (4), e0122936. doi: 10.1371/journal.pone.0122936

Pieterse, C. M., Van Der Does, D., Zamioudis, C., Leon-Reyes, A., and Van Wees, S. C. (2012). Hormonal modulation of plant immunity. *Annu. Rev. Cell Dev. Biol.* 28, 489–521. doi: 10.1146/annurev-cellbio-092910-154055

Saijo, Y., Tintor, N., Lu, X., Rauf, P., Pajerowska-Mukhtar, K., Haweker, H., et al. (2009). Receptor quality control in the endoplasmic reticulum for plant innate immunity. *EMBO J.* 28 (21), 3439–3449. doi: 10.1038/emboj.2009.263

Schmittgen, T. D., and Livak, K. J. (2008). Analyzing real-time PCR data by the comparative C(T) method. *Nat. Protoc.* 3 (6), 1101–1108. doi: 10.1038/nprot.2008.73

Sornaraj, P., Luang, S., Lopato, S., and Hrmova, M. (2015). Basic leucine zipper (bZIP) transcription factors involved in abiotic stresses: a molecular model of a wheat bZIP factor and implications of its structure in function. *Biochim. Biophys. Acta*. 180 (1), 46–56. doi: 10.1016/j.bbagen.2015.10.014

Sun, Z., Yang, D., Xie, L., Sun, L., Zhang, S., Zhu, Q., et al. (2013). Rice black-streaked dwarf virus P10 induces membranous structures at the ER and elicits the unfolded protein response in *Nicotiana benthamiana*. *Virology* 447 (1), 131–139. doi: 10.1016/j.virol.2013.09.001

Sun, L., Zhang, S. S., Lu, S. J., and Liu, J. X. (2015). Site-1 protease cleavage site is important for the ER stress-induced activation of membrane-associated transcription factor bZIP28 in *Arabidopsis*. *Sci. China Life Sci.* 58 (3), 270–275. doi: 10.1007/s11427-015-4807-6

Tajima, H., Iwata, Y., Iwano, M., Takayama, S., and Koizumi, N. (2008). Identification of an *Arabidopsis* transmembrane bZIP transcription factor involved in the endoplasmic reticulum stress response. *Biochem. Biophys. Res. Commun.* 374 (2), 242–247. doi: 10.1016/j.bbrc.2008.07.021

Takahashi, H., Kawakatsu, T., Wakasa, Y., Hayashi, S., and Takaiwa, F. (2012). A rice transmembrane bZIP transcription factor, OsbZIP39, regulates the endoplasmic reticulum stress response. *Plant Cell Physiol.* 53 (1), 144–153. doi: 10.1093/pcp/pcr157

Tateda, C., Ozaki, R., Onodera, Y., Takahashi, Y., Yamaguchi, K., Berberich, T., et al. (2008). NtbZIP60, an endoplasmic reticulum-localized transcription factor, plays a role in the defense response against bacterial pathogens in *Nicotiana tabacum*. *J. Plant Res.* 121 (6), 603–611. doi: 10.1007/s10265-008-0185-5

van Loon, L. C., Rep, M., and Pieterse, C. M. (2006). Significance of inducible defense-related proteins in infected plants. *Annu. Rev. Phytopathol.* 44, 135–162. doi: 10.1146/annurev.phyto.44.070505.143425

Wakasa, Y., Yasuda, H., Oono, Y., Kawakatsu, T., Hirose, S., Takahashi, H., et al. (2011). Expression of ER quality control-related genes in response to changes in BiP1 levels in developing rice endosperm. *Plant J.* 65 (5), 675–689. doi: 10.1111/j.1365-313X.2010.04453.x

Wan, A., Zhao, Z., Chen, X., He, Z., Jin, S., Jia, Q., et al. (2004). Wheat stripe rust epidemic and virulence of *Puccinia striiformis* f. sp. *tritici* in China in 2002. *Plant Dis.* 88 (8), 896–904. doi: 10.1094/PDIS.2004.88.8.896

Wang, D., Weaver, N. D., Kesarwani, M., and Dong, X. (2005). Induction of protein secretory pathway is required for systemic acquired resistance. *Science* 308 (5724), 1036–1040. doi: 10.1126/science.1108791

Wang, F., Lin, R., Feng, J., Chen, W., Qiu, D., and Xu, S. (2015). TaNAC1 acts as a negative regulator of stripe rust resistance in wheat, enhances susceptibility to *Pseudomonas syringae*, and promotes lateral root development in transgenic *Arabidopsis thaliana*. *Front. Plant Sci.* 6, 108. doi: 10.3389/fpls.2015.00108

Wang, B., Du, H., Zhang, Z., Xu, W., and Deng, X. (2017). BhbZIP60 from resurrection plant *Boea hygrometrica* is an mRNA splicing-activated endoplasmic reticulum stress regulator involved in drought tolerance. *Front. Plant Sci.* 8, 245. doi: 10.3389/fpls.2017.00245

Xu, H., Xu, W., Xi, H., Ma, W., He, Z., and Ma, M. (2013). The ER luminal binding protein (BiP) alleviates Cd(2+)-induced programmed cell death through endoplasmic reticulum stress-cell death signaling pathway in tobacco cells. *J. Plant Physiol.* 170 (16), 1434–1441. doi: 10.1016/j.jplph.2013.05.017

Yang, Y. G., Lv, W. T., Li, M. J., Wang, B., Sun, D. M., and Deng, X. (2013). Maize membrane-bound transcription factor Zmbzip17 is a key regulator in the cross-talk of ER quality control and ABA signaling. *Plant Cell Physiol.* 54 (12), 2020–2033. doi: 10.1093/pcp/pct142

Ye, C., Dickman, M. B., Whitham, S. A., Payton, M., and Verchot, J. (2011). The unfolded protein response is triggered by a plant viral movement protein. *Plant Physiol.* 156 (2), 741–755. doi: 10.1104/pp.111.174110

Yoshida, H., Matsui, T., Yamamoto, A., Okada, T., and Mori, K. (2001). XBP1 mRNA is induced by ATF6 and spliced by IRE1 in response to ER stress to produce a highly active transcription factor. *Cell* 107 (7), 881–891. doi: 10.1016/s0092-8674(01)00611-0

Yuan, C., Li, C., Yan, L., Jackson, A. O., Liu, Z., Han, C., et al. (2011). A high throughput *barley stripe mosaic virus* vector for virus induced gene silencing in monocots and dicots. *PloS One* 6 (10), e26468. doi: 10.1371/journal.pone.0026468

Zhou, Y., Xu, D., Jia, L., Huang, X., Ma, G., Wang, S., et al. (2017). Genome-wide identification and structural analysis of bZIP transcription factor genes in. *Brassica Napus. Genes (Basel)* 8, 288. doi: 10.3390/genes8100288

Conflict of Interest: The authors declare that the research was conducted in the absence of any commercial or financial relationships that could be construed as a potential conflict of interest.

frontiers in Plant Science

ORIGINAL RESEARCH
published: 28 November 2019
doi: 10.3389/fpls.2019.01448

Dual Mode of the Saponin Aescin in Plant Protection: Antifungal Agent and Plant Defense Elicitor

Lucie Trdá[1], Martin Janda[1,2,3], Denisa Macková[1,2], Romana Pospíchalová[1], Petre I. Dobrev[4], Lenka Burketová[1] and Pavel Matušinsky[5,6]*

[1] Laboratory of Pathological Plant Physiology, Institute of Experimental Botany of The Czech Academy of Sciences, Prague, Czechia, [2] Laboratory of Plant Biochemistry, Department of Biochemistry and Microbiology, University of Chemistry and Technology Prague, Prague, Czechia, [3] Department Genetics, Faculty of Biology, Biocenter, Ludwig-Maximilian-University of Munich (LMU), Martinsried, Germany, [4] Laboratory of Hormonal Regulations in Plants, Institute of Experimental Botany of The Czech Academy of Sciences, Prague, Czechia, [5] Department of Plant Pathology, Agrotest Fyto, Ltd, Kroměříž, Czechia, [6] Department of Botany, Faculty of Science, Palacký University in Olomouc, Olomouc, Czechia

Being natural plant antimicrobials, saponins have potential for use as biopesticides. Nevertheless, their activity in plant–pathogen interaction is poorly understood. We performed a comparative study of saponins' antifungal activities on important crop pathogens based on their effective dose (EC_{50}) values. Among those saponins tested, aescin showed itself to be the strongest antifungal agent. The antifungal effect of aescin could be reversed by ergosterol, thus suggesting that aescin interferes with fungal sterols. We tested the effect of aescin on plant–pathogen interaction in two different pathosystems: *Brassica napus* versus (fungus) *Leptosphaeria maculans* and *Arabidopsis thaliana* versus (bacterium) *Pseudomonas syringae* pv *tomato* DC3000 (*Pst* DC3000). We analyzed resistance assays, defense gene transcription, phytohormonal production, and reactive oxygen species production. Aescin activated *B. napus* defense through induction of the salicylic acid pathway and oxidative burst. This defense response led finally to highly efficient plant protection against *L. maculans* that was comparable to the effect of fungicides. Aescin also inhibited colonization of *A. thaliana* by *Pst* DC3000, the effect being based on active elicitation of salicylic acid (SA)-dependent immune mechanisms and without any direct antibacterial effect detected. Therefore, this study brings the first report on the ability of saponins to trigger plant immune responses. Taken together, aescin in addition to its antifungal properties activates plant immunity in two different plant species and provides SA-dependent resistance against both fungal and bacterial pathogens.

Keywords: ***Brassica napus*, *Leptosphaeria maculans*, salicylic acid, fungicide, *Pseudomonas syringae*, *Arabidopsis thaliana*, EC_{50}**

OPEN ACCESS

Edited by:
Ivan Baccelli, Istituto per la Protezione sostenibile delle Piante, Sede Secondaria Firenze, Italy

Reviewed by:
Eugenio Llorens, Tel Aviv University, Israel
Hidenori Matsui, Okayama University, Japan

****Correspondence:***
Lucie Trdá
lucie.trda@gmail.com;
trdal@ueb.cas.cz

Specialty section:
This article was submitted to Plant Microbe Interactions, a section of the journal Frontiers in Plant Science

Received: *16 August 2019*
Accepted: *17 October 2019*
Published: *28 November 2019*

Citation:
Trdá L, Janda M, Macková D, Pospíchalová R, Dobrev PI, Burketová L and Matušinsky P (2019) Dual Mode of the Saponin Aescin in Plant Protection: Antifungal Agent and Plant Defense Elicitor. Front. Plant Sci. 10:1448. doi: 10.3389/fpls.2019.01448

INTRODUCTION

Crop production is hampered by numerous plant diseases caused by diverse pathogenic microorganisms, such as fungi, bacteria or pests, affecting yield, harvest quality and safety. Although pesticides are currently employed to control crop pathogens and pests, growing problems of fungal resistance to fungicides appear to pose a serious future threat to agriculture (Fisher et al., 2018).

Moreover, alternatives to fungicides are needed that are less harmful to health and the environment. These might include more intensive employment of biological control, greater crop diversity (Zhu et al., 2000), or developing safer compounds with new modes of action (Burketová et al., 2015). Higher plants could constitute a great source of such compounds. Most plants produce a wide variety of antimicrobial secondary metabolites, including alkaloids, flavonoids, terpenes, organic acids, essential oils, and saponins that are involved in plant defense responses essential for plant protection against microbial or pest attack (Osbourn, 1996; Field et al., 2006; da Cruz Cabral et al., 2013; Matušinský et al., 2015).

Saponins occur in a wide range of plant species (Price et al., 1987; Moses et al., 2014). They comprise a structurally diverse family of triterpenoids, steroids or steroidal glycoalkaloids (Podolak et al., 2010; Moses et al., 2014). Saponins exhibit amphiphilic properties that are due to the linkage of a lipophilic triterpene derivative (sapogenin) to one or more hydrophilic glycoside moieties. Historically, plant extracts from *Saponaria officinalis* have been used for their soap properties (Hostettmann and Marston, 1995). Saponins have a broad spectrum of activities in living organisms. They are generally antimicrobial against bacteria and fungi invading plants (Gruiz, 1996; Zablotowicz et al., 1996; Papadopoulou et al., 1999; Barile et al., 2007; Hoagland, 2009; Moses et al., 2014), but they were also effectively applied against microbes associated with animals (Yang et al., 2006; Saleem et al., 2010). Furthermore, saponins exert insecticidal (Nielsen et al., 2010; Singh and Kaur, 2018), antiviral (Zhao et al., 2008), and molluscicidal (Huang et al., 2003) activities, as well as allelopathic activity towards other plant species (Waller et al., 1993).

Saponins are mainly considered to comprise a part of plants' antimicrobial defense system. The underlying mechanisms of their activity are understood to be based on their ability to form complexes with sterols present in the membrane of microorganisms and consequently to cause membrane perturbation (Steel and Drysdale, 1988; Morrissey and Osbourn, 1999; Augustin et al., 2011; Sreij et al., 2019). The antifungal activity of saponins has been known for decades (Turner, 1960; Wolters, 1966; Gruiz, 1996) and their activity against fungal plant pathogens of crops has been reported previously. For example, minutoside saponins and sapogenins, alliogenin, and neoagigenin, isolated from the bulbs of *Allium minutiflorum* showed antimicrobial activity against various soil-borne and air-borne fungal pathogens (Barile et al., 2007). Saponin alliospiroside extracted from *Allium cepa* protected strawberry plants against *Colletotrichum gloeosporioides*, thus indicating a potential to control anthracnose of the plant (Teshima et al., 2013). To date, however, only limited work has been reported toward quantifying antifungal activity against phytopathogenic fungi by establishing EC_{50} values (Saniewska et al., 2006; Porsche et al., 2018), and parallel comparisons with fungicides are often lacking. Moreover, effects on plants have been tested only by several studies (Hoagland et al., 1996; Hoagland, 2009). The goal of the present study was to investigate the potential of plant saponins as an alternative to fungicide treatment on crops.

We focus here mainly on the pathosystem of the crop *Brassica napus* (oilseed rape) and its devastating fungal hemibiotrophic pathogen *Leptosphaeria maculans*, an infectious agent of phoma stem canker in oilseed rape. Plants face microbial infections through an efficient immune system. Plant immunity is very complex, consisting of pathogen recognition by plant immune receptors, signaling events, such as reactive oxygen species (ROS) production or MAP kinase activation, which ultimately triggers such defense mechanisms as changes in gene transcription resulting in expression of antimicrobial proteins, phytohormone production, or callose accumulation (Dodds and Rathjen, 2010; Cook et al., 2015; Trdá et al., 2015). Signaling pathways of phytohormones, such as salicylic acid (SA), jasmonic acid (JA) or ethylene (ET) cross-communicate allowing the plant to finely regulate its immune responses (Glazebrook, 2005; Pieterse et al., 2009). Immune responses have been previously studied in *B. napus* (Šašek et al., 2012a; Šašek et al., 2012b; Lloyd et al., 2014; Nováková et al., 2014).

Plant treatment with diverse agents, including microbe-derived compounds, phytohormones and synthetic chemicals, can induce resistance to subsequent pathogen invasion both locally and systemically (Walters et al., 2013, Burketová et al., 2015). Such resistance, called systemic acquired resistance (SAR), is among others mediated and dependent on SA. SAR was inhibited in *npr1* or *ics1* mutant plants (Kachroo and Robin, 2013). SAR-inducing chemicals are employed in pest control. Benzothiadiazole (BTH) is a functional analog of salicylic acid (SA) and a synthetic inducer of resistance to pathogens (Friedrich et al., 1996; Walters et al., 2013). BTH activates the *B. napus* immune system and provides protection against *L. maculans* (Šašek et al., 2012a). We have previously shown that the phytohormone salicylic acid (SA) plays an important role upon *L. maculans* infection (Šašek et al., 2012b). SA's role in plant immunity is well established (Tsuda et al., 2013; Janda and Ruelland, 2015). Although SA can be involved also in response to some necrotrophic pathogens (Nováková et al., 2014), it is mostly connected with defense against biotrophic microorganisms (Glazebrook, 2005). Substantial knowledge about SA's role in plant disease resistance comes from studies using a model pathosystem involving *A. thaliana* and the bacteria *Pseudomonas syringae* pv tomato DC3000 (*Pst* DC3000) (Katagiri et al., 2002; Xin and He, 2013; Xin et al., 2018; Leontovyčová et al., 2019).

Here, we present a comprehensive and comparative study of antifungal activities against crop pathogens of three terpenoid saponins in comparison to fungicides in commercial use. We chose aescin as the best antifungal agent and further characterized its activity in plants. We show that aescin triggers plant defense by activating the SA pathway and oxidative burst, ultimately leading to highly efficient resistance of *B. napus* against the fungus *L. maculans*. The level of protection it provides is comparable to that of fungicides. In *A. thaliana*, aescin induces SA-dependent resistance to *Pst* DC3000. Therefore, we provide here evidence of aescin's dual mode of action in plant defense.

MATERIAL AND METHODS

Fungal Isolates and Cultivation

Fungal isolates (with the exception of *L. maculans* JN2) were acquired in the territory of the Czech Republic from

symptomatic crop tissue in the field during the period 2002–2015. *Microdochium nivale* (Mn177 and Mn30) and *Oculimacula yallundae* (Oy19 and Oy221) were isolated from the stem bases of wheat in 2013 (Matušinský et al., 2017). *Zymoseptoria tritici* (Zt88 and Zt96) was collected from the leaves of winter wheat in 2013, and *Fusarium culmorum* strains (Fc107 and Fc289) were collected from wheat grains after harvest in 2010 and 2002, respectively (Matušinský et al., 2015). *Pyrenophora teres* (Ptt52 and Ptt17) and *Ramularia collo-cygni* (Rcc11 and Rcc41) were collected from leaves of spring barley in 2013. *L. maculans* (Lm170, Lm1-Lm4) isolates were collected from leaves of oilseed rape during 2014–2015.

Pyrenophora teres and *R. collo-cygni* conidia were transferred from the symptomatic leaves to Petri dishes with potato dextrose agar (PDA) media containing 50 μg·ml^{-1} of ampicillin. Conidia were spread over the surface of media and cultivated for 24–96 h at 18°C. Single-spore microcolonies were transferred into new Petri dishes. In the case of *L. maculans*, a single pycnidium from a symptomatic leaf was transferred to a droplet of sterile water on a glass microscope slide. The pycnidium was crushed by a cover glass and a part of the conidia was spread using a sterile needle over a solid PDA medium. After 3 days at 18°C in darkness, single microcolonies were transferred to new PDA plates. The *L. maculans* isolate JN2, also referred to as v23.1.2 (Balesdent et al., 2001; Šašek et al., 2012b), was used for most of the assays. Conidia of isolates JN2 and JN2-sGFP (JN2 transformed using a pCAMBgfp construct (Šašek et al., 2012a) were obtained from sporulating mycelium 10 days old kept under a 14h/10h light/dark regime (150 μE·m^{-2}·s^{-1}, 22°C, 70% relative humidity) in a cultivation chamber as described by Šašek et al. (2012b). Conidia were stored in concentration 10^8 conidia·ml^{-1} at −20°C for up to 6 months.

Antifungal and Antibacterial Assays

The radial growth of fungal mycelium was analyzed on PDA plates using the agar dilution method. Mycelial discs, 2 mm in diameter, were cut from the margins of colonies 5 days old and transferred to medium supplemented with streptomycin sulfate (50 μg·ml^{-1}) and saponins (0, 10, 25, 50, and 100 μg·ml^{-1}). After incubation at 18°C in darkness for 3 days in cases of rapidly growing fungi (*F. culmorum, L. maculans, M. nivale*, and *P. teres*) and 14 days in case of slowly growing fungi (*O. yallundae, R. collo-cygni*, and *Z. tritici*), the colony diameters were measured and compared to control plates lacking a saponin. Each isolate was analyzed in four technical replicates (four mycelial discs per plate) and in three independent biological experiments.

The conidial growth of *L. maculans* JN2-GFP isolate was analyzed in Gamborg B5 medium (Duchefa) supplemented with 0.3% (w/v) sucrose and 10 mM MES buffer (pH 6.8) at the final concentration of 2500 conidia per well of black 96-well plate (Nunc®). Aescin was used in the concentration range 0–100 μg·ml^{-1}. Plates were incubated in darkness at 26°C for 4 days. Fluorescence was measured in eight wells for each treatment using a Tecan F200 fluorescence reader (Tecan, Männedorf, Switzerland) with 485/20 nm excitation filter and 535/25 nm emission filter. For both assays, the final concentration of EtOH in all treatments was 1% (v/v). Effective dose (EC_{50}) values were calculated by probit analysis (Finney, 1971) using Biostat software (AnalystSoft Inc., Walnut, CA, USA). For microscopic analysis, the content of each well was transferred to a microscopic slide and observed under a Leica DM 5000 B fluorescence microscope (Leica, Germany).

To monitor antibacterial activity of aescin, a fresh bacterial suspension (OD_{600} of 0.005) in liquid LB medium was prepared from *Pst* DC3000 culture grown overnight on LB agar plates. Aescin (10 μg·ml^{-1}) or EtOH (0.1%) was added to this suspension and OD_{600} was measured after 24 h, with three independent samples being used for each treatment.

Fungal Treatment for Gene Expression

For gene expression, 10^7 conidia of JN2-GFP were grown in 100 ml of Gamborg B5 medium (Duchefa, G0210, Haarlem, The Netherlands) supplemented with 3% (w/v) sucrose and 10 mM MES (pH 6.8) in Erlenmeyer flasks. Cultures were kept at 26°C in darkness and at constant shaking of 130 rpm in an orbital shaker (JeioTech, Seoul, Korea). The culture at day 7 was treated in sterile conditions with aescin, fungicide, or control (EtOH). The concentration of EtOH solvent was identical in each treatment. Samples were collected after 24 hours of treatment and processed as described for plant samples.

Plant Cultivation and Treatment

Brassica napus plants of cultivar (cv.) Columbus were grown in perlite nourished with Steiner's nutrient solution (Steiner, 1984) under a 14 h/10 h light/dark regime (25°C and 150 μE·m^{-2}·s^{-1}/22°C) and 30–50% relative humidity in a cultivation room. In all assays, chemical treatment was applied to 10 days old plants. Treatment was infiltrated into the abaxial side of cotyledons using a 1 ml plastic needleless syringe. At least six plants were used for each sample.

Arabidopsis thaliana Col-0 and NahG transgenic plants (Delaney et al., 1994) were grown in soil. Surface-sterilized seeds were sown in Jiffy 7 peat pellets and the plants cultivated under a short-day photoperiod (10 h/14 h light/dark regime) at 100–130 μE·m^{-2}·s^{-1}, 22°C and 70% relative humidity. They were watered with fertilizer-free distilled water as necessary. Plants 4 weeks old were used for all assays. Treatment was applied to three fully developed leaves from one plant, using a 1 ml needless syringe. At least six plants were used for each sample.

Except from concentration dependent assays, aescin was used at 25 μg·ml^{-1} and 10 μg·ml^{-1} concentrations for *B. napus* and *A. thaliana*, respectively. Treatment at these concentrations caused no evident leaf chlorosis symptoms. As a control treatment, EtOH at a corresponding concentration was used.

Plant Resistance Assays

For *B. napus- L. maculans* resistance assays, cotyledons were pre-treated with diverse treatments 4 days prior to infection. Upon infection, the pre-treated cotyledons of *B. napus* plants 14 days old were infiltrated by an aqueous conidial suspension of *L. maculans* JN2-GFP (10^5 conidia·ml^{-1}) as described by Šašek et al.

(2012a) using a 1 ml needleless syringe. Prior to inoculation true leaves were removed from plants to avoid cotyledon senescence. At least 12 plants were used per condition. The cotyledons were assessed 11 days after inoculation. The cotyledon areas and lesion areas therein were measured by image analysis using APS Assess 2.0 software (American Phytopathological Society, St. Paul, MN, USA). The relative lesion area was then calculated as the ratio of lesion area to whole leaf area. The hyphal colonization of cotyledons was assessed under a Leica DM5000 B fluorescence microscope (Leica, Germany).

For *A. thaliana* – *P. syringae* pv. tomato DC3000 resistance assays, leaves were pre-treated with aescin 24h prior to infection. The bacteria *Pst* DC3000 was cultivated overnight on lysogeny broth (LB) agar plates with rifampicin at 26°C, then resuspended in 10 mM $MgCl_2$ to an OD_{600} of 0.005. The bacterial suspension was infiltrated into three fully developed pre-treated leaves from one plant, using a 1 ml needless syringe. After 3 days, cut leaf discs (one disc per leaf, 0.6 cm in diameter) were collected from infected tissue, with three leaves from a single plant representing one sample. To determine bacterial content in leaves at 0 dpi, samples were collected 1 h after bacterial infiltration. Tissue was homogenized in tubes with silica beads using a FastPrep-24 instrument (MP Biomedicals, Santa Ana, CA, USA). The resulting homogenate was serially diluted and transferred onto LB agar plates with rifampicin. Grown bacterial colonies were counted after 24 h of incubation at 26°C.

Reactive Oxygen Species Detection

Treated cotyledons were detached and infiltrated under vacuum with diaminobenzidine tetrahydrochloride (DAB; Šašek et al., 2012b) aqueous solution (10 mg·ml^{-1}, Sigma–Aldrich), with DAB being solubilized in dimethylformamide. Cotyledons were kept in humid conditions in darkness at room temperature until reddish-brown staining appeared. Chlorophyll was removed using 96% EtOH, after which cotyledons were rehydrated and scanned.

Analysis of Plant Hormones

Levels of plant hormones were determined 24 hours post treatment in *B. napus* cotyledons. In each sample, 150 mg of fresh material from plant tissue was pooled from eight different plants, as previously described (Dobrev and Kaminek, 2002). Briefly, samples were homogenized with extraction reagent methanol/H_2O/formic acid (15:4:1, v:v:v) supplemented with stable isotope-labeled internal standards, each at 10 pmol per sample. Clarified supernatants were subjected to solid-phase extraction using Oasis MCX cartridges (Waters Co., Milford, MA, USA), eluates were evaporated to dryness, and the generated solids were dissolved in 30 µL of 15% (v/v) acetonitrile in water. Quantification was done on an Ultimate 3000 high-performance liquid chromatograph (HPLC; Dionex, Bannockburn, IL, USA) coupled to a 3200 Q TRAP hybrid triple quadrupole/linear ion trap mass spectrometer (MS; Applied Biosystems, Foster City, CA, USA), as described by Djilianov et al. (2013). Metabolite levels were expressed in pmol·g^{-1} fresh weight.

Gene Expression Analysis

Samples (both plant and fungi) were collected 24 hours post treatment. At least six plants were used for each sample for gene expression. Total RNA was isolated from 100 mg of frozen plant tissue or fungal mycelium using a Spectrum Plant Total RNA Kit (Sigma–Aldrich, St. Louis, MO, USA). Next, 1 µg of RNA was treated with a DNA-free Kit (Ambion, Austin, TX, USA) and reverse transcribe to cDNA with M-MLV RNase H Minus Point Mutant reverse transcriptase (Promega Corp., Fitchburg, WI, USA) and anchored oligo dT_{21} primer (Metabion, Martinsried, Germany). Gene transcription was quantified by q-PCR using LightCycler 480 SYBR Green I Master kit and LightCycler 480 (Roche, Basel, Switzerland). The PCR conditions were: 95°C for 10 minutes, followed by 45 cycles of 95°C for 10 s, 55°C for 20 s, and 72°C for 20 s, followed by a melting curve analysis. Relative transcription was calculated with efficiency correction and normalization to the corresponding housekeeping gene for each organism. LmERG3 (Q8J207) and LmERG11 (Q8J1Y7) proteins were retrieved from the Uniprot database and primers were designed for the corresponding genes using PerlPrimer v1.1.21 (Marshall, 2004). Primers are listed in **Supplementary Table 1**.

Chemical Treatments

Saponins aescin (E1378), hederagenin (H3916), and soyasaponin I (S9951), and fungicides metconazole, fluconazole, boscalid, and fluopyram (all purchased from Sigma–Aldrich, St. Louis, MO, USA) were dissolved in 99.8% ethanol (EtOH) as 10 mg·ml^{-1} stock solution. Tebuconazole, in the form of the commercially formulated product Horizon 250 EW (Bayer CropScience, Germany), was also prepared as 10 mg·ml^{-1} stock solution in EtOH. Ergosterol (Sigma, St. Louis, MO, USA) was prepared as 5 mM stock solution in EtOH and used at the final concentration of 25 µg·ml^{-1}. Benzothiadiazole (BTH) was used in the form of the commercially formulated product Bion 50 WG (Syngenta, Switzerland) and prepared directly into the working solutions. The commercial peptide flg22 (EZBiolab) was diluted in Milli-Q water and used at the final concentration of 1 µM. All stock solutions were stored at −20°C.

Statistical Analyses

If not stated otherwise, all experiments were repeated independently three times, with at least three independent samples (from independent biological material, cultivated under the same conditions). Using Statistica 12 software, statistical analyses were performed either by paired two-tailed Student's *t*-test or by analysis of variance in conjunction with Tukey's honestly significant difference multiple mean comparison *post hoc* test ($P < 0.05$).

RESULTS

Aescin Has the Highest Antifungal Activity Among Tested Saponins

Although saponins are well known to have antifungal activity (Gruiz, 1996; Moses et al., 2014), only very limited data is available

quantifying saponin antifungal activity by establishing EC_{50} values. We screened antifungal activity of the triterpenoid plant saponins aescin (from *Aesculus hippocastanum*), soyasaponin (from *Glycine max*), and hederagenin (from *Hedera helix*) against important fungal pathogens (*O. yallundae, M. nivale, Z. tritici, P. teres, R. collo-cygni, F. culmorum*, and *L. maculans*). These fungi infect such crop plants as wheat, barley, or oilseed rape. Our fungal collection consists of various naturally occurring isolates for each pathogen. To calculate EC_{50} values, we assessed the radial mycelial growth on solid media plates supplemented with saponins. All tested saponins displayed significant antifungal activity, with aescin's activity being the most efficient (**Figure 1A**). Differences in species sensitivity to saponins were observed (**Figure 1A**). As further analyzed for aescin, the activity on isolates varied among species but was mostly conserved within a given fungal species (**Figure 1B**). The fungi most sensitive to saponins were *M. nivale*, *P. teres*, and *L. maculans*, while *O. yallundae*, *R. collo-cygni, Z. tritici*, and *F. culmorum* showed only minor growth inhibition (**Figures 1A**, **B**; **Table 1**). Accordingly, while aescin EC_{50} values for *P. teres, M. nivale*, and *L. maculans* isolates occurred in the range of 11–21 $\mu g \cdot ml^{-1}$, 7–29 $\mu g \cdot ml^{-1}$, and 25–33 $\mu g \cdot ml^{-1}$, respectively, EC_{50} values for more-resistant fungal isolates exceeded 100 $\mu g \cdot ml^{-1}$ and could not be calculated precisely due to concentration limitations caused by saponin solubility (**Table 1**). It is noteworthy that fungal sensitivity (**Figure 1B**) did not correlate with hyphal thickness (**Supplementary Figure 1A**). Correlation between fungal growth rate and fungal sensitivity was observed, however, with the slowly growing isolates being the most resistant (**Supplementary Figure 1B**). In summary, all tested saponins inhibited growth of phytopathogenic fungi in a species-dependent manner, with the strongest growth inhibition provided by aescin.

Aescin Antifungal Activity Is Lower Than That of Commercial Fungicides

The biological activity of aescin was further studied on *L. maculans*, which is a destructive pathogen of *B. napus*. The antifungal activities (EC_{50} values) of aescin and synthetic fungicides were first compared. Several fungicides of different classes were tested, including triazolic sterol inhibitor tebuconazole, commonly used for *B. napus* protection against phoma stem canker (Child

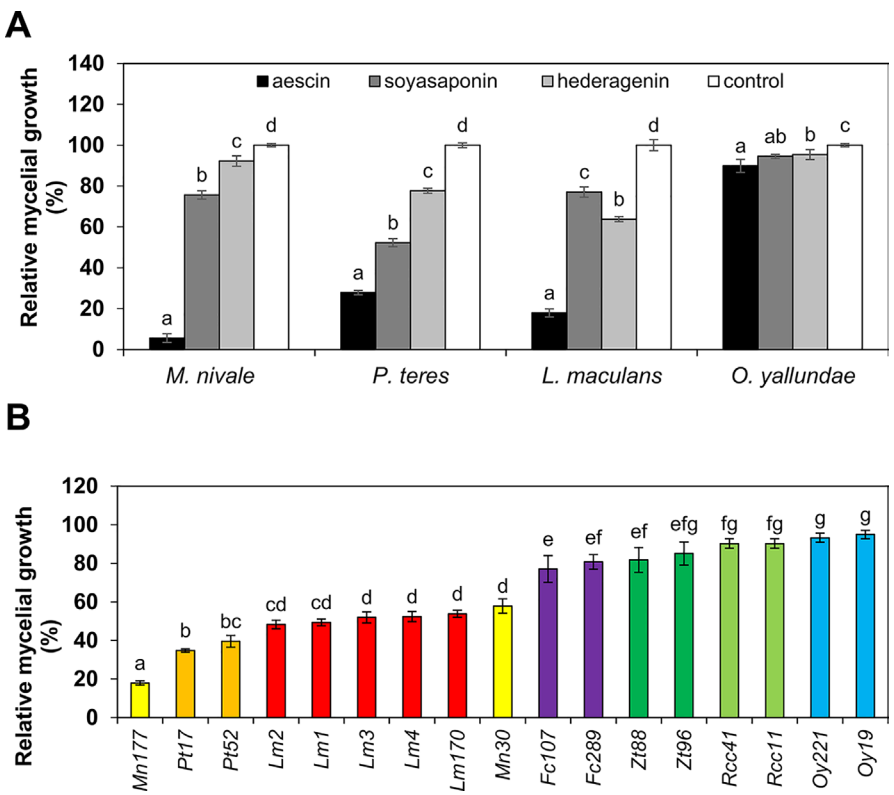

FIGURE 1 | Saponins inhibit mycelial growth of crop pathogens *in vitro* in a species-dependent manner. Relative growth of different fungal species assessed as percentage diameter of fungal colony cultivated on PDA medium supplemented with saponins. The control treatment (without saponins) was set as 100%. **(A)** Growth on aescin (black bars), soyasaponin (dark gray bars), and hederagenin (light gray bars) at 100 $\mu g \cdot ml^{-1}$, or on a control (without saponin; white bars). The following fungal isolates were used: Mn177, Pt52, Lm1, and Oy19. **(B)** Growth on aescin at the 25 $\mu g \cdot ml^{-1}$ rate compared to control-treated fungi. All data represent means ± SE from three independent experiments. Different letters above bars illustrate significant differences using ANOVA test in conjunction with Tukey's honestly significant difference multiple mean comparison *post hoc* test ($P < 0.05$). For (A), the statistical analyses were carried out separately within each fungal species (Fc, *Fusarium culmorum*; Lm, *Leptosphaeria maculans*; Mn, *Microdochium nivale*; Oy, *Oculimacula yallundae*; Pt, *Pyrenophora teres*; Rcc, *Ramularia collo-cygni*; Zt, *Zymoseptoria tritici*).

TABLE 1 | Effective dose (EC_{50}) values of saponins against pathogenic fungi.

Fungal species	Isolate	EC_{50} [μg·ml^{-1}]		
		Aescin	Soyasaponin	Hederagenin
Microdochium nivale	Mn30	29.40 ± 6.01	*na*	*na*
	Mn177	6.74 ± 0.84	>100.00	>100.00
Pyrenophora teres	Pt17	11.40 ± 9.51	*na*	*na*
	Pt52	20.79 ± 5.14	97.61 ± 8.83	> 100.00
Leptosphaeria maculans	Lm170	31.71 ± 3.29	*na*	*na*
	Lm1	28.62 ± 10.03	>100.00	>100.00
	Lm2	25.21 ± 3.25	*na*	*na*
	Lm3	33.11 ± 6.49	*na*	*na*
	Lm4	25.52 ± 0.88	*na*	*na*
Fusarium culmorum	Fc107	>100.00	*na*	*na*
	Fc289	>100.00	*na*	*na*
Zymoseptoria tritici	Zt88	>100.00	*na*	*na*
	Zt96	>100.00	*na*	*na*
Ramularia collo cygni	Rcc11	>100.00	*na*	*na*
	Rcc41	>100.00	*na*	*na*
Oculimacula yallundae	Oy19	>100.00	>100.00	>100.00
	Oy221	>100.00	*na*	*na*

EC_{50} values [μg·ml^{-1}] calculated by probit analysis for combinations of a given fungal pathogenic isolate and a given saponin, assessed as inhibition of mycelial radial growth on PDA medium with saponin. Data are expressed as means ± SE from three experiments. Cases of EC_{50} > 100.00 indicate that precise values above 100 μg ml^{-1} could not be calculated. na, not analyzed.

et al., 1993). For this purpose, fungal growth was measured as GFP fluorescence of germinating conidia of the *L. maculans* JN2 isolate expressing GFP (JN2-GFP) (Balesdent et al., 2001; Šašek et al., 2012a). In this setup, aescin was fully fungitoxic to the conidia at concentrations above 50 μg·ml^{-1} (**Figure 2A**) and demonstrated EC_{50} of 28.79 μg·ml^{-1} (**Figures 2A**, **B**) that was in agreement with EC_{50} obtained for the *L. maculans* field isolates (**Table 1**). EC_{50} values for the fungicides were mostly in a range from 0.018 μg·ml^{-1} to 0.087 μg·ml^{-1}, with metconazole being the most efficient (**Figure 2B**). On the other hand, fluconazole, was the least efficient (EC_{50} = 2.33 μg·ml^{-1}; **Figure 2B**). Overall, aescin inhibits conidial and mycelial growth of *L. maculans in vitro* and demonstrates antifungal activity 1 to 3 orders of magnitude lower than that of fungicides.

Antifungal Activity of Aescin Against *L. Maculans* Occurs Through Its Interaction With Sterols

Aescin's antimicrobial effect occurs through interference with membranes and interaction with sterols (Morrissey and Osbourn, 1999; Sreij et al., 2019). Therefore, we tested aescin's activity in the presence of ergosterol, a sterol naturally present in fungal membranes. Ergosterol markedly restored the growth of *L. maculans* JN2-GFP in the presence of aescin at all the inhibiting concentrations (**Figure 3A**), which was confirmed also by microscopic analysis of hyphae (**Figure 3B**) (**Supplementary Figure 2**). Growth inhibition caused by metconazole could not be reversed by the ergosterol supply (**Figure 3C**). Ergosterol itself did not significantly affect fungal growth (concentration 0 of **Figures 3A, C**). Inasmuch as triazole fungicides block biosynthesis of ergosterol (Sanati et al., 1997), transcription of *LmErg3* and *LmErg11* genes, identified as involved in ergosterol biosynthesis in *L. maculans* (Griffiths and Howlett, 2002), was assessed following aescin treatment of the fungus. The effect of aescin or fungicides was observed in 7-day-old *L. maculans* culture 24 h post treatment. While metconazole induced transcription of *LmErg3* and *LmErg11* genes by 7 times and 27 times, respectively, in excess of the control, aescin did not significantly upregulate transcription of these genes (**Figure 3D**). The data show that aescin interfered with the fungal ergosterol but not directly with its biosynthesis.

Aescin Pretreatment Confers Resistance in *B. napus* Against *L. maculans*

Given the antifungal activity of aescin, we further investigated whether pretreatment with aescin could efficiently protect *B. napus* against *L. maculans*. Pretreatment of *B. napus* cotyledons by leaf infiltration with aescin at rates of 25 μg·ml^{-1} and 10 μg·ml^{-1} 3 days prior to inoculation with *L. maculans* JN2-GFP efficiently reduced the cotyledon area covered by necrotic lesions (**Figures 4A, B**). The effect was comparable to those provided both by the fungicide metconazole at rate 2 μg·ml^{-1} and the plant defense inducer benzothiadiazole (BTH) at rate 30 μM. BTH activates the *B. napus* immune system and provides protection against *L. maculans* (Šašek et al., 2012a). The protection provided by aescin was even more efficient than was that induced by the fungicide tebuconazole at rate 2 μg·ml^{-1}. Aescin's protection was concentration dependent, and no significant effect was observed with aescin at the 2 μg·ml^{-1} level. Microscopic analyses (**Figure 4C**) revealed only a few restricted GFP-fluorescent hyphal zones in aescin- and metconazole-pretreated cotyledons, while the control treatment displayed extensive hyphal network all over the infected cotyledon and corresponding to the localization of necroses. We also showed that foliar spray of aescin aqueous solution is protective (**Supplementary Figure 3**), although higher concentration may be required compared to when

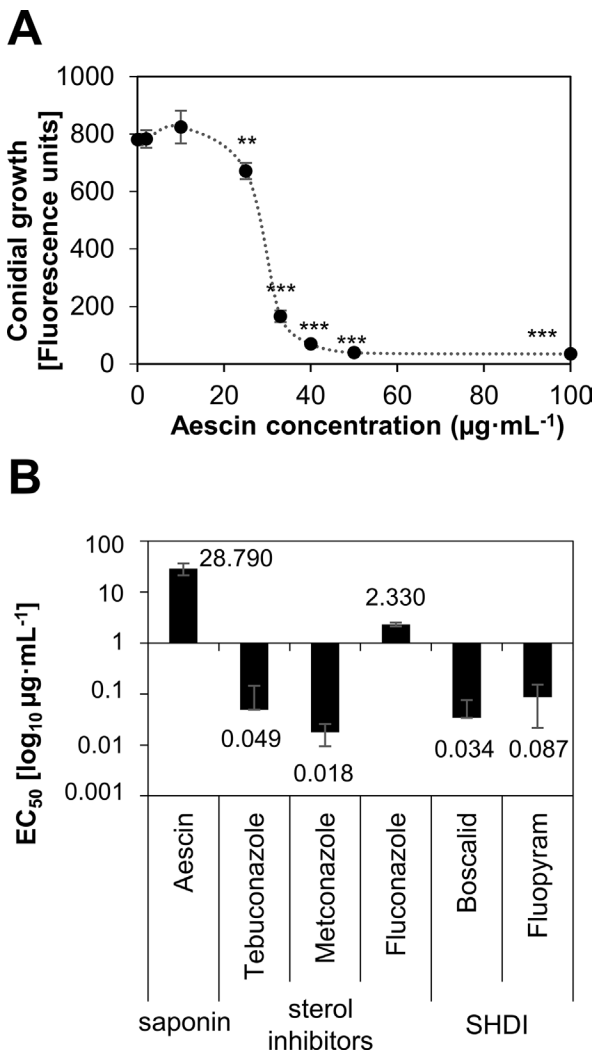

FIGURE 2 | Comparison of aescin and fungicide inhibitory activity against *L. maculans*. Growth of *L. maculans* JN2-GFP conidia *in vitro* in Gamborg liquid medium supplemented with aescin, fungicides, or control medium assessed as GFP fluorescence at 3 days. **(A)** The concentration-dependent curve for growth in the presence of aescin. Data are mean ± SE of absolute fluorescence units out of three experiments. Asterisks indicate significant differences between aescin treatment and control (0) using two-tailed Student's *t*-test (***P* < 0.01; ****P* < 0.001). **(B)** Calculated EC_{50} values [µg·ml^{-1}] ± SE at $\log_{10}$ base for aescin and different fungicides from sterol inhibitor (tebuconazole, metconazole, and fluconazole) and succinate dehydrogenase inhibitor (SHDI) classes (boscalid, fluopyram). Data are from three independent experiments.

infiltration is used. Taken together, our data demonstrate that aescin protects *B. napus* against *L. maculans* by inhibiting tissue colonization by fungal hyphae and necrosis formation. It is noteworthy that the treatment with aescin at concentration 25 µg·ml^{-1} decreased cotyledon growth to a similar extent as did 30 µM BTH (**Supplementary Figure 4**). At higher concentrations (above 50 µg·ml^{-1}), aescin caused chlorosis and necroses on leaves (**Supplementary Figure 4**). Treatment with 10 µg·ml^{-1} of aescin caused no obvious effects on cotyledon fitness (**Supplementary Figure 4**), however, and this concentration was still able to reduce *L. maculans* infection (**Figure 4A**).

Aescin Induces Defense Responses in *L. Maculans*, Governed by SA Pathway and Oxidative Burst

The fact that aescin can provide a higher level of plant protection than do fungicides having more potent antifungal activity suggested a possibility that aescin stimulates plant defense. Therefore, transcription of plant defense marker genes was determined in cotyledons 6 h and 24 h after treatment with aescin or BTH (**Figure 5A**). At both time points, aescin upregulated transcription of *BnPR1* and SA-specific transcription factor *BnWRKY70* genes previously characterized as being marker genes of activated SA pathway in *B. napus* (Šašek et al., 2012b). At 24 h, the level of induction was similar to that of BTH, but aescin and BTH induced defense genes with different kinetics. In contrast to BTH, aescin also upregulated transcription of the SA-biosynthetic gene for isochorismate synthase 1 (*BnICS1)*. Given the strong induction of *BnICS1* transcription, aescin's capacity to stimulate SA production was tested and compared to that of flg22, a well-characterized microbe-associated molecular pattern (MAMP) activating SA pathway in *A. thaliana* (Tsuda et al., 2008; Lloyd et al., 2014). Aescin application at the 25 µg·ml^{-1} rate to cotyledons led to a massive increase in SA 24 h after treatment, with SA content reaching even higher levels than those seen following treatment with 1 µM flg22 (**Figure 5B**). Other tested phytohormone metabolites were altered not at all or only slightly by aescin (**Figure 5C**). Aescin caused mild decrease in the *cis*-OPDA metabolite, the JA precursor (Dave and Graham, 2012), and auxin forms. In summary, based on gene transcription analysis and phytohormone measurement, it was apparent that aescin treatment activated the SA pathway.

Further defense responses were analyzed in aescin-treated *B. napus* cotyledons. At 24 h following treatment aescin triggered accumulation of ROS compared to the control treatment, as was visualized by brown-reddish precipitates in DAB staining assay (**Figure 5D**). The accumulation was induced to a similar extent as was that for the flg22 treatment and was concentration dependent (**Supplementary Figure 5**). Accordingly, at 24 h post treatment, aescin induced transcription of respiratory burst oxidase homolog *RbohD* and *RbohF* genes coding NADPH oxidases responsible for ROS production in plants after exposure to MAMPs (Torres et al., 2005; Qi et al., 2017) (**Figure 5E**). The fungicides tebuconazole and metconazole did not elicit transcription of any defense genes, nor did they trigger oxidative burst in *B. napus* cotyledons (**Supplementary Figures 6A**, **B**).

Aescin-Induced SA-Dependent Resistance to Bacterial Pathogen in *A. thaliana*

To exclude that the phenomenon of aescin-activated immunity is specific to the *B. napus–L. maculans* system, the activity of aescin was investigated also in an *A. thaliana* model system challenged by a hemibiotrophic bacterial pathogen, *Pst* DC3000. After 24 h of treatment with aescin at the 10 µg·ml^{-1} level, there

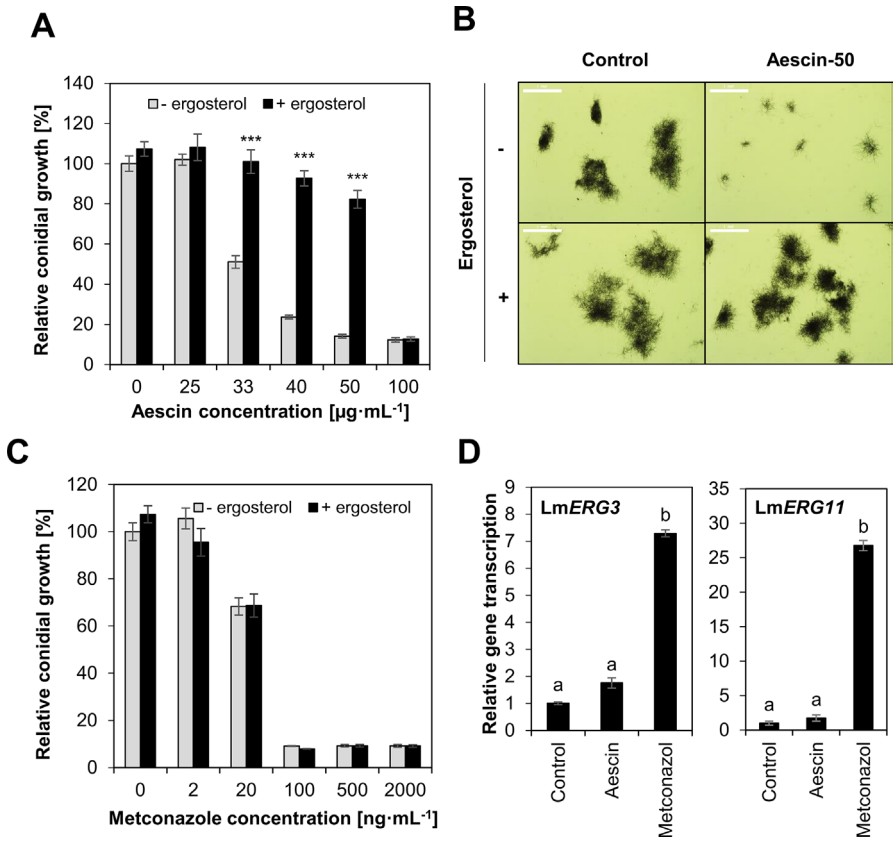

FIGURE 3 | Ergosterol reverts aescin-mediated growth inhibition of *L. maculans.* **(A–C)**. Growth of *L. maculans* JN2-GFP conidia *in vitro* in Gamborg liquid medium supplemented with aescin **(A**, **B)** or metconazole **(C)** in absence (gray bars) or presence (black bars) of ergosterol (25 µg·ml^{-1}). **(A**, **C)** Data are expressed as relative fluorescence units at 4 days of growth compared to control (0) without ergosterol, set as 100%. Data are expressed as means ± SE from three independent experiments. Asterisks indicate significant differences (***$P < 0.001$; two-tailed Student's *t*-test) between treatments with and without ergosterol for each concentration of aescin or metconazole. **(B)** Light microscopy of germinating hyphae at control and aescin at 50 µg·ml^{-1} rate at 5 days of growth in presence or absence of ergosterol (25 µg·ml^{-1}). Scale bar corresponds to 1 mm. **(D)** Relative transcription of ergosterol biosynthetic genes *LmERG3* and *LmERG11* at mycelium 7 days old and treated with aescin (100 µg·ml^{-1}) or metconazole (2 µg·ml^{-1}) for 24 h. Gene transcription was analyzed by qPCR, normalized to *LmTubulin*, then compared to control treatment. Data represent mean ± SE from one biological experiment (three biological replicates) representative of three. Different letters above bars illustrate significant differences using ANOVA test in conjunction with Tukey's honestly significant difference multiple mean comparison *post hoc* test ($P < 0.05$).

was upregulated transcription of *AtPR1* and *AtICS1* genes in *A. thaliana* leaves (**Figure 6A**). Aescin pretreatment for 24 h also led to induced resistance against bacterium *Pst* DC3000, observed as substantial decrease of both disease symptoms and bacterial titers in infected leaves (**Figure 6B**). For direct investigation of possible SA involvement in aescin-triggered resistance to Pst DC3000, we used NahG transgenic plants, in which low endogenous SA levels are maintained through the expression of SA-hydroxylase (Delaney et al., 1994). In NahG plants, the effect of aescin-induced resistance against *Pst* DC3000 was lost (**Figure 6B**).

Aescin did not impact the growth of *Pst* DC3000 cultivated *in vitro* (**Supplementary Figure 7A**). It also did not affect the bacterial titers in aescin-pretreated leaves sampled 1 h after infection with *Pst* DC3000 (**Supplementary Figure 7B**). In addition, co-inoculation of *A. thaliana* plants simultaneously with *Pst* DC3000 bacterium and aescin did not affect the bacterial colonization in the infected leaves (**Supplementary Figure 7C**). These data suggest that the bacterial resistance provided by aescin in *A. thaliana* is not due to a direct antibacterial effect. Together, these data show increased resistance of *A. thaliana* against *Pst* DC3000 induced by aescin treatment, which possibly acts through activating SA-dependent immune pathways.

DISCUSSION

Currently, field crops are protected from fungal pathogens by such fungicide compounds as benzimidazoles, sterol biosynthesis inhibitors, strobilurins, or succinate dehydrogenase inhibitors. Because the occurrence of synthetic pesticide residues is progressively degrading the health of living organisms and the environment even as fungicide resistance is developing, there is a clear need to discover "greener" antifungal agents. Our study was focused on plant-derived saponins as hypothetical new plant protectants.

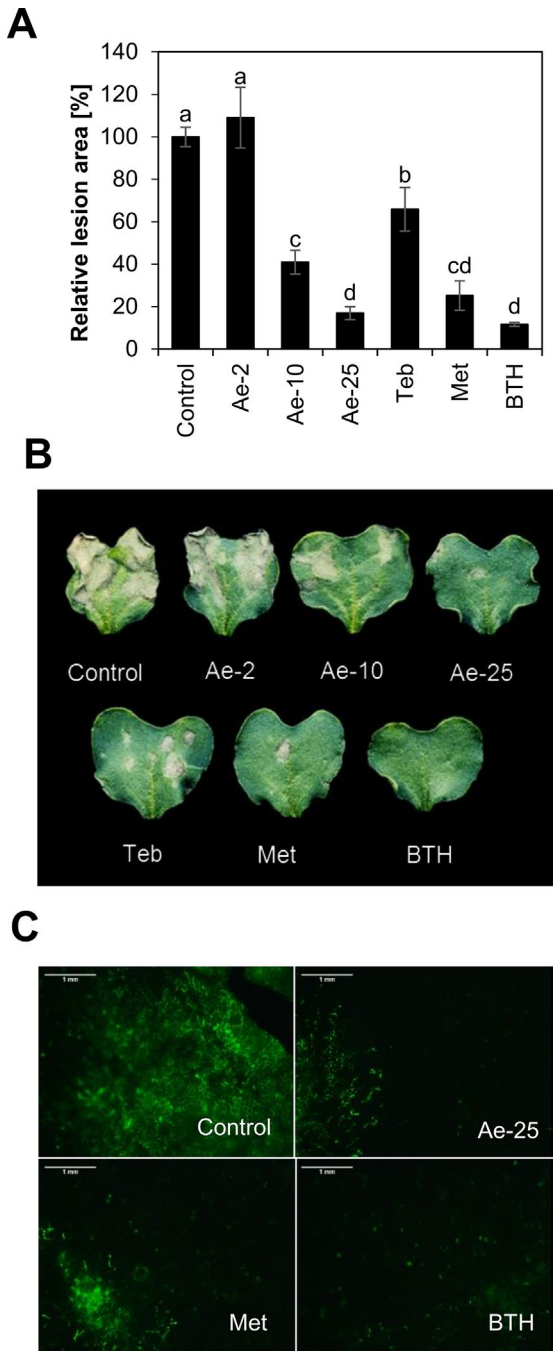

FIGURE 4 | Aescin pretreatment provides B. napus with efficient resistance against *L. maculans*. Cotyledons of *B. napus* were infiltrated by aqueous solutions of aescin (Ae; at 2, 10, and 25 μg·ml^{-1}), tebuconazole, metconazole (Teb and Met; both at 2 μg·ml^{-1}), BTH (30 μM), or a control 3 days prior to being infiltrated by conidial suspension of *L. maculans* JN2-GFP. The outcome was assessed at 12 days. **(A)** Quantification of the relative lesion area by image analysis is expressed as percentage. Control treatment was set as 100%. Data represent means ± SE from five independent experiments. Different letters above bars illustrate significant differences using ANOVA test in conjunction with Tukey's honestly significant difference multiple mean comparison *post hoc* test (P 0.05). **(B)** Panel with representative infected cotyledons. **(C)** Hyphal spread of JN2-GFP fungus in infected cotyledons. Scale bar corresponds to 1 mm.

Aescin: A Potent Antifungal Saponin

The effect of saponins on fungi has been widely studied (Gruiz, 1996; Barile et al., 2007; Hoagland, 2009; Saha et al., 2010; Teshima et al., 2013). Heretofore, however, there has been only few comprehensive studies of saponin activity against phytopathogens, including to determine EC_{50} values and compare more deeply saponin efficiency with that of synthetic fungicides.

EC_{50} values in the ranges 181–678 μg·ml^{-1} and 230–455 μg·ml^{-1} have been reported for the inhibitory activity of saponins of *Sapindus mukorossi* and *Diploknema butyracea,* respectively, on mycelial growth of phytopathogens *Rhizoctonia* sp. and *Sclerotinia* sp. (Saha et al., 2010). Minutosides extracted from *A. minutiflorum* have been shown to be highly inhibitory to spore germination of soil- and air-borne fungi (*Fusarium oxysporum, F. solani, Pythium ultimum, Rhizoctonia solani, Botrytis cinerea, Alternaria alternata, A. porri*, and *Trichoderma harzianum*) at 10–1000 μg·ml^{-1}, depending upon the individual fungal species and saponin (Barile et al., 2007). The antifungal activity of aescin, a saponin from horse chestnut *Aesculus hippocastanum*, has been characterized only poorly. Previous studies have reported both antibacterial activity of β-aescin towards soil *Rhizobium* bacteria (Zablotowicz et al., 1996) and its antifungal activity against Candida sp. (Franiczek et al., 2015). However, knowledge as to aescin's activity against phytopathogens has not previously been presented. Here, we tested the antifungal effect of aescin on seven species of phytopathogenic fungi causing crop losses in cereals and rapeseed. The activity was also tested in comparison to that of soyasaponin, hederagenin, and synthetic fungicides.

We have shown here that aescin displayed strong inhibitory effect against fungal growth, significantly impeding mycelial growth in all tested fungal isolates (**Figure 1A**). Aescin was highly active against *M. nivale*, *P. teres*, and *L. maculans,* exhibiting EC_{50} values below 50 μg·ml^{-1} (**Table 1**). Aescin also exhibited greater antifungal activity than did the other two saponins tested, soyasaponin and hederagenin (**Figure 1A**, **Table 1**). In light of these results and those of previous studies on other saponins, aescin emerges as a potent antifungal saponin. A parallel comparison of aescin's inhibitory activity with those of synthetic commercial fungicides was carried out on germinating *L. maculans* conidia. Aescin's EC_{50} was from 1 to 3 orders of magnitude greater in comparison to that of fungicides (**Figure 2**). Co-treatment with ergosterol, which reverses the effect of aescin but not the effect of fungicides, showed aescin to have a different mode of action on membranes compared to that of fungicides (**Figures 3A**, **C**).

We observed aescin activity to be variable in different fungal species, while it was mostly conserved among isolates within a given species (**Figure 1B**). Compared to other fungi, O. *yallundae* isolates were the most resistant to aescin and the other tested saponins (**Figure 1**, **Table 1**). This general resistance of *O. yallundae* independent of saponin type (**Figure 1A**) may reflect its different fungal morphology and physiology. A correlation was observed between growth rate and fungal sensitivity, and *O. yallundae* is a slowly growing fungus (**Supplementary Figure 1**). Furthermore, saponin-resistant fungi may contain membranes with low sterol content (Arneson and Durbin,

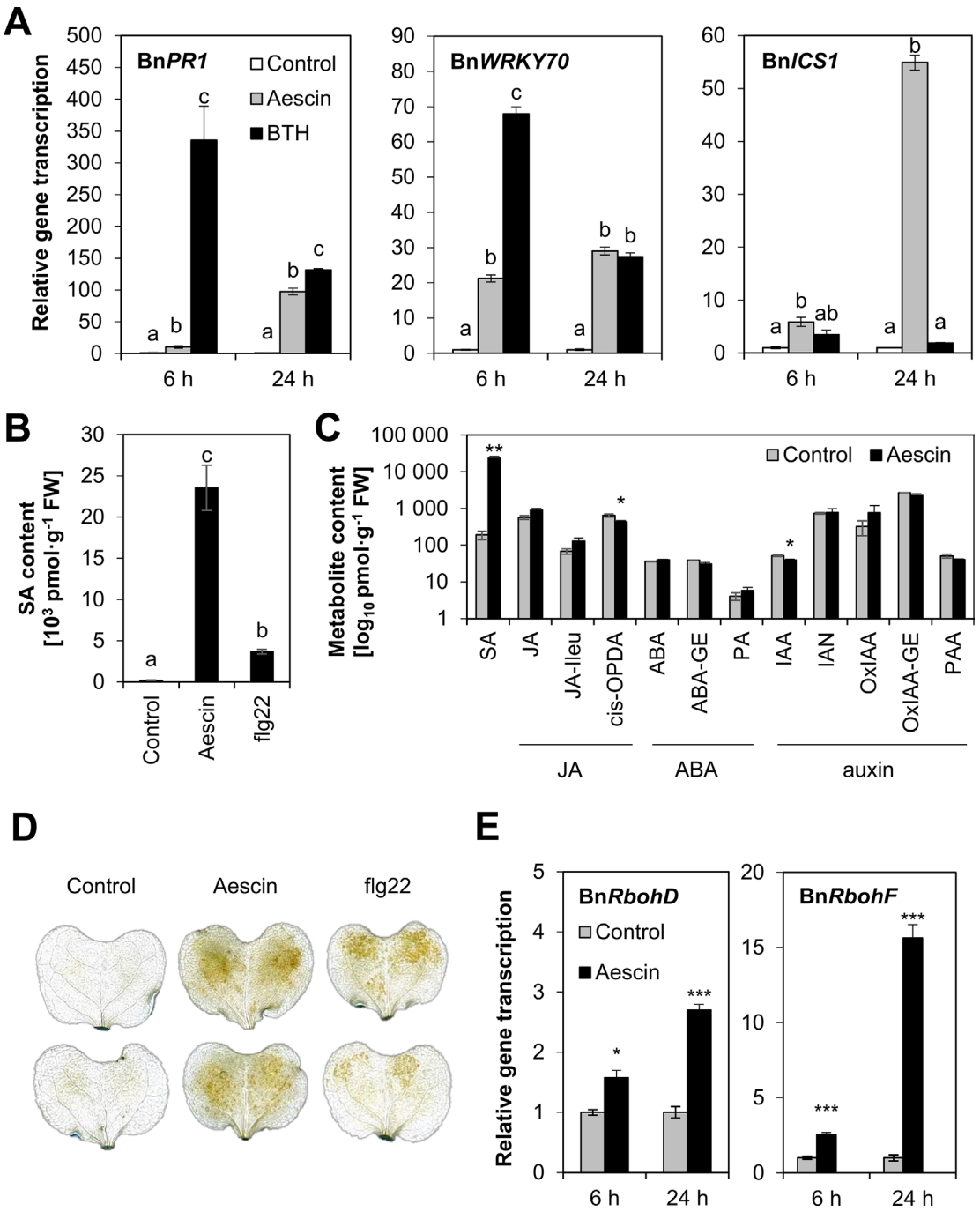

FIGURE 5 | Aescin treatment triggers defense responses in *B. napus*. Cotyledons of *B. napus* were infiltrated by aqueous solutions of aescin (25 μg·ml^{-1}), BTH (30 μM), flg22 (1 μM), or a control treatment. **(A)** Gene transcription of *pathogenesis-related BnPR1*, *BnWRKY70*, and *isochorismate-synthase 1 BnICS1* was analyzed by qPCR after 6 and 24 h of treatment, normalized to *BnActin* and *BnTIP41*, and compared to the corresponding control at 6 or 24 h (set as 1). Data represent mean ± SE from one biological experiment (four biological replicates), representative of three. **(B**, **C)** Content of salicylic acid (SA; **B**) and SA, JA, ABA- and auxin-derived hormones in control- or aescin-treated plants **(C)**. The content of hormones in plant tissue expressed as pmol·g^{-1} fresh weight ± SE was measured after 24 h. Data are means of four biological replicates. Experiment was repeated twice. SA, salicylic acid; JA, jasmonic acid; JA-Ile, JA-isoleucine; *cis*-OPDA, *cis*-12-oxo-phytodienoic acid; ABA, abscisic acid; ABA-GE, ABA-glucose ester; PA, phaseic acid; IAA, indole-3-acetic acid; OxIAA, oxo-IAA; OxIAA-GE, oxo-IAA-glucose ester; IAN, indole-3-acetonitrile; PAA, phenylacetic acid. **(D)** Oxidative burst visualized by DAB staining at 24 h post treatment. Images are representative of three experiments. **(E)** Transcription of respiratory burst oxidase homolog *RbohD* and *RbohF* genes following aescin treatment was analyzed at 6 or 24 h by qPCR, normalized to Bn*Actin* and Bn*TIP41*, and compared to the corresponding control (set as 1). Data represent means ± SE from one biological experiment (four biological replicates) representative of three. For **(A)** and **(B)**, different letters above bars illustrate significant differences using ANOVA test in conjunction with Tukey's honestly significant difference multiple mean comparison *post hoc* test (P 0.05). For **(A)**, the statistical analyses were carried out separately within each time point. For **(C)** and **(E)**, asterisks indicate significant differences between control and a given treatment (*$P < 0.05$; **$P < 0.01$; ***$P < 0.001$; two-tailed Student's *t*-test).

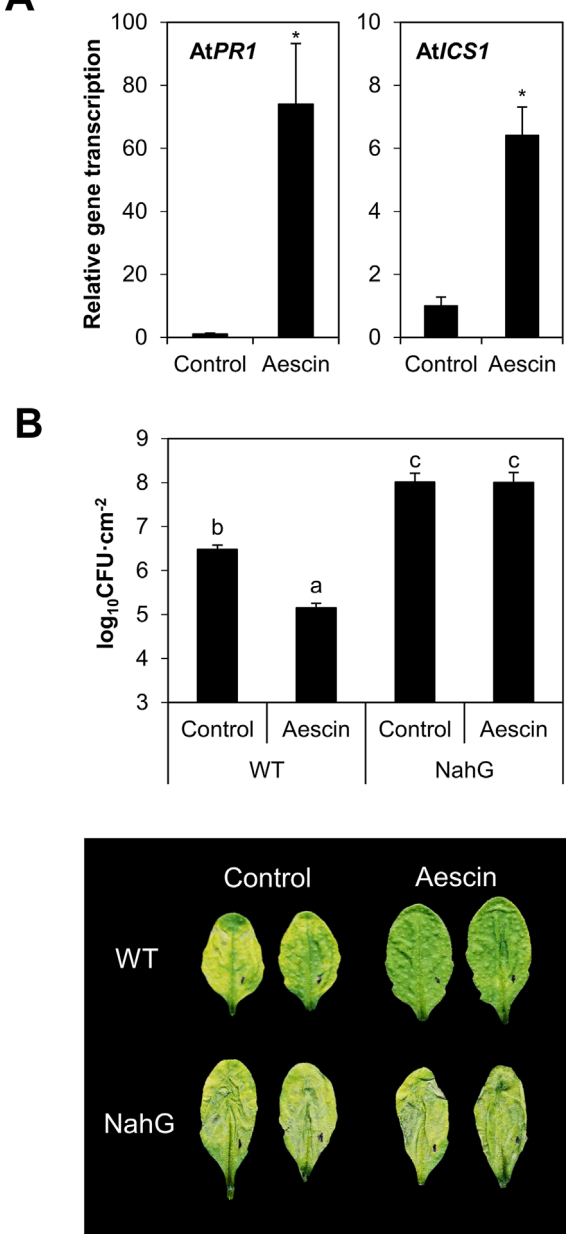

FIGURE 6 | Aescin pretreatment triggers defense gene transcription in *A. thaliana* and resistance against bacteria *Pseudomonas syringae* pv. tomato DC3000 (Pst DC3000). Leaves of Arabidopsis plants were infiltrated by aqueous solutions of aescin (10 μg·ml^{-1}) or a control treatment. **(A)** Gene transcription of *pathogenesis-related AtPR1* and *isochorismate-synthase 1 AtICS1* was analyzed by qPCR after 24 h of treatment, normalized to At*TIP41*, then compared to the control. Data represent mean ± SE from one biological experiment (four biological replicates), representative of three. Asterisks indicate significant differences *$P < 0.05$; two-tailed Student's *t*-test). **(B)** Bacterial growth of *Pst* DC3000 bacteria at 3 days post inoculation in infected leaves of wild type (WT) or NahG transgenic plants pretreated by aescin or control for 24 h. (*upper*) Bacterial titers within leaves. Data represent means of colony forming units (CFU) per cm^2 ± SE from six independent replicates of one experiment, representative of three. Different letters above bars illustrate statistical difference between samples using ANOVA with a Tukey honestly significant difference multiple mean comparison *post hoc* test ($P < 0.01$). (*lower*) A representative leaf for each treatment is shown.

1967; Barile et al., 2007) or fungal sterols with moieties bound only weakly by saponins (Steel and Drysdale, 1988). In general, fungi with defective sterol biosynthesis or in the presence of sterol inhibitors are more resistant to saponins (Olsen, 1973; Defago and Kern, 1983). Moreover, some fungi can cleave sugar moieties of saponins, thereby resulting in non-toxic molecules. For some saponins, a C3-attached sugar moiety or moieties can be critical for both permeabilizing membrane and antifungal properties of saponins (Morrissey and Osbourn, 1999). For instance, *Gaeumannomyces graminis* and *Gibberella pulicaris* produce avenacinase and alpha-chaconinase, respectively, and these detoxify their hosts' saponins (Bowyer et al., 1995; Becker and Weltring, 1998). To sum up, our study characterizes the fungistatic activity of aescin on different phytopathogenic fungi and provides a parallel comparison to fungicides.

Aescin: A Potent Plant Disease Control Agent

The role of saponins as plant-protecting compounds has been shown. Namely, avenacin triterpene glycosides protect oat roots against soil-borne fungal pathogens such as the *Gaeumannomyces graminis* causing disease "take all" in cereals (Papadopoulou et al., 1999). Saponin alliospiroside extracted from *A. cepa* protects strawberry plants against *C. gloeosporioides*, the causal agent of anthracnose (Teshima et al., 2013). Beta-amyrin-derived triterpene glycosides confer resistance in *Barbarea vulgaris* against flea beetle (*Phyllotreta nemorum*) (Nielsen et al., 2010). Here, we showed that pretreatment of *B. napus* cotyledons with aescin led to strong concentration-dependent plant protection against infection by the hemibiotrophic fungus *L. maculans* that causes phoma stem canker. This was demonstrated also by the reduced hyphal spread and necrosis formation in infected cotyledons pretreated with aescin (**Figure 4**).

Aescin induced transcription of SA-dependent genes in *B. napus*. Namely, aescin led to increased transcription of the SA biosynthetic gene *BnICS1* (**Figure 5A**) and caused great accumulation of SA (**Figure 5B**). Additionally, aescin triggered oxidative burst, as demonstrated by ROS accumulation and upregulated transcription of *BnRbohD* and *BnRbohF* genes (**Figure 5E**). Both SA and oxidative stress have antimicrobial properties (Lamb and Dixon, 1997). Aescin's dual mode of action combining antifungal and induced plant immune responses led to a very efficient inhibition of blackleg disease on *B. napus*. Aescin treatment provided plant resistance to a similar extent as did the fungicide metconazole or BTH (**Figure 4A**), a potent plant immunity inducer (Zhou and Wang, 2018). The key role played by triggering immunity in aescin-induced *B. napus* protection is seen in the fact that metconazole is greater than 1000 times more effective in its antifungal activity against *L. maculans* compared to aescin (**Figures 2B and 3A**, **C**). Overall, then, the plant defense activation may be an important part – and perhaps the crucial part – of aescin-induced plant protection. In the animal kingdom, various studies have shown that saponins induce immunity in vertebrates. Indeed, they are commonly used as vaccine adjuvants (Sun et al., 2009; Moses et al., 2014) because they stimulate antibody production (Soltysik et al., 1995),

production of cytotoxic T-lymphocytes or induce inflammasome (Marty-Roix et al., 2016). To the best of our knowledge, we are the first to show that saponins may induce plant immune responses.

SA Pathway: Target of Aescin-Triggered Immunity

Our data show that aescin activates the plant immune system, and specifically the SA pathway, in both *B. napus* and *A. thaliana*. The SA pathway was shown to be the main defense route activated in *B. napus* upon *L. maculans* infection (Potlakayala et al., 2007; Šašek et al., 2012b). Various microorganisms evolved strategies to disrupt SA-mediated defense (Qi et al., 2018). Some *L. maculans* effectors, such as AvrLm4-7, may target this pathway to weaken the host immune system (Nováková et al., 2016). *B. napus* plants transformed with the salicylate hydroxylase gene *nahG* have been shown to have compromised systemic acquired resistance against *L. maculans* and *P. syringae* pv. *maculicola* (Potlakayala et al., 2007). In comparison with SA, other tested phytohormone metabolites were not or much less affected in *B. napus*. Slight decrease in *cis*-OPDA metabolite might be caused by SA-mediated repression on JA pathways, as has been described for *A. thaliana* (Pieterse et al., 2009; Dave and Graham, 2012).

The crucial role of SA in aescin-triggered plant resistance against pathogens was shown using the *A. thaliana–P. syringae* model pathosystem (Katagiri et al., 2002). Leaf pretreatment with aescin strongly inhibited *Pst* DC3000 infection (**Figure 6B**). The protective effect of aescin relied on the active defense mechanisms of *A. thaliana* inasmuch as aescin did not exhibit direct antibacterial properties (**Supplementary Figure 7B**). Accordingly, the treatment with aescin simultaneously with the infection had no effect on *Pst* DC3000 infection (**Supplementary Figure 7A**), thus suggesting some time is required to activate the plant defense. Furthermore, NahG plants defective in SA pathway showed no effect of aescin on the bacterial infection (**Figure 6B**), thus demonstrating that a functional SA pathway is indispensable for aescin-induced *A. thaliana* resistance against *Pst* DC3000.

In conclusion, we report here broad-spectrum antifungal activity of aescin and the new finding that aescin elicits defense responses in *B. napus* and *A. thaliana* by triggering the SA pathway and oxidative burst. These responses lead ultimately to highly efficient protection of *B. napus* against the fungus *L. maculans* and of *A. thaliana* against the bacteria *Pst* DC3000. The effect of aescin against *L. maculans* is of an extent comparable to that provided by fungicide protection. Additionally, we showed that aescin provides protective activity as a foliar spray. Taken together, our results suggest that aescin may constitute an attractive bioactive molecule with dual mode of action that could be found suitable for field application.

DATA AVAILABILITY STATEMENT

The datasets generated for this study are available on request to the corresponding author.

AUTHOR CONTRIBUTIONS

LT and PM designed the experiments. LT, MJ, DM, RP, PD, and PM performed the experiments. LT, MJ, PD and PM analyzed the data. LT, MJ, and PM wrote the manuscript. LB revised the manuscript and provided a methodological and knowledge platform for studying the *L. maculans* and *B. napus* interaction, finances, and lab space for a substantial part of the work. All the authors discussed the results and commented on the manuscript.

FUNDING

The research leading to these results was supported by projects QJ1310226, QK1910197, MZE-RO1118, TA ČR GAMA PP1 TG03010009, by the Ministry of Education, Youth and Sports of the Czech Republic from the European Regional Development Fund-Project 'Centre for Experimental Plant Biology': No. CZ.02.1.01/0.0/0.0/16_019/0000738, and the European Structural and Investment Funds, OP RDE-funded project 'CHEMFELLS4UCTP' (No. CZ.02.2.69/0.0/0.0/17_050/0008485).

ACKNOWLEDGMENTS

The authors would like to thank T. Rouxel for *L. maculans* JN2 isolate, Andrea Kung Wai and English Editorial Services for editing, and Iva Trdá for her technical assistance that enabled us to complete the manuscript.

SUPPLEMENTARY MATERIAL

The Supplementary Material for this article can be found online at: https://www.frontiersin.org/articles/10.3389/fpls.2019.01448/full#supplementary-material

REFERENCES

Arneson, P. A., and Durbin, R. D. (1967). Hydrolysis of tomatine by Septoria lycopersici: a detoxification mechanism. *Phytopathology* 57, 1358–1360.

Augustin, J. M., Kuzina, V., Andersen, S. B., and Bak, S. (2011). Molecular activities, biosynthesis and evolution of triterpenoid saponins. *Phytochemistry* 72 (6), 435–457. doi: 10.1016/j.phytochem.2011.01.015

Balesdent, M. H., Attard, A., Ansan-Melayah, D., Delourme, R., Renard, M., and Rouxel, T. (2001). Genetic control and host range of avirulence toward Brassica napus Cultivars Quinta and Jet Neuf in Leptosphaeria maculans. *Phytopathology* 91 (1), 70–76. doi: 10.1094/PHYTO.2001.91.1.70

Barile, E., Bonanomi, G., Antignani, V., Zolfaghari, B., Sajjadi, S. E., Scala, F., et al. (2007). Saponins from Allium minutiflorum with antifungal activity. *Phytochemistry* 68 (5), 596–603. doi: 10.1016/j.phytochem.2006.10.009

Becker, P., and Weltring, K. M. (1998). Purification and characterization of alpha-chaconinase of Gibberella pulicaris. *FEMS Microbiol. Lett.* 167, 197–202. doi: 10.1111/j.1574-6968.1998.tb13228.x

Bowyer, P., Clarke, B. R., Lunness, P., Daniels, M. J., and Osbourn, A. E. (1995). Host-range of a plant-pathogenic fungus determined by a Saponin detoxifying enzyme. *Science* 267, 371–374. doi: 10.1126/science.7824933

Burketová, L., Trdá, L., Ott, P. G., and Valentová, O. (2015). Bio-based resistance inducers for sustainable plant protection against pathogens. *Biotechnol. Adv.* 33 (6 Pt 2), 994–1004. doi: 10.1016/j.biotechadv.2015.01.004

Child, R. D., Evans, D. E., Allen, J., and Arnold, G. M. (1993). Growth responses in oilseed rape (Brassica napus L.) to combined applications of the triazole chemicals triapenthenol and tebuconazole and interactions with gibberellin. *Plant Growth Regul.* 13 (2), 203–212. doi: 10.1007/BF00024263

Cook, D. E., Mesarich, C. H., and Thomma, B. P. (2015). Understanding plant immunity as a surveillance system to detect invasion. *Annu. Rev. Phytopathol.* 53, 541–563. doi: 10.1146/annurev-phyto-080614-120114

da Cruz Cabral, L., Fernandez Pinto, V., and Patriarca, A. (2013). Application of plant derived compounds to control fungal spoilage and mycotoxin production in foods. *Int. J. Food Microbiol.* 166 (1), 1–14. doi: 10.1016/j.ijfoodmicro.2013.05.026

Dave, A., and Graham, I. A. (2012). Oxylipin signaling: a distinct role for the Jasmonic acid precursor cis-(+)-12-Oxo-Phytodienoic Acid (cis-OPDA). *Front. Plant Sci.* 3, 42. doi: 10.3389/fpls.2012.00042

Defago, G., and Kern, H. (1983). Induction of Fusarium-solani mutants insensitive to Tomatine, their pathogenicity and aggressiveness to tomato fruits and pea-plants. *Physiol. Plant Pathol.* 22, 29–37. doi: 10.1016/S0048-4059(83)81035-2

Delaney, T. P., Uknes, S., Vernooij, B., Friedrich, L., Weymann, K., Negrotto, D., et al. (1994). A central role of salicylic Acid in plant disease resistance. *Science* 266 (5188), 1247–1250. doi: 10.1126/science.266.5188.1247

Djilianov, D. L., Dobrev, P. I., Moyankova, D. P., Vankova, R., Georgieva, D. T., Gajdošová, S., et al. (2013). Dynamics of endogenous phytohormones during desiccation and recovery of the resurrection plant species Haberlea rhodopensis. *J. Plant Growth Regul.* 32, 564–574. doi: 10.1007/s00344-013-9323-y

Dobrev, P. I., and Kaminek, M. (2002). Fast and efficient separation of cytokinins from auxin and abscisic acid and their purification using mixed-mode solid-phase extraction. *J. Chromatogr. A* 950 (1–2), 21–29. doi: 10.1016/S0021-9673(02)00024-9

Dodds, P. N., and Rathjen, J. P. (2010). Plant immunity: towards an integrated view of plant-pathogen interactions. *Nat. Rev. Genet.* 11 (8), 539–548. doi: 10.1038/nrg2812

Field, B., Jordán, F., and Osbourn, A. (2006). First encounters–deployment of defence-related natural products by plants. *New Phytol.* 172 (2), 193–207. doi: 10.1111/j.1469-8137.2006.01863.x

Finney, D. J. (1971). *Probit Analysis*. Cambridge: Cambridge University Press.

Fisher, M. C., Hawkins, N. J., Sanglard, D., and Gurr, S. J. (2018). Worldwide emergence of resistance to antifungal drugs challenges human health and food security. *Science* 360 (6390), 739–742. doi: 10.1126/science.aap7999

Franiczek, R., Glensk, M., Krzyzanowska, B., and Wlodarczyk, M. (2015). beta-Aescin at subinhibitory concentration (sub-MIC) enhances susceptibility of Candida glabrata clinical isolates to nystatin. *Med. Mycol.* 53, 845–851. doi: 10.1093/mmy/myv035

Friedrich, L., Lawton, K., Ruess, W., Masner, P., Specker, N., Rella, M. G., et al. (1996). A benzothiadiazole derivative induces systemic acquired resistance in tobacco. *Plant J.* 10, 61–70. doi: 10.1046/j.1365-313X.1996.10010061.x

Glazebrook, J. (2005). Contrasting mechanisms of defense against biotrophic and necrotrophic pathogens. *Annu. Rev. Phytopathol.* 43, 205–227. doi: 10.1146/annurev.phyto.43.040204.135923

Griffiths, K. M., and Howlett, B. J. (2002). Transcription of sterol Delta(5,6)-desaturase and sterol 14alpha-demethylase is induced in the plant pathogenic ascomycete, Leptosphaeria maculans, during treatment with a triazole fungicide. *FEMS Microbiol. Lett.* 217 (1), 81–87. doi: 10.1111/j.1574-6968.2002.tb11459.x

Gruiz, K. (1996). Fungitoxic activity of saponins: practical use and fundamental principles. *Adv. Exp. Med. Biol.* 404, 527–534. doi: 10.1007/978-1-4899-1367-8_43

Hoagland, R. E., Zablotowicz, R. M., and Reddy, K. N., (1996). "Studies of the Phytotoxicity of Saponins on Weed and Crop Plants," in *Saponins Used in Food and Agriculture. Advances in Experimental Medicine and Biology*, vol. 405 . Eds. Waller, G. R., and Yamasaki, K. (Boston, MA: Springer). doi: 10.1007/978-1-4613-0413-5_6

Hoagland, R. E. (2009). Toxicity of tomatine and tomatidine on weeds, crops and phytopathogenetic fungi. *Allelopathy J.* 23 (2), 425–436.

Hostettmann, K., and Marston, A., (1995). *Saponins*. Cambridge University Press. doi: 10.1017/CBO9780511565113

Huang, H. C., Liao, S. C., Chang, F. R., Kuo, Y. H., and Wu, Y. C. (2003). Molluscicidal saponins from Sapindus mukorossi, inhibitory agents of golden apple snails, Pomacea canaliculata. *J. Agric. Food Chem.* 51 (17), 4916–4919. doi: 10.1021/jf0301910

Janda, M., and Ruelland, E. (2015). Magical mystery tour: Salicylic acid signaling. *Environ. Exp. Bot.* 114, 117–128. doi: 10.1016/j.envexpbot.2014.07.003

Kachroo, A., and Robin, G. P. (2013). Systemic signaling during plant defense. *Curr. Opin. Plant Biol.* 16, 527–533.

Katagiri, F., Thilmony, R., He, S. Y. (2002). The Arabidopsis thaliana-pseudomonas syringae interaction. *Arabidopsis Book*. 1, e0039. doi: 10.1199/tab.0039

Lamb, C., and Dixon, R. A. (1997). The cxidative burst in plant disease resistance. *Annu. Rev. Plant Physiol. Plant Mol. Biol.* 48, 251–275. doi: 10.1199/tab.0039

Leontovyčová, H., Kalachova, T., Trdá, L., Pospíchalová, R., Lamparová, L., Dobrev, P. I., et al. (2019). Actin depolymerization is able to increase plant resistance against pathogens *via* activation of salicylic acid signalling pathway. *Sci. Rep.* 9 (1), 10397. doi: 10.1038/s41598-019-46465-5

Lloyd, S. R., Schoonbeek, H. J., Trick, M., Zipfel, C., and Ridout, C. J. (2014). Methods to study PAMP-triggered immunity in Brassica species. *Mol. Plant Microbe Interact.* 27 (3), 286–295. doi: 10.1094/MPMI-05-13-0154-FI

Marshall, O. J. (2004). PerlPrimer: cross-platform, graphical primer design for standard, bisulphite and real-time PCR. *Bioinformatics* 20 (15), 2471–2472. doi: 10.1093/bioinformatics/bth254

Marty-Roix, R., Vladimer, G. I., Pouliot, K., Weng, D., Buglione-Corbett, R., West, K., et al. (2016). Identification of QS-21 as an inflammasome-activating molecular component of saponin adjuvants. *J. Biol. Chem.* 291 (3), 1123–1136. doi: 10.1074/jbc.M115.683011

Matušinský, P., Svačinová, I., Jonavičiené, A., and Tvarůžek, L. (2017). Long-term dynamics of causative agents of stem base diseases in winter wheat and reaction of Czech Oculimacula spp. and Microdochium spp. populations to prochloraz. *Eur. J. Plant Pathol.* 148, 199–206. doi: 10.1007/s10658-016-1082-8

Matušinský, P., Zouhar, M., Pavela, R., and Nový, P. (2015). Antifungal effect of five essential oils against important pathogenic fungi of cereals. *Ind. Crops Prod.* 67, 208–215. doi: 10.1016/j.indcrop.2015.01.022

Morrissey, J. P., and Osbourn, A. E. (1999). Fungal resistance to plant antibiotics as a mechanism of pathogenesis. *Microbiol. Mol. Biol. Rev.* 63 (3), 708–724.

Moses, T., Papadopoulou, K. K., and Osbourn, A. (2014). Metabolic and functional diversity of saponins, biosynthetic intermediates and semi-synthetic derivatives. *Crit. Rev. Biochem. Mol. Biol.* 49 (6), 439–462. doi: 10.3109/10409238.2014.953628

Nielsen, J. K., Nagao, T., Okabe, H., and Shinoda, T. (2010). Resistance in the plant, Barbarea vulgaris, and counter-adaptations in flea beetles mediated by saponins. *J. Chem. Ecol.* 36 (3), 277–285. doi: 10.1007/s10886-010-9758-6

Nováková M, Sašek V, Dobrev PI, Valentová O, Burketová L. (2014). Plant hormones in defense response of Brassica napus to Sclerotinia sclerotiorum - reassessing the role of salicylic acid in the interaction with a necrotroph. *Plant Physiol. Biochem.* 80, 308–317. doi: 10.1016/j.plaphy.2014.04.019

Nováková, M., Šašek, V., Trdá, L., Krutinová, H., Mongin, T., Valentová, O., et al. (2016). Leptosphaeria maculans effector AvrLm4-7 affects salicylic acid (SA) and ethylene (ET) signalling and hydrogen peroxide (H2O2) accumulation in Brassica napus. *Mol. Plant Pathol.* 17, 818–831. doi: 10.1111/mpp.12332

Olsen, R. A. (1973). Triterpeneglycosides as inhibitors of fungal growth and metabolism.6. Effect of Aescin on fungi with reduced sterol contents. *Physiol. Plant* 29, 145–149. doi: 10.1111/j.1399-3054.1973.tb03082.x

Osbourn, A. (1996). Saponins and plant defence - A soap story. *Trends Plant Sci.* 1, 4–9. doi: 10.1016/S1360-1385(96)80016-1

Papadopoulou, K., Melton, R. E., Leggett, M., Daniels, M. J., and Osbourn, A. E. (1999). Compromised disease resistance in saponin-deficient plants. *Proc. Natl. Acad. Sci. U.S.A.* 96, 12923–12928. doi: 10.1073/pnas.96.22.12923

Pieterse, C. M., Leon-Reyes, A., Van der Ent, S., and Van Wees, S. C. (2009). Networking by small-molecule hormones in plant immunity. *Nat. Chem. Biol.* 5 (5), 308–316. doi: 10.1038/nchembio.164

Podolak, I., Galanty, A., and Sobolewska, D. (2010). Saponins as cytotoxic agents: a review. *Phytochem. Rev.* 9 (3), 425–474. doi: 10.1007/s11101-010-9183-z

Porsche, F. M., Molitor, D., Beyer, M., Charton, S., Andre, C., and Kollar, A. (2018). Antifungal activity of saponins from the fruit pericarp of Sapindus mukorossi against Venturia inaequalis and Botrytis cinerea. *Plant Dis.* 102 (5), 991–1000. doi: 10.1094/PDIS-06-17-0906-RE

Potlakayala, S. D., Reed, D. W., Covello, P. S., and Fobert, P. R. (2007). Systemic acquired resistance in canola is linked with pathogenesis-related gene expression and requires salicylic acid. *Phytopathology* 97, 794–802. doi: 10.1094/PHYTO-97-7-0794

Price, K. R., Johnson, I. T., Fenwick, G. R., and Malinow, M. R. (1987). The chemistry and biological significance of saponins in foods and feedingstuffs. *Crit. Rev. Food Sci. Nutr.* 26 (1), 27–135. doi: 10.1080/10408398709527461

Qi, J., Wang, J., Gong, Z., and Zhou, J. M. (2017). Apoplastic ROS signaling in plant immunity. *Curr. Opin. Plant Biol.* 38, 92–100. doi: 10.1016/j.pbi.2017.04.022

Qi, G., Chen, J., Chang, M., Chen, H., Hall, K., Korin, J., et al. (2018). Pandemonium breaks out: disruption of salicylic acid-mediated defense by plant pathogens. *Mol. Plant* 11 (12), 1427–1439. doi: 10.1016/j.molp.2018.10.002

Saha, S., Walia, S., Kumar, J., and Parmar, B. S. (2010). Structure-biological activity relationships in triterpenic saponins: the relative activity of protobassic acid and its derivatives against plant pathogenic fungi. *Pest Manage. Sci.* 66, 825–831. doi: 10.1002/ps.1947

Saleem, M., Nazir, M., Ali, M. S., Hussain, H., Lee, Y. S., Riaz, N., et al. (2010). Antimicrobial natural products: an update on future antibiotic drug candidates. *Nat. Prod Rep.* 27 (2), 238–254. doi: 10.1039/B916096E

Sanati, H., Belanger, P., Fratti, R., and Ghannoum, M. (1997). A new triazole, voriconazole (UK-109,496), blocks sterol biosynthesis in Candida albicans and Candida krusei. *Antimicrob. Agents Chemother.* 41, 2492–2496. doi: 10.1128/AAC.41.11.2492

Saniewska, A., Jarecka, A., Bialy, Z., and Jurzysta, M. (2006). Antifungal activity of saponins originated from Medicago hybrida against some ornamental plant pathogens. *Acta Agrobotanica* 59 (2), 51–58. doi: 10.5586/aa.2006.061

Šašek, V., Nováková, M., Dobrev, P. I., Valentová, O., and Burketová, L. (2012a). β-aminobutyric acid protects Brassica napus plants from infection by Leptosphaeria maculans. Resistance induction or a direct antifungal effect? *Eur. J. Plant Pathol.* 133, 279–289. doi: 10.1007/s10658-011-9897-9

Šašek, V., Nováková, M., Jindřichová, B., Boka, K., Valentová, O., and Burketová, L. (2012b). Recognition of avirulence gene AvrLm1 from hemibiotrophic ascomycete Leptosphaeria maculans triggers salicylic acid and ethylene signaling in Brassica napus. *Mol. Plant Microbe Interact.* 25, 1238–1250. doi: 10.1094/MPMI-02-12-0033-R

Singh, B., and Kaur, A. (2018). Control of insect pests in crop plants and stored food grains using plant saponins: a review. *LWT* 87, 93–101. doi: 10.1016/j.lwt.2017.08.077

Soltysik, S., Wu, J. Y., Recchia, J., Wheeler, D. A., Newman, M. J., Coughlin, R. T., et al. (1995). Structure-function studies of Qs-21 adjuvant - assessment of triterpene aldehyde and glucuronic-acid roles in adjuvant function. *Vaccine* 13, 1403–1410. doi: 10.1016/0264-410X(95)00077-E

Sreij, R., Dargel, C., Schweins, R., Prevost, S., Dattani, R., and Hellweg, T. (2019). Aescin-cholesterol complexes in DMPC model membranes: a DSC and temperature-dependent scattering study. *Sci. Rep.* 9 (1), 5542. doi: 10.1038/s41598-019-41865-z

Steel, C. C., and Drysdale, R. B. (1988). Electrolyte leakage from plant and fungal tissues and disruption of liposome membranes by alpha-tomatine. *Phytochemistry* 27, 1025–1030. doi: 10.1016/0031-9422(88)80266-8

Steiner, A. A. (1984). The Universal Nutrient Solution. *Proceedings of IWOSC 6th International Congress on Soilless Culture*, Netherlands: Wageningen. pp. 633–650, Wageningen, Netherlands. doi: 10.1016/j.vaccine.2009.01.091

Sun, H. X., Xie, Y., and Ye, Y. P. (2009). Advances in saponin-based adjuvants. *Vaccine* 27, 1787–1796. doi: 10.1016/j.vaccine.2009.01.091

Teshima, Y., Ikeda, T., Imada, K., Sasaki, K., El-Sayed, M. A., Shigyo, M., et al. (2013). Identification and biological activity of antifungal saponins from shallot (Allium cepa L. Aggregatum group). *J. Agric. Food Chem.* 61 (31), 7440–7445. doi: 10.1021/jf401720q

Torres, M. A., Jones, J. D., and Dangl, J. L. (2005). Pathogen-induced, NADPH oxidase-derived reactive oxygen intermediates suppress spread of cell death in Arabidopsis thaliana. *Nat. Genet.* 37 (10), 1130–1134. doi: 10.1038/ng1639

Trdá, L., Boutrot, F., Claverie, J., Brulé, D., Dorey, S., and Poinssot, B. (2015). Perception of pathogenic or beneficial bacteria and their evasion of host immunity: pattern recognition receptors in the frontline. *Front. Plant Sci.* 6, 219. doi: 10.3389/fpls.2015.00219

Tsuda, K., Sato, M., Glazebrook, J., Cohen, J. D., and Katagiri, F. (2008). Interplay between MAMP-triggered and SA-mediated defense responses. *Plant J.* 53 (5), 763–775. doi: 10.1111/j.1365-313X.2007.03369.x

Tsuda, K., Mine, A., Bethke, G., Igarashi, D., Botanga, C. J., Tsuda, Y., et al. (2013). Dual regulation of gene expression mediated by extended MAPK activation and salicylic acid contributes to robust innate immunity in Arabidopsis thaliana. *PloS Genet.* 9 (12), e1004015. doi: 10.1371/journal.pgen.1004015

Turner, E. M. C. (1960). The nature of the resistance of oats to the take-all fungus.3. Distribution of the inhibitor in oat seedlings. *J. Exp. Bot.* 11, 403–412. doi: 10.1093/jxb/11.3.403

Waller, G. R., Jurzysta, M., and Thorne, R. L. Z. (1993). Allelopathic activity of root Saponins from Alfalfa (Medicago-Sativa L) on weeds and wheat. *Bot. Bull. Acad. Sin.* 34, 1–11.

Walters, D. R., Ratsep, J., and Havis, N. D. (2013). Controlling crop diseases using induced resistance: challenges for the future. *J. Exp. Bot.* 64, 1263–1280. doi: 10.1093/jxb/ert026

Wolters, B. (1966). [On antimicrobial activity of plant steroids and triterpenes]. *Planta Med.* 14, 392–399. doi: 10.1055/s-0028-1100066

Xin, X. F., and He, S. Y. (2013). Pseudomonas syringae pv. tomato DC3000: a model pathogen for probing disease susceptibility and hormone signaling in plants. *Annu. Rev. Phytopathol.* 51, 473–498. doi: 10.1146/annurev-phyto-082712-102321

Xin, X. F., Kvitko, B., and He, S. Y. (2018). Pseudomonas syringae: what it takes to be a pathogen. *Nat. Rev. Microbiol.* 16 (5), 316–328. doi: 10.1038/nrmicro.2018.17

Yang, C. R., Zhang, Y., Jacob, M. R., Khan, S. I., Zhang, Y. J., and Li, X. C. (2006). Antifungal activity of C-27 steroidal saponins. *Antimicrob. Agents Chemother.* 50 (5), 1710–1714. doi: 10.1128/AAC.50.5.1710-1714.2006

Zablotowicz, R. M., Hoagland, R. E., and Wagner, S. C. (1996). Effect of saponins on the growth and activity of rhizosphere bacteria. *Saponins Used Food Agric.* 405, 83–95. doi: 10.1007/978-1-4613-0413-5_8

Zhao, Y. L., Cai, G. M., Hong, X., Shan, L. M., and Xiao, X. H. (2008). Anti-hepatitis B virus activities of triterpenoid saponin compound from Potentilla anserine L. *Phytomedicine* 15 (4), 253–258. doi: 10.1016/j.phymed.2008.01.005

Zhu, Y., Chen, H., Fan, J., Wang, Y., Li, Y., Chen, J., et al. (2000). Genetic diversity and disease control in rice. *Nature* 406 (6797), 718–722. doi: 10.1038/35021046

Zhou, M., and Wang, W. (2018). Recent advances in synthetic chemical inducers of plant immunity. *Front. Plant Sci.* 9, 1–10. doi: 10.3389/fpls.2018.01613

Conflict of Interest: Author Pavel Matusinsky is employed by company Agrotest Fyto, Ltd. The remaining authors declare that the research was conducted in the absence of any commercial or financial relationships that could be construed as a potential conflict of interest.

frontiers in Plant Science

ORIGINAL RESEARCH
published: 08 January 2020
doi: 10.3389/fpls.2019.01654

Functional Characterization of Invertase Inhibitors PtC/VIF1 and 2 Revealed Their Involvements in the Defense Response to Fungal Pathogen in *Populus trichocarpa*

Tao Su[1,2], *Mei Han*[1]*, *Jie Min*[1], *Huaiye Zhou*[1], *Qi Zhang*[3], *Jingyi Zhao*[3] *and Yanming Fang*[1,2]

[1] Co-Innovation Center for Sustainable Forestry in Southern China, College of Biology and the Environment, Nanjing Forestry University, Nanjing, China, [2] Key Laboratory of State Forestry Administration on Subtropical Forest Biodiversity Conservation, Nanjing Forestry University, Nanjing, China, [3] College of Forest, Nanjing Forestry University, Nanjing, China

OPEN ACCESS

Edited by:
Laura Bertini,
Università degli Studi della Tuscia, Italy

Reviewed by:
Jin Zhang,
Oak Ridge National Laboratory (DOE), United States
Guodong Wang,
Shaanxi Normal University, China
Mariangela Coppola,
University of Naples Federico II, Italy

***Correspondence:**
Mei Han
mei.han@cos.uni-heidelberg.de;
sthanmei@njfu.edu.cn

Specialty section:
This article was submitted to Plant Microbe Interactions, a section of the journal Frontiers in Plant Science

Received: 04 September 2019
Accepted: 22 November 2019
Published: 08 January 2020

Citation:
Su T, Han M, Min J, Zhou H, Zhang Q, Zhao J and Fang Y (2020) Functional Characterization of Invertase Inhibitors PtC/VIF1 and 2 Revealed Their Involvements in the Defense Response to Fungal Pathogen in Populus trichocarpa. Front. Plant Sci. 10:1654. doi: 10.3389/fpls.2019.01654

In higher plants, cell wall invertase (CWI) and vacuolar invertase (VI) were considered to be essential coordinators in carbohydrate partitioning, sink strength determination, and stress responses. An increasing body of evidence revealed that the tight regulation of CWI and VI substantially depends on the post-translational mechanisms, which were mediated by small proteinaceous inhibitors (C/VIFs, Inhibitor of β-Fructosidases). As yet, the extensive survey of the molecular basis and biochemical property of C/VIFs remains largely unknown in black cottonwood (*Populus trichocarpa* Torr. & A. Gray), a model species of woody plants. In the present work, we have initiated a systematic review of the genomic structures, phylogenies, *cis*-regulatory elements, and conserved motifs as well as the tissue-specific expression, resulting in the identification of 39 genes encoding C/VIF in poplar genome. We characterized two putative invertase inhibitors *PtC/VIF1* and *2*, showing predominant transcript levels in the roots and highly divergent responses to the selected stress cues including fusarium wilt, drought, ABA, wound, and senescence. *In silico* prediction of the signal peptide hinted us that they both likely had the apoplastic targets. Based on the experimental visualization *via* the transient and stable transformation assays, we confirmed that PtC/VIF1 and 2 indeed secreted to the extracellular compartments. Further validation of their recombinant enzymes revealed that they displayed the potent inhibitory affinities on the extracted CWI, supporting the patterns that act as the typical apoplastic invertase inhibitors. To our knowledge, it is the first report on molecular characterization of the functional C/VIF proteins in poplar. Our results indicate that PtC/VIF1 and 2 may exert essential roles in defense- and stress-related responses. Moreover, novel findings of the up- and downregulated C/VIF genes and functional enzyme activities enable us to further unravel the molecular mechanisms in the promotion of woody plant performance and adapted-biotic stress, underlying the homeostatic control of sugar in the apoplast.

Keywords: poplar, invertase inhibitor, sucrose, apoplast, pathogen, defense response, drought

INTRODUCTION

Sucrose synthesized in source leaves represents the primary form of carbon assimilates translocated *via* the phloem complex to non-photosynthetic sink organs (Koch, 2004). During the passage, two classes of sucrose-splitting enzymes intermediate the sucrose hydrolysis. Sucrose synthase (EC2.4.1.13, Susy) reversibly converts sucrose into UDP-glucose and fructose, both of which are utilized for the cell respiration and cellulose biosynthesis (Coleman et al., 2009). By contrast, invertase (EC 3.2.1.26) irreversibly catalyzes the cleavage of sucrose into its hexose (glucose and fructose) components, exerting a pivotal role in carbon utilization and distribution. After unloading into sink cells, sucrose is either taken up symplastically by intracellular trafficking pathway *via* plasmodesmata for the metabolic and synthetic processes (Rausch and Greiner, 2004), or it can also be apoplastically transported by sucrose transporters (SUTs) to the extracellular space for fungal colonization and defense-related responses (Roitsch et al., 2003; Doidy et al., 2012).

Evolutionary analyses between various cellular organisms suggested the presence of two smaller sub-families, acid invertase (AI) and cytosolic neutral/alkaline invertase (CI) distinguished by the properties of protein solubility, pH optima, and subcellular targets (Sturm, 2002; Wan et al., 2018). The AI sub-family is comprised of cell wall invertase (CWI) and vacuolar invertase (VI). The deduction of protein structure and domain revealed that CWI and VI are clustered to GH32 (glycoside hydrolase family 32) enzymes with an optimal pH of 3.5–5.0, sharing similar patterns of conserved motifs and catalytic domains (Van den Ende et al., 2009). It is worthwhile to note that AIs are all glycosylated enzymes and intrinsically stable; however, CI varies substantially from AI in molecular and biochemical properties and belongs to GH100 with an optimal pH of 6.8–9.0, appearing to be localized to cytosols, mitochondrion, plastids, and nucleus.

It has been long known that CIs compensate for the loss of Susy and AI activities, fulfilling roles in sucrose metabolism (Liu et al., 2015), cellulose biosynthesis (Rende et al., 2017; Barnes and Anderson, 2018), nitrogen uptake (Tamoi et al., 2010; Maruta et al., 2015), and reactive oxygen species (ROS) scavenging as well as osmotic stress adaptation (Xiang et al., 2011; Battaglia et al., 2017). However, AIs playing multi-faceted actions in source–sink interactions have received much more attention. The hexoses released by CWI or VI not only served as core metabolites and nutrient sources but also acted as key signaling molecules to impact on gene expression during developmental transitions and responding to environmental cues (Rolland et al., 2006; Ruan, 2014). The basic functions of VI in photoassimilate partitioning, cell expansion, and osmotic regulation have been implemented widely in a variety of plants (Klann et al., 1996; Kohorn et al., 2006; Sergeeva et al., 2006; Yu et al., 2008; Nägele et al., 2010; Morey et al., 2018). Suppression of VI activities showed a decrease of cold-induced sweetening (CIS), leading to improved processing qualities of potato tubers (Bhaskar et al., 2010; Zhu et al., 2016). Aside from the developmental functions, VI exerts important roles in stress tolerance (e.g. drought and cold) by sustaining the homeostasis of sugar metabolism (Qian et al., 2018; Weiszmann et al., 2018; Wei et al., 2019).

By contrast, apoplastic CWI splits sucrose into hexose components that were further translocated either into intracellular compartments for the transcriptional regulation, sugar metabolism, and polysaccharide biosynthesis or into extracellular space for the enhancement of sink capacity and stress responses (Bihmidine et al., 2013; Proels and Hückelhoven, 2014). The promotions of CWI on seed filling and fruit set have been well attempted in a wide range of plant species like maize, rice, tomato, cotton, and litchi (Chourey et al., 2006; Wang et al., 2008; Zanor et al., 2009; Wang and Ruan, 2012; Li et al., 2013; Zhang et al., 2018), indicating that CWIs facilitate the improvement of sink cell differentiation *via* multiple regulatory mechanisms of sugar metabolism and signaling. Recently, overexpressing *CWIs* in tobacco and tomato resulted in the deferral of leaf aging and drought avoidance (Balibrea Lara et al., 2004; Albacete et al., 2015). Also numerous reports also revealed that CWI plays central roles in defense and immune responses during plants–pathogen interactions (Swarbrick et al., 2006; Essmann et al., 2008; Kocal et al., 2008; Sun et al., 2014; Veillet et al., 2016), pointing out that CWI serves as a significant stress indicator and pathogenesis-related proteins.

Early research focused primarily on the induction of AI activities through the (post-) transcriptional increases in their corresponding gene transcripts (Ehness and Roitsch, 1997). However, given the protein glycosylation and discordant protein/transcript expression patterns, the tight control of AI may subject primarily to the post-translational mechanisms. Accumulating evidence has confirmed that CWI and VI activities were explicitly determined by the low-molecular-weight (15–23 kDa) proteinaceous inhibitors, namely C/VIFs (cell wall/vacuolar inhibitor of β-fructosidases) according to the targeting patterns. *In silico* analyses revealed that the C/VIF family is moderately conserved within one species and various plant species (Rausch and Greiner, 2004). C/VIFs and the structure-related PMEIs (pectin methylesterase inhibitors) belong to the same superfamily, enabling it with difficulties to distinguish them from sequence comparisons (Hothorn et al., 2004). However, an enigma of whether C/VIFs have genuine *in vivo* inhibitory activities against the targeted enzymes remains to be unlocked. Using the heterologous expression system, some CIFs were functionally dug out in tobacco, tomato, and maize (Greiner, 1998; Bate, 2004; Reca et al., 2008). After that, crystal analyses of complex uncovered that CIF used its small motifs (PKF) to target CWI through physical binding to substrate cleft in a pH-dependent manner (Hothorn et al., 2004; Hothorn et al., 2010).

Overexpression of VIF-encoded genes led to the insensitivity to CIS of potato tubers (Greiner et al., 1999; Brummell et al., 2011; Liu et al., 2013; Mckenzie et al., 2013), indicating that the functional capping VI restrained glucose release *via* the post-translational regulation. In addition to biotechnology relevance, recent reports suggested that the VIF-mediated sucrose metabolism conferred the alterations of fruit ripeness and drought stress tolerance (Chen et al., 2016; Qin et al., 2016).

By contrast, silencing of *CIF* expression also facilitated the improvements of seed filling, prolonged leaf green, and cold tolerance in tomato (Jin et al., 2009; Xu et al., 2017), highlighting that the post-translational control is necessary for hexoses to release to sink organs, particularly responding to stressors and phytohormone cues. These results corroborated the findings that the suppression of *CIF* expression resulted in increased seed production and germination (Su et al., 2016; Tang et al., 2017). An increasing body of evidence supported the notion that the C/VIF-mediated post-translational modulation of invertase commonly involves multiple cellular processes, metabolic pathways, and molecular regulation. Interestingly, the post-translational elevation of CWI activities and its components by native inhibitors in *Arabidopsis* contributed to a marked reduction of susceptibility and disease index to the bacterial and fungal pathogens (Bonfig et al., 2010; Siemens et al., 2011), indicating that the rapid rise of CWI acted as a significant signal of defense during the plant host and pathogen interactions.

Poplar has served as a model woody organism in perennial plants and forestry for research of biology and molecular physiology owning to high superiorities for plantation, biomass, and ecological functions (Jansson and Douglas, 2007). Despite the advances that have been made in a variety of plant species, little was known about genes encoding C/VIF and the enzyme properties in *P. trichocarpa*. In a bid to rectify this situation, we conducted a genome-wide survey of C/VIF candidates in the recently released genome of *P. trichocarpa* (Tuskan et al., 2006). Based on the conserved patterns and expression profiling, we reported the molecular isolation and functional characterization of two PtC/VIFs using the bacterial expressed recombinant proteins. Their subcellular targets were explored by ectopic expression of fluorescent fusions *via* transient and stable assays. Here, the demonstrated substantial regulation of gene transcripts upon various stressors concurrent with enzyme targeting activities provided a promising strategy for the future unraveling the *in vivo* roles of C/VIF family in poplar and other woody perennials.

MATERIALS AND METHODS

Plant Materials, Growth Conditions, and Stress Treatments

P. trichocarpa (genotype Nisqually-1) grows on standard pot in the growth chamber, using a temperature cycling between 22°C (night) and 26°C (day) under long-day conditions (16 h light/8 h dark, 20 μE) according to a previous report (Li et al., 2017; Su et al., 2019). *N. benthamiana* and *A. thaliana* (ecotype *Col-0*) plants were maintained in a growth chamber at 25°C under a light regime of 16 h and 200–300 μE of long-day conditions. Unless otherwise specified, vegetative tissues of eight-week-cultured *P. trichocarpa* and floral organs of field-grown *P. deltoids* were harvested for qRT-PCR according to a previous study (Bocock et al., 2008). The *in vitro P. trichocarpa* were cultured (25°C, 16/8 h day/night photoperiod, 20 μE) on wood plant medium (WPM) with 30 g l^{-1} sucrose, 0.1 mg l^{-1} IBA, and solidified with 8 g l^{-1} plant agar (Biofroxx). After a culturing for five weeks, seedlings were transferred to standard pots with mixtures of vermiculite:perlite:peat (1:1:3). For the infection of the fungal pathogen, roots peripheral areas of 8-week-cultured plants were inoculated with 20 ml *F. solani* spore suspensions (2.0×10^6 spore/ml) for 48 and 72 h. Similarly, plants were irrigated with 20 ml ABA (100 μM, dissolved in 10% ethanol) once a day for 4 days, and grown for 48 and 96 h. The drought stress was induced by water withholding treatments for 96 and 120 h. For wounding treatments, the mature leaves were physically punched and harvested after 2 and 6 h. Seasonal senescence leaves were harvested from plants grown in a growth chamber according to a previous study (Su et al., 2019). The frozen samples were ground in the liquid nitrogen and subjected to RNA and protein extraction, followed by qRT-PCR and functional assay.

Sequence Available, Gene Structure and Distribution, *Cis*-Element, and Conserved Motif

The previously described C/VIFs (Link et al., 2004; Tang et al., 2017) were collected as queries to search for the homologs in *P. trichocarpa* genome assembly (3.0) from the JGI gene catalog (Phytozome v12.1, https://phytozome.jgi.doe.gov/pz/portal.html) with the *E*-value cutoff set as 1e-5 and GenBank (https://www.ncbi.nlm.nih.gov/). The respective protein sequences were verified in Pfam (http://pfam.xfam.org/) by the HMMER program (3.1b2). The incomplete sequences with too short (<150 aa) and too long (>250 aa) length as well as sequences showing more than 98% identities were eliminated. The genomic structure was deduced by comparing the coding sequences (CDS) and corresponding DNA sequences using the GSDS (Hu et al., 2015). The chromosomal distribution of *PtC/VIFs* candidates was obtained from the PopGenIE (http://popgenie.org/chromosome-diagram) and was drawn with MapInspect (http://www.softsea.com/review/MapInspect.html). The conserved motifs were identified by the MEME program (http://meme-suite.org/index.html) with default settings except that the maximum widths of motifs were set to 50 (Bailey et al., 2006). Approximately 1.5-kb upstream regions were used to search for the *cis*-acting regulatory elements in the PlantCARE (http://bioinformatics.psb.ugent.be/webtools/plantcare/html/). The putative transcription factor (TF) binding sites were analyzed in the PlantTFDB 4.0 (http://planttfdb.cbi.pku.edu.cn/). Signal peptides and subcellular targeting sequences were deduced by online programs of PSORT (https://wolfpsort.hgc.jp/) and Phobius (http://phobius.binf.ku.dk/).

Transcriptomic Sequencing and Expression Analysis

Transcriptomic sequencing (RNA-seq) of eighteen vegetative and reproductive tissues (SRA: SRP077540) was collected from Phytozome (v12.1) (BioProject: PRJNA10772; Accession number: GCF_000002775.4). The Affymetrix expression data (BioProject: PRJNA112485; GEO: GSE13990) is accessible from Poplar eFP Browser (http://bar.utoronto.ca/efppop/cgi-

bin/efpWeb.cgi). Duplicate or triplicate samples of *P. trichocarpa* were used for microarray analysis (Wilkins et al., 2009). For the qRT-PCR analyses, RNA extraction and cDNA synthesis were performed according to the previous report (Han et al., 2013; Su et al., 2019). Total RNA was extracted using the RNeasy Plant Mini Kit (Qiagen, China). RNase-free DNase I (Qiagen, China) was used to remove genomic DNA. First-strand cDNA was synthesized using the PrimeScript II 1st Strand cDNA Synthesis Kit (Takara, China). For a standard qRT-PCR assay, samples were loaded to a TB green Premix ExTap™ Tli RNaseH Plus (Takara, China). The mixture was subjected to StepOnePlus™ Real-Time PCR System (AB, USA) with a three-step PCR using the cycling parameters: 95°C for 30 s, followed by 95°C for 5 s and 60°C for 30 s, for 40 cycles, and a melt cycle from 65 to 95°C. The primer amplification efficiency was evaluated with dilutions of cDNA, producing an R^2 value ≥ 0.99. The relative expression of the target gene was normalized by the geometric mean (Vandesompele et al., 2002) of three reference genes: *PtUBIC*, *Ptβ-Actin*, and *PtEF-1α*. The detailed primers used for targeting specific genes are listed in **Supplementary Table S1**.

Plant Transformation

The *Agrobacterium*-mediated transformation in *Arabidopsis* by floral dip has been described previously (Clough and Bent, 1998). Transformants were primarily screened by spraying BASTA® on seedlings grown in soil. The T2 homozygous generations were used for image analysis as indicated. For the transient transformation in tobacco (*N. benthamiana*), the *Agrobacterium* strain (*C58C1*) containing the appropriate constructs were grown overnight in 30 ml of YEB-medium supplemented with carbenicillin (50 μg ml^{-1}), rifampicin (100 μg ml^{-1}) and spectinomycin (50 μg ml^{-1}) until the stationary phase. After centrifugation at 3000 g for 30 min, the cells were re-suspended in 15 ml of infiltration buffer [10-mM 2-(N-morpholino) ethanesulfonic acid (MES), pH 5.9, 150-μM acetosyringone] and incubated with gentle agitation for 2 h at room temperature. The suspension cells were mixed with infiltration buffer and adjusted to OD600 = 1.0. The lower epidermis of 5-week-old tobacco leaves was infiltrated with *Agrobacterium* via a needless syringe. After two days of inoculation, the transformed regions were subject to confocal laser scanning microscopy (CLSM) for image analyses.

Subcellular Localizations

The analyses of subcellular localization were conducted according to a previous study (Tang et al., 2017). The CDS (stop codon omitted) of *PtC/VIF1* and *PtC/VIF2* were amplified by PCR using the primers containing the Gateway™ (Invitrogen, Germany) *attB1* and *attB2* recombinant sites (**Supplementary Table S1**). The respective PCR products were recovered and then inserted into the donor plasmid *pDONR201* and subsequently recombined with the binary destination vector *pB7YWG2.0*, yielding the *pB7C/VIF1-YFP* and *pB7C/VIF2-YFP* constructs. Half of the tobacco leaves were co-infiltrated with *A. tumefaciens* (*C58C1*), harboring the C-terminal YFP-fusion constructs and the *Arabidopsis* cell wall-localization marker (*pK7CIF1-RFP*). As a control, another half leaves were infiltrated with strain with null constructs. The visualization of fluorescent signals in the transgenic *Arabidopsis* roots was conducted according to a previous study (Su et al., 2016). The YFP was excited by a 514 nm laser line and the emitted fluorescent signal was collected by a 530–600 nm bandpass filter. The RFP was excited with a 543 nm laser line, and the emitted fluorescence was captured with a 560 nm long-pass filter. Images were analyzed by a Zeiss LSM 510 Meta inverted CLSM.

Heterologous Expression and Purification of PtC/VIF1 and 2

The protein purification was performed according to the previous reports (Link et al., 2004; Tang et al., 2017). The CDS (signal peptide omitted) of *PtC/VIF1* and *2* were amplified using primers containing the Gateway™ (Invitrogen, Germany) *attB1* and *attB2* recombinant sites (**Supplementary Table S1**) from the roots, followed by recombination with the destination vector *pETG-20A*, yielding 6x His-tagged thioredoxin A (TrxA) fusion constructs that were introduced into the *E. coli* strain Rosetta-gami™ (DE3) (Novagen, Germany) for recombinant protein induction and expression. Bacterial cells were harvested by centrifugation at 10,000 g for 15 min and lysed with 1/20 volume of lysis buffer (50-mM Na_2HPO_4/NaH_2PO_4, pH 7.0, 500-mM NaCl, 1% Triton X-100, 1 mg ml^{-1} lysozyme) and repeat the centrifugation at 15 000 g for 1 h. The supernatant was collected and mixed with 0.6 g Ni-TED Protino resin (Macherey-Nagel, Germany) and kept stirring at 4°C for 45 min to enable protein binding. After loading to the column, the resin was firstly washed with lysis buffer followed by washing buffer (50-mM Na_2HPO_4/NaH_2PO_4, pH 7.0, 500-mM NaCl, 10% glycerol). The bound TrxA-fusion proteins were then eluted with 10 volumes of the imidazole (250 mM) containing a washing buffer. Afterward, the eluted proteins were dialyzed against TEV protease cleavage buffer (50-mM Na_2HPO^4/NaH_2PO_4, pH 7.0, 200-mM NaCl) at 30°C for 3 h before loading to the column. A second elution was conducted to eliminate 6× His tags, yielding the finally purified recombinant proteins.

Invertase Extraction and Functional Assay

The acid invertase (CWI and VI) extraction and the functional assay were conducted according to the previous reports (Link et al., 2004; Tang et al., 2017). For CWI preparation, the root tissues were ground in the liquid nitrogen and homogenized in 500-μl extraction buffer (30-mM MOPS, 250-mM sorbitol, 10-mM $MgCl_2$, 10-mM KCl, and 1-mM PMSF, pH 6.0). After centrifugation for 10 min (8 000g, 4°C), the insoluble cell wall pellets were washed once with extraction buffer plus 1% Triton X-100, and twice with extraction buffer only, followed by the re-suspension in 500-μl assay buffer (20-mM triethanolamine, 7-mM citric acid, and 1-mM PMSF, pH 4.6). For VI preparation, endogenous sucrose in the soluble fraction was removed by precipitation of 4 volumes of ice-cold acetone (–20°C, 20 min). After centrifugation for 10 min (15,000 g, 4°C), the pellets were resolved in 1 volume of assay buffer. The inhibitory activities of

recombinant proteins were determined against the extracted CWI and VI. Variable amounts of purified recombinant proteins were mixed with suitable invertase preparations in assay buffer. A total amount of 200 µl mixtures was incubated at 37°C for 30 min to enable the complex formation and then mixed with 100 µl sucrose (100 mM) for 60 min. The reactions were terminated by sodium phosphate buffer (1 M, pH 7.5) and quickly boiled at 95°C for 5 min. The liberated glucose was quantitated by a coupled enzymatic-optical assay according to the Lambert–Beer Law and the enzyme activity was expressed in nkat g^{-1} fresh weight (1 nkat = 1 nmole glucose liberated/second). Each experiment was performed in a quadruplicate, one of which without the addition of the recombinant protein was calculated as the background of absorption.

RESULTS

Genome-Wide Identification of the Invertase Inhibitor Genes in *P. trichocarpa*

Using the reported C/VIFs in *Arabidopsis* and soybean as queries, the systematic BLAST was performed in Phytozome (v.12.1) database, retrieving a large number of homologs within the genome (v3.0) of *P. trichocarpa*. After removal of the redundant sequences, a total of 39 genes encoding C/VIF were identified and postulated to be as *C/VIF* candidates. As we are not able to distinguish C/VIF from PMEI based on the conserved sequence alone, all members were annotated as C/VIF/PMEI superfamily genes in our analyses. The accession ID, chromosomal location, CDS and open reading frame, protein size, molecular weights (MWs), isoelectric point (pI), deduced signal peptide, and subcellular targets are analyzed. We found that all members had no presence of the transcript variants (**Supplementary Table S2**). The translated protein sequences varied from 172 to 241 amino acid residues with theoretical MWs ranging from 18.42 to 26.60 kDa. Most of C/VIF candidates were predicted to contain the targeting peptides. An unrooted phylogenetic tree revealed that the *C/VIF* candidates were divided into two sub-families (**Figure 1A**). Further comparison of genomic structure and exon/intron organization revealed that they are all encoded by only one exon, whose length and locations are generally conserved (**Figure 1A**). Patterns of chromosomal locations revealed that all members were mapped on sixteen out of the 19 chromosomes (Chr) with the individual distribution from Chr1 to Chr16 (**Figure 1B**). Additionally, twice genome duplication events were assumed to occur in poplar (Tuskan et al., 2006). Based on the phylogenetic analyses, the 14 pairs of genes were clustered together with high protein sequence identities, of which two pairs of genes (Potri.015G128200/300 and Potri.002G194800/900) were identified to likely evolve as the consequence of tandem duplication as they were adjacent on a chromosome segment.

Regulatory elements within the gene promotor are the essential clues to characterize the environmental stimuli that modulate gene expression. *In silico* prediction was conducted in the PlantCARE database, resulting in findings of seven *cis*-regulatory elements associated with phytohormone regulation, and five of which involved in stress- and defense-related responses (**Figure 2**). ABA-responsive elements (ABRE) were found to more widely spread in the promotors of 27 genes, followed by the jasmonate (MeJA)-responsiveness elements (TGACG and CGTCA) and salicylic acid (SA)-responsive elements (TCA), which were identified in 20 genes. However, the gibberellin-responsive elements (GARE-motif, P-box, and TATC-box) and auxin-responsive elements (AuxRR-core/TGA-element) were rich in a small number of genes. By contrast, a few defense and stress-related *cis*-acting elements, including wounding (WUN-motif), TC-rich repeats, low temperature (LTR), and oxidation (as-1) were abundantly distributed in 10 to 16 genes. The TFs of MYB binding sites involved in carbon metabolism were listed. The characterization of prevalent *cis*-regulatory elements and the TF binding sites provided the clue that the molecular regulation of genes may depend on the crosstalk between phytohormones, stress, and nutrient sources.

Mining Conserved Motifs, Phylogenetic Evolution, and Expression Profiling

To gain insight into the conserved patterns, the full-length protein sequences were analyzed by Pfam (32.0) and MEME. Both C/VIF and PMEI family are homologous inhibitors containing targeting sequences and four cysteines (Cys) residues that have been verified the formation of two strictly conserved disulfide bridges to strengthen protein structure. All C/VIF candidates showed the same conserved PMEI/C/VIF domain (IPR035513; IPR034087), which is annotated with the functional inhibition on PME and/or invertase activities (**Figure 3**). Accordingly, a total of 15 sequence fragments were programmed to be as the putatively conserved motifs by MEME analyses. Interestingly, the motif-1 deduced in all members contains the first pair of Cys residues with the random insertion of eight amino acids. Other motifs containing the third and fourth Cys residues varied in the presence from 24 to 28 members (**Figure 3**). To further assess the evolutionary relationship and distinct origin, all members were aligned with the reported C/VIF and PMEI genes in the other nine plant species. The alignment of the full-length protein sequences revealed that all 53 homologs were categorized into two distinct sub-clades with well-supported bootstrap values, termed PMEI family and C/VIF family (**Figure 4**). Five of 19 *PtC/VIF* candidates within the C/VIF sub-clades were identified to be evolutionarily close to the three confirmed C/VIF paralogs in *Arabidopsis*, soybean, and sugar beet. By contrast, three of 20 *PtPMEI* candidates displayed similarities with genes in *Arabidopsis* and kiwi within the PMEI sub-clade (**Figure 4**).

To evaluate the tissue-specific expression patterns, all gene transcripts were examined using RNA-seq and microarray data that were obtained from the Phytozome (v12.1) and eFP database, respectively. The RNA-seq data demonstrated a significant variation of gene expression in vegetative and reproductive tissues. Approximately 12 genes were dominantly expressed in the roots, and more than 10 genes showed high expression levels in the leaves (**Figure 5A**). Interestingly,

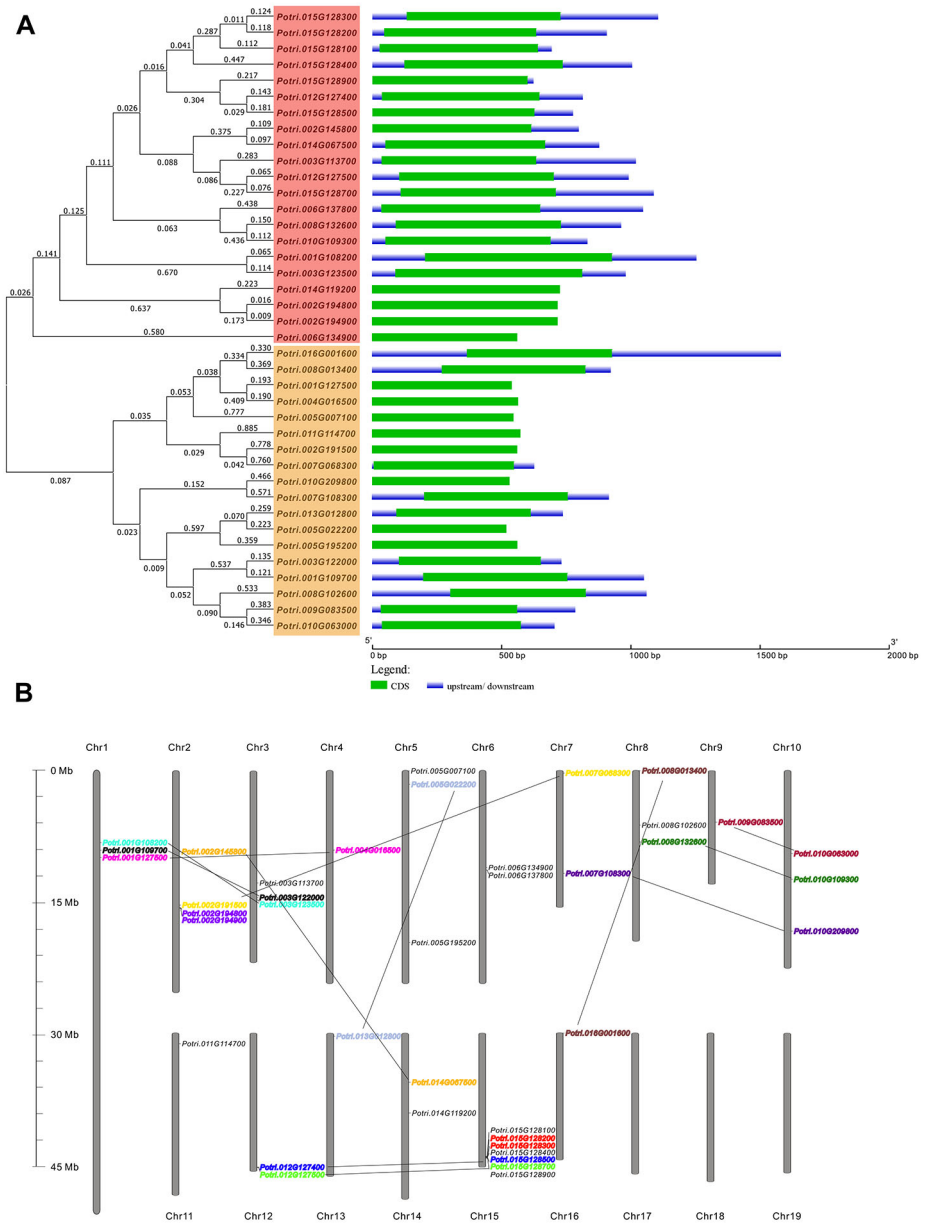

FIGURE 1 | Genomic structures and the chromosomal distribution of *PtC/VIF* candidate genes. **(A)** Gene structures showing the exon/intron organization that was analyzed by the online tool GSDS. The full-length sequences of mRNA were aligned by ClustalW Omega (https://www.ebi.ac.uk/Tools/msa/clustalo/) to generate the Neighbour-joining tree with branched length by a cladogram, and on the left, the gene classification was indicated. The lengths of exons are displayed proportionally to the scale on the bottom **(B)** Thirty-nine *PtC/VIF/PMEIs* were anchored on 16 chromosomes. Pairs of gene speculated to have undergone segmental/tandem duplication are lined and labeled in the same color.

fourteen genes appeared to be not expressed in the majority of developmental tissues, whereas they showed specific expression in floral tissues (e.g., catkins) (**Supplementary Figure S2**). The gene transcript abundance of all members in tissues were also compared by microarray, which was mostly compatible with the RNA-seq, particularly for those genes with high expression levels in roots (**Supplementary Figure S3**). However, seven C/VIF candidates have not been retrieved their expression patterns owning to the lack of probes for specific targeting (**Supplementary Table S2**). Accordingly, to reinforce the identity of gene expression in various tissues particularly in the roots and leaves, we further conducted the experimental measurement of gene expression levels by qRT-PCR using the *in vitro* cultured plants. A total of 21 *PtC/VIF* candidates were

FIGURE 2 | The *in silico* prediction of the *cis*-regulatory elements in the promoters. Upstream 1.5 kb sequences of each gene promoter were analyzed in the PlantCARE server. The stress- and phytohormone-related *cis*-regulatory elements are boxed in different colors.

verified their expression levels in the four selected vegetative tissues (roots, stem, young leaves, and mature leaves) (**Supplementary Figure S4**). Among these C/VIF candidates, six of them were identified to be predominantly expressed in the roots and 16 genes were detected the transcript abundance in the mature leaves or young leaves.

Molecular Characterization of *PtC/VIF1* and *2*

The collectively evolutionary analyses revealed that Potri.008G102600 (PtC/VIF1) and Potri.010G063000 (PtC/VIF2) were identified with significant homologies to the reported orthologous CIFs in tomato and *Arabidopsis*. PtC/VIF1 shows 33.56% protein sequence identities with SlINVINH1 (Jin et al., 2009) and PtC/VIF2 shows 45.75% protein sequence identities with AtCIF1 (Link et al., 2004). PtC/VIF1 and 2 displayed similar genomic patterns and shared 39.04% protein sequence identities. By removing the N-terminal targeting sequences, the deduced mature proteins were comprised of 148 and 146 amino acid residues for PtC/VIF1 and 2, respectively (**Supplementary Table S2**). The predicted MW for the mature PtC/VIF1 is 16.15 kDa with an acid pI of 4.76, and for PtC/VIF2, the MW is 15.69 kDa with a basic pI of 7.02. The multiple sequence alignment revealed that both PtC/VIF1 and 2 contained the motif-1 and the typical hallmarks, four Cys residues. However, only PtC/VIF2 showed the presence of a small motif (PKF) that was defined as a critical sequence for invertase–inhibitor interaction (Hothorn et al., 2010).

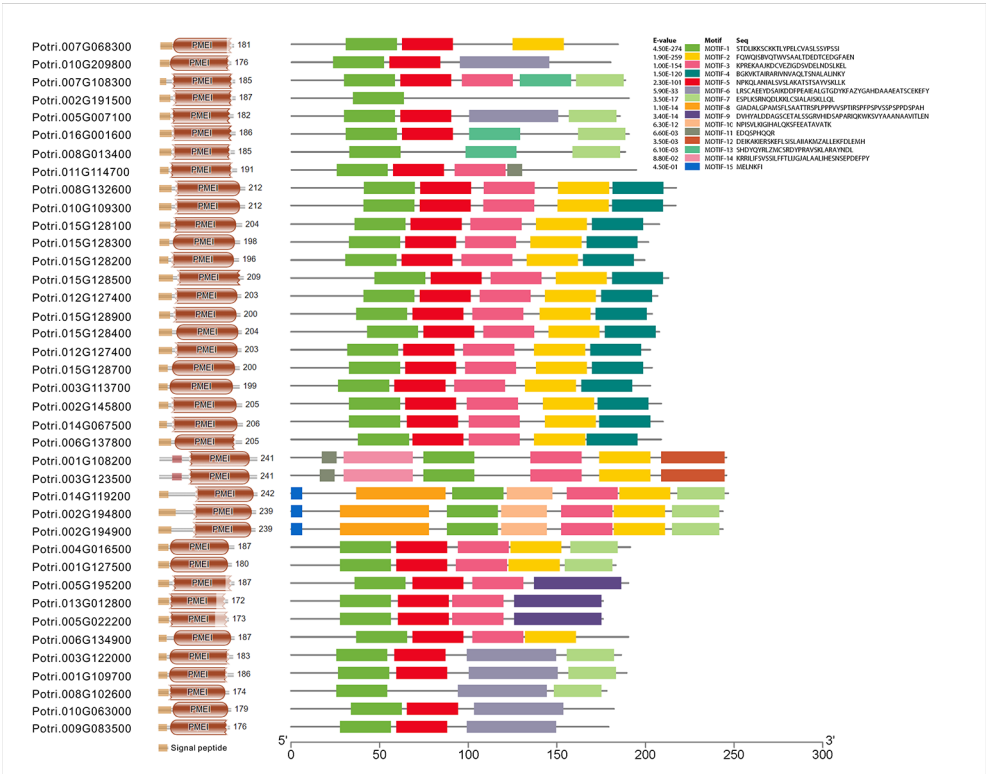

FIGURE 3 | The deduction of conserved motifs and amino acid residues. The distribution of signal peptides, conserved domain, and 15 motifs of 39 PtC/VIF/PMEIs was programmed by Pfam (32.0) and MEME. The motif-1 contains the first pair of Cys residues that were characterized to be involved in the formation of the disulfide bridge.

Accordingly, above RNA-seq and microarray data revealed their extremely high levels of expression in the roots (**Figure 5A** and **Supplementary Figures S2**, **S3**). Further qRT-PCR evaluation of the spatiotemporal expression patterns showed that *PtC/VIF1* was specifically expressed in the roots and stems (**Figure 5B**). By contrast, *PtC/VIF2* displayed predominant expression levels in the roots, followed by in the catkins and fruits (**Figure 5C**). These qRT-PCR results confirmed the tissue-specific expressions through the analyses of RNA-seq and microarray (**Figure 5A** and **Supplementary Figure S2**). The programed stress-related *cis*-regulatory elements within *PtC/VIF1* and *2* promoters allowed us to examine the effects on their expressions upon various environmental factors, including fusarium wilt (*F. solani*), drought, ABA, wound, and senescence. As shown in **Figures 5D and E**, after fungal inoculation of 72 hours, both *PtC/VIF1* and *2* expressions were significantly down-regulated in roots by the pathogenic *F. solani*. Under the drought stress conditions, *PtC/VIF1* showed a constant increase of expressions in the roots, whereas *PtC/VIF2* appeared to be promoted significantly when the time was extended to 96 hours. Additionally, *PtC/VIF2* expression in the roots displayed significant increases under the ABA treatments. By contrast, *PtC/VIF1* expression was markedly induced by the wounding stress. Interestingly, both *PtC/VIF1* and *2* displayed continuous promotions of the expression levels in responses to the seasonal leave senescence.

Apoplastic Targets of PtC/VIF1 and 2

The *in silico* prediction of target sequences of PtC/VIF1 and 2 suggested their subcellular localizations to the apoplast (**Figure 3** and **Supplementary Table S2**). To verify their primary targets, we expressed the fluorescent-labeled proteins in transient and stable transformation systems. For a transient assay, the C-terminal YFP fusion constructs (*35S: PtC/VIF1: YFP* and *35S: PtC/VIF2: YFP*) were co-introduced with a reported *Arabidopsis* cell wall-localization marker (*35S:AtCIF1: RFP*) into tobacco leaf epidermis (**Figures 6A–F**). The overlapped fluorescent signals revealed that distributions of the yellow fluorescence were observed around the cell periphery of the epidermis, suggesting that YFP fusions (green) were fully congruent with that of cells expressing the cell wall marker fused to RFP (red). However, there were no fluorescent signals were visualized from the vacuoles (**Figures 6C, F**). As an alternative approach, the same YFP fusion constructs were stably transformed into *Arabidopsis* and generate transgenic plants. As shown in **Figure 6G**, the YFP signals (green) were captured from the root epidermal cells. After the mannitol-triggered cell plasmolysis, the contracted vacuoles were visualized in the bright field of microscopy (**Figure 6I**).

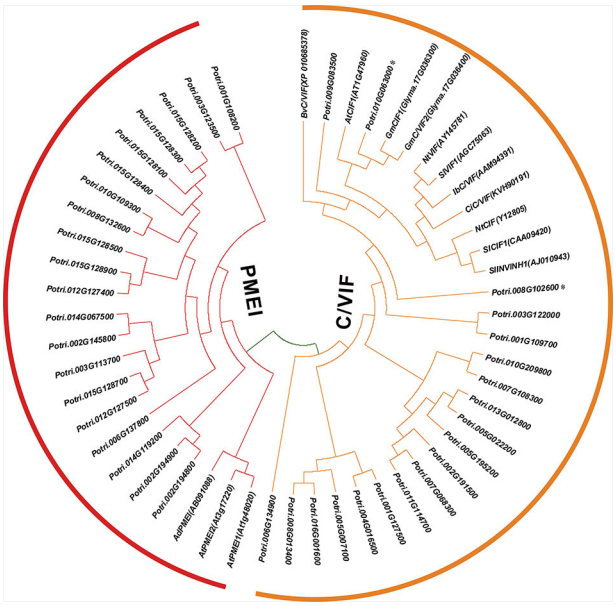

FIGURE 4 | Phylogenetic relationships of PMEI and C/VIF homologs between poplar and other plant species. Multiple protein sequences of PMEI/C/VIF were aligned with the other nine plant species by ClustalW. The unrooted phylogenetic tree was constructed by MEGA7 (https://www.megasoftware.net/) using the neighbor-joining method (Kumar et al., 2016). The evolutionary distances were computed using the Poisson correction method and are in the units of the number of amino acid substitutions per site. The percentage of replicate trees in which the associated taxa clustered together in the 1000 bootstrap test is shown next to the branches. The experimentally verified *PMEI* and *C/VIF* were reported in *N. tabacum* (Nt), *A. thaliana* (At), *B. vulgaris* (Bv), *I. batatas* (Ib), *C. intybus* (Ci), *G. max* (Gm), *S. lycopersicum* (Sl), *S. tuberosum* (St), and *A. deliciosa* (Ad). The accession numbers in Genbank are adjacent to the corresponding genes.

Concurrently, a fluorescent intercalating agent, PI (propidium iodide) was used to stain the cell wall. The captured yellow fluorescent signals from the overlapping of YFP fusion proteins (green) and PI staining (red) suggested that both PtC/VIF1 and 2 were localized to the apoplast (**Figure 6K** and **Supplementary Figure S1E**). Collectively, the image analyses of fluorescent fusions in tobacco leaves and transgenic *Arabidopsis* roots further supported the notion that PtC/VIF1 and 2 primarily targeted to the apoplast.

Inhibitory Activities of the PtC/VIF1 and 2

Given the conserved patterns and apoplastic localization of PtC/VIF1 and 2, we postulated that they might exert the functional inhibition on CWI activities. To specify their enzyme activities and targeting affinities, full-length CDS of *PtC/VIF1* and *2* with the removal of signal peptides were amplified and cloned into the *pETG-20A* vector to generate the 6xHis-tagged N-terminal TrxA-fusion constructs by the heterologous expression in the *E. coli* strain (**Figures 7A, B**). After induction by IPTG (Isopropyl β-d-1-thiogalactopyranoside), the TrxA-fusion proteins were harvested and further released through the cleavage of the TEV protease under the native conditions. As both TrxA and TEV protease contained His-tags, the released recombinant proteins were recovered by Ni-TED affinity chromatography to remove the tagged TrxA and TEV protease. Based on the gel images in **Figure 7C**, the size of finally purified PtC/VIF1 and 2 were close to the deduced MW of mature proteins (**Supplementary Table S2**). Furthermore, under the non-reducing conditions, the observed mobility shifts of recombinant PtC/VIF1 and 2 on SDS-PAGE suggested the synthesis of active intramolecular disulfide bridges (data not shown). To determine the inhibitory targeting activities *in vitro*, different concentrations of recombinant enzymes were incubated with fractions of the root extracted CWI and VI. For PtC/VIF1, the addition of 100 ng its recombinant enzymes demonstrated the maximum inhibition on CWI, showing a significant decrease of 98% activities, whereas no inhibitory effects were detected on VI activities (**Figure 7D**). By contrast, the input of approximately 800 ng of the recombinant PtC/VIF2 led to the maximum inhibition, causing a 95% suppression of CWI activities and, additionally, a 15% decreases of inhibition on VI activities (**Figure 7E**). Both of the recombinant PtC/VIF1 and 2 exhibited remarkably functional affinities on CWI rather than VI, prompting their potential roles as the apoplastic invertase inhibitors *in vitro*.

DISCUSSION

Emerging reports implicated that CWI and VI exert pivotal roles in maintaining sink capacity and stress acclimation. Since CWI and VI are intrinsically stable enzymes, the regulation of the enzyme activities depends mainly on the post-translational mechanisms that are mediated by the proteinaceous inhibitors (Ruan, 2014). The physiological roles and biotechnology relevance of C/VIF *via* fine-tuning of CWI or VI that modulates sugar metabolism and signaling in apoplast or vacuoles have been attempted in a variety of plants (Greiner et al., 1999; Jin et al., 2009; Liu et al., 2013; Qin et al., 2016; Su et al., 2016; Tang et al., 2017; Chen et al., 2019; Zhao et al., 2019). Hitherto, there is very little literature on molecular mechanisms of the functional genes in the model poplar tree owing to the recalcitrance. The complete genome sequence of *P. trichocarpa* has been released for a decade, and the genetic resource was well-annotated (Tuskan et al., 2006). However, the lack of the molecular basis of a specific gene family has impeded to unveil the physiological significance in the regulation of plant growth and development as well as the potential in the stress adaptation. Thus, the main objective of our work is to extend our knowledge on molecular and biochemical details of C/VIF family in woody plants.

In the present study, to explore the molecular background of C/VIF family genes, we identified a total of 39 candidate genes encoding PtC/VIF in the *Populus* genome (v3.0) of Phytozome 12.1. Analyses of the genomic patterns revealed that they were all intronless genes and had a similar length of the coding region. Approximately 14 gene pairs mapped on 13 chromosomes showed high identities, suggesting that the segmental and tandem duplication occurred commonly during the genome evolution in

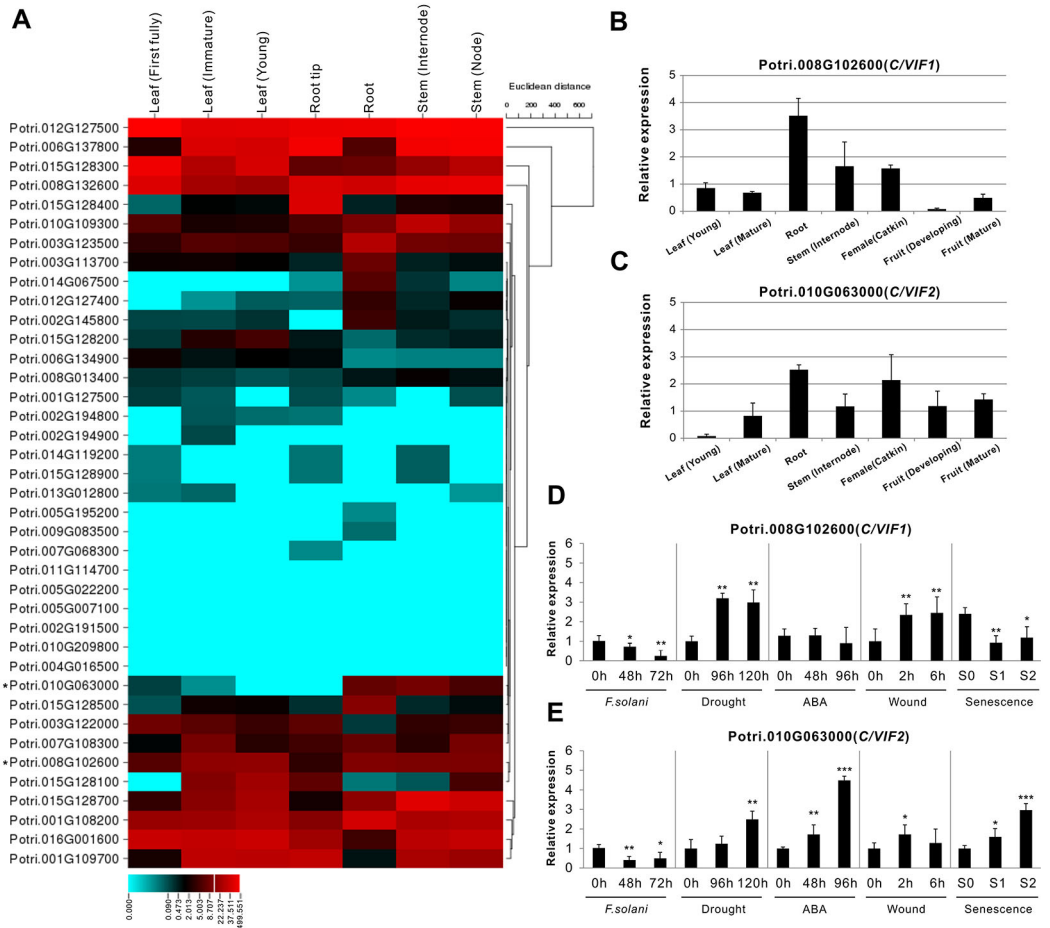

FIGURE 5 | Expression profiles of *PtC/VIF/PMEIs* in various tissues and effects on transcripts of *PtC/VIF1* and *2* upon stress factors. **(A)** Transcriptomic analyses in a heat map showing the transcript abundance of *PtC/VIF/PMEIs* in vegetative tissues of *P. trichocarpa*. **(B, C)** qRT-PCR analyses showing the tissue-specific expression and **(D, E)** the transcript effects of *PtC/VIF1* and *PtC/VIF2* upon the pathogenic *F. solani*, drought, ABA, wound, and seasonal senescence. The RNA-seq results were given in fragments per kilobase per million reads expression values. The heat map presented for RNA-seq was generated by the online program CIMminer (http://discover.nci.nih.gov/cimminer/home.do). Expression data represent mean values standard error (± SE) of at least three independent biological replicates for qRT-PCR. *PtActin*, *PtUBIC*, and *PtEFα1* were used as reference genes. The asterisks indicate significant differences in comparison with the control using Student's *t*-test: $^{***}p < 0.001$, $^{**}p < 0.01$, $^{*}p < 0.05$.

poplar (**Figures 1A, B**). The genome duplication is an important driver of species origination and diversification, facilitating genes in woody plants to acquire new functions and adapt various environmental factors (Jansson and Douglas, 2007; Bocock et al., 2008). Gene complexity and duplications may give rise to more challenges in the elucidation of functional roles for a unique gene in poplar. In combination with RNA-seq and microarray data, the qRT-PCR analyses of spatiotemporal expression suggested that all candidate genes were differentially expressed in vegetative and reproductive tissues. Additionally, we analyzed the conserved patterns of the PtC/VIF/PMEI protein through the multiple sequence alignment, resulting in the identification of conserved PMEI domain and 15 putative motifs (**Figure 3**). Interestingly, only motif-1 was identified to be evenly distributed among all *PtC/VIF* candidates, whereas other motifs appeared not to spread universally, reflecting that both C/VIF and PMEI family are moderately conserved enzymes.

Based on the phylogenetic comparison between *PtC/VIF* candidates and the functional reported homologs in other plant species, we characterized two putative invertase inhibitors, *PtC/VIF1* and *2*, showing distinguishing features of root-specific expression. The spatiotemporal expressions of CWI coupled with inhibitors and SUTs during the sink organ development have been demonstrated in a variety of plant species, suggesting that the co-expression is a typical pattern underlying the mechanisms of inhibitor-mediated post-translational regulation (Jin et al., 2009; Wang and Ruan, 2012; Su et al., 2016). The co-expression (localization) patterns of

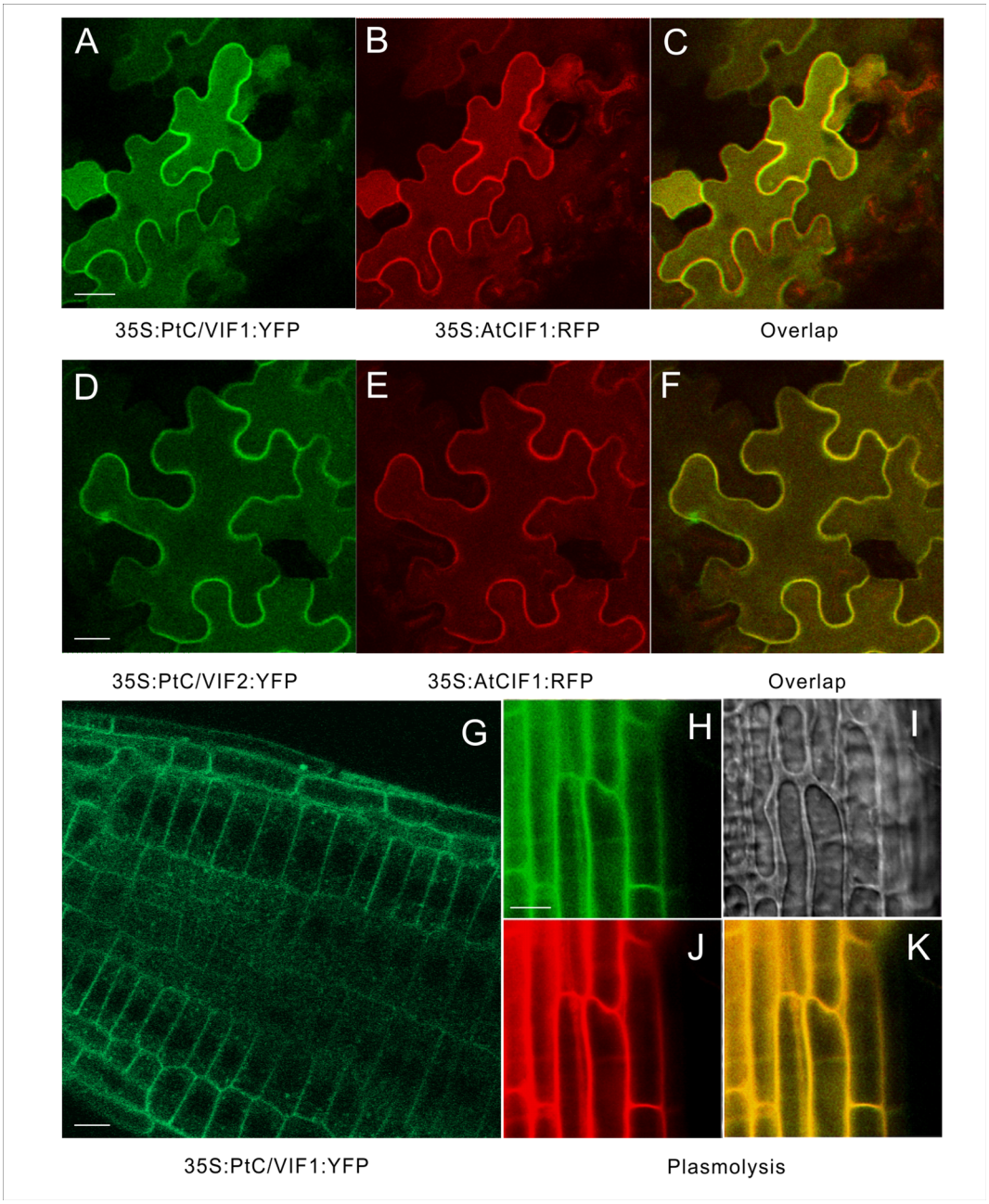

FIGURE 6 | Apoplastic localizations of PtC/VIF1 and 2 in tobacco and *Arabidopsis*. **(A-F)** Tobacco leaves were co-infiltrated with *A. tumefaciens* (C58C1) culture harboring the florescent fusion constructs of *35S: PtC/VIF1: YFP* and *35S:AtCIF1: RFP* or *35S: PtC/VIF2: YFP* and *35S:AtCIF1: RFP*. **(A, D)** Epidermal cells of tobacco leaf depicting YFP (green) fluorescence. **(B, E)** The red fluorescent signals of a cell wall marker AtCIF1. **(C, F)** The yellow fluorescent signals captured from the overlap of YFP and RFP fusion. **(G)** Images of CLSM in transgenic *Arabidopsis* showed the yellow fluorescent (green) signal of PtC/VIF1. Fluorescent images showing **(H)** YFP (green) signals, **(I)** the contracted vacuoles, **(J)** PI staining (red), and **(K)** the overlapping signals (yellow) from YFP and PI after plasmolysis (200 mM mannitol). PI (propidium iodide) was used as a marker to track the cell wall for fresh cells. The *Arabidopsis* seedlings grew for five days under short-day conditions and were harvested for the CLSM analysis.

invertase and the inhibitor provide the clues for the direct functional target. Such dispersed co-localization also contributes to the efficient transport of the hydrolyzed hexose to the sink fruits *via* modulation of the enzyme activities and sugar signaling (Palmer et al., 2015). Recent reports on evolutionary analyses suggested the presence of five CWI homologs and three VI homologs in the poplar genome (Bocock et al., 2008), which allowed us to reassess their expression patterns in our selected tissues. The RT-PCR validation revealed that three CWI genes (*PtCWI3*, *4*, and *5*)

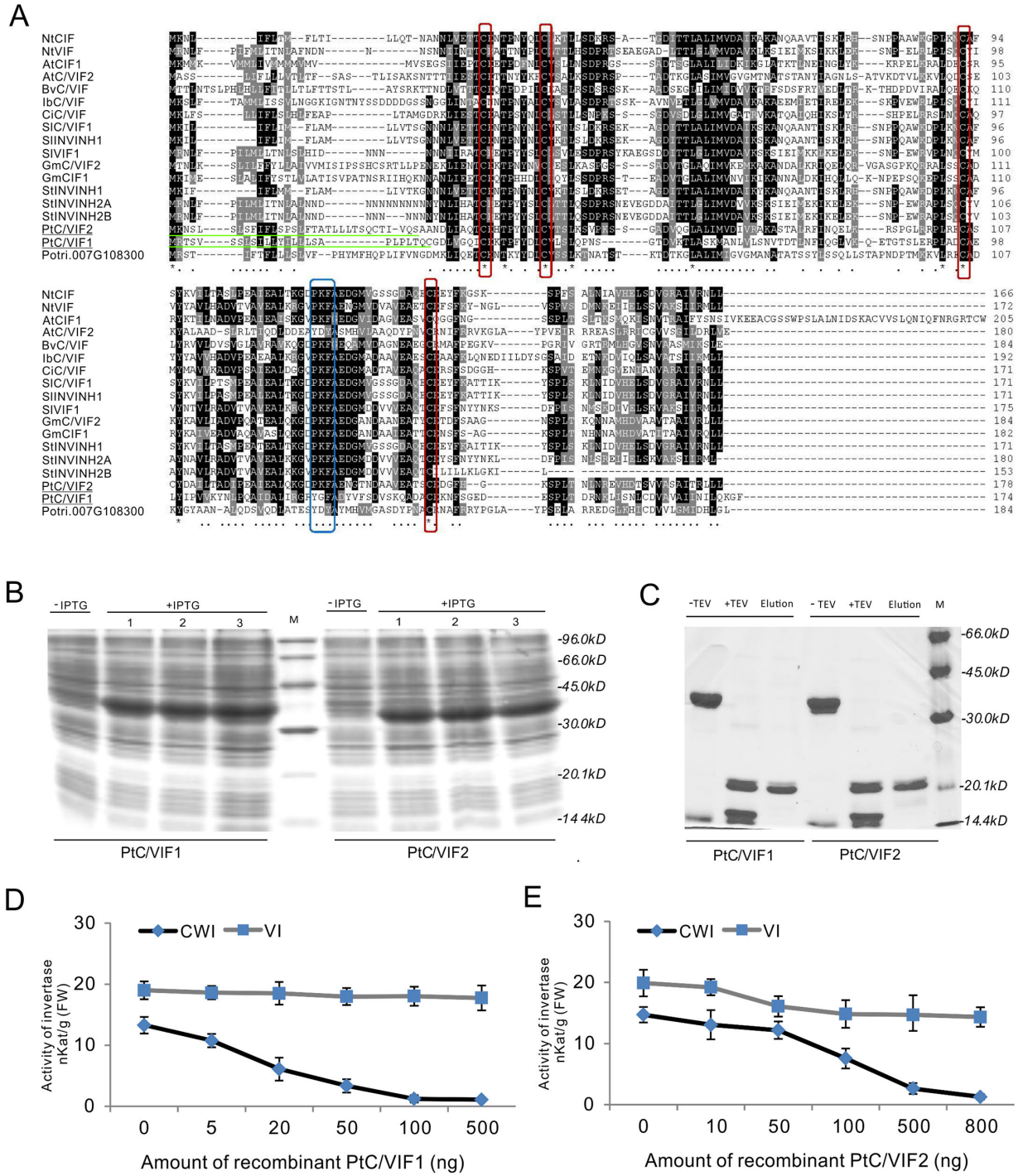

FIGURE 7 | The inhibitory functions *in vitro* of the recombinant PtC/VIF1 and 2. **(A)** Multiple sequence alignment of PtC/VIF homologs showed the presence of targeting sequences (underlined in green), the four Cys residues (boxed in red), and the reported small motif PKF (boxed in blue). **(B, C)** SDS-PAGE analyses showed the induction and purification of the recombinant proteins. **(D, E)** The functional activities *in vitro* of recombinant proteins were determined by the inhibition of CWI and VI, which were extracted from the roots. The minimum dose input caused maximum inhibitory activities of CWI and VI was 100 ng for the recombinant PtC/VIF1, and 800 ng for the recombinant PtC/VIF2. Determination of the functional enzyme activities represents means ± SE of at least four independent biological replicates.

showed transcript abundance in the roots and leaves (**Supplementary Figure S4**). These findings envisioned the potential co-expression of three *PtCWI* genes with *PtC/VIF1* or *2* in poplar normal growth. However, whether the co-expression patterns between inhibitor genes and *CWIs* are critical under the stress regime or which inhibitor(s) would target specific CWI gene(s) *in vivo* remains to be determined further.

As discussed previously, the differential expression profiles of *PtC/VIF1* and *2* in response to various stress factors indicated the complexities and crosstalk of phytohormone and environmental cues (**Figures 5D, E**). Increases in enzyme activities within the apoplastic space upon pathogen infection suggested that CWI served as an essential activator in plant defense regulation (Tauzin and Giardina, 2014). The depression of CIF-encoded gene expression contributed to fortify the hexose capacity, resulting in reduced disease symptoms in apoplastic space (Siemens et al., 2011; Veillet et al., 2016; Su et al., 2018). Under the infection of the *F. solani*, significant down-regulation of *PtC/VIF1* and *2* transcripts were observed after 72 hour inoculation, indicating that they both may be involved in the sucrose-mediated defense pathway. This finding reconciled the ongoing RNA-seq analyses, showing similar patterns of suppressed gene transcript levels among the majorly affected genes in roots with *F. solani* infection (data not shown). Interestingly, some research revealed that the boosting of pathogen innate invertase led to the reprogramed sucrose hydrolysis that may maintain the sugar demand to their benefit (Chang et al., 2017). Collectively, it remains to be deciphered whether CIFs indeed function in a manner of fine-tuning sucrose homeostasis and signaling during plant pathogenesis, or what specific factors and molecular mechanisms potentially perturb the inhibitor gene expression and subsequently, activate/deactivate the immune defense responses to apoplast-adapted stresses (Veillet et al., 2016; Naseem et al., 2017).

The dynamic processes of drought tolerance in plants involved sophisticated control of water influx, cellular osmosis, and sugar metabolism (Golldack et al., 2014). The accumulated storage sugars were also identified to be in correlation with the increase of AI transcripts upon the drought stress (Ji et al., 2010). Under abiotic conditions, the constant induction of *PtC/VIF1* transcript upon drought and wound in the roots suggested that it was dehydration- and wound-responsive gene. Recently, promising work in tomato revealed that significant elevation of CWI activities rather than the transcripts conferred the improvement of drought tolerance (Albacete et al., 2015), reflecting the roles of CIF in the post-translational regulation. Suppression of a tomato *CIF* expression can significantly delay the leaf senescence and fruit size (Jin et al., 2009). An extracellular invertase inhibitor, *AtCIF1* was reevaluated to act as the essential stimulator to be involved in seed germination and biomass control (Su et al., 2016), prompting that the post-translational modulation of CWI positively impacted on sink capacity. In accordance with this, the marked induction of *PtC/VIF2* transcript upon ABA and the seasonal senescence provided clues that *PtC/VIF2* may be a critical component in processing the nitrogen metabolism and remobilization during the leaf aging.

Sugar metabolism is a highly complex network in perennial woody plants and transferred between several intracellular or extracellular compartments for the metabolite biosynthesis, partitioning, and storage (Bocock et al., 2008). In the apoplast, the external supply of carbohydrates is much utilized by sink organs for the developmental and reproductive processes. However, the post-translational mechanisms underlying the regulation of acid invertase through proteinaceous inhibitors have received less attention in woody plants, mostly owing to the lack of extensive molecular basis and the biochemical reports. The recently updated genome assembling in *P. trichocarpa* enables us to mine the C/VIF family for the post-translational modulation in sucrose metabolism and stress response in poplar. Along with the comprehensive view of the genomic patterns and expression profiling, analyses of the phylogenies and conserved motifs revealed that PtC/VIF1 and 2 were closer to the reported C/VIF homologs, suggesting the potential action as invertase inhibitors *in vitro*. Based on the *in silico* analyses, they both were deduced ultimately to transport mature proteins to the apoplast. Thereafter, using the transient and stable expression of YFP-fusion proteins in tobacco and *Arabidopsis*, we observed the fluorescent signals from the cell wall, confirming the typical patterns of apoplast-localized proteins. However, further exploit of their subcellular localization and co-localization with targeting invertase in the cells of native poplar plants remain to be solved.

Accordingly, the comparative crystallographic approach revealed that the target specificity of homologous PMEI and C/VIF used similar structural modules to exert differentially inhibitory functions (Hothorn et al., 2004). However, it is still unreliable to predict the functional pattern from the sequence alone owing to the graded identities of conserved domains and motifs between C/VIF and PMEI family (Link et al., 2004; Zuma et al., 2018). Additional variation of residue combination also may impact on respective interface between C/VIF/PMEI and the targeting proteins (Hothorn et al., 2010), prompting the situation that the use of direct enzyme assay may be the optimized way to distinguish C/VIF from PMEI prior to unveiling the physiological roles in the regulation of plant development and stress tolerance (Wolf et al., 2003; Link et al., 2004). Thus, to examine the specific enzyme properties and targeting affinities, a functional inhibition assay was implemented through the heterologous expression and purification of recombinant proteins in *E.coli*. Based on the functional determination of the enzyme activities, PtC/VIF1 and 2 were confirmed to exhibit a large proportion of inhibitory activities on the extracted CWI rather than VI, further corroborating their roles as the genuine apoplastic invertase inhibitors.

CONCLUSIONS

Thus far, there has been ongoing interest in the improvement of poplar performance with strengthened pathogen resistance and

stress tolerance remains a significant challenge for modern agriculture and forestry. Accumulated evidence has prompted that the small inhibitory proteins exert fundamental roles in plant growth and development as well as the regulation of sucrose metabolism and homeostasis through the fine-tuning of the acid invertase activities. Here, we described molecular and genetic details of PtC/VIF family is essential to implicate how genes influence the phenotypes. The spatiotemporal expression patterns of PtC/VIF-encoded genes may confer functional specificity and diversity in response to stress stimuli and environmental cues in woody plants. Among these candidates, *PtC/VIF1* and *2* represent the first invertase inhibitor genes to be characterized in woody plants. Taken together, a remarkable feature of functional PtC/VIF1 and 2 contribute to in-depth unraveling the roles *in vivo* and the post-translational mechanisms underlying the molecular interaction with their targeting enzymes. Further work will attempt to evaluate the possible phenotypes of genetically constructed mutants under stress exposure, and in the long term, it may facilitate the increases of apoplast-adapted pathogen infection and diverse abiotic stressors.

DATA AVAILABILITY STATEMENT

The microarray data: GEO: GSE13990 (https://www.ncbi.nlm.nih.gov/gds/?term=GSE13990); BioProject: PRJNA112485 (https://www.ncbi.nlm.nih.gov/bioproject/?term=GSE13990. 15.01.2009). The RNA-seq data: Accession number: AARH00000000.3 (30.11.2018); BioProject: PRJNA10772 (https://www.ncbi.nlm.nih.gov/bioproject/PRJNA10772/), GCF_000002775.4 (https://www.ncbi.nlm.nih.gov/assembly/GCA_000002775.3 24.01.2018) contains a large number of RNA-seq data, of which, the accession number corresponding to our manuscript in SRA is SRP077540 (https://www.ncbi.nlm.nih.gov/sra/?term=SRP077540), including the detailed different SRA_run (Leaf_FFE: SRR3727130, 32, and 40; Leaf_Immature: SRR3727123, 25, and 39; Leaf_Young: SRR3727116, 21, and 33; Stem_Node: SRR3727110, 17, and 38; Stem_Inode: SRR3727120, 24, and 41; Roots: SRR3727119, 35, and 36; Roottip: SRR3727111, 15, and 22.

AUTHOR CONTRIBUTIONS

TS and MH designed the experiment, collected and analyzed all of the data. TS and MH prepared the initial draft of the manuscript and developed the concept. MH and YF were responsible for approving the final draft of the manuscript. TS conducted the image analyses of CLSM and protein purification. JM and HZ performed the qRT-PCR analysis and enzyme assay. QZ and JZ assisted JM and HZ with the experiment conduction. HZ was responsible for plant culture *in vitro*. TS did much work on the bioinformatics analysis, including conserved domain and promoter analyses, RNA-seq collection, and heat map construction. All authors have reviewed the manuscript.

FUNDING

This research was supported by the Natural Science Foundation of China (NSFC) (31870589; 31700525), the Natural Science Foundation of Jiangsu Province (NSFJ) (BK20170921), the Scientific Research Foundation for High-Level Talents of Nanjing Forestry University (SRFNFU) (GXL2017011; GXL2017012), the Priority Academic Program Development of Jiangsu Higher Education Institutions (PAPD), and the Undergraduate Innovation and Entrepreneurship Training Programs in NFU (2018NFUSPITP044).

ACKNOWLEDGMENTS

The authors would like to thank NSFC, NSFJ, and SRFNFU for funding this research. Our thanks also go to the Key Laboratory of State Forestry Administration on Subtropical Forest Biodiversity Conservation, the Co-Innovation Center for Sustainable Forestry in Southern China, and PAPD for the instrument support. Thanks go to the JGI Plant Gene Atlas project conducted by the U.S. Department of JGI was supported by the U.S DOE Office of Science (no. DE-AC02-05CH11231). We also appreciate the critical comments on manuscript preparation by Prof. Dr. Thomas Rausch and Dr. Sebastian Wolf from the Centre of Organismal Studies (COS), Heidelberg University.

SUPPLEMENTARY MATERIAL

The Supplementary Material for this article can be found online at: https://www.frontiersin.org/articles/10.3389/fpls.2019.01654/full#supplementary-material

REFERENCES

Albacete, A., Cantero-Navarro, E., Großkinsky, D. K., Arias, C. L., Balibrea, M. E., Bru, R., et al. (2015). Ectopic overexpression of the cell wall invertase gene CIN1 leads to dehydration avoidance in tomato. *J. Exp. Bot.* 66, 863–878. doi: 10.1093/jxb/eru448

Bailey, T. L., Williams, N., Misleh, C., and Li, W. W. (2006). MEME: discovering and analyzing DNA and protein sequence motifs. *Nucleic Acids Res.* 34, W369–W373. doi: 10.1093/nar/gkl198

Balibrea Lara, M. E., Gonzalez Garcia, M.-C., Fatima, T., Ehneß, R., Lee, T. K., Proels, R., et al. (2004). Extracellular invertase is an essential component of cytokinin-mediated delay of senescence. *Plant Cell* 16, 1276–1287. doi: 10.1105/tpc.018929

Barnes, W. J., and Anderson, C. T. (2018). Cytosolic invertases contribute to cellulose biosynthesis and influence carbon partitioning in seedlings of Arabidopsis thaliana. *Plant J.* 94, 956–974. doi: 10.1111/tpj.13909

Bate, N. J. (2004). An invertase inhibitor from maize localizes to the embryo surrounding region during early kernel development. *Plant Physiol.* 134, 246–254. doi: 10.1104/pp.103.027466

Battaglia, M. E., Martin, M. V., Lechner, L., Martínez-Noël, G. M. A., and Salerno, G. L. (2017). The riddle of mitochondrial alkaline/neutral invertases: a novel Arabidopsis isoform mainly present in reproductive tissues and involved in

root ROS production. *PloS One* 12, e0185286. doi: 10.1371/journal.pone.0185286

Bhaskar, P. B., Wu, L., Busse, J. S., Whitty, B. R., Hamernik, A. J., Jansky, S. H., et al. (2010). Suppression of the vacuolar invertase gene prevents cold-induced sweetening in potato. *Plant Physiol.* 154, 939–948. doi: 10.1104/pp.110.162545

Bihmidine, S., Hunter, C. T., Johns, C. E., Koch, K. E., and Braun, D. M. (2013). Regulation of assimilate import into sink organs: update on molecular drivers of sink strength. *Front. Plant Sci.* 4, 177. doi: 10.3389/fpls.2013.00177

Bocock, P. N., Morse, A. M., Dervinis, C., and Davis, J. M. (2008). Evolution and diversity of invertase genes in Populus trichocarpa. *Planta* 227, 565–576. doi: 10.1007/s00425-007-0639-3

Bonfig, K. B., Gabler, A., Simon, U. K., Luschin-Ebengreuth, N., Hatz, M., Berger, S., et al. (2010). Post-translational derepression of invertase activity in source leaves via down-regulation of invertase inhibitor expression is part of the plant defense response. *Mol. Plant* 3, 1037–1048. doi: 10.1093/mp/ssq053

Brummell, D. A., Chen, R. K. Y., Harris, J. C., Zhang, H., Hamiaux, C., Kralicek, A. V., et al. (2011). Induction of vacuolar invertase inhibitor mRNA in potato tubers contributes to cold-induced sweetening resistance and includes spliced hybrid mRNA variants. *J. Exp. Bot.* 62, 3519–3534. doi: 10.1093/jxb/err043

Chang, Q., Liu, J., Lin, X., Hu, S., Yang, Y., Li, D., et al. (2017). A unique invertase is important for sugar absorption of an obligate biotrophic pathogen during infection. *New Phytol.* 215, 1548–1561. doi: 10.1111/nph.14666

Chen, S. F., Liang, K., Yin, D. M., Ni, D. A., Zhang, Z. G., and Ruan, Y. L. (2016). Ectopic expression of a tobacco vacuolar invertase inhibitor in guard cells confers drought tolerance in Arabidopsis. *J. Enzyme Inhib. Med. Chem.* 31, 1381–1385. doi: 10.3109/14756366.2016.1142981

Chen, L., Liu, X., Huang, X., Luo, W., Long, Y., Greiner, S., et al. (2019). Functional characterization of a drought-responsive invertase inhibitor from maize (Zea mays L.). *Int. J. Mol. Sci.* 20, 4081. doi: 10.3390/ijms20174081

Chourey, P. S., Jain, M., Li, Q. B., and Carlson, S. J. (2006). Genetic control of cell wall invertases in developing endosperm of maize. *Planta*. 223, 159–167. doi: 10.1007/s00425-005-0039-5

Clough, S. J., and Bent, A. F. (1998). Floral dip: a simplified method for Agrobacterium-mediated transformation of Arabidopsis thaliana. *Plant J.* 16, 735–743. doi: 10.1046/j.1365-313x.1998.00343.x

Coleman, H. D., Yan, J., and Mansfield, S. D. (2009). Sucrose synthase affects carbon partitioning to increase cellulose production and altered cell wall ultrastructure. *Proc. Natl. Acad. Sci.* 106, 13118–13123. doi: 10.1073/pnas.0900188106

Doidy, J., Grace, E., Kühn, C., Simon-Plas, F., Casieri, L., and Wipf, D. (2012). Sugar transporters in plants and in their interactions with fungi. *Trends Plant Sci.* 17, 413–422. doi: 10.1016/j.tplants.2012.03.009

Ehness, R., and Roitsch, T. (1997). Co-ordinated induction of mRNAs for extracellular invertase and a glucose transporter in Chenopodium rubrum by cytokinins. *Plant J.* 11, 539–548. doi: 10.1046/j.1365-313X.1997.11030539.x

Essmann, J., Schmitz-Thom, I., Schön, H., Sonnewald, S., Weis, E., and Scharte, J. (2008). RNA interference-mediated repression of cell wall invertase impairs defense in source leaves of tobacco. *Plant Physiol.* 147, 1288–1299. doi: 10.1104/pp.108.121418

Golldack, D., Li, C., Mohan, H., and Probst, N. (2014). Tolerance to drought and salt stress in plants: unraveling the signaling networks. *Front. Plant Sci.* 5, 151. doi: 10.3389/fpls.2014.00151

Greiner, S., Rausch, T., Sonnewald, U., and Herbers, K. (1999). Ectopic expression of a tobacco invertase inhibitor homolog prevents cold-induced sweetening of potato tubers. *Nat. Biotechnol.* 17, 708–711. doi: 10.1038/10924

Greiner, S. (1998). Cloning of a tobacco apoplasmic invertase inhibitor. proof of function of the recombinant protein and expression analysis during plant development. *Plant Physiol.* 116, 733–742. doi: 10.1104/pp.116.2.733

Han, M., Heppel, S. C., Su, T., Bogs, J., Zu, Y., An, Z., et al. (2013). Enzyme inhibitor studies reveal complex control of methyl-d-erythritol 4-phosphate (MEP) pathway enzyme expression in catharanthus roseus. *PloS One* 8, e62467. doi: 10.1371/journal.pone.0062467

Hothorn, M., Wolf, S., Aloy, P., Greiner, S., and Scheffzek, K. (2004). Structural insights into the target specificity of plant invertase and pectin methylesterase inhibitory proteins. *Plant Cell.* 16, 3437–3447. doi: 10.1105/tpc.104.025684

Hothorn, M., Van den Ende, W., Lammens, W., Rybin, V., and Scheffzek, K. (2010). Structural insights into the pH-controlled targeting of plant cell-wall invertase by a specific inhibitor protein. *Proc. Natl. Acad. Sci.* 107, 17427–17432. doi: 10.1073/pnas.1004481107

Hu, B., Jin, J., Guo, A.-Y., Zhang, H., Luo, J., and Gao, G. (2015). GSDS 2.0: an upgraded gene feature visualization server. *Bioinformatics* 31, 1296–1297. doi: 10.1093/bioinformatics/btu817

Jansson, S., and Douglas, C. J. (2007). Populus : a model system for plant biology. *Annu. Rev. Plant Biol.* 58, 435–458. doi: 10.1146/annurev.arplant.58.032806.103956

Ji, X., Shiran, B., Wan, J., Lewis, D. C., Jenkins, C. L. D., Condon, A. G., et al. (2010). Importance of pre-anthesis anther sink strength for maintenance of grain number during reproductive stage water stress in wheat. *Plant Cell Environ.* 33, 926–942. doi: 10.1111/j.1365-3040.2010.02130.x

Jin, Y., Ni, D.-A., and Ruan, Y.-L. (2009). Posttranslational elevation of cell wall invertase activity by silencing its inhibitor in tomato delays leaf senescence and increases seed weight and fruit hexose level. *Plant Cell* 21, 2072–2089. doi: 10.1105/tpc.108.063719

Klann, E. M., Hall, B., and Bennett, A. B. (1996). Antisense acid invertase (TIV1) gene alters soluble sugar composition and size in transgenic tomato fruit. *Plant Physiol.* 112, 1321–1330. doi: 10.1104/pp.112.3.1321

Kocal, N., Sonnewald, U., and Sonnewald, S. (2008). Cell wall-bound invertase limits sucrose export and is involved in symptom development and inhibition of photosynthesis during compatible interaction between tomato and Xanthomonas campestris pv vesicatoria. *Plant Physiol.* 148, 1523–1536. doi: 10.1104/pp.108.127977

Koch, K. (2004). Sucrose metabolism: regulatory mechanisms and pivotal roles in sugar sensing and plant development. *Curr. Opin. Plant Biol.* 7, 235–246. doi: 10.1016/j.pbi.2004.03.014

Kohorn, B. D., Kobayashi, M., Johansen, S., Riese, J., Huang, L. F., Koch, K., et al. (2006). An Arabidopsis cell wall-associated kinase required for invertase activity and cell growth. *Plant J.* 46, 307–316. doi: 10.1111/j.1365-313X.2006.02695.x

Kumar, S., Stecher, G., and Tamura, K. (2016). MEGA7: Molecular Evolutionary Genetics Analysis Version 7.0 for Bigger Datasets. *Mol. Biol. Evol.* 33, 1870–1874. doi: 10.1093/molbev/msw054

Li, B., Liu, H., Zhang, Y., Kang, T., Zhang, L., Tong, J., et al. (2013). Constitutive expression of cell wall invertase genes increases grain yield and starch content in maize. *Plant Biotechnol. J.* 11, 1080–1091. doi: 10.1111/pbi.12102

Li, S., Zhen, C., Xu, W., Wang, C., and Cheng, Y. (2017). Simple, rapid and efficient transformation of genotype Nisqually-1: A basic tool for the first sequenced model tree. *Sci. Rep.* 7, 2638. doi: 10.1038/s41598-017-02651-x

Link, M., Rausch, T., and Greiner, S. (2004). In Arabidopsis thaliana, the invertase inhibitors AtC/VIF1 and 2 exhibit distinct target enzyme specificities and expression profiles. *FEBS Lett.* 573, 105–109. doi: 10.1016/j.febslet.2004.07.062

Liu, X., Lin, Y., Liu, J., Song, B., Ou, Y., Zhang, H., et al. (2013). StInvInh2 as an inhibitor of StvacINV1 regulates the cold-induced sweetening of potato tubers by specifically capping vacuolar invertase activity. *Plant Biotechnol. J.* 11, 640–647. doi: 10.1111/pbi.12054

Liu, S., Lan, J., Zhou, B., Qin, Y., Zhou, Y., Xiao, X., et al. (2015). HbNIN2, a cytosolic alkaline/neutral-invertase, is responsible for sucrose catabolism in rubber-producing laticifers of Hevea brasiliensis (para rubber tree). *New Phytol.* 206, 709–725. doi: 10.1111/nph.13257

Maruta, T., Miyazaki, N., Nosaka, R., Tanaka, H., Padilla-Chacon, D., Otori, K., et al. (2015). A gain-of-function mutation of plastidic invertase alters nuclear gene expression with sucrose treatment partially via GENOMES UNCOUPLED1-mediated signaling. *New Phytol.* 206, 1013–1023. doi: 10.1111/nph.13309

Mckenzie, M. J., Chen, R. K. Y., Harris, J. C., Ashworth, M. J., and Brummell, D. A. (2013). Post-translational regulation of acid invertase activity by vacuolar invertase inhibitor affects resistance to cold-induced sweetening of potato tubers. *Plant Cell Environ.* 36, 176–185. doi: 10.1111/j.1365-3040.2012.02565.x

Morey, S. R., Hirose, T., Hashida, Y., Miyao, A., Hirochika, H., Ohsugi, R., et al. (2018). Genetic evidence for the role of a rice vacuolar invertase as a molecular sink strength determinant. *Rice.* 11, 6. doi: 10.1186/s12284-018-0201-x

Nägele, T., Henkel, S., Hörmiller, I., Sauter, T., Sawodny, O., Ederer, M., et al. (2010). Mathematical modeling of the central carbohydrate metabolism in Arabidopsis reveals a substantial regulatory influence of vacuolar invertase on whole plant carbon metabolism. *Plant Physiol.* 153, 260–272. doi: 10.1104/pp.110.154443

Naseem, M., Kunz, M., and Dandekar, T. (2017). Plant–pathogen maneuvering over apoplastic sugars. *Trends Plant Sci.* 22, 740–743. doi: 10.1016/j.tplants.2017.07.001

Palmer, W. M., Ru, L., Jin, Y., Patrick, J. W., and Ruan, Y. L. (2015). Tomato ovary-to-fruit transition is characterized by a spatial shift of mrnas for cell wall invertase and its inhibitor with the encoded proteins localized to sieve elements. *Mol. Plant*. 8, 315–328. doi: 10.1016/j.molp.2014.12.019

Proels, R. K., and Hückelhoven, R. (2014). Cell-wall invertases, key enzymes in the modulation of plant metabolism during defence responses. *Mol. Plant Pathol.* 15, 858–864. doi: 10.1111/mpp.12139

Qian, W., Xiao, B., Wang, L., Hao, X., Yue, C., Cao, H., et al. (2018). CsINV5, a tea vacuolar invertase gene enhances cold tolerance in transgenic Arabidopsis. *BMC Plant Biol.* 18, 228. doi: 10.1186/s12870-018-1456-5

Qin, G., Zhu, Z., Wang, W., Cai, J., Chen, Y., Li, L., et al. (2016). A tomato vacuolar invertase inhibitor mediates sucrose metabolism and influences fruit ripening. *Plant Physiol.* 172, 1596–1611. doi: 10.1104/pp.16.01269

Rausch, T., and Greiner, S. (2004). Plant protein inhibitors of invertases. *Biochim. Biophys. Acta-Proteins Proteomics* 1696, 253–261. doi: 10.1016/j.bbapap.2003.09.017

Reca, I. B., Brutus, A., D'Avino, R., Villard, C., Bellincampi, D., and Giardina, T. (2008). Molecular cloning, expression and characterization of a novel apoplastic invertase inhibitor from tomato (Solanum lycopersicum) and its use to purify a vacuolar invertase. *Biochimie* 90, 1611–1623. doi: 10.1016/j.biochi.2008.04.019

Rende, U., Wang, W., Gandla, M. L., Jönsson, L. J., and Niittylä, T. (2017). Cytosolic invertase contributes to the supply of substrate for cellulose biosynthesis in developing wood. *New Phytol.* 214, 796–807. doi: 10.1111/nph.14392

Roitsch, T., Balibrea, M. E., Hofmann, M., Proels, R., and Sinha, A. K. (2003). Extracellular invertase: key metabolic enzyme and PR protein. *J. Exp. Bot.* 54, 513–524. doi: 10.1093/jxb/erg050

Rolland, F., Baena-Gonzalez, E., and Sheen, J. (2006). Sugar sensing and signaling in plants: conserved and novel mechanisms. *Annu. Rev. Plant Biol.* 57, 675–709. doi: 10.1146/annurev.arplant.57.032905.105441

Ruan, Y.-L. (2014). Sucrose metabolism: gateway to diverse carbon use and sugar signaling. *Annu. Rev. Plant Biol.* 65, 33–67. doi: 10.1146/annurev-arplant-050213-040251

Sergeeva, L. I., Keurentjes, J. J. B., Bentsink, L., Vonk, J., van der Plas, L. H. W., Koornneef, M., et al. (2006). Vacuolar invertase regulates elongation of Arabidopsis thaliana roots as revealed by QTL and mutant analysis. *Proc. Natl. Acad. Sci.* 103, 2994–2999. doi: 10.1073/pnas.0511015103

Siemens, J., González, M. C., Wolf, S., Hofmann, C., Greiner, S., Du, Y., et al. (2011). Extracellular invertase is involved in the regulation of clubroot disease in Arabidopsis thaliana. *Mol. Plant Pathol.* 12, 247–262. doi: 10.1111/j.1364-3703.2010.00667.x

Sturm, A. (2002). Invertases. Primary structures, functions, and roles in plant development and sucrose partitioning. *Plant Physiol.* 121, 1–8. doi: 10.1104/pp.121.1.1

Su, T., Wolf, S., Han, M., Zhao, H., Wei, H., Greiner, S., et al. (2016). Reassessment of an Arabidopsis cell wall invertase inhibitor AtCIF1 reveals its role in seed germination and early seedling growth. *Plant Mol. Biol.* 90, 137–155. doi: 10.1007/s11103-015-0402-2

Su, T., Han, M., Min, J., Chen, P., Mao, Y., Huang, Q., et al. (2018). Genome-wide survey of invertase encoding genes and functional characterization of an extracellular fungal pathogen-responsive invertase in glycine max. *Int. J. Mol. Sci.* 19, 2395. doi: 10.3390/ijms19082395

Su, T., Han, M., Min, J., Cao, D., Zhai, G., Zhou, H., et al. (2019). Genome-wide characterization of AspATs in populus: gene expression variation and enzyme activities in response to nitrogen perturbations. *Forests* 10, 449. doi: 10.3390/f10050449

Sun, L., Yang, D. L., Kong, Y., Chen, Y., Li, X. Z., Zeng, L. J., et al. (2014). Sugar homeostasis mediated by cell wall invertase GRAIN INCOMPLETE FILLING 1 (GIF1) plays a role in pre-existing and induced defence in rice. *Mol. Plant Pathol.* 15, 161–173. doi: 10.1111/mpp.12078

Swarbrick, P. J., Schulze-Lefert, P., and Scholes, J. D. (2006). Metabolic consequences of susceptibility and resistance (race-specific and broad-spectrum) in barley leaves challenged with powdery mildew. *Plant Cell Environ.* 29, 1061–1076. doi: 10.1111/j.1365-3040.2005.01472.x

Tamoi, M., Tabuchi, T., Demuratani, M., Otori, K., Tanabe, N., Maruta, T., et al. (2010). Point mutation of a plastidic invertase inhibits development of the photosynthetic apparatus and enhances nitrate assimilation in sugar-treated Arabidopsis seedlings. *J. Biol. Chem.* 285, 15399–15407. doi: 10.1074/jbc.M109.055111

Tang, X., Su, T., Han, M., Wei, L., Wang, W., Yu, Z., et al. (2017). Suppression of extracellular invertase inhibitor gene expression improves seed weight in soybean (Glycine max). *J. Exp. Bot.* 68, 469–482. doi: 10.1093/jxb/erw425

Tauzin, A. S., and Giardina, T. (2014). Sucrose and invertases, a part of the plant defense response to the biotic stresses. *Front. Plant Sci.* 5, 293. doi: 10.3389/fpls.2014.00293

Tuskan, G. A., Difazio, S., Jansson, S., Bohlmann, J., Grigoriev, I., Hellsten, U., et al. (2006). The genome of black cottonwood, Populus trichocarpa (Torr. \& Gray). *Science* (80-.), 1596. doi: 10.1126/science.1128691

Van den Ende, W., Lammens, W., Van Laere, A., Schroeven, L., and Le Roy, K. (2009). Donor and acceptor substrate selectivity among plant glycoside hydrolase family 32 enzymes. *FEBS J.* 276, 5788–5798. doi: 10.1111/j.1742-4658.2009.07316.x

Vandesompele, J., De Preter, K., Pattyn, F., Poppe, B., Van Roy, N., De Paepe, A., et al. (2002). Accurate normalization of real-time quantitative RT-PCR data by geometric averaging of multiple internal control genes. *Genome Biol.* 3, 1–12. doi: 10.1186/gb-2002-3-7-research0034

Veillet, F., Gaillard, C., Coutos-Thévenot, P., and La Camera, S. (2016). Targeting the AtCWIN1 gene to explore the role of invertases in sucrose transport in roots and during botrytis cinerea infection. *Front. Plant Sci.* 7, 1899. doi: 10.3389/fpls.2016.01899

Wan, H., Wu, L., Yang, Y., Zhou, G., and Ruan, Y. L. (2018). Evolution of sucrose metabolism: the dichotomy of invertases and beyond. *Trends Plant Sci.* 23, 163–177. doi: 10.1016/j.tplants.2017.11.001

Wang, L., and Ruan, Y.-L. (2012). New insights into roles of cell wall invertase in early seed development revealed by comprehensive spatial and temporal expression patterns of GhCWIN1 in cotton. *Plant Physiol.* 160, 777–787. doi: 10.1104/pp.112.203893

Wang, E., Wang, J., Zhu, X., Hao, W., Wang, L., Li, Q., et al. (2008). Control of rice grain-filling and yield by a gene with a potential signature of domestication. *Nat. Genet.* 40, 1370–1374. doi: 10.1038/ng.220

Wei, T., Wang, Y., Xie, Z., Guo, D., Chen, C., Fan, Q., et al. (2019). Enhanced ROS scavenging and sugar accumulation contribute to drought tolerance of naturally occurring autotetraploids in Poncirus trifoliata. *Plant Biotechnol. J.* 17, 1394–1407. doi: 10.1111/pbi.13064

Weiszmann, J., Fürtauer, L., Weckwerth, W., and Nägele, T. (2018).). Vacuolar sucrose cleavage prevents limitation of cytosolic carbohydrate metabolism and stabilizes photosynthesis under abiotic stress. *FEBS J.* 285, 4082–4098. doi: 10.1111/febs.14656

Wilkins, O., Nahal, H., Foong, J., Provart, N. J., and Campbell, M. M. (2009). Expansion and diversification of the populus R2R3-MYB family of transcription factors. *Plant Physiol.* 149, 981–993. doi: 10.1104/pp.108.132795

Wolf, S., Grsic-Rausch, S., Rausch, T., and Greiner, S. (2003). Identification of pollen-expressed pectin methylesterase inhibitors in Arabidopsis. *FEBS Lett.* 555, 551–555. doi: 10.1016/S0014-5793(03)01344-9

Xiang, L., Le Roy, K., Bolouri-Moghaddam, M.-R., Vanhaecke, M., Lammens, W., Rolland, F., et al. (2011). Exploring the neutral invertase–oxidative stress defence connection in Arabidopsis thaliana. *J. Exp. Bot.* 62, 3849–3862. doi: 10.1093/jxb/err069

Xu, X., Hu, Q., Yang, W., and Jin, Y. (2017). The roles of cell wall invertase inhibitor in regulating chilling tolerance in tomato. *BMC Plant Biol.* 17, 195. doi: 10.1186/s12870-017-1145-9

Yu, X., Wang, X., Zhang, W., Qian, T., Tang, G., Guo, Y., et al. (2008). Antisense suppression of an acid invertase gene (MAI1) in muskmelon alters plant growth and fruit development. *J. Exp. Bot.* 59, 2969–2977. doi: 10.1093/jxb/ern158

Zanor, M. I., Osorio, S., Nunes-Nesi, A., Carrari, F., Lohse, M., Usadel, B., et al. (2009). RNA interference of LIN5 in tomato confirms its role in controlling brix content, uncovers the influence of sugars on the levels of fruit hormones, and demonstrates the Importance of sucrose cleavage for normal fruit development and fertility. *Plant Physiol.* 150, 1204–1218. doi: 10.1104/pp.109.136598

Zhang, J., Wu, Z., Hu, F., Liu, L., Huang, X., Zhao, J., et al. (2018). Aberrant seed development in Litchi chinensis is associated with the impaired expression of cell wall invertase genes. *Hortic. Res.* 5, 39. doi: 10.1038/s41438-018-0042-1

Zhao, H., Greiner, S., Scheffzek, K., Rausch, T., and Wang, G. (2019). A 6&1-FEH encodes an enzyme for fructan degradation and interact with invertase inhibitor protein in maize (Zea mays L.). *Int. J. Mol. Sci.* 20, 3807. doi: 10.3390/ijms20153807

Zhu, X., Gong, H., He, Q., Zeng, Z., Busse, J. S., Jin, W., et al. (2016). Silencing of vacuolar invertase and asparagine synthetase genes and its impact on acrylamide formation of fried potato products. *Plant Biotechnol. J.* 14, 709–718. doi: 10.1111/pbi.12421

Zuma, B., Dana, M. B., and Wang, D. (2018). Prolonged expression of a putative invertase inhibitor in micropylar endosperm suppressed embryo growth in arabidopsis. *Front. Plant Sci.* 9, 61. doi: 10.3389/fpls.2018.00061

Conflict of Interest: The authors declare that the research was conducted in the absence of any commercial or financial relationships that could be construed as a potential conflict of interest.

frontiers in Plant Science

REVIEW
published: 24 January 2020
doi: 10.3389/fpls.2019.01741

Modulation of the Root Microbiome by Plant Molecules: The Basis for Targeted Disease Suppression and Plant Growth Promotion

Alberto Pascale[1†], *Silvia Proietti*[2†], *Iakovos S. Pantelides*[3*] and *Ioannis A. Stringlis*[4*]

[1] Department of Agricultural Sciences, University of Naples Federico II, Naples, Italy, [2] Department of Ecological and Biological Sciences, University of Tuscia, Viterbo, Italy, [3] Department of Agricultural Sciences, Biotechnology and Food Science, Cyprus University of Technology, Limassol, Cyprus, [4] Plant-Microbe Interactions, Department of Biology, Science4Life, Utrecht University, Utrecht, Netherlands

OPEN ACCESS

Edited by:
Paulo José Pereira Lima Teixeira, University of São Paulo, Brazil

Reviewed by:
Ka Wai Ma, Max Planck Institute for Plant Breeding Research, Germany
Kei Hiruma, Nara Institute of Science and Technology (NAIST), Japan

***Correspondence:**
Iakovos S. Pantelides
iakovos.pantelides@cut.ac.cy
Ioannis A. Stringlis
I.Stringlis@uu.nl

[†]These authors share first authorship

Specialty section:
This article was submitted to Plant Microbe Interactions, a section of the journal Frontiers in Plant Science

Received: 30 September 2019
Accepted: 11 December 2019
Published: 24 January 2020

Citation:
Pascale A, Proietti S, Pantelides IS and Stringlis IA (2020) Modulation of the Root Microbiome by Plant Molecules: The Basis for Targeted Disease Suppression and Plant Growth Promotion. Front. Plant Sci. 10:1741. doi: 10.3389/fpls.2019.01741

Plants host a mesmerizing diversity of microbes inside and around their roots, known as the microbiome. The microbiome is composed mostly of fungi, bacteria, oomycetes, and archaea that can be either pathogenic or beneficial for plant health and fitness. To grow healthy, plants need to surveil soil niches around the roots for the detection of pathogenic microbes, and in parallel maximize the services of beneficial microbes in nutrients uptake and growth promotion. Plants employ a palette of mechanisms to modulate their microbiome including structural modifications, the exudation of secondary metabolites and the coordinated action of different defence responses. Here, we review the current understanding on the composition and activity of the root microbiome and how different plant molecules can shape the structure of the root-associated microbial communities. Examples are given on interactions that occur in the rhizosphere between plants and soilborne fungi. We also present some well-established examples of microbiome harnessing to highlight how plants can maximize their fitness by selecting their microbiome. Understanding how plants manipulate their microbiome can aid in the design of next-generation microbial inoculants for targeted disease suppression and enhanced plant growth.

Keywords: plant defense, plant growth promotion, plant molecules, root exudation, root microbiome, microbiota, disease suppression, microbial inoculants

INTRODUCTION

Plants are sessile organisms anchored in the soil by their roots. In terrestrial ecosystems, plants are the main food producers supporting most of the other life. In nature, plants are continuously exposed to various biotic stresses caused by pathogens or pests and adverse environmental conditions, such as drought, soil salinity, extreme temperatures, nutrient deficiencies, or exposure to heavy metals (De Coninck et al., 2015; Antoniou et al., 2017; Hacquard et al., 2017). To survive biotic stresses, plants have evolved an array of sophisticated immune responses which protect plant cells from the challenges they confront (Pieterse et al., 2012; Pieterse et al., 2014). For decades, the interactions between plants and pathogens were studied under the prism of an

individual plant–microbe relationship, ignoring the complexity of such interactions and the involvement of many other groups of microorganisms that affect the outcome of infection (Mendes et al., 2011; Berendsen et al., 2012; Bulgarelli et al., 2013). Over the last years, focus has been diverted to the effect of the plant-associated microbial communities on plant growth and health. Increasing evidence suggests that services provided by plant-associated microorganisms can broaden immune functions of the plant host (Vannier et al., 2019). It has even been postulated that plants actively recruit soil microorganisms by releasing compounds in the rhizosphere that selectively stimulate microorganisms that are beneficial to plant growth and health (Reinhold-Hurek et al., 2015; Sasse et al., 2017). Here, we review the current understanding on the composition and activity of the root-associated microbial communities, and we discuss how different plant molecules can shape the structure of these communities providing also with examples on the interactions between plants and soilborne fungi.

Plants and Microbiome

Game of Biomes: Plants Roots and Their Microbiome

Plants harbor a mesmerizing diversity of microbes both in their aboveground and their belowground tissues that are collectively known as plant microbiota, while the genomes of the microbiota living in close association with plants are commonly referred to as the plant microbiome (Berendsen et al., 2012; Bulgarelli et al., 2013). This review will focus on the interactions of the microbiome with the root, which is the plant organ "hidden" in the soil that mediates key functions for plant longevity and fitness (De Coninck et al., 2015). Some of these functions are the fixation of a plant in a position, the uptake and storage of nutrients and water from the soil and the mediation of the interaction with soil-inhabiting microbes (**Figure 1**). Roots and their surrounding soil constitute one of the most rich and diverse ecosystems on Earth. The grand concentration of microbial life in the thin soil layer surrounding the roots, known as the rhizosphere, is explained by the release of carbon-rich products of photosynthesis which are a vital food source for the attracted microbes (Bais et al., 2006; Sasse et al., 2017). Rhizodeposits are quite diverse and include organic acids, amino acids, sugars, products of secondary metabolism, and even the release of dying root cap border cells (Dakora and Phillips, 2002; Bais et al., 2006; Driouich et al., 2013). Root-derived exudates, apart from supporting microbial proliferation in the rhizosphere, are also responsible for the formation of distinct microbial assemblages between soil and the rhizosphere, a phenomenon described as the "rhizosphere effect" (Hiltner, 1904; Berendsen et al., 2012). The microbes proliferating in the rhizosphere are therefore exposed to plant-derived compounds and signaling molecules

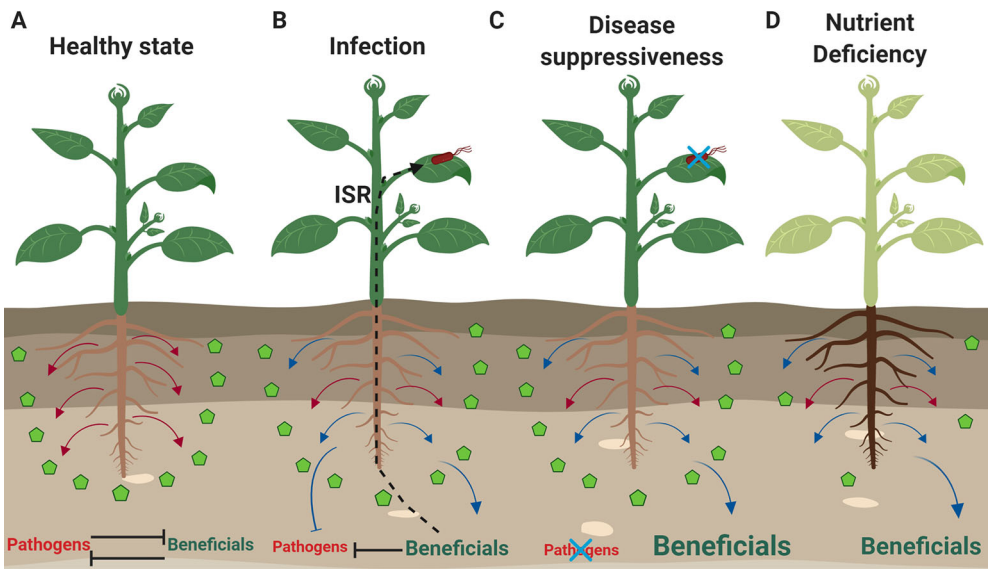

FIGURE 1 | Plants respond to different environmental stresses and modulate their microbiome. **(A)** Plants not experiencing any biotic stress and having access to nutrients (green pentagons), release constitutively exudates (red arrows) that allow them to sustain a balance in the rhizosphere between pathogenic and beneficial microbes. **(B)** Upon infection by a pathogen (red microbe), the exudation profile of roots changes and stress-induced exudates (blue arrows) aid the plants in inhibiting pathogenic growth in the rhizosphere, while selecting at the same time for beneficial microbes. Some of these beneficial microbes when they establish themselves in the rhizosphere, can trigger ISR that can help plants deal with pathogenic infections in the leaves. **(C)** In the case of soil suppressiveness or "cry-for-help" conditions, there is establishment of beneficial rhizosphere communities that are further supported by the release of stress-induced exudates. Under these conditions, soilborne and foliar pathogens fail to cause disease. **(D)** Plants experiencing nutrient deficiencies (e.g. iron, nitrogen, phosphate) change the metabolomic profile of their roots to either make nutrients more available and soluble or to attract beneficial microbes (e.g. rhizobia, AMF, PGPR) that can help them deal with the nutrient deficiency. Font size indicates the abundance of beneficial or pathogenic subsets of the microbiota under different conditions. The figure was designed with Biorender (https://biorender.com).

and represent a subset of the highly complex microbial communities of the bulk soil (Berendsen et al., 2012). A next layer of selection occurs when microbes grow on the root surface (rhizoplane) or inside roots (endosphere) and in turn less diverse microbial communities are observed (Bulgarelli et al., 2013; Reinhold-Hurek et al., 2015; Hacquard et al., 2017). These layers of selection are critical considering that the root-associated microbiota consist of microbes that can assist plants in nutrient assimilation, or enhance their growth and defense potential, but also of microbes that can be detrimental for plant health (Lugtenberg and Kamilova, 2009; Pieterse et al., 2014; De Coninck et al., 2015). Therefore, the maintenance of a balance between plant health and the accommodation of this plethora of microbes in the root rhizosphere requires a coordination of complex processes in the rhizosphere where all partners benefit (Zamioudis and Pieterse, 2012).

The Identity of Root-Associated Microbiomes

The last decade several studies unearthed the composition of root-associated microbial communities. Most of these studies employed next-generation sequencing of microbial marker genes like 16S rRNA for bacteria and the nuclear ribosomal internal transcribed spacer (ITS) region for fungi (Claesson et al., 2010; Schoch et al., 2012) which is known as amplicon sequencing (Sharpton, 2014), while others used shotgun metagenomics sequencing where not only selected microbial marker genes but all DNA present in an environmental sample is sequenced (Sessitsch et al., 2012; Ofek-Lalzar et al., 2014; Bai et al., 2015; Bulgarelli et al., 2015; Stringlis et al., 2018b). The latter approach allows not only for the taxonomic profiling of the root-associated microbial communities but also for the functional characterization of the microbiome (Sharpton, 2014). These culture-independent methodologies allowed the characterization of the microbiota in both the rhizosphere but also in the endosphere of different plant species. In the case of bacteria, analysis at phylum level revealed that the microbiota of healthy *Arabidopsis thaliana* (hereafter Arabidopsis) plants originates from the more diverse soil communities, and is dominated by the phyla Proteobacteria, Actinobacteria, Bacteroidetes and less by Firmicutes (Bulgarelli et al., 2012; Lundberg et al., 2012). Similarly, the root microbiome of closely related species belonging to the Brassicaceae family (*Cardamine hirsuta*, *Arabidopsis halleri*, *Arabidopsis lyrata* and *Arabis alpina*) display quite similar root microbial assemblages with those of Arabidopsis (Schlaeppi et al., 2014; Dombrowski et al., 2017). In plant species not related to Arabidopsis, such as barley, citrus, rice, *Lotus japonicus*, poplar, sugarcane, and tomato, the phyla Proteobacteria, Actinobacteria, Bacteroidetes, and Firmicutes constitute the highest proportion among the identified bacteria (Bulgarelli et al., 2015; Edwards et al., 2015; De Souza et al., 2016; Zgadzaj et al., 2016; Beckers et al., 2017; Zhang et al., 2017; Kwak et al., 2018). For fungal communities, studies in Arabidopsis, *Arabis alpina*, poplar, and sugarcane have shown that mostly the phyla Ascomycota, Basidiomycota and less Zygomycota, and Glomeromycota dominate the root microbiota of their host plants (Shakya et al., 2013; De Souza et al., 2016; Almario et al., 2017; Robbins et al., 2018; Bergelson et al., 2019). The high representation of selected bacterial and fungal phyla in roots and rhizospheres of different hosts suggests that members of these phyla constitute competitive and adaptable colonizers under various soil types and locations (Muller et al., 2016). Indeed, sequencing of microbiome DNA and RNA from the rhizosphere and the root of *Brassica napus* and citrus demonstrated that phyla Proteobacteria, Actinobacteria, Acidobacteria and Bacteroidetes are really active in the root and the rhizosphere and assimilate most of the carbon released by the roots (Gkarmiri et al., 2017; Zhang et al., 2017). Metatranscriptomics, functional studies or labelling of carbon absorption revealed that overrepresentation of specific fungal phyla in the rhizosphere correlates with their increased activity around the roots or services they provide to the host plants (Vandenkoornhuyse et al., 2007; Turner et al., 2013; Almario et al., 2017; Gonzalez et al., 2018).

Interactions of Plants With Beneficial and Pathogenic Microbes

Beneficial Associations With Plants

Symbiotic Plant-Microbe Associations. Research has unearthed that intimate interactions of plants with beneficial microbes first occurred millions of years ago. The first land plants were colonized by ancestral filamentous fungi that facilitated water absorption and nutrient acquisition for the host plant, while fungi received back photosynthetically-fixed carbon (Field et al., 2015; Martin et al., 2017). This symbiotic association coevolved in such a successful direction since more than 90% of living plant species form symbioses with mycorrhizal fungi, of which about 80% are classified as arbuscular mycorrhizal fungi (AMF) (Parniske, 2008; Bonfante and Genre, 2010). As obligate biotrophs, AMF need to sense the presence of the host plants to complete their lifecycle. The root-exuded plant hormone strigolactone has been recognized as the stimulatory signal for AMF mycelium metabolism and branching and its concentration gradient from the roots reveal the proximity to the host plant (Parniske, 2008; Bonfante and Genre, 2010). Intriguingly, AMF signaling pathways are very similar to the one that coordinates the well-known symbiosis between the paraphyletic group of rhizobial bacteria and leguminous plants and are therefore named common signaling symbiotic pathways (CSSPs) (Maclean et al., 2017; Martin et al., 2017). In rhizobia, the symbiotic association begins with the perception of specific root-exuded iso-flavonoid compounds by the microbes that stimulates root nodule formation (Begum et al., 2001; Oldroyd, 2013; Poole et al., 2018). Once symbiosis is established there is continuous exchange of nutrients between the host plant and the microbes. AMF can uptake the consistently low water-soluble inorganic orthophosphate (Pi) from soils and transport Pi through the extraradical mycelium network and fungal arbuscules inside the root. AMF can also uptake and transport other major nutrients; for example nitrogen is transferred in the forms of nitrate, ammonium, and amino acids inside plants by using specialized transporters (Parniske, 2008; Bonfante and Genre, 2010; Maclean et al., 2017). In exchange, AMF receive the entire carbon

requirements from plants, through specific fungal hexose transporters and fatty acids (Jiang et al., 2017; Maclean et al., 2017). In rhizobia-leguminous plants symbiosis, rhizobia reduce atmospheric N_2 to ammonia inside the root nodules and secrete it to plants, while plants provide rhizobia with dicarboxylates (Poole et al., 2018).

Nutrient Uptake and Growth Promotion by Beneficial Microbes. Plants can acquire nutrients even in the absence of symbiosis with AMF or rhizobia. Enhanced nutrient acquisition in plants is a very common mechanism of phytostimulation (Lugtenberg and Kamilova, 2009; Finkel et al., 2017; Jacoby et al., 2017; Verbon et al., 2017) and a wide array of microbes can accomplish this function in non-mycorrhizal plants (Almario et al., 2017; Castrillo et al., 2017; Fabianska et al., 2019). The non-host plant Arabidopsis acquires Pi through its natural root endophytic symbiont *Colletotrichum tofieldiae* (Hiruma et al., 2016). Hiruma and colleagues (2016) demonstrated that Pi translocation is the main plant growth promotion mechanism provided by *C. tofieldiae* and this mechanism is governed by the plant phosphate starvation status and requires intact immune system of the plant. Endophytic fungi belonging to the order of Sebacinales, such as *Serendipita indica* (formerly known as *Piriformospora indica*) can also promote plant growth through Pi acquisition (Yadav et al., 2010; Weiss et al., 2016). Similarly, *Trichoderma* fungi can produce chelating metabolites that solubilize phosphate and increase its acquisition by plants to promote plant growth (Altomare et al., 1999; De Jaeger et al., 2011). Nitrogen acquisition is mediated on non-leguminous plants by other microbes which are not belonging in the N-fixing bacteria group (Jacoby et al., 2017; Martin et al., 2017). Evidence also accumulates that during root colonization selected beneficial microbes can hijack the iron deficiency response of plants. In this case, following bacterial colonization there is induction of the expression of genes with a role in iron uptake, and these genes are commonly used by plants to mobilize and uptake iron, when this element is present in unavailable forms in the soil (Zamioudis et al., 2015; Zhou et al., 2016; Martinez-Medina et al., 2017; Verbon et al., 2017).

Beneficial microbes can promote plant growth by affecting the hormonal balance of plants. This beneficial effect can be induced by the secretion of microbial small secondary metabolites (SM) that can act as hormone-like plant growth regulators, or by the production of SM and proteins that enable microbes to modulate the signaling of plant defense hormones to successfully colonize plant tissues (Verbon and Liberman, 2016; Patkar and Naqvi, 2017; Manganiello et al., 2018; Stringlis et al., 2018c). Numerous microbial species among plant associated bacteria and fungi can produce indole-3-acetic acid (IAA) or auxin-mimicking molecules that play a direct role on plant growth and development (Duca et al., 2014; Garnica-Vergara et al., 2016). Other microbial phytohormones or phytohormone-like molecules, such as cytokinins, gibberellins and analogues of defense-related hormones, such as salicylic acid (SA) or jasmonic acid (JA)-isoleucine are mainly produced to facilitate microbial colonization through modulation of plant immunity (Schafer et al., 2009; Stringlis et al., 2018c). Moreover, many plant beneficial microorganisms produce 1-aminocyclopropane-1-carboxylate (ACC) deaminase that cleaves ACC, the immediate biosynthetic precursor of ethylene (ET) in plants, and promote plant growth presumably by lowering plant ET which can reach inhibitory levels for plant growth when subjected to stress conditions (Viterbo et al., 2010; Brotman et al., 2013; Glick, 2014; Stringlis et al., 2018c).

Induced Systemic Resistance. Another well-studied mechanism of elevated plant defense potential is the so-called induced systemic resistance (ISR) which is triggered by beneficial members of the root microbiome to a wide range of plant hosts making them resistant against various pathogenic threats (Pieterse et al., 2014). Systemic activation of plant defenses is ensured by a complex network of defense-related hormone signaling pathways, which brings the message of a beneficial interaction, in different plants organs (Pieterse et al., 2009; Pieterse et al., 2014). The ISR phenomenon has been firstly described for bacteria of the genus *Pseudomonas,* and this mechanism has been distinguished from "systemic acquired resistance" (SAR) which is induced by pathogens (Pieterse et al., 2014). ISR has also been described for many plant growth-promoting bacteria (PGPR) of the genus *Bacillus* and *Serratia* and plant growth-promoting fungi (PGPF) of the genus *Trichoderma, Fusarium, Serendipita* and AMF (Harman et al., 2004; Kloepper et al., 2004; Shoresh et al., 2010; Jung et al., 2012; Pieterse et al., 2014) and is determined by the perception of microbial secreted SM (Ongena and Jacques, 2008; Raaijmakers et al., 2010; Manganiello et al., 2018; Stringlis et al., 2018c). Interestingly, ISR is characterized by the activation of defense responses only after pathogen attack, saving the plant from a great energy consumption. This mechanism of "upon attack" defense activation is known as priming and is an energy-saving evolutionary strategy that allows plants to silently alert their immune system until a challenge by pathogens or insects occurs. Following this challenge, plants will deploy all the cellular responses faster and/or stronger resulting in a more efficient and effective resistance (Pieterse et al., 2014; Martinez-Medina et al., 2016).

All the beneficial associations presented above are based on the interaction between the host plant and a single beneficial microbe. Modern holistic approaches aim to correlate plant health to the entire plant-associated microbial community. In this case, microbial genes are considered as an extension of the plant genetic repertoire and perform specific functions benefiting plant growth, reproduction and disease resistance (Vandenkoornhuyse et al., 2015; Hassani et al., 2018). Community level-based metagenomic studies can elucidate whether there is functional redundancy or overlapping genomic traits in most microbes promoting plant growth or inducing systemic resistance, enabling in this way the discovery of novel PGPR or PGPF (Lugtenberg and Kamilova, 2009; Pieterse et al., 2014; Bai et al., 2015; Zeilinger et al., 2016; Berendsen et al., 2018; Duran et al., 2018).

Plant-Pathogen Interactions

During plant life, roots support beneficial associations with soil-inhabiting microbes but need to cope at the same time with the

infections caused by pathogenic microorganisms. Soilborne pathogens can affect hundreds of plant species, including economically important crops, and cause significant monetary losses due to significant reduction in yield and quality. For many crops, losses are estimated at 10%–20% of the attainable yield (Pimentel et al., 1991; Okubara and Paulitz, 2005; De Coninck et al., 2015). However, crop losses are often underestimated as soilborne pathogens are not an immediate concern for growers and their practices in many cases lead to increased inoculum reservoirs in soils (Chellemi et al., 2016). Also, their economic importance is expected to significantly rise due to the increasing implementation of conservation tillage or no-till farming practices in many countries (De Coninck et al., 2015) and the climate change that can increase their geographical range on Earth (Cheng et al., 2019). Soilborne pathogens reside in the soil for short or extended periods, and survive as saprophytes on plant residues and organic matter or as resting structures (e.g. sclerotia, chlamydospores, oospores, melanized mycelia) until triggered to grow by root exudates (Bruehl, 1987; Bais et al., 2006; De Coninck et al., 2015). For example, phenolic acids, sugars, and free amino acids in root exudates from watermelon significantly increased spore germination and sporulation of *F. oxysporum* f. sp. *niveum* (Hao et al., 2010). Similarly, tomato root exudates stimulated microconidia germination of the tomato pathogens *F. oxysporum* f. sp. *lycopersici* and *F. oxysporum* f. sp. *radicis-lycopersici* and the level of stimulation was affected by plant age (Steinkellner et al., 2005). Moreover, root exudates can be detected by fungal pathogens enabling fungal hyphae to orient their growth towards the root. For example, the chemotropic response of *F. oxysporum* towards tomato roots was recently characterized and involves the catalytic activity of root-secreted class III peroxidases (Turrà et al., 2015). Under favorable environmental conditions, soilborne pathogens invade plants through the root system and in most cases roots and other belowground parts are directly affected; however, symptoms are often visible on above ground parts of plants (Koike et al., 2003). Plants infected by soilborne pathogens suffer from root rots, inhibition of root development, stunted growth, seedling damping-off, stem and collar rots, wilting or even plant death (De Coninck et al., 2015; Katan, 2017). Diseases caused by soilborne plant pathogens are notoriously difficult to control for several reasons: many soilborne pathogens produce persistent resting structures that can survive in the soil for many years even in the absence of a susceptible host (Katan, 2017); measures targeting resting structures (e.g. chemical fumigation) are unsuitable for large-scale application due to public health and environmental issues and ban on chemical fumigants (Yadeta and Thomma, 2013); application of pesticides is often insufficient because of the poor accessibility in soil matrix (De Coninck et al., 2015); some of the soilborne pathogens infect a wide range of host plants rendering cultural control measures ineffective (Antoniou et al., 2017). Moreover, in order to establish a parasitic relationship with the plants, pathogens must interact with the complex rhizosphere community that also influences the outcome of the infection (Raaijmakers et al., 2009). Pathogens are negatively affected by co-inhabiting microorganisms through antibiosis and competition for nutrients, processes that usually involve secreted molecules. Snelders et al. (2018) proposed that pathogens can fight back by delivering effector proteins which target the rhizosphere communities instead of the plant to ultimately facilitate host colonization by the pathogen. Soilborne pathogens include species of fungi, oomycetes, bacteria, viruses and nematodes (Katan, 2017). The most important soilborne fungal pathogens are *Fusarium oxysporum* (Michielse and Rep, 2009), *Fusarium solani* (Coleman, 2016), *Rhizoctonia solani* (Gonzalez et al., 2011), *Verticillium* spp. (Klosterman et al., 2009), and *Sclerotinia sclerotiorum* (Bolton et al., 2006) and destructive soilborne oomycetes are *Phytophthora* spp. (Van West et al., 2003; Lamour et al., 2012) and *Pythium* spp. (Van West et al., 2003). Among many soil bacteria that are beneficial, there are only a few groups that infect the plant roots. Examples are *Ralstonia solanacearum* (Peeters et al., 2013) and the causal agent of crown gall *Agrobacterium tumefaciens* (Anand et al., 2008) that require a natural opening or wound to penetrate into the plant and cause infection. Only a small number of viruses can infect roots and like bacteria, they require an opening to achieve penetration. They generally survive only in the living tissues of the host plant or in their vectors. In soil, viruses are transmitted by zoosporic fungi (Campbell, 1996) or by nematodes (Brown et al., 1995).

How Do Plants Select Microbes and Defend Against Pathogens

Effect of Root Exudates on Root-Associated Microbiome

Plants produce and exude *via* their roots various metabolites that can affect the assembly of the root microbiome before even microbes reach the root surface where they confront with the plant immune system (Sasse et al., 2017). The age and developmental stage of the plant influence exudation and subsequently the microbes proliferating around roots. Exudates of Arabidopsis plants collected at different plant age varied in sugar levels which affected accordingly microbial functions related with sugar and secondary metabolism (Chaparro et al., 2013). It was also shown that Arabidopsis plants during the early and late stage of their development can influence the abundance of Actinobacteria, Bacteroidetes and Cyanobacteria and microbial activity as well (Chaparro et al., 2014). Functions aligning with pathogens were more represented at early developmental stages while later developmental stages were dominated by functions related with antibiosis and chemotaxis and aligned to beneficial microbes, suggesting a selective pressure during plant aging towards microbes that provide their hosts with important services. In this direction, a recent study elegantly demonstrated that exudates change during the growth cycle of *Avena barbata* with sucrose levels are high at earlier stages while amino acids and defense molecules are released more at later developmental stages (Zhalnina et al., 2018). Using exometabolomics, this study showed that selected metabolites including aromatic organic acids (nicotinic, shikimic, salicylic,

cinnamic, and IAA) are responsible for the proliferation or not of specific microbes around the roots during the different growth stages of the host plant (Zhalnina et al., 2018).

Different rhizodeposits have been shown to influence the microbiome composition. Studies on how plants select root-associated microbes/microbiota are summarized in **Table 1**. Biosynthesis of aliphatic and indolic glucosinolates, that are components of the chemical defense of plants, occurs in the vascular stele (Xu et al., 2017). Early studies demonstrated that root exudation of aliphatic glucosinolates can affect the rhizospheric microbial communities (Bressan et al., 2009), while indolic glucosinolates accumulate in Arabidopsis root upon pathogen infection (Bednarek et al., 2005). Combinations of exudates collected from Arabidopsis plants growing *in vitro* and applied in soil in the absence of plants revealed differential effects of phenolic compounds on the abundance of bacterial taxa (Badri et al., 2013). More specifically, phenolics seemed to have the biggest effect on the growth and attraction of bacterial operational taxonomic units (OTUs), followed by amino acids and sugars. A role of phenolics in affecting soil microbial diversity was also demonstrated with an Arabidopsis ABC transporter mutant (*abcg30*) which releases more phenolics but shows a reduced export of sugars (Badri et al., 2009). In soil in which *abcg30* plants were grown, an increased abundance of PGPR or bacteria involved in heavy metal remediation was observed compared to wild type Col-0 plants, suggesting a role for phenolics in attracting beneficial microbes. More recent studies suggested that coumarins, which are also phenolic compounds, can shape the rhizosphere microbiome and display differential toxicity against beneficial and pathogenic microbes (Stringlis et al., 2018b; Stringlis et al., 2019a; Voges et al., 2019). Next to phenolics, more chemical players have been found to contribute in the balance between roots and the microbiome, including benzoxazinoids (Hu et al., 2018; Cotton et al., 2019), triterpenes (Huang et al., 2019), and camalexin (Koprivova et al., 2019). Other naturally occurring exudates, like flavonoids and strigolactones, act as signaling compounds for the establishment of well-characterized symbiotic interactions of plant hosts with rhizobia and AMF (Akiyama et al., 2005; Subramanian et al., 2007). Moreover, border cells and border-like cells that are forming an extra root layer between the root tip and soil have been shown to affect a group of soilborne bacteria, because of proteins synthesized and released through them (Driouich et al., 2013). Arabinogalactan proteins were identified among the secreted molecules and were found to regulate *Rhizobium* and *Agrobacterium* attachment on roots (Gaspar et al., 2004; Vicre et al., 2005; Xie et al., 2012). Different parts of the root can release a different blend of exudates that can favor the colonization by selected members of the microbiome (Baetz and Martinoia, 2014). Studies using modern techniques like microfluidics and bacterial biosensors responsive to selected root exudates have revealed the preferential colonization of the root elongation zone and of lateral roots by bacteria of the genera *Bacillus* and *Rhizobium* (Massalha et al., 2017; Pini et al., 2017).

Structural Root Defenses and Microbiome

Plants have developed various ways to restrict microbial growth and colonization on plant tissues, once microbes overcome niche competition with other microbes in the rhizosphere and can successfully grow in root exudates. In leaves, an armory of structural and chemical defense mechanisms have evolved to prevent disease caused by colonization of harmful microbes inside plant tissues (Senthil-Kumar and Mysore, 2013). These structural defense components include the cuticle, lignin, suberin and deposition of callose and are also present in the roots. Roots are plant organs characterized by radial organization where each concentric layer corresponds to a different tissue (Wachsman et al., 2015). Lignin fortifies the xylem of *Arabidopsis* roots (Van De Mortel et al., 2008; Naseer et al., 2012) and going outwards from the root core, lignin-composed Casparian strips (CS) and the hydrophobic polymer suberin make the endodermis a barrier between the xylem and the soil (Naseer et al., 2012; Geldner, 2013). Recognition of microbes or of microbial elicitors can induce callose deposition in the epidermal cells of the root (Millet et al., 2010; Jacobs et al., 2011; Hiruma et al., 2016). Finally, cutin as a waxy polymer of the cuticle coating the epidermis, has barrier-like properties like suberin and is present in the primary and lateral roots (Berhin et al., 2019). Evidence suggests that plant defense components exert some selective pressure on the microbes that can colonize the inner tissues of the root. The first seminal studies on the root microbiome field demonstrated that the endosphere microbiota is a fraction of the rhizosphere microbiota, and structural defense components might have a role in this observation (Bulgarelli et al., 2012; Lundberg et al., 2012). Other structural modifications of the root system like emergence of lateral roots or formation of root hairs might be involved in creating micro-niches that host distinct subsets of the root microbiota. A study in barley comparing wild type and mutant plants for root hair formation revealed that the microbial community in root hair mutants was simpler and less diverse compared to the microbial communities assembled in the roots of wild type barley plants (Robertson-Albertyn et al., 2017). Despite the presence of structural defense components in roots and their dynamic contribution in plant growth, information on their role in the assembly of the root microbiome is still limited.

Interplay Between Plant Immunity and the Microbiome

Root Immune System

As already mentioned in this review, soil microbial populations consist of a mix of beneficial and pathogenic microbes. Hence, plants need to successfully recognize them and subsequently reprogram their defense strategies to allow or block their colonization (Zamioudis and Pieterse, 2012; Yu et al., 2019a). To effectively and timely perceive microbial signals, plants have evolved a multilayered detection system that leads, depending on the trigger, to the activation of downstream defense responses (Dodds and Rathjen, 2010). In the first layer of this defense system, surface-localized pattern recognition receptors (PRRs)

TABLE 1 | Representative studies where plants under different stresses can select/modulate the assembly of the root-associated microbiome. For each study (when possible) the trigger leading to plant activity that modulates the microbiome, the identified mechanism of action, the effect on the microbiome, the host plant and the reference is mentioned.

Trigger	Mechanisms	Effect	Host	Reference
Pathogen-triggered				
Fusarium oxysporum f. sp. *lycopersici*	Disease -induced recruitment from suppressive compost	Enrichment of Proteobacteria, Actinobacteria, and Firmicutes (*Bacillus*)	Tomato	Antoniou et al., 2017
Hyaloperonospora arabidopsidis/ *Pseudomonas syringae* pv. *tomato*	Legacy-mediated development of soil suppressiveness	Assemblage of beneficial rhizosphere microbiome	Arabidopsis/ Tomato	Berendsen et al., 2018/ Yuan et al., 2018
Rhizoctonia solani	Activation of bacterial stress responses and activation of antagonistic traits that restrict pathogen infection	Shifts in microbiome composition and enrichment of *Oxalobacteraceae*, *Burkholderiaceae*, *Sphingobacteriaceae,* and *Sphingomonadaceae*	Sugar beet	Chapelle et al., 2016
Botrytis cinerea	Chemoattraction induced by root-exuded peroxidases and oxylipins	Attraction of *Trichoderma harzianum and* inhibition of *Fusarium oxysporum*	Tomato; Cucumber	Lombardi et al., 2018
Rhizoctonia solani	Pathogen-induced taxa enrichment from suppressive soils	Recruitment of specific taxa from rhizosphere of sugar beet infected with *Rhizoctonia solani*	Sugar beet	Mendes et al., 2011
Pseudomonas syringae pv. *tomato*	Root-secreted malic acid	Recruitment of *Bacillus subtilis* FB17	Arabidopsis	Rudrappa et al., 2008
Fusarium oxysporum f. sp. *lini*	Disease-induced recruitment of beneficial microbes from *Fusarium* suppressive soils	Increase of taxa associated to Fusarium wilt suppressiveness	Flax	Siegel-Hertz et al., 2018
Huanglongbing (HLB) caused by *Candidatus Liberibacter* spp.	Putative mechanisms: HLB significantly altered the structure or functional potential of the citrus endosphere	Decrease in abundance of taxa and loss of functions in the rhizoplane-rhizosphere enriched microbiome of HLB- infected citrus roots	Citrus	Zhang et al., 2017
Insects-triggered				
Aphids	Elicitation of plant immunity *via* SA/JA systemic signaling and expression of pathogenesis-related (PR) proteins in roots	Recruitment of the beneficial bacteria *Bacillus subtilis* and decrease of the population of *Ralstonia solanacearum*	Pepper	Lee et al., 2012
Whitefly	Whitefly infestation elicited SA and JA signaling in above and below ground tissues and overexpression of PR genes in the roots resulting in a differential microbiome assembly	The differential microbiome assembly induced resistance against to *Xanthomonas axonopodis* pv. *vesicatoria* and *Ralstonia solanacearum*	Pepper	Yang et al., 2011
Abiotic stress/nutrient deficiency-triggered				
Phosphate deficiency	Phosphate starvation response *via* PHR1 and PHL1 and PHO2	Differential assemblage of bacterial and fungal microbiota	Arabidopsis	Castrillo et al., 2017/ Fabianska et al., 2019
Gradients of phosphate, salinity, pH, temperature	-	Assembly of different modules of co-occurring strains	Arabidopsis	Finkel et al., 2019
wounding; salt stress	Chemoattraction induced by root-exuded peroxidases and oxylipins	Exudates attracted *Trichoderma harzianum* and showed deterrent activity against *Fusarium oxysporum*	Tomato; Cucumber	Lombardi et al., 2018
Iron deficiency/ colonization by PGPR	Increased accumulation and secretion of the coumarin scopoletin exerts selective antimicrobial activity in rhizosphere	Differential microbiome assembly, repelling potential against phytopathogens and thus, recruiting potential beneficial microbes	Arabidopsis	Stringlis et al., 2018b
Iron deficiency	Catecholic coumarins show differential antimicrobial activity	Shift in microbial composition of SynCom *in vitro*	Arabidopsis	Voges et al., 2019
Endogenous/exogenous plant-derived molecules-triggered				
-	Overexpression of genes involved biosynthesis and transport of root-exuded secondary metabolites	Greater abundance of potentially beneficial bacteria	Arabidopsis	Badri et al., 2009
-	Differential exudation of root secondary metabolites regulated by Benzoxazinoids (BXs)	Enrichment of *Methylophilaceae, Nitrosomonadaceae, Oxalobactereraceae, Syntrophobacteriaceae,* and *Gaiellaceae*	Maize	Cotton et al., 2019
-	Benzoxazinoids (BXs) drive plant-soil feedback	BXs shape the microbiota of the next generation of plants	Maize	Hu et al., 2018
-	Differential secretion of triterpene-derived metabolites by altering triterpene gene cluster	Differential assembly of Arabidopsis root microbiome	Arabidopsis	Huang et al., 2019

(Continued)

TABLE 1 | Continued

Trigger	Mechanisms	Effect	Host	Reference
Pathogen-triggered				
-	Microbial sulfatase cleaves root-exuded sulfate esters produced by the camalexin biosynthetic pathway	Stimulation of microbial sulfatase activity in soil and is required for the plant growth-promoting effects of several bacterial strains	Arabidopsis	Koprivova et al., 2019
-	Assembly of differential microbiome between tomato cultivars susceptible and resistant to *Ralstonia solanacearum*	Enrichment of *Flavobacterium* in the microbiome of tomato cultivars resistant to *Ralstonia*, *Flavobacterium* application confers resistance to susceptible cultivar	Tomato	Kwak et al., 2018
SA	Compromised innate immune system impairing SA biosynthetic pathway	SA-dependent modulation of root microbiome and enrichment of *Flavobacterium*, *Terracoccus,* and *Streptomyces* in SA-treated roots and bulk soils	Arabidopsis	Lebeis et al., 2015
-	DIMBOA Benzoxazinoids (BXs) induce chemotaxis-associated genes in *Pseudomonas putida*	Enhanced rhizosphere colonization by *P. putida*	Maize	Neal et al., 2012
ACC; JA	ACC and JA application, induced altered expression of PRR and RLK and cell wall biosynthesis and maintenance related genes	Inhibition of the secondary stage of root colonization by *Laccaria bicolor*	Poplar	Plett et al., 2014b

perceive conserved microbe-derived molecules, called microbe-associated molecular patterns (MAMPs). In Arabidopsis, some MAMP/PRR pairs are well defined (Couto and Zipfel, 2016). Bacterial flagellin and the immunogenic epitope of flagellin flg22 are perceived by receptor kinase FLAGELLIN-SENSING 2 (FLS2) (Gomez-Gomez and Boller, 2000), while ELONGATION FACTOR-TU RECEPTOR (EFR) recognizes bacterial elongation factor Tu and its derived immunogenic peptide elf18 (Kunze et al., 2004). Additionally, CHITIN ELICITOR RECEPTOR KINASE 1 (CERK1) and LYSIN MOTIF CONTAINING RECEPTOR-LIKE KINASE 5 (LYK5) recognize hepta- or octamers of the fungal elicitor chitin (Miya et al., 2007; Cao et al., 2014). The recognition of a MAMP leads to the induction of immune responses in the host plant that constitute the first layer of defense referred to as MAMP-triggered immunity (MTI). Based on their timing, the activated immune responses range from instant [medium alkalization, oxidative burst (ROS), protein phosphorylation] and early (ethylene biosynthesis, defense gene activation) to late (callose deposition and growth inhibition) (Boller and Felix, 2009). All these processes aim to halt any further growth of a microbe on/in plant tissues and have been elucidated by the extensive study of pathogen perception in the aerial plant tissues. During the last decade, many studies have shown that roots can perceive MAMPs and generate MAMP-specific responses such as callose deposition, camalexin biosynthesis, and induction of defence-related genes similar to leaves (Millet et al., 2010; Jacobs et al., 2011; Wyrsch et al., 2015; Poncini et al., 2017; Stringlis et al., 2018a; Marhavy et al., 2019). Constitutive activation of PRRs in microbe- and elicitor-enriched environments like roots and the surrounding rhizosphere could result in unnecessary MTI that in turn could cause growth and yield inhibition of plants (Gomez-Gomez et al., 1999; Vos et al., 2013). For this, different researchers aimed to define the involvement of different plant organs in flg22 perception by its receptor FLS2 (Beck et al., 2014) and the contribution of different root tissues in the induction of MTI upon flg22 elicitation (Wyrsch et al., 2015). Interestingly, inner tissues show higher expression of the FLS2 receptor and stronger MAMP responses (ROS production and induction of defense genes) compared to epidermal tissues. However, it's not only the plant side that adapts to the presence of MAMPs, but the microbes themselves adapt to the presence of PRRs. Only a small fraction of the genomes of the culturable microbiome of Arabidopsis (3%–6%) contains genes coding for flg22 or elf18 peptides, while the peptide cold shock protein 22 (csp22) recognized by Solanaceae and not by Arabidopsis is present in 25% of the isolated Arabidopsis-associated microbes (Wang et al., 2016; Hacquard et al., 2017). This suggests that the presence of PRRs in roots exerts a selective pressure on the root-associated microbes that need to develop mechanisms to mask the presence of their MAMPs and achieve colonization. Some PRRs can also identify "self" molecules known as host-derived damage-associated molecular patterns (DAMPs). In response to cellular rupture by nematodes or fungal attack, DAMPs are released and can induce strong tissue specific responses in the roots of Arabidopsis (Poncini et al., 2017; Marhavy et al., 2019). Considering the potential of DAMPs to induce stronger defense responses in the roots compared to MAMPs (Poncini et al., 2017), their role in the assembly of the root microbiome and on how plants discriminate between beneficial and pathogenic root colonizers should be expected.

Suppression of Root Defenses by Beneficial Microbes. Signaling pathways of defense hormones SA and JA have been long-involved in responses of plants to infection by pathogens or colonization by beneficial microbes (Pieterse et al., 2012; Zamioudis and Pieterse, 2012; Pieterse et al., 2014) and studies using mutants for these hormonal pathways have demonstrated their role in shaping the root microbiome (Carvalhais et al., 2015; Lebeis et al., 2015). Beneficial members of the root microbiota have developed different strategies to suppress MTI and/or manipulate the homeostasis of defense hormones to achieve colonization and provide their host with benefits (Zamioudis and Pieterse, 2012; Yu et al., 2019a). Symbiotic mycorrhizal and ectomycorrhizal fungi *Rhizophagus irregularis* and *Laccaria bicolor* secrete mutualism

effectors that manipulate ET and JA hormonal signaling pathways (Kloppholz et al., 2011; Plett et al., 2011; Plett et al., 2014a; Plett et al., 2014b), while effectors of endophytic fungus *Serendipita indica* target JA signaling to achieve defense suppression (Jacobs et al., 2011; Akum et al., 2015). JA signaling is also upregulated by PGPF *Trichoderma* spp. to suppress activation of immune responses during early colonization of the root (Brotman et al., 2013). Beneficial bacteria employ different strategies to manipulate the host and accomplish colonization. The type III secretion system (T3SS) is important in the establishment of symbiosis between rhizobia and their legume partners (Zamioudis and Pieterse, 2012). T3SS is a multicomponent apparatus that Gram negative bacteria, mostly pathogenic, use to secrete effector molecules into host cells aiming to restrict the defense responses mounted due to their recognition and achieve host colonization (Galan and Collmer, 1999). *Sinorhizobium fredii* HH103 with defective T3SS is unable to suppress SA-dependent defenses and subsequently fails to promote nodulation on its legume host (Jimenez-Guerrero et al., 2015). Non-symbiotic PGPR such as *Pseudomonas fluorescens* SBW25, *Pseudomonas brassicacearum* Q8r1-96 and *Pseudomonas simiae* WCS417 and other root-associated Pseudomonads, are also equipped with T3SS, however its role in root colonization remains elusive (Preston et al., 2001; Mavrodi et al., 2011; Loper et al., 2012; Berendsen et al., 2015; Stringlis et al., 2019b). Nevertheless, beneficial microbes can employ other mechanisms independent of secretion systems to mask their presence in the rhizosphere. Pathogenic bacteria *Pseudomonas aeruginosa* and *Pseudomonas syringae* release the extracellular alkaline protease AprA which degrades flagellin monomers, and allows microbes to have their MAMPs undetected by the immune system of both mammals and plants (Bardoel et al., 2011; Pel et al., 2014). Plant-beneficial bacteria have AprA homologs in their genomes so a role of this protease in their interaction with roots is possible (Pel et al., 2014). More recently, Yu et al. (2019b) suggested another mode of plant manipulation where beneficial rhizobacteria of the genus *Pseudomonas* spp. produce organic acids during root colonization that lower the environmental pH and in turn suppress root immune responses following recognition of the flg22 peptide.

Phenomena Where Selection Occurs

Building Up of Disease Suppressiveness

Soil microbial communities provide silently their valuable services in terrestrial ecosystems by increasing ecosystem resilience, making soil more resistant to any disturbance-induced damages due to environmental changes (Berendsen et al., 2012). Disease suppression is a well-known microbiome-mediated phenomenon that provides a first line of defense against infections by the soilborne pathogens (Weller et al., 2002). Disease suppressive soils have been originally defined as "soils in which the pathogen does not establish or persist, establishes but causes little or no damage, or establishes and causes disease for a while but thereafter the disease is less important, although the pathogen may persist in the soils" (Baker and Cook, 1974). In contrast, in conducive soils the disease occurs readily. Two types of soil suppressiveness have been characterized: "general" and "specific" suppression. In general suppression, growth and activity of pathogens are inhibited to some extent and the suppressiveness is attributed to the antagonistic activity of the collective microbial community that is often associated with competition for available resources (Mazzola, 2002; Weller et al., 2002; Cook, 2014). General suppressiveness is enhanced by the incorporation of organic amendments or other management practices that increase the total microbial activity and competition in the soil (Weller et al., 2002; Bonanomi et al., 2010). It is often effective against a broad range of pathogens and is not transferable between soils (Cook and Rovira, 1976; Weller et al., 2002). General suppressiveness is a pre-existing characteristic of soils and is fundamentally microbiological in nature (Weller et al., 2002; Raaijmakers and Mazzola, 2016). Specific suppression occurs when individual species or specific subsets of soil microorganisms interfere with the infection cycle of a pathogen (Weller et al., 2002; Berendsen et al., 2012). The biotic nature of specific suppression is also demonstrated as it can be eliminated through soil pasteurization or biocides. In contrast to general suppressiveness, specific suppressiveness can be transferred by introducing very small amounts (1%–10%) of suppressive soil into a conducive soil (Cook and Rovira, 1976; Mendes et al., 2011; Raaijmakers and Mazzola, 2016; Schlatter et al., 2017). Specific suppression is superimposed over the general suppression and is more effective (Berendsen et al., 2012). In some soils specific suppression is retained for prolonged periods even when soils are left bare, whereas in other soils it is induced by continuous monoculture of a susceptible host after a disease outbreak (Berendsen et al., 2012; Raaijmakers and Mazzola, 2016). Induction of specific suppression requires multilateral interactions between plants, soil microbiome and pathogens and is mechanistically complex. The interaction between plant and pathogen that occurs before a disease outbreak may induce the release of pathogen- or plant-derived metabolites that lead to alterations in microbiota composition and activation of pathogen-suppressive microorganisms (Chapelle et al., 2016). In recent years, many studies using new culture-independent technologies started to unravel the identity of responsible microorganisms in disease suppressive soils (Gomez Exposito et al., 2017). For instance, suppressiveness towards *Verticillium dahliae* was mainly associated with higher abundances of Actinobacteria and *Oxalobacteraceae* (Cretoiu et al., 2013). Another study regarding fungi revealed significant differences in the fungal community composition between suppressive and non-suppressive soil for the disease caused by *R. solani* AG 8; *Xylaria*, *Bionectria,* and *Eutypa* were more abundant in the suppressive soil whereas *Alternaria* and *Davidiella* dominated the non-suppressive soil (Penton et al., 2014). Also, higher abundances of the Phyla Actinobacteria, Proteobacteria, Acidobacteria, Gemmatimonadetes, and Nitrospirae were found in soil with specific suppressiveness to Fusarium wilt of strawberry (Cha et al., 2016). More recently, it was shown that fungal and bacterial diversity differed significantly between a suppressive and a conducive soil of Fusarium wilt whereas several of the fungal and bacterial genera known for their activity against *F. oxysporum* were detected exclusively or more abundantly in the Fusarium wilt-suppressive soil (Siegel-Hertz

et al., 2018). Interestingly, studies analyzing the rhizobacterial community composition in soils suppressive or conducive to *R. solani* revealed that relative abundance of specific bacterial taxa is a more important indicator of suppressiveness than the exclusive presence or absence of specific bacterial families (Mendes et al., 2011; Chapelle et al., 2016). In a study by Hu et al. (2016) defined *Pseudomonas* species consortia were introduced into naturally complex microbial communities to assess the importance of the *Pseudomonas* community diversity for the suppression of *R. solanacearum* in the tomato rhizosphere. Only the most dense and diverse *Pseudomonas* communities reduced pathogen density in the rhizosphere and decreased the disease incidence due to both intensified resource competition and interference with the pathogen. Recently, Wei et al. (2019) demonstrated that the composition and functioning of the initial soil microbiome predetermines future disease outcome of *R. solanacearum* on tomato plants. Plant survival was associated with specific bacterial species, including the highly antagonistic *Pseudomonas* and *Bacillus* bacteria together with specific rare taxa. The mechanism behind the suppression could be the production of antibiotics, as high abundance of genes encoding non-ribosomal peptide and polyketide synthases was found in the initial microbiomes associated with healthy plants. Intriguingly, they also demonstrated that this capacity can be transferred to the next generation of plants through soil transplantation opening a new avenue of exploiting microbiomes for disease resistance.

Microbiome Modulation by Coumarins, Benzoxazinoids, and Other Root-Exuded Molecules

Coumarins

Coumarins are phenolic compounds produced *via* the phenylpropanoid pathway and have been extensively studied for their role in disease resistance (Stringlis et al., 2019a) but also for their involvement in responses of dicotyledonous plants to iron deficiency (Tsai and Schmidt, 2017a). Coumarins are produced when iron is unavailable in the soil around the roots and their exudation increases to make iron more available before it is imported inside the roots (Tsai and Schmidt, 2017b; Tsai and Schmidt, 2017a). Coumarins with pronounced production/exudation in response to iron deficiency are scopolin, scopoletin, esculin, esculetin, fraxetin and sideretin (Jin et al., 2007; Rodriguez-Celma et al., 2013; Fourcroy et al., 2014; Schmid et al., 2014; Schmidt et al., 2014; Fourcroy et al., 2016; Rajniak et al., 2018; Tsai et al., 2018). Recent studies have suggested their role also in shaping microbiome composition around the roots (Stringlis et al., 2018b; Voges et al., 2019). Stringlis et al. (2018b) showed that both under iron deficiency and colonization of roots by beneficial rhizobacteria that induce ISR, there is increased accumulation of coumarins inside the roots. Components of the production and exudation of coumarins in this study were genes with a key role in ISR, such as the root-specific transcription factor MYB72 and beta-glucosidase gene *BGLU42* (Verhagen et al., 2004; Van Der Ent et al., 2008; Zamioudis et al., 2014; Stringlis et al., 2018b). More specifically, in *myb72* mutant plants no coumarin accumulation was observed inside the roots, while in *bglu42* mutant plants there was reduced exudation of coumarin scopoletin. Analysis of the rhizosphere microbiomes in these mutants plants, the coumarin biosynthesis mutant *f6′h1* (Kai et al., 2008; Schmid et al., 2014) and wild-type plants revealed that coumarins can affect the composition of the microbiome around the roots (Stringlis et al., 2018b). There was increase in the relative abundance of Proteobacteria but decrease of Firmicutes in the *f6′h1* rhizosphere compared to wild-type plants rhizosphere. Further experiments showed that coumarin scopoletin was inhibiting the growth of soilborne pathogens whereas rhizobacteria that induce ISR were insensitive to its antimicrobial activity (Stringlis et al., 2018b; Stringlis et al., 2019a). Voges et al. (2019) showed that coumarins can shape the composition of a synthetic bacterial community inoculated in *in vitro* grown plants and there was enrichment of a *Pseudomonas* strain in *f6′h1* compared to wild-types plants growing under iron deficiency. In this study, it was suggested that the antimicrobial effect of catecholic coumarins fraxetin and sideretin, produced downstream of scopoletin (Rajniak et al., 2018; Tsai et al., 2018), are due to the hydrogen peroxide deriving from catecholic coumarins at conditions of iron deficiency (Voges et al., 2019).

Benzoxazinoids

Benzoxazinoids are a class of compounds, quite abundant in the roots of maize, with a documented role in the attraction of beneficial microbes in the rhizosphere (Neal et al., 2012) and the defense responses of plants to various pathogenic threats (Ahmad et al., 2011). Recently, studies have focused on characterizing how benzoxazinoids can shape the assembly of root-associated bacterial and fungal communities (Hu et al., 2018; Cotton et al., 2019). Hu et al. (2018) using a benzoxazinoids deficient maize mutant observed that different bacterial and fungal communities assemble in the roots of the mutants compared to wild-type maize. Despite the prominent changes in bacterial and fungal microbiome the authors didn't assess the effects of benzoxazinoids on specific bacterial/fungal taxa. Release of benzoxazinoids and the subsequent microbiome changes were sufficient to provide plants of a next generation growing in this soil with protection against a herbivore insect. Next–generation maize plants growing in soil with and without benzoxazinoids displayed distinct bacterial and fungal communities both in the root and the rhizosphere. Actinobacteria OTUs and some Ascomycota and Glomeromycota OTUs were mostly responsible for root and rhizosphere separation but the effects on plant fitness were more strongly associated with changes in bacteria than fungi in the rhizosphere of these next-generation plants (Hu et al., 2018). There was increase of a subset of Proteobacteria in soils with benzoxazinoids, while Chloroflexi OTUs were enriched in soils without benzoxazinoids. In the case of fungal communities, Ascomycota OTUs were present in both soils with and without benzoxazinoids. Interestingly, Glomeromycota OTUs seemed to be less abundant in soils with benzoxazinoids. In the study by Cotton et al. (2019), the effect of benzoxazinoids on the metabolomic profile of roots and microbiome assembly was assessed. Metabolomic profiles of mutants in benzoxazinoids production were different compared to those of wild type plants, indicating a role of benzoxazinoids in the metabolic response of maize roots. The microbiome analysis revealed enrichment or depletion of

bacterial and fungal OTUs between the rhizospheres of wild type and mutant plants and the authors correlated the changes in the microbial abundance with metabolites present in the roots of wild type and mutant plants (Cotton et al., 2019). Studies like those presented herein on coumarins and benzoxazinoids enrich our understanding on how specific exudates shape root-associated microbial communities, and unlocking how a beneficial microbiome can be selected *via* exudation could allow us to breed for plants that can manipulate their microbiome to maximize growth and health benefits (Vannier et al., 2019).

Triterpenes and Camalexin

As already mentioned in section *Effect of Root Exudates on Root-Associated Microbiome*, triterpenes and camalexin were recently found to be involved in microbiome shaping (Huang et al., 2019; Koprivova et al., 2019). Triterpenes are products of plant metabolism with involvement in disease resistance and with antimicrobial activity (Papadopoulou et al., 1999). Triterpenes are synthesized *via* the mevalonate pathway and can accumulate in plant tissues as triterpene glycosides (Thimmappa et al., 2014). Huang et al. (2019) observed that triterpenes thalianin and arabidin are produced in roots and biosynthetic genes for their production are induced following treatment of roots with MeJA. Microbiome analysis of thalianin and arabidin mutants and wild-type plants revealed the assembly of distinct root microbial communities in the absence of triterpenes. These differences were explained by the enrichment of Bacteroidetes and the depletion of Deltaproteobacteria in the roots of triterpene mutants compared with the roots of wild type plants (Huang et al., 2019). In the study of Koprivova et al. (2019), the authors performed a genome wide association study (GWAS) and measured microbial sulfatase activity in the soil where 172 accessions of Arabidopsis were grown. Through this screen the authors found single-nucleotide polymorphisms (SNPs) explaining differences in microbial sulfatase activity. Some of these SNPs were in gene *CYP71A27* and a mutant of this gene displayed reduced microbial sulfatase activity and impaired production of antimicrobial compound camalexin. Interestingly, the authors observed that beneficial rhizobacteria could promote growth in wild-type plants but only beneficial rhizobacteria without sulfatase activity could promote growth in *cyp71a27* mutants. The fact that beneficial rhizobacterium *Pseudomonas* sp. CH267 could promote growth in wild-type plants but not in nine Arabidopsis accessions with variation in the amino acid sequence of CYP71A27, suggested that camalexin is required in the interaction of roots with microbes in order the plants to have a benefit (Koprivova et al., 2019).

"Cry for Help" During Infection of Plants

Plants experiencing infection by phytopathogens or insects, actively recruit beneficial members from the rhizosphere microbiota that will help them overcome biotic stresses, a phenomenon defined as "cry for help" (Bakker et al., 2018). Studies have shown that the build-up of a beneficial microbial community in the root is mediated by changes in gene expression and alterations in root exudation responsive to pathogen attack (**Figure 1**). Rudrappa et al. (2008) showed that infection of Arabidopsis leaves by *Pseudomonas syringae* pv. *tomato* (Pst) induced the root exudation of malic acid that in turn favored the recruitment of the beneficial *Bacillus subtilis* strain FB17 which triggers ISR in Arabidopsis against Pst. Tomato plants experiencing different stresses produced exudates that acted as chemoattractants for the beneficial fungus *Trichoderma harzianum* (Lombardi et al., 2018). Other studies have shown that aphid feeding or whitefly infestation of pepper and tobacco leaves can cause a transcriptional reprogramming in roots and changes in the root microbiome composition which makes plants more resistant to foliar and soilborne pathogens (Yang et al., 2011; Lee et al., 2012; Lee et al., 2018). Recently, Berendsen et al. (2018) demonstrated that Arabidopsis leaf infection by the biotrophic oomycete *Hyaloperonospora arabidopsidis* (Hpa) can lead to the enrichment of three bacterial taxa (*Xanthomonas* spp., *Stenotrophomonas* spp., and *Microbacterium* spp.) in the rhizosphere. Isolation of these microbes and inoculation of Arabidopsis showed that these three microbes together could induce ISR against Hpa and promote plant growth, indicating the active recruitment of beneficial microbes by infected plants. Microbiome changes were also apparent in Arabidopsis infected with *Pseudomonas syringae* and those changes were attributed to changes in root exudation (Yuan et al., 2018). In these studies, the beneficial effect in plant health due to microbiome changes could be transferred to the offspring of the infected plants that displayed increased levels of resistance to these pathogens (Berendsen et al., 2018; Yuan et al., 2018). These findings indicate that in soils with infected plants changes in exudation and the microbiome lead to the build-up of a microbial legacy that is inherited to the next generations of plants growing in this soil and favors their survival under phytopathogenic pressure (Bakker et al., 2018). Considering the continuity of plant-pathogens interactions during the lifetime of a plant in a field, a functional "loop" should be in action: when plants experience stress they respond with changes in exudation that can favor the selection of beneficial microbial members from the rhizosphere which in turn can help the plants deal with the stress (Liu et al., 2019a). Future studies should elucidate how different exudates contribute in the microbial recruitment and the subsequent soilborne legacy described above, considering the involvement of coumarins (Stringlis et al., 2018b; Stringlis et al., 2019a), malic acid (Rudrappa et al., 2008), benzoxazinoids (Hu et al., 2018; Cotton et al., 2019), and camalexin (Koprivova et al., 2019) in the selection of beneficial microbes in the rhizosphere.

Rhizosphere Microbiome as a Source of Benefits for the Plant

Beneficial Effects Against Biotic Stresses

It is well documented that plant genotype exerts strong influence on the overall composition of root associated communities through plant root exudates (Bulgarelli et al., 2012; Badri et al., 2013; Matthews et al., 2019). Recent evidence suggest that root exudates attract beneficial and pathogen-suppressing microbes or reshape microbiome assembly in the plant rhizosphere to suppress disease symptoms (Kwak et al., 2018; Mendes et al., 2018). The study of Mendes et al. (2018) using common bean

cultivars with variable levels of resistance has shown that rhizobacteria belonging to *Pseudomonadaceae*, *Bacillaceae*, *Solibacteraceae*, and *Cytophagaceae* families were more abundant in the rhizosphere of the Fusarium-resistant cultivar. Kwak et al. (2018) analyzed the rhizosphere microbiomes of a resistant and a susceptible tomato variety to the soilborne pathogen *R. solanacearum* to assess the role of plant-associated microorganisms in disease resistance and proved that transplantation of rhizosphere microbiota from resistant plants suppressed disease symptoms in susceptible plants. By comparing the metagenomes of the rhizosphere from resistant and susceptible plants a flavobacterial genome was identified to be far more abundant in the resistant plant rhizosphere. The isolated flavobacterium could suppress *R. solanacearum* in pot experiments with a susceptible tomato variety suggesting that selection of native microbiota can protect plants from root pathogens. Recently, it was shown that in natural populations of Arabidopsis, the plants are protected against root-inhabiting filamentous eukaryotes because of the presence of the co-residing bacterial root microbiota that is essential for plant survival (Duran et al., 2018). In another microbiome study, the occurrence of potato common scab caused by *Streptomyces* was correlated with the composition and putative function of the soil microbiome (Shi et al., 2019). The community composition of the geocaulosphere soil samples revealed that *Geobacillus*, *Curtobacterium*, and unclassified *Geodermatophilaceae* were the most abundant genera that were significantly negatively correlated with the scab severity level, the estimated absolute abundance of pathogenic *Streptomyces*, and *txtAB* gene copy number (biosynthetic gene of the scab phytotoxin). In contrast, *Variovorax*, *Stenotrophomonas*, and *Agrobacterium* were the most abundant genera that were positively correlated with these three parameters.

Direct pathogen suppression by rhizospheric microorganisms has been extensively reported (Mendes et al., 2011; Santhanam et al., 2015; Cha et al., 2016; Hu et al., 2016). Pathogen growth is affected by several and highly diverse mechanisms including microbial competition (for resources or space) (Zelezniak et al., 2015), secretion of antimicrobial compounds (Chen et al., 2018; Helfrich et al., 2018; Stringlis et al., 2018b; Koprivova et al., 2019) and hyperparasitism (Parratt and Laine, 2018). As mentioned previously, members of the rhizosphere microbiome can alter plant growth by producing phytohormones which modulate endogenous plant hormone levels (Stringlis et al., 2018c). In a recent study, two synthetic microbial communities were designed and consisted of bacterial strains that show ACC deaminase activity and produce an array of hormones and enzymes *in vitro* and also show antimicrobial activity against *F. oxysporum* f. sp. *lycopersici*. Inoculation of these synthetic communities in a poor substrate enhanced the growth of tomato plants and reduced symptoms caused by *F. oxysporum* f. sp. *lycopersici* (Tsolakidou et al., 2019a). In another study, endophytic *Enterobacteriaceae* strains engineered to express ACC deaminase activity on the bacterial cell walls did not show any activity against a pathogenic strain of *Fusarium oxysporum* f. sp. *cubense in vitro*. However, they promoted banana plant growth and increased resistance to banana Fusarium wilt suggesting that engineering the interactions between plants with their microbiome can provide valuable tools to deal with plant pathogens that are difficult to control (Liu et al., 2019b). Pathogenic microbes can employ similar strategies with beneficial microbes to colonize their hosts. For example, overexpression of *ACC deaminase* gene in *V. dahliae* significantly lowered ACC levels in the roots of infected tomato plants and increased both its virulence and the fungal biomass in the vascular tissues of plants (Tsolakidou et al., 2019b). Therefore, future studies need to address how functions shared by both beneficial and pathogenic microbes are perceived by the plants and how plants can maintain a balance in the rhizosphere.

Beneficial Effects Against Abiotic Stresses

Accumulating evidence suggests that the rhizosphere microbiome is not only involved in coping with biotic stresses but is also involved in protection of plants against abiotic stresses (**Figure 1**). Rhizosphere bacteria have been shown to elicit so-called induced systemic tolerance to high salinity, drought and nutrient deficiency or excess (Yang et al., 2009; Rolli et al., 2015). A recent study found a diverse range of root-associated bacteria of soybean and wheat, including *Pseudomonas* spp., *Pantoea* spp., and *Paraburkholderia* spp., showing mechanisms involved in improved nutrient uptake, growth, and stress tolerance like phosphate solubilization, nitrogen fixation, indole acetic acid and ACC deaminase production (Rascovan et al., 2016). Accumulation of heavy metals, hydrocarbons and pesticides in soil can cause deterioration of soil properties and have negative impact on plant growth or make the plant unsuitable for consumption (Kuiper et al., 2004). Interestingly, Sessitsch et al. (2012) found enrichment of microbial functions for the degradation of aromatic compounds in the metagenomes of endophytes, highlighting a potential for bioremediation. Understanding how microbiome dynamics and functions can change in response to perturbations can open new avenues to engineer microbial communities also for bioremediation purposes (Perez-Garcia et al., 2016; Eng and Borenstein, 2019). Indeed, soil tillage and compost amendment of contaminated soils could stimulate the indigenous microbial communities which are naturally adapted to the pollutants of these soils (Ventorino et al., 2019). In another study the modification of the microbiota assemblage following the introduction of a natural and diverse microbiome transplant in an oil-contaminated soil led to more efficient contaminant degradation compared to the introduction of an artificial microbial selection (Bell et al., 2016). Phytoremediation is the use of plants to extract, sequester, or detoxify pollutants. This practice is often associated with the microbial bioremediation since the presence of plants can stimulate the microbial population in the rhizosphere, improve physical and chemical properties of the soil and increase contacts between microbes and soil contaminants (Kuiper et al., 2004). In a recent work, Fan and colleagues found that inoculation of *Robinia pseudoacacia* with

rhizobia, significantly affected rhizosphere microbial population and functions and also improved the phytoremediation capacity of the plants (Fan et al., 2018).

Plant Microbiome as a Source of Variability in Plant Breeding

The efforts of plant breeding practices have always been directed towards the selection of desirable phenotypic traits, such as higher yield associated with improved edible characteristics. This domestication process, progressively led to the loss of allelic diversity, also named as genetic erosion of domesticated plants (Perez-Jaramillo et al., 2016; Pieterse et al., 2016). Recent studies indicated that in several plant species the rhizosphere microbiome composition may have been affected in domesticated plants as compared to their wild relatives (Perez-Jaramillo et al., 2017; Perez-Jaramillo et al., 2018; Pérez-Jaramillo et al., 2019). For common bean, it was shown that relative abundance of Bacteroidetes was increased in wild accessions whereas Actinobacteria and Proteobacteria were enriched in modern accessions and this shifting was associated with plant genotypic and specific root morphological traits (Perez-Jaramillo et al., 2017). Interestingly, the transition of common bean from a native to an agricultural soil led to a gain of rhizobacterial diversity and to a stronger effect of the bean genotype on rhizobacterial assembly (Pérez-Jaramillo et al., 2019). In a study using 33 strains of sunflower (*Helianthus annuus*) with varying degrees of domestication it was found that rhizosphere fungal communities were more strongly influenced by host genetic factors and plant breeding than bacterial communities. They also found that there was a minimal vertical transmission of fungi from seeds to adult plants (Leff et al., 2017). A survey of the bacterial community structure of 3 barley accessions also pointed to a small but significant role of the host genotype on root-associated community composition (Bulgarelli et al., 2015). Perez-Jaramillo et al. (2018) conducted a meta-analysis integrating metagenomics data of 6 independent studies with the aim of addressing whether plant domestication affected the composition of the root-associated microbiome in various crop plant species and observed consistent enrichment of Actinobacteria and Proteobacteria in modern varieties in contrast to the enrichment of Bacteroidetes in their wild relatives. This evidence indicates that modern agriculture may not utilize the full potential the associated microbiome may offer. In this framework, wild relatives have been suggested to provide new perspective into plant genes associated with microbiome assembly, and this knowledge could open new horizons for future breeding strategies (Perez-Jaramillo et al., 2018).

Engineering Microbial Inoculants to Suppress Disease and Support Plant Growth: From the Lab to the Field

The Prospect of Using Synthetic Communities to Promote Plant Health

The successful application of microbial consortia as inoculants to protect plants from stresses and enhance their productivity relies mainly on the ability of microorganisms that show promise in the lab to overcome hurdles and retain their characteristics when applied in the field (Sessitsch et al., 2019). The rationale behind this strategy is twofold: the selection and combination i) of distantly related microorganisms with different or complementing characteristics tailored to promote plant growth and suppress pathogens, or tolerate different plant genotypes or environmental conditions (Compant et al., 2019), or ii) of closely related strains in order to expand the diversity of resources that these strains use (Wei et al., 2015; Hu et al., 2016). Species-rich communities are often more efficient and more productive than species-poor communities as they use limiting resources more efficiently (Loreau et al., 2001). For instance, the introduction of high diversity *Pseudomonas* consortia reduced *R. solanacearum* density in the rhizosphere of tomato plants and decreased the disease incidence due to interference and intensified resource competition with the pathogen. Interestingly, increasing diversity of the introduced *Pseudomonas* consortia also increased their survival (Hu et al., 2016). Furthermore, increasing the richness of *Pseudomonas* consortia resulted in enhanced accumulation of plant biomass and more efficient assimilation of nutrients in tomato plants; diversity effects were more important than the identity of the *Pseudomonas* strain and the observed plant growth promotion was associated with elevated production of plant hormones, siderophores, and solubilization of phosphorus *in vitro* (Hu et al., 2017). In contrast, increasing genotypic richness of *P. fluorescens* communities increased disproportionally the antagonistic interactions, causing community collapse and resulted in loss of *Medicago sativa* protection against the oomycete *Pythium ultimum* (Becker et al., 2012). It was recently proposed that microbial synthetic communities can be used as inoculants to produce plant growth substrates with desired characteristics such as biocontrol of targeted pathogens and plant growth promotion (Tsolakidou et al., 2019a). The composition of the synthetic communities was a determinant factor for the growth of plants and pathogen inhibition. The synthetic community consisting of different bacterial genera promoted the growth of tomato plants but failed to protect plants against Fusarium wilt. The synthetic community consisting of *Bacillus* isolates suppressed Fusarium wilt symptoms and enhanced tomato growth but to a lesser extent as compared to the more diverse synthetic community (Tsolakidou et al., 2019a).

There is a substantial number of studies suggesting that complex inocula can provide plants with increased disease resistance and growth promotion effects as compared to single strains (Rolli et al., 2015; Santhanam et al., 2015; Wei et al., 2015; Molina-Romero et al., 2017; Niu et al., 2017; Berendsen et al., 2018; Tsolakidou et al., 2019a). Bacterial strains that show little or no effects as single inoculants can exhibit plant growth promotion effects when used in a consortium (Raaijmakers and Weller, 1998; Berendsen et al., 2018).

The prospect of using microbial mixtures as plant inoculants that can positively affect plant properties is an emerging field of research (**Figure 2**). However, the complexity of experimentation is exponentially increasing when using synthetic microbial

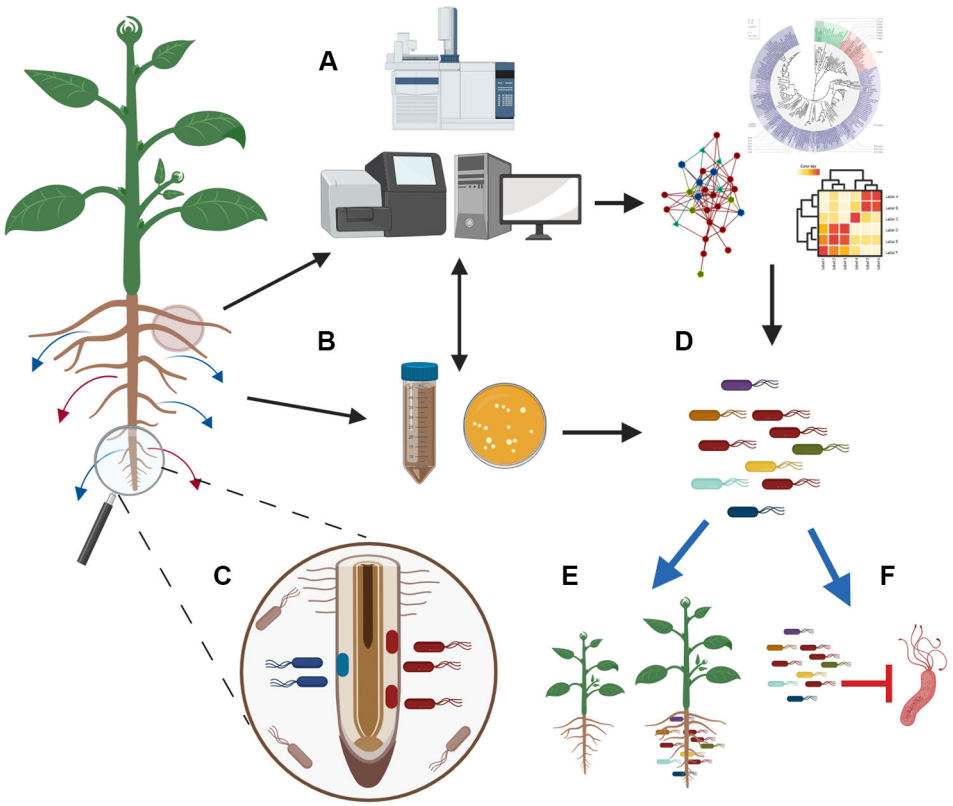

FIGURE 2 | Integration of modern technologies to engineer microbial inoculants that boost plant growth and suppress pathogens. Plants respond to stresses and change their exudation. To unravel how changes in exudation affect microbiome composition and functions, we need to couple advance metabolomic techniques with metagenomics sequencing **(A)** and culture-based methodologies **(B)**. At the same time, there is promise for the use of exometabolomics methodologies and spatial metabolomics that can help in finding where specific exudates are produced and how the microbes around the exudation site are affected **(C)**. Analysis of the generated data in depth will allow the characterization of the microbial communities that respond to exudates and the identification of networks that will reveal how microbes interact and contribute in the microbiome assembly **(A)**. The parallel isolation of a representative fraction of the root microbiome **(B)** will allow to link descriptive data with the isolated microbes and will guide the design of synthetic communities **(D)**. Testing of these synthetic communities with different hosts under different conditions (e.g. biotic/abiotic stress/*in vitro*/in soil/in field) will facilitate the selection of synthetic communities that can promote plant growth **(E)** and suppress pathogens **(F)** in a consistent and reproducible manner. The figure was designed with Biorender (https://biorender.com/).

communities as compared to single strain inoculants. Thus, successful implementation of microbial consortia with desired host outputs will depend on our understanding of how microorganisms interact with one another and with their hosts in natural ecosystems. To this direction, synthetic microbial communities have been widely adopted for fundamental discoveries in plant microbiomes research as a reductionist approach to simplify and especially control each component of this complex system (Bai et al., 2015; Lebeis et al., 2015; Finkel et al., 2019). Indeed, as cleverly postulated by Vorholt and colleagues (2017), the true strength of a synthetic community is that each member of the community can be singularly added or substituted, and this can be even accomplished at a functional level by silencing or expressing specific genes.

However, controlling each member of a large community would bring to a factorial number of possible combinations, making it impossible to control. Recently, Paredes and colleagues (2018) developed a machine learning computational approach to design a bacterial synthetic community. This method was based on the "cry-for-help" theory, consisting in the construction of a neural-network model that received as inputs the growth rate of a pool of bacterial isolates grown with the root exudates of phosphate starved plants, and the phosphate content of shoots of plants in binary interaction with each one of these single bacterial isolates. This method allowed to design a synthetic community with consistent predictable plant phenotypes. In parallel, the construction of the synthetic community based on the "cry-for-help" carried out by Berendsen and colleagues (2018) was more based on a plant-driven approach, where plants effectively attracted a consortium of beneficial bacteria which in turn produced desirable plant phenotypes. These examples show that the identification of microbes that mostly respond to plant stress signals can be used as reliable predictors for the discovery of beneficial microbes.

Techniques and Workflows to Harness Plants and Engineer Beneficial Microbiomes

Engineering microbiomes to promote plant fitness and health is an emerging scientific field and an approach holding great promise towards the realization of sustainable future agriculture. However, there are many aspects and technical limitations that need to be considered to effectively exploit this technology. Here, we aim to summarize some of these considerations that are extensively discussed in a recent review by Lawson et al. (2019). First, to unravel mechanisms underlying the interactions between hosts and microbiomes, multiple omics techniques need to be integrated (Jansson and Baker, 2016). Metabolomics, metagenomics, plant transcriptomics, metatranscriptomics, and plant genetics are some of the approaches that combined can disentangle the complex interactions occurring between members of the holobiont. A thorough description of these methodologies are beyond the scope of this review, but some recent focused reviews are available for further reading (Van Dam and Bouwmeester, 2016; Levy et al., 2018; O' Banion et al., 2019; Rodriguez et al., 2019). Here, we report some examples where application of a multi-omics approach revealed how selected plant exudates produced under natural or under stress conditions can affect the colonization of roots by specific microbes. Hu et al. (2018) combined metabolomics and amplicon-based metagenomics analysis on two maize genotypes (wild type and a benzoxazinoids precursor mutant) and revealed how the defense-related benzoxazinoids metabolites structure the bacterial and fungal community of the maize rhizosphere. Stringlis et al. (2018b) also exploited the combination of shotgun metagenomics and metabolomics on an array of Arabidopsis mutants to demonstrate that root exudation of coumarins can shape the rhizosphere microbiome. Similarly, Huang et al. (2019) utilized metabolomics and metagenomics to reveal the effect that root-exuded triterpenes have on microbiota composition of the root. On the track of the work by Berendsen et al. (2018); Yuan et al. (2018) revealed the metabolic drivers of the "legacy effect" by combining metabolomics of the root exudates of infected plants with metagenomics analysis of the rhizospheres of these plants. Furthermore, in an elegant combination of exometabolomics, metagenomics and comparative genomics, Zhalnina et al. (2018) demonstrated how temporal dynamic exudation of root metabolites during different plant developmental stages assembled specific microbial communities and enriched for specific microbial functions. In a next step, we need to link how released plant molecules can affect microbial activity and unearth how plant secretions can define which root niches can be colonized by beneficial microbes while at the same time excluding the pathogenic ones (Jacoby and Kopriva, 2018; Levy et al., 2018).

Furthermore, as the blend of root exudates is strictly dependent on plant genotype, it is expectable that different plants attract different microbes that can produce similar effects on different hosts, due to the redundancy of functions of the microbiome. Considering this, we propose to use desirable microbiome functions as selective markers to identify potential beneficial microbes. By exposing different plant species to the same stress conditions, a comparative metatranscriptomics approach would allow the identification of common functions expressed by microbiomes upon the sensing of stress plant signals. Metatranscriptomics has already been used to highlight the most active members of microbiomes in different plant species or to identify bacterial genes expressed during different Arabidopsis life stages (Turner et al., 2013; Chaparro et al., 2014). To date, only a few metatranscriptomics studies have been conducted, due to the difficulties of mapping metatranscripts to reference genomes and metagenomes. Again, in this case, using synthetic communities composed of whole-genome sequenced members would facilitate this task. Associating these studies with detailed metabolomic analysis of root exudates from stressed plants would then make the integration of multi-omics techniques more and more reliable (**Figure 2**). All together these strategies would produce an incredible amount of data that still need to be interpreted. For this reason, it is necessary to develop bioinformatics techniques that would allow the reduction and summarization of these data. System biology approaches based on correlation networks have been proposed to discover microbial associations where positive and negative correlations can be used to infer possible synergistic or antagonistic interactions (Agler et al., 2016; Poudel et al., 2016; Van Der Heijden and Hartmann, 2016). With this methodology, it is also possible to identify the so-called microbial hub taxa which represent the most interactive nodes in the networks. In this direction, Agler et al. (2016) established a computational method which identified the plant pathogen *Albugo* and the fungus *Dioszegia* as microbial hubs in the microbiome of Arabidopsis phyllosphere. In a further experiment, through the artificial manipulation of the microbiome it was also demonstrated that the microbes identified as the hubs of the network, also represented "keystone taxa" as they drove the composition and function of the microbiome. The concept of "keystone" also has been adopted by Niu et al. (2017) when studying the contribution of individual members of a microbial synthetic community on the rhizosphere of maize plants. In this case, the removal of a singular member caused the collapse of the community functioning with the respective decrease of the richness indexes. These results clearly highlighted that some microbial individuals play a key role in shaping microbial communities on plant hosts.

Another very powerful computational approach is the use of metagenome-wide association study (MWAS). This method derives from the genome-wide association's studies, which rely on the construction of linear mixed models to relate genotypic variations to quantitative observed phenotypes. MWAS have been typically used in human metagenomics studies, i.e. to identify microbial taxa or microbial functions associated with a host phenotypic trait which could be a disease or the host metabolomics profile, by integrating a multi-omics approach (Gilbert et al., 2016). Genome-wide association approach has also been used in the study of plant-microbe interactions, i.e. to identify Arabidopsis loci associated with the ability of plants to maximize benefit from the interaction with the beneficial

Pseudomonas strain WCS417 (Wintermans et al., 2016). In a plant-microbiome context, Beilsmith and colleagues (2019) propose to use MWAS to find associations between host genes and microbial taxa. MWAS could be very useful to find functional associations between either microbial genes and host genes, or microbial genes and host phenotype, which could also include root exudation profiles.

Finally, to build synthetic microbial communities with consistent beneficial effects for plants in the field, it is essential to understand whether a specific trait of a single strain is expressed in a community level and under multiple contexts (different environmental conditions, hosts, other microorganisms, etc.) (Vannier et al., 2019). This is crucial considering that single strains or synthetic communities that have beneficial effects *in vitro* and under controlled conditions might behave in a different manner in the field. We need also to be aware that the increasing complexity of the synthetic community decreases the feasibility of the large-scale industrial production of microbial inoculants. This should be considered in future plant-microbiome studies with a translational intent, since a number of methodologies and tools need to be combined to design small and effective synthetic communities that can provide the host plants with consistent and predictable outcomes.

AUTHOR CONTRIBUTIONS

All authors have contributed to the structure and writing of this review, have read and approved it for publication.

FUNDING

The authors gratefully acknowledge MIUR (Ministry for Education, University and Research) for financial support (MIUR- PRIN 2017, grant number PROSPECT 2017JLN833_005).

REFERENCES

Agler, M. T., Ruhe, J., Kroll, S., Morhenn, C., Kim, S. T., Weigel, D., et al. (2016). Microbial hub taxa link host and abiotic factors to plant microbiome variation. *PloS Biol.* 14, e1002352. doi: 10.1371/journal.pbio.1002352

Ahmad, S., Veyrat, N., Gordon-Weeks, R., Zhang, Y., Martin, J., Smart, L., et al. (2011). Benzoxazinoid metabolites regulate innate immunity against aphids and fungi in maize. *Plant Physiol.* 157, 317–327. doi: 10.1104/pp.111.180224

Akiyama, K., Matsuzaki, K., and Hayashi, H. (2005). Plant sesquiterpenes induce hyphal branching in arbuscular mycorrhizal fungi. *Nature* 435, 824–827. doi: 10.1038/nature03608

Akum, F. N., Steinbrenner, J., Biedenkopf, D., Imani, J., and Kogel, K. H. (2015). The *Piriformospora indica* effector PIIN_08944 promotes the mutualistic Sebacinalean symbiosis. *Front. Plant Sci.* 6, 906. doi: 10.3389/fpls.2015.00906

Almario, J., Jeena, G., Wunder, J., Langen, G., Zuccaro, A., Coupland, G., et al. (2017). Root-associated fungal microbiota of nonmycorrhizal *Arabis alpina* and its contribution to plant phosphorus nutrition. *Proc. Natl. Acad. Sci. U. S. A.* 114, 9403–9412. doi: 10.1073/pnas.1710455114

Altomare, C., Norvell, W. A., Bjorkman, T., and Harman, G. E. (1999). Solubilization of phosphates and micronutrients by the plant-growth-promoting and biocontrol fungus *Trichoderma harzianum* Rifai 1295-22. *Appl. Environ. Microbiol.* 65, 2926–2933. doi: 10.1128/aem.65.7.2926-2933.1999

Anand, A., Uppalapati, S. R., Ryu, C. M., Allen, S. N., Kang, L., Tang, Y., et al. (2008). Salicylic acid and systemic acquired resistance play a role in attenuating crown gall disease caused by *Agrobacterium tumefaciens*. *Plant Physiol.* 146, 703–715. doi: 10.1104/pp.107.111302

Antoniou, A., Tsolakidou, M. D., Stringlis, I. A., and Pantelides, I. S. (2017). Rhizosphere microbiome recruited from a suppressive compost improves plant fitness and increases protection against vascular wilt pathogens of tomato. *Front. Plant Sci.* 8, 2022. doi: 10.3389/fpls.2017.02022

Badri, D. V., Quintana, N., El Kassis, E. G., Kim, H. K., Choi, Y. H., Sugiyama, A., et al. (2009). An ABC transporter mutation alters root exudation of phytochemicals that provoke an overhaul of natural soil microbiota. *Plant Physiol.* 151, 2006–2017. doi: 10.1104/pp.109.147462

Badri, D. V., Chaparro, J. M., Zhang, R., Shen, Q., and Vivanco, J. M. (2013). Application of natural blends of phytochemicals derived from the root exudates of Arabidopsis to the soil reveal that phenolic-related compounds predominantly modulate the soil microbiome. *J. Biol. Chem.* 288, 4502–4512. doi: 10.1074/jbc.M112.433300

Baetz, U., and Martinoia, E. (2014). Root exudates: the hidden part of plant defense. *Trends Plant Sci.* 19, 90–98. doi: 10.1016/j.tplants.2013.11.006

Bai, Y., Muller, D. B., Srinivas, G., Garrido-Oter, R., Potthoff, E., Rott, M., et al. (2015). Functional overlap of the Arabidopsis leaf and root microbiota. *Nature* 528, 364–369. doi: 10.1038/nature16192

Bais, H. P., Weir, T. L., Perry, L. G., Gilroy, S., and Vivanco, J. M. (2006). The role of root exudates in rhizosphere interactions with plants and other organisms. *Annu. Rev. Plant Biol.* 57, 233–266. doi: 10.1146/annurev.arplant.57.032905.105159

Baker, K. F., and Cook, R. J. (1974). *Biological control of plant pathogens* (San Francisco, USA: WH Freeman and Company). doi: 10.1017/S001447970000661X

Bakker, P. A. H. M., Pieterse, C. M. J., De Jonge, R., and Berendsen, R. L. (2018). The soil-borne legacy. *Cell* 172, 1178–1180. doi: 10.1016/j.cell.2018.02.024

Bardoel, B. W., Van Der Ent, S., Pel, M. J., Tommassen, J., Pieterse, C. M. J., Van Kessel, K. P., et al. (2011). *Pseudomonas* evades immune recognition of flagellin in both mammals and plants. *PloS Pathog.* 7, e1002206. doi: 10.1371/journal.ppat.1002206

Beck, M., Wyrsch, I., Strutt, J., Wimalasekera, R., Webb, A., Boller, T., et al. (2014). Expression patterns of *FLAGELLIN SENSING 2* map to bacterial entry sites in plant shoots and roots. *J. Exp. Bot.* 65, 6487–6498. doi: 10.1093/jxb/eru366

Becker, J., Eisenhauer, N., Scheu, S., and Jousset, A. (2012). Increasing antagonistic interactions cause bacterial communities to collapse at high diversity. *Ecol. Lett.* 15, 468–474. doi: 10.1111/j.1461-0248.2012.01759.x

Beckers, B., Op De Beeck, M., Weyens, N., Boerjan, W., and Vangronsveld, J. (2017). Structural variability and niche differentiation in the rhizosphere and endosphere bacterial microbiome of field-grown poplar trees. *Microbiome* 5, 25. doi: 10.1186/s40168-017-0241-2

Bednarek, P., Schneider, B., Svatos, A., Oldham, N. J., and Hahlbrock, K. (2005). Structural complexity, differential response to infection, and tissue specificity of indolic and phenylpropanoid secondary metabolism in Arabidopsis roots. *Plant Physiol.* 138, 1058–1070. doi: 10.1104/pp.104.057794

Begum, A. A., Leibovitch, S., Migner, P., and Zhang, F. (2001). Specific flavonoids induced nod gene expression and pre-activated nod genes of *Rhizobium leguminosarum* increased pea (*Pisum sativum* L.) and lentil (*Lens culinaris* L.) nodulation in controlled growth chamber environments. *J. Exp. Bot.* 52, 1537–1543. doi: 10.1093/jexbot/52.360.1537

Beilsmith, K., Thoen, M. P. M., Brachi, B., Gloss, A. D., Khan, M. H., and Bergelson, J. (2019). Genome-wide association studies on the phyllosphere microbiome: embracing complexity in host-microbe interactions. *Plant J.* 97, 164–181. doi: 10.1111/tpj.14170

Bell, T. H., Stefani, F. O., Abram, K., Champagne, J., Yergeau, E., Hijri, M., et al. (2016). A diverse soil microbiome degrades more crude oil than specialized bacterial assemblages obtained in culture. *Appl. Environ. Microbiol.* 82, 5530–5541. doi: 10.1128/AEM.01327-16

Berendsen, R. L., Pieterse, C. M. J., and Bakker, P. A. H. M. (2012). The rhizosphere microbiome and plant health. *Trends Plant Sci.* 17, 478–486. doi: 10.1016/j.tplants.2012.04.001

Berendsen, R. L., Van Verk, M. C., Stringlis, I. A., Zamioudis, C., Tommassen, J., Pieterse, C. M. J., et al. (2015). Unearthing the genomes of plant-beneficial *Pseudomonas* model strains WCS358, WCS374 and WCS417. *BMC Genomics* 16, 539. doi: 10.1186/s12864-015-1632-z

Berendsen, R. L., Vismans, G., Yu, K., Song, Y., De Jonge, R., Burgman, W. P., et al. (2018). Disease-induced assemblage of a plant-beneficial bacterial consortium. *ISME J.* 12, 1496–1507. doi: 10.1038/s41396-018-0093-1

Bergelson, J., Mittelstrass, J., and Horton, M. W. (2019). Characterizing both bacteria and fungi improves understanding of the *Arabidopsis* root microbiome. *Sci. Rep.* 9, 24. doi: 10.1038/s41598-018-37208-z

Berhin, A., De Bellis, D., Franke, R. B., Buono, R. A., Nowack, M. K., and Nawrath, C. (2019). The root cap cuticle: a cell wall structure for seedling establishment and lateral root formation. *Cell* 176, 1367–1378. doi: 10.1016/j.cell.2019.01.005

Boller, T., and Felix, G. (2009). A renaissance of elicitors: perception of microbe-associated molecular patterns and danger signals by pattern-recognition receptors. *Annu. Rev. Plant Biol.* 60, 379–406. doi: 10.1146/annurev.arplant.57.032905.105346

Bolton, M. D., Thomma, B. P. H. J., and Nelson, B. D. (2006). *Sclerotinia sclerotiorum* (Lib.) de Bary: biology and molecular traits of a cosmopolitan pathogen. *Mol. Plant Pathol.* 7, 1–16. doi: 10.1111/j.1364-3703.2005.00316.x

Bonanomi, G., Antignani, V., Capodilupo, M., and Scala, F. (2010). Identifying the characteristics of organic soil amendments that suppress soilborne plant diseases. *Soil Biol. Biochem.* 42, 136–144. doi: 10.1016/j.soilbio.2009.10.012

Bonfante, P., and Genre, A. (2010). Mechanisms underlying beneficial plant-fungus interactions in mycorrhizal symbiosis. *Nat. Commun.* 1, 48. doi: 10.1038/ncomms1046

Bressan, M., Roncato, M. A., Bellvert, F., Comte, G., Haichar, F. Z., Achouak, W., et al. (2009). Exogenous glucosinolate produced by *Arabidopsis thaliana* has an impact on microbes in the rhizosphere and plant roots. *ISME J.* 3, 1243–1257. doi: 10.1038/ismej.2009.68

Brotman, Y., Landau, U., Cuadros-Inostroza, A., Tohge, T., Fernie, A. R., Chet, I., et al. (2013). *Trichoderma*-plant root colonization: escaping early plant defense responses and activation of the antioxidant machinery for saline stress tolerance. *PloS Pathog.* 9, e1003221. doi: 10.1371/journal.ppat.1003221

Brown, D. J., Robertson, W. M., and Trudgill, D. L. (1995). Transmission of viruses by plant nematodes. *Annu. Rev. Phytopathol.* 33, 223–249. doi: 10.1146/annurev.py.33.090195.001255

Bruehl, G. W. (1987). *Soilborne plant pathogens* (New York, USA: Macmillan Publishing Company). doi: 10.1086/415660

Bulgarelli, D., Rott, M., Schlaeppi, K., Ver Loren Van Themaat, E., Ahmadinejad, N., Assenza, F., et al. (2012). Revealing structure and assembly cues for Arabidopsis root-inhabiting bacterial microbiota. *Nature* 488, 91–95. doi: 10.1038/nature11336

Bulgarelli, D., Schlaeppi, K., Spaepen, S., Ver Loren Van Themaat, E., and Schulze-Lefert, P. (2013). Structure and functions of the bacterial microbiota of plants. *Annu. Rev. Plant Biol.* 64, 807–838. doi: 10.1146/annurev-arplant-050312-120106

Bulgarelli, D., Garrido-Oter, R., Munch, P. C., Weiman, A., Droge, J., Pan, Y., et al. (2015). Structure and function of the bacterial root microbiota in wild and domesticated barley. *Cell Host Microbe* 17, 392–403. doi: 10.1016/j.chom.2015.01.011

Campbell, R. N. (1996). Fungal transmission of plant viruses. *Annu. Rev. Phytopathol.* 34, 87–108. doi: 10.1146/annurev.phyto.34.1.87

Cao, Y., Liang, Y., Tanaka, K., Nguyen, C. T., Jedrzejczak, R. P., Joachimiak, A., et al. (2014). The kinase LYK5 is a major chitin receptor in Arabidopsis and forms a chitin-induced complex with related kinase CERK1. *eLife* 3, e03766. doi: 10.7554/eLife.03766

Carvalhais, L. C., Dennis, P. G., Badri, D. V., Kidd, B. N., Vivanco, J. M., and Schenk, P. M. (2015). Linking jasmonic acid signaling, root exudates, and rhizosphere microbiomes. *Mol. Plant-Microbe Interact.* 28, 1049–1058. doi: 10.1094/MPMI-01-15-0016-R

Castrillo, G., Teixeira, P. J., Paredes, S. H., Law, T. F., De Lorenzo, L., Feltcher, M. E., et al. (2017). Root microbiota drive direct integration of phosphate stress and immunity. *Nature* 543, 513–518. doi: 10.1038/nature21417

Cha, J. Y., Han, S., Hong, H. J., Cho, H., Kim, D., Kwon, Y., et al. (2016). Microbial and biochemical basis of a Fusarium wilt-suppressive soil. *ISME J.* 10, 119–129. doi: 10.1038/ismej.2015.95

Chaparro, J. M., Badri, D. V., Bakker, M. G., Sugiyama, A., Manter, D. K., and Vivanco, J. M. (2013). Root exudation of phytochemicals in Arabidopsis follows specific patterns that are developmentally programmed and correlate with soil microbial functions. *PloS One* 8, e55731. doi: 10.1371/journal.pone.0055731

Chaparro, J. M., Badri, D. V., and Vivanco, J. M. (2014). Rhizosphere microbiome assemblage is affected by plant development. *ISME J.* 8, 790–803. doi: 10.1038/ismej.2013.196

Chapelle, E., Mendes, R., Bakker, P. A. H. M., and Raaijmakers, J. M. (2016). Fungal invasion of the rhizosphere microbiome. *ISME J.* 10, 265–268. doi: 10.1038/ismej.2015.82

Chellemi, D. O., Gamliel, A., Katan, J., and Subbarao, K. V. (2016). Development and deployment of systems-based approaches for the management of soilborne plant pathogens. *Phytopathology* 106, 216–225. doi: 10.1094/PHYTO-09-15-0204-RVW

Chen, Y., Wang, J., Yang, N., Wen, Z., Sun, X., Chai, Y., et al. (2018). Wheat microbiome bacteria can reduce virulence of a plant pathogenic fungus by altering histone acetylation. *Nat. Commun.* 9, 3429. doi: 10.1038/s41467-018-05683-7

Cheng, Y. T., Zhang, L., and He, S. Y. (2019). Plant-microbe interactions facing environmental challenge. *Cell Host Microbe* 26, 183–192. doi: 10.1016/j.chom.2019.07.009

Claesson, M. J., Wang, Q., O'sullivan, O., Greene-Diniz, R., Cole, J. R., Ross, R. P., et al. (2010). Comparison of two next-generation sequencing technologies for resolving highly complex microbiota composition using tandem variable 16S rRNA gene regions. *Nucleic Acids Res.* 38, e200. doi: 10.1093/nar/gkq873

Coleman, J. J. (2016). The *Fusarium solani* species complex: ubiquitous pathogens of agricultural importance. *Mol. Plant Pathol.* 17, 146–158. doi: 10.1111/mpp.12289

Compant, S., Samad, A., Faist, H., and Sessitsch, A. (2019). A review on the plant microbiome: Ecology, functions, and emerging trends in microbial application. *J. Adv. Res.* 19, 29–37. doi: 10.1016/j.jare.2019.03.004

Cook, R. J., and Rovira, A. D. (1976). Role of bacteria in biological control of *Gaeumannomyces graminis* by suppressive soils. *Soil Biol. Biochem.* 8, 269–273. doi: 10.1094/PHYTO-03-17-0111-RVW

Cook, R. J. (2014). *Plant health management: Pathogen suppressive soils.* (Amsterdam, Netherlands: Elsevier). doi: 10.1016/0038-0717(76)90056-0

Cotton, T. E. A., Petriacq, P., Cameron, D. D., Meselmani, M. A., Schwarzenbacher, R., Rolfe, S. A., et al. (2019). Metabolic regulation of the maize rhizobiome by benzoxazinoids. *ISME J.* 13, 1647–1658. doi: 10.1038/s41396-019-0375-2

Couto, D., and Zipfel, C. (2016). Regulation of pattern recognition receptor signalling in plants. *Nat. Rev. Immunol.* 16, 537–552. doi: 10.1038/nri.2016.77

Cretoiu, M. S., Korthals, G. W., Visser, J. H., and Van Elsas, J. D. (2013). Chitin amendment increases soil suppressiveness toward plant pathogens and modulates the actinobacterial and oxalobacteraceal communities in an experimental agricultural field. *Appl. Environ. Microbiol.* 79, 5291–5301. doi: 10.1128/AEM.01361-13

Dakora, F. D., and Phillips, D. A. (2002). Root exudates as mediators of mineral acquisition in low-nutrient environments. *Plant Soil* 245, 35–47. doi: 10.1023/A:1020809400075

De Coninck, B., Timmermans, P., Vos, C., Cammue, B. P., and Kazan, K. (2015). What lies beneath: belowground defense strategies in plants. *Trends In Plant Sci.* 20, 91–101. doi: 10.1016/j.tplants.2014.09.007

De Jaeger, N., De La Providencia, I. E., De Boulois, H. D., and Declerck, S. (2011). *Trichoderma harzianum* might impact phosphorus transport by arbuscular mycorrhizal fungi. *FEMS Microbiol. Ecol.* 77, 558–567. doi: 10.1111/j.1574-6941.2011.01135.x

De Souza, R. S., Okura, V. K., Armanhi, J. S., Jorrin, B., Lozano, N., Da Silva, M. J., et al. (2016). Unlocking the bacterial and fungal communities assemblages of sugarcane microbiome. *Sci. Rep.* 6, 28774. doi: 10.1038/srep28774

Dodds, P. N., and Rathjen, J. P. (2010). Plant immunity: towards an integrated view of plant-pathogen interactions. *Nat. Rev. Genet.* 11, 539–548. doi: 10.1038/nrg2812

Dombrowski, N., Schlaeppi, K., Agler, M. T., Hacquard, S., Kemen, E., Garrido-Oter, R., et al. (2017). Root microbiota dynamics of perennial *Arabis alpina* are dependent on soil residence time but independent of flowering time. *ISME J.* 11, 43–55. doi: 10.1038/ismej.2016.109

Driouich, A., Follet-Gueye, M. L., Vicre-Gibouin, M., and Hawes, M. (2013). Root border cells and secretions as critical elements in plant host defense. *Curr. Opin. Plant Biol.* 16, 489–495. doi: 10.1016/j.pbi.2013.06.010

Duca, D., Lorv, J., Patten, C. L., Rose, D., and Glick, B. R. (2014). Indole-3-acetic acid in plant-microbe interactions. *Antonie Van Leeuwenhoek* 106, 85–125. doi: 10.1007/s10482-013-0095-y

Duran, P., Thiergart, T., Garrido-Oter, R., Agler, M., Kemen, E., Schulze-Lefert, P., et al. (2018). Microbial interkingdom interactions in roots promote Arabidopsis survival. *Cell* 175, 973–983. doi: 10.1016/j.cell.2018.10.020

Edwards, J., Johnson, C., Santos-Medellin, C., Lurie, E., Podishetty, N. K., Bhatnagar, S., et al. (2015). Structure, variation, and assembly of the root-associated microbiomes of rice. *Proc. Natl. Acad. Sci. U.S.A.* 112, 911–920. doi: 10.1073/pnas.1414592112

Eng, A., and Borenstein, E. (2019). Microbial community design: methods, applications, and opportunities. *Curr. Opin. Biotechnol.* 58, 117–128. doi: 10.1016/j.copbio.2019.03.002

Fabianska, I., Gerlach, N., Almario, J., and Bucher, M. (2019). Plant-mediated effects of soil phosphorus on the root-associated fungal microbiota in *Arabidopsis thaliana*. *New Phytol.* 221, 2123–2137. doi: 10.1111/nph.15538

Fan, M., Xiao, X., Guo, Y., Zhang, J., Wang, E., Chen, W., et al. (2018). Enhanced phytoremdiation of *Robinia pseudoacacia* in heavy metal-contaminated soils with rhizobia and the associated bacterial community structure and function. *Chemosphere* 197, 729–740. doi: 10.1016/j.chemosphere.2018.01.102

Field, K. J., Pressel, S., Duckett, J. G., Rimington, W. R., and Bidartondo, M. I. (2015). Symbiotic options for the conquest of land. *Trends Ecol. Evol.* 30, 477–486. doi: 10.1016/j.tree.2015.05.007

Finkel, O. M., Castrillo, G., Paredes, S. H., Salas Gonzalez, I., and Dangl, J. L. (2017). Understanding and exploiting plant beneficial microbes. *Curr. Opin. Plant Biol.* 38, 155–163. doi: 10.1016/j.pbi.2017.04.018

Finkel, O. M., Salas-González, I., Castrillo, G., Law, T. F., Conway, J. M., Teixeira, P. J. P. L., et al. (2019). Root development is maintained by specific bacteria-bacteria interactions within a complex microbiome. *bioRxiv* 645655. doi: 10.1101/645655

Fourcroy, P., Siso-Terraza, P., Sudre, D., Saviron, M., Reyt, G., Gaymard, F.,, et al. (2014). Involvement of the ABCG37 transporter in secretion of scopoletin and derivatives by Arabidopsis roots in response to iron deficiency. *New Phytol.* 201, 155–167. doi: 10.1111/nph.12471

Fourcroy, P., Tissot, N., Gaymard, F., Briat, J. F., and Dubos, C. (2016). Facilitated Fe nutrition by phenolic compounds excreted by the Arabidopsis ABCG37/PDR9 transporter requires the IRT1/FRO2 high-affinity root Fe(2+) transport system. *Mol. Plant* 9, 485–488. doi: 10.1016/j.molp.2015.09.010

Galan, J. E., and Collmer, A. (1999). Type III secretion machines: bacterial devices for protein delivery into host cells. *Science* 284, 1322–1328. doi: 10.1126/science.284.5418.1322

Garnica-Vergara, A., Barrera-Ortiz, S., Munoz-Parra, E., Raya-Gonzalez, J., Mendez-Bravo, A., Macias-Rodriguez, L., et al. (2016). The volatile 6-pentyl-2H-pyran-2-one from Trichoderma atroviride regulates Arabidopsis thaliana root morphogenesis *via* auxin signaling and Ethylene Insensitive 2 functioning. *New Phytol.* 209, 1496–1512. doi: 10.1111/nph.13725

Gaspar, Y. M., Nam, J., Schultz, C. J., Lee, L. Y., Gilson, P. R., Gelvin, S. B., et al. (2004). Characterization of the Arabidopsis lysine-rich arabinogalactan-protein *AtAGP17* mutant (*rat1*) that results in a decreased efficiency of Agrobacterium transformation. *Plant Physiol.* 135, 2162–2171. doi: 10.1104/pp.104.045542

Geldner, N. (2013). The endodermis. *Annu. Rev. Plant Biol.* 64, 531–558. doi: 10.1146/annurev-arplant-050312-120050

Gilbert, J. A., Quinn, R. A., Debelius, J., Xu, Z. Z., Morton, J., Garg, N., et al. (2016). Microbiome-wide association studies link dynamic microbial consortia to disease. *Nature* 535, 94–103. doi: 10.1038/nature18850

Gkarmiri, K., Mahmood, S., Ekblad, A., Alstrom, S., Hogberg, N., and Finlay, R. (2017). Identifying the active microbiome associated with roots and rhizosphere soil of oilseed rape. *Appl. Environ. Microbiol.* 83, e01938–e01917. doi: 10.1128/AEM.01938-17

Glick, B. R. (2014). Bacteria with ACC deaminase can promote plant growth and help to feed the world. *Microbiol. Res.* 169, 30–39. doi: 10.1016/j.micres.2013.09.009

Gomez Exposito, R., De Bruijn, I., Postma, J., and Raaijmakers, J. M. (2017). Current insights into the role of rhizosphere bacteria in disease suppressive soils. *Front. Microbiol.* 8, 2529. doi: 10.3389/fmicb.2017.02529

Gomez-Gomez, L., and Boller, T. (2000). FLS2: an LRR receptor-like kinase involved in the perception of the bacterial elicitor flagellin in Arabidopsis. *Mol. Cell* 5, 1003–1011. doi: 10.1016/s1097-2765(00)80265-8

Gomez-Gomez, L., Felix, G., and Boller, T. (1999). A single locus determines sensitivity to bacterial flagellin in *Arabidopsis thaliana*. *Plant J.* 18, 277–284. doi: 10.1046/j.1365-313x.1999.00451.x

Gonzalez, M., Pujol, M., Metraux, J. P., Gonzalez-Garcia, V., Bolton, M. D., and Borras-Hidalgo, O. (2011). Tobacco leaf spot and root rot caused by *Rhizoctonia solani* Kuhn. *Mol. Plant Pathol.* 12, 209–216. doi: 10.1111/j.1364-3703.2010.00664.x

Gonzalez, E., Pitre, F. E., Page, A. P., Marleau, J., Guidi Nissim, W., St-Arnaud, M., et al. (2018). Trees, fungi and bacteria: tripartite metatranscriptomics of a root microbiome responding to soil contamination. *Microbiome* 6, 53. doi: 10.1186/s40168-018-0432-5

Hacquard, S., Spaepen, S., Garrido-Oter, R., and Schulze-Lefert, P. (2017). Interplay between innate immunity and the plant microbiota. *Annu. Rev. Phytopathol.* 55, 565–589. doi: 10.1146/annurev-phyto-080516-035623

Hao, W. Y., Ren, L. X., Ran, W., and Shen, Q. R. (2010). Allelopathic effects of root exudates from watermelon and rice plants on *Fusarium oxysporum* f.sp. *niveum*. *Plant Soil* 336, 485–497. doi: 10.1007/s11104-010-0505-0

Harman, G. E., Howell, C. R., Viterbo, A., Chet, I., and Lorito, M. (2004). Trichoderma species–opportunistic, avirulent plant symbionts. *Nat. Rev. Microbiol.* 2, 43–56. doi: 10.1038/nrmicro797

Hassani, M. A., Duran, P., and Hacquard, S. (2018). Microbial interactions within the plant holobiont. *Microbiome* 6, 58. doi: 10.1186/s40168-018-0445-0

Helfrich, E. J. N., Vogel, C. M., Ueoka, R., Schafer, M., Ryffel, F., Muller, D. B., et al. (2018). Bipartite interactions, antibiotic production and biosynthetic potential of the *Arabidopsis* leaf microbiome. *Nat. Microbiol.* 3, 909–919. doi: 10.1038/s41564-018-0200-0

Hiltner, L. (1904). Uber neure Erfahrungen und probleme aufdem gebeit der bodenbackteriologie und unter besonderer berucksichtigung der grundungung und brache. *Arb. Dtsch. Landwirtsch. Gesellschaft* 98, 59–78.

Hiruma, K., Gerlach, N., Sacristan, S., Nakano, R. T., Hacquard, S., Kracher, B., et al. (2016). Root endophyte *Colletotrichum tofieldiae* confers plant fitness benefits that are phosphate status dependent. *Cell* 165, 464–474. doi: 10.1016/j.cell.2016.02.028

Hu, J., Wei, Z., Friman, V. P., Gu, S. H., Wang, X. F., Eisenhauer, N., et al. (2016). Probiotic diversity enhances rhizosphere microbiome function and plant disease suppression. *MBio* 7, e01790–e01716. doi: 10.1128/mBio.01790-16

Hu, J., Wei, Z., Weidner, S., Friman, V. P., Xu, Y. C., Shen, Q. R., et al. (2017). Probiotic *Pseudomonas* communities enhance plant growth and nutrient assimilation *via* diversity-mediated ecosystem functioning. *Soil Biol. Biochem.* 113, 122–129. doi: 10.1016/j.soilbio.2017.05.029

Hu, L., Robert, C. A. M., Cadot, S., Zhang, X., Ye, M., Li, B., et al. (2018). Root exudate metabolites drive plant-soil feedbacks on growth and defense by shaping the rhizosphere microbiota. *Nat. Commun.* 9, 2738. doi: 10.1038/s41467-018-05122-7

Huang, A. C., Jiang, T., Liu, Y. X., Bai, Y. C., Reed, J., Qu, B., et al. (2019). A specialized metabolic network selectively modulates Arabidopsis root microbiota. *Science* 364, eaau6389. doi: 10.1126/science.aau6389

Jacobs, S., Zechmann, B., Molitor, A., Trujillo, M., Petutschnig, E., Lipka, V., et al. (2011). Broad-spectrum suppression of innate immunity is required for colonization of Arabidopsis roots by the fungus *Piriformospora indica*. *Plant Physiol.* 156, 726–740. doi: 10.1104/pp.111.176446

Jacoby, R. P., and Kopriva, S. (2018). Metabolic niches in the rhizosphere microbiome: new tools and approaches to analyse metabolic mechanisms of plant-microbe nutrient exchange. *J. Exp. Bot.* 70, 1087–1094. doi: 10.1093/jxb/ery438

Jacoby, R., Peukert, M., Succurro, A., Koprivova, A., and Kopriva, S. (2017). The role of soil microorganisms in plant mineral nutrition-current knowledge and future directions. *Front. Plant Sci.* 8, 1617. doi: 10.3389/fpls.2017.01617

Jansson, J. K., and Baker, E. S. (2016). A multi-omic future for microbiome studies. *Nat. Microbiol.* 1, 16049. doi: 10.1038/nmicrobiol.2016.49

Jiang, Y., Wang, W., Xie, Q., Liu, N., Liu, L., Wang, D., et al. (2017). Plants transfer lipids to sustain colonization by mutualistic mycorrhizal and parasitic fungi. *Science* 356, 1172–1175. doi: 10.1126/science.aam9970

Jimenez-Guerrero, I., Perez-Montano, F., Monreal, J. A., Preston, G. M., Fones, H., Vioque, B., et al. (2015). The *Sinorhizobium (Ensifer) fredii* HH103 type 3 secretion system suppresses early defense responses to effectively nodulate soybean. *Mol. Plant-Microbe Interact.* 28, 790–799. doi: 10.1094/MPMI-01-15-0020-R

Jin, C. W., You, G. Y., He, Y. F., Tang, C., Wu, P., and Zheng, S. J. (2007). Iron deficiency-induced secretion of phenolics facilitates the reutilization of root apoplastic iron in red clover. *Plant Physiol.* 144, 278–285. doi: 10.1104/pp.107.095794

Jung, S. C., Martinez-Medina, A., Lopez-Raez, J. A., and Pozo, M. J. (2012). Mycorrhiza-induced resistance and priming of plant defenses. *J. Chem. Ecol.* 38, 651–664. doi: 10.1007/s10886-012-0134-6

Kai, K., Mizutani, M., Kawamura, N., Yamamoto, R., Tamai, M., Yamaguchi, H., et al. (2008). Scopoletin is biosynthesized *via* ortho-hydroxylation of feruloyl CoA by a 2-oxoglutarate-dependent dioxygenase in *Arabidopsis thaliana*. *Plant J.* 55, 989–999. doi: 10.1111/j.1365-313X.2008.03568.x

Katan, J. (2017). Diseases caused by soilborne pathogens: biology, management and challenges. *J. Plant Pathol.* 99, 305–315. doi: 10.4454/jpp.v99i2.3862

Kloepper, J. W., Ryu, C. M., and Zhang, S. (2004). Induced systemic resistance and promotion of plant growth by *Bacillus* spp. *Phytopathology* 94, 1259–1266. doi: 10.1094/PHYTO.2004.94.11.1259

Kloppholz, S., Kuhn, H., and Requena, N. (2011). A secreted fungal effector of *Glomus intraradices* promotes symbiotic biotrophy. *Curr. Biol.* 21, 1204–1209. doi: 10.1016/j.cub.2011.06.044

Klosterman, S. J., Atallah, Z. K., Vallad, G. E., and Subbarao, K. V. (2009). Diversity, pathogenicity, and management of *Verticillium* species. *Annu. Rev. Phytopathol.* 47, 39–62. doi: 10.1146/annurev-phyto-080508-081748

Koike, S., Subbarao, K., Davis, R. M., and Turini, T. (2003). Vegetable diseases caused by soilborne pathogens. UCANR Publications. 8099:12.

Koprivova, A., Schuck, S., Jacoby, R. P., Klinkhammer, I., Welter, B., Leson, L., et al. (2019). Root-specific camalexin biosynthesis controls the plant growth-promoting effects of multiple bacterial strains. *Proc. Natl. Acad. Sci. U. S. A.* 116, 15735–15744. doi: 10.1073/pnas.1818604116

Kuiper, I., Lagendijk, E. L., Bloemberg, G. V., and Lugtenberg, B. J. (2004). Rhizoremediation: a beneficial plant-microbe interaction. *Mol. Plant-Microbe Interact.* 17, 6–15. doi: 10.1094/MPMI.2004.17.1.6

Kunze, G., Zipfel, C., Robatzek, S., Niehaus, K., Boller, T., and Felix, G. (2004). The N terminus of bacterial elongation factor Tu elicits innate immunity in Arabidopsis plants. *Plant Cell* 16, 3496–3507. doi: 10.1105/tpc.104.026765

Kwak, M. J., Kong, H. G., Choi, K., Kwon, S. K., Song, J. Y., Lee, J., et al. (2018). Rhizosphere microbiome structure alters to enable wilt resistance in tomato. *Nat. Biotechnol.* 36, 1100–1109. doi: 10.1038/nbt.4232

Lamour, K. H., Stam, R., Jupe, J., and Huitema, E. (2012). The oomycete broad-host-range pathogen *Phytophthora capsici*. *Mol. Plant Pathol.* 13, 329–337. doi: 10.1111/j.1364-3703.2011.00754.x

Lawson, C. E., Harcombe, W. R., Hatzenpichler, R., Lindemann, S. R., Loffler, F. E., O'malley, M. A., et al. (2019). Common principles and best practices for engineering microbiomes. *Nat. Rev. Microbiol.* 17, 725–741. doi: 10.1038/s41579-019-0255-9

Lebeis, S. L., Paredes, S. H., Lundberg, D. S., Breakfield, N., Gehring, J., Mcdonald, M., et al. (2015). Salicylic acid modulates colonization of the root microbiome by specific bacterial taxa. *Science* 349, 860–864. doi: 10.1126/science.aaa8764

Lee, B., Lee, S., and Ryu, C. M. (2012). Foliar aphid feeding recruits rhizosphere bacteria and primes plant immunity against pathogenic and non-pathogenic bacteria in pepper. *Ann. Bot.* 110, 281–290. doi: 10.1093/aob/mcs055

Lee, H. R., Lee, S., Park, S., Van Kleeff, P. J. M., Schuurink, R. C., and Ryu, C. M. (2018). Transient expression of whitefly effectors in *Nicotiana benthamiana* leaves activates systemic immunity against the leaf pathogen *Pseudomonas syringae* and soil-borne pathogen *Ralstonia solanacearum*. *Front. Ecol. Evol.* 6, 90. doi: 10.3389/fevo.2018.00090

Leff, J. W., Lynch, R. C., Kane, N. C., and Fierer, N. (2017). Plant domestication and the assembly of bacterial and fungal communities associated with strains of the common sunflower, *Helianthus annuus*. *New Phytol.* 214, 412–423. doi: 10.1111/nph.14323

Levy, A., Conway, J. M., Dangl, J. L., and Woyke, T. (2018). Elucidating bacterial gene functions in the plant microbiome. *Cell Host Microbe* 24, 475–485. doi: 10.1016/j.chom.2018.09.005

Liu, H., Macdonald, C. A., Cook, J., Anderson, I. C., and Singh, B. K. (2019a). An ecological loop: Host microbiomes across multitrophic interactions. *Trends Ecol. Evol.* 34, 1118–1130. doi: 10.1016/j.tree.2019.07.011

Liu, Y., Zhu, A., Tan, H., Cao, L., and Zhang, R. (2019b). Engineering banana endosphere microbiome to improve Fusarium wilt resistance in banana. *Microbiome* 7, 74. doi: 10.1186/s40168-019-0690-x

Lombardi, N., Vitale, S., Turra, D., Reverberi, M., Fanelli, C., Vinale, F., et al. (2018). Root exudates of stressed plants stimulate and attract *Trichoderma* soil fungi. *Mol. Plant-Microbe Interact.* 31, 982–994. doi: 10.1094/MPMI-12-17-0310-R

Loper, J. E., Hassan, K. A., Mavrodi, D. V., Davis Ii, E. W., Lim, C. K., Shaffer, B. T., et al. (2012). Comparative genomics of plant-associated *Pseudomonas* spp.: insights into diversity and inheritance of traits involved in multitrophic interactions. *PloS Genet.* 8, e1002784. doi: 10.1371/journal.pgen.1002784

Loreau, M., Naeem, S., Inchausti, P., Bengtsson, J., Grime, J. P., Hector, A., et al. (2001). Biodiversity and ecosystem functioning: current knowledge and future challenges. *Science* 294, 804–808. doi: 10.1126/science.1064088

Lugtenberg, B., and Kamilova, F. (2009). Plant-growth-promoting rhizobacteria. *Annu. Rev. Microbiol.* 63, 541–556. doi: 10.1146/annurev.micro.62.081307.162918

Lundberg, D. S., Lebeis, S. L., Paredes, S. H., Yourstone, S., Gehring, J., Malfatti, S., et al. (2012). Defining the core *Arabidopsis thaliana* root microbiome. *Nature* 488, 86–90. doi: 10.1038/nature11237

Maclean, A. M., Bravo, A., and Harrison, M. J. (2017). Plant signaling and metabolic pathways enabling arbuscular mycorrhizal symbiosis. *Plant Cell* 29, 2319–2335. doi: 10.1105/tpc.17.00555

Manganiello, G., Sacco, A., Ercolano, M. R., Vinale, F., Lanzuise, S., Pascale, A., et al. (2018). Modulation of tomato response to *Rhizoctonia solani* by *Trichoderma harzianum* and its secondary metabolite harzianic Acid. *Front. In Microbiol.* 9, 1966. doi: 10.3389/fmicb.2018.01966

Marhavy, P., Kurenda, A., Siddique, S., Denervaud Tendon, V., Zhou, F., Holbein, J., et al. (2019). Single-cell damage elicits regional, nematode-restricting ethylene responses in roots. *EMBO J.* 38, e100972. doi: 10.15252/embj.2018100972

Martin, F. M., Uroz, S., and Barker, D. G. (2017). Ancestral alliances: Plant mutualistic symbioses with fungi and bacteria. *Science* 356, eaad4501. doi: 10.1126/science.aad4501

Martinez-Medina, A., Flors, V., Heil, M., Mauch-Mani, B., Pieterse, C. M. J., Pozo, M. J., et al. (2016). Recognizing plant defense priming. *Trends Plant Sci.* 21, 818–822. doi: 10.1016/j.tplants.2016.07.009

Martinez-Medina, A., Van Wees, S. C. M., and Pieterse, C. M. J. (2017). Airborne signals by *Trichoderma* fungi stimulate iron uptake responses in roots resulting in priming of jasmonic acid-dependent defences in shoots of *Arabidopsis thaliana* and *Solanum lycopersicum*. *Plant Cell Environ.* 40, 2691–2705. doi: 10.1111/pce.13016

Massalha, H., Korenblum, E., Malitsky, S., Shapiro, O. H., and Aharoni, A. (2017). Live imaging of root-bacteria interactions in a microfluidics setup. *Proc. Natl. Acad. Sci. U. S. A.* 114, 4549–4554. doi: 10.1073/pnas.1618584114

Matthews, A., Pierce, S., Hipperson, H., and Raymond, B. (2019). Rhizobacterial community assembly patterns vary between crop species. *Front. Microbiol.* 10, 581. doi: 10.3389/fmicb.2019.00581

Mavrodi, D. V., Joe, A., Mavrodi, O. V., Hassan, K. A., Weller, D. M., Paulsen, I. T., et al. (2011). Structural and functional analysis of the type III secretion system from *Pseudomonas fluorescens* Q8r1-96. *J. Bacteriol.* 193, 177–189. doi: 10.1128/JB.00895-10

Mazzola, M. (2002). Mechanisms of natural soil suppressiveness to soilborne diseases. *Antonie Van Leeuwenhoek* 81, 557–564. doi: 10.1023/A:1020557523557

Mendes, R., Kruijt, M., De Bruijn, I., Dekkers, E., Van Der Voort, M., Schneider,? J.?H., et al. (2011). Deciphering the rhizosphere microbiome for disease-suppressive bacteria. *Science* 332, 1097–1100. doi: 10.1126/science.1203980

Mendes, L. W., Raaijmakers, J. M., De Hollander, M., Mendes, R., and Tsai, S. M. (2018). Influence of resistance breeding in common bean on rhizosphere

microbiome composition and function. *ISME J.* 12, 212–224. doi: 10.1038/ismej.2017.158

Michielse, C. B., and Rep, M. (2009). Pathogen profile update: *Fusarium oxysporum*. *Mol. Plant Pathol.* 10, 311–324. doi: 10.1111/j.1364-3703.2009.00538.x

Millet, Y. A., Danna, C. H., Clay, N. K., Songnuan, W., Simon, M. D., Werck-Reichhart, D., et al. (2010). Innate immune responses activated in Arabidopsis roots by microbe-associated molecular patterns *Plant Cell* 22, 973–990. doi: 10.1105/tpc.109.069658

Miya, A., Albert, P., Shinya, T., Desaki, Y., Ichimura, K., Shirasu, K., et al. (2007). CERK1, a LysM receptor kinase, is essential for chitin elicitor signaling in Arabidopsis. *Proc. Natl. Acad. Sci. U.S.A.* 104, 19613–19618. doi: 10.1073/pnas.0705147104

Molina-Romero, D., Baez, A., Quintero-Hernandez, V., Castaneda-Lucio, M., Fuentes-Ramirez, L. E., Bustillos-Cristales, M. D. R., et al. (2017). Compatible bacterial mixture, tolerant to desiccation, improves maize plant growth. *PloS One* 12, e0187913. doi: 10.1371/journal.pone.0187913

Muller, D. B., Vogel, C., Bai, Y., and Vorholt, J. A. (2016). The plant microbiota: systems-level insights and perspectives. *Annu. Rev. Genet.* 50, 211–234. doi: 10.1146/annurev-genet-120215-034952

Naseer, S., Lee, Y., Lapierre, C., Franke, R., Nawrath, C., and Geldner, N. (2012). Casparian strip diffusion barrier in *Arabidopsis is* made of a lignin polymer without suberin. *Proc. Natl. Acad. Sci. U.S.A.* 109, 10101–10106. doi: 10.1073/pnas.1205726109

Neal, A. L., Ahmad, S., Gordon-Weeks, R., and Ton, J. (2012). Benzoxazinoids in root exudates of maize attract *Pseudomonas putida* to the rhizosphere. *PloS One* 7, e35498. doi: 10.1371/journal.pone.0035498

Niu, B., Paulson, J. N., Zheng, X., and Kolter, R. (2017). Simplified and representative bacterial community of maize roots. *Proc. Natl. Acad. Sci. U. S. A.* 114, 2450–2459. doi: 10.1073/pnas.1616148114

O' Banion, B., O' Neal, L., Alexandre, G., and Lebeis, S. (2019). Bridging the gap between single-strain and community-level plant-microbe chemical interactions. *Mol. Plant-Microbe Interact.* doi: 10.1094/MPMI-1004-1019-0115-CR

Ofek-Lalzar, M., Sela, N., Goldman-Voronov, M., Green, S. J., Hadar, Y., and Minz, D. (2014). Niche and host-associated functional signatures of the root surface microbiome. *Nat. Commun.* 5, 4950. doi: 10.1038/ncomms5950

Okubara, P. A., and Paulitz, T. C. (2005). Root defense responses to fungal pathogens: a molecular perspective. *Plant and Soil*, 274, 215–226. doi: 10.1007/s11104-004-7328-9

Oldroyd, G. E. (2013). Speak, friend, and enter: signalling systems that promote beneficial symbiotic associations in plants. *Nat. Rev. Microbiol.* 11, 252–263. doi: 10.1038/nrmicro2990

Ongena, M., and Jacques, P. (2008). *Bacillus* lipopeptides: versatile weapons for plant disease biocontrol. *Trends Microbiol.* 16, 115–125.

Papadopoulou, K., Melton, R. E., Leggett, M., Daniels, M. J., and Osbourn, A. E. (1999). Compromised disease resistance in saponin-deficient plants. *Proc. Natl. Acad. Sci. U. S. A.* 96, 12923–12928. doi: 10.1073/pnas.96.22.12923

Paredes, S. H., Gao, T. X., Law, T. F., Finkel, O. M., Mucyn, T., Teixeira, P. J. P. L., et al. (2018). Design of synthetic bacterial communities for predictable plant phenotypes. *PloS Biol.* 16, e2003962. doi: 10.1371/journal.pbio.2003962

Parniske, M. (2008). Arbuscular mycorrhiza: the mother of plant root endosymbioses. *Nat. Rev. Microbiol.* 6, 763–775. doi: 10.1038/nrmicro1987

Parratt, S. R., and Laine, A. L. (2018). Pathogen dynamics under both bottom-up host resistance and top-down hyperparasite attack. *J. Appl. Ecol.* 55, 2976–2985. doi: 10.1111/1365-2664.13185

Patkar, R. N., and Naqvi, N. I. (2017). Fungal manipulation of hormone-regulated plant defense. *PloS Pathog.* 13, e1006334. doi: 10.1371/journal.ppat.1006334

Peeters, N., Guidot, A., Vailleau, F., and Valls, M. (2013). *Ralstonia solanacearum*, a widespread bacterial plant pathogen in the post-genomic era. *Mol. Plant Pathol.* 14, 651–662. doi: 10.1111/mpp.12038

Pel, M. J., Van Dijken, A. J., Bardoel, B. W., Seidl, M. F., Van Der Ent, S., Van Strijp, J. A., et al. (2014). *Pseudomonas syringae* evades host immunity by degrading flagellin monomers with alkaline protease AprA. *Mol. Plant-Microbe Interact.* 27, 603–610. doi: 10.1094/MPMI-02-14-0032-R

Penton, C. R., Gupta, V. V., Tiedje, J. M., Neate, S. M., Ophel-Keller, K., Gillings, M., et al. (2014). Fungal community structure in disease suppressive soils assessed by 28S LSU gene sequencing. *PloS One* 9, e93893. doi: 10.1371/journal.pone.0093893

Perez-Garcia, O., Lear, G., and Singhal, N. (2016). Metabolic network modeling of microbial interactions in natural and engineered environmental systems. *Front. Microbiol.* 7, 673. doi: 10.3389/fmicb.2016.00673

Pérez-Jaramillo, J. E., Mendes, R., and Raaijmakers, J. M. (2016). Impact of plant domestication on rhizosphere microbiome assembly and functions. *Plant Mol. Biol.* 90, 635–644. doi: 10.1007/s11103-015-0337-7

Pérez-Jaramillo, J. E., Carrion, V. J., Bosse, M., Ferrao, L. F. V., De Hollander, M., Garcia, A.a.F., et al. (2017). Linking rhizosphere microbiome composition of wild and domesticated *Phaseolus vulgaris* to genotypic and root phenotypic traits. *ISME J.* 11, 2244–2257. doi: 10.1038/ismej.2017.85

Perez-Jaramillo, J. E., Carrion, V. J., De Hollander, M., and Raaijmakers, J. M. (2018). The wild side of plant microbiomes. *Microbiome* 6, 143. doi: 10.1186/s40168-018-0519-z

Pérez-Jaramillo, J. E., De Hollander, M., Ramírez, C. A., Mendes, R., Raaijmakers, J. M., and Carrión, V. J. (2019). Deciphering rhizosphere microbiome assembly of wild and modern common bean (*Phaseolus vulgaris*) in native and agricultural soils from Colombia. *Microbiome* 7, 114.

Pieterse, C. M. J., Leon-Reyes, A., Van Der Ent, S., and Van Wees, S. C. M. (2009). Networking by small-molecule hormones in plant immunity. *Nat. Chem. Biol.* 5, 308–316. doi: 10.1038/nchembio.164

Pieterse, C. M. J., Van Der Does, D., Zamioudis, C., Leon-Reyes, A., and Van Wees, S. C. M. (2012). Hormonal modulation of plant immunity. *Annu. Rev. Cell Dev. Biol.* 28, 489–521. doi: 10.1146/annurev-cellbio-092910-154055

Pieterse, C. M. J., Zamioudis, C., Berendsen, R. L., Weller, D. M., Van Wees, S. C. M., and Bakker, P. A. H. M. (2014). Induced systemic resistance by beneficial microbes. *Annu. Rev. Phytopathol.* 52, 347–375. doi: 10.1146/annurev-phyto-082712-102340

Pieterse, C. M. J., De Jonge, R., and Berendsen, R. L. (2016). The soil-borne supremacy. *Trends Plant Sci.* 21, 171–173. doi: 10.1016/j.tplants.2016.01.018

Pimentel, D. L., McLaughlin, A., Zepp, B., Lakitan, T., Kraus, P., Kleinman, F., et al. (1991). Environmental and economic effects of reducing pesticide use. *Bioscience*, 41, 492–409. doi: 10.2307/1311747

Pini, F., East, A. K., Appia-Ayme, C., Tomek, J., Karunakaran, R., Mendoza-Suarez, M., et al. (2017). Bacterial biosensors for *in vivo* spatiotemporal mapping of root secretion. *Plant Physiol.* 174, 1289–1306. doi: 10.1104/pp.16.01302

Plett, J. M., Kemppainen, M., Kale, S. D., Kohler, A., Legue, V., Brun, A., et al. (2011). A secreted effector protein of *Laccaria bicolor* is required for symbiosis development. *Curr. Biol.* 21, 1197–1203. doi: 10.1016/j.cub.2011.05.033

Plett, J. M., Daguerre, Y., Wittulsky, S., Vayssieres, A., Deveau, A., Melton, S. J., et al. (2014a). Effector MiSSP7 of the mutualistic fungus *Laccaria bicolor* stabilizes the Populus JAZ6 protein and represses jasmonic acid (JA) responsive genes. *Proc. Natl. Acad. Sci. U. S. A.* 111, 8299–8304. doi: 10.1073/pnas.1322671111

Plett, J. M., Khachane, A., Ouassou, M., Sundberg, B., Kohler, A., and Martin, F. (2014b). Ethylene and jasmonic acid act as negative modulators during mutualistic symbiosis between *Laccaria bicolor* and Populus roots. *New Phytol.* 202, 270–286. doi: 10.1111/nph.12655

Poncini, L., Wyrsch, I., Denervaud Tendon, V., Vorley, T., Boller, T., Geldner, N., et al. (2017). In roots of *Arabidopsis thaliana*, the damage-associated molecular pattern AtPep1 is a stronger elicitor of immune signalling than flg22 or the chitin heptamer. *PloS One* 12, e0185808. doi: 10.1371/journal.pone.0185808

Poole, P., Ramachandran, V., and Terpolilli, J. (2018). Rhizobia: from saprophytes to endosymbionts. *Nat. Rev. Microbiol.* 16, 291–303. doi: 10.1038/nrmicro.2017.171

Poudel, R., Jumpponen, A., Schlatter, D. C., Paulitz, T. C., Gardener, B. B., Kinkel, L. L., et al. (2016). Microbiome networks: a systems framework for identifying candidate microbial assemblages for disease management. *Phytopathology* 106, 1083–1096. doi: 10.1094/PHYTO-02-16-0058-FI

Preston, G. M., Bertrand, N., and Rainey, P. B. (2001). Type III secretion in plant growth-promoting *Pseudomonas fluorescens* SBW25. *Mol. Microbiol.* 41, 999–1014. doi: 10.1046/j.1365-2958.2001.02560.x

Raaijmakers, J. M., and Mazzola, M. (2016). Soil immune responses. *Science* 352, 1392–1393. doi: 10.1126/science.aaf3252

Raaijmakers, J. M., and Weller, D. M. (1998). Natural plant protection by 2,4-diacetylphloroglucinol - producing *Pseudomonas* spp. in take-all decline soils. *Mol. Plant-Microbe Interact.* 11. doi: 10.1094/MPMI.1998.11.2.144

Raaijmakers, J. M., Paulitz, T. C., Steinberg, C., Alabouvette, C., and Moenne-Loccoz, Y. (2009). The rhizosphere: a playground and battlefield for soilborne pathogens and beneficial microorganisms. *Plant Soil* 321, 341–361. doi: 10.1007/s11104-008-9568-6

Raaijmakers, J. M., De Bruijn, I., Nybroe, O., and Ongena, M. (2010). Natural functions of lipopeptides from *Bacillus* and *Pseudomonas*: more than surfactants and antibiotics. *FEMS Microbiol. Rev.* 34, 1037–1062. doi: 10.1111/j.1574-6976.2010.00221.x

Rajniak, J., Giehl, R. F. H., Chang, E., Murgia, I., Von Wiren, N., and Sattely, E. S. (2018). Biosynthesis of redox-active metabolites in response to iron deficiency in plants. *Nat. Chem. Biol.* 14, 442–450. doi: 10.1038/s41589-018-0019-2

Rascovan, N., Carbonetto, B., Perrig, D., Diaz, M., Canciani, W., Abalo, M., et al. (2016). Integrated analysis of root microbiomes of soybean and wheat from agricultural fields. *Sci. Rep.* 6, 28084. doi: 10.1038/srep28084

Reinhold-Hurek, B., Bunger, W., Burbano, C. S., Sabale, M., and Hurek, T. (2015). Roots shaping their microbiome: global hotspots for microbial activity. *Annu. Rev. Phytopathol.* 53, 403–424. doi: 10.1146/annurev-phyto-082712-102342

Robbins, C., Thiergart, T., Hacquard, S., Garrido-Oter, R., Gans, W., Peiter, E., et al. (2018). Root-associated bacterial and fungal community profiles of *Arabidopsis thaliana* are robust across contrasting soil P levels. *Phytobiomes J.* 2, 24–34. doi: 10.1094/PBIOMES-09-17-0042-R

Robertson-Albertyn, S., Alegria Terrazas, R., Balbirnie, K., Blank, M., Janiak, A., Szarejko, I., et al. (2017). Root hair mutations displace the barley rhizosphere microbiota. *Front. Plant Sci.* 8, 1094. doi: 10.3389/fpls.2017.01094

Rodriguez, P. A., Rothballer, M., Chowdhury, S. P., Nussbaumer, T., Gutjahr, C., and Falter-Braun, P. (2019). Systems biology of plant-microbiome interactions. *Mol. Plant* 12, 804–821. doi: 10.1016/j.molp.2019.05.006

Rodriguez-Celma, J., Lin, W. D., Fu, G. M., Abadia, J., Lopez-Millan, A. F., and Schmidt, W. (2013). Mutually exclusive alterations in secondary metabolism are critical for the uptake of insoluble iron compounds by Arabidopsis and *Medicago truncatula*. *Plant Physiol.* 162, 1473–1485. doi: 10.1104/pp.113.220426

Rolli, E., Marasco, R., Vigani, G., Ettoumi, B., Mapelli, F., Deangelis, M. L., et al. (2015). Improved plant resistance to drought is promoted by the root-associated microbiome as a water stress-dependent trait. *Environ. Microbiol.* 17, 316–331. doi: 10.1111/1462-2920.12439

Rudrappa, T., Czymmek, K. J., Pare, P. W., and Bais, H. P. (2008). Root-secreted malic acid recruits beneficial soil bacteria. *Plant Physiol.* 148, 1547–1556. doi: 10.1104/pp.108.127613

Santhanam, R., Luu, V. T., Weinhold, A., Goldberg, J., Oh, Y., and Baldwin, I. T. (2015). Native root-associated bacteria rescue a plant from a sudden-wilt disease that emerged during continuous cropping. *Proc. Natl. Acad. Sci. U.?S.?A.* 112, 5013–5020. doi: 10.1073/pnas.1505765112

Sasse, J., Martinoia, E., and Northen, T. (2017). Feed your friends: do plant exudates shape the root microbiome? *Trends Plant Sci.* 23, 25–41. doi: 10.1016/j.tplants.2017.09.003

Schafer, P., Pfiffi, S., Voll, L. M., Zajic, D., Chandler, P. M., Waller, F., et al. (2009). Manipulation of plant innate immunity and gibberellin as factor of compatibility in the mutualistic association of barley roots with *Piriformospora indica*. *Plant J.* 59, 461–474. doi: 10.1111/j.1365-313X.2009.03887.x

Schlaeppi, K., Dombrowski, N., Garrido-Oter, R., Ver Loren Van Themaat, E., and Schulze-Lefert, P. (2014). Quantitative divergence of the bacterial root microbiota in *Arabidopsis thaliana* relatives. *Proc. Natl. Acad. Sci. U. S. A.* 111, 585–592. doi: 10.1073/pnas.1321597111

Schlatter, D., Kinkel, L., Thomashow, L., Weller, D., and Paulitz, T. (2017). Disease suppressive soils: new insights from the soil microbiome. *Phytopathology* 107, 1284–1297. doi: 10.1094/PHYTO-03-17-0111-RVW

Schmid, N. B., Giehl, R. F., Doll, S., Mock, H. P., Strehmel, N., Scheel, D., et al. (2014). Feruloyl-CoA 6'-Hydroxylase1-dependent coumarins mediate iron acquisition from alkaline substrates in Arabidopsis. *Plant Physiol.* 164, 160–172. doi: 10.1104/pp.113.228544

Schmidt, H., Gunther, C., Weber, M., Sporlein, C., Loscher, S., Bottcher, C., et al. (2014). Metabolome analysis of *Arabidopsis thaliana* roots identifies a key metabolic pathway for iron acquisition. *PloS One* 9, e102444. doi: 10.1371/journal.pone.0102444

Schoch, C. L., Seifert, K. A., Huhndorf, S., Robert, V., Spouge, J. L., Levesque, C. A., et al. (2012). Nuclear ribosomal internal transcribed spacer (ITS) region as a universal DNA barcode marker for *Fungi*. *Proc. Natl. Acad. Sci. U. S. A.* 109, 6241–6246. doi: 10.1073/pnas.1117018109

Senthil-Kumar, M., and Mysore, K. S. (2013). Nonhost resistance against bacterial pathogens: retrospectives and prospects. *Annu. Rev. Phytopathol.* 51, 407–427. doi: 10.1146/annurev-phyto-082712-102319

Sessitsch, A., Hardoim, P., Doring, J., Weilharter, A., Krause, A., Woyke, T., et al. (2012). Functional characteristics of an endophyte community colonizing rice roots as revealed by metagenomic analysis. *Mol. Plant-Microbe Interact.* 25, 28–36. doi: 10.1094/MPMI-08-11-0204

Sessitsch, A., Pfaffenbichler, N., and Mitter, B. (2019). Microbiome applications from lab to field: Facing complexity. *Trends Plant Sci.* 24, 194–198. doi: 10.1016/j.tplants.2018.12.004

Shakya, M., Gottel, N., Castro, H., Yang, Z. K., Gunter, L., Labbe, J., et al. (2013). A multifactor analysis of fungal and bacterial community structure in the root microbiome of mature *Populus deltoides* trees. *PloS One* 8, e76382. doi: 10.1371/journal.pone.0076382

Sharpton, T. J. (2014). An introduction to the analysis of shotgun metagenomic data. *Front. Plant Sci.* 5, 209. doi: 10.3389/fpls.2014.00209

Shi, W., Li, M., Wei, G., Tian, R., Li, C., Wang, B., et al. (2019). The occurrence of potato common scab correlates with the community composition and function of the geocaulosphere soil microbiome. *Microbiome* 7, 14. doi: 10.1186/s40168-019-0629-2

Shoresh, M., Harman, G. E., and Mastouri, F. (2010). Induced systemic resistance and plant responses to fungal biocontrol agents. *Annu. Rev. Phytopathol.* 48, 21–43. doi: 10.1146/annurev-phyto-073009-114450

Siegel-Hertz, K., Edel-Hermann, V., Chapelle, E., Terrat, S., Raaijmakers, J. M., and Steinberg, C. (2018). Comparative microbiome analysis of a Fusarium wilt suppressive soil and a Fusarium wilt conducive soil from the Chateaurenard region. *Front. Microbiol.* 9, 568. doi: 10.3389/fmicb.2018.00568

Snelders, N. C., Kettles, G. J., Rudd, J. J., and Thomma, B. P. H. J. (2018). Plant pathogen effector proteins as manipulators of host microbiomes? *Mol. Plant Pathol.* 19, 257–259. doi: 10.1111/mpp.12628

Steinkellner, S., Mammerler, R., and Vierheilig, H. (2005). Microconidia germination of the tomato pathogen *Fusarium oxysporum* in the presence of root exudates. *J. Plant Interact.* 1, 23–30. doi: 10.1080/17429140500134334

Stringlis, I. A., Proietti, S., Hickman, R., Van Verk, M. C., Zamioudis, C., and Pieterse, C. M. J. (2018a). Root transcriptional dynamics induced by beneficial rhizobacteria and microbial immune elicitors reveal signatures of adaptation to mutualists. *Plant J.* 93, 166–180. doi: 10.1111/tpj.13741

Stringlis, I. A., Yu, K., Feussner, K., De Jonge, R., Van Bentum, S., Van Verk, M. C., et al. (2018b). MYB72-dependent coumarin exudation shapes root microbiome assembly to promote plant health. *Proc. Natl. Acad. Sci. U. S. A.* 115, E5213–E5222. doi: 10.1073/pnas.1722335115

Stringlis, I. A., Zhang, H., Pieterse, C. M. J., Bolton, M. D., and De Jonge, R. (2018c). Microbial small molecules - weapons of plant subversion. *Natural Product Rep.* 35, 410–433. doi: 10.1039/c7np00062f

Stringlis, I. A., De Jonge, R., and Pieterse, C. M. J. (2019a). The age of coumarins in plant-microbe interactions. *Plant Cell Physiol.* 60, 1405–1419. doi: 10.1093/pcp/pcz076

Stringlis, I. A., Zamioudis, C., Berendsen, R. L., Bakker, P. A. H. M., and Pieterse, C. M. J. (2019b). Type III secretion system of beneficial rhizobacteria *Pseudomonas simiae* WCS417 and *Pseudomonas defensor* WCS374. *Front. Microbiol.* 10, 1631. doi: 10.3389/fmicb.2019.01631

Subramanian, S., Stacey, G., and Yu, O. (2007). Distinct, crucial roles of flavonoids during legume nodulation. *Trends In Plant Sci.* 12, 282–285. doi: 10.1016/j.tplants.2007.06.006

Thimmappa, R., Geisler, K., Louveau, T., O'maille, P., and Osbourn, A. (2014). Triterpene biosynthesis in plants. *Annu. Rev. Plant Biol.* 65, 225–257. doi: 10.1146/annurev-arplant-050312-120229

Tsai, H. H., and Schmidt, W. (2017a). Mobilization of iron by plant-borne coumarins. *Trends Plant Sci.* 22, 538–548. doi: 10.1016/j.tplants.2017.03.008

Tsai, H. H., and Schmidt, W. (2017b). One way. Or another? Iron uptake in plants. *New Phytol.* 214, 500–505. doi: 10.1111/nph.14477

Tsai, H. H., Rodriguez-Celma, J., Lan, P., Wu, Y. C., Velez-Bermudez, I. C., and Schmidt, W. (2018). Scopoletin 8-hydroxylase-mediated fraxetin production is crucial for iron mobilization. *Plant Physiol.* 177, 194–207. doi: 10.1104/pp.18.00178

Tsolakidou, M.-D., Stringlis, I. A., Fanega-Sleziak, N., Papageorgiou, S., Tsalakou, A., and Pantelides, I. S. (2019a). Rhizosphere-enriched microbes as a pool to design synthetic communities for reproducible beneficial outputs. *FEMS Microbiol. Ecol.* 95, fiz138. doi: 10.1093/femsec/fiz138

Tsolakidou, M. D., Pantelides, I. S., Tzima, A. K., Kang, S., Paplomatas, E. J., and Tsaltas, D. (2019b). Disruption and overexpression of the gene encoding ACC (1-aminocyclopropane-1-carboxylic acid) deaminase in soil-borne fungal pathogen *Verticillium dahliae* revealed the role of ACC as a potential regulator of virulence and plant defense. *Mol. Plant-Microbe Interact.* 32, 639–653. doi: 10.1094/MPMI-07-18-0203-R

Turner, T. R., Ramakrishnan, K., Walshaw, J., Heavens, D., Alston, M., Swarbreck, D., et al. (2013). Comparative metatranscriptomics reveals kingdom level changes in the rhizosphere microbiome of plants. *ISME J.* 7, 2248–2258. doi: 10.1038/ismej.2013.119

Turrà, D., El Ghalid, M., Rossi, F., and Di Pietro, A. (2015). Fungal pathogen uses sex pheromone receptor for chemotropic sensing of host plant signals. *Nature* 527, 521–524. doi: 10.1038/nature15516

Van Dam, N. M., and Bouwmeester, H. J. (2016). Metabolomics in the rhizosphere: Tapping into belowground chemical communication. *Trends Plant Sci.* 21, 256–265. doi: 10.1016/j.tplants.2016.01.008

Van De Mortel, J. E., Schat, H., Moerland, P. D., Ver Loren Van Themaat, E., Van Der Ent, S., Blankestijn, H., et al. (2008). Expression differences for genes involved in lignin, glutathione and sulphate metabolism in response to cadmium in *Arabidopsis thaliana* and the related Zn/Cd-hyperaccumulator *Thlaspi caerulescens*. *Plant Cell Environ.* 31, 301–324. doi: 10.1111/j.1365-3040.2007.01764.x

Van Der Ent, S., Verhagen, B. W., Van Doorn, R., Bakker, D., Verlaan, M. G., Pel, M. J., et al. (2008). *MYB72 is* required in early signaling steps of rhizobacteria-induced systemic resistance in Arabidopsis. *Plant Physiol.* 146, 1293–1304. doi: 10.1104/pp.107.113829

Van Der Heijden, M. G., and Hartmann, M. (2016). Networking in the plant microbiome. *PloS Biol.* 14, e1002378. doi: 10.1371/journal.pbio.1002378

Van West, P., Appiah, A. A., and Gow, N. A. R. (2003). Advances in research on oomycete root pathogens. *Physiol. Mol. Plant Pathol.* 62, 99–113. doi: 10.1016/S0885-5765(03)00044-4

Vandenkoornhuyse, P., Mahe, S., Ineson, P., Staddon, P., Ostle, N., Cliquet, J. B., et al. (2007). Active root-inhabiting microbes identified by rapid incorporation of plant-derived carbon into RNA. *Proc. Natl. Acad. Sci. U. S. A.* 104, 16970–16975. doi: 10.1073/pnas.0705902104

Vandenkoornhuyse, P., Quaiser, A., Duhamel, M., Le Van, A., and Dufresne, A. (2015). The importance of the microbiome of the plant holobiont. *New Phytol.* 206, 1196–1206. doi: 10.1111/nph.13312

Vannier, N., Agler, M., and Hacquard, S. (2019). Microbiota-mediated disease resistance in plants. *PloS Pathog.* 15, e1007740. doi: 10.1371/journal.ppat.1007740

Ventorino, V., Pascale, A., Fagnano, M., Adamo, P., Faraco, V., Rocco, C., et al. (2019). Soil tillage and compost amendment promote bioremediation and biofertility of polluted area. *J. Cleaner Prod.* 239, 118087. doi: 10.1016/j.jclepro.2019.118087

Verbon, E. H., and Liberman, L. M. (2016). Beneficial microbes affect endogenous mechanisms controlling root development. *Trends Plant Sci.* 21, 218–229. doi: 10.1016/j.tplants.2016.01.013

Verbon, E. H., Trapet, P. L., Stringlis, I. A., Kruijs, S., Bakker, P. A. H. M., and Pieterse, C. M. J. (2017). Iron and immunity. *Annu. Rev. Phytopathol.* 55, 355–375. doi: 10.1146/annurev-phyto-080516-035537

Verhagen, B. W., Glazebrook, J., Zhu, T., Chang, H. S., Van Loon, L. C., and Pieterse, C. M. J. (2004). The transcriptome of rhizobacteria-induced systemic resistance in Arabidopsis. *Mol. Plant-Microbe Interact.* 17, 895–908. doi: 10.1094/MPMI.2004.17.8.895

Vicre, M., Santaella, C., Blanchet, S., Gateau, A., and Driouich, A. (2005). Root border-like cells of Arabidopsis. Microscopical characterization and role in the interaction with rhizobacteria. *Plant Physiol.* 138, 998–1008. doi: 10.1104/pp.104.051813

Viterbo, A., Landau, U., Kim, S., Chernin, L., and Chet, I. (2010). Characterization of ACC deaminase from the biocontrol and plant growth-promoting agent *Trichoderma asperellum* T203. *FEMS Microbiol. Lett.* 305, 42–48. doi: 10.1111/j.1574-6968.2010.01910.x

Voges, M., Bai, Y., Schulze-Lefert, P., and Sattely, E. S. (2019). Plant-derived coumarins shape the composition of an Arabidopsis synthetic root microbiome. *Proc. Natl. Acad. Sci. U.S.A.* 116, 12558–12565. doi: 10.1073/pnas.1820691116

Vorholt, J. A., Vogel, C., Carlstrom, C. I., and Muller, D. B. (2017). Establishing causality: opportunities of synthetic communities for plant microbiome research. *Cell Host Microbe* 22, 142–155. doi: 10.1016/j.chom.2017.07.004

Vos, I. A., Pieterse, C. M. J., and Van Wees, S. C. M. (2013). Costs and benefits of hormone-regulated plant defences. *Plant Pathol.* 62, 43–55. doi: 10.1111/ppa.12105

Wachsman, G., Sparks, E. E., and Benfey, P. N. (2015). Genes and networks regulating root anatomy and architecture. *New Phytol.* 208, 26–38. doi: 10.1111/nph.13469

Wang, L., Albert, M., Einig, E., Furst, U., Krust, D., and Felix, G. (2016). The pattern-recognition receptor CORE of Solanaceae detects bacterial cold-shock protein. *Nat. Plants* 2, 16185. doi: 10.1038/nplants.2016.185

Wei, Z., Yang, T., Friman, V. P., Xu, Y., Shen, Q., and Jousset, A. (2015). Trophic network architecture of root-associated bacterial communities determines pathogen invasion and plant health. *Nat. Commun.* 6, 8413. doi: 10.1038/ncomms9413

Wei, Z., Gu, Y., Friman, V. P., Kowalchuk, G. A., Xu, Y., Shen, Q., et al. (2019). Initial soil microbiome composition and functioning predetermine future plant health. *Sci. Adv.* 5, eaaw0759. doi: 10.1126/sciadv.aaw0759

Weiss, M., Waller, F., Zuccaro, A., and Selosse, M. A. (2016). Sebacinales - one thousand and one interactions with land plants. *New Phytol.* 211, 20–40. doi: 10.1111/nph.13977

Weller, D. M., Raaijmakers, J. M., Gardener, B. B., and Thomashow, L. S. (2002). Microbial populations responsible for specific soil suppressiveness to plant pathogens. *Annu. Rev. Phytopathol.* 40, 309–348. doi: 10.1146/annurev.phyto.40.030402.110010

Wintermans, P. C., Bakker, P. A. H. M., and Pieterse, C. M. J. (2016). Natural genetic variation in *Arabidopsis* for responsiveness to plant growth-promoting rhizobacteria. *Plant Mol. Biol.* 90, 623–634. doi: 10.1007/s11103-016-0442-2

Wyrsch, I., Dominguez-Ferreras, A., Geldner, N., and Boller, T. (2015). Tissue-specific FLAGELLIN-SENSING 2 (FLS2) expression in roots restores immune responses in Arabidopsis *fls2* mutants. *New Phytol.* 206, 774–784. doi: 10.1111/nph.13280

Xie, F., Williams, A., Edwards, A., and Downie, J. A. (2012). A plant arabinogalactan-like glycoprotein promotes a novel type of polar surface attachment by *Rhizobium leguminosarum*. *Mol. Plant-Microbe Interact.* 25, 250–258. doi: 10.1094/MPMI-08-11-0211

Xu, D., Hanschen, F. S., Witzel, K., Nintemann, S. J., Nour-Eldin, H. H., Schreiner, M., et al. (2017). Rhizosecretion of stele-synthesized glucosinolates and their catabolites requires GTR-mediated import in Arabidopsis. *J. Exp. Bot.* 68, 3205–3214. doi: 10.1093/jxb/erw355

Yadav, V., Kumar, M., Deep, D. K., Kumar, H., Sharma, R., Tripathi, T., et al. (2010). A phosphate transporter from the root endophytic fungus *Piriformospora indica* plays a role in phosphate transport to the host plant. *J. Biol. Chem.* 285, 26532–26544. doi: 10.1074/jbc.M110.111021

Yadeta, K. A., and Thomma, B. P. H. J. (2013). The xylem as battleground for plant hosts and vascular wilt pathogens. *Front. Plant Sci.* 4, 97. doi: 10.3389/fpls.2013.00097

Yang, J., Kloepper, J. W., and Ryu, C. M. (2009). Rhizosphere bacteria help plants tolerate abiotic stress. *Trends Plant Sci.* 14, 1–4. doi: 10.1016/j.tplants.2008.10.004

Yang, J. W., Yi, H. S., Kim, H., Lee, B., Lee, S., Ghim, S. Y., et al. (2011). Whitefly infestation of pepper plants elicits defence responses against bacterial pathogens in leaves and roots and changes the below-ground microflora. *J.? Ecol.* 99, 46–56. doi: 10.1111/j.1365-2745.2010.01756.x

Yu, K., Pieterse, C. M. J., Bakker, P. A. H. M., and Berendsen, R. L. (2019a). Beneficial microbes going underground of root immunity. *Plant Cell Environ.* 42, 2860–2870. doi: 10.1111/pce.13632

Yu, K., Tichelaar, R., Liu, Y., Savant, N., Lagendijk, E., Van Kuijk, S., et al. (2019b). Rhizopshere-associated *Pseudomonas* suppress local root immune responses

by gluconic acid-mediated lowering of environmental pH. *Curr. Biol.* 29, 3913–3920. doi: 10.1016/j.cub.2019.09.015

Yuan, J., Zhao, J., Wen, T., Zhao, M., Li, R., Goossens, P., et al. (2018). Root exudates drive the soil-borne legacy of aboveground pathogen infection. *Microbiome* 6, 156. doi: 10.1186/s40168-018-0537-x

Zamioudis, C., and Pieterse, C. M. J. (2012). Modulation of host immunity by beneficial microbes. *Mol. Plant-Microbe Interact.* 25, 139–150. doi: 10.1094/MPMI-06-11-0179

Zamioudis, C., Hanson, J., and Pieterse, C. M. J. (2014). β-Glucosidase BGLU42 is a MYB72-dependent key regulator of rhizobacteria-induced systemic resistance and modulates iron deficiency responses in Arabidopsis roots. *New Phytol.* 204, 368–379. doi: 10.1111/nph.12980

Zamioudis, C., Korteland, J., Van Pelt, J. A., Van Hamersveld, M., Dombrowski, N., Bai, Y., et al. (2015). Rhizobacterial volatiles and photosynthesis-related signals coordinate *MYB72* expression in Arabidopsis roots during onset of induced systemic resistance and iron-deficiency responses. *Plant J.* 84, 309–322. doi: 10.1111/tpj.12995

Zeilinger, S., Gupta, V. K., Dahms, T. E., Silva, R. N., Singh, H. B., Upadhyay, R. S., et al. (2016). Friends or foes? Emerging insights from fungal interactions with plants. *FEMS Microbiol. Rev.* 40, 182–207. doi: 10.1093/femsre/fuv045

Zelezniak, A., Andrejev, S., Ponomarova, O., Mende, D. R., Bork, P., and Patil, K. R. (2015). Metabolic dependencies drive species co-occurrence in diverse microbial communities. *Proc. Natl. Acad. Sci. U. S. A.* 112, 6449–6454. doi: 10.1073/pnas.1421834112

Zgadzaj, R., Garrido-Oter, R., Jensen, D. B., Koprivova, A., Schulze-Lefert, P., and Radutoiu, S. (2016). Root nodule symbiosis in *Lotus japonicus* drives the establishment of distinctive rhizosphere, root, and nodule bacterial communities. *Proc. Natl. Acad. Sci. U. S. A.* 113, 7996–8005. doi: 10.1073/pnas.1616564113

Zhalnina, K., Louie, K. B., Hao, Z., Mansoori, N., Da Rocha, U. N., Shi, S., et al. (2018). Dynamic root exudate chemistry and microbial substrate preferences drive patterns in rhizosphere microbial community assembly. *Nat. Microbiol.* 3, 470–480. doi: 10.1038/s41564-018-0129-3

Zhang, Y., Xu, J., Riera, N., Jin, T., Li, J., and Wang, N. (2017). Huanglongbing impairs the rhizosphere-to-rhizoplane enrichment process of the citrus root-associated microbiome. *Microbiome* 5, 97. doi: 10.1186/s40168-017-0304-4

Zhou, C., Guo, J., Zhu, L., Xiao, X., Xie, Y., Zhu, J., et al. (2016). *Paenibacillus polymyxa* BFKC01 enhances plant iron absorption *via* improved root systems and activated iron acquisition mechanisms. *Plant Physiol. Biochem.* 105, 162–173. doi: 10.1016/j.plaphy.2016.04.025

Conflict of Interest: The authors declare that the research was conducted in the absence of any commercial or financial relationships that could be construed as a potential conflict of interest.

frontiers in Plant Science

ORIGINAL RESEARCH
published: 30 April 2020
doi: 10.3389/fpls.2020.00461

Heterologous Expression of PKPI and Pin1 Proteinase Inhibitors Enhances Plant Fitness and Broad-Spectrum Resistance to Biotic Threats

David Turrà[1], Stefania Vitale[1], Roberta Marra[1,2], Sheridan L. Woo[2,3,4] and Matteo Lorito[1,2,3]**

[1] Department of Agricultural Sciences, University of Naples Federico II, Naples, Italy, [2] Task Force on Microbiome Studies, University of Naples Federico II, Naples, Italy, [3] Institute for Sustainable Plant Protection, National Research Council, Naples, Italy, [4] Department of Pharmacy, University of Naples Federico II, Naples, Italy

OPEN ACCESS

Edited by:
Ivan Baccelli,
Istituto per la Protezione Sostenibile delle Piante, Sede Secondaria Firenze, Italy

Reviewed by:
Marie-Claire Goulet,
Laval University, Canada
Patricia Castro,
Universidad de Córdoba, Spain

***Correspondence:**
David Turrà
davturra@unina.it
Matteo Lorito
lorito@unina.it

Specialty section:
This article was submitted to Plant Microbe Interactions, a section of the journal Frontiers in Plant Science

Received: 27 September 2019
Accepted: 27 March 2020
Published: 30 April 2020

Citation:
Turrà D, Vitale S, Marra R, Woo SL and Lorito M (2020) Heterologous Expression of PKPI and Pin1 Proteinase Inhibitors Enhances Plant Fitness and Broad-Spectrum Resistance to Biotic Threats. Front. Plant Sci. 11:461. doi: 10.3389/fpls.2020.00461

Kunitz-type (PKPI) and Potato type I (Pin1) protease inhibitors (PIs) are two families of serine proteinase inhibitors often associated to plant storage organs and with well known insecticidal and nematicidal activities. Noteworthy, their ability to limit fungal and bacterial pathogenesis *in vivo* or to influence plant physiology has not been investigated in detail. To this aim, we generated a set of PVX-based viral constructs to transiently and heterologously express two potato *PKPI* (*PKI1*, *PKI2*) and three potato *Pin1* (*PPI3A2*, *PPI3B2*, *PPI2C4*) genes in *Nicotiana benthamiana* plants, a widely used model for plant-pathogen interaction studies. Interestingly, transgenic plants expressing most of the tested PIs showed to be highly resistant against two economically important necrotrophic fungal pathogens, *Botrytis cinerea* and *Alternaria alternata*. Unexpectedly, overexpression of the *PKI2* Kunitz-type or of the *PPI2C4* and *PPI3A2* Potato type I inhibitor genes also lead to a dramatic reduction in the propagation and symptom development produced by the bacterial pathogen *Pseudomonas syringae*. We further found that localized expression of *PPI2C4* and *PKI2* in *N. benthamiana* leaves caused an increase in cell expansion and proliferation which lead to tissue hypertrophy and trichome accumulation. In line with this, the systemic expression of these proteins resulted in plants with enhanced shoot and root biomass. Collectively, our results indicate that PKPI and Pin1 PIs might represent valuable tools to simultaneously increase plant fitness and broad-spectrum resistance toward phytopathogens.

Keywords: *Pin1*, *PKPI*, plant cell proliferation, *Pseudomonas syringae*, *Alternaria alternata*, *Botrytis cinerea*, disease resistance

INTRODUCTION

PKPI and Pin1 are among the most abundant naturally occurring plant serine proteinase inhibitors (PIs). Large amounts of these inhibitors accumulate in plant reproductive and storage organs, as in the case of *Solanum tuberosum* (Heibges et al., 2003; van den Broek et al., 2004). Nevertheless, their genes are also transcribed, however at lower levels, in all other plant tissues (Kuo et al., 1984; Lincoln et al., 1987; Jofuku and Goldberg, 1989; Heitz et al., 1993; Wang et al., 2003, 2008; Turrà et al., 2009). Serine PIs expression apart from being regulated at developmental, spatial and species-specific level (Lee et al., 1986; Rosahl et al., 1986; Balandin et al., 1995; Singh et al., 2009; Tamhane et al., 2009; Turrà et al., 2009), is boosted up by various external stimuli including wounding, insect feeding and microbial infections (Mello et al., 2001; van Loon et al., 2006; Turrà and Lorito, 2011), being one of the best-characterized defense reactions activated by the plant in response to pathogen and insect attack. Many studies on the effect of serine PIs, either artificially introduced into diets or heterologously expressed in transgenic plants, have shown the ability of these proteins to reduce the growth and development of a wide range of herbivorous insects and pathogenic nematodes mainly by interfering with nutrient digestibility and fertility (Jongsma et al., 1995; Urwin et al., 1995; Altpeter et al., 1999; Andrade et al., 2003; Cai et al., 2003; Srinivasan et al., 2005).

Besides, few serine PIs have also shown inhibitory activity against bacteria and fungi *in vitro* by reducing their growth or conidial germination and hyphal swelling, respectively (Lorito et al., 1994; Dunaevsky et al., 1996; Chen et al., 1999; Soares-Costa et al., 2002; Kim et al., 2005; Hermosa et al., 2006; Kim et al., 2006; Di Cera, 2009). However, while serine PIs insecticidal and nematicidal activities have been efficiently proven *in planta*, their ability to alter plant resistance against fungal or bacterial pathogens *in vivo* has remained elusive.

Proteases and PIs play important roles in plant-pathogen interactions; nevertheless, testimony for their endogenous role in plants is relatively recent and our current understanding of the diverse physiological processes regulated by PIs is rapidly expanding (van der Hoorn, 2008; Turrà and Lorito, 2011; Grosse-Holz and van der Hoorn, 2016). To date, protease-PI interactions have been shown to regulate many diverse aspects of the plant life cycle including senescence and programmed cell death (PCD), leaf trichome density and branching, seed and flower development and sieve element maturation (Solomon et al., 1999; Xu et al., 2001; Sin and Chye, 2004; Pak and Van Doorn, 2005; Liu et al., 2006; Xie et al., 2007; Luo et al., 2009; Boex-Fontvieille et al., 2015; Rustgi et al., 2017).

As proteolysis is a fundamental process in all living beings, in order to avoid undesired side-effects plants must carefully control endogenous protease activity in both a timely and a spatial manner (van der Hoorn, 2008; Turrà and Lorito, 2011). In a previous work from our group, we have shown that *PI* gene members of the *Pin1* and *PKPI* families are differentially expressed in *Solanum tuberosum* var. Desireè plants upon abiotic or biotic insults, or in a tissue-dependent manner, thus indicating a possible role for these PIs as both endogenous- and defense-related plant regulators (Turrà et al., 2009).

In this study, the effect of transient expression of different members of the *Pin1* and *PKPI* families on plant resistance toward fungal and bacterial pathogens and on plant physiology is reported. When heterologously expressed in *Nicotiana benthamiana*, different potato *PKPI* and *Pin1* genes confer protection against *B. cinerea* and *A. alternata*, two agronomically important pathogens. Moreover, *in vivo* assays designed to challenge PIs-expressing plants with *Pseudomonas syringae* pv. *tabaci* also revealed enhanced plant resistance to bacterial attack. In addition to this, overexpression of two of these serine *PI* genes also caused severe developmental effects on *N. benthamiana* plants, including over-accumulation of trichomes and growth enhancement. These phenotypes were accompanied by the high inhibitory activity of total soluble proteins (TSP) extracted from transformed leaf patches toward yet unknown proteases present in the *N. benthamiana* leaf apoplast. Based on these results, we propose that Pin1 and PKPIs are critically involved in host resistance and modulation of plant physiology.

MATERIALS AND METHODS

Microbial Strains, Plants, and Culture Conditions

Nicotiana benthamiana plants were cultivated and maintained at 25°C in a phytocabinet under 16/8 h light-dark photoperiod.

Agrobacterium tumefaciens GV3101, *Escherichia coli* DH5α and a rifampicin-resistant strain of *P. syringae* pv. *tabaci* were routinely grown in Luria-Bertani (LB) media (Sambrook and Russell, 2001) with appropriate antibiotics at 28°C, 37°C, or 28°C, respectively. All bacterial DNA transformations were performed by electroporation using standard protocols (Sambrook and Russell, 2001).

Conidia of the pathogenic fungi *B. cinerea* and *A. alternata* were harvested respectively from malt extract peptone agar (MEP) (Difco, Detroit, MI, United States) or potato dextrose agar (PDA) (Sigma-Aldrich, St. Louis, MO, United States) plates, after 1 week of incubation at 25°C, as previously described (Hermosa et al., 2006).

Construction of PVX::*PI* Gene Fusions

To amplify full-length cDNAs of *PKI1*, *PKI2*, *PPI3A2*, *PPI3B2,* and *PPI2C4* genes (Hermosa et al., 2006; Turrà et al., 2009), total RNA was extracted from 100 mg of *Solanum tuberosum* var. Desireè sprouts using the TRI Reagent (Ambion, Austin, TX, United States). First-strand cDNA was synthesized using the Reverse Transcription System kit (Promega, Madison, WI, United States) and 1 μg random primers for every 2 μg of total RNA, following the supplier's instructions. The *PKPI* and *Pin1* derivatives were amplified by PCR using the oligonucleotide combinations indicated in **Supplementary Table S1**, subcloned into pGEM-T Easy vector (Promega), and ligated into the *Cla*I and *Sal*I sites of the *A. tumefaciens* binary PVX vector pGR106 (Lu et al., 2003).

Constructs containing the inserts in sense orientation were designated PVX::*PKI1*, PVX::*PKI2*, PVX::*PPI3A2*, PVX::*PPI3B2,* and PVX::*PPI2C4*. The obtained binary vectors, the pGR106

vector without any insert and the pGR208 vector (Rairdan et al., 2008), *gfp* cDNA ligated in the same vector, were transformed into *A. tumefaciens* strain GV3101. pGR106 and pGR208 vectors were used as PVX controls.

Transient Expression of *PIs* Genes in *N. benthamiana* and *in vivo* Resistance Assay on PVX-Infected Plants

N. benthamiana seedlings at the fourth true-leaf stage were used for *A. tumefaciens* infiltration. To evaluate local effects of PI overexpression, *A. tumefaciens* overnight cultures diluted to an OD600 of 0.25 with sterile distilled water were used to infiltrate the abaxial side of the leaf (using a needleless 5 ml syringe). Alternatively, to achieve systemic transformation of plants, third and fourth leaves of 2–3-week-old *N. benthamiana* seedlings were wounded twice along the midvein with a sterile wooden toothpick previously streaked over an *A. tumefaciens* culture grown on solid agar medium.

For *P. syringae* infection, 5 days after *A. tumefaciens* syringe-infiltration, the same leaf areas were infiltrated (the abaxial side of the leaf) with 40 μl of a 1×10^8 *P. syringae* cells/ml culture (adjusted with sterile distilled H_2O to OD600 = 0.24). After 2, 4, 7, and 9 days, the necrotic zone around the inoculation site was imaged. Every treatment was repeated at least 6 times and on at least three different plants. A separate round of experiments was used to quantify *P. syringae* growth in the agroinfiltrated leaves. Ten μl of a *P. syringae* cell suspension (OD600 = 0.24) was applied to needle-pricked leaves. Plants were covered with clear polyethylene bags and sealed around the base using elastic bands, to keep humidity. After 1, 3, and 6 days, six leaf discs (0.8 cm diameter) per treatment were excised from inoculated areas, pooled and ground (Ultra-Turrax T25 basic, IKA Labortechnik, Germany) in 10 mM $MgSO_4$ (1 ml/disc), by keeping the tube in an ice bath. An aliquot of the homogenate was plated on LB-rifampicin agar at three different dilutions (10^{-3}, 10^{-4}, and 10^{-5}) and colonies were counted 1 and 2 days after incubation at 28°C. Another aliquot (15 μl) of the homogenate was mixed with 110 μl of LB-rifampicin and incubated in 96-well microtiter plates at 28°C (120 rpm for 16 h). Optical density at 550 nm was then measured with a Bio-Rad microplate reader (Bio-Rad, Richmond, CA, United States). *P. syringae* inoculation was independently repeated on at least six leaves of at least three different plants.

For *B. cinerea* and *A. alternata* infections, upper leaves of systemically transformed *N. benthamiana* plants (11 days after *A. tumefaciens* toothpick inoculation) were challenged with 10 μl of germination solution (20 mM glucose, 20 mM potassium phosphate) containing 10^5 or 10^7 conidia/ml of *B. cinerea* or *A. alternata*, respectively. All plants were covered with transparent polyethylene bags and sealed around the base using elastic bands, to keep humidity. The appearance of necrotic spots was assessed 2, 4, and 6 days after inoculation and disease incidence recorded.

Each pathogen–PVX construct combination was assayed on at least four different leaves of at least three different plants. All infection assays were repeated at least twice. Data are presented as mean values ± SD of different experiments. To assess statistical differences between control (PVX::*gfp*) and PI expressing samples a Yates' corrected chi-squared test (two-sided) was used. Statistical differences between treatments at each time point were assessed by one-way ANOVA with *post hoc* Tukey HSD Tests.

RT-PCR Analysis of PIs Expression

For RT-PCR validation of transient PI expression, total RNA was isolated from 100 mg of control (PVX::*gfp*) and PIs transformed *N. benthamiana* leaves (5 days post agroinfiltration) using the TRI Reagent (Ambion). RT-PCR was performed on equal amounts of total RNA using the Reverse Transcription System kit (Promega) and of 1 μg random primers for each 2 μg total RNA, following the supplier's instructions. Two microliters of first-strand cDNA solution were used as a template for RT-PCR experiments. Amplifications of *Pin1*, *PKPI,* and β-*tubulin* gene transcripts were performed as indicated earlier (Turrà et al., 2009). Plasmid DNA of the cloned cDNAs *PPI3B2* and *PKI1* (Turrà et al., 2009) were used as positive controls and PCR products of the constitutively expressed β-*tubulin* gene used as a quantitative control. Amplifications were repeated in independent occasions on neo-synthesized cDNA from at least three independently repeated experiments.

Protein Extractions

For the extraction of the TSP, ten grams of untransformed or of locally transformed *N. benthamiana* leaf areas (7 days after *A. tumefaciens* syringe-inoculation) were ground with an Ultra-Turrax Homogenizer in 30 ml of 0.1 M sodium phosphate buffer (pH 6.8) by keeping the tube in an ice bath. The slurry was incubated 1h on ice under occasional shaking, filtered through four layers of cheesecloth, and cleared by centrifugation at 50,000 g for 1 h at 4°C in a Beckman L7-65 Ultracentrifuge (Beckman, Milan, Italy).

Apoplastic fluids (AF) were prepared from *N. benthamiana* leaves according to the method of Moehnke et al. (2008), with minor modifications. Briefly, 10 g of leaf material was vacuum-infiltrated for 2 min with 100 ml infiltration buffer [100 mM Tris/HCl (pH 7.5), 10 mM $MgCl_2$]. Leaves were then dried with sterile paper towels and placed into the barrel of a 50 ml syringe. The syringe was subsequently inserted into a 50 ml falcon tube with the needle hub facing downwards and spun at 2,000 g for 10 min at 4°C. After centrifugation, AF was collected from the bottom of the centrifuge tube.

All protein extracts were subjected to filtration and dialysis by using Centriprep YM-3 devices (Amicon Corporation, Danvers, MA, United States), filter sterilized (0.22 μm) and stored at −20°C if not immediately used. Protein concentrations were determined by a Bradford DC protein assay (Bio-Rad) using bovine serum albumin as a standard.

In vitro Evaluation of Plant Crude Extracts Activity

Inhibition assays of *N. benthamiana* TSP and AF proteolytic activities by TSP extracted from PVX::*gfp*, PVX::*PKI2,* and PVX::*PPI2C4* transformed *N. benthamiana* leaf areas were

carried out in microtiter plates by using azocasein (Sigma-Aldrich) as chromogenic substrate and in-gel protease assays using the Bio-Rad zymogram buffer system, following the previously described procedures (Tian et al., 2004; Hermosa et al., 2006). For the first method, a total of 20 μg of TSP and AF from untransformed plants were preincubated with 20 μg of TSP from PVX-transformed plants in a volume of 250 μl for 30 min at room temperature, and followed by incubation with 200 μl of 1% azocasein (w/v) at 37°C for 1 h. The reaction was halted by adding an equal volume of 10% (w/v) TCA. After 10 min on ice, the reaction mixture was centrifuged for 10 min at 13,000 g and the supernatant mixed with an equal volume of 1 M NaOH. The optical density at 450 nm was then determined with a Bio-Rad microplate reader. The percentage of the remaining protease activity was therefore plotted relative to that of TSP and AF samples from untransformed plants incubated with TSP extracted from PVX:*gfp* transformed plants. Experiments were performed in triplicate and repeated in at least two independent occasions. Data represent the mean value [±SD (standard deviation)] across all experiments. Statistical differences between treatments were assessed by one-way ANOVA with *post hoc* Tukey HSD Tests.

For zymogen in-gel protease assays, 20 μg of TSP from mock- (H_2O) and PVX-infiltrated *N. benthamiana* leaf areas were mixed with zymogram sample buffer and loaded on a 10% SDS-polyacrylamide gel without boiling or addition of reducing reagents. Following electrophoresis, the gel was incubated in 1x zymogram renaturation buffer for 30 min. Then the gel was incubated in 1x zymogram development buffer for 18 h at 37°C before staining with 0.5% Coomassie Brilliant Blue. Areas of protease activity were revealed as cleared bands on a blue background.

To assess the antifungal activity of plant crude extracts, 10 μl of a solution of 10^7 conidia/ml of *B. cinerea* or *A. alternata* were mixed with 40 μl of plant crude extracts (50 μg/ml) and 40 μl of Potato Dextrose Broth (PDB). After 48 h of incubation at 28°C in a 96-well microtiter plate, the change in optical density at 550 nm was determined using a Bio-Rad microplate reader. Each experiment was repeated at least three times and data presented as the percentage of growth inhibition relative to that of the PVX:*gfp* transformed plants. Data correspond to mean values (± SD) across all experiments. Statistical differences between treatments were assessed by one-way ANOVA with *post hoc* Tukey HSD Tests.

Determination of Plant Growth and Analysis of Leaf Surface Expansion

The effect of PI transient expression on *N. benthamiana* shoot and root growth was evaluated in pot experiments. Seedlings were grown *in vitro* at 23°C under 24 h fluorescent lighting (3,500–6,000 lux) on Murashige and Skoog (MS) salt medium (ICN Pharmaceuticals Inc., Cleveland, OH, United States), and 1% bacto-agar (Difco, Detroit, MI, United States) first and then transferred to soil in 10 cm diameter pots and left to grow in a phytocabinet as described above. Plantlets at the fourth-leaf stage were *A. tumefaciens* toothpick inoculated, as described above. Complete shoots and roots were collected separately (21 days after agroinfection). Roots were briefly rinsed to remove attached sand, quickly dried with a paper towel, incubated for 72 h at 75°C and weighted to estimate the dry weight. Experiments were repeated twice (n = 10). Data correspond to mean values (± SD) across all experiments. Statistical differences between treatments were assessed by one-way ANOVA with *post hoc* Tukey HSD Tests.

To determine leaf disc surface expansion and leaf strip curvature of PI transformed leaf areas, the methods were adapted from those of Gevaudant and coworkers (Gevaudant et al., 2007). Briefly, fully developed PVX-transformed *N. benthamiana* leaf areas (7 days after *A. tumefaciens* syringe-inoculation) were used. Leaf discs (1 cm diameter) and strips (2 × 10 mm) were cut from the interveinal region and incubated for 24 h at room temperature in 10 mM Sucrose, 10 mM KCl, and 0.5 mM 2-(N-Morpholino)ethanesulfonic acid hemisodium salt (MES), pH 6.0. Leaf discs were photographed with a digital camera before and after the treatment and their surface estimated as their pixel content, by the use of the ImageJ software (Collins, 2007). Differences in surface increase between treatments and controls (PVX::*gfp*) were expressed as a percentage of the initial disc area. Leaf strip curvature was estimated as the angle made by the two tangents to the two terminal parts of each strip. Each experiment was repeated three times on at least 15 leaf discs or strips per treatment. Statistical differences between treatments were assessed by one-way ANOVA with *post hoc* Tukey HSD Tests.

For microscopic analysis of cell size and nuclei density, adaxial epidermis from agroinfiltrated (7, 13, and 20 days after *A. tumefaciens* syringe-infiltration) *N. benthamiana* leaf areas was used. Briefly, entire leaves were detached and immersed for 1 h in 1% (v/v) Tween 20 before peeling off the adaxial epidermis from the agro-infiltrated area. Tissues were mounted in water and observed with an Axioskop2 Plus microscope (Zeiss, Milan, Italy). Cell size measurement was performed by using the ImageJ software (Collins, 2007). For nuclear visualization, leaf epidermis was stained with 4′,6-diamidino-2-phenylindole (DAPI; 1 μg/ml) for 20 min, and mounted in 50% (v/v) phosphate-buffered saline (PBS)-glycerol for observation. Quantification of epidermial cell size and nuclear density was repeated at least four times on 500 cells/leaf per treatment. To assess statistical differences between control (PVX and PVX:*gfp*) and PI expressing samples a Yates' corrected chi-squared test (two-sided) was used.

Sequence Data and Bioinformatic Analysis

BLAST searches were performed in the NCBI database[1]. Signal peptide and extracellular localization predictions were performed by using the SignalP and WoLF PSORT softwares, respectively (Emanuelsson et al., 2007; Horton et al., 2007).

[1]http://www.ncbi.nlm.nih.gov

Sequence data from this article can be found in the GenBank data library under accession numbers DQ087220 (*PKI1*), JX878493 (*PKI2*), DQ087224 (*PPI3A2*), DQ087221 (*PPI3B2*), DQ087223 (*PPI2C4*).

RESULTS

Potato *Kunitz* and *Pin1* PIs Are Efficiently Expressed in *Nicotiana benthamiana* Plants

Five PCR fragments corresponding to three previously characterized (*PPI3A2*, *PPI3B2,* and *PPI2C4*) full-length *Pin1* cDNAs and two full-length *Kunitz* cDNAs, one of them previously characterized (*PKI1*) and a novel one (*PKI2*) were amplified from potato sprouts (Turrà et al., 2009). BlastX analysis of the latter gene indicated about 95% identity with the *S. tuberosum P1H5* gene (AAM10743) and 94% identity with *PKI1*. All amplified PIs were predicted to be secreted to the apoplast according to the SignalP and WoLF PSORT prediction tools.

Recombinant PVX plasmids containing the full-length cDNA of all of the above mentioned *PI* genes were used for transient transformation of *N. benthamiana* plants. For local expression of *PI* genes, the method of transient *Agrobacterium*-mediated expression by leaf infiltration was chosen. Transgene expression in agroinfiltrated leaf patches was confirmed 5 days after agro-infiltration by extracting total RNA and performing RT-PCR using PI specific oligonucleotides (**Supplementary Table S1**) followed by DNA sequence analysis (**Figures 1A,B**). For systemic transgene expression, a toothpick-inoculation system was used. In this case transgene expression in the upper non-inoculated parts of the plant was verified by monitoring GFP fluorescence 5, 7, 11, 14, and 21 DPI with the PVX::*gfp* viral construct. All inoculated plants displayed systemic GFP expression starting from 11 DPI (**Figure 1C**).

Transient Expression of *Kunitz* and *Pin1* Inhibitor Genes Increases Plant Resistance Toward the Fungal Pathogens *Botrytis cinerea* and *Alternaria alternata*

To evaluate the effect of Kunitz and Pin1 expression on plant resistance toward fungal pathogens, plants systemically transformed with PVX::*gfp* and PVX::*PIs* were challenge-inoculated with suspensions of *B. cinerea* and *A. alternata* spores. Necrotic symptoms 6 days postinoculation are shown in **Figures 2A**, **3A**. The size of the disease lesions was also measured after 2, 4, and 6 days in the case of *B. cinerea* and after 4 and 6 days in the case of *A. alternata* infection (**Figures 2B**, **3B**).

While *B. cinera* symptoms developed markedly on PVX::*PPI3A2* transformed plants, those expressing the *PKI1* or *PKI2*, *PPI3B2,* and *PPI2C4* genes exhibited partial or almost complete disease resistance, respectively (**Figure 2A**). Noteworthy, the reduction in the severity of necrotic lesions ranged from 87% (PVX::*PKI2*) to 100% (PVX::*PPI3B2*) 6 days after spore inoculation when compared to the control (PVX::*gfp*) treated plants (**Figure 2B**).

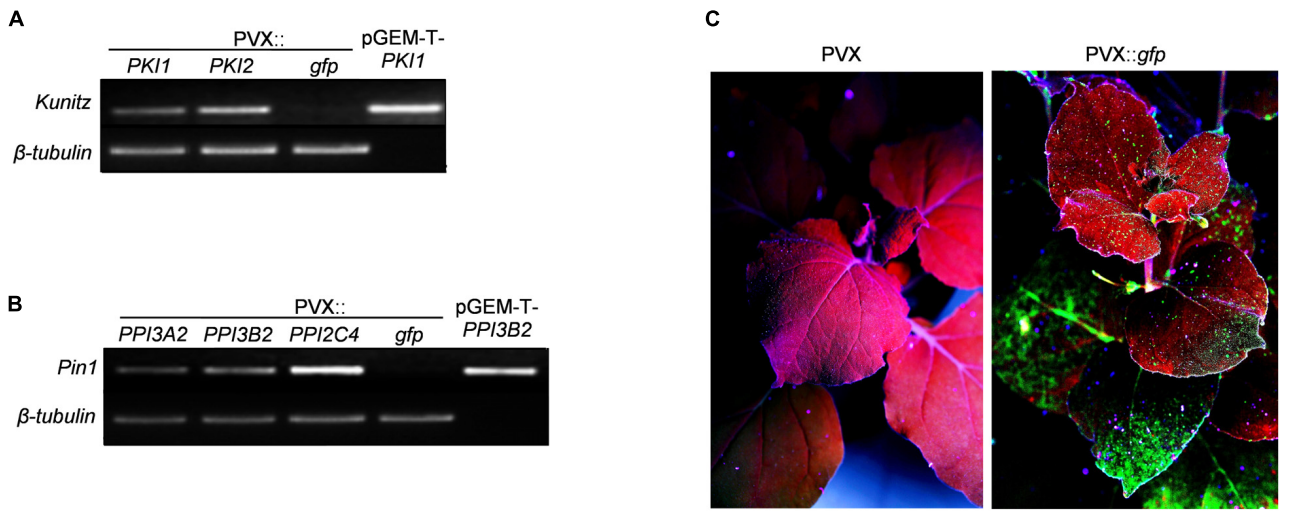

FIGURE 1 | Functional validation of PVX-mediated gene expression. **(A,B)** RT-PCR analysis of potato *PKPI* and *Pin1* expression in control (PVX::*gfp*) and in *PKI1*, *PKI2* **(A)** or *PPI3A2*, *PPI3B2*, *PPI2C4* **(B)** transiently expressing *Nicotiana benthamiana* plants. Total RNA was extracted from *N. benthamiana* leaves 5 days after *Agrobacterium tumefaciens* infiltration and subjected to RT-PCR analysis. Plasmids pGEM-T-*PKI1* **(A)** and pGEM-T-*PPI3B2* **(B)** were used as positive amplification controls. The β-*tubulin* gene was used to confirm an equal amount of total RNA among samples. Each sample consisted of leaf tissues pooled from at least four independently transformed plants. Representative results from three independent experiments are shown. **(C)** Systemic transgene expression was validated by analyzing GFP fluorescence in newly formed *N. benthamiana* leaves at different time intervals 11 days after toothpick inoculation of basal leaves with a colony of *A. tumefaciens* carrying either the pGR106 (PVX control) or the pGR106-*gfp* (PVX::*gfp*) plasmid. Photographs in **(C)** are representatives of UV-irradiated *N. benthamiana* plants 11 dpi.

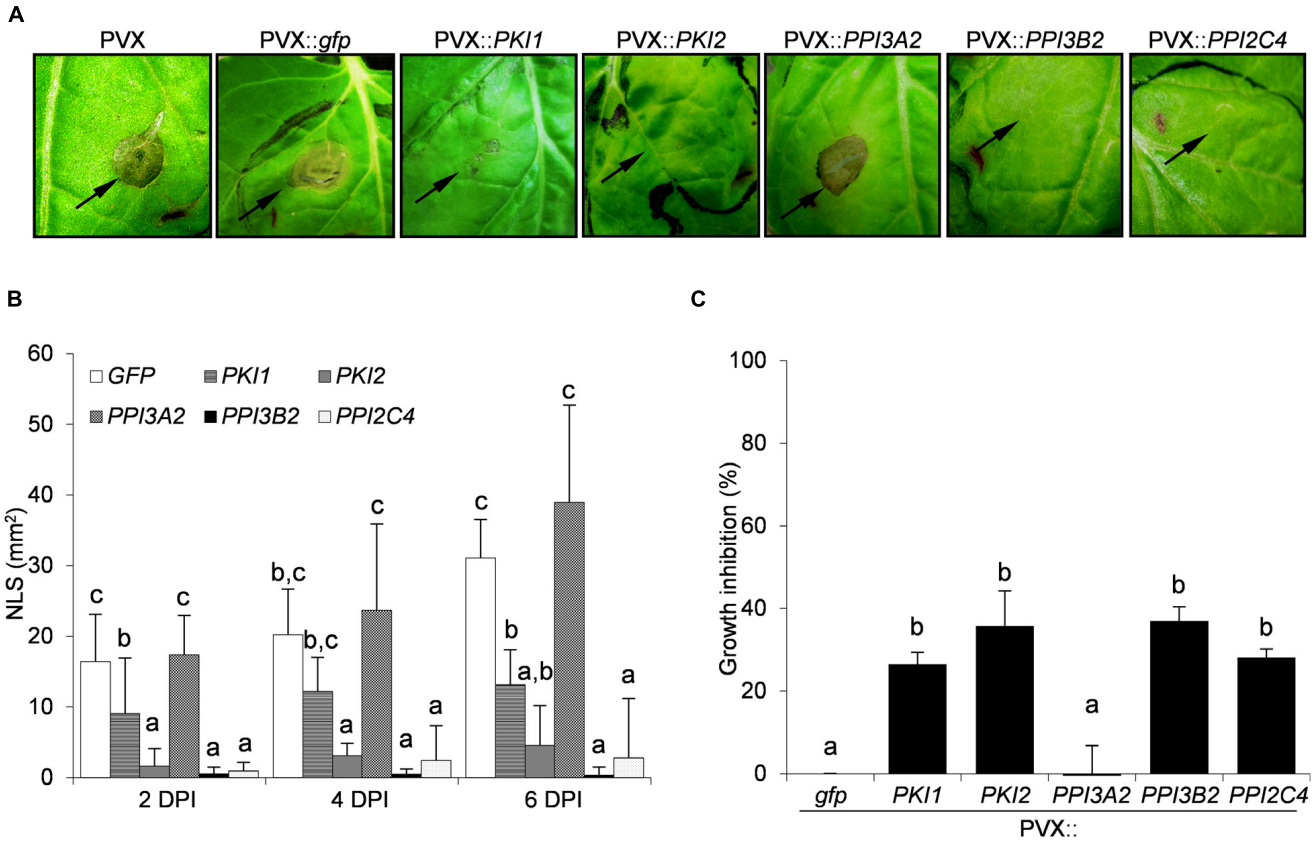

FIGURE 2 | Transient expression of *PKI2* Kunitz and of *PPI3B2* and *PPI2C4* Pin1 inhibitor genes increases plant resistance toward the fungal pathogen *Botrytis cinerea*. Third and fourth leaves of *Nicotiana benthamiana* plants were toothpick inoculated with *Agrobacterium tumefaciens* carrying the indicated viral constructs. After 11 days, the upper leaves showing systemic viral symptoms were challenged with 10 μl of germination solution (20 mM glucose, 20 mM potassium phosphate) supplemented with 10^5 conidia/ml of *Botrytis cinerea*. **(A)** Representative pictures of necrotic lesions (NLS) observed 6 days after *B. cinerea* inoculation on the indicated PVX-transformed *N. benthamiana* plants. **(B)** Severity of necrotic lesions recorded 2, 4, and 6 days after *B. cinerea* inoculation (DPI) on the indicated PVX-transformed *N. benthamiana* plants. Values are the means of four independent inoculations repeated on at least three plants; error bars represent the standard deviation. Mock inoculated plants (H_2O), PVX and PVX::*gfp* transformed plants were used as negative controls. Different letters indicate significant differences ($P < 0.01$) among treatments at each DPI according to One-way ANOVA with *post hoc* Tukey HSD Test. **(C)** *In vitro* inhibitory activity of total soluble proteins (TSP; 50 μg/ml) extracted from PVX-transformed *N. benthamiana* leaf areas toward *B. cinerea*. Fungal growth inhibition was measured as the reduction of the optical density at 550 nm relative to the control treatment (TSP extracted from PVX::*gfp* transformed plants). Values are the means of triplicate determinations; error bars represent the standard deviation. Different letters indicate significant differences ($P < 0.05$) among the different treatments according to One-way ANOVA with *post-hoc* Tukey HSD Test.

Differently from *B. cinerea* infection, no symptoms developed on any of the *A. alternata* challenged leaves 2 days post-infection (data not shown). Marked necrotic areas started to appear 4 days post-infection on PVX::*PPI3B2*, PVX::*PPI2C4,* and PVX::*gfp* transformed plants, while those expressing *PKI2*, *PKI1,* and *PPI3A2* genes exhibited a significant increase of disease resistance (PVX::*PKI1*, 84%; PVX::*PKI2*, 93%; PVX::*PPI3A2*, 68%). Six days post-infection all PI expressing plants showed significantly increased resistance (varying between 50 and 66%) when compared to the control ones (PVX::*gfp*) (**Figure 3B**).

To understand if the inhibition of *B. cinerea* and *A. alternata* growth on PI-expressing *N. benthamiana* plants depended on the chemical composition of leaf TSP, the *in vitro* inhibitory activity of TSP extracted from PIs-transformed *N. benthamiana* leaf areas was compared to that of PVX::*gfp* transformed ones. Data reported in **Figures 2C**, **3C** show that all TSP extracted from PI-transformed plants were able to reduce the growth of both fungal pathogens, except those from *PPI3A2*-expressing plants that selectively inhibited *A. alternata* but not *B. cinerea* proliferation.

Transient Expression of *PKI2*, *PPI3A2,* and *PPI2C4 PI* Genes Increases Plant Resistance Toward the Bacterial Pathogen *Pseudomonas syringae* pv. *tabaci*

To determine whether *Kunitz* and *Pin1* gene overexpression confers protection against bacterial phytopathogens in *N. benthamiana* plants, a cell suspension of *P. syringae* pv. *tabaci* was syringe-infiltrated into the abaxial side of PVX::*PIs* or PVX::*gfp* transformed leaf areas. Chlorotic and

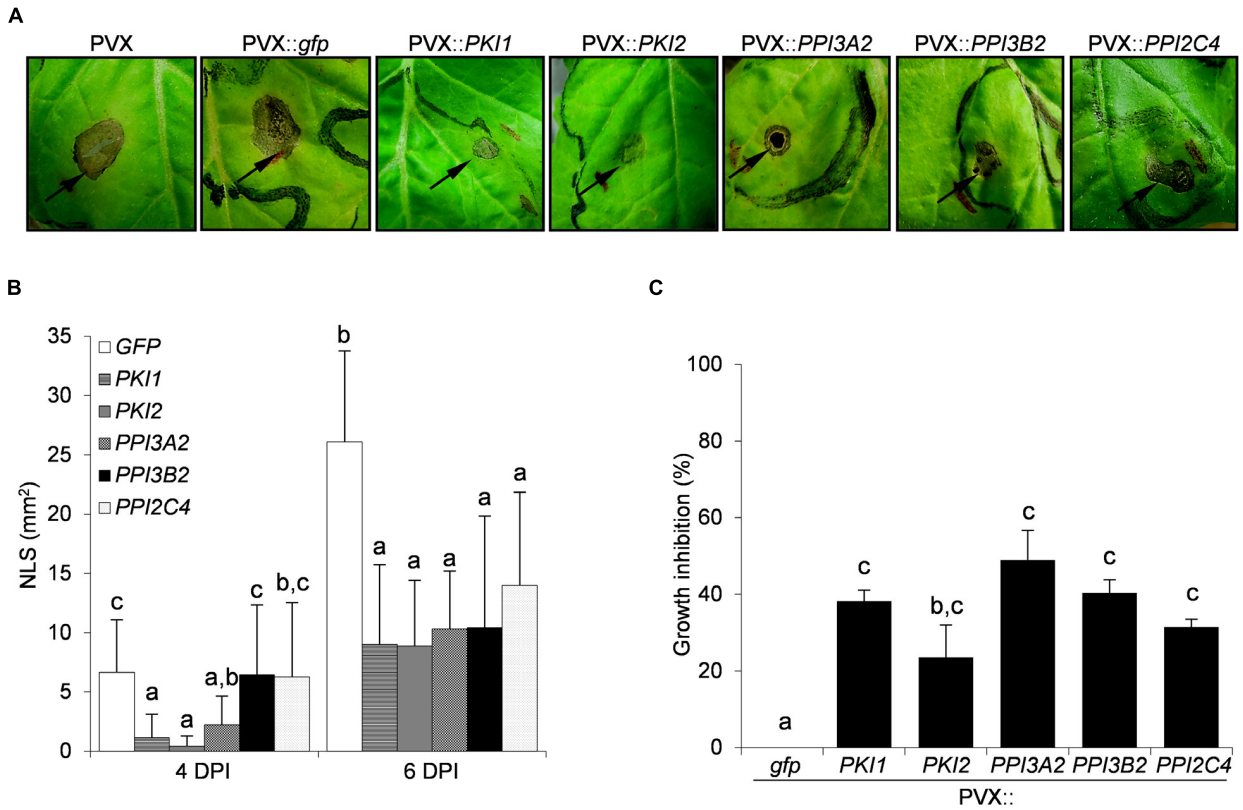

FIGURE 3 | Transient expression of several *Kunitz* and *Pin1* genes increases plant resistance toward the fungal pathogen *Alternaria alternata*. Third and fourth leaves of *Nicotiana benthamiana* plants were toothpick inoculated with *Agrobacterium tumefaciens* carrying the indicated viral constructs. After 11 days, the upper leaves showing systemic viral symptoms were challenged with 10 μl of germination solution (20 mM glucose, 20 mM potassium phosphate) supplemented with 10^7 spores/ml of *A. alternata*. **(A)** Representative pictures of necrotic lesions (NLS) observed 6 days after *A. alternata* inoculation (DPI) on the indicated PVX-transformed *N. benthamiana* plants. **(B)** Severity of necrotic lesions recorded 4 and 6 days after *A. alternata* infection on the indicated PVX-transformed *N. benthamiana* plants. Values are the means of four independent inoculations repeated on at least three plants; error bars represent the standard deviation. Mock inoculated plants (H_2O), PVX and PVX::*gfp* transformed plants were used as negative controls. Different letters indicate significant differences ($P < 0.01$) among treatments at each DPI according to One-way ANOVA with *post-hoc* Tukey HSD Test. **(C)** *In vitro* inhibitory activity of total soluble proteins (TSP) extracted from PVX-transformed *N. benthamiana* leaf areas toward *A. alternata*. Fungal growth inhibition was measured as the reduction of the optical density at 550 nm relative to the control treatment (TSP extracted from PVX::*gfp* transformed plants). Values are the means of triplicate determinations; error bars represent the standard deviation. Different letters indicate significant differences ($P < 0.05$) among the different treatments according to One-way ANOVA with *post-hoc* Tukey HSD Test.

necrotic symptoms markedly developed on PVX::*gfp* and PVX::*PKI1* transformed plants 7 days post-infection (**Figure 4A**). Interestingly, while a mild reduction of symptoms was observed on PVX::*PPI3A2*- and PVX::*PPI3B2*-infected plants, in those expressing the *PKI2* or the *PPI2C4* gene only a small necrosis surrounding the point of inoculation, comparable to that observed in the water inoculated leaves (data not shown), was visible (**Figure 4A**).

As necrotic lesions showed an irregular outline and it was difficult to exactly determine the area of necrosis, the number of surviving *P. syringae* cells in infected leaves was quantified (**Figures 4B,C**). Leaf discs were collected from distinct infiltrated areas from each treated plant, homogenized and plated on LB-rifampicin agar at three different dilutions (10^{-3}, 10^{-4}, and 10^{-5}). Alternatively, a 10^{-3} dilution was mixed with LB-rifampicin in 96 well-plates and incubated with constant shaking at 28°C for 16 h. Colony counting and optical density readings retrieved similar results, reported in **Figures 4B,C**. No inhibition of bacterial growth was observed 6 days after inoculation in PVX::*PKI1*-transformed plants when compared to control ones (PVX::*gfp*). Strikingly, a strong reduction of *P. syringae* population was detected in plants transformed with the PVX::*PPI3B2* and PVX::*PPI3A2* vectors (∼40–60%), and complete resistance was observed in those transformed with the *PKI2* and *PPI2C4* genes. As expected, mock infiltrated leaves showed no necrotic symptoms and no bacterial colonies grew after plating their homogenates.

Transient Expression of *PPI2C4* and *PKI2* Genes Alters Plant Development

PVX::*PKI2* and PVX::*PPI2C4* transiently transformed *N. benthamiana* plants showed, in contrast to the untransformed and PVX::*gfp* transformed plants, several developmental abnormalities. Hypertrophy and unusual accumulation of trichomes were observed in locally transformed leaf areas

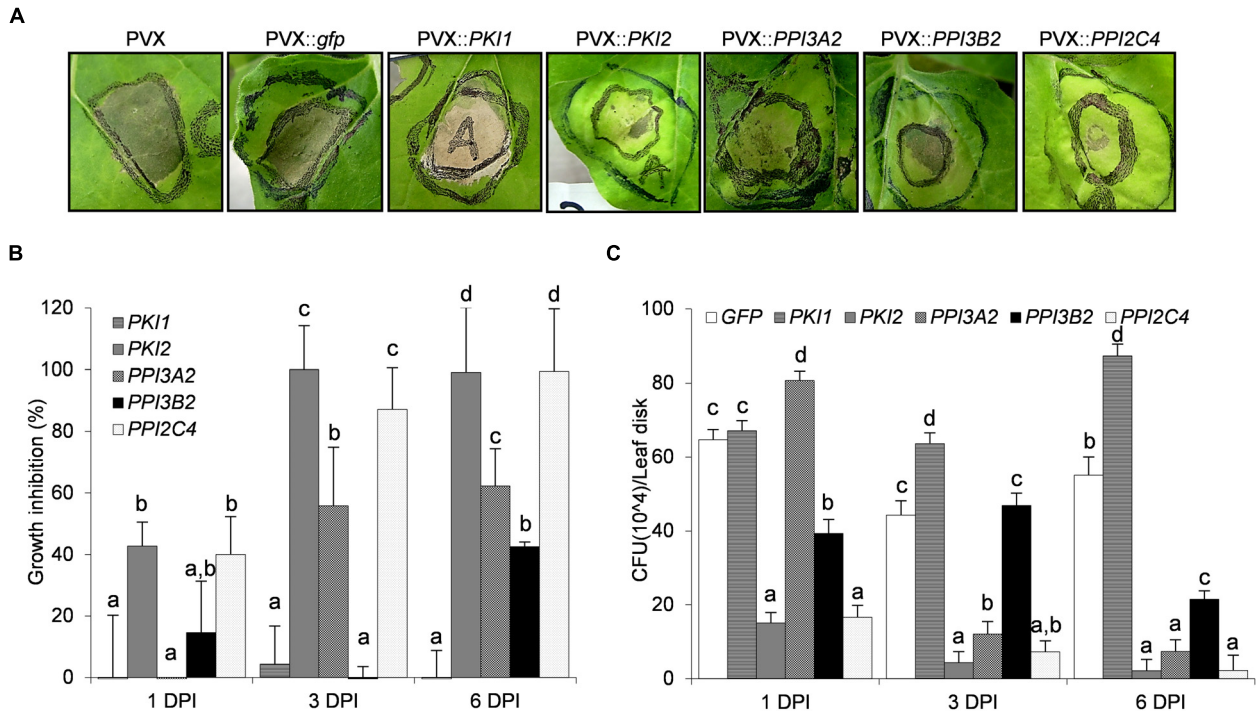

FIGURE 4 | Transient expression of *PKI2* Kunitz inhibitor and of *PPI3A2* and *PPI2C4* Pin1 inhibitor genes increases plant resistance toward the bacterial pathogen *Pseudomonas syringae* pv. *tabaci*. Fully developed leaves of *Nicotiana benthamiana* plants were syringe-infiltrated with a solution of *Agrobacterium tumefaciens* carrying the indicated viral constructs. After 5 days, the previously transformed leaf areas were challenge infiltrated with 40 μl of a 1×10^8 *P. syringae* pv. *tabaci* cells/ml culture **(A)** or needle-pricked and 10 μl of the same *P. syringae* cell suspension were applied at the center of the wounded area **(B,C)**. **(A)** Representative pictures of chlorotic and necrotic symptoms observed 7 days after *P. syringae* pv. *tabaci* infiltration. **(B,C)** The number of surviving bacterias 1, 3, and 6 days after leaf infection with *P. syringae* was determined. Leaf disks (0.8 cm diameter) were excised from the inoculated areas, ground in 10 mM $MgSO_4$ and homogenates were either serially diluted, plated and colonies counted on LB-rifampicin agar **(C)** or mixed with the LB-rifampicin and optical density (OD) at 550 nm determined after 16 h of incubation **(B)** ($P < 0.001$). *P. syringae* growth inhibition in **(B)** is expressed in percentage as the reduction in OD of the PVX::*PI* treated samples compared to the control ones (PVX::*gfp*). In all cases values are the means of four independent inoculations repeated on at least three different plants; error bars represent the standard deviation. Mock inoculated plants (H_2O), PVX and PVX::*gfp* transformed plants were used as negative controls. Different letters indicate significant differences ($P < 0.01$) among the different treatments according to One-way ANOVA with *post hoc* Tukey HSD Test.

21 days after syringe-infiltration (**Figures 5A–C**). Because these macroscopic phenotypes are indicative of a role of PKI2 and PPI2C4 serine PIs in the regulation of cell division and plant development, we tested whether locally transformed *N. benthamiana* leaves showed higher rates of cell expansion. Interestingly, leaf discs from PVX::*PKI2* and PVX::*PPI2C4* transformed plants expanded twice as much as the control ones (PVX::*gfp*) in a 24 h incubation period (**Figure 5D**). In an additional set of experiments, leaf strip curvature or epinasty, a phenotype often related to cell expansion (Keller and Van Volkenburgh, 1997), was analyzed by measuring the curvature of leaf strips excised from PVX-transformed patches 24 h after incubation. Notably, PPI2C4- and PKI2-expressing leaf strips bent 3–4-fold more than GFP-expressing ones (**Figure 5E**), indicating leaf asymmetrical expansion, with the adaxial surface growing faster than the abaxial one.

To confirm the relevance of PKI2 and PPI2C4 proteins in the regulation of plant development, *N. benthamiana* seedlings were systemically transformed with the PVX::*PKI2* and PVX::*PPI2C4* viral constructs. Morphological analyses showed that PKI2- and PPI2C4-overexpressing plants grew faster, developed bigger root systems and leaves and exhibited an increase in root and shoot dry weight of more than three and two times, respectively, when compared to controls (**Figures 5F–J**).

Effects of PI Expression on *Nicotiana benthamiana* Endogenous Protease Activity, Epidermal Cell Expansion, and Division

To ask whether the hypertrophic phenotype observed in PKI2 and PPI2C4 expressing leaves reflects induction of cell division, we performed a detailed microscopic analysis of the adaxial epidermis of PVX::*PPI2C4* and PVX::*gfp* agroinfiltrated patches 7, 13, and 21 DPI. While no alterations of cell morphology could be observed, an increase in the average cell size before (7 DPI) and in nuclear density after (13 DPI) was detected in PPI2C4 expressing plants (**Figures 6A–C,F**). Accordingly, *PPI2C4* expression also lead to the appearance of tight clusters of small-sized cells, some of which being trichomes (**Figures 6D,E**), 13 DPI. Similar results were obtained in PVX::*PKI2* expressing leaves (data not shown). As expected, none of these changes

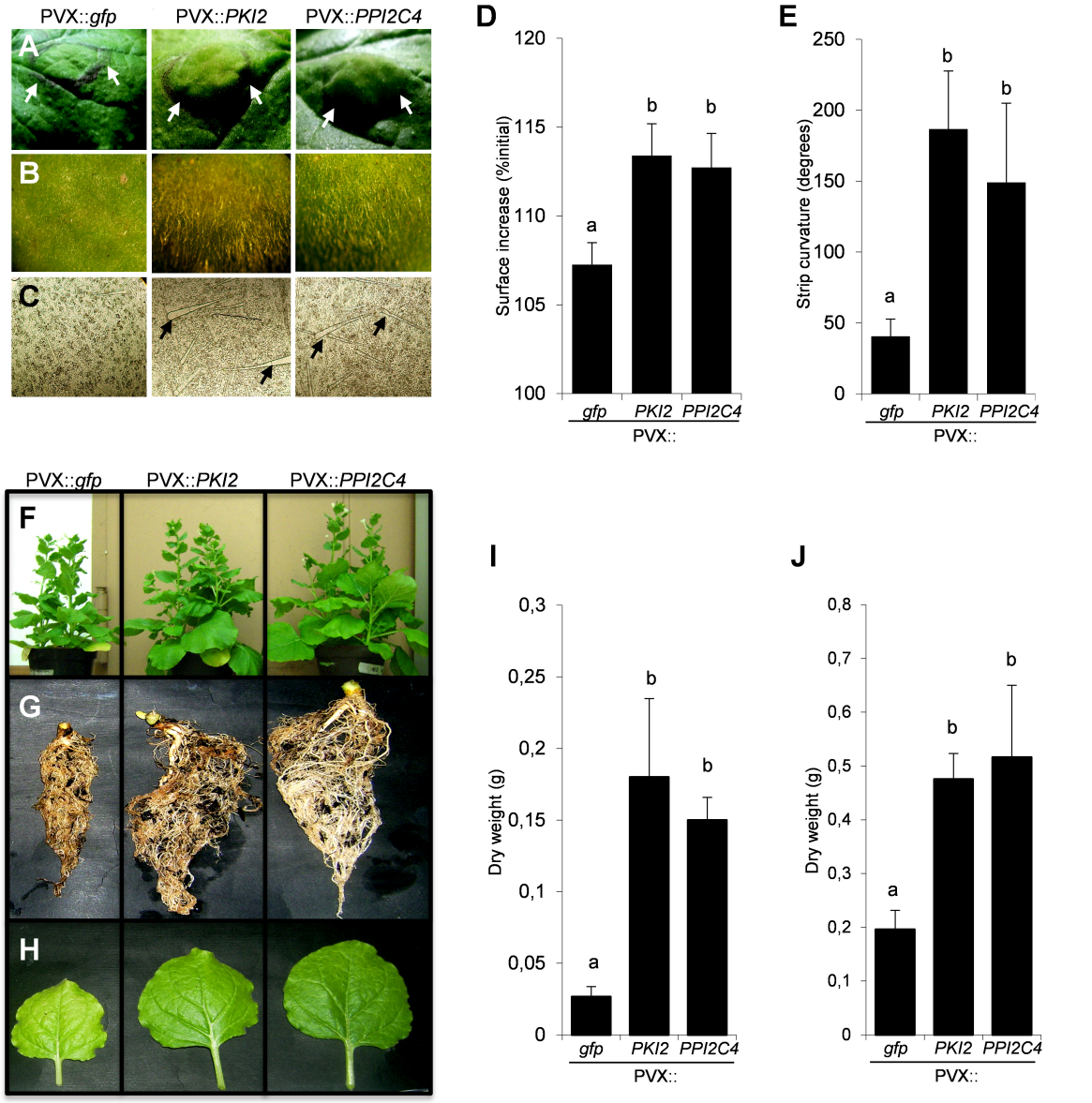

FIGURE 5 | Transient expression of *PKI2* and *PPI2C4* genes enhances plant growth and trichome accumulation. **(A,B)** Representative pictures of *Nicotiana benthamiana* transformed leaf areas 21 days after syringe-infiltration with a solution of *Agrobacterium tumefaciens* carrying the indicated viral constructs. Note the leaf area enlargement **(A)** and overaccumulation of trichomes **(B)** in PVX::*PKI2* and PVX::*PP12C4* transformed leaves. **(C)** Stereomicroscopic view (40X) of adaxial leaf epidermal cells shows higher number and bigger size of trichomes in PVX::*PKI2* and PVX::*PPI2C4* transformed leaf areas. **(D,E)** Curvature of leaf strips and area increase of leaf discs. Leaf strips and discs (1 × 1 cm) from transiently transformed leaf areas (7 days after *A. tumefaciens* syringe-infiltration) were incubated for 24 h as indicated in section "Materials and Methods". Images were taken before and after incubation and the strip curvature **(E)** and the increase of leaf disc area **(D)** (expressed as a percentage of the initial leaf disc area) were calculated. Values are the means of 15 different leaf strips or discs measurements repeated in three independent experiments; error bars represent the standard deviation. Different letters indicate significant differences ($P < 0.01$) according to One-way ANOVA with *post hoc* Tukey HSD Test. **(F–J)** Effects of systemic *PKI2* and *PPI2C4* over-expression on plant growth. Third and fourth leaves of 2–3-week-old *N. benthamiana* seedlings were tooth-pick incoculated with the indicated viral constructs. PVX or PVX::*gfp* transformed plants were used as controls. Representative pictures of entire plants **(F),** root systems **(G)** and newly formed leaves **(H)**, and measurement of root **(I)** and shoot **(J)** dry weight 21 days after *A. tumefaciens* inoculation. Values are the means of 10 different measurements repeated in three independent experiments; error bars represent the standard deviation. Different letters indicate significant differences ($P < 0.01$) according to One-way ANOVA with *post hoc* Tukey HSD Test.

was observed in control PVX (data not shown) or PVX::*gfp* transformed leaves.

To understand if misregulation of cell division in these plants was associated with an alteration of the endogenous protease activity, TSP from mock- (H_2O) and PVX-infiltrated *N. benthamiana* leaf areas were either directly used in a in-gel protease assay (**Figure 7A**) or the first extracts mixed with the latter's to measure the residual protease activity

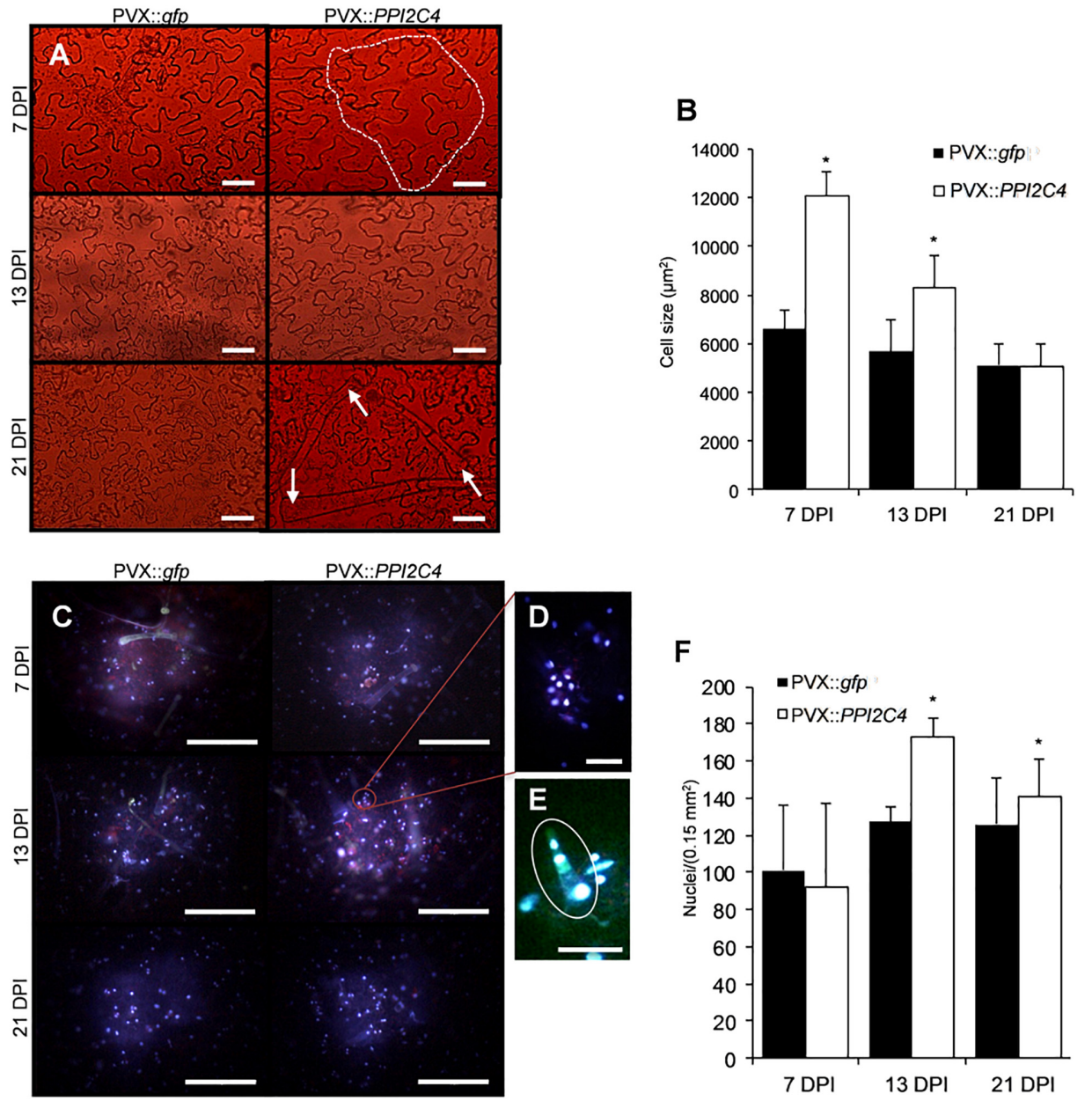

FIGURE 6 | Effect of *PPI2C4* gene overexpression on epidermal cell division and trichome accumulation. **(A,C,D,E)** Representative pictures of *Nicotiana benthamiana* transformed epidermal cells under light microscopy **(A)** or fluorescence microcopy (DAPI staining) **(C–E)**, 7, 13 and 21 days after syringe-infiltration (DPI) with a solution of *Agrobacterium tumefaciens* carring the indicated viral constructs. **(D)** Magnification of **(C)** to show details of clustered nuclei. **(E)** Magnification of a neoforming trichome observed 13 DPI in PVX::*PPI2C4* transformed leaves. Note the bigger size of epidermal cells 7 DPI (circled) and number of trichomes 21 DPI (pointed with arrowheads) in PVX:: *PPI2C4* transformed leaves. Scale bar, 10 μm in **(A,D,E)** and 50 μm in **(C)**. **(B,F)** Cell size **(B)** and number of nuclei **(F)** in transformed adaxial leaf epidemis (n = 500 cells, in at least four leaves) 7, 13, and 21 DPI (*$P < 0.0001$ versus PVX::*gfp* according to Yates' corrected chi-squared test).

(**Figure 7B**). Similar results were obtained in these two assays. In the first case, an additional protease band was clearly visible in the GFP-expressing sample and in the mock-inoculated control, but not in the TSP from PVX::*PKI2* and PVX::*PPI2C4* transformed plants (**Figure 7A**). In the second case, TSP from PKI2- and PPI2C4-expressing samples showed 100 and 60% higher inhibitory activities, respectively, than those from control plants (GFP expressing). Interestingly, TSP from PKI2- and PPI2C4-expressing samples also showed a high degree of inhibition (90%) toward *N. benthamiana* apoplastic protease activity, when compared to the GFP-expressing controls (**Figure 7C**).

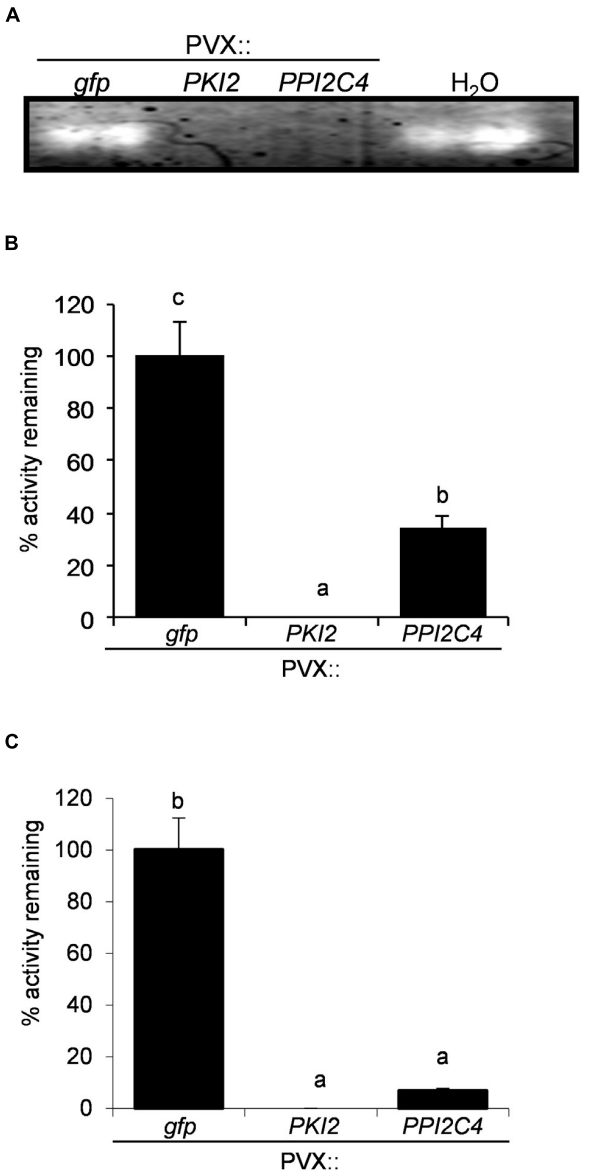

FIGURE 7 | *PKI2* and *PPI2C4* inhibit *Nicotiana benthamiana* apoplastic proteasic activity. **(A)** Zymogen in-gel protease assays of total soluble proteins (TSP) extracted from mock- (H_2O) and PVX-infiltrated *Nicotiana benthamiana* leaf areas (7 days after syringe-infiltration). **(B,C)** TSP **(B)** or intercellular fluids **(C)** isolated from untransformed *N. benthamiana* plant leaves were incubated with TSP extracted from PVX-transformed *N. benthamiana* leaf areas (7 days after syringe-infiltration) and the remaining protease activity was analyzed by measuring the change in optical density at 450 nm after 1 h of incubation in the presence of a 1% (w/v) azocasein solution. Values are the means of triplicate determinations; error bars represent the standard deviation. Different letters indicate significant differences ($P < 0.05$) according to One-way ANOVA with *post hoc* Tukey HSD Test.

DISCUSSION

Hydrolysis and protein synthesis, as well as the regulation of these physiological processes, are fundamental phenomena impacting both plant development and susceptibility/resistance to pathogens (Rawlings et al., 2004, 2014; Turrà and Lorito, 2011; Grosse-Holz and van der Hoorn, 2016). Indeed, several members of the serine protease group, a widely distributed set of extracellular and intracellular proteolytic enzymes, act as pathogenicity factors in different plant pathogens including fungi, oomycetes, bacteria, insects, and nematodes (Ryan, 1990; Urwin et al., 1995; Atkinson et al., 2003; Gvozdeva et al., 2004; Lopez-Solanilla et al., 2004; Hermosa et al., 2006; Pekkarinen et al., 2007; Luo et al., 2009; Thomas and van der Hoorn, 2018). Besides, serine proteases also regulate a panoply of endogenous processes in plants including innate immunity, cell death and nitrogen uptake (Kohli et al., 2012; Grosse-Holz and van der Hoorn, 2016; Salvesen et al., 2016; Balakireva and Zamyatnin, 2018). Interestingly, inhibitors of these enzymes, especially those belonging to the multigene PI families *PKPI* and *Pin1* have been shown to accumulate in plant tissues in a highly precise spatial and temporal manner and following both abiotic and biotic threats (Hermosa et al., 2006; Wang et al., 2008; Singh et al., 2009; Turrà et al., 2009; Boex-Fontvieille et al., 2015; Rustgi et al., 2017). These findings together with the increasing evidence of their inhibitory activity both *in vitro* and *in vivo* toward insects and nematodes, and *in vitro* toward fungi and bacteria is indicative of a possible multitasking activity of these PI families in both the regulation of plant physiology and biochemical defense responses (Duan et al., 1996; Cai et al., 2003; Vila et al., 2005; Turrà and Lorito, 2011; Quilis et al., 2013). However, a clear correlation between *PKPI* and *Pin1* expression and *in planta* modulation of developmental processes or resistance toward fungal or bacterial pathogens is currently missing. We have previously shown that extracellular proteases secreted by the fungal pathogen *B. cinerea* mainly belong to the serine protease class (Hermosa et al., 2006). We further identified, from the complex set of plant-produced PIs, different protein products belonging to the PKPI and Pin1 serine proteinase inhibitor families and showing high inhibitory activity on both fungal growth and disease development when exogenously supplemented to the fungal inoculum source (Hermosa et al., 2006). Now, to demonstrate their efficacy *in vivo* toward fungal plant pathogens, we have heterologously expressed different potato *PKPI* and *Pin1* genes in *N. benthamiana*, a model system to study the effect of transgene expression on plant-pathogen interactions (Goodin et al., 2008). Consistent with our previous findings, all tested *PIs* genes (except the *Pin1 PPI3A2*) efficiently reduced the *in vitro* growth and increased plant resistance toward two fungal pathogens, *B. cinerea* and *A. alternata*. Noteworthy, no *B. cinerea* symptoms developed at all, even 6 days postinoculation, on *N. benthamiana* plants transformed with PPI3B2, the potato Pin1 inhibitor formerly identified for its strong antifungal activity on *B. cinerea in vitro* (Hermosa et al., 2006). To understand if *in planta* over-expression of *PKPI* and *Pin1* genes could also alter plant resistance toward bacterial phytopathogens, we challenged *N. benthamiana* transformed plants with the bacterial pathogen *P. syringae* pv. *tabaci*. Interestingly, bacteria survival in PKI2-, PPI3A2-, PPI3B2-, and PPI2C4-expressing plants dropped over time and necrotic symptoms barely developed on PKI2 and PPI2C4 transformed leaves, suggesting that PKPI and Pin1 PIs might act by exerting either a direct and/or indirect

antiproliferative activity on *Pseudomonas*. This hypothesis is supported by two lines of evidence. First, several studies have already shown the importance of *Pseudomonas* spp. cysteine and serine proteases in the degradation of both structural and soluble host plant proteins and virulence (Engel et al., 1998; Axtell et al., 2003; Hotson and Mudgett, 2004). Second, uninfected PKI2-, and PPI2C4-transformed areas from fully developed leaves enlarged abruptly and accumulated higher amounts of trichomes, epidermal cells specialized in defending the plant from both biotic and abiotic stresses (Wagner, 1991; Amme et al., 2005). Importantly, this phenotype was accompanied by an increase in epidermial cell growth and division in PVX:*PPI2C4* agroinfiltrated leaves and an overall shoot and root size in systemically transformed plants, indicative for an endogenous inhibitory activity of these PIs, as also shown by TSP activity on apoplastic proteases.

Overall our findings show for the first time that specific members of the Pin1 and PKPI PI families might act as multifunctional proteins playing fundamental roles in both the regulation of important plant physiological processes such as cell development and differentiation as well as wide-spectrum disease resistance against fungal and bacterial pathogens. These results might represent a framework for the future selection of *Pin1* and *PKPI* genes to be used either individually or in gene pyramiding approaches to obtain fast-growing trees or crops with broad-resistance to biotic threats.

DATA AVAILABILITY STATEMENT

All datasets generated for this study are included in the article/**Supplementary Material**.

AUTHOR CONTRIBUTIONS

DT, SV, SW, and ML designed and conceived the study, and wrote the manuscript. DT, SV, and RM performed the experiments and analyzed the data. All authors read and approved the final version of the manuscript for publication.

FUNDING

This work was supported by the following projects: MIURPON (Grant No. Linfa 03PE_00026_1; Grant No. Marea 03PE_00106); MIUR-GPS (Grant No. Sicura DM29156); POR FESR CAMPANIA 2014/2020- O.S. 1.1 (Grant No. Bioagro CUP B63D18000270007); MISE (Grant No. Protection F/050421/01-03/X32); PRIN 2017 (Grant No. PROSPECT 2017JLN833); Regione Veneto PSR 2014-2020 (Grant No. DIVINE 3589659) and Regione Campania PSR 2014-2020 (Grant No. ABC 2015.15.17221.5692).

ACKNOWLEDGMENTS

We gratefully thank D. Baulcombe (Sainsbury Laboratory, Norwich, United Kingdom) for the PVX-based expression vectors pgR106 and pgR208 and the *A. tumefaciens* strain GV3101.

SUPPLEMENTARY MATERIAL

The Supplementary Material for this article can be found online at: https://www.frontiersin.org/articles/10.3389/fpls.2020.00461/full#supplementary-material

REFERENCES

Altpeter, F., Diaz, I., McAuslane, H., Gaddour, K., Carbonero, P., and Vasil, I. (1999). Increased insect resistance in transgenic wheat stably expressing trypsin inhibitor CMe. *Mol. Breed.* 5, 53–63. doi: 10.1023/A:1009659911798

Amme, S., Rutten, T., Melzer, M., Sonsmann, G., Vissers, J. P., Schlesier, B., et al. (2005). A proteome approach defines protective functions of tobacco leaf trichomes. *Proteomics* 5, 2508–2518. doi: 10.1002/pmic.200401274

Andrade, S. A., Santomauro-Vaz, E. M., Lopes, A. R., Chudzinski-Tavassi, A. M., Juliano, M. A., Terra, W. R., et al. (2003). Bauhinia proteinase inhibitor-based synthetic fluorogenic substrates for enzymes isolated from insect midgut and caterpillar bristles. *Biol. Chem.* 384, 489–492.

Atkinson, H. J., Urwin, P. E., and McPherson, M. J. (2003). Engineering plants for nematode resistance. *Annu. Rev. Phytopathol.* 41, 615–639.

Axtell, M. J., Chisholm, S. T., Dahlbeck, D., and Staskawicz, B. J. (2003). Genetic and molecular evidence that the *Pseudomonas syringae* type III effector protein AvrRpt2 is a cysteine protease. *Mol. Microbiol.* 49, 1537–1546. doi: 10.1046/j.1365-2958.2003.03666.x

Balakireva, A. V., and Zamyatnin, A. A. (2018). Indispensable role of proteases in plant innate immunity. *Int. J. Mol. Sci.* 19:629. doi: 10.3390/ijms19020629

Balandin, T., van der Does, C., Albert, J. M., Bol, J. F., and Linthorst, H. J. (1995). Structure and induction pattern of a novel proteinase inhibitor class II gene of tobacco. *Plant Mol. Biol.* 27, 1197–1204. doi: 10.1007/bf00020893

Boex-Fontvieille, E., Rustgi, S., Reinbothe, S., and Reinbothe, C. (2015). A Kunitz-type protease inhibitor regulates programmed cell death during flower development in *Arabidopsis thaliana*. *J. Exp. Bot.* 66, 6119–6135. doi: 10.1093/jxb/erv327

Cai, D., Thurau, T., Tian, Y., Lange, T., Yeh, K. W., and Jung, C. (2003). Sporamin-mediated resistance to beet cyst nematodes (*Heterodera schachtii* Schm.) is dependent on trypsin inhibitory activity in sugar beet (*Beta vulgaris* L.) hairy roots. *Plant Mol. Biol.* 51, 839–849.

Chen, Z. Y., Brown, R. L., Lax, A. R., Cleveland, T. E., and Russin, J. S. (1999). Inhibition of plant-pathogenic fungi by a corn trypsin inhibitor overexpressed in *Escherichia coli*. *Appl. Environ. Microbiol.* 65, 1320–1324. doi: 10.1128/aem.65.3.1320-1324.1999

Collins, T. J. (2007). ImageJ for microscopy. *Biotechniques* 43(1 Suppl.), 25–30.

Di Cera, E. (2009). Serine proteases. *IUBMB Life* 61, 510–515. doi: 10.1002/iub.186

Duan, X., Li, X., Xue, Q., Abo-el-Saad, M., Xu, D., and Wu, R. (1996). Transgenic rice plants harboring an introduced potato proteinase inhibitor II gene are insect resistant. *Nat. Biotechnol.* 14, 494–498. doi: 10.1038/nbt0496-494

Dunaevsky, Y. E., Pavlukova, E. B., and Belozersky, M. A. (1996). Isolation and properties of anionic protease inhibitors from buckwheat seeds. *Biochem. Mol. Biol. Int.* 40, 199–208. doi: 10.1080/15216549600201692

Emanuelsson, O., Brunak, S., von Heijne, G., and Nielsen, H. (2007). Locating proteins in the cell using TargetP, SignalP and related tools. *Nat. Protoc.* 2, 953–971. doi: 10.1038/nprot.2007.131

Engel, L. S., Hill, J. M., Caballero, A. R., Green, L. C., and O'Callaghan, R. J. (1998). Protease IV, a unique extracellular protease and virulence factor from *Pseudomonas aeruginosa*. *J. Biol. Chem.* 273, 16792–16797. doi: 10.1074/jbc.273.27.16792

Gevaudant, F., Duby, G., von Stedingk, E., Zhao, R., Morsomme, P., and Boutry, M. (2007). Expression of a constitutively activated plasma membrane H+-ATPase alters plant development and increases salt tolerance. *Plant Physiol.* 144, 1763–1776. doi: 10.1104/pp.107.103762

Goodin, M. M., Zaitlin, D., Naidu, R. A., and Lommel, S. A. (2008). *Nicotiana benthamiana*: its history and future as a model for plant–pathogen interactions. *Mol. Plant Microbe Interact.* 21, 1015–1026. doi: 10.1094/mpmi-21-8-1015

Grosse-Holz, F. M., and van der Hoorn, R. A. L. (2016). Juggling jobs: roles and mechanisms of multifunctional protease inhibitors in plants. *New Phytol.* 210, 794–807. doi: 10.1111/nph.13839

Gvozdeva, E. L., Ievleva, E. V., Gerasimova, N. G., Ozeretskovskaia, O. L., and Valueva, T. A. (2004). Exoproteinases of the oomycete Phytophthora infestans. *Prikl. Biokhim. Mikrobiol.* 40, 194–200.

Heibges, A., Glaczinski, H., Ballvora, A., Salamini, F., and Gebhardt, C. (2003). Structural diversity and organization of three gene families for Kunitz-type enzyme inhibitors from potato tubers (*Solanum tuberosum* L.). *Mol. Genet. Genomics* 269, 526–534. doi: 10.1007/s00438-003-0860-0

Heitz, T., Geoffroy, P., Stintzi, A., Fritig, B., and Legrand, M. (1993). cDNA cloning and gene expression analysis of the microbial proteinase inhibitor of tobacco. *J. Biol. Chem.* 268, 16987–16992.

Hermosa, M. R., Turrà, D., Fogliano, V., Monte, E., and Lorito, M. (2006). Identification and characterization of potato protease inhibitors able to inhibit pathogenicity and growth of *Botrytis cinerea*. *Physiol. Mol. Plant Pathol.* 68, 138–148. doi: 10.1016/j.pmpp.2006.09.004

Horton, P., Park, K. J., Obayashi, T., Fujita, N., Harada, H., Adams-Collier, C. J., et al. (2007). WoLF PSORT: protein localization predictor. *Nucleic Acids Res.* 35, W585–W587. doi: 10.1093/nar/gkm259

Hotson, A., and Mudgett, M. B. (2004). Cysteine proteases in phytopathogenic bacteria: identification of plant targets and activation of innate immunity. *Curr. Opin. Plant Biol.* 7, 384–390. doi: 10.1016/j.pbi.2004.05.003

Jofuku, K. D., and Goldberg, R. B. (1989). Kunitz trypsin inhibitor genes are differentially expressed during the soybean life cycle and in transformed tobacco plants. *Plant Cell* 1, 1079–1093. doi: 10.1105/tpc.1.11.1079

Jongsma, M. A., Bakker, P. L., Peters, J., Bosch, D., and Stiekema, W. J. (1995). Adaptation of *Spodoptera exigua* larvae to plant proteinase inhibitors by induction of gut proteinase activity insensitive to inhibition. *Proc. Natl. Acad. Sci. U.S.A.* 92, 8041–8045. doi: 10.1073/pnas.92.17.8041

Keller, C. P., and Van Volkenburgh, E. (1997). Auxin-induced epinasty of tobacco leaf tissues (a nonethylene-mediated response). *Plant Physiol.* 113, 603–610. doi: 10.1104/pp.113.2.603

Kim, J. Y., Park, S. C., Kim, M. H., Lim, H. T., Park, Y., and Hahm, K. S. (2005). Antimicrobial activity studies on a trypsin-chymotrypsin protease inhibitor obtained from potato. *Biochem. Biophys. Res. Commun.* 330, 921–927. doi: 10.1016/j.bbrc.2005.03.057

Kim, M. H., Park, S. C., Kim, J. Y., Lee, S. Y., Lim, H. T., Cheong, H., et al. (2006). Purification and characterization of a heat-stable serine protease inhibitor from the tubers of new potato variety "Golden Valley". *Biochem. Biophys. Res. Commun.* 346, 681–686. doi: 10.1016/j.bbrc.2006.05.186

Kohli, A., Narciso, J. O., Miro, B., and Raorane, M. (2012). Root proteases: reinforced links between nitrogen uptake and mobilization and drought tolerance. *Physiol. Plant* 145, 165–179. doi: 10.1111/j.1399-3054.2012.01573.x

Kuo, T. M., Pearce, G., and Ryan, C. A. (1984). Isolation and characterization of proteinase inhibitor I from etiolated tobacco leaves. *Arch. Biochem. Biophys.* 230, 504–510. doi: 10.1016/0003-9861(84)90430-2

Lee, J. S., Brown, W. E., Graham, J. S., Pearce, G., Fox, E. A., Dreher, T. W., et al. (1986). Molecular characterization and phylogenetic studies of a wound-inducible proteinase inhibitor I gene in *Lycopersicon* species. *Proc. Natl. Acad. Sci. U.S.A.* 83, 7277–7281. doi: 10.1073/pnas.83.19.7277

Lincoln, J. E., Cordes, S., Read, E., and Fischer, R. L. (1987). Regulation of gene expression by ethylene during *Lycopersicon esculentum* (tomato) fruit development. *Proc. Natl. Acad. Sci. U.S.A.* 84, 2793–2797. doi: 10.1073/pnas.84.9.2793

Liu, J., Xia, K. F., Zhu, J. C., Deng, Y. G., Huang, X. L., Hu, B. L., et al. (2006). The nightshade proteinase inhibitor IIb gene is constitutively expressed in glandular trichomes. *Plant Cell Physiol.* 47, 1274–1284. doi: 10.1093/pcp/pcj097

Lopez-Solanilla, E., Bronstein, P. A., Schneider, A. R., and Collmer, A. (2004). HopPtoN is a *Pseudomonas syringae* Hrp (type III secretion system) cysteine protease effector that suppresses pathogen-induced necrosis associated with both compatible and incompatible plant interactions. *Mol. Microbiol.* 54, 353–365. doi: 10.1111/j.1365-2958.2004.04285.x

Lorito, M., Broadway, R. M., Hayes, C. K., Woo, S. L., Noviello, C., Williams, D. L., et al. (1994). Proteinase inhibitors from plants as a novel class of fungicides. *Mol. Plant Microbe Interact.* 7, 525–527.

Lu, R., Malcuit, I., Moffett, P., Ruiz, M. T., Peart, J., Wu, A. J., et al. (2003). High throughput virus-induced gene silencing implicates heat shock protein 90 in plant disease resistance. *EMBO J.* 22, 5690–5699. doi: 10.1093/emboj/cdg546

Luo, Y., Caldwell, K. S., Wroblewski, T., Wright, M. E., and Michelmore, R. W. (2009). Proteolysis of a negative regulator of innate immunity is dependent on resistance genes in tomato and *Nicotiana benthamiana* and induced by multiple bacterial effectors. *Plant Cell* 21, 2458–2472. doi: 10.1105/tpc.107.056044

Mello, G. C., Oliva, M. L., Sumikawa, J. T., Machado, O. L., Marangoni, S., Novello, J. C., et al. (2001). Purification and characterization of a new trypsin inhibitor from *Dimorphandra mollis* seeds. *J. Protein Chem.* 20, 625–632.

Moehnke, M. H., Midoro-Horiuti, T., Goldblum, R. M., and Kearney, C. M. (2008). The expression of a mountain cedar allergen comparing plant-viral apoplastic and yeast expression systems. *Biotechnol. Lett.* 30, 1259–1264. doi: 10.1007/s10529-008-9665-x

Pak, C., and Van Doorn, W. G. (2005). Delay of Iris flower senescence by protease inhibitors. *New Phytol.* 165, 473–480. doi: 10.1111/j.1469-8137.2004.01226.x

Pekkarinen, A. I., Longstaff, C., and Jones, B. L. (2007). Kinetics of the inhibition of fusarium serine proteinases by barley (*Hordeum vulgare* L.) inhibitors. *J. Agric. Food Chem.* 55, 2736–2742. doi: 10.1021/jf0631777

Quilis, J., Lopez-Garcia, B., Meynard, D., Guiderdoni, E., and San Segundo, B. (2013). Inducible expression of a fusion gene encoding two proteinase inhibitors leads to insect and pathogen resistance in transgenic rice. *Plant Biotechnol. J.* 12, 367–377. doi: 10.1111/pbi.12143

Rairdan, G. J., Collier, S. M., Sacco, M. A., Baldwin, T. T., Boettrich, T., and Moffett, P. (2008). The coiled-coil and nucleotide binding domains of the Potato Rx disease resistance protein function in pathogen recognition and signaling. *Plant Cell* 20, 739–751. doi: 10.1105/tpc.107.056036

Rawlings, N. D., Tolle, D. P., and Barrett, A. J. (2004). Evolutionary families of peptidase inhibitors. *Biochem. J.* 378(Pt 3), 705–716. doi: 10.1042/bj20031825

Rawlings, N. D., Waller, M., Barrett, A. J., and Bateman, A. (2014). MEROPS: the database of proteolytic enzymes, their substrates and inhibitors. *Nucleic Acids Res.* 42, D503–D509. doi: 10.1093/nar/gkt953

Rosahl, S., Eckes, P., Schell, J., and Willmitzer, L. (1986). Organ-specific gene expression in potato: isolation and characterization of tuber-specific cDNA sequences. *Mol. Gen. Genet.* 202, 368–373. doi: 10.1007/bf00333264

Rustgi, S., Boex-Fontvieille, E., Reinbothe, C., von Wettstein, D., and Reinbothe, S. (2017). Serpin1 and WSCP differentially regulate the activity of the cysteine protease RD21 during plant development in *Arabidopsis thaliana*. *Proc. Natl. Acad. Sci. U.S.A.* 114, 2212–2217. doi: 10.1073/pnas.1621496114

Ryan, C. A. (1990). Protease inhibitors in plants: genes for improving defenses against insects and pathogens. *Annu. Rev. Phytopathol.* 28, 425–449. doi: 10.1146/annurev.py.28.090190.002233

Salvesen, G. S., Hempel, A., and Coll, N. S. (2016). Protease signaling in animal and plant-regulated cell death. *FEBS J.* 283, 2577–2598. doi: 10.1111/febs.13616

Sambrook, J., and Russell, D. W. (2001). *Molecular Cloning: A Laboratory Manual*. Cold Spring Harbor, NY: Cold Spring Harbor Laboratory Press.

Sin, S. F., and Chye, M. L. (2004). Expression of proteinase inhibitor II proteins during floral development in *Solanum americanum*. *Planta* 219, 1010–1022. doi: 10.1007/s00425-004-1306-6

Singh, A., Sahi, C., and Grover, A. (2009). Chymotrypsin protease inhibitor gene family in rice: Genomic organization and evidence for the presence of a bidirectional promoter shared between two chymotrypsin protease inhibitor genes. *Gene* 428, 9–19. doi: 10.1016/j.gene.2008.09.028

Soares-Costa, A., Beltramini, L. M., Thiemann, O. H., and Henrique-Silva, F. (2002). A sugarcane cystatin: recombinant expression, purification, and antifungal activity. *Biochem. Biophys. Res. Commun.* 296, 1194–1199. doi: 10.1016/s0006-291x(02)02046-6

Solomon, M., Belenghi, B., Delledonne, M., Menachem, E., and Levine, A. (1999). The involvement of cysteine proteases and protease inhibitor genes in the regulation of programmed cell death in plants. *Plant Cell* 11, 431–444.

Srinivasan, A., Giri, A. P., Harsulkar, A. M., Gatehouse, J. A., and Gupta, V. S. (2005). A Kunitz trypsin inhibitor from chickpea (*Cicer arietinum* L.) that exerts anti-metabolic effect on podborer (*Helicoverpa armigera*) larvae. *Plant Mol. Biol.* 57, 359–374. doi: 10.1007/s11103-004-7925-2

Tamhane, V. A., Giri, A. P., Kumar, P., and Gupta, V. S. (2009). Spatial and temporal expression patterns of diverse Pin-II proteinase inhibitor genes in *Capsicum annuum* Linn. *Gene* 442, 88–98. doi: 10.1016/j.gene.2009.04.012

Thomas, E. L., and van der Hoorn, R. A. L. (2018). Ten prominent host proteases in plant-pathogen interactions. *Int. J. Mol. Sci.* 19:639. doi: 10.3390/ijms19020639

Tian, M., Huitema, E., Da Cunha, L., Torto-Alalibo, T., and Kamoun, S. (2004). A Kazal-like extracellular serine protease inhibitor from *Phytophthora infestans* targets the tomato pathogenesis-related protease P69B. *J. Biol. Chem.* 279, 26370–26377. doi: 10.1074/jbc.m400941200

Turrà, D., Bellin, D., Lorito, M., and Gebhardt, C. (2009). Genotype-dependent expression of specific members of potato protease inhibitor gene families in different tissues and in response to wounding and nematode infection. *J. Plant Physiol.* 166, 762–774. doi: 10.1016/j.jplph.2008.10.005

Turrà, D., and Lorito, M. (2011). Potato type I and II proteinase inhibitors: modulating plant physiology and host resistance. *Curr. Protein Pept. Sci.* 12, 374–385. doi: 10.2174/138920311796391151

Urwin, P. E., Atkinson, H. J., Waller, D. A., and McPherson, M. J. (1995). Engineered oryzacystatin-I expressed in transgenic hairy roots confers resistance to *Globodera pallida*. *Plant J.* 8, 121–131. doi: 10.1046/j.1365-313x.1995.08010121.x

van den Broek, L. A., Pouvreau, L., Lommerse, G., Schipper, B., Van Koningsveld, G. A., and Gruppen, H. (2004). Structural characterization of potato protease inhibitor I (Cv. Bintje) after expression in *Pichia pastoris*. *J. Agric. Food Chem.* 52, 4928–4934.

van der Hoorn, R. A. (2008). Plant proteases: from phenotypes to molecular mechanisms. *Annu. Rev. Plant Biol.* 59, 191–223. doi: 10.1146/annurev.arplant.59.032607.092835

van Loon, L. C., Rep, M., and Pieterse, C. M. (2006). Significance of inducible defense-related proteins in infected plants. *Annu. Rev. Phytopathol.* 44, 135–162. doi: 10.1146/annurev.phyto.44.070505.143425

Vila, L., Quilis, J., Meynard, D., Breitler, J. C., Marfa, V., Murillo, I., et al. (2005). Expression of the maize proteinase inhibitor (mpi) gene in rice plants enhances resistance against the striped stem borer (*Chilo suppressalis*): effects on larval growth and insect gut proteinases. *Plant Biotechnol. J.* 3, 187–202. doi: 10.1111/j.1467-7652.2004.00117.x

Wagner, G. J. (1991). Secreting glandular trichomes: more than just hairs. *Plant Physiol.* 96, 675–679. doi: 10.1104/pp.96.3.675

Wang, H. Y., Huang, Y. C., Chen, S. F., and Yeh, K. W. (2003). Molecular cloning, characterization and gene expression of a water deficiency and chilling induced proteinase inhibitor I gene family from sweet potato (*Ipomoea batatas* Lam.) leaves. *Plant Sci.* 165, 191–203. doi: 10.1016/s0168-9452(03)00158-4

Wang, J., Shi, Z. Y., Wan, X. S., Shen, G. Z., and Zhang, J. L. (2008). The expression pattern of a rice proteinase inhibitor gene OsPI8-1 implies its role in plant development. *J. Plant Physiol.* 165, 1519–1529. doi: 10.1016/j.jplph.2007.08.008

Xie, J., Ouyang, X. Z., Xia, K. F., Huang, Y. F., Pan, W. B., Cai, Y. P., et al. (2007). Chloroplast-like organelles were found in enucleate sieve elements of transgenic plants overexpressing a proteinase inhibitor. *Biosci. Biotechnol. Biochem.* 71, 2759–2765. doi: 10.1271/bbb.70362

Xu, Z. F., Qi, W. Q., Ouyang, X. Z., Yeung, E., and Chye, M. L. (2001). A proteinase inhibitor II of *Solanum americanum* is expressed in phloem. *Plant Mol. Biol.* 47, 727–738.

Conflict of Interest: The authors declare that the research was conducted in the absence of any commercial or financial relationships that could be construed as a potential conflict of interest.

frontiers in Plant Science

ORIGINAL RESEARCH
published: 08 May 2020
doi: 10.3389/fpls.2020.00529

Arabidopsis Plants Sense Non-self Peptides to Promote Resistance Against *Plectosphaerella cucumerina*

Julia Pastor-Fernández, Jordi Gamir, Victoria Pastor, Paloma Sanchez-Bel, Neus Sanmartín, Miguel Cerezo and Víctor Flors*

Metabolic Integration and Cell Signaling Laboratory, Plant Physiology Section, Unidad Asociada al Consejo Superior de Investigaciones Científicas (EEZ-CSIC)-Department of Ciencias Agrarias y del Medio Natural, Universitat Jaume I, Castellón, Spain

Peptides are important regulators that participate in the modulation of almost every physiological event in plants, including defense. Recently, many of these peptides have been described as defense elicitors, termed phytocytokines, that are released upon pest or pathogen attack, triggering an amplification of plant defenses. However, little is known about peptides sensing and inducing resistance activities in heterologous plants. In the present study, exogenous peptides from solanaceous species, Systemins and HypSys, are sensed and induce resistance to the necrotrophic fungus *Plectosphaerella cucumerina* in the taxonomically distant species *Arabidopsis thaliana.* Surprisingly, other peptides from closer taxonomic clades have very little or no effect on plant protection. *In vitro* bioassays showed that the studied peptides do not have direct antifungal activities, suggesting that they protect the plant through the promotion of the plant immune system. Interestingly, tomato Systemin was able to induce resistance at very low concentrations (0.1 and 1 nM) and displays a maximum threshold being ineffective above at higher concentrations. Here, we show evidence of the possible involvement of the JA-signaling pathway in the Systemin-Induced Resistance (Sys-IR) in Arabidopsis. Additionally, Systemin treated plants display enhanced *BAK1* and *BIK1* gene expression following infection as well as increased production of ROS after PAMP treatment suggesting that Systemin sensitizes Arabidopsis perception to pathogens and PAMPs.

Keywords: systemin, induced resistance, Arabidopsis, LC-MS, *Plectoshaerella cucumerina*

OPEN ACCESS

Edited by:
Laura Bertini,
University of Tuscia, Italy

Reviewed by:
Antonio Molina,
Polytechnic University of Madrid, Spain
Pierre Pétriacq,
Université de Bordeaux, France
Lenka Burketova,
Institute of Experimental Botany, Academy of Sciences of the Czech Republic, Czechia

***Correspondence:**
Víctor Flors
flors@uji.es

Specialty section:
This article was submitted to Plant Microbe Interactions, a section of the journal Frontiers in Plant Science

Received: *05 November 2019*
Accepted: *07 April 2020*
Published: *08 May 2020*

Citation:
Pastor-Fernández J, Gamir J, Pastor V, Sanchez-Bel P, Sanmartín N, Cerezo M and Flors V (2020) Arabidopsis Plants Sense Non-self Peptides to Promote Resistance Against Plectosphaerella cucumerina. Front. Plant Sci. 11:529. doi: 10.3389/fpls.2020.00529

INTRODUCTION

Plants are constantly challenged by changes in their environment, such as biotic and abiotic stresses. To respond to biotic challenges, such as chewing insects or pathogen attack, plants have developed complex strategies that allow them to mount a proper defense response. Plants can sense pathogens by recognizing the so-called pathogen-associated molecular patterns (PAMPs), which are exogenous molecules that belong to specific classes of microbes, such as flagellin (Flg22) and Elf18 from bacteria or chitin from fungi. PAMPs are recognized by membrane pattern recognition receptors (PRRs), triggering a first layer of inducible plant defense referred to as PAMP-triggered immunity (PTI) that includes reactive oxygen species (ROS) and Ca^{2+}

burst, mitogen-activated protein kinases (MAPKs) activation, phytohormones production and transcriptomic and metabolomic reprogramming (Saijo et al., 2018; Hou et al., 2019).

Plants are also able to recognize host-derived molecules that are released from disrupted cells after pest or pathogen attack and bind to PRRs on intact cells, triggering the amplification of immune signaling. These molecules are known as damage-associated molecular patterns (DAMPs) and include, on the one hand, cell wall fragments that are released after cellular damage caused, for example, by herbivores and, on the other hand, peptide molecules that are released and rapidly activated upon pest or pathogen challenge and cause the amplification of immune signaling (Hou et al., 2019).

Although many peptides have been described as DAMPs, recent studies include these peptides in a new classification. Classic DAMPs are cell debris that are passively released after a cellular disruption and are usually components of the cell wall, such as oligogalacturonides (OGs) and xyloglucan oligosaccharides. Nevertheless, peptides are usually actively synthesized, processed and released by cells under a stress situation that does not include cell damage; these peptides are secondary endogenous danger signals, also named phytocytokines due to their similarity to mammalian cytokines (Gust et al., 2017).

Exposure to danger signals, such as PAMPs, DAMPs or phytocytokines, as well as many other stimuli, produces an alarm state in the plant, enhancing defense capacity locally and systemically that protects the plant against future attack (Gust et al., 2017; Yu et al., 2017; Hou et al., 2019). This state is called induced resistance (IR) and can be triggered by pathogenic and non-pathogenic microbes, herbivores and chemicals, leading to systemic acquired resistance (SAR), or by plant beneficial microbes, including plant growth-promoting rhizobacteria and fungi, leading induced systemic resistance (ISR) (Pieterse et al., 2014). The state of induced resistance is characterized by the rapid activation of latent defense mechanisms, for instance, the production of antimicrobial proteins, and confers protection against a broad spectrum of threats (Pieterse et al., 2014).

An increasing number of plant peptides have been described as defense elicitors. These peptides are released upon pest or pathogen attack and usually derived from the processing of larger precursor proteins, secreted into the extracellular space and bind to specific membrane receptors, triggering a cascade of plant defenses and causing an amplification of the plant immune response (Yamaguchi and Huffaker, 2011; Albert, 2013).

Systemin was the first signaling peptide described in plants (Pearce et al., 1991). Systemin is an 18 aa peptide found in tomato plants that is part of in a 200 aa precursor protein, Prosystemin. Systemin is released upon wounding or herbivory and induces the accumulation of protease inhibitors (PIs) in local and systemic leaves and volatile signaling that attract natural predators of the pest (Corrado et al., 2007). There is also evidence of the role of Systemin in defense against pathogenic fungi (De la Noval et al., 2007; Coppola et al., 2015, 2019). The hydroxyproline-rich systemins (HypSys) are peptides found in tomato and tobacco that trigger physiological responses that are similar to those triggered by tomato Systemin (Pearce et al., 2001; Pearce and Ryan, 2003). In Arabidopsis, elicitor peptides (Peps) were described as endogenous amplifiers of innate immunity that induce the transcription of defense-related genes, such as defensin *PDF1.2* and *PR1*, and activate the synthesis of reactive oxygen species (ROS; e.g., H_2O_2) (Huffaker et al., 2006; Klauser et al., 2013). AtPep1 participates in plant resistance against several pathogens, including *Botrytis cinerea, Pseudomonas syringae* pv. DC3000 and *Phytophthora infestans* (Huffaker et al., 2006; Yamaguchi et al., 2010; Liu et al., 2013), and contributes to JA-mediated defense against herbivory (Klauser et al., 2015). Another family of peptides, PAMP-induced peptides (PIPs), were identified in Arabidopsis and are induced by pathogens and elicitors. More specifically, when PIP1 and PIP2 are externally applied, they lead to enhanced immune responses and resistance to *Pseudomonas syringae* and *Fusarium oxysporum* (Hou et al., 2014). Likewise, three short peptides from Soybean, GmPep914, GmPep890, and GmSubPep, were found to alkalinize the cellular media and induce pathogen-related genes, such as *Chitinase 1* and *Chalcone Synthas*e, and genes involved in phytoalexin synthesis and production (Pearce et al., 2010; Yamaguchi et al., 2011).

Some peptides that were initially thought to be involved in different physiological events have been later found to have a role in defense responses. The Arabidopsis GRIM RIPER peptide (GRIp) is involved not only in the response to ozone but also in the resistance to bacterial pathogen PstDC3000 (Wrzaczek et al., 2009). Likewise, the IDA-LIKE 6 (IDL6) mature peptide was studied for its role in controlling floral organ abscission and lateral root emergence and was later found to be involved in the mediation of Arabidopsis susceptibility to *Pst* DC3000 (Wang et al., 2017). The peptides from rapid alkalinization factors (RALFs) were shown to positively and negatively regulate plant immunity through the RLK Feronia (FER) receptor (Stegmann et al., 2017). Recently, the plant pentapeptide, phytosulfokine (PSK), was found to enhance auxin-dependent immune responses through cytosolic Ca^{2+} signaling in tomato (Zhang et al., 2018).

Interestingly, some studies have reported peptide sensing and signaling in heterologous plant species. Although a report claims that tobacco cells do not respond to exogenous systemin treatment (Scheer et al., 2003), a later study showed that tobacco calli and suspension cells responded to Systemin by both MAPK activation and weak-medium alkalinization (Malinowski et al., 2009). In addition, it was also reported that constitutive expression of the tomato prosystemin gene in tobacco considerably affected the synthesis of host proteins, several of which are involved in protection against pathogens (Rocco et al., 2008). On the other hand, tobacco cells transformed with the AtPep1 receptor PEPR1 responded to nanomolar concentrations of AtPep1, producing a strong alkalinization of the cell culture medium, suggesting a capacity of tobacco to activate Pep1 signaling (Yamaguchi et al., 2006). More surprisingly, Zhang et al. (2017), reported that tomato Systemin was sensed by Arabidopsis plants, leading to an inhibition of seedling root growth and the expression of the plant defensin *PDF1.2*. Moreover, the expression of the tomato prosystemin

gene in Arabidopsis conferred resistance to the necrotrophic fungus *Botrytis cinerea* (Zhang et al., 2017).

These findings suggest that some plants may be able to sense exogenous peptides and that there could be a common receptor-mediated intracellular signaling pathway in response to peptides.

Small peptides have recently received attention since they are involved in almost all physiological plants processes. The vast agronomical potential of peptides is limited by the studies focused on plant species-self peptides. We tested whether exogenous treatment with peptides produced from different plant species are sensed and able to protect Arabidopsis plants. Hence, the goal of this study was to identify peptides from phylogenetically distant species with plant-resistance inducing activities against necrotrophic fungal pathogens.

MATERIALS AND METHODS

Plant Material and Growth Conditions

Seeds of wild type *Arabidopsis thaliana* Col-0 ecotype were sterilized for 30 s with 70% ethanol, followed by 15 min of a 10% bleach solution, and finally, 4–5 washes with sterile distilled water to remove the sterilization solution. Sterile seeds were sown *in vitro* 24-well plates in medium containing 4.9 g/L basal Murashige and Skoog (1962) salt mixture, 1% sucrose and 6 g/L Agar and 5.7 of pH. The plates were placed in a growth chamber with 9 h light period at 24°C and 15 h of darkness at 18°C; a dark surface was placed beneath the plates.

For the mutant screenings, the same procedure was carried out. The mutant *sid2.1* (Nawrath and Métraux, 1999) was kindly provided by M. Nishimura (Stanford University, CA, United States), *jar1* (Matthes et al., 2010) by Jurriaan Ton (University of Sheffield, United Kingdom), and *jin1* (Lorenzo et al., 2004) and *pad4.1* (Nishimura et al., 2003) were provided by Brigitte Mauch-Mani (University of Neuchâtel, Switzerland) and the mutant perp1 was obtained from SALK collection (SALK_059281) and previously described by Flury et al. (2013).

Tomato seeds (*Solanum lycopesicum* L. cv. Money Maker) were sterilized by 15 min shaking in a solution of 75% bleach containing 0.1% of Tween, followed by 4–5 washes with sterile distilled water to remove the sterilization solution. The seeds were sown in 100 ml pots containing 30 ml of solid MS medium (described above). The pots were then placed in a growth chamber with 16 h light period at 26°C and 8 h of darkness at 18°C; a dark surface was placed beneath the plates.

Peptide Treatment, Pathogen Inoculation and Infection Quantification by Trypan Blue Staining

The plants were treated 2 weeks after sowing with a range of peptide concentrations from 0.1 to 20 nM (final concentration) by adding the peptides to the medium. Twenty four hours after peptide treatment, plants were challenged with 5×10^3 spores/ml of *Plectosphaerella cucumerina* by drop inoculation (1 µl per leaf). In Arabidopsis plants, BABA was used as a positive control at a concentration of 1 ppm (1 mg/L) (Pastor et al., 2013).

For the infection quantification, the plants were collected 5 days after infection and dead cells were stained using trypan blue (Ton and Mauch-Mani, 2004). The infection levels were quantified by a disease rating, measured as a percentage of infected leaf surface according to a scale (0 = healthy leaves; 1 = leaves with less than 25% of diseased surface; 2 = leaves with 25–50%; 3 = leaves with 50–75% of diseased surface; 4 = leaves with more than 75% diseased surface). A minimum of 6 plants per condition and 4 leaves per plant were analyzed. All experiments were repeated a minimum of three times.

Fungal Biomass Quantification

Infection quantification was also determined by measuring a fungal constitutive gene related to a plant constitutive gene. Arabidopsis tissue of plants treated either with water or 0.1 nM systemin was collected for DNA extraction 48 h after pathogen infection. For the DNA extraction, a simple and rapid protocol was followed (Edwards et al., 1991). A Quantitative Real-Time PCR (qPCR) was performed with a Maxima SYBR Green/ROX qPCR Master Mix (2X) (Thermo Scientific), using a StepOne instrument (Applied Biosystems). A ratio was calculated of the expression of *PcTUBULIN*, as a constitutive gene of *P. cucumerina*, relative to the expression of *AtUBIQUITIN21,* a constitutive gene of Arabidopsis, following the ΔCt method. Primer sequences are listed in **Supplementary Table S1**.

In vitro Antifungal Assays

Sterile 12-well plates were filled with PDB1/2 medium containing the peptides at the concentration of 20 nM, the highest concentration used in the screenings. A solution with *Plectosphaerella cucumerina* spores was added to each well to a final concentration of 10^4 spores/ml in each well, and the plates were placed in a shaker until the next day. To measure the fungal growth, absorbance at 600 nm was measured 24 h after pathogen inoculation. This method was adapted from Broekaert et al. (1990). A commercial fungicidal was used as a positive control of growth inhibition.

ROS Production Measurement

H_2O_2 production after treatments was determined in leaf discs using a luminol-based assay as previously described (Torres et al., 2013). Two different experiments were performed. Firstly, to determine the ROS production in response to Systemin treatments, a group of leaf discs (6 mm diameter; $n = 8$) obtained from 6-week-old plants were stored with 150 ml of water. After 24 h the water was replaced by water (blanc) or Systemin at different concentrations (0.1, 1, 10, 100, and 1000 nM) in a 96-well titer plate (one disc/well) with a solution containing luminol (Sigma-Aldrich; 100 µM) and horseradish peroxidase (Sigma-Aldrich; 1 µg mL^{-1}). Secondly, to test whether Systemin treated plants were sensitive to PAMPs, the leaf discs were maintained overnight either with water or with increasing concentrations of systemin (0.1, 1, 10, 100, and 1000 nM). Twenty four hours later, H_2O_2 production was triggered by adding 100 nM flg22 to the leaf discs. Plates were analyzed for 1 h using a Luminoskan 96 microplate luminometer (Thermo Fisher Scientific) and a signal

integration time of 1.5 s. Luminescence was expressed in Relative Luminescence Units.

Targeted HPLC-MS for Hormonal Analysis

For hormonal analyses, 120 mg of freeze-dried material sampled at 48 hpi was powdered in liquid nitrogen and homogenized with 1 ml of MeOH: H_2O (0.01%HCOOH) (10:90). Crystal balls were added to each sample and tubes were placed in shaker during 2.5 min at 30 Hz. Then, samples were centrifuged and the supernatant was collected into a new tube.

A mix of internal standards with salicylic acid-d5 (SA-d5), dehydrojasmonic acid (dhJA), and jasmonate-isoleucine-d6 (JA-Ile-d6) was added to each sample. To quantify precisely, external calibration curves were prepared with each pure compound (quantification, SA-d5 for SA, dhJA for JA and JA-Ile-d6 for JA-Ile). The targeted hormonal analysis was performed in an Acquity ultraperformance liquid chromatography system (UPLC; Waters, Mildford, MA, United States) coupled to a triple quadrupole mass spectrometer (Xevo TQS, Waters Micromass, Manchester, United Kingdom). The column used for the LC separation was a UPLC Kinetex 2.6 μm EVO C18 100 Å, 2.1 × 50 mm (Phenomenex). Conditions and solvent gradients used in this chromatographic analysis were the same as described in Sánchez-Bel et al. (2018).

RNA Extraction and RT-qPCR Analysis

Two days post-inoculation (48 hpi), the leaves were collected, powdered in liquid nitrogen and stored at −80°C. For the RNA extraction, 1 ml of Trizol was added to 100 mg of grounded leaves. After centrifugation, the supernatant was transferred to a new tube, and 0.22 ml of CHCl3 was added. The samples were centrifuged, and the supernatant was collected in a new tube; 0.35 ml of isopropanol, 0.35 ml of 0.8 M citrate and 1.2 mM NaCl were added and mixed vigorously. After centrifugation, the supernatant was removed, and the pellet was washed twice with 70% EtOH. The pellet was dried and dissolved in nuclease-free water.

The synthesis of cDNA was performed using a High Capacity cDNA Reverse Transcription Kit (Applied Biosystems). Quantitative Real-Time PCR (qPCR) was performed with a Maxima SYBR Green/ROX qPCR Master Mix (2X) (Thermo Fisher Scientific), using a StepOne instrument (Applied Biosystems).

The ΔCt method was used to analyze the gene expression data. The housekeeping genes *UBIQUITIN21 (At5g25760)* and *PP2A (At1g13320)* were used to normalize the expression values.

The sequences of the primers are shown in **Supplementary Table S1**.

Peptide Extraction

One day after peptide treatment, the seedlings were collected, powdered with liquid nitrogen and stored at −80°C. Fresh material (250 mg) was homogenized in a tube with 1.5 ml of Phenol/TRIS and saturated (ACROS Organic, ref. 327125000) at pH 8. The suspension was incubated at room temperature for 20 min, crystal balls were added to each sample and the tubes were placed in a shaker for 2.5 min at 30 Hz.

The tubes were centrifuged 2 min at 21.900 RCF. After centrifugation, the liquid phase was filtered using a hydrophilic PVDF filter with a 25 mm diameter and a pore size of 0.45 μm (FILTER-LAB). After filtration, 6 volumes of pure cold acetone (Scharlau, AC0312, PharmPur®) were added to each sample, and the samples were stored overnight at −20°C.

The precipitate was recovered the next day and washed twice with cold acetone. The liquid phase was discarded, and the pellet was dried. The final residue was re-suspended in 500 μl of a solution of 0.1% HCOOH in H_2O: acetonitrile (9:1, v/v) and injected into the TQS-MS/MS instrument (Xevo TQS, Waters Micromass, Manchester, United Kingdom).

Reagents and Standards

Supergradient HPLC-grade acetonitrile was purchased from Scharlab (AC 0331). Formic acid was obtained from J.T. Baker (Deventer, Holland, 6037). Methanol (HPLC grade), and trypan blue were purchased from Sigma[1]. Peptide standards of Systemin, Pep1, HypSysI, HypSysII, HypSysII, PotSysI, PotSysII, PepSys, NishSys, Pep914, Pep890, and Systemin-P13AT17A were purchased from Biomatik[2].

Optimization of a Multi-Residue Targeted Quantitative LC-MS Method for Small Peptide Analysis

High-performance liquid chromatography (HPLC) was performed using a Waters Xevo TQ-S. A protocol that was adapted from Pastor et al. (2018) was followed. Aliquots of 20 μl were injected into the system through a reversed column Aeris PEPTIDE 3.6 μ XB-C18 (150 × 4.6 mm) from Phenomenex, at a flow rate of 0.3 ml min^{-1}.

The peptides were eluted with a gradient of ACN (organic phase) and Milli-Q water containing 0.1% HCOOH (aqueous phase), starting with 5:95 (v/v), linearly increasing to 35:65 (v/v) over 10 min and plateauing at 95:5 (v/v) 1 min later. The gradient was maintained in isocratic conditions for 1 min before the column was left to equilibrate for 3 min in order to reach initial conditions, for a total of 15 min per sample. The effluents originating from the HPLC were introduced into a triple quadrupole mass spectrometer (Xevo TQS, Waters Micromass, Manchester, United Kingdom) equipped with T-Wave devices and an ESI interface operated in positive mode. The cone and desolvation gas was nitrogen. The nebulizer gas flow was set to 250 L h^{-1} and the desolvation gas flow at 1200 L h^{-1}. For operation in tandem MS/MS mode, the collision gas was pure 99.995% argon (Praxair, Madrid, Spain), at a pressure of 4×10^{-3} bar in the collision cell. The desolvation gas temperature was 650°C, the source temperature was set to 150°C, and the capillary voltage was 3.2 kV. The mass spectrometer was set to multiple reaction monitoring (MRM) mode, and the data were acquired

[1] www.sigmaaldrich.com

[2] https://www.biomatik.com/

and processed using the MassLynx v4.1 software (Waters, Manchester, United Kingdom).

For the selection of the precursor and daughter ions of each peptide, peptide standards direct infusion was performed in a Waters Xevo TQ-S instrument, and masses showing the highest signal were selected for fragmentation and daughter ion characterization. Optimal conditions and appropriate cone and collision energies were determined to obtain the characteristic transitions for each peptide. Second, the retention time for each peptide was characterized by injecting aliquots of the standard peptides in a range of concentrations to construct calibration curves for each peptide. To quantitatively determine the peptides, an HPLC–MS/MS method was validated regarding the selectivity, linearity, precision, limit of detection (LOD) and quantification (LOQ). The transitions with higher signal intensities were selected as follows: HypSysI (519.8>498.2); HypSysII (595.5>494.6), HypSys III (518.3>394.2); Systemin (503.2>614.3); Potsys I (498.7>816.3); PotSys II (491.7>816.3); PepSys (395.8>392.2), and NishSys (506.3>515.3).

Statistical Analysis

Statgraphics-plus software for Windows V.5 (Statistical Graphics Corp., MD, United States) was used to determine the statistical analysis by one-way analysis of variance (ANOVA) otherwise indicated in the figure legends. Means are shown with standard errors and their comparative was performed using Fisher's least significant difference (LSD) at 99.5%. Graphs show the averages of one of the experiments. Each experiment contained a minimum of 6 plants per treatment and was repeated at least three times.

RESULTS

Peptides From Different Plant Species Are Uptaken and Induce Resistance Against *Plectosphaerella cucumerina* in *Arabidopsis thaliana*

Plant peptides are involved in the majority of physiological plant processes. Most peptides that have been studied are peptides involved in plant growth and development. However, although there are some reports related to plant defense and induced resistance triggered by peptides, there remain large unexplored potentials of many peptides that may confer resistance against a wide range of pathogens and insects.

In a first attempt, we tested peptides for their potential activities in inducing plant resistance against fungal pathogens. To achieve this goal, we selected peptides from different plant species that were found to be involved in plant defense and performed screening bioassays of induced-resistance in the *Arabidopsis thaliana-Plectosphaerella cucumerina* pathosystem.

Pep1 from *Arabidopsis thaliana* (Huffaker et al., 2006; Yamaguchi et al., 2006; Klauser et al., 2015) and systemin from tomato were comparatively tested for induced resistance. As expected, Arabidopsis plants treated with AtPep1, which is known to function as an elicitor of plant defense in response to pathogens, exhibited significantly reduced severity

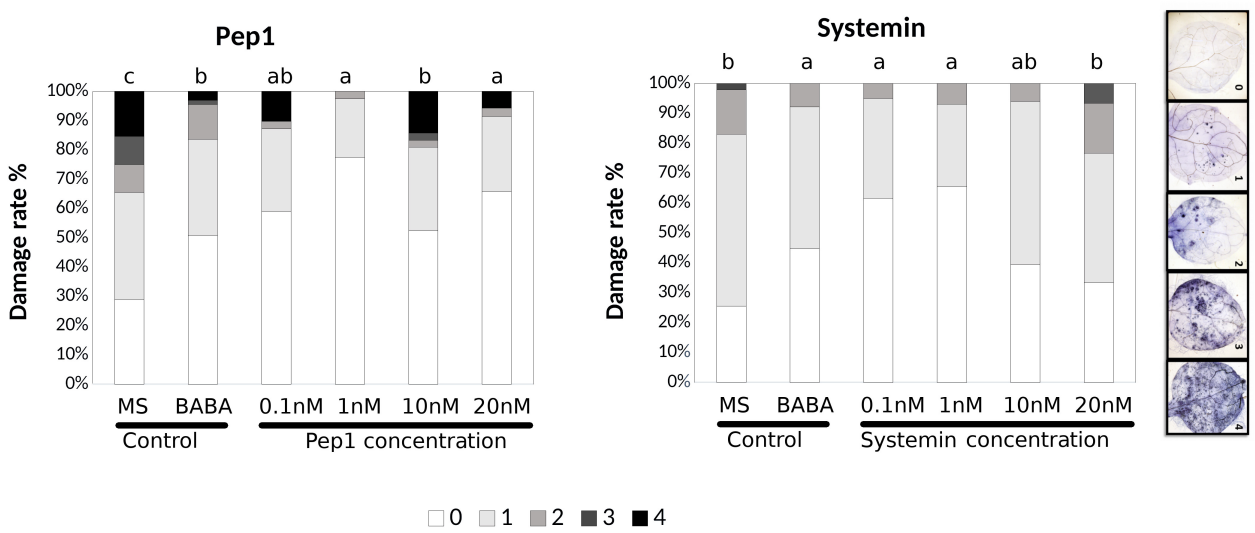

FIGURE 1 | Pep1 and Systemin induced-resistance assays against *Plectosphaerella cucumerina* in Arabidopsis plants. Infection levels 5 days after inoculation quantified by a disease rating in trypan blue stained leaves, measured as a percentage of the infected leaf surface. Arabidopsis Col-0 plants were treated with increasing concentrations of Pep1 or Systemin (0.1, 1, 10, and 20 nM) 24 h before infection with 1 μl droplets of 5 × 10E3 spores/ml of *P. cucumerina* BMM. ß-amino butyric acid (BABA) at 1 ppm was used as a positive control. Colors mean % of diseased leaves in a scale (0 = healthy leaves; 1 = leaves with less than 25% of diseased surface; 2 = leaves with 25–50%; 3 = leaves with 50–75% of the diseased surface, 4 = leaves with more than 75% of the surface diseased). Different letters indicate statistically significant differences (ANOVA, Fisher's Least Significant Difference (LSD) test; $P < 0.05$, $n = 24$). The experiment had 6 plants per treatment and was repeated at least three times with similar results.

TABLE 1 | Peptides Induced-Resistance assays summary table.

Peptide	Species of origin	0.1 nM	1 nM	10 nM	20 nM
Pep1	Arabidopsis	+	+	+	+
Systemin	Tomato	+	+	−	−
PepSys	Pepper	+	+	−	−
NishSys	Nightshade	−	+	−	−
PotSys I	Potato	−	−	−	−
PotSys II	Potato	+	−	−	−
HypSys I	Tomato	−	−	+	+
HypSys II	Tomato	−	−	+	+
HypSys III	Tomato	−	−	−	+
AFP1	Radish	−	−	−	+
AFP2	Radish	−	−	−	+
Pep914	Soybean	−	−	−	−
Pep890	Soybean	−	−	−	−

Peptides tested, their species of origin and the results obtained in the induce-resistance assays are shown in the table. (+) indicates effective plant protection and (–) indicates control levels of disease.

of infection compared with water-treated controls at any of the concentrations tested (**Figure 1** and **Table 1**). Systemin is an 18 aa peptide that has a function similar to that of AtPep1, although this peptide is mostly related to wounding and defense against insects in tomato (Fürstenberg-Hägg et al., 2013). Surprisingly, Systemin at very low concentrations (0.1 and 1 nM) was able to protect the plant against the necrotrophic fungus (**Figure 1**). Note that Pep1 and Systemin at the lowest concentrations (0.1 nM) protected plants to an extent similar to the protection conferred by □-amino butyric acid (BABA), a well-known inducer of resistance (Pastor et al., 2013). Subsequently, Systemins from other solanaceous species (potato, pepper, nightshade; **Supplementary Figure S1**; Constabel et al., 1998) were also tested. PepSys, NishSys and PotSysII were able to induce resistance at the same concentration as tomato Systemin. Note that all these peptides are produced in species that are taxonomically distant from *Arabidopsis thaliana* (**Supplementary Figure S1**). Moreover, we tested three short peptides from tomato, namely, HypSys I, HypSys II, and HypSys III, with functions in the defense against biotic stresses, although with a different sequence from Systemin. Arabidopsis plants were less sensitive to these peptides, although the plants treated with HypSysI and HypSysII at concentrations above 10 nM or with HypSys III at concentrations above 20 nM were also protected (**Figure 2** and **Table 1**). These results suggest that Arabidopsis senses and responds to heterologous peptides.

The previous peptides were shown to function as DAMPs, stimulating the defensive responses following sensing of PAMPs. In addition, there are other peptides involved in defense display direct antimicrobial activity rather than activating signaling cascades. Two antimicrobial peptides (AMPs; AFP1, and AFP2) from radish that were described to be active against a broad spectrum of fungi were also tested for their ability to protect Arabidopsis against *P. cucumerina* (Terras et al., 1992; **Supplementary Figure S2**). AFP-treated plants showed significant levels of protection only at the highest concentration tested (20 nM) (**Supplementary Figure S3**). Finally, two short peptides from Soybean described as defense signals, GmPep914 and GmPep890, were also tested against *P. cucumerina*. These peptides lead to alkalinization of the medium and the activation of defense-related genes (Yamaguchi et al., 2011). None of these peptides succeeded in protecting Arabidopsis plants at any of the concentrations tested (**Supplementary Figure S3**). Interestingly, plants treated with 0.1 and 1 nM of GmPep91 are more susceptible to the fungus. This result correlates with the one shown in the antifungal assays (**Figure 3**) in which the fungal growth was higher in the presence of GmPep91. It is likely that the fungus is using this peptide as a source of amino acids.

It was previously shown that the T17A and P13AT17A truncated Systemin proteins were not functional at inducing resistance in tomato against fungal pathogens (Pearce et al., 1993; Xu et al., 2018). Furthermore, Sys-P13AT17A also failed to inhibit seedling root growth in Arabidopsis plants (Zhang et al., 2017). However, Sys-P13AT17A induced resistance in Arabidopsis against *P. cucumerina* at the same level as the natural tomato peptide (**Supplementary Figure S4**A). Alternatively, the functionality of the Arabidopsis peptide Pep1 was tested in tomato against *B. cinerea* and showed no significant protection (**Supplementary Figure S4B**).

Although it has been shown that some peptides and resistance inducers can produce direct cell death, in our experimental conditions, at all the concentrations used we did not observe any cell death in mock-infected plants following trypan blue staining. Therefore, we can assure that the cell death observed in our experiments is due to the infection.

Few methods for small peptides determination in solanaceous are found along the literature (Mucha et al., 2019). To further confirm the uptake and the presence of the non-self peptides that were able to induce resistance in Arabidopsis we developed a multi-residue analytical method based on the one described in Pastor et al. (2018). In this regard, a fast and accurate quantitative multi-residue method for the simultaneous determination of small peptides was developed. It was observed that the chromatographic standard peptides in plant complex matrices behaved very, similarly, to pure standard preparations, making it feasible to identify these peptides in any plant material following root treatments. With this method, we were able to detect and measure them in Arabidopsis plant samples after 24 h of the peptides' treatment (**Supplementary Figure S5**).

The Sequence Homology of Studied Peptides Is Not Linked to Their IR Activity

To determine whether the results in the screening assay of induced resistance could be explained by the phylogenetic proximity to *Arabidopsis thaliana* or sequence identity with the AtPep1, we performed multiple sequence alignment of the amino acid sequences of the peptides tested and built a phylogenetic tree based on the peptide sequences provided by the UniProt database.

By performing a Clustal Omega multiple sequence alignment, we discovered that the different peptides used in the screening have very low or nonexistent sequence homology with AtPep1

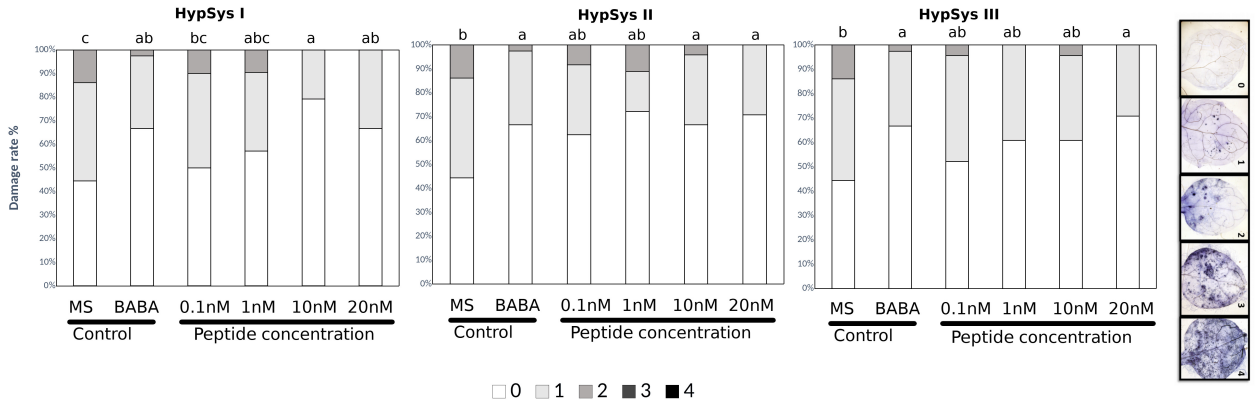

FIGURE 2 | HypSys peptides induced-resistance assays against *Plectosphaerella cucumerina* in Arabidopsis plants. Infection levels 5 days after inoculation quantified by a disease rating in trypan blue stained leaves, measured as a percentage of the infected leaf surface. Arabidopsis Col-0 plants were treated with increasing concentrations of HypSysI, HypSysII, and HypSysII (0.1, 1, 10, and 20 nM) 24 h before infection with 1 μl droplets of 5 × 10E3 spores/ml of *P. cucumerina* BMM. ß-amino butyric acid (BABA) at 1 ppm was used as a positive control. Colors mean % of diseased leaves in a scale (0 = healthy leaves; 1 = leaves with less than 25% of diseased surface; 2 = leaves with 25–50%; 3 = leaves with 50–75% of the diseased surface, 4 = leaves with more than 75% of the surface diseased). Different letters indicate statistically significant differences (ANOVA, Fisher's Least Significant Difference (LSD) test; $P < 0.05$, $n = 24$). The experiment had 6 plants per treatment and was repeated at least three times with similar results.

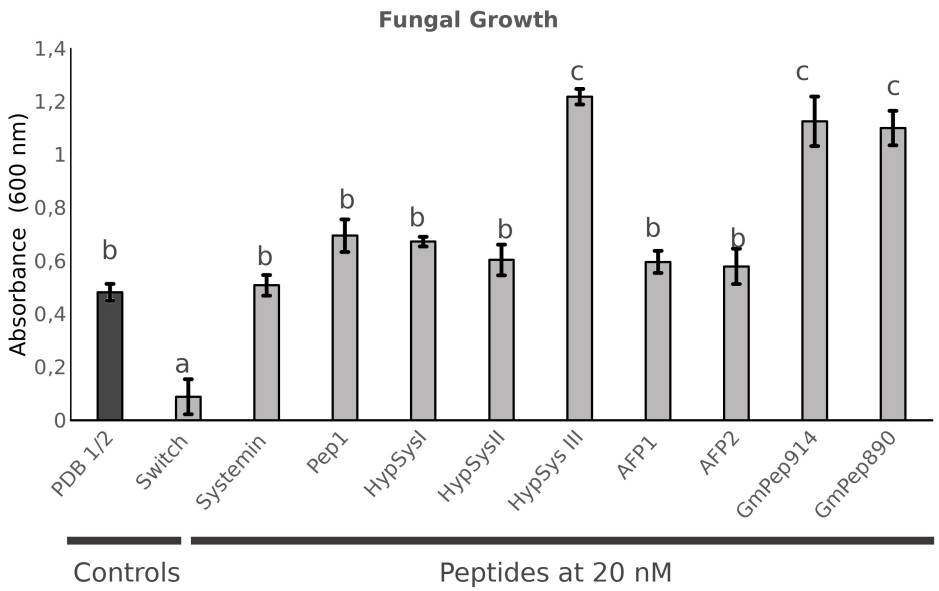

FIGURE 3 | *In vitro* antifungal assays. *Plectosphaerella cucumerina* growth measured after 24 h growing in liquid medium containing each peptide at a concentration of 20 nM. Fungal growth was measured as the level of turbidity (absorbance 600 nM). A commercial fungicidal (Switch) was used as a positive control. Bars represent mean ± standard error (SD), $n = 3$. Different letters indicate statistically significant differences (ANOVA, Fisher's Least Significant Difference (LSD) test; $P < 0.05$, $n = 3$).

or with the other peptides tested (**Supplementary Figure S6**). Interestingly, the species that clade closer to Arabidopsis in the phylogenetic tree are those whose peptides either minimally protected (AFPs from radish) or failed to induce resistance (Peps from Soybean) against the fungus (**Supplementary Figure S1**). By comparison (**Supplementary Figure S1** and **Table 1**), a correlation between the phylogenetic distance and effectively induced resistance against *P. cucumerina* in *Arabidopsis* was not observed.

In addition, we analyzed if the tested non-self peptides shared common motifs with AtPep1 that would account for their effectiveness in Arabidopsis. Using the Prosite database[3], we found that Sys, PotSys1, PotSys2, PepSys, HypSys3, and Pep1 showed a serine protein kinase C phosphorylation site (red boxes in **Supplementary Figure S6**). Alternatively, AFP1 and AFP2 shared an N-myristoylation site (blue box). All these protein sites

[3]http://wwwuser.cnb.csic.es/~pazos/cam97/

are patterns which have a high probability of occurrence, still they could not explain the different results obtained in the resistance induction assays (**Supplementary Figure S6**).

The Studied Peptides Do Not Display Any Direct Antifungal Activity Against *P. cucumerina*

Because most peptides tested can protect Arabidopsis against the necrotrophic fungus, they likely exert either an induced resistance or a direct antimicrobial effect. To test this possibility, an *in vitro* assay to measure fungal growth in the presence of each peptide was performed. For the assay, we filled sterile 12-well plates with 3 ml of LB medium containing the peptide at the highest concentration (20 nM) to examine the toxic antimicrobial effect. Spores of *P. cucumerina* were added to each well, and fungal growth was measured 24 hpi by assessing the turbidity of the medium at 600 nm. A commercial fungicide (Switch®; Syngenta, 37.5% w/w cyprodinil and 25% w/w fludioxonil) at a concentration of 0.6 $g.L^{-1}$ was used as a positive control (**Figure 3**). None of the peptides tested demonstrated antifungal activity against the necrotroph (**Figure 3**). Surprisingly, some of the peptides enhanced fungal growth, suggesting that the fungus may use the peptides as a source of amino acids.

These results suggest that the peptides induce resistance through the promotion of the plant immune system.

Alterations in the Hormonal Imbalance May Contribute to Systemin-IR

For subsequent analysis, we focus on the tomato Systemin peptide since it was effective on inducing resistance at very low concentrations (**Table 1**). To further confirm Sys-IR using a different method for the infection quantification, fungal biomass related to the plant tissue was confirmed that it was significantly lower in plants treated with 0.1 nM Systemin (**Supplementary Figure S7**).

In a first approach to understand the likely mechanisms of Systemin-IR in Arabidopsis, SA and JA as the main hormones regulating defense pathways were quantified (**Figure 4A**). In tomato, Systemin was shown to accumulate upon herbivory and was linked to JA-dependent responses (Sun et al., 2011; Fürstenberg-Hägg et al., 2013). In Arabidopsis, 0.1 nM Systemin treatments triggered an increase in SA, JA and JA-Ile in the absence of infection compared to water-treated plants. In contrast, following infection, the hormonal levels in Arabidopsis plants treated with Systemin remained similar to the levels before the infection. These observations suggest that SA- and JA-dependent pathways may contribute to Systemin-IR, however, the hormonal changes triggered by Systemin take place independently of the infection.

To complement the previous observations on the hormonal imbalances, we performed an analysis of *ICS1, LOX2,* and *PDF1.2* gene expression (**Figure 4B**). The JA-biosynthesis gene *LOX2* was boosted by systemin in the presence of infection displaying a priming profile (Mauch-Mani et al., 2017), whereas PDF1.2 gene expression was triggered by the treatment independently of the infection. *ICS1* expression levels increased due to the infection being significantly higher only in plants treated with Systemin.

To be more confident about the role of both hormonal pathways, mutants impaired in the SA and JA-related pathways were treated and infected (**Figure 5**). Interestingly, only those mutants altered in the JA responses were impaired in the Systemin-IR, while the SA-related *pad 4.1* and *sid2.1* mutants were protected by the peptide.

Based on these results, although SA is induced by Systemin treatments, the gene expression and the mutant analysis suggest that, like in tomato, JA-dependent responses may regulate Systemin-IR in Arabidopsis. However, JA functions in Systemin-IR may likely happen coordinately with other yet unknown mechanisms to contribute to the observed induced resistance phenotype.

Systemin Enhances PTI Responses in Arabidopsis

To gain knowledge on the perception and signaling of tomato Systemin in Arabidopsis we analyzed some well-known PTI responses. On the one hand, we measured the expression of the *BAK1* and *BIK1* membrane receptors as PTI markers in Arabidopsis plants treated with systemin and challenged with spores of *P. cucumerina* (**Figure 6**). None of the tested genes was directly induced by systemin treatments. However, both PTI markers were strongly upregulated in treated plants after infection (**Figure 6**), showing a typical priming profile.

On the other hand, we measured ROS production induced by Systemin and a PAMP challenge after 24 h systemin treatment (**Figure 7**). A wide range of Systemin concentrations was used (0.1, 1, 10, 100, and 1000 nM). Systemin treatments in the absence of a PAMP did not induce the production of H_2O_2 (**Figure 7** and **Supplementary Figure S8**) but ROS production was significantly induced when plants that were treated with Systemin 24 h before and challenged with flg22 (**Figure 7**). The induction was higher with increasing concentrations of Systemin showing a maximum threshold (100 nM). When Systemin was applied at higher concentrations the ROS accumulation decayed to levels similar to 0.1 nM os Systemin. This result shows a dose-threshold response of Arabidopsis to Systemin, resembling the protection pattern that we observed in the IR assays (**Figure 1** and **Table 1**). The results commented above suggest that Arabidopsis perceives tomato Systemin but in a non-canonnical perception unlike classical DAMPs such as Pep1. To further study this hypothesis we confirmed that the mutant pepr1 displays a wild-type phenotype of Sys-IR (**Supplementary Figure S9**), hence this reinfoced a PEPR1-independent function of systemin.

DISCUSSION

The understanding of small peptides as signaling molecules in plants has grown significantly in the last few years. In the present study, the role of Arabidopsis self and non-self peptides in inducing resistance against *P. cucumerina* has been analyzed. Reasonably, self-peptides are active in protecting Arabidopsis, but surprisingly, other heterologous peptides, such as Systemins

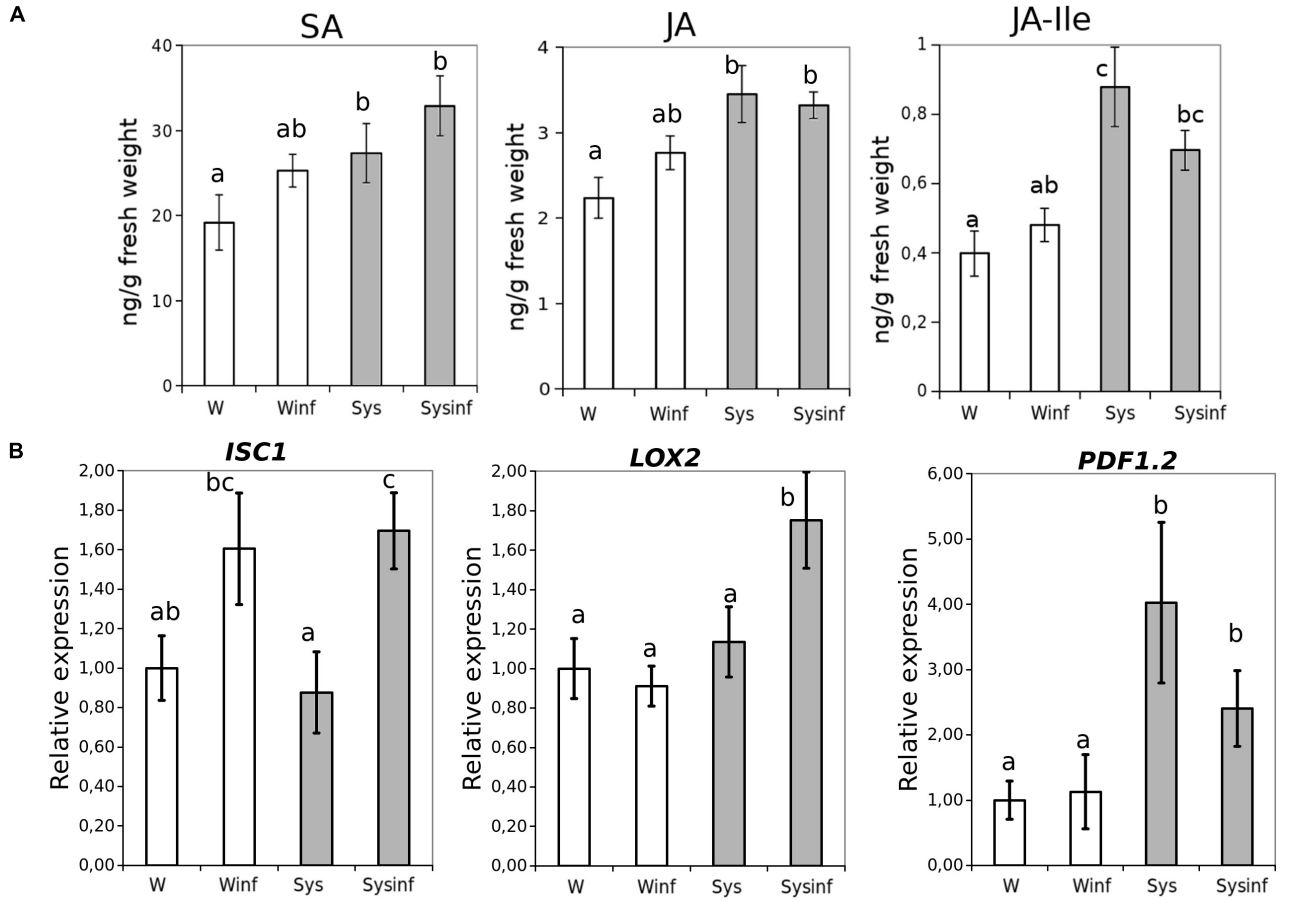

FIGURE 4 | Systemin treatment impact in hormonal profiles. **(A)** Salicylic acid (SA), Jasmonic acid (JA) and JA-isoleucine (JA-ile) hormone quantitative levels (ng/g fresh weight) measured in Arabidopsis seedlings 48 h after *P. cucumerina* infection in control (W) control infected (W inf) 24 h Systemin-pretreated (Sys) and 24 h Systemin-pretreated infected (Sys inf) plants by targeted HPLC-MS analysis. **(B)** Quantitative reverse transcription-polymerase chain reaction analysis of *ICS1*, *LOX2,* and *PDF1.2* in seedlings 48 h after *P. cucumerina* infection in Water plants "W," water infected plants "W inf," 0.1 nM Systemin treated plants "Sys" and Sys infected plants "Sys inf." Bars represent mean ± standard error (SD), $n = 6$. Different letters represent statistically significant differences. (ANOVA, Fisher's Least Significant Difference (LSD) test; $P < 0.05$, $n = 6$).

from Solanum species, protect Arabidopsis in the nanomolar range. Besides, other peptides from phylogenetically distant plant species are also active in defense, although to a different extent.

Alternatively, most knowledge of small peptides functioning throughout the plant physiology has been generated by studying the gene expression of their respective propeptides. However, the post-translational processing of these propeptides is tightly regulated, which makes the analytical characterization and quantification of the active peptides essential. For this reason, we have generated a multi-residue UPLC coupled to mass spectrometry method for the simultaneous analysis of small plant peptides (15–20 amino acids).

Small peptides were shown to participate in plant defense as amplifiers of PAMP sensing; therefore, they were suggested to function as DAMPs, which are also known as phytocytokines (Gust et al., 2017). For instance, PIPs from Arabidopsis were shown to amplify flg22 responses and resistance to *PstDC3000* (Hou et al., 2014), and similarly, elf18 responses increased upon co-treatment with RALF17 (Stegmann et al., 2017). Previous studies described the functionality of the Arabidopsis endogenous peptide Pep1 in the defense against fungal pathogens, such as *B. cinerea* (Liu et al., 2013). In the current study, Pep1 exogenously applied in a range from 0.1 to 20 nM was found to protect plants against *P. cucumerina*. Pep1, at the concentrations tested, was as functional as the well-known priming agent □-amino butyric acid (BABA). In parallel, a screening of non-self peptides for induced resistance against the necrotroph was performed. The screening included peptides from other Brassicaceae, such as AFP1 and 2 (Terras et al., 1992), Solanaceae, such as Systemin, PepSys, NishSys, PotSysI and II (Constabel et al., 1998), HypSys I, II, and III (Pearce and Ryan, 2003), and Fabaceae, such as Pep914 and 890 (Yamaguchi et al., 2011). Unexpectedly, the solanum peptides were the most effective in protecting Arabidopsis. Systemin-induced resistance from tomato and pepper and PEP1-IR were as strong as that induced by BABA-IR and Pep1-IR at the very low concentrations of 0.1 and 1 nM. In contrast, a Systemin from potato (PotSysI) and peptides from soybean (Pep914 and 890)

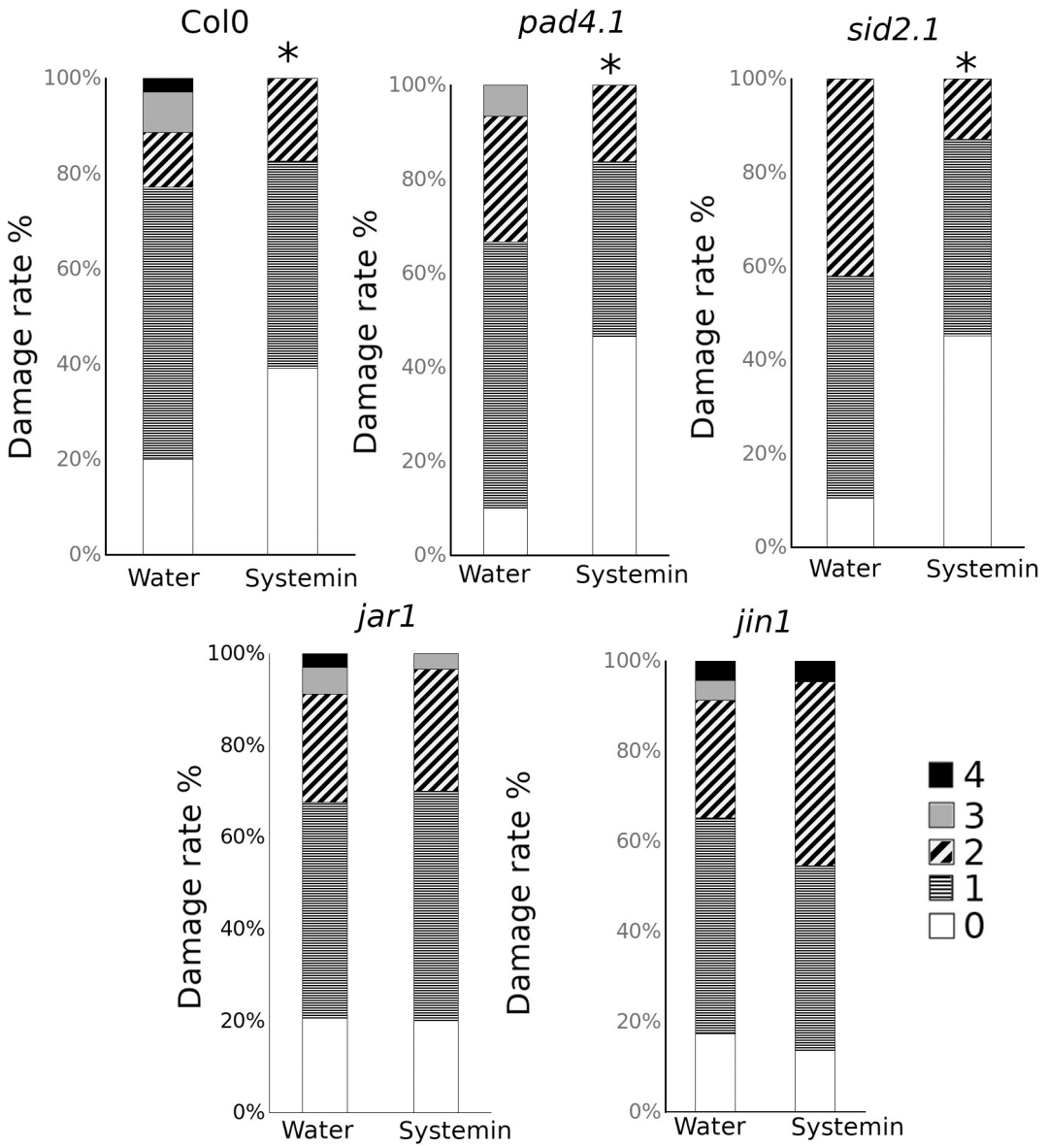

FIGURE 5 | Sys-IR assays in mutants impaired in the SA and JA-related pathways. Col-0, *pad4.1*, *sid2.1*, *jar1,* and jin1 plants were challenged with 1 μl droplets of 5 × 10E3 spores/ml of *P. cucumerina* BMM 24 h after treatment with 0.1 nM Systemin. Infection levels were quantified 5 days after inoculation by a disease rating in trypan blue stained leaves, measured as a percentage of the infected leaf surface. Colors mean % of diseased leaves in a scale (0 = healthy leaves; 1 = leaves with less than 25% of diseased surface; 2 = leaves with 25–50%; 3 = leaves with 50–75% of the diseased surface, 4 = leaves with more than 75% of the surface diseased). Asterisks mean statistical significant differences; *T*-test; $P < 0.05$, $n = 12$). The experiment had 12 plants per treatment and was repeated at least three times with similar results.

did not induce resistance at the concentrations studied. HypSys I, II, and III as well as AFP1 and 2 demonstrated protection only at the highest concentrations. These observations suggest that either Arabidopsis has specific receptor(s) for heterologous plant peptides, which is rather unlikely, or that other yet unknown receptors may bind nonspecifically other small peptides. Further research is needed to clarify this hypothesis.

Because induced resistance was observed, a double analysis of the peptides was performed. The likely link between phylogenetic proximity of the plant species that produce the peptides and the effectiveness inducing resistance was studied. The phylogenetic distance of radish is closer to Arabidopsis compared with tomato, pepper or soybean, although systemins from tomato and pepper were the most effective. Hence, the protection conferred by the tested peptides may not be related to the phylogenetic proximity of the plant species. Second, the sequence homology and the motifs contained in the peptides were also studied. Any of these biochemical properties were linked to higher efficiency in protection. In fact, Pep1 from Arabidopsis shares higher sequence homology with AFPs and Pep from soybean, while

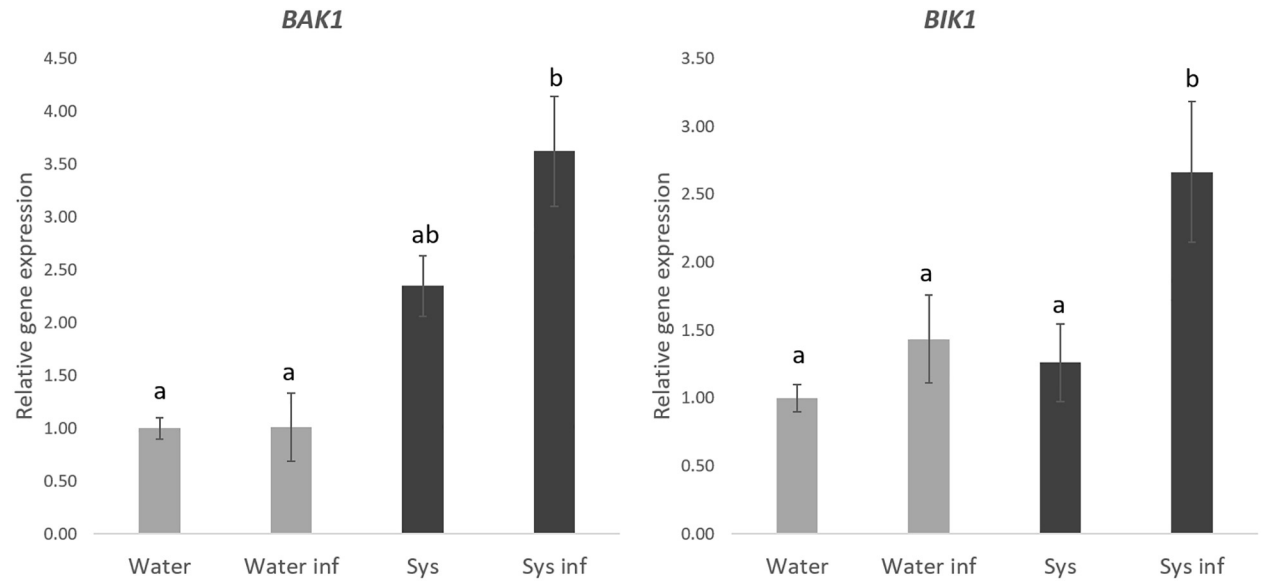

FIGURE 6 | Systemin treatment impact in ***BAK1*** and ***BIK1*** gene expression. Quantitative reverse transcription-polymerase chain reaction (qPCR)analysis of *BAK1* and *BIK1* in seedlings 48 h after *P. cucumerina* infection in normal water plants "W," water infected plants "W inf," 0.1 nM Systemin treated "Sys" and Sys infected plants "Sys inf" plants. Bars represent mean ± standard error (SD), $n = 6$. Different letters represent statistically significant differences (ANOVA, Fisher's Least Significant Difference (LSD) test; $P < 0.05$, $n = 6$).

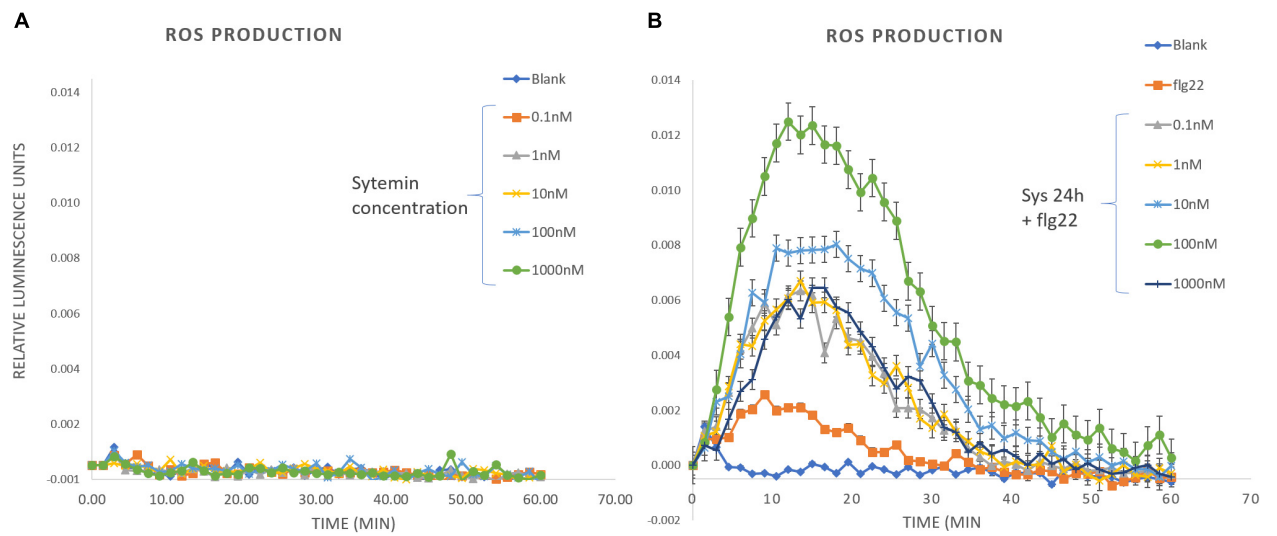

FIGURE 7 | ROS production in response to Systemin and PAMP challenge. H_2O_2 production was measured during 1 h in leaf disks after elicitation with **(A)** Systemin at different concentrations and **(B)** 100 nM flg22 in leaf disks that were pre-treated for 24 h with different concentrations of Systemin. Luminescence was expressed in Relative Luminescence Units. Slopes represent the means of each time-point ± standard error (SD), $n = 8$.

Systemin, PepSys and PotSysI and II share very high sequence homology. Note that Systemin and PepSys treatments induced strongly Arabidopsis resistance against the fungus, while PotSysI treatment was ineffective. Alternatively, the only motif shared by these small peptides was a phosphorylation site that was present in Systemin, PepSys, Pep1, PotSys1, PotSys2, and HypSys3. Therefore, neither a conserved sequence nor specific motifs can explain the differential function in Arabidopsis protection.

To fully exclude the possibility that these peptides protect Arabidopsis by inhibiting *P. cucumerina* growth or germination, the *in vitro* antimicrobial effect of all peptides at the highest concentration was tested. None of the small peptides inhibited fungal growth, although surprisingly some of them promoted mycelium expansion, such as HypSys III from tomato and Pep914 and 890 from soybean. These peptides may function as additional nutritional sources for the fungus, which would explain its

enhanced growth. Especially surprising was the absence of an antimicrobial effect of the antifungal peptides AFP1 and 2, since their inhibitory properties against several fungi, including the necrotroph *B. cinerea,* have been previously shown, although at concentrations higher than those used in our tests (Terras et al., 1992; De Lucca et al., 1999; Thevissen et al., 2012). Regarding the remaining peptides, any of them either promoted or reduced fungal growth, which suggest they protect Arabidopsis through activation of the plant immunity.

Under our experimental conditions, Pep1 treatments protected Arabidopsis plant at any of the concentrations tested (0.1–20 nM). Nevertheless, Systemin treatments significantly protected Arabidopsis at the very low doses of 0.1 and 1 nM, but it was not active at the higher concentrations.

This mode of action has been previously reported for some well-known resistance inducers and phytohormones. BABA shows a threshold of protection against *Phytophthora infestans* between 1 and 10 mM while 0.1 and 20 mM are less effective (Floryszak-Wieczorek et al., 2015). Moreover, BABA-induced callose accumulation in response to PAMPs has also a maximum in the range of 1–5 ppm, while decays at higher concentrations (Pastor et al., 2013). Similarly, BTH was shown to protect better a low doses triggering PAL and inducing coumarin accumulation (Katz et al., 1998). Regarding phytohormones, as an example, brassinosteroid showed maximum threshold on promoting root elongation, while they trigger root elongation at low doses (0.05–0.1 nM) they fail above 1 nM (Müssig et al., 2003). Therefore we can assume that Systemin-IR in arabidopsis acts in a dose-threshold manner, what was also confirmed by the ROS assays.

There are reports of enhanced resistance of transgenic Arabidopsis plants overexpressing the Prosystemin gene (Zhang et al., 2017). The overexpression of Prosystemin has a strong impact on the Arabidopsis transcriptome with upregulation of stress-related genes. Prosystemin is a 200 amino acid peptide that is processed in tomato by phytaspases. Subsequently, leucine aminopeptidase A removes the terminal Leu, releasing the active form of systemin (Beloshistov et al., 2017). Despite the functionality of overexpression of prosystemin in Arabidopsis, it is still unknown whether the propeptide is active by itself or whether other Arabidopsis phytaspases and a LapA-like protein can process Prosystemin. In the present experiments, it was shown that not only Systemin but also its truncated form Sys-P13AT17A (Pearce et al., 1993) are sensed by Arabidopsis. This result suggests that a core of amino acids in the peptide may be responsible for the non-specific perception and downstream signaling in Arabidopsis since the truncated forms are entirely impaired in inducing resistance in tomato (Pearce et al., 1993; Xu et al., 2018).

Conversely, Pep1 treatments did not protect tomato plants against *B. cinerea*. Thus, it appears that tomato very specifically senses Systemin but not Pep1, while Arabidopsis can sense Pep1 though its known receptors (PEPR1 and 2) and Systemin through an unknown mechanism. In this regard, not only Systemin but also several other tested peptides, such as PepSys, NighSys, HypSys I, II, and III, can induce resistance in Arabidopsis, although at higher concentrations. This finding reinforces the hypothesis that Arabidopsis may have alternative non-specific receptors for non-self peptides. It is tempting to hypothesize that extracellular peptides, as it has been shown for DNA, ATP or oxylipins released form the membrane may function as danger signals, although not all peptides exert the same activity.

As a first approach to decipher mechanisms underlying Sys-IR, a hormonal analysis showed that SA- and JA-related signaling could be involved. Despite their antagonism, both SA and JA increased following Systemin treatments in Arabidopsis. The active hormone JA-Ile was also triggered following Systemin treatments. Accordingly, several hormone-related genes, such as *LOX2* and *PDF1.2* from the JA-dependent pathway, were also induced by Systemin treatments. The hormone induction and the gene expression have consistent behavior in the activation of both pathways in Systemin-treated plants upon infection, indicating that a more complex regulation of defenses may occur following Systemin sensing that indeed has an impact on hormonal signaling. Note that the PEPR pathway co-activates SA- and JA/ET- mediated immune branches in Arabidopsis (Ross et al., 2014). Despite the induction of SA levels after Systemin treatments, the mutant analysis showed that SA-impaired mutants were fully protected suggesting that JA-dependent responses are behind Sys-IR in Arabidopsis. Similarly, Systemin treatments have been shown to trigger JA-dependent responses in tomato (Ryan, 2000; Sun et al., 2011; Fürstenberg-Hägg et al., 2013) and involve the upstream oxylipin pathway following herbivory. Thus, the JA induction following Systemin treatments appears to be a conserved molecular response in Arabidopsis and tomato.

To understand Systemin perception in Arabidopsis we analyzed both *BAK1* and *BIK1* gene expression and the generation of ROS. Following Systemin treatment any of the studied markers were directly induced. However, following *P. cucumerina* infection both transcripts increased significantly and additionally flg22 application in Systemin-treated plants induced strong increases in ROS production. To strengthen these observations, we confirmed that Sys-IR is functional in the mutant *pepr1*, hence PEPR1-independent. Note that it was reported previously that systemin effects on root architecture in Arabidopsis is also PEPR1-independent (Zhang et al., 2017). This suggests that Arabidopsis senses Systemin although it is inducing a non-canonical function compared with endogenous peptidic DAMPs such as Pep1/2 that directly induce responses. Although Systemin clearly amplifies PAMP/pathogen response, it is likely that the low doses used do not trigger direct responses resembling priming defense as it has been previously suggested for other priming stimuli (Mauch-Mani et al., 2017; Wilkinson et al., 2019).

Much of the understanding of the function of peptides in plant immunity has been based on propeptide gene expression. In very few cases, the processing of these propeptides, the final receptors and signaling cascades have only been recently discovered (Yamaguchi et al., 2006; Hou et al., 2014; Wang et al., 2018; Xu et al., 2018). Following the propeptide translation, proteolytic processing is involved in the cleavage and release of the active peptide from a larger precursor. Non-self peptides should not be specifically processed in Arabidopsis, since they are not naturally present, although it could be possible that they can be processed by other non-specific phytaspases or peptidases

that are ubiquitous among plants. Using a multi-residue chromatographic method we have confirmed the uptake and systemic transport of the heterologous peptides in Arabidopsis.

CONCLUSION

In conclusion, Systemin and other related peptides that are not produced in Arabidopsis can induce resistance against *P. cucumerina,* triggering protection at very low doses and to a comparable extent as the protection provided by BABA, which indicated that Arabidopsis can sense non-self peptides from phylogenetically distant plant species that are not related in structure or sequence. Furthermore, we show evidence that the JA-dependent signaling mediates Systemin-Induced Resistance that amplifies PAMP receptor expression and ROS production in the presence of a challenge. Pre-challenge induction may prepare the plant for subsequent exposure. These findings open future research to decipher the mechanisms underlying Sys-IR in Arabidopsis.

DATA AVAILABILITY STATEMENT

All datasets generated for this study are included in the article/**Supplementary Material**.

AUTHOR CONTRIBUTIONS

JP-F performed most bioassays of IR and peptide treatments. JG and VP developed the LC-MS methods and contributed to the writing of results and methods. PS-B contributed to writing, interpretation, motif, and peptide sequence analysis. NS performed assays with tomato and the mutant screenings. MC contributed to PCR analysis. VF contributed to writing, supervised the research, designed experiments, and performed hormonal analysis.

FUNDING

This work was funded by the Plan de Promoción de la Investigación Universitat Jaume I UJI-B2016-43; the Spanish Ministry MICIU; RTI2018-094350-B-C33; the grant to JP-F 19I045 from the Plan Propio de Investigación Universitat Jaume I and PRIMA-INTOMED.

ACKNOWLEDGMENTS

We thank the SCIC of the Universitat Jaume I and the financial support to GVA GV/2018//115 and IDIFEDER/2018/01.

SUPPLEMENTARY MATERIAL

The Supplementary Material for this article can be found online at: https://www.frontiersin.org/articles/10.3389/fpls.2020.00529/full#supplementary-material

FIGURE S1 | Systemins from Solanaceous species induced-resistance assays against *Plectosphaerella cucumerina* in Arabidopsis plants. Infection levels 5 days after inoculation quantified by a disease rating in trypan blue stained leaves, measured as a percentage of the infected leaf surface. Arabidopsis Col-0 plants were treated with increasing concentrations of PotSys (potato systemin), PepSys (pepper systemin), NishSys (nightshade systemin) (0.1, 1, 10, and 20 nM) 24 h before infection with 1 μl droplets of 5 × 10E3 spores/ml of *P. cucumerina* BMM. ß-amino butyric acid (BABA) at 1 ppm was used as a positive control. Colors mean % of diseased leaves in a scale (0 = healthy leaves; 1 = leaves with less than 25% of diseased surface; 2 = leaves with 25–50%; 3 = leaves with 50–75% of the diseased surface, 4 = leaves with more than 75% of the surface diseased). Different letters indicate statistically significant differences (ANOVA, Fisher's Least Significant Difference (LSD) test; $P < 0.05$ $n = 6$). The experiment had 6 plants per treatment and was repeated at least three times with similar results.

FIGURE S2 | Antimicrobial peptides from radish induced-resistance assays against *Plectosphaerella cucumerina* in Arabidopsis plants. Infection levels 5 days after inoculation quantified by a disease rating in trypan blue stained leaves, measured as a percentage of the infected leaf surface. Arabidopsis Col-0 plants were treated with increasing concentrations of AFP1 and AFP2 (0.1, 1, 10, and 20 nM) 24 h before infection with 6 μl droplets of 5 × 10E3 spores/ml of *P. cucumerina* BMM. ß-amino butyric acid (BABA) at 1 ppm was used as a positive control. Colors mean % of diseased leaves in a scale (0 = healthy leaves; 1 = leaves with less than 25% of diseased surface; 2 = leaves with 25–50%; 3 = leaves with 50–75% of the diseased surface, 4 = leaves with more than 75% of the surface diseased). Different letters indicate statistically significant differences (ANOVA, Fisher's Least Significant Difference (LSD) test; $P < 0.05$, $n = 6$). The experiment had 6 plants per treatment and was repeated at least three times with similar results.

FIGURE S3 | Soybean peptides induced-resistance assays against *Plectosphaerella cucumerina* in Arabidopsis plants. Infection levels 5 days after inoculation quantified by a disease rating in trypan blue stained leaves, measured as a percentage of the infected leaf surface. Arabidopsis Col-0 plants were treated with increasing concentrations of GmPep914 and GmPep890 (0.1, 1, 10, and 20 nM) 24 h before infection with 1 μl droplets of 5×10^3 spores/ml of *P. cucumerina* BMM. Colors mean % of diseased leaves in a scale (0 = healthy leaves; 1 = leaves with less than 25% of diseased surface; 2 = leaves with 25–50%; 3 = leaves with 50–75% of the diseased surface, 4 = leaves with more than 75% of the surface diseased). Different letters indicate statistically significant differences (ANOVA, Fisher's Least Significant Difference (LSD) test; $P < 0.05$, $n = 6$). The experiment had 6 plants per treatment and was repeated at least three times with similar results.

FIGURE S4 | Induced- Resistance assays of Sys-P13AT17A in Arabidopsis and AtPep1 in tomato. Infection levels of Arabidopsis Col-0 plants treated with 0.1 nM of truncated Systemin (Sys-P13AT17A) **(A)** and tomato wild-type plants treated with increasing concentrations of AtPep1 (0.1, 1, 10, and 20 nM) **(B)** 24 h before infection. Infection was quantified 5 days after inoculation with 1 μl droplets of 5×10^3 spores/ml of *P. cucumerina* BMM by a disease rating in trypan blue stained leaves, measured as a percentage of the infected leaf surface. Colors mean % of diseased leaves in a scale (0 = healthy leaves; 1 = leaves with less than 25% of diseased surface; 2 = leaves with 25–50%; 3 = leaves with 50–75% of the diseased surface, 4 = leaves with more than 75% of the surface diseased). Different letters indicate statistically significant differences (ANOVA, Fisher's Least Significant Difference (LSD) test; $P < 0.05$, $n = 6$). The experiment had 6 plants per treatment and was repeated at least three times with similar results.

FIGURE S5 | Peptides measured by HPLC-MS *in planta.* **(A)** total ion current (TIC) in ESI (+) of a mix of peptide standards and **(B)** HPLC–MS/MS chromatograms of specific transitions for each peptide of study detected in Arabidopsis plants 24 h after peptide treatment. Aliquots of 20 μl of a standard mix of 300 $\mu l.L^{-1}$ were injected into the LC-MS system through a reversed column, at a flow rate of 0.3 ml min^{-1}. After data recording, chromatograms were generated using the Maslynx 4.1 (Waters) software.

FIGURE S6 | Peptides phylogenetic tree and multiple alignment based on their amino acid sequence. Phylogenetic tree and multiple alignment were performed

using the Clustal Omega multiple alignment of the EMBL-EBI online tool (https://www.ebi.ac.uk/Tools/msa/clustalo/) using the peptides amino acid sequence provided by the Uniprot database. Numbers on the right indicate peptides' length (number of aminoacids). Highlighted in boxes are the motifs found in each peptide using the Prosite Database (http://wwwuser.cnb.csic.es/~pazos/cam97/). Red boxes indicate the Serine Protein Kinase C phosphorylation sites, blue box indicate N-myristoylation sites.

FIGURE S7 | *P. cucumerina* Infection quantification by measuring fungal biomass. A ratio of *PcTUBULIN* relative to *AtUBIQUITIN21* was calculated after performing a qPCR from gDNA of Arabidopsis infected plant samples 48 h after pathogen inoculation in watered plants and plants treated with 0.1 nM systemin 24 h before inoculation of *P. cucumerina.* Bars represent mean ± standard error (SD), $n = 6$. Asterisks mean statistical significant differences; *T*-test; $P < 0.05$, $n = 6$.

FIGURE S8 | ROS production areas in response to Systemin and PAMP challenge. H_2O_2 production was measured during 1 h in leaf disks after elicitation with Systemin at different concentrations and with 100 nM flg22 in leaf disks that were pre-treated for 24 h with different concentrations of Systemin. Luminescence was expressed in Relative Luminescence Units. Bars represent means of peak areas ± standard error (SD), $n = 8$. Different letters represent statistically significant differences. (ANOVA, Fisher's Least Significant Difference (LSD) test; $P < 0.05$, $n = 8$).

FIGURE S9 | Sys-IR assays in the *pepr1* mutant. Col-0 and *pepr1* plants were challenged with 1 μl droplets of 5 × 10E3 spores/ml of *P. cucumerina* BMM 24 h after treatment with 0.1 nM Systemin. Infection levels were quantified 5 days after inoculation by a disease rating in trypan blue stained leaves, measured as a percentage of the infected leaf surface. Colors mean % of diseased leaves in a scale (0 = healthy leaves; 1 = leaves with less than 25% of diseased surface; 2 = leaves with 25–50%; 3 = leaves with 50–75% of the diseased surface, 4 = leaves with more than 75% of the surface diseased). Asterisks mean statistical significant differences; *T*-test; $P < 0.05$, $n = 12$). The experiment had 12 plants per treatment and was repeated at least three times with similar results.

TABLE S1 | Primers used for the qPCR analysis of gene expression and *Plectosphaerella cucumerina* quantification.

REFERENCES

Albert, M. (2013). Peptides as triggers of plant defence. *J. Exp. Bot.* 64, 5269–5279. doi: 10.1093/jxb/ert275

Beloshistov, R. E., Dreizler, K., Galiullina, R. A., Alexander, I., Tuzhikov, A. I., Serebryakova, M. V., et al. (2017). Phytaspase-mediated precursor processing and maturation of the wound hormone systemin. *New Phytol.* 218, 1167–1178. doi: 10.1111/nph.14568

Broekaert, W. F., Terras, F. W. G., Cammue, B. P. A., and Vandedeyden, J. (1990). An automated quantitative assay for fungal growth inhibition. *FEMS Microbiol. Lett.* 69, 55–60. doi: 10.1111/j.1574-6968.1990.tb04174.x

Constabel, C. P., Yip, L., and Ryan, C. A. (1998). Prosystemin from potato, black nightshade, and bell pepper: primary structure and biological activity of predicted systemin polypeptides. *Plant Mol. Biol.* 36, 55–62. doi: 10.1023/A:1005986004615

Coppola, M., Corrado, G., Coppola, V., Cascone, P., Martinelli, R., Digilio, M. C., et al. (2015). Prosystemin overexpression in tomato enhances resistance to different biotic stresses by activating genes of multiple signaling pathways. *Plant Mol. Biol. Rep.* 33, 1270–1285. doi: 10.1007/s11105-014-0834-x

Coppola, M., Di Lelio, I., Romanelli, A., Gualtieri, L., Molisso, D., Ruocco, M., et al. (2019). Tomato plants treated with systemin peptide show enhanced levels of direct and indirect defense associated with increased expression of defense-related genes. *Plants* 8:395. doi: 10.3390/plants8100395

Corrado, G., Sasso, R., Pasquariello, M., Iodice, L., Carretta, A., Cascone, P., et al. (2007). Systemin regulates both systemic and volatile signaling in tomato plants. *J. Chem. Ecol.* 33, 669–681. doi: 10.1007/s10886-007-9254-9

De la Noval, B., Pérez, E., Martínez, B., León, O., Martínez-Gallardo, N., and Délano-Frier, J. (2007). Exogenous systemin has a contrasting effect on disease resistance in mycorrhizal tomato (Solanum lycopersicum) plants infected with necrotrophic or hemibiotrophic pathogens. *Mycorrhiza* 17, 449–460. doi: 10.1007/s00572-007-0122-9

De Lucca, A. J., Jacks, T. J., and Broekaert, W. J. (1999). Fungicidal and binding properties of three plant peptides. *Mycopathologia* 144, 87–91. doi: 10.1023/A:1007018423603

Edwards, K., Johnstone, C., and Thompson, C. (1991). A simple and rapid method for the preparation of plant genomic DNA for PCR analysis. *Nucleic Acids Res.* 19:1349. doi: 10.1093/nar/19.6.1349

Floryszak-Wieczorek, J., Arasimowicz-Jelonek, M., and Abramowski, D. (2015). BABA-primed defense responses to Phytophthora infestans in the next vegetative progeny of potato. *Front. Plant Sci.* 6:844. doi: 10.3389/fpls.2015.00844

Flury, P., Klauser, D., Schulze, B., Boller, T., and Bartels, S. (2013). The anticipation of danger: microbe-associated molecular pattern perception enhances atpep-triggered oxidative burst. *Plant Physiol.* 161, 2023–2035. doi: 10.1104/pp.113.216077

Fürstenberg-Hägg, J., Zagrobelny, M., and Bak, S. (2013). Plant defense against insect herbivores. *Int. J. Mol. Sci.* 14, 10242–10297. doi: 10.3390/ijms140510242

Gust, A., Pruit, R., and Nürnberger, T. (2017). Sensing danger: key to plant immunity. *Trends Plant Sci.* 22, 779–791. doi: 10.1016/j.tplants.2017.07.005

Hou, S., Liu, Z., Shen, H., and Wu, D. (2019). Damage-associated molecular pattern-triggered immunity in plants. *Front. Plant Sci.* 10:646. doi: 10.3389/fpls.2019.00646

Hou, S., Wang, X., Chen, D., Yang, X., Wang, M., Turrà, D., et al. (2014). The secreted peptide PIP1 amplifies immunity through receptor-like kinase 7. *PLoS Pathog.* 10:e1004331. doi: 10.1371/journal.ppat.1004331

Huffaker, A., Pearce, G., and Ryan, C. A. (2006). An endogenous peptide signal in Arabidopsis activates components of the innate immune response. *Proc. Natl. Acad. Sci. U.S.A.* 103, 10098–10103. doi: 10.1073/pnas.0603727103

Katz, V. A., Thulke, O. U., and Conrath, U. (1998). A benzothiadiazole primes parsley cells for augmented elicitation of defense responses. *Plant Physiol.* 117, 1333–1339. doi: 10.1104/pp.117.4.1333

Klauser, D., Desurmont, G. A., Glauser, G., Vallat, A., Flury, P., Boller, T., et al. (2015). The Arabidopsis Pep-PEPR system is induced by herbivore feeding and contributes to JA-mediated plant defence against herbivory. *J. Exp. Bot.* 66, 5327–5336. doi: 10.1093/jxb/erv250

Klauser, D., Flury, P., Boller, T., and Bartels, S. (2013). Several MAMPs, including chitin fragments, enhance AtPep-triggered oxidative burst independently of wounding. *Plant Signal. Behav.* 8:e25346. doi: 10.4161/psb.25346

Liu, Z., Wu, Y., Yang, F., Zhang, Y., Chen, S., Xie, Q., et al. (2013). BIK1 interacts with PEPRs to mediate ethylene-induced immunity. *Proc. Natl. Acad. Sci. U.S.A.* 110, 6205–6210. doi: 10.1073/pnas.1215543110

Lorenzo, O., Chico, J. M., Sanchez-Serrano, J. J., and Solano, R. (2004). Jasmonate-insensitive1 encodes a MYC transcription factor essential to discriminate between different jasmonateregulated defence responses in *Arabidopsis*. *Plant Cell* 16, 1938–1950. doi: 10.1105/tpc.022319

Malinowski, R., Higgins, R., Luo, Y., Piper, L., Nazir, A., Bajwa, V. S., et al. (2009). The tomato brassinosteroid receptor BRI1 increases binding of systemin to tobacco plasma membranes, but is not involved in systemin signaling. *Plant Mol. Biol.* 70, 603–616. doi: 10.1007/s11103-009-9494-x

Matthes, M. C., Bruce, T. J., Ton, J., Verrier, P. J., Pickett, J. A., and Napier, J. A. (2010). The transcriptome of cis-jasmone-induced resistance in *Arabidopsis thaliana* and its role in indirect defence. *Planta* 232, 1163–1180. doi: 10.1007/s00425-010-1244-4

Mauch-Mani, B., Baccelli, I., Luna, E., and Flors, V. (2017). Defense priming: an adaptive part of induced resistance. *Anuu. Rev. Plant Biol.* 68, 485–512. doi: 10.1146/annurev-arplant-042916-041132

Mucha, P., Ruczynski, J., Dobkowski, M., Ewelina Backtrog, E., and Rekowski, P. (2019). Capillary electrophoresis study of systemin peptides spreading in tomato plant. *Electrophoresis* 40, 336–342. doi: 10.1002/elps.201800206

Murashige, T., and Skoog, F. (1962). A revised medium for rapid growth and bio assays with tobacco tissue cultures. *Physiol. Plant* 15, 473–497. doi: 10.1111/j.1399-3054.1962.tb08052.x

Müssig, C., Shin, G., and Altmann, T. (2003). Brassinosteroids promote root growth in *Arabidopsis*. *Plant Physiol.* 133, 1261–1271. doi: 10.1104/pp.103.028662

Nawrath, C., and Métraux, J. P. (1999). Salicylic acid induction-deficient mutants of *Arabidopsis* express PR-2 and PR-5 and accumulate high levels of camalexin after pathogen inoculation. *Plant Cell* 11, 1393–1404. doi: 10.1105/tpc.11.8.1393

Nishimura, M. T., Stein, M., Hou, B. H., Vogel, J. P., Edwards, H., and Somerville, S. (2003). Loss of a callose synthase results in salicylic acid-dependent disease resistance. *Science* 301, 969–972. doi: 10.1126/science.1086716

Pastor, V., Luna, E., Ton, J., Cerezo, M., García-Agustín, P., and Flors, V. (2013). Fine tuning of reactive oxygen species homeostasis regulates primed immune responses in *Arabidopsis*. *MPMI* 26, 1334–1344. doi: 10.1094/MPMI-04-13-0117-R

Pastor, V., Sánchez-Bel, P., Gamir, J., Pozo, M. J., and Flors, V. (2018). Accurate and easy method for Systemin quantification and examining metabolic changes under different endogenous levels. *Plant Methods* 14:33. doi: 10.1186/s13007-018-0301-z

Pearce, G., Johnson, S., and Ryan, C. A. (1993). Structure-activity of deleted and substituted systemin, an 18-amino acid polypeptide inducer of plant defensive. *Genes* 268, 212–216.

Pearce, G., Moura, D. S., Stratmann, J., and Ryan, C. A. (2001). Production of multiple plant hormones from a single polyprotein precursor. *Nature* 411, 817–820. doi: 10.1038/35081107

Pearce, G., and Ryan, C. A. (2003). Systemic signaling in tomato plants for defense against herbivores. Isolation and characterization of three novel defense signalling glycopeptide hormones coded in a single precursor gene. *J. Biol. Chem.* 278, 30044–30050. doi: 10.1074/jbc.M304159200

Pearce, G., Strydom, D., Johnson, S., and Ryan, C. A. (1991). A polypeptide from tomato leaves induces wound-inducible proteinase inhibitor proteins. *Science* 253, 895–897. doi: 10.1126/science.253.5022.895

Pearce, G., Yamaguchi, Y., Barona, G., and Ryan, C. A. (2010). A subtilisin-like protein from soybean contains an embedded, cryptic signal that activates defense-related genes. *Proc. Natl. Acad. Sci. U.S.A.* 107, 14921–14925. doi: 10 1073/pnas.1007568107

Pieterse, M. J. C., Zamioudis, C., Berendsen, R. L., Weller, D. M., Van Wees, C. M. S., and Bakker, A. H. M. P. (2014). Induced systemic resistance by beneficial microbes. *Annu. Rev. Phytopathol.* 52, 347–375. doi: 10.1146/annurev-phyto-082712-102340

Rocco, M., Corrado, G., Arena, S., D'Ambrosio, C., Tortiglione, C., Sellaroli, S., et al. (2008). The expression of tomato prosystemin gene in tobacco plants highly affects host proteomic repertoire. *J. Proteom.* 71, 176–185. doi: 10.1016/j.jprot.2008.04.003

Ross, A., Yamada, K., Hiruma, K., Yamashita-Yamada, M., Lu, X., Takano, Y., et al. (2014). The Arabidopsis PEPR pathway couples local and systemic plant immunity. *EMBO J.* 33, 62–75. doi: 10.1002/embj.201284303

Ryan, C. A. (2000). The systemin signaling pathway: differential activation of plant defensive genes. *Biochim. Biophys. Acta* 1477, 112–121. doi: 10.1016/s0167-4838(99)00269-1

Saijo, Y., Loo, P. E., and Yasuda, S. (2018). Pattern recognition receptors and signalling in plant-microbe interactions. *Plant J.* 93, 592–613. doi: 10.1111/tpj.13808

Sánchez-Bel, P., Sanmartín, N., Pastor, V., Mateu, D., Cerezo, M., Vidal-Albalat, A., et al. (2018). Mycorrhizal tomato plants fine tunes the growth-defence balance upon N depleted root environaments. *Plant Cell Environ.* 41, 406–420. doi: 10.1111/pce.13105

Scheer, J. M., Pearce, G., and Ryan, C. A. (2003). Generation of systemin signaling in tobacco by transformation with the tomato systemin receptor kinase gene. *Proc. Natl. Acad. Sci. U.S.A.* 100, 10114–10117. doi: 10.1073/pnas.1432910100

Stegmann, M., Monaghan, J., Smakowska-Luzan, E., Rovenich, H., Lehner, A., Holton, N., et al. (2017). The receptor kinase FER is a RALF-regulated scaffold controlling plant immune signaling. *Science* 355, 287–289. doi: 10.1126/science.aal2541

Sun, J., Jiang, H., and Li, C. (2011). Systemin/jasmonate-mediated systemic defense signaling in tomato. *Mol. Plant.* 4, 607–615. doi: 10.1093/mp/ssr008

Terras, F. R. G., Schoofs, H. M. E., De Bolle, M. F. C., Van Leuven, F., Rees, S. B., et al. (1992). Analysis of two novel classes of plant antifungal proteins from radish (*Raphanus sativus* L.) Seeds. *J. Biol. Chem.* 267, 15301–15309. doi: 10.1016/j.peptides.2008.08.008

Thevissen, K., de Mello Tavares, P., Xu, D., Blankenship, J., Vandenbosch, D., Idkowiak-Baldys, J., et al. (2012). The plant defensin RsAFP2 induces cell wall stress, septin mislocalization and accumulation of ceramides in *Candida albicans*. *Mol. Microbiol.* 84, 166–180. doi: 10.1111/j.1365-2958.2012.08017.x

Ton, J., and Mauch-Mani, B. (2004). Beta-amino-butyric acid-induced resistance against necrotrophic pathogens is based on ABA-dependent priming for callose. *Plant J.* 38, 119–130. doi: 10.1111/j.1365-313X.2004.02028.x

Torres, M. A., Morales, J., Sánchez-Rodríguez, C., Molina, A., and Dangl, J. L. (2013). Functional interplay between *Arabidopsis* NADPH oxidases and heterotrimeric g protein. *MPMI* 26, 686–694. doi: 10.1094/MPMI-10-12-0236-R

Wang, L., Einig, E., Almeida-Trapp, M., Albert, M., Fliegmann, J., Mithöfer, A., et al. (2018). The systemin receptor SYR1 enhances resistance of tomato against herbivorous insects. *Nature Plants* 4, 152–156. doi: 10.1038/s41477-018-0106-0

Wang, X., Hou, S., Wu, Q., Lin, M., Acharya, B. R., Wu, D., et al. (2017). IDL6-HAE/HSL2 impacts pectin degradation and resistance to *Pseudomonas* syringae pv tomato DC3000 in *Arabidopsis* leaves. *Plant J.* 89, 250–263. doi: 10.1111/tpj.13380

Wilkinson, S. W., Magerøy, M. H., López Sánchez, A., Smith, L. M., Furci, L., Cotton, T. E. A., et al. (2019). Surviving in a hostile world: plant strategies to resist pests and diseases. *Ann. Rev. Phytopathol.* 57, 505–529. doi: 10.1146/annurev-phyto-082718-095959

Wrzaczek, M., Brosche, M., Kollist, H., and Kangasjarvi, J. (2009). *Arabidopsis* GRI is involved in the regulation of cell death induced by extracellular ROS. *Proc. Natl. Acad. Sci. U.S.A.* 106, 5412–5417. doi: 10.1073/pnas.0808980106

Xu, S., Liao, C., Jaiswal, N., Lee, S., Yun, D., Lee, S. Y., et al. (2018). Tomato PEPR1 ORTHOLOGUE RECEPTOR-LIKE KINASE1 regulates responses to systemin, necrotrophic fungi and insect herbivory. *Plant Cell Adv.* 30, 2214–2229. doi: 10.1105/tpc.17.00908

Yamaguchi, Y., Barona, G., Ryan, C. A., and Pearce, G. (2011). GmPep914, an eight-amino acid peptide isolated from soybean leaves, activates defense-related genes. *Plant Physiol.* 156, 932–942. doi: 10.1104/pp.111.173096

Yamaguchi, Y., and Huffaker, A. (2011). Endogenous peptide elicitors in higher plants. *Curr. Opin. Plant Biol.* 14, 351–357. doi: 10.1016/j.pbi.2011.05.001

Yamaguchi, Y., Huffaker, A., Bryan, A. C., Tax, F. E., and Ryan, C. A. (2010). PEPR2 is a second receptor for the Pep1 and Pep2 peptides and contributes to defense responses in *Arabidopsis*. *Plant Cell* 22, 508–522. doi: 10.1105/tpc.109.068874

Yamaguchi, Y., Pearce, G., and Ryan, C. A. (2006). The cell surface leucine-rich repeat receptor for AtPep1, an endogenous peptide elicitor in Arabidopsis, is functional in transgenic tobacco cells. *Proc. Natl. Acad. Sci. U.S.A.* 103, 10104–10109. doi: 10.1073/pnas.0603729103

Yu, X., Feng, B., He, P., and Shan, L. (2017). From chaos to harmony: response and signaling upon microbial pattern recognition. *Annu. Rev. Phytopathol.* 55, 5.1–5.29. doi: 10.1146/annurev-phyto-080516-035649

Zhang, H., Hu, Z., Lei, C., Zheng, C., Wang, J., Shao, S., et al. (2018). A plant phytosulfokine peptide initiates auxin-dependent immunity through cytosolic Ca(2+) signaling in tomato. *Plant Cell* 30, 652–667. doi: 10.1105/tpc.170 0537

Zhang, H., Yu, P., Zhao, J., Jiang, H., Wang, H., Zhu, Y., et al. (2017). Expression of tomato prosystemin gene in *Arabidopsis* reveals systemic translocation of its mRNA and confers necrotrophic fungal resistance. *New Phytol.* 217, 799–812. doi: 10.1111/nph.14858

Conflict of Interest: The authors declare that the research was conducted in the absence of any commercial or financial relationships that could be construed as a potential conflict of interest.

frontiers in Plant Science

ORIGINAL RESEARCH
published: 30 June 2020
doi: 10.3389/fpls.2020.00716

TaRac6 Is a Potential Susceptibility Factor by Regulating the ROS Burst Negatively in the Wheat–*Puccinia striiformis* f. sp. *tritici* Interaction

Qiong Zhang[1†], Xinmei Zhang[2†], Rui Zhuang[1], Zetong Wei[1], Weixue Shu[1], Xiaojie Wang[1] and Zhensheng Kang[1*]*

[1] State Key Laboratory of Crop Stress Biology for Arid Areas, College of Plant Protection, Northwest A&F University, Yangling, China, [2] College of Life Sciences, Northwest A&F University, Yangling, China

OPEN ACCESS

Edited by:
Silvia Proietti,
University of Tuscia, Italy

Reviewed by:
Oswaldo Valdes-Lopez,
National Autonomous University of Mexico, Mexico
Matthew Rouse,
United States Department of Agriculture-Agricultural Research Service, United States
Steven Whitham,
Iowa State University, United States

***Correspondence:**
Xiaojie Wang
wangxiaojie@nwsuaf.edu.cn
Zhensheng Kang
kangzs@nwsuaf.edu.cn

[†] These authors have contributed equally to this work

Specialty section:
This article was submitted to Plant Microbe Interactions, a section of the journal Frontiers in Plant Science

Received: 24 October 2019
Accepted: 06 May 2020
Published: 30 June 2020

Citation:
Zhang Q, Zhang X, Zhuang R, Wei Z, Shu W, Wang X and Kang Z (2020) TaRac6 Is a Potential Susceptibility Factor by Regulating the ROS Burst Negatively in the Wheat–Puccinia striiformis f. sp. tritici Interaction. Front. Plant Sci. 11:716. doi: 10.3389/fpls.2020.00716

Rac/Rop proteins play important roles in the regulation of cell growth and plant defense responses. However, the function of Rac/Rop proteins in wheat remains largely unknown. In this study, a small G protein gene, designated as *TaRac6*, was characterized from wheat (*Triticum aestivum*) in response to *Puccinia striiformis* f. sp. *tritici* (*Pst*) and was found to be highly homologous to the Rac proteins identified in other plant species. Transient expression analyses of the TaRac6-GFP fusion protein in *Nicotiana benthamiana* leaves showed that TaRac6 was localized in the whole cell. Furthermore, transient expression of TaRac6 inhibited Bax-triggered plant cell death (PCD) in *N. benthamiana*. Transcript accumulation of *TaRac6* was increased at 24 h post-inoculation (hpi) in the compatible interaction between wheat and *Pst*, while it was not induced in an incompatible interaction. More importantly, silencing of *TaRac6* by virus induced gene silencing (VIGS) enhanced the resistance of wheat (Suwon 11) to *Pst* (CYR31) by producing fewer uredinia. Histological observations revealed that the hypha growth of *Pst* was markedly inhibited along with more H_2O_2 generated in the *TaRac6*-silenced leaves in response to *Pst*. Moreover, transcript levels of *TaCAT* were significantly down-regulated, while those of *TaSOD* and *TaNOX* were significantly up-regulated. These results suggest that *TaRac6* functions as a potential susceptibility factor, which negatively regulate the reactive oxygen species (ROS) burst in the wheat–*Pst* interaction.

Keywords: TaRac6, wheat, *Puccinia striiformis* f. sp. *tritici*, reactive oxygen species, susceptibility factor

INTRODUCTION

Small GTP-binding proteins are proteins that have a molecular weight of 20–40 kd. They constitute a superfamily with five families—Ras, Ran, Rab, Rho, and Arf—which includes more than 100 members (Takai et al., 2001). The Rho family in animals is further divided into three subfamilies: Rho, Rac, and CDC42. However, because the Rho family in plants more closely resembles the Rac subfamily in animals, they are also called Rac-like or Rop-like (Rac/Rop) proteins (Winge et al., 2000).

The Rac/Rop protein family contains five highly conserved G-boxes and a C-terminal motif (Wennerberg et al., 2005). One G-box is the binding region of downstream effectors. The function of the other four G-boxes is to bind GTP/GDP and to hydrolyze GTP to GDP. The C-terminal motifs are related to the function of GTPase and the subcellular localization (Williams, 2003). Based on its C-terminal motifs, Rac/Rop proteins may be divided into two types (Winge et al., 2000): Type I have a conserved CaaL motif (a: aliphatic amino acid), while Type II lack the CaaL motif (Lavy et al., 2002) but have a cysteine domain to the membrane (Kawano et al., 2014). All type-I Rac/Rop proteins are prenylated (Lavy et al., 2002). Prenylation is required for membrane attachment and function of type I Rops, while type II Rops with the cysteine domain are attached to the plasma membrane by S-acylation. The prenylation of Rops determines their stable distribution between the plasma membrane and cytoplasm but has little effect on the dynamics of membrane interaction. In addition, the prenylation of type I Rops has only a small effect on ROP function. The mechanism of type II ROP S-acylation and membrane attachment is unique to plants and likely responsible for the viability of plants in the absence of CaaL prenylation activity. Type I ROPs affect the cell structure, primarily on the adaxial side, while type II ROPs induce a novel cell division phenotype (Sorek et al., 2011).

There are two states of Rac/Rop: the GTP-bound state Rac/Rop and GDP-bound state Rac/Rop, with the former being active and the latter being inactive (Vetter and Wittinghofer, 2001). GTPase-activating proteins (GAPs) reconvert the active Rac/Rop to an inactive state by promoting GTPase activity. The guanine nucleotide dissociation inhibitor (GDI) inhibits GDP-bound to GTP-bound, and guanine nucleotide exchange factors (GEFs) release GDP from Rac/Rop and bind Rac/Rop to GTP. The active Rac/Rop are able to interact with downstream effectors to function.

The Rac/Rop family is an important signal transduction regulator in plants, participating in various key life processes, including plant cell polarity, cell growth, morphological development, cytoplasmic division, signal transduction of hormones, and resistance to adversity (Schiene et al., 2000; Vernoud et al., 2003; Berken, 2006; Kawano et al., 2010a,b; Kawano and Shimamoto, 2013). However, the functioning of Rac/Rop family members in the interaction between plants and pathogens are still largely unknown. In rice (*Oryza sativa*), seven Rac/Rop family genes have been isolated (Miki et al., 2005). Among them, *OsRac1* plays a positive role in blast resistance but overexpressed transgenic plants of *OsRac4*, *OsRac5*, and *OsRac6* showed greater susceptibility to rice blast, whereas *OsRac3* and *OsRac7* may not participate in plant disease responses (Jung et al., 2006; Chen et al., 2010). OsRac1 contributes to disease resistance by regulating reactive oxygen species (ROS) and the biosynthesis of chitin and lignin (Wong et al., 2004; Kawasaki et al., 2006; Akamatsu et al., 2013). Additionally, several proteins, such as OsMAPK6, CERK1, GEF1, and SPL11, were found to be associated with Rac/Rop proteins participating in the interaction between plants and their pathogens (Lieberherr et al., 2005; Akamatsu et al., 2013; Liu et al., 2015). In barley (*Hordeum vulgare*), six Rac/Rop family genes were isolated, of which *HvRacB* was confirmed to be able to promote the susceptibility of barley to *Blumeria graminis* f. sp. *hordei* (*Bgh*) (Schultheiss et al., 2002, 2003). Furthermore, HvRacB was shown to affect barley's resistance to *Bgh* by modulating the reorganization of actin (Opalski et al., 2005). Thus, different members of the same Rac/Rop family can play distinct roles in shaping how plants respond to pathogenic attacks and infection. Hence, it is of great significance to explore the mechanisms underpinning the Rac/Rop family genes' involvement in plant responses to pathogens.

Wheat stripe rust, caused by *Puccinia striiformis* f. sp. *tritici* (*Pst*), is among the most devastating diseases afflicting wheat (Chen et al., 2014), having become one the most important biotic problems threatening wheat production worldwide (Schwessinger, 2017). A better understanding of host–pathogen interactions will lay a theoretical foundation to formulate new strategies for the sustainable control of stripe rust. Analysis of cDNA library data revealed a Rac/Rop homologous gene in wheat that was up regulated in a compatible interaction (Ma et al., 2009). Yet, the function of this Rac/Rop gene in wheat's response to *Pst* is still unknown. In this study, we report on this Rac/Rop family gene, designated as *TaRac6,* which was located to the whole cell and inhibited cell death induced by Bax. The function of *TaRac6* was further analyzed using VIGS (virus induced gene silencing), which demonstrated that *TaRac6* could regulate the resistance of wheat to *Pst* negatively by affecting the ROS burst. These results lay a foundation to explore the functioning of plant Rac/Rop proteins under pathogen infection.

MATERIALS AND METHODS

Preparation of Plant Materials, Wheat Stripe Rust and Bacterial

Wheat and tobacco (*Nicotiana benthamiana*) plants were planted at 16°C and 23°C, respectively, under 60% relative humidity. The *Pst* isolates CYR31 and CYR23 were cultured on wheat cultivars 'Suwon11' and 'Mingxian169,' respectively (Kang et al., 2002). The *Escherichia coli* strain JM109 was cultured in Luria-Bertani (LB) culture medium overnight at 37°C in the dark. The *Agrobacterium tumefaciens* strain GV3101 was cultured in LB at 30°C in the dark for 1–2 days.

Sequence Analysis of TaRac6

The protein features were predicted in NCBI[1]. Protein molecular weight was predicted by ExPASy[2]. SignalP 4.1[3] was used to predict protein signal peptide. TMHMM Server v. 2.0[4] was used to predict transmembrane helices in proteins. PSORT[5] was used to predict subcellular localization. cNLS Mapper (nls-mapper.iab.keio.ac.jp/cgi-bin/NLS_Mapper_form.cgi#opennewwindow) was used to

[1]https://www.ncbi.nlm.nih.gov

[2]https://web.expasy.org/compute_pi/

[3]http://www.cbs.dtu.dk/services/SignalP/

[4]http://www.cbs.dtu.dk/services/TMHMM-2.0/#opennewwindow

[5]https://wolfpsort.hgc.jp/

predict nuclear location signal. The software DNAMAN6.0 was used to align multiple sequences. The Phylogenetic tree was produced with the MEGA5 using the neighbor-joining approach. The fragment used for VIGS was aligned with the whole genome information of wheat[6] and *Pst*[7] to ensure sequence specificity.

Plasmid Construction

Primers used for plasmid construction are listed in **Supplementary Table S1**. The ORF sequence of *TaRac6* was cloned into the pCAMBIA-1302 and pBinGFP2 vectors to verify its subcellular localization. pCAMBIA-1302 vector was used to express GFP at the C-terminus of TaRac6 (TaRac6-GFP^C) and pBinGFP2 at the N-terminus (GFP^N-TaRac6). To silence *TaRac6*, a specific 183-bp fragment containing a 13-bp untranslated region and a 170-bp fragment of a translated region was constructed into the BSMV-γ vector. To overexpress *TaRac6* in *N. benthamiana*, the ORF sequence was inserted into the PVX vector pGR106.

RNA Extraction and Quantitative RT-PCR

The fresh urediniospores of CYR23 (incompatible interaction) and CYR31 (compatible interaction) were inoculated on the first leaves of 7-day-old wheat seedlings (Suwon11) with an inoculation needle. After inoculation, wheat seedlings were cultured in dark for 24 h with 100% humidity, and then transferred to a greenhouse at 15°C with a 16 h photoperiod. The leaves inoculated with CYR23 and CYR31 were sampled at 0, 12, 24, 48, 72, and 120 h post-inoculation (hpi), respectively. Total RNA from each sample was extracted using the MiniBEST Universal RNA Extraction Kit (TaKaRa, Kusatsu, Japan). The quality of obtained RNA was checked by electrophoresis. As described by Feng et al. (2011), first-strand cDNA was synthesized using Oligo dT Primer.

The primers used for the qRT-PCR can be found in **Supplementary Table S1**. Elongation factor 1α (EF-1α) of wheat was selected as the inner reference gene (Ling et al., 2007). The procedure of qRT-PCR followed that of Feng et al. (2011). The results were analyzed using the $2^{-\Delta\Delta CT}$ method (Livak and Schmittgen, 2012), with three independent biological replicates.

Transient Expression Assays for Subcellular Localization

GV3101 carrying pCAMBIA-1302-TaRac6-GFP^C, pCAMBIA-1302-GFP, pBinGFP2-GFP^N-TaRac6 or 35S-mCherry plasmids were cultured in LB (50 μg/mL kanamycin and 50 μg/mL rifampicin) for 1–2 days. The cells were collected and suspended as described by Zhao et al. (2018). GFP, GFP^N-TaRac6, TaRac6-GFP^C of *A. tumefaciens* were co-injected into leaves of tobacco plants 4–6 weeks old with mCherry, respectively. Two days later plant tissue samples were harvested. The GFP images were taken under a LSM510 Confocal Microscope (Zeiss, Germany) with 488 nm laser lines. The mCherry images were taken under a LSM510 Confocal Microscope (Zeiss, Germany) with 584 nm laser lines.

[6]http://plants.ensembl.org/Triticum_aestivum/Info/Index

[7]http://fungi.ensembl.org/Puccinia_graminis/Info/Index

The expression of TaRac6-GFP^C and GFP^N-TaRac6 were further confirmed by western blot. The total proteins of injected tobacco leaves were extracted using the Native lysis buffer (Solarbio, Beijing, China). Specifically, 10 μL PMSF (100 mM) and 10 μL protease inhibitor cocktail (EDTA-Free, 100 × in DMSO) were added per ml of lysate. The extraction of total protein and the western blot procedure used are described in Zhao et al. (2018).

Inhibition Assay of PCD Induced by Bax

The pGR106-TaRac6, pGR106-eGFP (negative control), and pGR106-Avr1b (positive control, Dou et al., 2008) were respectively transformed into GV3101 (Hellens et al., 2000). Details on the treatment of the positive transformant can be found in Zhao et al. (2018). The *A. tumefaciens* cell suspensions of pGR106-TaRac6, pGR106-eGFP, and pGR106-Avr1b were injected separately into *N. benthamiana* leaves using sterile syringes. Then, 24 h later, the agrobacterium suspension containing the Bax gene was injected again at the same location. The tobacco leaves were sampled at 3 days post inoculation (dpi). The total RNA and cDNA of all samples at 3 dpi with Bax were obtained using the procedural methods described above. qRT-PCR was used to detect the transcription levels of *N. benthamiana* defense-related genes (*PR1α, PR2,* and *PR5*). The *N. benthamiana* housekeeping gene *NbActin* was selected as the inner reference gene. The results were analyzed by the $2^{-\Delta\Delta CT}$ method (Livak and Schmittgen, 2012), using three independent biological replicates. Symptoms were observed 5–7 days later. Leaves were decolorized by ethanol/glacial acetic acid (v/v, 1:1).

BSMV-Mediated *TaRac6* Gene Silencing

The VIGS (virus induced gene silencing) system was implemented as described by Holzberg et al. (2002). 'Suwon11' was the cultivar used for the experiment. To silence TaRac6, BSMV: α + β + γ-TaRac6 was used to inoculate wheat seedlings. BSMV: α + β + γ was used as the control. About 30 seedlings were inoculated with each treatment. Ten days after virus inoculation, fresh CYR31 urediniospores were inoculated onto the fourth leaf. The wheat seedlings were cultured as described by Zhao et al. (2018). Their fourth leaves were sampled at 24 hpi and 48 hpi, to detect the gene-silencing efficiency and to observe the hyphae lengths and H_2O_2 accumulation at the histological level. The RNA of the fourth leaves inoculated with BSMV: α + β + γ and BSMV: α + β + γ-TaRac6 were isolated, and the qRT-PCR was used to assess the silencing efficiency and expression of the *TaCAT*, *TaSOD* and *TaNOX* genes. Cytological analyses of *Pst* growth and the host response in the control and *TaRac6*-silenced wheat plants were carried out as described by Zhao et al. (2018). Thirty-five infection sites from three leaves per treatment were used to calculate the hyphal length and H_2O_2 accumulation. Only the infected sites with substomatal vesicles under the stomata were considered to be successfully infected. Wheat germ agglutinin conjugated to Alexa Fluor 488 (Invitrogen, Carlsbad, CA, United States) was used to stain the *Pst* infection structures as described in Ayliffe et al. (2011). The length of hyphae and accumulation of H_2O_2 were each

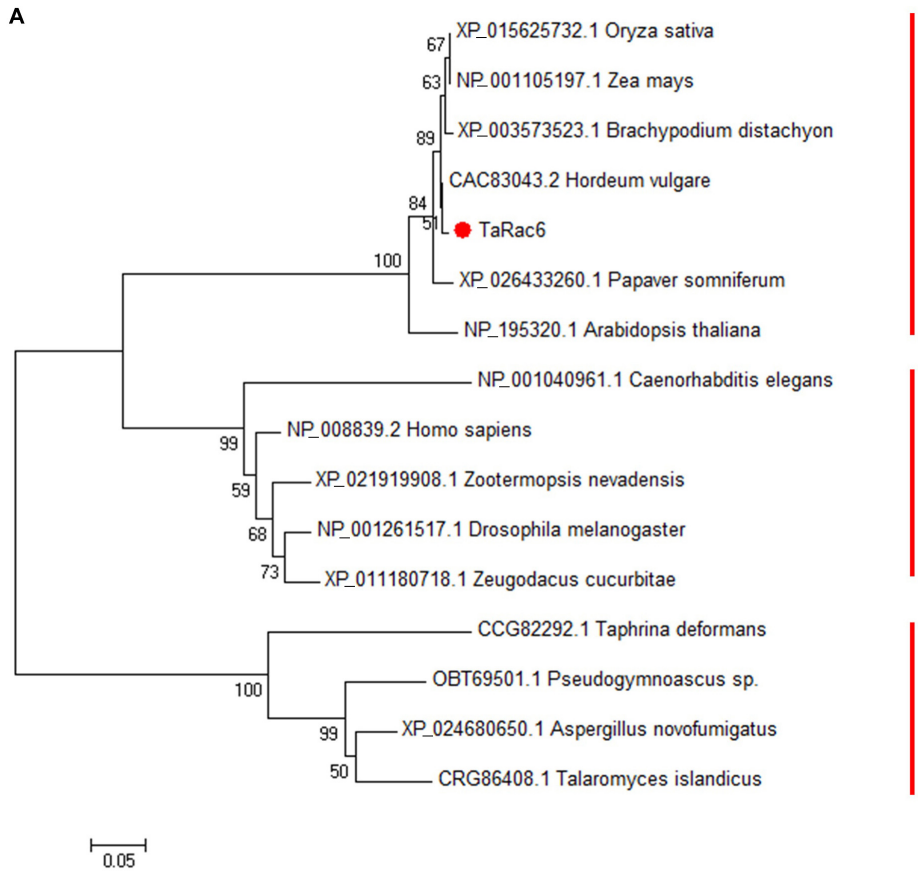

B

MSASRFIKCVTVGDGAVGKTCMLISYTSNTFPTDYVPTVFDNFSANVVVDGNT

VNLGLWDTAGQEDYNRLRPLSYRGADVFLLAFSLISKASYENVSKKWIPELKH

YAPGVPIILVGTKLDLRDDKQFFVDHPGAVPITTAQGEELKKLIGAPYYIECSSKT

QLNVKGVFDAAIKVVLAPPKAKKKKKAQRGACSIL

FIGURE 1 | Amino acid sequences analysis and characterization. **(A)** The Phylogenetic tree of TaRac6 and RAC/ROP proteins from various eukaryotes was carried out using the MEGA5 by neighbor-joining approach. Branches are labeled with GenBank accession numbers and the corresponding name of each eukaryotic species. XP_015625732.1 (OsRac6), NP_001105197.1 (ZmRop9), XP_003573523.1 (BdRac6), CAC83043.2 (HvRopB), XP_026433260.1 (PsRac6), NP_195320.1 (AtRac6), NP_001040961.1 (CeRac2), NP_008839.2 (HsRac1), XP_021919908.1 (ZnRac1), NP_001261517.1 (DmRac2), XP_011180718.1 (ZcRac1), and CCG82292.1 (TdRho2). **(B)** Conserved domain of the *TaRac6* protein. The red boxes indicate G1–G5 boxes. The yellow box indicates the CxxL motif. The sequence underlined with a black line indicates the Rho domain.

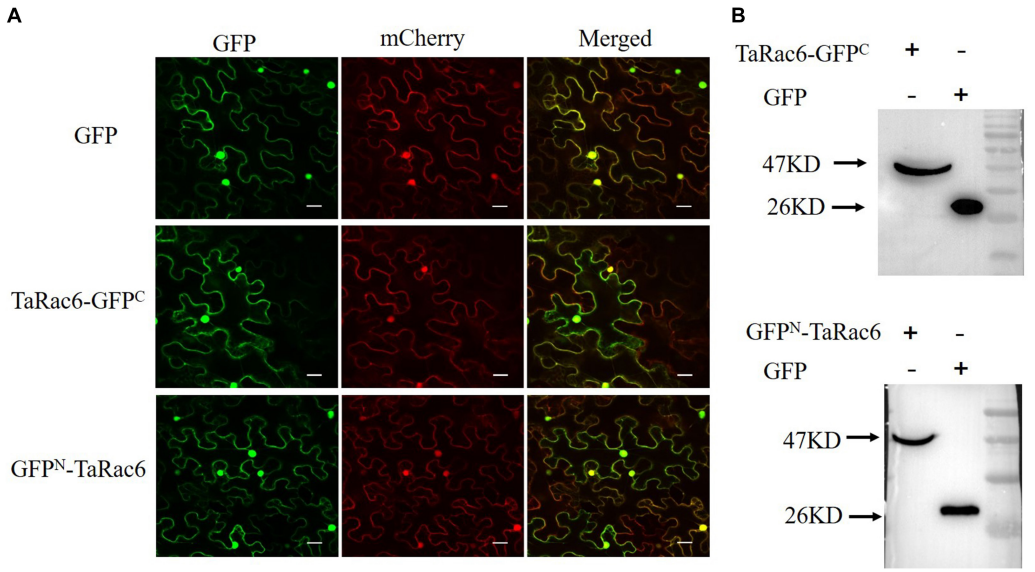

FIGURE 2 | Subcellular localization of TaRac6 in tobacco leaves. **(A)** The green fluorescent protein (GFP), TaRac6-GFP^C, and the GFP^N-TaRac6 fusion protein were transiently expressed in *Nicotiana benthamiana* with mCherry, respectively. Signals of both were detected throughout the cell. **(B)** Western blot was used to analyze the GFP, TaRac6-GFP^C, and GFP^N-TaRac6 fusion protein. Bars = 20 μm.

observed under an Olympus BX-51 microscope. The wheat phenotypes were observed 14 days after the *Pst* inoculation (dpi). For each treatment, six inoculated leaves were used to observe the phenotype. The phenotype was quantified by calculating the uredinium number within 1 cm^2 area for one leaf. To avoid bias among the leaf samples, test points were randomly selected from the six treated plants. To estimate changes in the fungal biomass, DNA quantification of the single-copy target genes *PsEF1* (from *Pst*) and *TaEF1* (from wheat) was further measured using qRT-PCR as previously described (Panwar et al., 2013; Liu et al., 2016). Three independent biological replicates were performed.

RESULTS

Sequence Analysis of TaRac6

An up-regulated transcript in the cDNA library of the compatible interaction between wheat and *Pst* was isolated (Ma et al., 2009), and designated as *TaRac6* based on the Blast results in NCBI (see foot note 1). BlastN analyses in the *Triticum aestivum* genome sequence showed that there are three copies of this gene in the wheat genome, located on 6A, 6B, and 6D. The cDNA sequence of the three copies obtained in Suwon11 are highly similar (**Supplementary Figure S1**) and encodes the same proteins (**Supplementary Figure S2**). The three copies of *TaRac6* encode the same 197 amino acids, which showed high homology with the Rac/Rop proteins from other plants (**Supplementary Figure S3**). TaRac6 has no signal peptide or transmembrane domain predicted by the SignalP 4.1 and TMHMM Server. It was predicted to be located in the plasma membrane, cytoplasm, and Chloroplast and has a nuclear localization signal predicted by the PSORT and cNLS Mapper. The protein features analysis indicated that TaRac6 contained a Rop-like domain (**Supplementary Figure S4**). Phylogenetic analysis indicated that *TaRac6* and other plant Rho-related GTPases clustered together (**Figure 1A**). As a protein in the Rac/Rop GTPase family, TaRac6 contains five G boxes and a CxxL motif, which is the typical motif of the Rac/Rop protein belonging to Type I (**Figure 1B**).

TaRac6 Is Localized in Plasma Membrane, Cytoplasm, and Nucleus

The control GFP, the TaRac6-GFP^C, or the GFP^N-TaRac6 were transiently expressed in tobacco leaves with 35S-mCherry, respectively. The fluorescence of TaRac6-GFP^C was observed in the plasma membrane, cytoplasm, and nuclear region of *N. benthamiana*. Similarly, the signal of TaRac6-GFP^N was also detected in the whole cell of *N. benthamiana* (**Figure 2A**). Western blot assays indicated that the TaRac6-GFP^C and TaRac6-GFP^N fusion proteins were successfully expressed in *N. benthamiana* (**Figure 2B**).

Transient Expression of TaRac6 Inhibits Cell Death in Tobacco

Cell death is associated with plant resistance to invasion and spread by pathogens (Van Doorn et al., 2011). Bax is a death-promoting member of the Bcl-2 family of proteins which trigger cell death when expressed in plants (Lacomme and Santa Cruz, 1999). Bax-triggered cell death has similar physiological characteristics to plant hypersensitive responses (Lacomme and Santa Cruz, 1999). To determine whether TaRac6 could induce cell death or inhibit Bax-induced cell death to affect plant defense response, TaRac6 was transiently overexpressed in tobacco leaves with the Bax system. When Bax was expressed in tobacco leaves, the cells showed obvious necrosis. By contrast, cell death induced

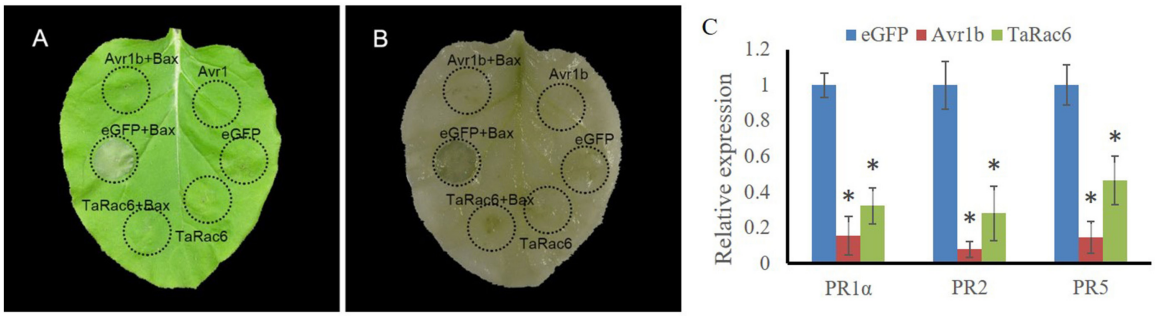

FIGURE 3 | Transient expression of TaRac6 inhibited Bax-induced plant cell death in tobacco. **(A)** Tobacco leaves were injected with *Agrobacterium tumefaciens* cells containing pGR106-eGFP (negative control), pGR106-TaRac6, or pGR106-Avr1b (positive control); 24 h later, *A. tumefaciens* cells containing Bax were injected into the tobacco leaves. Photos were taken 5 days later. **(B)** Leaves were decolorized by ethanol/glacial acetic acid (1:1, v/v). **(C)** Transcription level changes of *N. benthamiana* defense-related genes *PR1α, PR2,* and *PR5* in tobacco leaves when Bax was co-expressed with pGR106-eGFP, pGR106-TaRac6, or pGR106-Avr1b at 3dpi. *NbActin* was selected as the inner reference gene. Three independent biological replications were performed to calculate each of the mean values. Vertical bars represent the standard deviation. $^*P < 0.05$.

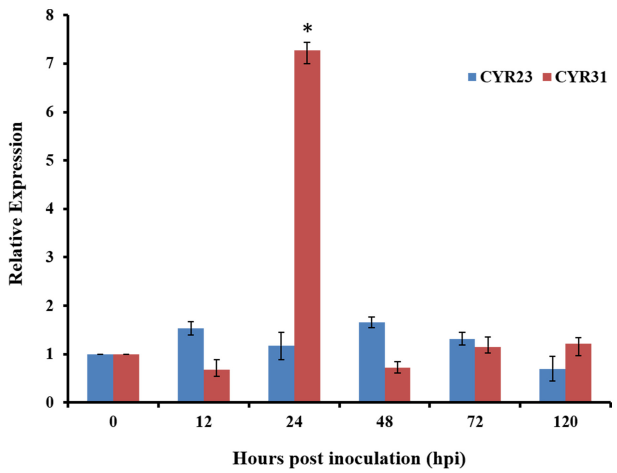

FIGURE 4 | Transcript profiles of *TaRac6* in wheat inoculated with *Pst*. Expression pattern analyses of *TaRac6* during the different developing stages of the incompatible interaction (CYR23) and compatible interaction (CYR31) were calculated using the $2^{-\Delta\Delta CT}$ method. Three independent biological replications were performed to calculate each of the mean values. The wheat gene *TaEF-1α* was used to normalize the qRT-PCR data. Vertical bars represent the standard deviation. $^*P < 0.05$.

by Bax was starkly inhibited when TaRac6 and Bax were co-expressed. However, no cell death was observed in the leaves injected with Avr1b, which served as the positive control. The transcription levels of *PR1α, PR2, and PR5* were reduced in tobacco leaves when Bax was co-expressed with pGR106-TaRac6 or pGR106-Avr1b, compared to pGR106-eGFP (**Figure 3**). These results indicated that TaRac6 could play an important role in inhibiting cell death.

TaRac6 Is Highly Expressed in the Compatible Wheat–Pst Interaction

To determine whether *TaRac6* participate in wheat-*Pst* interactions, qRT-PCR was used to detect the expression of *TaRac6* in the compatible and incompatible interaction of wheat–*Pst*. The expression of *TaRac6* was up-regulated in the compatible interaction of wheat–*Pst* (CYR31). The transcript level of *TaRac6* at 24 hpi was approximately 7.2-fold that of the control (0 hpi). However, the transcript level of *TaRac6* was almost unchanged in the incompatible interaction (**Figure 4**). The result indicated that *TaRac6* played an important role in the compatible interaction between wheat and *Pst*.

Silencing BSMV-TaRac6 Increased the Resistance of Wheat

The BSMV-VIGS system was used to silence the expression of *TaRac6* and thereby to characterize its function in the wheat–*Pst* interaction. Compared with the control leaves inoculated with FES-buffer, leaves inoculated with the vector of BSMV-γ and BSMV-TaRac6 displayed chlorotic striping at 10 days post-virus inoculation (dpvi) (**Figures 5Aa–c**). A bleaching phenotype was observed in PDS-silenced plants (**Figures 5A,d**), which suggested that the BSMV-VIGS system was effective. Race CYR31 was inoculated on the fourth leaf of wheat (Suwon 11), and 14 days later the leaves pre-inoculated with the FES-buffer and control leaves continued to display the typical compatible phenotype (**Figures 5A,e,f**); however, the susceptibility level of *TaRac6*-silenced leaves was significantly decreased (**Figures 5A,g**). The uredinia number in *TaRac6*-silenced leaves was reduced by approximately 30% relative to the control (BSMV-γ) (**Figure 5B**). Fungal DNA content was used as a proxy for *Pst* biomass in the leaves. The *Pst* DNA content was significantly reduced in *TaRac6*-silenced leaves indicating that fungal growth was inhibited (**Figure 5C**). To determine whether the phenotypic changes were caused by *TaRac6*'s silencing, qRT-PCR was used to detect the silencing efficiency compared with leaves inoculated with BSMV-γ. The transcript level of *TaRac6* was reduced by 67% and 71% at 24 hpi and 48 hpi, respectively (**Figure 5D**). This result indicated that the *TaRac6* gene had been successfully silenced. To determine whether the phenotypic changes between control and *TaRac6*-silenced plants are associated with fungal

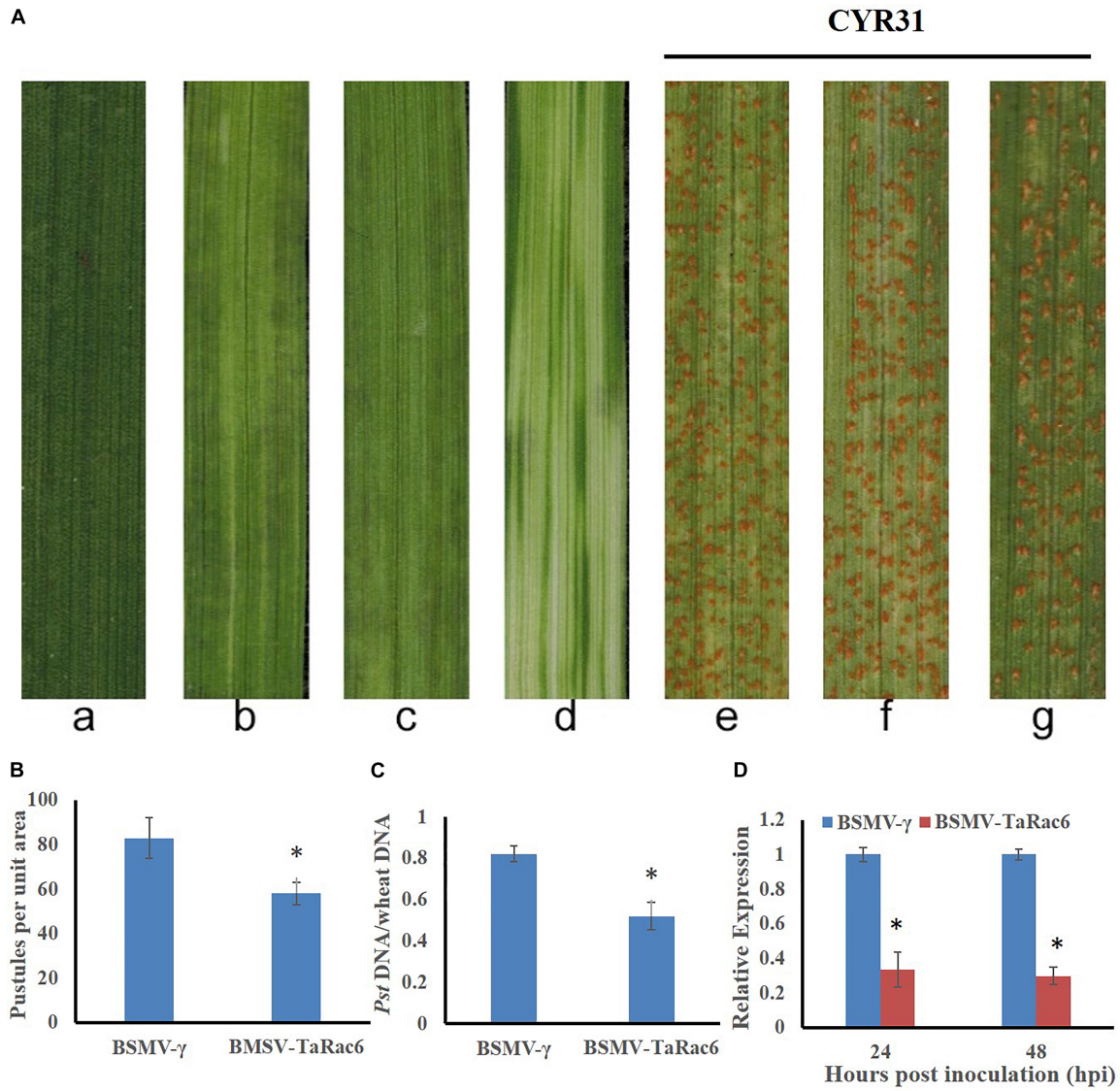

FIGURE 5 | Functions of *TaRac6* silencing by virus induced gene silencing (VIGS) in the compatible interaction between wheat (Suwon 11) and stripe rust pathogen (CYR31). **(A)** Phenotypes of the fourth leaves inoculated with the FES-buffer **(a)**, BSMV-γ **(b)**, BSMV-*TaRac6***(c)**, or BSMV-PDS **(d)** at 12 days post-virus treatment. Phenotypes of the fourth leaves inoculated with CYR31 at 14-day post inoculation that had been pre-inoculated with the FES-buffer **(e)**, BSMV-γ **(f)**, or BSMV-*TaRac6* **(g)**. **(B)** Quantification of the uredinium density at 14 dpi with *Pst*. Means and standard deviations were calculated from three independent replicates. Six treated leaves were used to calculate the uredinium number per replicate. $^*P < 0.05$. **(C)** Fungal biomass was measured with total genomic DNA extracted from control and TaRac6-silenced wheat plants using qRT-PCR. Means and standard deviations were calculated from three independent replicates. Samples were taken at 14-day post inoculation with *Pst*. $^*P < 0.05$. **(D)** Silencing efficiency in the *TaRac6*-knockdown plants inoculated with CYR31 were calculated using the $2^{-\Delta\Delta CT}$ method. Three independent biological replications were performed to calculate the standard deviations and mean values. The wheat gene *TaEF-1α* was used to normalize the qRT-PCR data. Vertical bars represent the standard deviation. $^*P < 0.05$.

growth and development, *Pst* infection structures were stained and observed by microscopy. Histological analysis revealed a shorter hyphal length in *TaRac6*-silenced plants than that in control leaves (**Figure 6**). The accumulation of reactive oxygen species is considered to be the earliest inducing event in the plant-pathogens interaction, which controls and inhibits the growth of pathogens (Camejo et al., 2016). Therefore, to clarify whether the silencing of *TaRac6* led to the changes in host resistance level to *Pst*, DAB staining was used to detect the accumulation of H_2O_2 in leaves, the H_2O_2 accumulation area was significantly increased in *TaRac6*-silenced plants when compared with the control (BSMV-γ) at both 24 hpi and 48 hpi (**Figures 7A,B**).

To investigate the expression of genes known to control ROS accumulation, we selected *TaNOX*, *TaSOD*, and *TaCAT*. NOX enzymes are known to generate H_2O_2 (Lambeth, 2004), SOD catalyzes the conversion of superoxide anion to O_2 and H_2O_2 (Fukai and Ushio-Fukai, 2011), and CAT is the major H_2O_2 scavenging enzyme (Yang and Poovaiah, 2002). To explore the

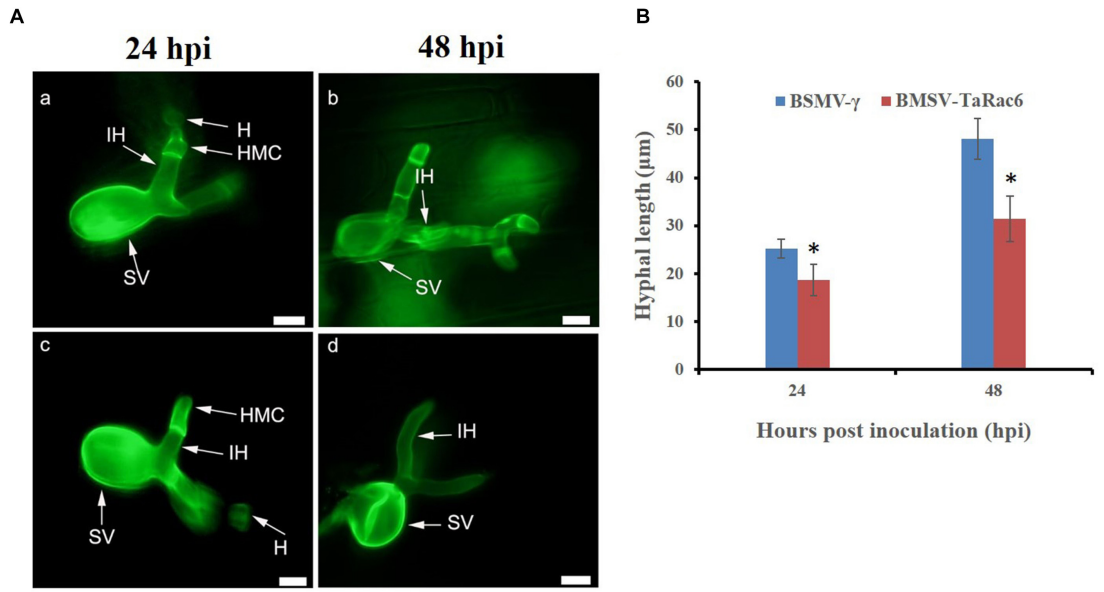

FIGURE 6 | Histological observation of fungal growth in the *TaRac6*-knockdown plants inoculated with CYR31. **(A)** Microscopic observation of wheat pre-inoculated with BSMV-γ **(a,b)** and BSMV-*TaRac6* **(c,d)**. Wheat leaves inoculated with race CYR31 at 24 hpi and 48 hpi, respectively. The histological changes were stained with wheat germ agglutinin (WGA) and observed under a fluorescent microscope. H, haustoria; HMC, haustoria mother cell; IH, infection hypha; SV, substomatal vesicle. **(B)** Histological statistical analysis of hyphae lengths in the *TaRac6*-knockdown plants inoculated with CYR31 compared to BSMV-γ at 24 hpi and 48 hpi. The average distance was calculated from the substomatal vesicles to hyphal tips from 35 infection sites of three leaves. Means and standard deviations were calculated from three independent replicates. *$P < 0.05$. Bars = 10 μm.

reason of the H_2O_2 accumulation in *TaRac6*-silenced plants, qRT-PCR was used to analyze the transcript level of these ROS-related genes in comparison with the control plants. In the *TaRac6*-silenced plants, the expression of *TaSOD* and *TaNOX* increased compared with that in control leaves (BSMV-γ), while the transcript level of *TaCAT* was down-regulated in the *TaRac6*-knockdown wheat (**Figure 7C**). Altogether, the above results indicated that *TaRac6* might increase wheat susceptibility to *Pst* by inhibiting the production of H_2O_2.

DISCUSSION

The Rac/Rop signaling pathway has a significant role in regulating many organism activities (Takai et al., 2001). The Rac/Rop proteins of rice, *Medicago sativa*, and barley (*Hordeum vulgare*) are known to be critical for the establishment of those plants' defense systems (Schiene et al., 2000; Schultheiss et al., 2003; Kawasaki et al., 2006; Chen et al., 2010). As in animals, such proteins can regulate the production of H_2O_2 by activating the NADPH oxidase at the plasma membrane (Park et al., 2000; Jones et al., 2007). Yet the function and mechanisms of similar Rac/Rop members in the response of plants to their pathogens remains largely understudied.

In this study, TaRac6 was isolated and characterized from wheat plants, and the involvement of *TaRac6* in wheat's response to *Pst* was experimentally investigated. Sequence analysis showed that the TaRac6 contains a CxxL motif at its C-terminal. According to the C-terminal motif, Rac/Rop GTPases comprise two types. Type I proteins have a CxxL motif, while Type II possess a cysteine motif to anchor the membrane (Winge et al., 2000). On the basis of this protein domain, TaRac6 constituted a Type I protein, with further analysis showing that it occurred in the whole cell. In earlier work, Type II proteins of *A. thaliana* were found mainly localized at the plasma membrane (Lavy et al., 2002). Generally, however, unlike type II proteins, type I Rac/Rop proteins are more often detected in the whole cell, including its plasma membrane, cytoplasm, and nucleus (Chen et al., 2010).

Our phylogenetic analysis indicated that *TaRac6* encodes nearly the same amino acids as HvRacB and OsRac6. HvRacB was identified as a negative regulator of barley defense to *Bgh* (Schultheiss et al., 2003), and the expression of constitutively activated HvRacB made barley more susceptible to *Bgh* (Schultheiss et al., 2005; Pathuri et al., 2008). The RNAi lines of *HvRacB* markedly induced barley's resistance to *Bgh* by restricting the formation of haustoria (Hoefle et al., 2011). Finally, overexpression of *OsRac6* enhanced susceptibility of rice to blast (Jung et al., 2006). Thus, in light of those findings, our results strongly suggest that TaRac6 is a potential susceptibility factor in wheat.

Bax-triggered plant cell death has similar physiological characteristics to plant HR. The cell death promoting function of Bax in plants correlated with accumulation of the defense-related protein PR1, suggesting that Bax activated an endogenous cell-death program in plants (Lacomme and Santa Cruz, 1999). This system has been used to successfully determine gene functioning as related to HR (Abramovitch et al., 2003; Wang et al., 2011). In our study, *TaRac6* was able to inhibit the cell

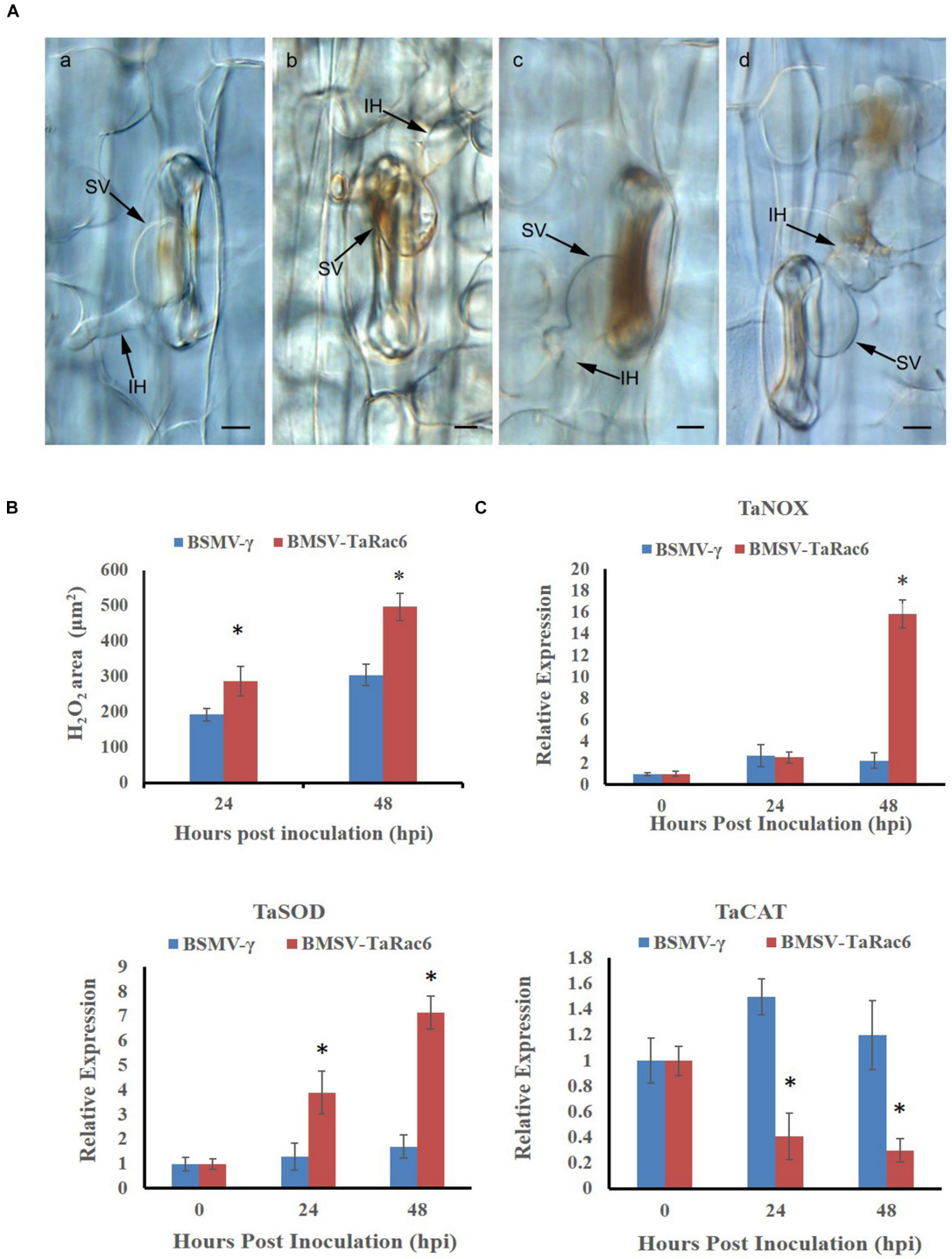

FIGURE 7 | Histological observation of H_2O_2 accumulation by the 3, 3′-diaminobenzidine (DAB) staining. **(A)** (**a,b**) shows the histological of H_2O_2 accumulation in the control leaves at 24 hpi and 48 hpi, respectively; **(c,d)** shows the histological H_2O_2 accumulation in *TaRac6*-silenced leaves at 24 hpi and 48 hpi, respectively. IH, infection hypha; SV, substomatal vesicle. Bars = 10 μm. **(B)** Histological statistical analysis of H_2O_2 areas in the *TaRac6*-knockdown plants inoculated with CYR31 compared to BSMV-γ at 24 hpi or 48 hpi, respectively. The production of H_2O_2 was stained by the DAB and the average staining area was calculated at 35 infection sites. Statistical differences were assessed using Student's *t* tests. $^*P < 0.05$. **(C)** The qRT-PCR analysis of *TaCAL*, *TaSOD* and *TaNOX* in the *TaRac6*-knockdown plants inoculated with CYR31 using the $2^{-\Delta\Delta CT}$ method. TaCAT, catalase (AKP21073.1); TaSOD, superoxide dismutase (JX398977.1). TaNOX, NADPH oxidase RBOHa (BK010636.1). BSMV-γ pre-inoculation plants served as the control. Three independent biological replications were performed to calculate the standard deviations and mean values. The wheat gene *TaEF-1α* was used to normalize the qRT-PCR data. Vertical bars represent the standard deviation. $^*P < 0.05$.

death induced by Bax and the transcription levels of *PR1α*, *PR2,* and *PR5* were reduced in tobacco leaves when Bax was co-expressed with pGR106-TaRac6 or pGR106-Avr1b, compared to pGR106-eGFP, which indicated that TaRac6 could inhibit the Bax-triggered cell-death.

To define the potential role of *TaRac6* in the wheat–*Pst* interaction, qRT-PCR was used to detect the transcript level of *TaRac6*. This showed that *TaRac6* was highly induced in the compatible interaction, especially at 24 hpi, which is a critical time-point in the compatible interaction, marked by the formation of haustoria (Kang et al., 2002). The VIGS results also showed increased resistance when *TaRac6* was silenced. According to the results of histological observation and expression analysis of ROS-related enzymes, we speculated that silencing *TaRac6* drove an increase in H_2O_2 production. More ROS limited the normal expansion of hyphal at the infected sites, resulting in decreased sporulation. Thus, TaRac6 could affect the susceptibility of wheat to *Pst* by inhibiting the cell death triggered by the ROS burst. In rice and other plants, Rac proteins can regulate the production of H_2O_2 (Park et al., 2000; Jones et al., 2007).

As an important signaling molecule in plant cells, ROS is not only involved in programmed cell death, but also more importantly related to the formation of plant defense (Neill et al., 2002). In plants, Rac proteins have been shown to affect hydrogen peroxide production by regulating the activity of NADPH oxidase, which is necessary for the production of ROS (Bokoch and Diebold, 2002). Under hypoxic conditions, Rops are rapidly activated in *Arabidopsis*, resulting in ROP-dependent H_2O_2 production (Baxter-Burrell et al., 2002). In soybean cells, the Rac protein participated in the regulation of ROS production (Park et al., 2000). Overexpression of cotton GhRac13 promoted the production of H_2O_2 and then affected the formation of secondary walls of cotton cells (Potikha et al., 1999). It was speculated that Rac/Rops in dicotyledon may contribute to the ROS generation, however, the function of Rac/Rops to ROS generation in monocotyledon varies. In this study, TaRAC6 was demonstrated to play a negative role in wheat to *Pst* by inhibiting the H_2O_2 accumulation. Similarly, the mutant of *OsRac1* promotes ROS accumulation and cell death to increase the rice resistance (Kawasaki et al., 1999; Ono et al., 2001). The production of H_2O_2 mediated by CA-OsRac1 could be inhibited by DPI (NADPH oxidase inhibitor), indicating that NADPH oxidase downstream of OsRac1 regulated the production of H_2O_2 (Kawasaki et al., 1999). OsRac1 could interact with the NLR protein Pit to generate ROS and HR. The results showed that OsRac1 is required for Pit-mediated resistance to rice blast fungus (Kawano et al., 2010b). However, Rac genes in *Zea mays* could induce the production of ROS (Hassanain et al., 2000). What is more, constitutively activated mutant HvRacB has no significant effect on ROS production; it partially inhibited F-actin polarization distribution to *Bgh* invasion sites to prevent the invasion (Opalski et al., 2005). Another study further inferred that HvRacB could activate a ROP-binding protein kinase HvRBK1, which functioned in basal resistance to powdery mildew by affecting microtubule organization (Huesmann et al., 2012). In *Arabidopsis*, overexpression of *AtRac1* blocked the depolymerization of actin filaments during stomatal closure (Lemichez et al., 2001). In Barley, HvRacB was proven not only to regulate the reorganization of actin filaments to enhance susceptibility to *Bgh*, but also to affect stomata closure in ABA response (Schultheiss et al., 2005). Moreover, stomatal closure could be induced by ABA signaling in guard cells, which requires ROS formation to interact with Ca^{2+}-channels (Kwak et al., 2006; Li et al., 2006). These results indicate that the plant Rac protein not only participates in regulating the production of ROS, but also affects the opening and closing of stoma. In this study, silencing of *TaRac6* could reduce ROS accumulation of wheat to improve the infection of *Pst*. As we know, *Pst* infects wheat leaves through stoma (Wang et al., 2007). Whether *TaRac6* plays a role in stomatal opening and closing and whether it affects the infection of *Pst* by affecting stomatal opening and closing needs be further explored.

CONCLUSION

In conclusion, *TaRac6* was characterized in wheat's response to *Pst*. As a type I Rac/Rop GTPase, TaRac6 was located in the whole cell, where it could inhibit the cell death induced by Bax. More importantly, *TaRac6* plays a role in governing the level of wheat susceptibility to *Pst* by affecting the ROS burst. This finding is of great significance in advancing the full functional exploration of Rac/Rop in plant responses to pathogens, and it lays a foundation for breeding disease-resistance in wheat by modifying its susceptibility genes.

DATA AVAILABILITY STATEMENT

The raw data supporting the conclusions of this article will be made available by the authors, without undue reservation, to any qualified researcher.

AUTHOR CONTRIBUTIONS

ZK and XW designed the experiments. QZ performed most of the experiments, analyzed the data, and wrote the manuscript. XZ, RZ, ZW, WS, XW, and ZK assisted in the experiments and discussed the results. All authors contributed to the article and approved the submitted version.

FUNDING

This study was financially supported by the "111 Project" from the Ministry of Education of China (B07049) and the National Natural Science Foundation of China (No. 31620103913) to ZK.

ACKNOWLEDGMENTS

We thank Dr. Hao Feng for providing suggestions on how to improve the manuscript.

SUPPLEMENTARY MATERIAL

The Supplementary Material for this article can be found online at: https://www.frontiersin.org/articles/10.3389/fpls.2020.00716/full#supplementary-material

FIGURE S1 | Multiple alignment of the cDNA sequence of the three copies of *TaRac6* isolated from wheat cultivar "Suwon11."

FIGURE S2 | Multiple alignment of the encoding sequence of the three copies of TaRac6.

FIGURE S3 | Multiple alignment of TaRac6 against homologous amino acid sequences from other plant species. The red boxes indicate the G1–G5 boxes. The yellow box indicates the CxxL motif. Ta, *Triticum aestivum;* Os, *Oryza sativa*; Zm, *Zea mays*; At, *Arabidopsis thaliana*; Zm, *Zea mays*; Bd, *Brachypodium distachyon*. Different colors indicate homology levels of amino acids. The pink shading indicates at least 75% amino acid homology. Light blue shading indicates at least 50% amino acid homology.

FIGURE S4 | The protein feature of TaRac6.

FIGURE S5 | The original image file for western blot of TaRac6.

REFERENCES

Abramovitch, R. B., Kim, Y. J., Chen, S., Dickman, M. B., and Martin, G. B. (2003). *Pseudomonas* type III effector AvrPtoB induces plant disease susceptibility by inhibition of host programmed cell death. *EMBO J.* 22, 60–69. doi: 10.1093/emboj/cdg006

Akamatsu, A., Wong, H. L., Fujiwara, M., Okuda, J., Nishide, K., Uno, K., et al. (2013). An OsCEBiP/OsCERK1-OsRacGEF1-OsRac1 module is an essential early component of Chitin-induced rice immunity. *Cell Host Microbe.* 13, 465–476. doi: 10.1016/j.chom.2013.03.007

Ayliffe, M., Devilla, R., Mago, R., White, R., Talbot, M., Pryor, A., et al. (2011). Nonhost resistance of rice to rust pathogens. *Mol. Plant Microbe Interact.* 24:1143. doi: 10.1094/MPMI-04-11-0100

Baxter-Burrell, A., Yang, Z., Springer, P., and Bailey-Serres, J. (2002). RopGAP4-dependent rop GTpase rheostat control of arabidopsis oxygen deprivation tolerance. *Science* 296, 2026–2028. doi: 10.1126/science.1071505

Berken, A. (2006). ROPs in the spotlight of plant signal transduction. *Cell Mol. Life Sci.* 63, 2446–2459. doi: 10.1007/s00018-006-6197-1

Bokoch, G., and Diebold, B. (2002). Current molecular models for NADPH oxidase regulation by Rac GTPase. *Blood* 100, 2692–2695. doi: 10.1182/blood-2002-04-1149

Camejo, D., Guzmán-Cedeño, Á, and Moreno, A. (2016). Reactive oxygen species, essential molecules, during plant-pathogen interactions. *Plant Physiol. Biochem.* 103, 10–23. doi: 10.1016/j.plaphy.2016.02.035

Chen, L., Shiotani, K., Togashi, T., Miki, D., Aoyama, M., Wong, H. L., et al. (2010). Analysis of the Rac/Rop small GTPase family in rice: expression, subcellular localization and role in disease resistance. *Plant Cell Physiol.* 51, 585–595. doi: 10.1093/pcp/pcq024

Chen, W., Wellings, C., Chen, X., Kang, Z., and Liu, T. (2014). Wheat stripe (yellow) rust caused by *Puccinia striiformis* f. sp. tritici. *Mol. Plant Pathol.* 15, 433–446. doi: 10.1111/mpp.12116

Dou, D., Kale, S., Wang, X., Jiang, R., Bruce, N., Arredondo, F., et al. (2008). RXLR-Mediated entry of Phytophthora sojae effector Avr1b into Soybean cells does not require pathogen-encoded machinery. *Plant Cell* 20, 1930–1947. doi: 10.1105/tpc.107.056093

Feng, H., Wang, X., Sun, Y., Wang, X., Chen, X., Guo, J., et al. (2011). Cloning and characterization of a calcium binding EF-hand protein gene TaCab1 from wheat and its expression in response to *Puccinia striiformis* f. sp. tritici and abiotic stresses. *Mol. Biol. Rep.* 38, 3857–3866. doi: 10.1007/s11033-010-0501-8

Fukai, T., and Ushio-Fukai, M. (2011). Superoxide dismutases: role in redox signaling, vascular function, and diseases. *Antioxid. Redox. Signal.* 15, 1583–1606. doi: 10.1089/ars.2011.3999

Hassanain, H., Sharma, Y., Moldovan, L., Khramtsov, V., Berliner, L., Duvick, J., et al. (2000). Plant Rac proteins induce superoxide production in mammalian cells. *Biochem. Biophys. Res. Commun.* 272, 783–788. doi: 10.1006/bbrc.2000.2791

Hellens, R. P., Edwards, E. A., Leyland, N. R., Bean, S., and Mullineaux, P. M. (2000). pGreen: a versatile and flexible binary Ti vector for Agrobacterium-mediated plant transformation. *Plant Mol. Biol.* 42, 819–832. doi: 10.1023/a:1006496308160

Hoefle, C., Huesmann, C., Schultheiss, H., Börnke, F., Hensel, G., Kumlehn, J., et al. (2011). A barley ROP GTPase ACTIVATING PROTEIN associates with microtubules and regulates entry of the barley powdery mildew fungus into leaf epidermal cells. *Plant Cell* 23, 2422–2439. doi: 10.1105/tpc.110.082131

Holzberg, S., Brosio, P., Gross, C., and Pogue, G. P. (2002). Barley stripe mosaic virus-induced gene silencing in a monocot plant. *Plant J.* 30, 315–327. doi: 10.1046/j.1365-313x.2002.01291.x

Huesmann, C., Reiner, T., Hoefle, C., Preuss, J., Jurca, M., Domoki, M., et al. (2012). Barley ROP binding kinase1 is involved in microtubule organization and in basal penetration resistance to the barley powdery mildew fungus. *Plant Physiol.* 159, 311–320. doi: 10.1104/pp.111.191940

Jones, M. A., Raymond, M. J., Yang, Z., and Smirnoff, N. (2007). NADPH oxidase-dependent reactive oxygen species formation required for root hair growth depends on ROP GTPase. *J. Exp. Bot.* 58, 1261–1270. doi: 10.1093/jxb/erl279

Jung, Y. H., Agrawal, G. K., Rakwal, R., Kim, J. A., Lee, M. O., Choi, P. G., et al. (2006). Functional characterization of OsRacB GTPase-a potentially negative regulator of basal disease resistance in rice. *Plant Physiol. Biochem.* 44, 68–77. doi: 10.1016/j.plaphy.2005.12.001

Kang, Z., Huang, L., and Buchenauer, H. (2002). Ultrastructural changes and localization of lignin and callose in compatible and incompatible interactions between wheat and Puccinia striiformis. *J. Plant Dis. Prot.* 109, 25–37.

Kawano, Y., Akamatsu, A., Hayashi, K., Housen, Y., Okuda, J., Yao, A., et al. (2010a). Activation of a Rac GTPase by the NLR family disease resistance protein Pit plays a critical role in rice innate immunity. *Cell Host Microbe* 7, 362–375. doi: 10.1016/j.chom.2010.04.010

Kawano, Y., Chen, L., and Shimamoto, K. (2010b). The function of Rac small GTPase and associated proteins in rice innate immunity. *Rice* 3, 112–121. doi: 10.1007/s12284-010-9049-4

Kawano, Y., Kaneko-Kawano, T., and Shimamoto, K. (2014). Rho family GTPase-dependent immunity in plants and animals. *Front. Plant Sci.* 5:522. doi: 10.3389/fpls.2014.00522

Kawano, Y., and Shimamoto, K. (2013). Early signaling network in rice PRR and R-mediated immunity. *Curr. Opin. Plant Biol.* 16, 496–504. doi: 10.1016/j.pbi.2013.07.004

Kawasaki, T., Henmi, K., Ono, E., Hatakeyama, S., Iwano, M., Satoh, H., et al. (1999). The small GTP-binding protein Rac is a regulator of cell death in plants. *Proc. Natl. Acad. Sci. U.S.A.* 96, 10922–10926. doi: 10.1073/pnas.96.19.10922

Kawasaki, T., Koita, H., Nakatsubo, T., Hasegawa, K., Wakabayashi, K., Takahashi, H., et al. (2006). Cinnamoyl-CoA reductase, a key enzyme in lignin biosynthesis, is an effector of small GTPase Rac in defense signaling in rice. *Proc. Natl. Acad. Sci. U.S.A.* 103, 230–235. doi: 10.1073/pnas.0509875103

Kwak, J., Nguyen, V., and Schroeder, J. (2006). The role of reactive oxygen species in hormonal responses. *Plant Physiol.* 141, 323–329. doi: 10.1104/pp.106.079004

Lacomme, C., and Santa Cruz, S. (1999). Bax-induced cell death in tobacco is similar to the hypersensitive response. *Proc. Natl. Acad. Sci. U.S.A.* 96, 7956–7961. doi: 10.1073/pnas.96.14.7956

Lambeth, J. D. (2004). NOX enzymes and the biology of reactive oxygen. *Nat. Rev. Immunol.* 4, 181–189. doi: 10.1038/nri1312

Lavy, M., Bracha-Drori, K., Sternberg, H., and Yalovsky, S. (2002). A cell-specific, prenylation-independent mechanism regulates targeting of type II RACs. *Plant Cell* 14, 2431–2450. doi: 10.1105/tpc.005561

Lemichez, E., Wu, Y., Sanchez, J. P., Mettouchi, A., Mathur, J., and Chua, N. H. (2001). Inactivation of AtRac1 by abscisic acid is essential for stomatal closure. *Genes Dev.* 15, 1808–1816. doi: 10.1101/gad.900401

Li, S., Assmann, S., and Albert, R. (2006). Predicting essential components of signal transduction networks: a dynamic model of guard cell abscisic acid signaling. *PLoS Biol.* 4:e312. doi: 10.1371/journal.pbio.0040312

Lieberherr, D., Thao, N. P., Nakashima, A., Umemura, K., Kawasaki, T., and Shimamoto, K. (2005). A sphingolipid elicitor-inducible mitogen-activated protein kinase is regulated by the small GTPase OsRac1 and heterotrimeric G-Protein in rice. *Plant Physiol.* 138, 1644–1652. doi: 10.1104/pp.104.057414

Ling, P., Wang, M., Chen, X., and Campbell, K. G. (2007). Construction and characterization of a full-length cDNA library for the wheat stripe rust pathogen (*Puccinia striiformis* f. sp. tritici). *BMC Genomics* 8:145. doi: 10.1186/1471-2164-8-145

Liu, J., Guan, T., Zheng, P., Chen, L., Yang, Y., Huai, B., et al. (2016). An extracellular Zn-only superoxide dismutase from Puccinia striiformis confers enhanced resistance to host-derived oxidative stress. *Environ. Microbiol.* 18:4118. doi: 10.1111/1462-2920.13451

Liu, J., Park, C., He, F., Nagano, M., Wang, M., Bellizzi, M., et al. (2015). The RhoGAP SPIN6 associates with SPL11 and OsRac1 and negatively regulates programmed cell death and innate immunity in rice. *PLoS Pathog.* 11:e1004629. doi: 10.1371/journal.ppat.1004629

Livak, K. J., and Schmittgen, T. D. (2012). Analysis of relative gene expression data using real-time quantitative PCR and the 2(-Delta C(T)) Method. *Methods* 25, 402–408. doi: 10.1006/meth.2001.1262

Ma, J., Huang, X., Wang, X., Chen, X., Qu, Z., Huang, L., et al. (2009). Identification of expressed genes during compatible interaction between stripe rust (Puccinia striiformis) and wheat using a cDNA library. *BMC Genomics* 10:586. doi: 10.1186/1471-2164-10-586

Miki, D., Itoh, R., and Shimamoto, K. (2005). RNA silencing of single and multiple members in a gene family of rice. *Plant Physiol.* 138, 1903–1913. doi: 10.1104/pp.105.063933

Neill, S., Desikan, R., and Hancock, J. (2002). Hydrogen peroxide signaling. *Curr. Opin. Plant Biol.* 5, 388–395. doi: 10.1016/S1369-5266(02)00282-0

Ono, E., Wong, H., Kawasaki, T., Hasegawa, M., Kodama, O., and Shimamoto, K. (2001). Essential role of the small GTPase Rac in disease resistance of rice. *Proc. Natl. Acad. Sci. U.S.A.* 98, 759–764. doi: 10.1073/pnas.021273498

Opalski, K. S., Schultheiss, H., Kogel, K. H., and Hückelhoven, R. (2005). The receptor-like MLO protein and the RAC/ROP family G-protein RACB modulate actin reorganization in barley attacked by the biotrophic powdery mildew fungus *Blumeria graminis* f.sp. hordei. *Plant J.* 41, 291–303. doi: 10.1111/j.1365-313X.2004.02292.x

Panwar, V., Mccallum, B., and Bakkeren, G. (2013). Endogenous silencing of Puccinia triticina pathogenicity genes through in planta-expressed sequences leads to the suppression of rust diseases on wheat. *Plant J.* 73:521. doi: 10.1111/tpj.12047

Park, J., Choi, H. J., Lee, S., Lee, T., Yang, Z., and Lee, Y. (2000). Rac-related GTP-binding protein in elicitor-induced reactive oxygen generation by suspension-cultured soybean cells. *Plant Physiol.* 124, 725–732. doi: 10.1104/pp.124.2.725

Pathuri, I. P., Zellerhoff, N., Schaffrath, U., Hensel, G., Kumlehn, J., Kogel, K., et al. (2008). Constitutively activated barley ROPs modulate epidermal cell size, defense reactions and interactions with fungal leaf pathogens. *Plant Cell Rep.* 27, 1877–1887. doi: 10.1007/s00299-008-0607-9

Potikha, T., Collins, C., Johnson, D., Delmer, D., and Levine, A. (1999). The involvement of hydrogen peroxide in the differentiation of secondary walls in cotton fibers. *Plant Physiol.* 119, 849–858. doi: 10.1104/pp.119.3.849

Schiene, K., Pühler, A., and Niehaus, K. (2000). Transgenic tobacco plants that express an antisense construct derived from a Medicago sativa cDNA encoding a Rac-related small GTP-binding protein fail to develop necrotic lesions upon elicitor infiltration. *Mol. Gen. Genet.* 263, 761–770. doi: 10.1007/s004380000248

Schultheiss, H., Dechert, C., Kogel, K. H., and Hückelhoven, R. (2002). A small GTP binding host protein is required for entry of powdery mildew fungus into epidermal cells of barley. *Plant Physiol.* 128, 1447–1454. doi: 10.1104/pp.010805

Schultheiss, H., Dechert, C., Kogel, K. H., and Hückelhoven, R. (2003). Functional analysis of barley RAC/ROP G-protein family members in susceptibility to the powdery mildew fungus. *Plant J.* 36, 589–601. doi: 10.1046/j.1365-313x.2003.01905.x

Schultheiss, H., Hensel, G., Imani, J., Broeders, S., Sonnewald, U., Kogel, K. H., et al. (2005). Ectopic expression of constitutively activated RACB in barley enhances susceptibility to powdery mildew and abiotic stress. *Plant Physiol.* 139, 353–362. doi: 10.1104/pp.105.066613

Schwessinger, B. (2017). Fundamental wheat stripe rust research in the 21st century. *New Phytol.* 213, 1625–1631. doi: 10.1111/nph.14159

Sorek, N., Gutman, O., Bar, E., Abu-Abied, M., Feng, X., Runing, M., et al. (2011). Differential effects of prenylation and S-acylation on type I and II ROPS membrane interaction and function. *Plant Physiol.* 155, 706–720. doi: 10.1104/pp.110.166850

Takai, Y., Sasaki, T., and Matozaki, T. (2001). Small GTP-binding proteins. *Physiol. Rev.* 81, 153–208. doi: 10.1152/physrev.2001.81.1.153

Van Doorn, W. G., Beers, E. P., Dangl, J. L., Tong, V. E. F., Gallois, P., Nishimura, I. H., et al. (2011). Morphological classification of plant cell deaths. *Cell Death. Differ* 18, 1241–1246. doi: 10.1038/cdd.2011.36

Vernoud, V., Horton, A. C., Yang, Z., and Nielsen, E. (2003). Analysis of the small GTPase gene superfamily in *Arabidopsis*. *Plant Physiol.* 131, 1191–1208. doi: 10.1104/pp.013052

Vetter, I. R., and Wittinghofer, A. (2001). The guanine nucleotide-binding switch in three dimensions. *Science* 294, 1299–1304. doi: 10.1126/science.1062023

Wang, C., Huang, L., Buchenauer, H., Han, Q., Zhang, H., and Kang, Z. (2007). Histochemical studies on the accumulation of reactive oxygen species (O2- and H2O2) in the incompatible and compatible interaction of wheat-*Puccinia striiformis* f. sp. tritici. *Physiol. Mol. Plant Pathol.* 71, 230–239. doi: 10.1016/j.pmpp.2008.02.006

Wang, Q., Han, C., Ferreira, A. O., Yu, X., Ye, W., Tripathy, S., et al. (2011). Transcriptional Programming and Functional Interactions within the Phytophthora sojae RXLR Effector Repertoire. *Plant Cell* 23, 2064–2086. doi: 10.1105/tpc.111.086082

Wennerberg, K., Rossman, K. L., and Der, C. J. (2005). The Ras superfamily at a glance. *J. Cell Sci.* 118, 843–846. doi: 10.1242/jcs.01660

Williams, C. L. (2003). The polybasic region of Ras and Rho family small GTPases: a regulator of protein interactions and membrane association and a site of nuclear localization signal sequences. *Cell. Signal.* 15, 1071–1080. doi: 10.1016/s0898-6568(03)00098-6

Winge, P., Brembu, T., Kristensen, R., and Bones, A. M. (2000). Genetic structure and evolution of RAC-GTPases in *Arabidopsis thaliana*. *Genetics* 156, 1959–1971.

Wong, H. L., Sakamoto, T., Kawasaki, T., Umemura, K., and Shimamoto, K. (2004). Down-regulation of Metallothionein, a reactive oxygen scavenger, by the small GTPase OsRac1 in rice. *Plant Physiol.* 135, 1447–1456. doi: 10.1104/pp.103.036384

Yang, T., and Poovaiah, B. W. (2002). Hydrogen peroxide homeostasis: activation of plant catalase by calcium/calmodulin. *Proc. Natl. Acad. Sci. U.S.A.* 99, 4097–4102. doi: 10.1073/pnas.052564899

Zhao, M., Wang, J., Ji, S., Chen, Z., Xu, J., Tang, C., et al. (2018). Candidate effector Pst_8713 impairs the plant immunity and contributes to virulence of *Puccinia striiformis* f. sp. tritici. *Front. Plant Sci.* 9:1294. doi: 10.3389/fpls.2018.01294

Conflict of Interest: The authors declare that the research was conducted in the absence of any commercial or financial relationships that could be construed as a potential conflict of interest.

Advantages of publishing in Frontiers

OPEN ACCESS
Articles are free to read for greatest visibility and readership

FAST PUBLICATION
Around 90 days from submission to decision

HIGH QUALITY PEER-REVIEW
Rigorous, collaborative, and constructive peer-review

TRANSPARENT PEER-REVIEW
Editors and reviewers acknowledged by name on published articles

Frontiers
Avenue du Tribunal-Fédéral 34
1005 Lausanne | Switzerland

Visit us: www.frontiersin.org
Contact us: frontiersin.org/about/contact

REPRODUCIBILITY OF RESEARCH
Support open data and methods to enhance research reproducibility

DIGITAL PUBLISHING
Articles designed for optimal readership across devices

FOLLOW US
@frontiersin

IMPACT METRICS
Advanced article metrics track visibility across digital media

EXTENSIVE PROMOTION
Marketing and promotion of impactful research

LOOP RESEARCH NETWORK
Our network increases your article's readership